Mathematical Modelling of Mass Transfer in Food Packaging Systems

A thesis presented in partial fulfilment of the requirements for the degree of

Master of Engineering in Bioprocess Engineering

at Massey University, Palmerston North, New Zealand

Jacus Kruger

2011

ABSTRACT

Food packaging is of critical importance for New Zealand food exports. One function of food packaging is to preserve the quality of food products during shipping and distribution, a key aspect of which is the control of mass transfer (in particular moisture). As such moisture transfer is an important consideration in the design of food packaging. However traditional food packaging selection has often involved a quantitative or "trial and error" approach. Mathematical models present a useful alternative, allowing changes to current system properties as well as the design of new systems to be investigated prior to physical testing. The objectives of this study were to: investigate the processes and considerations involved in food packaging selection, formulate mathematical models that can be used to predict moisture transfer in food packaging systems, and present potential applications for the developed mathematical models.

To obtain a broad understanding of food packaging, the properties of common packaging materials used in the food industry as well as current consumer and technological trends were reviewed. Considerations involved in food packaging selection were then investigated, including general considerations followed by a focus on mass transfer and barrier properties. It was found that, although theory allowing the quantitative selection of food packaging barrier properties is fairly comprehensive, it is common industry practice to select packaging qualitatively. This suggested that many food packaging systems are sub-optimised. Several phenomena not generally considered in food packaging selection were also investigated as required for the formulation of the mathematical models.

Review of literature revealed significant gaps regarding data of food packaging barrier properties. Therefore, to assist with the identification of specific applications for the mathematical models, a summary of the barrier property requirements of various food products was produced. As part of this work a table of the barrier properties of food packaging materials presented in a standard format was compiled.

Mathematical models were developed describing various mass transfer processes in food packaging systems. Firstly moisture transfer in a standard food package system was considered, consisting of a food product enclosed in a single individual packaging layer which may contain perforations. Further models were developed extending the standard system to include systems with two individual packaging layers that each may contain perforations, as well as packages containing food powders where mass transfer in the food powder is also significant. Systems with perforations in contact with food powder or centred on a relatively small isolated air pocket were also considered, where a localised two-dimensional moisture profile results. Finally, a food package consolidation model was developed to allow optimisation of such systems. Formulation of each model involved development of a conceptual system (including the identification of key processes and properties, and specifying assumptions), formulation of a mathematical model, a numerical or analytical solution using MATLAB® software, and validation against experimental observations.

Several potential applications for the developed mathematical models were identified. A particular focus was placed on food powder systems with perforated packaging, such as those for which dense phase filling is used. This may include flours, sugar, soy powders, dairy powders, and other industrial or commercial food ingredients. Many high moisture content food products were also identified as having conceptually similar packaging systems, such as fresh produce, dairy products, meat products, and seafood. However it was noted that some extensions to the mathematical models may be required in some cases.

ACKNOWLEDGEMENTS

I would like to express a sincere thank you to the following people and organisations that supported me during this project:

Firstly, to my chief supervisor Prof. **John Bronlund** for his kind and supportive guidance, and considerable efforts arranging support for this project. Also to my co-supervisors **Tom Robertson** and **Chris Hartwell** for their knowledge, experience and guidance.

To **SCION** for providing the financial support for this project, and **Fonterra Co-operative Group Limited** for providing test samples.

To **Massey Staff**, including **Sue Nicolson**, **Garry Radford**, **Steve Glasgow**, and **John Edwards** for assisting with experimental trials and **Linda Lowe** for administrative support.

And lastly, to my friends and family for support and encouragement during this project.

Jacus Kruger **November 2011**

TABLE OF CONTENTS

NOMENCLATURE

A_{bag} = Surface area of paperboard bag (m^2)

A_f = Surface area of food powder (m^2)

$A_{f,air}$ = Area of air pocket in contact with food powder (m^2)

$A_{f,r}$ = Area of node in radial direction (m^2)

$A_{f,x}$ = Area of node in axial direction (m^2)

$A_{f,x,air}$ = Area of node in axial direction in contact with air pocket (m^2)

A_{lnr} = Surface area of polymer liner (m^2)

A_{pkg} = Package surface area (m^2)

$A_{prf,bag}$ = Total area of perforation(s) in paperboard bag (m^2)

A_{prf} = Total area of perforation(s) in packaging (m^2)

$A_{prf,lnr}$ = Total area of perforation(s) in polymer liner (m^2)

A_{stk} = Contact area of mass stacked on top of food package (m^2)

b_{lin} = Slope of linear isotherm of food (-)

C_{BET} = Guggenheim constant for BET isotherm of food (-)

C_{GAB} = Guggenheim constant for GAB isotherm of food (-)

c_{lin} = Constant for linear isotherm of food ((kg water).(kg solids)$^{-1)}$

$D_{0,bag,n}^{H_2O}$ = Pre-exponential factor of diffusivity of water vapour in nth layer of paperboard bag ($m^2.s^{-1}$)

$D_{0,lnr,n}^{H_2O}$ = Pre-exponential factor of diffusivity of water vapour in nth layer of polymer liner ($m^2.s^{-1}$)

$D_{0,pkg,n}^{H_2O}$ = Pre-exponential factor of diffusivity of water vapour in nth layer of packaging ($m^2.s^{-1}$)

$D_{air}^{H_2O}$ = Diffusivity of water vapour in air ($m^2.s^{-1}$)

$D_{bag,n}^{H_2O}$ = Diffusivity of water vapour in n^{th} layer of paperboard bag ($m^2.s^{-1}$)

$D_{eff}^{H_2O}$ = Effective diffusivity of water vapour in food powder ($m^2.s^{-1}$)

$D_{lnr,n}^{H_2O}$ = Diffusivity of water vapour in n^{th} layer of polymer liner ($m^2.s^{-1}$)

$D_{pkg,n}^{H_2O}$ = Diffusivity of water vapour in n^{th} layer of packaging ($m^2.s^{-1}$)

d_{prf} = Average diameter of perforations (m)

$d_{prf,bag}$ = Average diameter of perforation(s) in paperboard bag (m)

$d_{prf,lnr}$ = Average diameter of perforation(s) in polymer liner (m)

$D^{H_2O}_{ref,bag,n}$ = Reference diffusivity of water vapour in nth layer of paperboard bag (m^2.s^{-1})

$D^{H_2O}_{ref,lnr,n}$ = Reference diffusivity of water vapour in nth layer of polymer liner (m^2.s^{-1})

$D^{H_2O}_{ref,pkg,n}$ = Reference diffusivity of water vapour in nth layer of packaging (m^2.s^{-1})

$E^{H_2O}_{D,lnr,n}$ = Activation energy of diffusion of water vapour in nth layer of polymer liner (J.mol^{-1})

$E^{H_2O}_{D,pkg,n}$ = Activation energy of diffusion of water vapour in nth layer of packaging (J.mol^{-1})

$E^{H_2O}_{D,bag,n}$ = Activation energy of diffusion of water vapour in nth layer of paperboard bag (J.mol^{-1})

$E^{H_2O}_{P,bag,n}$ = Activation energy of permeation of water vapour in nth layer of paperboard bag (J.mol^{-1})

$E^{H_2O}_{P,lnr,n}$ = Activation energy of permeation of water vapour in nth layer of polymer liner (J.mol^{-1})

$E^{H_2O}_{P,pkg,n}$ = Activation energy of permeation of water vapour in nth layer of packaging (J.mol^{-1})

g = Acceleration due to gravity (m.s^{-1})

J = Total number of nodes per layer (-)

j = Node number (-)

$J^{H_2O}_{prf}$ = Diffusive flux of water vapour through perforation(s) in packaging (mol.m^{-2}.s^{-1})

$J^{H_2O}_{prf,bag}$ = Diffusive flux of water vapour through perforation(s) in paperboard bag (mol.m^{-2}.s^{-1})

$J^{H_2O}_{prf,lnr}$ = Diffusive flux of water vapour through perforation(s) in polymer liner (mol.m^{-2}.s^{-1})

K = Total number of nodes in radial direction of food powder (-)

k = Node number in radial direction (-)

K_{air} = Node number in radial direction positioned at edge of air pocket (-)

k_{GAB} = Constant for GAB isotherm of food (-)

M = Moisture content of food ((kg water).(kg solids)$^{-1}$)

$M_{0,GAB}$ = Moisture content of monolayer for GAB isotherm ((kg water).(kg solids)$^{-1}$)

$M_{0,GAB}$ = Moisture content of monolayer for GAB isotherm of food ((kg water).(kg solids)$^{-1}$)

$M_{1,BET}$ = Moisture content of monolayer for BET isotherm of food ((kg water).(kg solids)$^{-1}$)

M_i = Initial moisture content of food product ((kg water).(kg solids)$^{-1}$)

$M_{r,air}$ = Molecular mass of dry air (kg.mol^{-1})

M_{r,H_2O} = Molecular mass of water (kg.mol^{-1})

m_s = Mass of solids in food product (kg)

m_{stk} = Mass stacked on top of food package (kg)

N = Total number of packaging layers (-)

N_{bag} = Total number of layers in paperboard bag (-)

N_{lnr} = Total number of layers in polymer liner (-)

$p_0^{H_2O}$ = Saturated water vapour pressure (Pa)

$P_{0,bag,n}^{H_2O}$ = Pre-exponential factor of permeability of water vapour in nth layer of paperboard bag (mol.m.m^{-2}.s^{-1}.Pa^{-1})

$P_{0,lnr,n}^{H_2O}$ = Pre-exponential factor of permeability of water vapour in nth layer of polymer liner (mol.m.m^{-2}.s^{-1}.Pa^{-1})

$P_{0,pkg,n}^{H_2O}$ = Pre−exponential factor of permeability of water vapour in nth layer of packaging (mol.m.m^{-2}.s^{-1}.Pa^{-1})

$p_a^{H_2O}$ = Water vapour pressure in ambient air (Pa)

$p_{ap}^{H_2O}$ = Water vapour pressure in air pocket (Pa)

p_{atm} = Atmospheric pressure (Pa)

$p_{bag}^{H_2O}$ = Water vapour pressure in paperboard bag (Pa)

$p_{bag,i}^{H_2O}$ = Initial water vapour pressure in paperboard bag (Pa)

$P_{bag,n}^{H_2O}$ = Permeability of water vapour in nth layer of paperboard bag (mol.m.m^{-2}.s^{-1}.Pa^{-1})

$p_{bh}^{H_2O}$ = Water vapour pressure in bag headspace (Pa)

$p_f^{H_2O}$ = Water vapour pressure in food (Pa)

$p_{f,i}^{H_2O}$ = Initial water vapour pressure in food (Pa)

$p_{lh}^{H_2O}$ = Water vapour pressure in liner headspace (Pa)

$p_{lnr,i}^{H_2O}$ = Initial water vapour pressure in polymer liner (Pa)

$p_{lnr,j}^{H_2O}$ = Water vapour pressure in j^{th} node of polymer liner (Pa)

$P_{lnr,n}^{H_2O}$ = Permeability of water vapour in n^{th} layer of polymer liner (mol.m.m^{-2}.s^{-1}.Pa^{-1})

p_{ph}^{air} = Pressure of air in package headspace (Pa)

$p_{pkg}^{H_2O}$ = Water vapour pressure in packaging (Pa)

$p_{pkg,i}^{H_2O}$ = Initial water vapour pressure in packaging (Pa)

$P_{pkg,n}^{H_2O}$ = Permeability of water vapour in n^{th} layer of packaging (mol.m.m^{-2}.s^{-1}.Pa^{-1})

R = Ideal gas constant (8.314 m^3.Pa.K^{-1}.mol^{-1} or J.K^{-1}.mol^{-1})

r = Spatial position in food powder in radial direction (m)

R_f = Thickness of food powder in radial direction (m)

RH_a = Ambient relative humidity (%)

$S_{0,bag,n}^{H_2O}$ = Pre-exponential factor of solubility of water vapour in n^{th} layer of paperboard bag (mol.m^{-3}.Pa^{-1})

$S_{0,lnr,n}^{H_2O}$ = Pre-exponential factor of solubility of water vapour in n^{th} layer of polymer liner (mol.m^{-3}.Pa^{-1})

$S_{0,pkg,n}^{H_2O}$ = Pre−exponential factor of solubility of water vapour in n^{th} layer of packaging (mol.m^{-3}.Pa^{-1})

$S_{air}^{H_2O}$ = Solubility of water vapour in air (mol.m^{-3}.Pa^{-1})

$S_{bag,n}^{H_2O}$ = Solubility of water vapour in n^{th} layer of paperboard bag (mol.m^{-3}.Pa^{-1})

$S_{f}^{H_2O}$ = Solubility of water vapour in food powder (mol.m^{-3}.Pa^{-1})

$S_{lnr,n}^{H_2O}$ = Solubility of water vapour in n^{th} layer of polymer liner (mol.m^{-3}.Pa^{-1})

$S_{pkg,n}^{H_2O}$ = Solubility of water vapour in n^{th} layer of packaging (mol.m^{-3}.Pa^{-1})

$S_{ref,bag,n}^{H_2O}$ = Reference solubility of water vapour in n^{th} layer of paperboard bag (mol.m^{-3}.Pa^{-1})

$S_{ref,lnr,n}^{H_2O}$ = Reference solubility of water vapour in n^{th} layer of polymer liner (mol.m^{-3}.Pa^{-1})

$S_{ref,pkg,n}^{H_2O}$ = Reference solubility of water vapour in n^{th} layer of packaging (mol.m^{-3}.Pa^{-1})

T = Temperature (K)

t = Time (s)

$T_{ref,D_{bag}^{H_2O},n}$ = Temperature of reference diffusivity of water vapour in nth layer of paperboard bag (K)

$T_{ref,D_{lnr}^{H_2O},n}$ = Temperature of reference diffusivity of water vapour in nth layer of polymer liner (K)

$T_{ref,D_{pkg}^{H_2O},n}$ = Temperature of reference diffusivity of water vapour in nth layer of packaging (K)

$T_{ref,S_{bag}^{H_2O},n}$ = Temperature of reference solubility of water vapour in nth layer of paperboard bag (K)

$T_{ref,S_{lnr}^{H_2O},n}$ = Temperature of reference solubility of water vapour in nth layer of polymer liner (K)

$T_{ref,S_{pkg}^{H_2O},n}$ = Temperature of reference solubility of water vapour in nth layer of packaging (K)

V_{air} = Volume of air in package headspace (m^3)

x = Spatial position (m)

$X_{bag,n}$ = Thickness of nth layer of paperboard bag (m)

X_f = Thickness of food powder (m)

$X_{lnr,n}$ = Thickness of nth layer of polymer liner (m)

X_n = Thickness of nth layer of packaging (m)

X_T = Total thickness of packaging (m)

$X_{T,bag}$ = Total thickness of paperboard bag (m)

$X_{T,lnr}$ = Total thickness of polymer liner (m)

$X_{T,pkg}$ = Total thickness of packaging (m)

$\Delta H_{S,bag,n}^{H_2O}$ = Partial molar enthalpy of sorption of water vapour in nth layer of paperboard bag (J.mol^{-1})

$\Delta H_{S,lnr,n}^{H_2O}$ = Partial molar enthalpy of sorption of water vapour in nth layer of polymer liner (J.mol^{-1})

$\Delta H_{S,pkg,n}^{H_2O}$ = Partial molar enthalpy of sorption of water vapour in nth layer of packaging (J.mol^{-1})

Δr_f = Width of node in radial direction of food powder (m)

$\Delta x_{bag,n}$ = Width of node in nth layer of paperboard bag (m)

Δx_f = Width of node in food powder (m)

$\Delta x_{lnr,n}$ = Width of node in nth layer of polymer liner (m)

$\Delta x_{pkg,n}$ = Width of node in nth layer of packaging (m)

ε = Porosity of food powder (-)

ρ_{air} = Density of air (kg.m^3)

LIST OF FIGURES

LIST OF TABLES

Chapter 1

INTRODUCTION

1.1 BACKGROUND

The New Zealand food industry is a significant contributor to the country's economy. Of particular importance are food exports, which account for a large proportion of sales. Due to the relatively remote location of New Zealand to international markets, the success of food exports has been largely based on an ability to preserve food product quality during shipping and distribution (Robertson, 2006). Food packaging has commonly been used for this purpose, and is an integral part of most food exports.

A key aspect of food packaging selection is mass transfer, in particular of moisture. It is well known that such factors can have a significant effect on the quality and shelf life characteristics of food products (Comyn, 1985; Brody, 2000; Robertson, 2006). As such the effect of mass transfer on the quality preservation of food has been researched extensively, and many current food packaging systems are designed to control mass transfer to increase product stability. However traditional food packaging selection in terms of barrier properties has often involved a qualitative approach leading to sub-optimised systems, or "trial and error" based design requiring significant capital expenditure (Coles et al., 2003; Robertson, 2006). This is further complicated by the long shelf life of many food products which may be upwards of one year, for which long term testing is often not feasible. A useful alternative is the use of mathematical models, which allow changes to current system properties as well as the design of new systems to be investigated prior to physical testing. Mathematical models therefore present potential for significant cost savings for industrial users.

Basic models of food packaging design in terms of mass transfer are fairly common (Robertson, 2006; Comyn 1985). However such theory contains many simplifications to allow practical utilisation for standard food packaging systems. Many industrial applications are expected to involve more complex mass transfer phenomena such as concentration

dependent barrier properties, non-constant temperatures, multiple layers with different properties and diffusion through perforations, for which basic food packaging design models would not be adequate. Therefore it will be necessary to produce more complex mathematical models for such scenarios.

The true value of the developed mathematical models will be for industrial applications. A key part of this study will therefore be to identify potential applications and demonstrate how the mathematical models can be applied for such scenarios, thereby increasing the likelihood of industry adoption. To aid the identification of potential applications it is first necessary to investigate the standard processes and considerations involved in food packaging selection, as well as the barrier property requirements of current food packaging systems. Food packaging selection involves many considerations in addition to mass transfer, and some of these may be conflicting. Investigating these considerations should provide some appreciation of the practical limitations of food packaging optimisation, as well as highlight areas for potential improvement. If potential industrial applications can be indentified and the mathematical models applied, industry uptake and use of the models is more likely.

1.2 OBJECTIVES

The objectives of this study were to:

- Investigate the processes and considerations involved in food packaging selection, and the requirements of current food packaging systems (in particular with respect to barrier properties).

- Formulate mathematical models that can be used to predict mass transfer in food packaging systems and the effect on food product shelf life, with a focus on moisture transfer.

- Present potential applications for the developed mathematical models, and demonstrate their utilisation.

If mathematical models of mass transfer in food packaging systems can be developed and target industrial applications identified, optimisation of current and future food packaging systems may be achieved.

Chapter 2

LITERATURE REVIEW

2.1 INTRODUCTION

To obtain an understanding of the processes and considerations involved in food packaging, the properties of common packaging materials used in the food industry were firstly reviewed. A large range of materials are used for food packaging, however not all these materials are relevant to this study. Outlining the properties of common packaging materials will direct the focus of this investigation, as well as assisting with the identification of potential applications for the mathematical models. Current consumer and technological trends in food packaging were also briefly investigated to ensure work carried out was relevant for future applications.

Food packaging selection involves many considerations in addition to barrier requirements. To gain an appreciation for other aspects of food packaging selection, general considerations were reviewed briefly. However barrier properties are the focus of this study and therefore were discussed in more detail.

Comprehensive theory exists for predicting the shelf life and barrier properties of packaged food systems, and can be used for food packaging selection. This theory forms the basis for mathematical models of water vapour/gas transfer in a packaged food. Two key aspects need to be considered: the effect of the gas/water vapour on the shelf life of the food product, and the rate of mass transfer of the gas/water vapour through the packaging material.

The basic theory for water vapour/gas transfer in packaged food systems contains many underlying assumptions and simplifications to increase its practical utilisation. However, these assumptions are not always valid, and this could affect the accuracy of predictions by mathematical models that are based on such theory. Formulating mathematical models for a broad range of food package systems will therefore require

additional knowledge to what is commonly used for food packaging selection. Detailed theory of the permeation of water vapour/gas through packaging materials will therefore need to be covered, including non-simplified expressions, the effect of temperature, and mass transfer through perforations. Similarly, more complex interactions between the food product and the water vapour/gas will also need to be considered, such as respiration.

Therefore, the objectives of this review were to:

- Review existing food packaging materials and investigate current consumer and technological trends.

- Investigate the processes and considerations involved in food packaging selection, with an emphasis on barrier properties.

- Review existing theory of food packaging design that can be used to determine the shelf life and barrier property requirements, as well as model mass transfer in packaged food systems (in particular moisture).

- Investigate more complex phenomena that may be required for formulating a mathematical model of the gas headspace inside a range of packaged food systems.

2.2 OVERVIEW OF FOOD PACKAGING

2.2.1 Outline of Food Packaging

Modern food packaging has four key functions: containment of the food product, protection of the product from the outside environment (and the environment from the product), convenience, and communication (Robertson, 2006). Whilst all these functions are crucial in the development of food packaging, this study is primarily concerned with the protection of the food product. Robertson (2006) suggests the environment outside the

food package consists of three different types: the physical environment in which physical damage can be caused to the product, the ambient environment including heat, water and water vapour, gases, light and biological contaminants, and the human environment where the food package interacts with people. Again this study is predominantly concerned with the ambient environment, specifically water vapour and gases such as oxygen and carbon dioxide.

2.2.2 Common Existing Food Packaging Materials

2.2.2.1 Paper and Paperboard

Paper and paperboard (alternatively termed fibreboard) are the most common type of packaging materials worldwide (Song et al., 2003), and accounted for 44% of the total mass of packaging materials consumed in New Zealand in 2008 (Packaging Council of New Zealand, 2009). These are materials that consist of a "network of natural cellulosic fibres" (Dury-Brun et al., 2006). Paper and paperboard are produced from pulp fibre, most of which is derived from wood. They are therefore commonly regarded as sustainable materials since most of the raw materials are renewable. Paper-based materials are also largely recyclable and biodegradable, and as such are generally more appreciated by consumers than other packaging materials (Dury-Brun et al., 2006). Another particular advantage of paper-based materials is that they are generally easily printable. However, they are usually highly permeable to water, gases (including oxygen and carbon dioxide), organic solvents, fatty substances, and volatile flavours and aromas. Therefore many food packaging applications that use paper-based materials require additional barrier materials such as plastics or metals (Coles et al., 2003). It should also be noted that paper materials generally have a higher carbon dioxide loading on the atmosphere than most other packaging materials (expect glass), which is increasingly accepted as a more accurate representation of environmental impact than sustainability or biodegradability (T. R. Robertson, personal communication, 16 September, 2009).

Paper-based materials are usually termed paperboard when the grammage (mass per unit area) exceeds 200-224 $g.m^{-2}$ (Coles et al., 2003; Robertson, 2006). Paper and paperboard packaging is used to produce various types of packaging, including flexible packaging such as beverage cartons, bags and pouches, and rigid packaging such as folding cartons and corrugated paperboard (Robertson, 2006; Brody, 2000). These can be used for dry food products (for example cereals, biscuits, bread, tea, coffee, sugar, and flour), frozen and chilled foods, liquid foods and beverages, chocolate and sugar confectionary, fast foods, and fresh produce (such as fruit, vegetables, meat, and fish) (Coles et al., 2003). However it should be noted that uncoated paper based packaging is generally only used where a very short shelf life is acceptable, or for relatively stable foods.

2.2.2.2 Polymers

The terms plastics or polymers are "generic terms for materials based on macromolecular organic compounds obtained from molecules with lower molecular weight or by chemical alteration of natural macromolecular compounds" (Robertson, 2006). Polymers are widely used for packaging materials because they are mouldable under certain conditions, generally chemically inert, cost effective, and lightweight, as well as being recyclable. They can also be produced in various colours and levels of transparency, and with various degrees of heat resistance, heat sealing ability, and barrier properties (Coles et al., 2003). Polymers are permeable to small molecules such as water vapour, gases and organic vapours; however the degree of permeability ranges significantly (Robertson, 2006). Plastic materials represented 21% of the total mass of packaging materials consumed in New Zealand in 2008 (Packaging Council of New Zealand, 2009). Polymers are used for a wide range of food packaging applications, including rigid plastic containers such as bottles, jars, and tubs, flexible films such as bags, sachets and pouches, and films or coatings with selective barrier properties (Coles et al., 2003; Brody, 2000).

Polymers commonly used in New Zealand for food packaging include poly(ethylene terephthalate) (PET), high density polyethylene (HDPE), low density polyethylene (LDPE), polypropylene (PP), polystyrene (PS), and ethylene vinyl alcohol (EVOH). The properties,

common uses, and approximate range of permeabilities to water vapour and oxygen of these polymers are outlined in Table 2-1.

Table 2-1: Properties, common uses, and approximate range of permeabilities to water vapour and oxygen of polymers commonly used in New Zealand for food packaging (Robertson, 2006; Coles et al., 2003; Piringer & Baner, 1999; Plastics Design Library, 1995).

Polymer	Properties	Common Uses	Water Vapour Permeability * (amol.m.m^{-2}.s^{-1}.Pa^{-1}) ¶	Oxygen Permeability † (amol.m.m^{-2}.s^{-1}.Pa^{-1}) ¶
PET	Transparent, high tensile strength, high chemical resistance, light weight, high puncture resistance	Bottles, trays	37,700 - 116,000	11.9
HDPE	Readily heat sealable, hard, high strength, good chemical stability, good barrier to water vapour, lower impact resistance, not transparent	Bottles	14,500	356 (22.8°C)
LDPE	Readily heat sealable, tough, high impact resistance, good chemical stability, good barrier to water vapour, partly transparent, high permeability to gases	Bottles, caps, tubs, dispensers, films, coatings	37,700 - 43,500	1,020 (23°C)
PP	Transparent, good thermal resistance, heat sealable, becomes brittle below 0°C, sensitive to oxygen, good water vapour barrier, not heat sealable	Bottle closures, bottles, tubs, films	14,500 - 37,700	2.04
PS	Hard, high transparency, resistant to many chemicals, printable, brittle, high permeability to gases and vapours	Tubs	324,000	658 (22.8°C)

EVOH	High barrier to gases including oxygen, high strength when dry, printable, high water vapour permeability, sensitive to moisture	High barrier films or coatings	53,200-305,000	0.0142-0.275

* Water vapour permeability values are at 40°C and 90% RH (Plastics Design Library, 1995)

† Oxygen permeability values are at 20°C and 0% RH unless otherwise noted (Plastics Design Library, 1995)

¶ a = atto = 10^{-18} (refer to Table 2-4)

2.2.2.3 Metals

Metal materials are commonly used for the packaging of foods, mainly as foils and cans. Foils usually consist of aluminium or aluminium alloys and are almost always used in combination with other materials. Where a packaging material consists mainly of aluminium foil, extruded layers of polyethylene are common on both surfaces to protect the aluminium and to provide a heat seal layer. Food packaging applications of aluminium foils include chocolate, potato chips and instant coffee packaging (Lord, 2003). Aluminium sheets thicker than 25.4 μm are practically impermeable, although they maintain good barrier properties below this thickness (Robertson, 2006). A vacuum-deposited coating of aluminium with a thickness in the nanometer range is another technology with reported good barrier properties (Lange & Wyser, 2003). Metal cans are produced from steel or aluminium, and can be constructed as either three- or two-piece containers. Cans are practically impermeable and allow severe heat processing of the food product, which can significantly extend the shelf life of the product to 2-3 years or more. Common food packaging applications of metal cans include beverages (such as soft drinks and beer), and processed foods (Coles et al., 2003). The disadvantage of metal materials is that they are relatively expensive, both in terms of the raw material and processing.

It is believed that, due to the relatively high cost of metals, most applications of metal foils would require very high barrier properties. Such packaging systems will generally not be relevant to this study.

2.2.2.4 Glass

Glass has traditionally been used to produce rigid containers such as bottles and jars for storing relatively high moisture content foods. Particularly important characteristics of glass are that it is transparent, impermeable, and chemically resistant to all food products, which are desirable for many food packaging applications (Coles et al., 2003). However, glass is relatively heavy, brittle, and requires a large amount of energy for production, which is also linked to a very high carbon dioxide loading on the atmosphere. Its importance as a packaging material for many commodity products has therefore been declining (Brody, 2000). Nonetheless, through developments such as increasing the strength and decreasing the weight of glass, glass containers have remained in common use as a food packaging material (Robertson, 2006). Also, it has been found that consumers generally perceive glass packaged products as being of a higher quality. As a result, the use of glass for packaging materials in New Zealand has in fact increased from an estimated 84,000 tonnes in 1994 to 229,151 tonnes in 2008 (Packaging Council of New Zealand, 2009). Current food products commonly packed in glass containers include instant coffee, spices, processed baby foods, premixed products, jams and spreads (Coles et al., 2003).

Again, as for metal foils, most applications of glass for food packaging would require very high barrier properties to justify the high cost. Therefore glass packaging materials will also generally not be relevant to this investigation.

2.2.2.5 Barrier Films and Coatings

Barrier films or coatings are commonly used in combination with other packaging materials, particularly for plastic packaging. These films or coatings provide the required barrier properties, while other materials make up the bulk of the packaging. As a result other packaging considerations can be optimised to a greater level while still providing the required protection in terms of shelf life. Polymers are the most common material used for water vapour/gas barriers in food packaging applications, which is mainly attributed to the significantly lower cost than other barrier materials. However, where very high barrier

properties are essential, polymers are often not suitable and metal or glass materials are generally required (Coles et al., 2003; Lange & Wyser, 2003).

Common barrier materials include aluminium foil or vacuum deposited coatings, and lamination or co-extrusion of high barrier polymers such as poly(vinylidene chloride) (PVdC), ethylene vinyl alcohol (EVOH), poly(vinyl alcohol) (PVAL), and polyamide (PA). A common problem encountered with high gas barrier polymers (other than PVdC) is their sensitivity to water; as a result these are often placed between water barrier layers (Lange & Wyser, 2003).

Currently a major focus of research in packaging technology is biopolymers (Akbari et al., 2007). According to Robertson (2006), the standard definition for a biopolymer is "a degradable plastic in which the degradation process results in lower molecular weight fragments produced by the action of naturally-occurring microorganisms such as bacteria, fungi and algae." One such technology is biobased nanocomposites, which are produced from the integration of nanoclay particles into polymers (Akbari et al., 2007). The aim is to produce materials with satisfactory barrier properties which also appeal to growing environmentally conscious markets.

2.2.3 Consumer and Technological Trends

2.2.3.1 Consumer

According to Euromonitor International (2005), consumers are increasingly concerned about the need for sustainability. Many consumers prefer less bulky food packaging, and a preference for recycled materials is growing. Similarly, there is growing concern about company practice with regards to environmental issues. Lange & Wyser (2003) reported an increasing desire by consumers to avoid aluminium and chlorine based packaging materials for environmental reasons. This is linked to the high amount of energy required to produce aluminium, and the potential of toxic dioxins produced by the

combustion of PVDC, PVC and similar chlorine containing polymers (although this is a fairly misunderstood and largely debated subject (Buekens & Huang, 1998)). These trends suggest that markets for biodegradable and recyclable food packaging, and packaging produced from sustainable raw materials should grow. However, it is believed that this trend is largely driven by supermarkets rather than consumers (T. R. Robertson, personal communication, 16 September, 2009).

Other consumer trends that have been indentified include a growing demand for organic food products, or fresher products with a shorter shelf-life. Sales of organic packaged food in Australia rose from AUD$193.6 million in 2002 to AUD$327.8 million in 2007 (Euromonitor International, 2009). This is based on the perception by many consumers that fresh foods and organic produce is safer than conventionally processed foods (Euromonitor International, 2005; Lange & Wyser, 2003). Markets for fresh food products can therefore be expected to continue to grow. Lange & Wyser (2003) also suggested an increasing demand for more convenient packaging with good opening and re-closing function, as well as allowing the food product to be prepared in the packaging.

2.2.3.2 Technological

Lange & Wyser (2003) identified contradictory demands for higher processing line speeds and a reduction in packaging material consumption by some food manufacturers. Increasing processing speeds places greater stress and strain on the packaging, and there is therefore a demand for thinner and stronger packaging. However, there is also a problem of increased food waste as a result of more product failures due to reductions in packaging (T. R. Robertson, personal communication, 16 September, 2009). Furthermore, partly due to the consumer trends involving sustainability there are also increasingly stringent environmental standards related to food packaging that food manufacturers will have to meet. Some opportunities and threats for companies to achieving sustainability are summarised in Table 2-2.

Table 2-2: Opportunities and threats for companies to achieving sustainability (Euromonitor International, 2005).

Opportunities	Threats
• Consumer awareness of bad company practise will continue to grow, due to efforts by campaigners and media coverage. • Companies will be forced or volunteer to meet increasingly stringent environmental standards. • Consumers will increase recycling efforts as a result of local government initiatives and growing environmental awareness. • Large manufacturers will continue to add more fair trade and organic brands to their portfolios, driven by growing consumer demand. • Organic and fair trade items will graduate from commodities to incorporate more sophisticated items, thus adding value to the segment. • The cost of organic and fair trade products will come down as distribution becomes more widespread through mass retail outlets. • Retailers will make more efforts to stock fair trade and organic products, and source more locally in response to consumer and governmental demands.	• Increasing globalisation and competition will continue to force companies to cut costs by using cheap labour and resources, and intensive farming methods. • More large companies may look to circumvent strict Fair Trade regulations by launching their own versions of ethical products. This may undermine confidence in fair trade as a whole. • Organic industry will be faced with the challenge of meeting consumer demands for healthy, safe, and convenient products while staying committed to all-natural and organic ingredients. • Organic and fair trade products will still be perceived as too expensive by many consumers. • Retail industry will continue to consolidate and become more competitive, thus increasing distribution area as food is sourced from further away and transported to fewer distribution centres.

Another common trend in the food packaging industry has been the replacement of glass with plastic for commodity products due to the cost savings associated with the actual lower material cost, weight reduction, and reduced breakage. However, there are several requirements that need to be met by any replacement packaging materials, including low oxygen and water vapour permeability, chemical resistance, heat-resistance and recyclability, depending on the application. Finally, many oxygen barrier layers currently used in packaging are sensitive to water and are generally placed between two moisture

barriers, which is costly. There is therefore a demand for oxygen barriers that retain their properties in the presence of water, particularly for applications where moisture transfer is not of importance (Lange & Wyser, 2003).

2.2.4 Discussion

Consumer trends suggest growing markets for biodegradable and recyclable food packaging, and packaging produced from sustainable raw materials. Currently work is being carried out on the development of biopolymer-based coatings that can be applied to paperboard packaging materials (Akbari et al., 2007; Sorrentino et al., 2007; J. E. Bronlund, personal communication, 9 July, 2009). Mass transfer, in particular moisture, will be a key issue in the development of such packaging technologies. Food packaging systems where these technologies are applied therefore present potential applications for the mathematical models to be developed.

2.3 FOOD PACKAGING SELECTION

2.3.1 Introduction

The selection of food packaging involves several considerations, including technical requirements, cost, consumer considerations, legislative requirements and environmental aspects. Many of these factors are conflicting, and the optimal packaging system may be a combination of suboptimal factors (Coles et al., 2003). This could impact on potential applications for the mathematical models to be developed. Such general food packaging considerations were briefly investigated.

2.3.2 General Considerations

2.3.2.1 Technical

The technical requirements of food product packaging are arguably the most important from a food manufacturer's point of view. This aspect of packaging selection is the focus of this investigation and involves protecting the investment made in the production of the food product (Robertson, 2006). The packaging needs to provide sufficient protection and/or preservation during storage and distribution to ensure the required shelf-life is met, and to minimise product waste due to damage. Considerations are dependent on the food product and the environment(s) it will encounter, and may include physical, chemical, biochemical, biological and microbial protection (Coles et al., 2003). Some common technical considerations include strength, flexibility, impact resistance, hardness, transparency, chemical resistance, printability, and heat sealability, which often have a significant bearing on the type of packaging material used. Mass transfer, including moisture, is also included in technical requirements.

2.3.2.2 Cost

Cost is a major consideration in food packaging selection, and places significant restrictions on the type of packaging. However, it should be noted that this not only includes direct costs (such as the cost of the packaging material and those associated with the required packaging process), but also indirect costs, including those associated with storage, transportation, supply, energy consumption, labour, line efficiency, investment, sales, quality control, and waste (Coles et al., 2003; Lange & Wyser, 2003). Therefore a food manufacturer needs to consider the total costs involved with the product packaging. For example, a more expensive packaging material may be feasible if it leads to a lower total cost (Lange & Wyser, 2003). This can particularly be a problem in large companies where the person(s) responsible for purchasing packaging may be well removed from the actual use of the packaging, and hence indirect costs may not be considered. Considerations of costs

associated with product packaging are not expected to be directly relevant to this investigation.

2.3.2.3 Consumer

Consumer considerations include marketing of the food product, communication, and how the product packaging will be used by the consumer. For marketing, aspects such as aesthetics, brand competition, and perceived quality need to be considered. Specific function and convenience provided by the packaging are also of importance (Brody, 2000; Coles et al., 2003). These considerations were not covered for this study unless they had a bearing on the work being carried out.

2.3.2.4 Legislation

Food product packaging needs to meet legislative requirements, such as regulations regarding food hygiene and labelling. Of particular importance in terms of the packaging material is migration from the packaging to the food product (Coles et al., 2003). Environmental regulations are also becoming increasingly strict. The New Zealand regulations for a food product and its packaging are outlined in the *Australia New Zealand Food Standards Code* (Commonwealth of Australia, 2007). Legislative requirements are not in the scope of this investigation.

2.3.2.5 Environmental

Environmental considerations are becoming increasingly important in the packaging selection process, and with the growing consumer concern of sustainability these considerations are also gaining some alignment with consumer requirements. Environmental considerations include energy and raw material requirements, ratio of package weight to product weight, reusability, recyclability, biodegradability, and waste

produced (Coles et al., 2003; Lyijynen et al., 2003). Again, such considerations are not expected to be directly relevant to this investigation.

2.3.3 Discussion

It is clear that there are many considerations that need to be made when selecting food packaging, and the most important considerations will largely depend on the intended application. Key issues that will likely need to be addressed for a coated paper/paperboard packaging material include recyclability, sustainability, migration of contaminants, strength, cost, and barrier properties. These issues will all have a significant bearing on the success of any such technology being developed. However, for this study only water vapour and gas barrier properties will be investigated.

2.4 SELECTING BARRIER PROPERTIES OF FOOD PACKAGING

2.4.1 Introduction

To determine the barrier property requirements of food packaging, two aspects need to be considered: the effect of water vapour/gas on the shelf life of the food product, and the rate of mass transfer of water vapour/gas into the package, including through the packaging material. These will be discussed in turn, followed by integrated concepts which allow required barrier properties to be calculated. Actual industry practice will also be discussed briefly.

2.4.2 Food Product Shelf Life

All food products undergo deteriorative changes which lead to a reduction in the quality of the product, and which can make the product unfit or unsafe for consumption. However, it should also be noted that some changes in foods are favourable, and optimal

product quality may occur at some stage during distribution or storage (for example ripening of fresh produce). The purpose of altering the barrier properties of packaging materials is to extend the shelf life of the food product by reducing the rate of deteriorative changes. The transfer of water vapour, oxygen, and carbon dioxide can have a significant effect on the rate of these changes. Many foods are particularly sensitive to one or more specific gas. To determine the optimum barrier properties of the food packaging, some understanding of how the quality of the product is affected by these factors is required.

2.4.2.1 Water Activity

Water activity (a_w) is a measure of the amount of free water that is available in a system, and which can therefore facilitate chemical and biochemical reactions. This is not the same as moisture content, which is a measure of the total water present in the system. This difference arises from the fact that water exists in various states and associates with other constituents in various ways. Particularly in food systems the relationship of water activity to moisture content can be complex (Fennema, 1996; Coles et al., 2003; Robertson, 2006). For the practical purposes of this study, the water activity of a system can mathematically be defined as:

$$a_w = \frac{p_i^{H_2O}}{p_0^{H_2O}} \quad \textbf{(2-1)}$$

where:

a_w = Water activity (-)

$p_i^{H_2O}$ = Vapour pressure of water exerted by the system (Pa)

$p_0^{H_2O}$ = Saturated vapour pressure of pure water at the same temperature (Pa)

In foods, water activity can have a significant effect on several types of changes, including: microbial growth, enzymatic reactions, nonenzymatic browning, lipid oxidation, textural and other structural changes (Iglesias & Chirife, 1982). The relative rates of some deteriorative reactions that affect food stability during storage are illustrated in Figure 2-1. The specific effects and mechanisms involved in these changes are not in the scope of this

study; however it should be suffice to say that the water activity of a food product is a significant determinant of its stability, quality and safety.

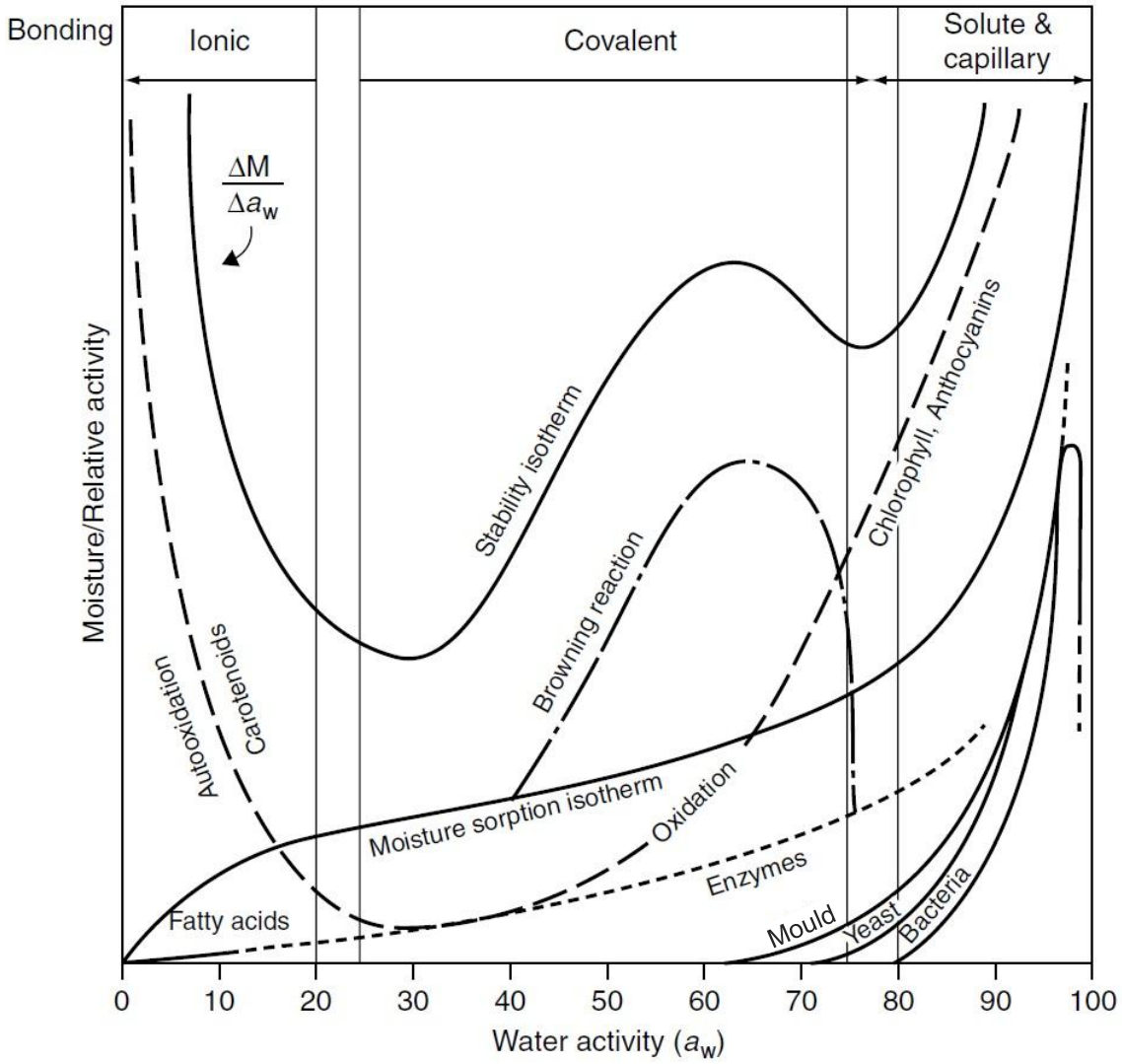

Figure 2-1: Relative rates of deteriorative reactions that affect food stability during storage (Rahman, 1995).

2.4.2.2 Moisture Sorption Isotherms

The relationship of water activity to moisture content of a system at any given temperature can be described by a moisture sorption isotherm. Schematic representations of typical moisture sorption isotherms for a food material are shown in Figure 2-2. This diagram also illustrates the common phenomenon of hysteresis, where the moisture sorption isotherm during desorption (removal of water) is different from that during

adsorption (addition of water) (Fennema, 1996). Depending on the food product being considered, this effect can potentially cause significant errors in a mathematical model. Obviously for moisture sensitive foods where the purpose of the packaging is to reduce the rate of moisture increase an adsorption isotherm will be required, and for applications of moisture loss from fresh foods a desorption isotherm will need to be used.

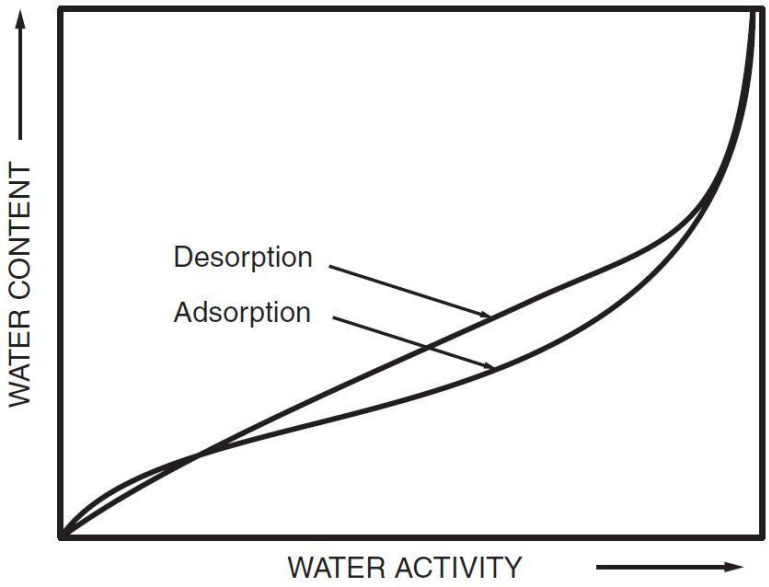

Figure 2-2: Schematic representation of typical moisture sorption isotherms for a food material (Eskin & Robinson, 2001).

Robertson (2006) described a method of predicting the shelf life of a low-moisture food product based on the equilibrium moisture content of the food if exposed to external package conditions (M_e), the initial moisture content (M_i), and the critical moisture content (M_c). These are depicted in Figure 2-3. The end of the product shelf life is reached when the moisture content of the food reaches the critical moisture content, after which the water activity of the food is too high to sufficiently reduce stability changes, or other changes have occurred. This method will be covered in more detail in Section 2.4.4.1. A similar method should be applicable to high moisture foods where the moisture loss is a major determinant of shelf life.

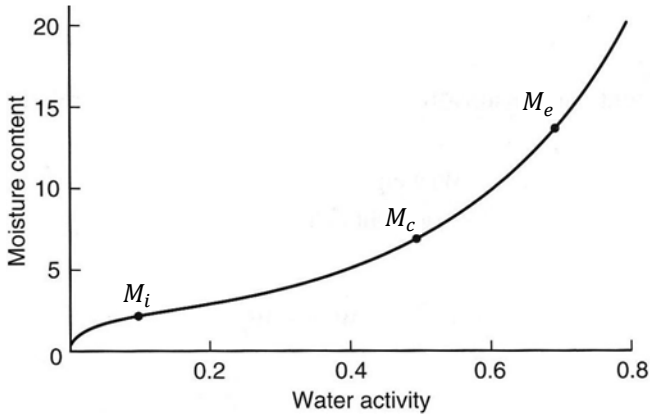

Figure 2-3: Typical moisture sorption isotherm for a low-moisture food, where M_i = initial moisture content, M_c = critical moisture content, M_e = equilibrium moisture content (Robertson, 2006).

Several mathematical equations of moisture sorption isotherm curves have been developed. The most relevant equation depends on the food product, the water activity range of interest, and other practical considerations (Robertson, 2006; Iglesias & Chirife, 1982). Some commonly used equations are outlined below. It should be noted that none of these equations are expected to be accurate at very high water activities (a_w > 0.95), therefore they will need to be used with caution for very high moisture foods (such as fresh produce).

2.4.2.2.1 Linear Model

$$M = b_{lin}a_w + c_{lin} \quad \textbf{(2-2)}$$

where:

M = Moisture content ((kg of water).(kg of solids)$^{-1}$)

b_{lin} = Slope of linear isotherm (-)

c_{lin} = Constant for linear isotherm ((kg of water).(kg of solids)$^{-1}$)

The linear model involves treating the isotherm as a linear function at a particular point of the curve (Robertson, 2006). This greatly simplifies calculations, however depending on the application this simplification would generally only be applicable over very small water activity intervals.

2.4.2.2.2 Brunauer-Emmett- Teller Model (BET)

$$\frac{M}{M_{1,BET}} = \frac{C_{BET} a_w}{(1 - a_w)(1 - a_w + C_{BET} a_w)} \quad \textbf{(2-3)}$$

where:

$M_{1,BET}$ = Moisture content of monolayer for BET isotherm ((kg of water).(kg of solids)$^{-1}$)

C_{BET} = Guggenheim constant for BET isotherm (-)

The BET equation is commonly used for low-moisture foods and generally fits water sorption data over a water activity range of 0.1 to 0.35 (Eskin & Robinson, 2001; Al-Muhtaseb et al., 2002).

2.4.2.2.3 Guggenheim-Anderson-de Boer Model (GAB)

$$\frac{M}{M_{0,GAB}} = \frac{C_{GAB} k_{GAB} a_w}{(1 - k_{GAB} a_w)(1 - k_{GAB} a_w + C_{GAB} k_{GAB} a_w)} \quad \textbf{(2-4)}$$

where:

$M_{0,GAB}$ = Moisture content of monolayer for GAB isotherm ((kg of water).(kg of solids)$^{-1}$)

C_{GAB} = Guggenheim constant for GAB isotherm (-)

k_{GAB} = Constant for GAB isotherm (-)

The GAB model is an extension of the BET equation and has been found to fit experimental sorption data for almost all food materials up to a high water activity of about 0.9 (Eskin & Robinson, 2001; Al-Muhtaseb et al., 2002).

2.4.2.3 Oxygen and Carbon Dioxide

Oxidation reactions are major mechanisms of quality degradation in many foods. However, oxygen and carbon dioxide can also significantly affect other deteriorative changes, including microbial growth, respiration and colour changes (Fennema, 1996; Robertson, 2006). The kinetics of these changes vary significantly. In terms of shelf life, acceptable levels of oxygen or carbon dioxide transfer are often expressed as a maximum amount gained or lost by the product, beyond which the extent of deteriorative changes have been sufficient to make the food product unacceptable (Robertson, 2006).

2.4.3 Packaging

To select an appropriate packaging material and type for a specific food product application it is necessary to know the transfer rate(s) of the gas(es) of interest through the materials. The rate of transfer of a gas through a permeable material is dependent on the thickness of the material, its surface area, and the difference in partial pressure of the gas on either side of the material. A standardised value known as the permeability can be used to compare and calculate the transfer rate of a specific gas through various packaging materials.

2.4.3.1 Permeability

Robertson (2006) indicated that steady state permeation through a uniform packaging film can be expressed as:

$$\frac{Q}{t} = \frac{P}{X} A \Delta p \qquad \textbf{(2-5)}$$

where:

Q = Amount of permeant (mol)

t = Time (s)

P = Permeability of permeating species in packaging (mol.m.m^{-2}.s^{-1}.Pa^{-1})

X = Thickness of packaging (m)

A = Surface area of packaging (m^2)

Δp = Difference in vapour pressure of permeant across packaging (Pa)

P/X is often referred to as a single term known as the permeance ($mol.m^{-2}.s^{-1}.Pa^{-1}$).

Assumptions made in the derivation of this expression include: permeation is at steady state, Henry's law applies (therefore solubility is constant and independent of concentration), diffusivity is also constant and independent of concentration, and permeation is in one dimension only (Robertson, 2006). The assumption of steady state relies on constant internal and external vapour pressures, a constant temperature, steady state being reached in a relatively short time, and that the absorption capacity of the film itself is not significant. Also, permeation in one direction only applies to uniform packaging materials where each individual layer has a constant thickness.

The permeability value is dependent on the conditions at which it is determined, particularly temperature. In industry, permeability values determined at 38°C and 90% relative humidity are often used to give a "worst case" analysis, and/or because this is often the only data available. However, for food products distributed in a temperate climate, 25°C and 75% relative humidity may be more appropriate (Robertson, 2006).

Permeability is determined using several different methods and is reported in many different units. Banks et al. (1995) proposed reporting values in SI units, and using SI prefixes to clarify comparison of values. It was also suggested that the quantity of permeant be reported in moles to allow better comparison of different gases. Using this convention, permeability values are reported as $mol.m.m^{-2}.s^{-1}.Pa^{-1}$, permeance values as $mol.m^{-2}.s^{-1}.Pa^{-1}$, and transfer rates in either $mol.m^{-2}.s^{-1}$ or $mol.m.m^{-2}.s^{-1}$. A list of conversion factors determined from first principles is shown in Table 2-3. Conversion factors are based on the assumption that the ideal gas law applies. A list of SI prefixes that may be used in this investigation is shown in Table 2-4.

Table 2-3: Factors for converting alternative permeability, permeance and transfer rate units to the proposed SI units (p_T = total system pressure (Pa), T = temperature (K), M_r = molecular mass of the permeating species (g.mol^{-1})). For oxygen transfer, these conversion factors assume a 100% concentration difference across the film; if an atmospheric oxygen concentration was used, the conversion factor needs to be divided by 0.2095.

Variable	SI Unit	Original Unit	Conversion Factor
Permeability	mol.m.m^{-2}.s^{-1}.Pa^{-1}	mL.cm.cm^{-2}.s^{-1}.(cm Hg)$^{-1}$	$9.023 \times 10^{-9}\ p_T/T$
Permeability	mol.m.m^{-2}.s^{-1}.Pa^{-1}	mL.mm.m^{-2}.day^{-1}.atm^{-1}	$1.374 \times 10^{-20}\ p_T/T$
Permeability	mol.m.m^{-2}.s^{-1}.Pa^{-1}	mL.mil.100 in.$^{-2}$.day^{-1}.atm^{-1}	$5.410 \times 10^{-21}\ p_T/T$
Permeability	mol.m.m^{-2}.s^{-1}.Pa^{-1}	mL.mm.cm^{-2}.s^{-1}.(cm Hg)$^{-1}$	$9.023 \times 10^{-10}\ p_T/T$
Permeability	mol.m.m^{-2}.s^{-1}.Pa^{-1}	g.mm.m^{-2}.day^{-1}.atm^{-1}	$1.143 \times 10^{-13}\ /M_r$
Permeance	mol.m^{-2}.s^{-1}.Pa^{-1}	g.100 in.$^{-2}$.day^{-1}.atm^{-1}	$1.771 \times 10^{-9}\ /M_r$
Permeance	mol.m^{-2}.s^{-1}.Pa^{-1}	g.m^{-2}.day^{-1}.bar^{-1}	$1.157 \times 10^{-10}\ /M_r$
Permeance	mol.m^{-2}.s^{-1}.Pa^{-1}	g.m^{-2}.day^{-1}.atm^{-1}	$1.143 \times 10^{-10}\ /M_r$
Permeance	mol.m^{-2}.s^{-1}.Pa^{-1}	mL.m^{-2}.day^{-1}.atm^{-1}	$1.374 \times 10^{-17}\ p_T/T$
Permeance	mol.m^{-2}.s^{-1}.Pa^{-1}	mL.m^{-2}.day^{-1}.bar^{-1}	$1.392 \times 10^{-17}\ p_T/T$
Transfer Rate	mol.m.m^{-2}.s^{-1}	g.mm.m^{-2}.day^{-1}	$1.157 \times 10^{-8}\ /M_r$
Transfer Rate	mol. m^{-2}.s^{-1}	g.m^{-2}.day^{-1}	$1.157 \times 10^{-5}\ /M_r$
Transfer Rate	mol.m.m^{-2}.s^{-1}	g.mil.100 in.$^{-2}$.day^{-1}	$4.557 \times 10^{-9}\ /M_r$
Transfer Rate	mol.m^{-2}.s^{-1}	mL.m^{-2}.day^{-1}	$1.392 \times 10^{-12}\ p_T/T$

Table 2-4: List of SI prefixes (Lukens, 2000).

Prefix	Symbol	Factor
milli	m	10^{-3}
micro	μ	10^{-6}
nano	n	10^{-9}
pico	p	10^{-12}
femto	f	10^{-15}
atto	a	10^{-18}

2.4.3.2 Multiple Layers

Packaging consisting of multiple layers can generally be regarded as providing resistances to gas or vapour transfer in series. Therefore the following relationship can be derived (Comyn, 1985):

$$\frac{X_T}{P_T} = \frac{X_1}{P_1} + \frac{X_2}{P_2} + \frac{X_3}{P_3} + \cdots \quad \textbf{(2-6)}$$

where:

P_T = Total permeability of permeating species in packaging film (mol.m.m^{-2}.s^{-1}.Pa^{-1})

P_1, P_2, P_3 = Permeability of permeating species in each individual layer (mol.m.m^{-2}.s^{-1}.Pa^{-1})

X_T = Total thickness of packaging film (m)

X_1, X_2, X_3 = Thickness of each individual packaging layer (m)

2.4.3.3 Concentration Dependence of Diffusivity and Solubility

Robertson (2006) indicated that diffusivity and solubility are relatively independent of concentration for many gases, including oxygen and to a certain extent carbon dioxide. However, this is not the case where significant interaction occurs between the polymer and permeant, such as water in hydrophilic films.

Vahdat & Sullivan (2001) suggested that the concentration-dependence of the diffusivity of a permeating species in a polymeric material can be represented by:

$$D = D(0)e^{\beta C} \quad \textbf{(2-7)}$$

where:

β = A constant (-)

$D(0)$ = Diffusivity as concentration approaches zero (m^2.s^{-1})

Comyn (1985) indicated that the above equation is generally only applicable where Henry's law is a reasonable approximation at low concentrations or sufficiently high temperatures. It was noted that for systems in which Henry's law is not a reasonable approximation, the concentration-dependence of the diffusivity is generally more complex. However, a similar expression was proposed in terms of vapour partial pressure:

$$D = D_0 exp\left(\alpha \frac{p}{p_0}\right) \quad \textbf{(2-8)}$$

where:

α = A constant (-)

Del Nobile et al. (2003) proposed the following relationship to describe the dependence of the water vapour diffusion coefficient on the concentration of water:

$$D = A_1 exp\left[\frac{-1}{A_2 + A_3 C}\right] \quad \textbf{(2-9)}$$

where:

A_1 = A constant (-)

A_2 = A constant (-)

A_3 = A constant (-)

Comyn (1985) suggested that where the solubility of a permeating species can not be approximated by Henry's law, a sorption isotherm similar to that for food products (Section 2.4.2.2) can be used to represent its concentration-dependence. Some common isotherms are represented graphically in Figure 2-4, where the solubility is equal to the adsorbed concentration divided by the vapour pressure (Equation 2-17).

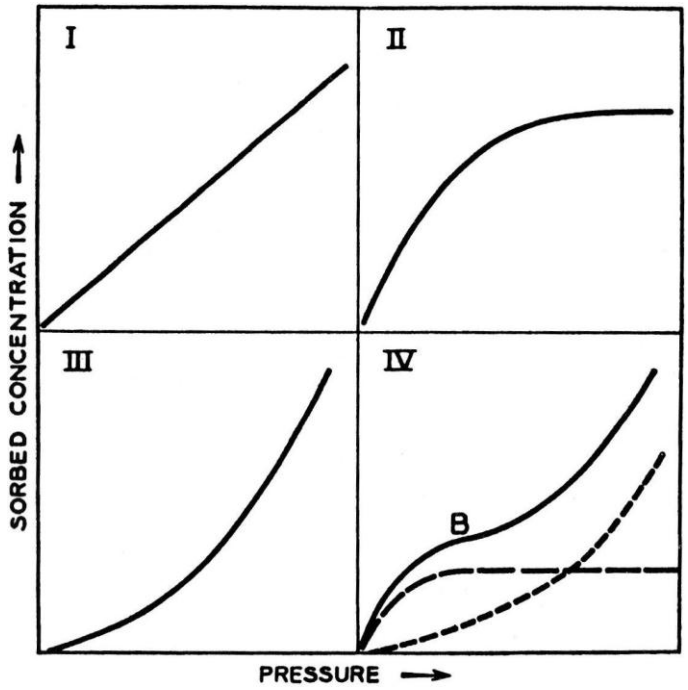

Figure 2-4: Common isotherms of the relationship between vapour pressure and adsorbed concentration, where (I) is Henry's law, (II) is the Langmuir equation, (III) is the Flory-Huggins equation, and (IV) is the BET equation (Comyn, 1985).

2.4.4 Integrated Concepts

2.4.4.1 Water-Sensitive Foods

Using relationships covered earlier, a series of expressions can be derived that allow the shelf life of a food product to be estimated. Alternatively, these expressions can be used to predict required barrier properties to achieve a specified shelf life. This derivation is described in detail by Robertson (2006), and will be represented here as it is fundamental to current packaging barrier selection. It should be noted that these expressions are limited by the restrictions and assumptions made in the derivation of the original relationships.

Firstly, the expression for steady-state permeation for a low-moisture content food can be written in terms of mass transfer of water as follows:

$$\frac{dm_{H_2O}}{dt} = \frac{P}{X} M_{r,H_2O} A\left(p_1^{H_2O} - p_2^{H_2O}\right) \quad \textbf{(2-10)}$$

where:

m_{H_2O} = Mass of water vapour (kg)

t = Time (s)

M_{r,H_2O} = Molecular mass of water (0.01802 kg.mol^{-1})

$p_1^{H_2O}$ = Vapour pressure of water vapour outside food package (Pa)

$p_2^{H_2O}$ = Vapour pressure of water vapour inside food package (Pa)

Note that the molecular mass of water was included since permeability is expressed here in mol.m.m^{-2}.s^{-1}.Pa^{-1}.

As described earlier, the moisture content can be written in terms of vapour pressure using the moisture sorption isotherm of the food product. For illustrative purposes and simplicity, a linear isotherm will be assumed. However, a similar approach can be used for any sorption isotherm. Therefore rearranging Equation 2-2 gives:

$$p = \frac{p_0}{b_{lin}}(M - c_{lin}) \quad \textbf{(2-11)}$$

Expressing Equation 2-10 in terms of moisture content and substituting Equation 2-11 for water vapour pressure gives:

$$\frac{dm_{H_2O}}{dt} = \frac{dMm_s}{dt} = \frac{P}{X} M_{r,H_2O} A \left[\frac{p_0 M_e}{b_{lin}} - \frac{p_0 M}{b_{lin}}\right] \quad \textbf{(2-12)}$$

Where:

M_e = Equilibrium moisture content ((kg of water).(kg of solids)$^{-1}$)

This expression can then be simplified and integrated as follows. Integration can become fairly complex for other moisture sorption isotherms and numerical integration may be necessary.

$$\int_{M_i}^{M} \frac{1}{M_e - M} dM = \int_0^t \frac{P}{X} \frac{M_{r,H_2O} A}{m_s} \frac{p_0}{b_{lin}} dt \quad \textbf{(2-13)}$$

This results in the final expression which relates the moisture content to time:

$$ln\left[\frac{M_e - M_i}{M_e - M}\right] = \frac{P}{X}\frac{M_{r,H_2O}A}{m_s}\frac{p_0}{b_{lin}}t \quad \textbf{(2-14)}$$

When the moisture content is equal to the critical moisture content, M_c, the shelf life of the food product can be estimated by the time, t (Robertson, 2006).

2.4.4.2 Oxygen-Sensitive Foods

A similar approach to that covered above for water-sensitive food products can be used to determine the shelf life or required barrier properties for oxygen-sensitive foods (or other gases including carbon dioxide) (Robertson, 2006). However the procedure is simplified by the fact that oxygen is generally readily utilised (the rate of oxygen consumption will be equal to the rate of ingress into the food package). As a result the oxygen concentration inside the food package will remain zero, and a sorption isotherm is not required. In this case the steady-state permeation equation can be integrated directly to give:

$$\frac{Q_{O_2}}{t} = \frac{P}{X}A\left(p_1^{O_2} - p_2^{O_2}\right) \quad \textbf{(2-15)}$$

where:

Q_{O_2} = Amount of oxygen transferred across packaging film (mol)

$p_1^{O_2}$ = Partial pressure of oxygen outside food package (Pa)

$p_2^{O_2}$ = Partial pressure of oxygen inside food package (Pa)

When the amount of oxygen transferred is equal to the maximum amount permissible (taking into account the initial amount of oxygen present in the package), the shelf life of the food product can be estimated by the time, t (Robertson, 2006).

2.4.5 Industry Practice

In industry, based on personal observation, the selection of packaging materials in terms of barrier properties often (although not always) appear to involve a relatively

qualitative approach. Companies mainly seem to select barrier polymers based on previous experience of similar products. Also, generally only one or a very few types of polymers are used for a specific barrier function (such as ethylene vinyl alcohol (EVOH) for a high oxygen barrier). This approach avoids the costs associated with quantitatively determining the required barrier properties for each food product; however it may lead to food packaging that is not optimised (the food packaging may either provide under- or over-protection). Under-protection will lead to a shorter shelf life than what is achievable or required; alternatively, over-protection could mean unnecessarily higher material costs.

It was noted that the availability of polymer films appeared to be a significant determinant of the type of packaging material used, particularly for companies that convert polymer films obtained from other manufacturers. Films with higher barrier properties than what is required may often be used because they are more readily available and sometimes more cost effective. This is linked to the costs associated with having to change the processing conditions of a production line to produce a different type of film. For example, a film with relatively many layers may be used because it is commonly produced for other purposes, even if not all the properties of the film are required to the same extent.

2.5 MODELLING OF INTERNAL FOOD PACKAGE CONDITIONS

2.5.1 Introduction

The basic theory of water vapour/gas transfer in packaged food systems is useful for practical purposes such as barrier selection and shelf life estimation in relatively simple systems. However, as indicated earlier, this theory contains many underlying assumptions and simplifications which may not be valid for all scenarios to be considered for the mathematical model (these are outlined in Section 2.4.3.1). The purpose of this section is therefore to address detailed theory of permeation not previously covered, as well as other concepts that may be needed for the modelling process. In particular, transient permeation involving concentration and temperature dependence will need to be addressed. Other

concepts of importance include mass transfer through perforations, heat transfer, the effect of multiple permeating species, and more complex interactions between the food and water vapour/gas, such as respiration.

2.5.2 Packaging

2.5.2.1 Permeation

The generalised model for unsteady-state diffusion is given by Fick's second law, and is analogous to heat transfer. Of primary importance to this investigation is one-dimensional unsteady-state diffusion through an infinite slab, which has the following form (Cleland, 2000):

$$\frac{\partial C}{\partial t} = \frac{\partial}{\partial x}\left(D(C)\frac{\partial C}{\partial x}\right) \quad \textbf{(2-16)}$$

where:

C = Concentration of permeant (mol.m^{-3})

x = Spatial position in x-direction (m)

D = Diffusivity (m^2.s^{-1})

At sufficiently low concentrations Henry's law is a reasonable approximation, which states the concentration of the diffusing species is directly proportional to its vapour pressure. The proportionality constant is known as the solubility:

$$C = Sp \quad \textbf{(2-17)}$$

where:

S = Solubility (mol.m^{-3}.Pa^{-1})

p = Vapour pressure (Pa)

However, at higher concentrations the relationship of concentration to vapour pressure may be more complex. In this case it is generally considered more accurate to express the driving force in terms of vapour pressure rather than concentration (Comyn, 1985). Therefore Fick's second law can be rewritten as:

$$S(p)\frac{\partial p}{\partial t} = \frac{\partial}{\partial x}\left(D(p)S(p)\frac{\partial p}{\partial x}\right) \quad \textbf{(2-18)}$$

The product of diffusivity and solubility is the permeability (Comyn, 1985). As a result Equation 2-18 can alternatively be expressed as:

$$S(p)\frac{\partial p}{\partial t} = \frac{\partial}{\partial x}\left(P(p)\frac{\partial p}{\partial x}\right) \quad \textbf{(2-19)}$$

where:

P = Permeability (mol.m.m^{-2}.s^{-1}.Pa^{-1})

2.5.2.2 Perforations

Perforations are common in many food packaging systems, and will have a significant bearing on moisture transfer. Fishman et al. (1996) suggested that when the diameter of a perforation is greater than 1×10^{-5} m, gas transfer can be treated as ordinary molecular diffusion in a cylindrical pathway filled with air. At steady-state the diffusive flux follows Fick's first law:

$$J_{prf} = D\frac{\Delta C}{L} \quad \textbf{(2-20)}$$

where:

J_{prf} = Diffusive flux of permeant through perforation (mol.m^{-2}.s^{-1})

D = Diffusivity (m^2.s^{-1})

ΔC = Difference in concentration of permeant across packaging (mol.m^{-3})

L = Path length (m)

The mean free-path of gas molecules at atmospheric pressure has been found to be about 1×10^{-7} m (Fishman et al., 1996). This suggests that when the diameter of perforations is greater than 1×10^{-7} m, gas transfer would occur by diffusion and convection. The analysis of these mechanisms is said to be very complex (Singh & Oliveira, 1994); however if the distance between macropores is much greater than their radius, the path length can be approximated by the sum of the length of the pore and the pore radius (Fishman et al., 1996; Techavises & Hikida, 2008).

Robertson (2006) suggested that gas flow through very small pores (diameter less than 1×10^{-7} m) follows Knudsen's law (Geankoplis, 2003):

$$J_{prf} = \frac{48.5 d_{prf}}{RTL}\left(\frac{T}{1000 M_r}\right)^{0.5} \Delta p \quad \textbf{(2-21)}$$

where:

d_{prf} = Diameter of perforation (m)

R = Ideal gas constant (8.314 $m^3.Pa.K^{-1}.mol^{-1}$)

T = Absolute temperature (K)

M_r = Molecular mass of diffusing gas ($kg.mol^{-1}$)

The derivation of permeability suggests that it should be independent of film thickness. However, it should be noted that pinholes can become significant in very thin films (<10 µm), which will affect the permeability. Similarly, affects of film thickness on the morphology of polymeric films has also been reported (Comyn, 1985).

2.5.2.3 Temperature Dependence

Kesting & Fritzsche (1993) suggested that the temperature dependence of the diffusivity of gases in a polymeric material can be expressed as an Arrhenius type relationship:

$$D = D_0 exp\left(-\frac{E_D}{RT}\right) \quad \textbf{(2-22)}$$

where:

D_0 = Diffusivity pre−exponential factor ($m^2.s^{-1}$)

E_D = Activation energy of diffusion ($J.mol^{-1}$)

A typical value of the activation energy of diffusion for water vapour includes 41,800 $J.mol^{-1}$ for polyvinyl chloride (Doty et al., 1946).

Ghosal & Freeman (1994) proposed a van't Hoff type relationship for the temperature dependence of the solubility of gases in polymers:

$$S = S_0 exp\left(-\frac{\Delta H_s}{RT}\right) \quad \textbf{(2-23)}$$

where:

S_0 = Solubility pre−exponential factor (mol.m^{-3}.Pa^{-1})

ΔH_S = Partial molar enthalpy of sorption (J.mol^{-1})

A typical value of the partial molar enthalpy of sorption for water vapour includes −31,000 J.mol^{-1} for polyvinyl chloride (Doty et al., 1946).

A similar expression can therefore be derived for the temperature dependence of permeability, which is the product of the diffusivity and solubility (Singh & Oliveira, 1994; Kesting & Fritzsche, 1993):

$$P = P_0 exp\left(-\frac{E_P}{RT}\right) \quad \textbf{(2-24)}$$

where:

P_0 = Permeability pre−exponential factor (mol.m.m^{-2}.s^{-1}.Pa^{-1})

E_P = Activation energy of permeation, which is the sum of E_D and ΔH_S (J.mol^{-1})

Example values of the activation energy of permeation for water vapour include 0 J.mol^{-1} for polystyrene, 9,830 J.mol^{-1} for polyvinyl chloride, and 73,200 J.mol^{-1} for poly(vinylidene chloride) (Doty et al., 1946).

Singh & Oliveira (1994) indicated that this is similar to the temperature dependence of produce respiration rate:

$$r = r_0 exp\left(-\frac{E_r}{RT}\right) \quad \textbf{(2-25)}$$

where:

r = Respiration rate (mol.s^{-1})

r_0 = Respiration rate pre−exponential factor (mol.s^{-1})

E_r = Activation energy of respiration (J.mol^{-1})

2.5.2.4 Temperature Profile

Temperature variations during the storage and distribution of a packaged food are common. Therefore it may not always be valid to assume a constant temperature, particularly when there are significant temperature fluctuations or large temperature differences or peaks. Where a constant temperature can not be assumed, the temperature-time profile that the product experiences during its storage and distribution will need to be considered. Similarly, heat transfer within the packaged food system may also need to be modelled where this is relatively slow. The generalised model for one-dimensional unsteady-state heat transfer through a slab is analogous to the mass transfer model (Cleland, 2008):

$$\rho(\theta)c_p(\theta)\frac{\partial\theta}{\partial t} = \frac{\partial}{\partial x}\left(\lambda(\theta)\frac{\partial\theta}{\partial x}\right) \quad \textbf{(2-26)}$$

where:

θ = Temperature (°C)

ρ = Density (kg.m^{-3})

c_p = Specific heat capacity (J.kg^{-1}.K^{-1})

λ = Thermal conductivity (W.m^{-1}.K^{-1})

2.5.2.5 Effect of One Permeating Species on Another

As mentioned earlier, the sensitivity of some packaging materials to water vapour, particularly in terms of oxygen permeability, is a common problem in food packaging. Packaging materials that are particularly sensitive to water vapour include poly(vinyl alcohol), uncoated cellulose, and nylon 6. More generally, permeation through a polymer can be regarded as a series of activated jumps from one cavity within the polymer to another. Therefore any agent that increases the size or number of these cavities increases the rate of permeation (Robertson, 2006). In the case of water, this is a result of swelling or plasticization (Comyn, 1985). Consequently, where this interaction is significant, the permeation of multiple permeating species will need to be considered simultaneously.

2.5.3 Food Product

2.5.3.1 Gas Utilisation/Production

Oxygen sensitive foods are generally two to four times more sensitive to oxygen in terms of shelf life than water sensitive foods are to moisture. Also, the amount of oxygen in air is usually 32 times higher than in the same volume of oxygen saturated water (Robertson, 2006). Therefore the oxygen initially inside a package containing an oxygen sensitive food product will likely be significant, and will need to be considered in a mathematical model. Oxygen and carbon dioxide utilisation/production are often modelled in terms of a single degradation mechanism, usually respiration in fresh produce (Tanner et al., 2002; Fonseca et al., 2002; Lee et al., 1991; Fishman et al., 1995), or some major oxygen-dependent reaction such as lipid-oxidation in potato chips (Quast et al., 2006) or vitamin C degradation in apple juice (Barront et al., 1993). Robertson (2006) suggests that for foods that are very resistant to gas diffusion (for example oxygen diffusion through very dense foods such as butter) the rate of diffusion in the food may need to be considered.

2.5.3.2 Respiration

For respiring produce the effect of respiration will need to be taken into account as it will have a significant effect on the concentrations of water vapour, oxygen and carbon dioxide. Various models for the rate of respiration have been developed; the relevant model is dependent on the application. Fishman et al. (1995) suggested an uncompetitive inhibition model:

$$r_{O_2} = \frac{V_m C_{O_2}}{K_M + C_{O_2} + K_i C_{O_2} C_{CO_2}} \quad \textbf{(2-27)}$$

where:

r_{O_2} = Rate of oxygen consumption (mol.s^{-1})

C_{O_2} = Concentration of oxygen (mol.m^{-3})

C_{CO_2} = Concentration of carbon dioxide (mol.m^{-3})

V_m = Maximal rate of Michaelis–Menten reaction (mol.s^{-1})

K_M = Michaelis constant (%)

K_i = Coefficient of inhibition ($\%^{-1}$)

When the respiratory quotient (RQ) is close to one, the rate of carbon dioxide production, r_{CO_2}, can be approximated by the rate of oxygen consumption, r_{O_2}.

Similarly, Conte et al. (2009) proposed a simplified version of the Michaelis-Menten equation:

$$r_{O_2} = A_{M1} exp\left(-A_{M2} C_{CO_2}\right) C_{O_2} \quad \textbf{(2-28)}$$

$$r_{CO_2} = K_1 \left\{A_{M1} exp\left(-A_{M2} C_{CO_2}\right) C_{O_2}\right\} \quad \textbf{(2-29)}$$

where:

A_{M1} = Maximum oxygen consumption rate ($mol.s^{-1}$)

A_{M2} = A constant (-)

K_1 = Ratio of moles of carbon dioxide produced to moles of oxygen consumed (-)

2.5.3.3 Multi-Domain Foods

Multi-domain foods are foods that consist of regions with different physical and chemical compositions, such as a breakfast cereal containing raisins (Roca et al., 2008; Labuza & Hyman, 1998). It is common for these different regions to have a different initial water activity, in which case the food system may not only be in a transient state with the surrounding environment, but also between the individual regions in the food itself. Of particular importance to this investigation is the situation where the water activity of one food component is higher than the critical water activity of a lower water activity component (or lower than the critical water activity of a higher water activity component). In this case moisture transfer within the food product will eventually be sufficient to make one component (and therefore the entire food product) unacceptable or unsafe for consumption, regardless of the rate of moisture transfer through the packaging of the food. Nonetheless, since the diffusion of water within a food is usually much greater than permeation through polymer packaging, any differences in the water activity of different

components could have a significant effect on the shelf life of the product, and will therefore need to be considered in a mathematical model of such a system.

Guillard et al. (2003) developed a mathematical model to simulate a two-component food system, which was successfully validated by experimental measurements of a sponge cake with a fresh filling scenario. This model was further developed by Roca et al. (2008) to include an air gap of varying thickness at the interface of the two components, which was similarly validated. The general approach was to model transient diffusion in one-dimension, which can be expressed in terms of moisture content for component z:

$$\frac{\partial M_z}{\partial t} = \frac{\partial}{\partial x}\left(D_z(M_z)\frac{\partial M_z}{\partial x}\right) \quad \textbf{(2-30)}$$

In the case of an air gap, it was proposed that instantaneous mass transfer across the gap can be assumed; however, mass transfer at the surface of each food component does need to be considered (Roca et al., 2008). If it is assumed that the ideal gas law applies, the expression for mass transfer at the surface can be rearranged to give:

$$-D_z\rho_z\frac{dM_z}{dx} = \frac{k_z M_z}{RT}\Delta p \quad \textbf{(2-31)}$$

where:

k_z = Mass transfer coefficient at the surface of component z ($m.s^{-1}$)

ρ_z = Density of component z ($kg.m^{-3}$)

The moisture isotherm of each component can then be related to mass transfer at its surface.

2.6 DISCUSSION

The literature review process revealed significant gaps in available literature regarding the barrier properties of food packaging. Of particular note was the lack of a concise summary of the barrier property requirements of foods. Some such data are

available in literature, however are fairly scarce and scattered, making comparison of various systems difficult. It is believed that a summary of this information would be very beneficial to this study, and will likely also aid future investigations. Therefore it is proposed that a summary of the barrier property requirements of various food products be produced as part of this investigation. A table presented by Robertson (2006) would provide a good basis for such a summary.

It was noted that available data of the barrier property requirements of food products is largely qualitative. This provides a general indication, but is not ideal for the intended purpose. Therefore it will likely be necessary to quantitatively determine the barrier property requirements for some food packaging systems as part of this investigation. One method which may be used for this purpose involves referring to the properties of given packaging materials. Data of the barrier properties of existing packaging materials to water vapour and gases such as oxygen are relatively common in literature, however these are reported in a large variety of formats and is again fairly scattered. Therefore it would also be beneficial to compile a comprehensive table of available data of the barrier properties of food packaging materials reported in a standard format. Data compiled by Plastics Design Library (1995) would provide a useful foundation for this work.

2.7 SUMMARY

The properties of common packaging materials used in the food industry were reviewed. Of most importance to this investigation will be polymer and paper-based materials due to their relative permeability to gases/water vapour and their importance to New Zealand food exports. Consumer trends were also investigated, and indicate growing markets for biodegradable and recyclable food packaging, and packaging produced from sustainable raw materials. This suggests that food packaging systems with biopolymer-based materials may present potential applications for the mathematical models.

General considerations involved in food packaging selection were briefly investigated, including technical, cost, consumer, legislative, and environmental considerations. In terms of barrier properties, theory allowing the barrier requirements of food packaging to be determined quantitatively is fairly comprehensive. Such theory was discussed in detail. It was found that it is common industry practise to use a qualitative approach to food packaging design, suggesting that many food packaging systems are likely to be overdesigned.

Several phenomena not generally considered in food packaging selection were investigated to allow a much broader range of packaged food systems to be accurately modelled. In terms of the food packaging itself, these included transient permeation, perforations, temperature variations, concentration dependence, and the affect of one permeating species on another. More complex interactions between the food product and water vapour/gas were also explored, including gas utilisation/production, respiration of fresh produce, and multi-domain foods.

To assist with the identification of specific applications for the mathematical models, it was proposed that a summary of the barrier property requirements of food products be produced. Data of the barrier properties of food packaging materials is also to be compiled.

Chapter 3

BARRIER REQUIREMENTS OF FOOD PRODUCTS

3.1 INTRODUCTION

In the previous chapter it was identified that no clear quantitative summary of the barrier property requirements of food products exists in literature. Therefore it was proposed that such a summary be produced to aid this investigation. It was also suggested that a table of the barrier properties of food packaging materials presented in a standard format be compiled as part of this work. This chapter will outline the work carried out to produce these reference tools, including the methodology used to determine the data presented.

3.2 BARRIER PROPERTIES OF FOOD PACKAGING MATERIALS

The barrier properties of a large range of food packaging materials were compiled from literature into a tabular form. Water vapour, oxygen and carbon dioxide barrier properties were included. All values were converted to SI units of $mol.m.m^{-2}.s^{-1}.Pa^{-1}$ (refer to Table 2-3). Only data from sources which specified relevant test conditions and other required information were considered. The finalised compilation can be found in Appendix A.

3.3 DETERMINING BARRIER REQUIREMENTS OF FOODS

3.3.1 Methodology

Five methods for determining the barrier property requirements of packaging for a range of foods were investigated: researching literature data, obtaining information directly

from food packaging manufacturers or from food producers, estimating requirements based on calculations, and experimentally measuring the properties of existing food products. These methods are discussed in more detail.

3.3.1.1 Literature

The easiest method of determining the packaging barrier property requirements of selected food products is obtaining this information directly from literature. Unfortunately this type of data is very scarce, and where it does exist it is generally indicative only and mostly qualitative.

Data of the barrier properties of packaging materials, particularly polymer materials, is fairly abundant. Therefore, if the packaging material(s) of a specific food product is(are) known, the barrier properties of the packaging can potentially be determined. However for many packaging films, particularly multi-layer films, it is very difficult to determine the type of polymers used and the thickness of each layer. Also, there are a vast range of polymers used in modern packaging films with numerous processing variations that produce different barrier properties, and individual layers may consist of blends of different polymers with potentially indistinct layer boundaries. It should similarly be noted that the methods used to determine barrier properties vary significantly, and reporting errors are common, which makes comparison of values difficult. Nonetheless, using literature data to determine barrier properties could be used to obtain a general indication of barrier requirements.

3.3.1.2 Information from Food Packaging Manufacturers

It was hoped that the barrier property requirements of food products would be obtainable from food packaging manufacturers. However, it was found that food packaging manufacturers often select packaging with a focus on other packaging requirements, and barrier properties are generally based on previous experience with similar food products and rough estimates. Food packaging manufacturers therefore generally do not have

specific data of permeability values required for specific food products, or prefer to keep this information in-house.

Another option is obtaining information of the type of packaging films used for food products from food packaging manufacturers and determining the barrier properties from literature data. Unfortunately in many cases the specifications of a packaging film, including the number of layers, the type of materials, and the thickness of each layer, for a specific food product is commercially sensitive information, which makes obtaining such data very difficult.

3.3.1.3 Information from Food Producers

Obtaining barrier property requirements directly from food producers was another method that was investigated. An ideal situation would be where a food producer carries out shelf life testing of their products, from which barrier requirements can be determined or calculated. However, it was found that in many cases food producers obtain advice on the type of packaging from food packaging manufacturers, who will often recommend barrier properties based on previous experience (as discussed previously). Where shelf life testing is carried out, such information would be very valuable if obtainable, although again companies are likely to keep any such information in-house.

3.3.1.4 Calculation from Food Requirements

Calculating the required water vapour barrier properties for a food product requires some key information, including: the moisture sorption isotherm, initial moisture content, critical moisture content, mass of solids, and shelf life of the food product. Some estimation of the storage and distribution conditions is also required (temperature and relative humidity), as well as the surface area and possibly film thickness of the package. Some of this data is available from literature, or can be determined from food products, although values such as the initial and critical moisture contents are more difficult to obtain. It should

also be noted that values are relatively specific for a specific food product. However, it is believed that this method should give a good estimation of the required barrier properties if non-specific data is used.

A similar approach can be used for a gas (such as oxygen or carbon dioxide), which requires data on the maximum quantity of the gas permissible inside the food package. However, such literature data is generally more difficult to obtain than for water vapour.

An example calculation to determine the water vapour barrier requirements for a standard consumer sized package of corn flakes is outlined below.

Example: Water vapour barrier requirement of corn flakes.

A summary of the parameters used to calculate the water vapour barrier requirement of corn flakes in a standard consumer sized package is summarised in Table 3-1.

Table 3-1: Data used to predict the water vapour permeability requirement of corn flakes in a standard consumer size package.

Parameter	Symbol	Value	Units
Initial moisture content	M_i	0.0357 [a]	(kg water).(kg solids)$^{-1}$
Critical moisture content	M_c	0.062 [a]	(kg water).(kg solids)$^{-1}$
GAB parameters at 25°C	$M_{0,GAB}$	0.066 [a]	(kg water).(kg solids)$^{-1}$
	k_{GAB}	0.897 [a]	-
	C_{GAB}	2.31 [a]	-
Mass of product	m	310 [b]	g
Shelf life	θ_s	180 [b]	days
Surface area of packaging film	A_{pkg}	0.1403 [c]	m^2
Thickness of packaging film	X_T	52.2 [c]	µm
Mass of solids	m_s	299.3 [d]	g
Molecular mass of water	M_{r,H_2O}	18.02	g.mol^{-1}
Saturated vapour pressure of water vapour	p_0	2341 [e]	Pa
Equilibrium moisture content	M_e	0.1667 [e]	(kg water).(kg solids)$^{-1}$

[a] Obtained from literature (Farroni et al., 2008; Azanha & Faria, 2005). The GAB isotherm of corn flakes at 20°C was assumed to be the same as at 25°C. [b] Obtained from food product information. [c] Measured data. [d] Calculated data. [e] Calculated based on assumed ambient storage conditions of 20°C and 75% RH.

The GAB isotherm equation can be rearranged to make the vapour pressure of water vapour the subject as shown in Section 4.3.2.3.1. Then substituting Equation 4-9 for water vapour pressure in the steady-state permeation equation (Equation 2-5) gives the following differential equation for the rate of change of moisture content of the corn flakes:

$$\frac{dM}{dt} = \frac{P_{pkg}^{H_2O}}{X_T} M_{r,H_2O} A_{pkg} \frac{p_0^{H_2O}}{m_s} \left[\left(\frac{-B_2(M_e) - \sqrt{B_2(M_e)^2 - 4B_1}}{2B_1} \right) - \left(\frac{-B_2(M) - \sqrt{B_2(M)^2 - 4B_1}}{2B_1} \right) \right] \quad \textbf{(3-1)}$$

where:

$$B_1 = {k_{GAB}}^2 (1 - C_{GAB}) \quad \textbf{(3-2)}$$

$$B_2(M_e) = k_{GAB} \left(C_{GAB} - C_{GAB} \frac{M_{0,GAB}}{M_e} - 2 \right) \quad \textbf{(3-3)}$$

$$B_2(M) = k_{GAB}\left(C_{GAB} - C_{GAB}\frac{M_{0,GAB}}{M} - 2\right) \quad \textbf{(3-4)}$$

Equation 3-1 was solved by numerical integration using Euler's method with 100 steps, and the solution is shown in Figure 3-1. The moisture content of the corn flakes equals the critical moisture content of 0.062 (g water).(g solids)$^{-1}$ after 180 days when the water vapour permeability is equal to 3.08×10^{-15} mol.m.m^{-2}.s^{-1}.Pa^{-1}. This corresponds to a water vapour transfer rate of 0.215 g.m^{-2}.day^{-1} at 20°C and 0-75% RH gradient.

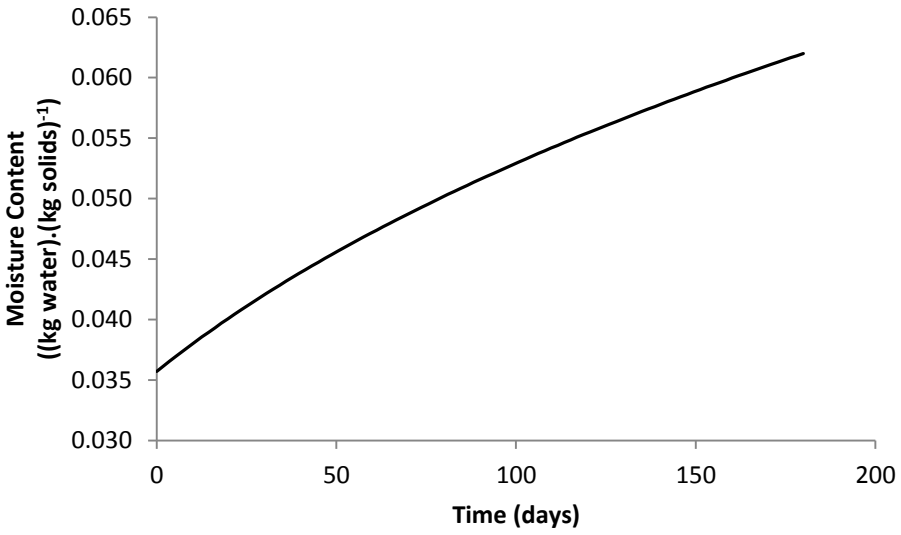

Figure 3-1: Plot of numerically predicted moisture content ((kg water).(kg solids)$^{-1}$) of corn flakes in a permeable package versus storage time (days) using Euler's method.

3.3.1.5 Experimental Measurement

To determine the barrier requirements of existing food products the barrier properties can be measured directly. Ideally the entire food package needs to be tested; however this is not always practical and determining the water vapour gradient in the packaging can be difficult. Therefore it if often more useful to test the barrier properties of a small section of the packaging. Several standards exist for testing barrier properties (Robertson, 2006). The ASTM E96 standard test consisting of the desiccant cup method was

used for most water vapour permeability tests in this investigation. The specific experimental procedure is outlined below.

A humidity chamber containing pure water (100% RH) inside a polystyrene bin was placed in an incubator room at approximately 20°C and allowed to come to equilibrium. A 100 mm by 100 mm square test sample was cut from a packaging sample. Dry silica gel beads were placed in a permeability dish to cover the bottom of each dish, the test sample placed over the dish, and the dish sealed. A sealed permeability dish is shown in Figure 3-2. The dish was weighed to 0.0001 g and placed in the humidity chamber. Humidity chambers containing test samples are shown in Figure 3-3. Measurements of temperature and relative humidity were logged at 15 minute intervals, and the dish weighed daily for approximately 14 days. This procedure was replicated three times for each packaging sample. This method was repeated for blank samples consisting of 3 layers of aluminium foil as a control to determine the level of moisture transfer occurring by other means.

Water vapour transfer rates were calculated from the average slope of mass versus time for each sample, minus that of the blank sample. Test conditions, including temperature and relative humidity gradient across the packaging sample were determined from the average of logged measurements.

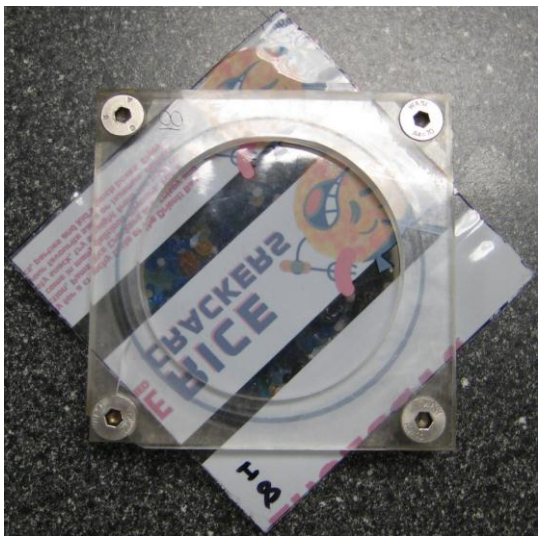

Figure 3-2: Sealed permeability dish.

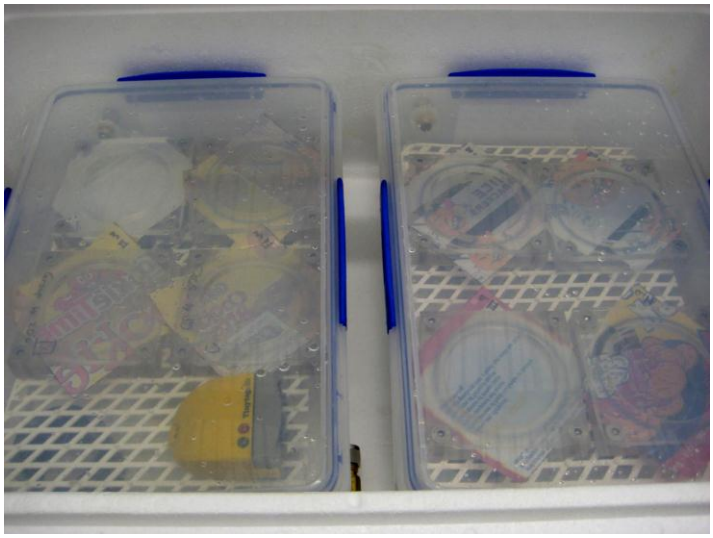

Figure 3-3: Desiccating chambers containing test samples.

Since food packaging is generally selected based on multiple considerations (refer to Section 2.3), it is believed that many food products may have packaging with barrier properties that are not optimised. Therefore the water vapour permeability values determined using this method may not necessarily be optimised values. However, since the packaging is currently in use, the barrier properties should be acceptable. It should also be noted that the types of packaging for a single food product type can vary significantly, and therefore a representative sample may be difficult to obtain.

3.3.2 Summary of Food Barrier Requirements

The storage conditions, packaging material(s) and water vapour barrier properties of various food products are summarised in Table 3-2. This table is an extension of a table previously compiled by Robertson (2006). Water vapour transfer rate (WVTR) requirements of various foods determined using both the calculation and experimental measurement methods were included in the table. These indicated that the two methods often produced significantly different results, although values were generally in the same order of magnitude. Differences may be due to the large range of literature data required for the calculation method, which may not necessarily be representative of the actual food product. Similarly, the experimental method does not consider seals in the packaging, additional packaging used for exporting products, or other real world factors.

Table 3-2: Storage conditions, packaging material(s), and water vapour barrier properties of various food products.

FOOD PRODUCT	PRODUCT DESCRIPTION	PRODUCT MASS (g)	TYPICAL/ESTIMATED STORAGE	
			TEMPERATURE (°C)	TIME (days)
DAIRY PRODUCTS				
Fluid milk			2 - 5	2 - 8
Fermented milk			2 - 5	16 - 18
Milk Powder			18	365
Milk powder	Pams Instant Skim Milk Powder	400	18	365
Milk powder	Pams Instant Skim Milk Powder	400	18	365
Milk powder	Industrial Skim Milk Powder	-	18	-
Fresh cheese			< 5	7 - 56
Fresh cheese	Mainland Special Reserve Traditional Feta†	200	< 5	180
Semi soft and hard cheeses			< 5	7 - 126
Hard cheese	Te Mata Cheese Company Mild Cheese	1,000	< 5	270
Hard Cheese	Industrial Cheese	20,000	< 5	-
Mould ripened cheeses			< 5	7 - 56
Soft cheese	Signature Range Classic Camembert Cheese	125	< 5	30
Butter, oil, dairy spreads			< 5	42
Butter	Tararua Butter	500	< 5	270
OTHER ANIMAL DERIVED PRODUCTS				
Red meats, modified atmosphere			0 - 5	6 - 14
Red meats, no control			0 - 5	1 - 4
Other meats			0 - 5	1 - 42
Cured meat products			5	28
Cured meat	Verkerks Hot Beef†	100	< 5	60
Cured fish products			5	28
Fish, high fat			0 - 5	1 - 7
Fish, low fat			0 - 5	1 - 7
Eggs			2 - 12	25 - 28
Pastas (fresh)			2 - 5	28
HORTICULTURAL PRODUCTS				
Root crops			0 - 18	7
Most vegetables			0 - 18	7
Most fruits and some vegetables			0 - 18	7

PACKAGING MATERIAL(S)	SURFACE AREA (m^2)	THICKNESS (µm)	METHOD	REQUIRED BARRIER PROPERTIES		REQUIRED WVTR * ($g.m^{-2}.day^{-1}$)	REF.
				H_2O	O_2		
LDPE bottle				High	High		[1]
				High	High		[1]
				High	High		[1]
polymer film/vacuum deposited aluminium	0.0704	83.3	Expt.			2.3 ± 0.4	
polymer film/vacuum deposited aluminium	0.0704	83.3	Calc.			0.0668	[6]
paperboard bag/polymer liner	-	97.2	Expt.			1.8 ± 0.4	
				High	High		[1]
polymer film	0.016	67.8	Expt.			1.9 ± 0.4	
	0.00553	52.2				3.9 ± 0.4	
				High/low	High		[1]
polymer film	0.0672	68.3	Expt.			2.2 ± 0.4	
polymer film	0.428	111	Expt.			1.2 ± 0.5	
				High	High		[1]
polymer film	0.018	75	Expt.			56.1 ± 1.1	
paper, aluminium foil, HIPS, PVC				(High)	High		[1]
paper	0.0396	69.4	Expt.			290 ± 17 ¶	
				(High)	High		[1]
				(High)	Low		[1]
				(High)	High		[1]
				(High)	High		[1]
polymer film	0.0287	76.1	Expt.			2.5 ± 0.3	
	0.0287	125				1.8 ± 0.4	
				(High)	High		[1]
				Low	High		[1]
				Low	High		[1]
				High	High		[1]
				(High)	High		[1]
polymer film, fibreboard carton				High	High		[1]
polymer film, fibreboard carton				High	High		[1]
polymer film, fibreboard carton				High	High		[1]

FOOD PRODUCT	PRODUCT DESCRIPTION	PRODUCT MASS (g)	TYPICAL/ESTIMATED STORAGE	
			TEMPERATURE (°C)	TIME (days)
DRY PRODUCTS				
Flour/grains			2 - 18	1095
Flour	Pams High Grade Flour	1,500	18	270
Rice	Sun Rice Medium Grain White Rice	1,000	18	730
Powders, high fat			18	365
Powders, low fat			18	365
Breakfast cereals			18	365
Corn flakes	Kellogg's Corn Flakes	310	18	180
Corn flakes	Kellogg's Corn Flakes	310	18	180
Pastas (dried)			18	30 - 180
Spaghetti	Diamond Spaghetti	500	18	730
Spices and herbs			18	180
Snack foods			18	365
Corn chips	Bluebird Corn Nachos	360	18	180
Coffees/teas			5 - 18	365
Breads			5 - 18	1 - 84
Tortillas	Old El Paso Tortillas	240	18	30
Garlic Bread	La Famiglia Garlic Bread	375	< 5	30
Cakes			5 - 18	1 - 120
Sponge cake	Ernest Adams Un-Filled Sponge	225	18	14
Pancakes	Golden Buttermilk Pancakes	360	18	3
Crackers and biscuits			18	120
Biscuits	CookieTime Cookie Bites	250	18	90
Biscuits	CookieTime Cookie Bites	250	18	90
Biscuits (fresh)	Choc Chip Biscuits	400	18	180
Crackers	Pams Rice Crackers	100	18	270
Crackers	Pams Rice Crackers	100	18	270
Chocolates			2 - 18	180 - 365
Chocolate	Whittaker's Peanut Block	250	18	365
Confectionary			18	365
Confectionary	The Natural Confectionary Co. Sour Squirms	180	18	365
Sugar			18	
White sugar		3,000	18	-

PACKAGING MATERIAL(S)	SURFACE AREA (m^2)	THICKNESS (µm)	METHOD	REQUIRED BARRIER PROPERTIES		REQUIRED WVTR * ($g.m^{-2}.day^{-1}$)	REF.
				H_2O	O_2		
fibreboard bag, wax coating, polymer film				High	-		[1]
fibreboard bag	0.095	121	Expt.			134 ± 10	
polymer film	0.0783	64.4	Expt.			2.4 ± 0.3	
				High	High		[1]
				High	High		[1]
fibreboard, wax coating, HDPE liner				High	High		[1]
fibreboard bag, polymer liner	0.14	52.2	Expt.			0.6 ± 0.3	
fibreboard bag, polymer liner	0.14	52.2	Calc.			0.215	[4,5]
				High	-		[1]
polymer film	0.0522	53.3	Expt.			1.3 ± 0.5	
				High	(High)		[1]
				High	High		[1]
polymer film	0.19	41.7	Expt.			1.5 ± 0.4	
				High	High		[1]
				High	High		[1]
polymer film	0.114	68.3	Expt.			0.8 ± 0.3	
polymer film	0.116	48.3	Expt.			2.9 ± 0.3	
				High	High		[1]
polymer film	0.0792	38.3	Expt.			2.1 ± 0.4	
polymer film	0.103	33.3	Expt.			1.6 ± 0.4	
				High	-		[1]
polymer film	0.0743	65.6	Expt.			0.7 ± 0.3	
polymer film	0.0743	65.6	Calc.			28.4	[2]
polymer film	0.0624	33.9	Expt.			0.8 ± 0.3	
polymer film	0.0652	70	Expt.			1.1 ± 0.4	
polymer film	0.0652	70	Calc.			2.06	[3]
				-	-		[1]
aluminium foil/ paper	0.05	66.7	Expt.			1.4 ± 0.4	
polymer films (PP, RCF), waxed paper				High	-		
polymer film	0.0442	60.8	Expt.			2.2 ± 0.4	
paper, waxed paper				High	-		
paper	0.126	169	Expt.			102 ± 5	

FOOD PRODUCT	PRODUCT DESCRIPTION	PRODUCT MASS (g)	TYPICAL/ESTIMATED STORAGE	
			TEMPERATURE (°C)	TIME (days)
BEVERAGES				
Water			18	365
Juice			5 - 18	5 - 365
Carbonated drinks (beer and soft drinks)			5 - 18	180 - 365
FROZEN FOODS				
High fat products			-18	365
Low fat products			-18	730
OTHERS				
High fat products (dressing, sauce, etc)			5 - 18	365
Ready meals			2 - 5	3-21
PET FOOD				
Dry biscuits			18	
Dog biscuits	Pedigree Adult Complete Nutrition	1,250	18	-

WVTR = water vapour transfer rate, Expt. = experimental measurement, Calc. = calculation, Ref. = reference(s)

* Water vapour transfer rates are at 20°C and 100% RH gradient unless otherwise noted.

† Packaging consists of more than one component in a parallel configuration.

¶ The measured WVTR was limited by the experimental method and therefore represents a minimum value.

References: [1] Robertson (2006), [2] Guillard et al. (2004), [3] Sirpatrawan (2009), [4] Farroni et al. (2008), [5] Azanha & Faria (2005), [6] Shrestha et al. (2007)

	PACKAGING MATERIAL(S)	SURFACE AREA (m^2)	THICKNESS (µm)	METHOD	REQUIRED BARRIER PROPERTIES		REQUIRED WVTR * ($g.m^{-2}.day^{-1}$)	REF.
					H_2O	O_2		
	PET bottle				High	-		[1]
	PET, glass bottle				High	High		[1]
	PET, aluminium can, glass bottle				High	High		[1]
					High	High		[1]
					High	High		[1]
					High	High		[1]
					High	High		[1]
					High	-		
	Paperboard	0.152	601	Expt.			8.8 ± 0.6	

The relative water vapour barrier requirements of various food products are illustrated in Figure 3-4. To gain some indication of the relationship between moisture content and water vapour barrier properties, food products were placed in order of approximate increasing moisture content. Somewhat surprisingly, most food products had similar water vapour barrier properties, although perhaps slightly increasing with moisture content. Sugar was a particularly notable exception to this trend, with a very low relative moisture barrier and moisture content. This may be due to the tested sample being only for local supply, which is unlikely representative of packaging for exported products.

It is important to note that the specific barrier requirements are dependent on various aspects of the food package, including storage and distribution conditions, the size of the food package, and the required shelf life of the product. Therefore the actual barrier requirements for individual applications may vary significantly for a particular type of food. The effects of varying package size and product shelf life on water vapour barrier requirements are illustrated for corn flakes in Figure 3-5 and Figure 3-6 respectively. Package size is represented by the ratio of surface area to volume, which decreases with increasing size. For this example the relative dimensions of the various package sizes were assumed to remain constant; although this may not necessarily be true, it does provide reasonable approximation of surface area to volume ratios.

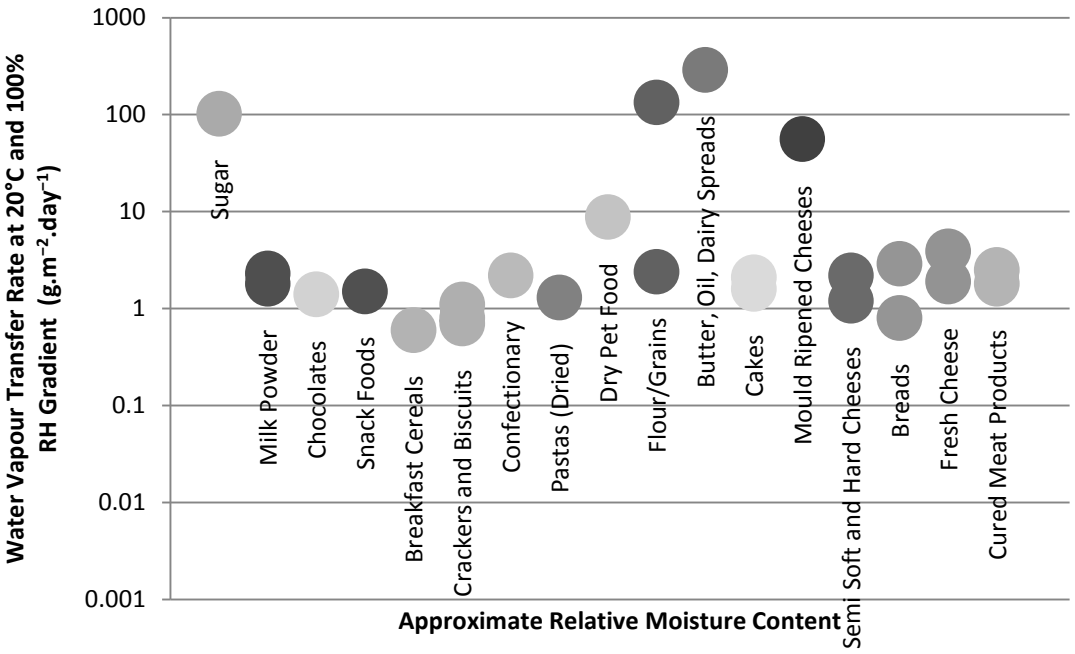

Figure 3-4: Plot of water vapour transfer rate requirements of various food products in order of approximate relative moisture content.

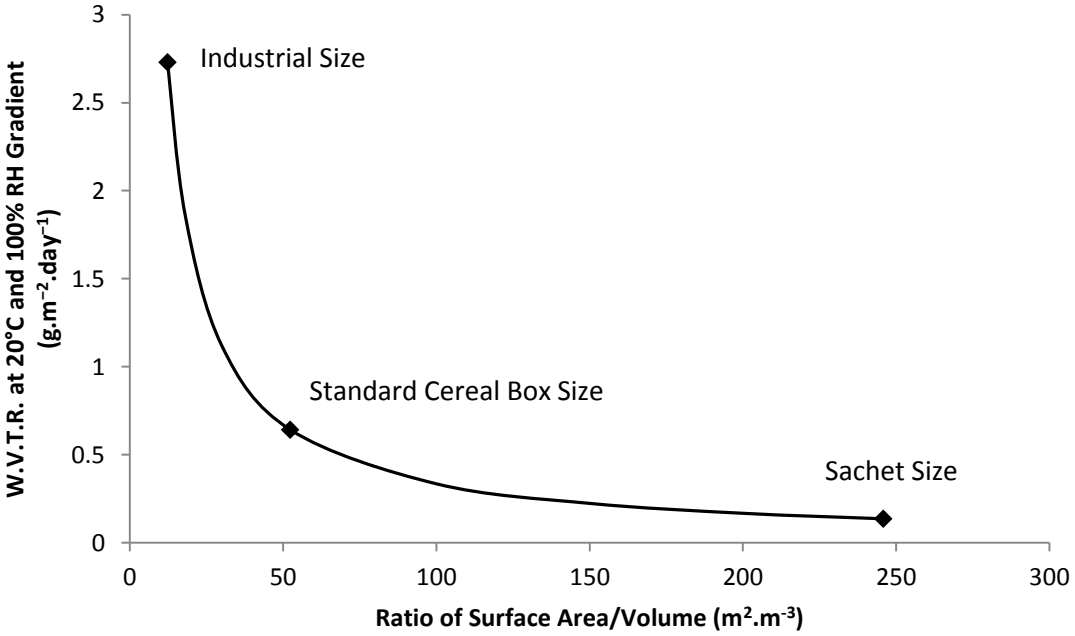

Figure 3-5: Plot of water vapour transfer rate requirements for packages of corn flakes with varying surface area to volume ratios.

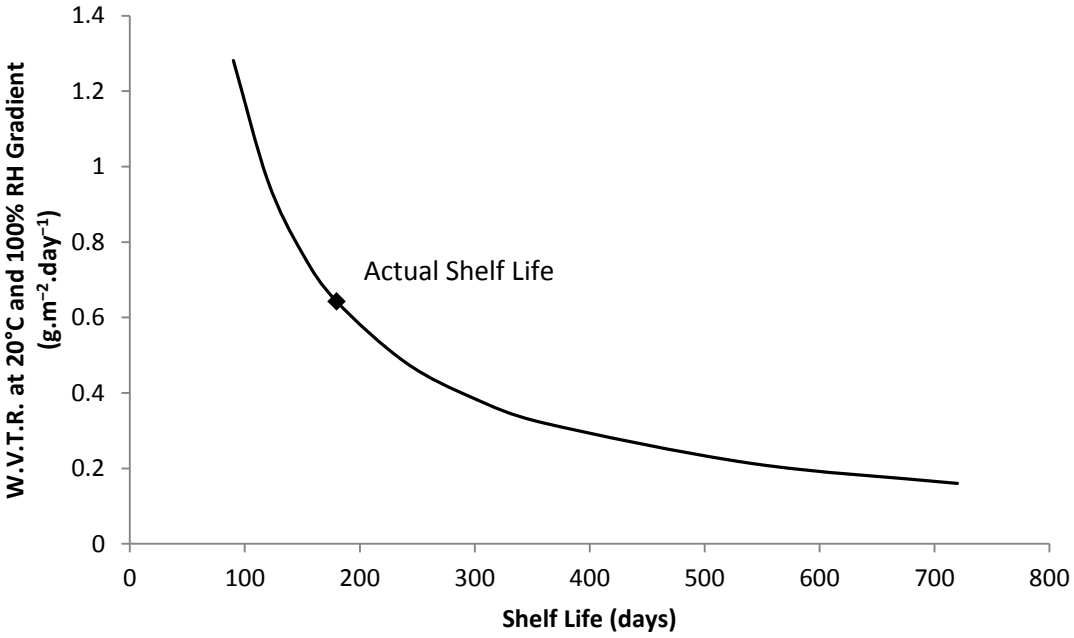

Figure 3-6: Plot of water vapour transfer rates required to achieve various shelf lives for corn flakes.

3.4 IDENTIFICATION OF POTENTIAL TARGET MARKETS

A summary of the quantities and value of major New Zealand food exports is shown in Table 3-3. It is clear from this table that horticultural produce make up a large proportion of New Zealand food exports. Due to respiration, these products often require perforated packaging to provide the necessary modified atmosphere conditions. Perforations allow the rate of transfer of various gases such as oxygen and carbon dioxide to be regulated to extend a favourable gas composition inside the food package (Fishman et al., 1996). Such packaging would also facilitate moisture loss, affecting product quality and value. Perforations therefore need to be a key focus point in the design of such packaging, for which quantitative design tools may be particularly helpful.

It should be noted that the figures of estimated number of packages exported are rough estimates only, since such data is very difficult to obtain. These values were calculated by assuming all exports of each type of produce were in a single package size, and did not take into account other forms of packaging that may be used for export (such as

bulk bins). It should therefore be used with caution, but is useful as a general indication or for comparative purposes.

Table 3-3: Summary of major New Zealand food exports and packaging quantities.

Industry	Produce	Annual export quantity (tonnes)	Export value (NZ $ million, fob)	Major form of packaging for export	Approximate export package size (kg)	Estimated number of packages exported annually [a]	Data year	Ref.
Horticulture								
	Apples	421,000	342	Corrugated fibreboard carton with polymer liner and 3 moulded-pulp 'Friday' trays	18.5	22,800,000 (with 68,300,000 'Friday' trays)	2007	[1,4]
	Kiwifruit	288,000	765	Corrugated fibreboard tray with polymer liner	3.6	80,000,000	2007	[1]
	Other fresh fruit	109,000	89	-	-	-	2007	[1]
	Onions	210,000	121	-	-	-	2007	[1]
	Squash	123,000	66	-	-	-	2007	[1]
	Other fresh vegetables		74	-	-	-	2007	[1]
	Other fresh fruit	109,000	89	-	-	-	2007	[1]
Dairy								
	Butter	370,000	1,033	Corrugated fibreboard carton with polymer liner	25	14,800,000	2006	[2,5]
	Cheese	270,000	1,147	Corrugated fibreboard carton with polymer liner	20	13,500,000	2006	[2,5]
	Whole milk powder	630,000	1,920	Paperboard bag with polymer liner	25	25,200,000	2006	[2]
	Skim milk powder	250,000	816	Paperboard bag with polymer liner	25	10,000,000	2006	[2]
Meat								
	Beef	480,000	1,904	Corrugated fibreboard carton with polymer liner	20	24,000,000	2004	[3,6]
	Lamb	380,000	-	Corrugated fibreboard carton with polymer liner	20	19,000,000	2004	[3]
	Mutton	70,000	-	Corrugated fibreboard carton with polymer liner	20	3,500,000	2004	[3]
Seafood								
	Mussels	-	203	-	-	-	2008	[7]
	Rock Lobster	-	180	-	-	-	2008	[7]
	Hoki	-	151	-	-	-	2008	[7]

[a] Approximate values only.

References: [1] Horticulture & Food Research Institute of New Zealand (2007), [2] Stringleman, H. & Scrimgeour, F. (2009), [3] Meat Industry Association of New Zealand (2010), [4] Ministry of Agriculture and Forestry (2007), [5] New Zealand Trade and Enterprise (2007a), [6] New Zealand Trade and Enterprise (2007b), [7] New Zealand Trade and Enterprise (2009)

3.5 DISCUSSION

It was previously suggested that industry practice often involves multiple considerations, or a qualitative approach to barrier property selection (Section 2.3). This was further indicated by the summary of food barrier requirements, since barrier properties calculated from food requirements seldom agreed with those measured experimentally. As a result it is likely that many commercial and industrial food packaging systems are currently either under- or over-designed. Such scenarios present possible applications for the mathematical models that will be developed as tools to aid the optimisation of current packaging systems.

There was also some indication that, where quantitative packaging selection methods are used, such methods often only consider “worst case” conditions. This approach ensures adequate protection of the food product, however often leads to over-protection. It may therefore be necessary to consider actual scenarios for this investigative work. Again the models could be used to optimise such systems.

A common packaging method used in industry, particularly for food powders, is dense phase filling. This process usually results in a large volume of air being added to the food package. Many food powders, such as sugar, flour and milk powder, therefore require breathable or perforated packaging to allow consolidation after filling. This is somewhat evident for flour and sugar in Figure 3-4 (although these products are for local markets and therefore have a relatively short shelf life). A similar scenario is expected for non-food powders such as concrete, which are conceptually very similar in terms of mass transfer. Moisture transfer will be of key importance in the preservation of product quality in such packaging systems since the perforations facilitate additional moisture ingress into the package. As a result these packaging systems present significant potential as applications for the moisture transfer models.

3.6 SUMMARY

A summary of the barrier property requirements of various foods was compiled. Five methods for determining the barrier property requirements were investigated, including researching literature data, obtaining information directly from food packaging manufacturers or from food producers, estimating requirements based on calculation, and experimentally measuring the properties of existing food products. An extensive table of the barrier properties of various packaging materials was also produced.

Barrier properties calculated from food requirements seldom agreed with those measured experimentally, suggesting a significant proportion of food packaging may be under- or over-designed. This presents potential applications for the mathematical models that will be developed. Further applications may be for powders packed using dense phase filling, where breathable packaging is required.

It is clear that there are many potential applications for mathematical models of moisture transfer in food package systems, particularly for systems with perforations. A good starting point would therefore be a standard model for packaging with perforations and one or more layers, but with appropriate simplifications. This standard model can then be extended as required for systems in which some of these simplifications are not adequate. It is expected that packaging with multiple layers separated by an air gap may need to be considered separately for some scenarios, as well as moisture transfer within the food itself. Multi-dimensional models of moisture transfer through perforations will also likely need to be considered.

Chapter 4

DEVELOPMENT OF A STANDARD FOOD PACKAGE MOISTURE TRANSFER MODEL

4.1 INTRODUCTION

This chapter outlines the development of a standard food package moisture transfer model. The standard food package system consists of a food product within an enclosed package which may contain perforations. This model forms the basis for other more complex models discussed later; consequently later sections may often refer back to work presented here due to similarities or repetition. It is expected that the standard system presented here should itself be applicable to a large range of food products.

The purpose of the model is to predict the internal headspace gas composition of a food package; in particular the relative humidity (RH) and thus the moisture content of the food product. Changes in the internal headspace gas composition will be dependent on the packaging barrier properties, integrity of the package, characteristics of the food product, and the ambient environment to which the package is exposed.

The objectives of work covered in this chapter were to:

- Develop a conceptual moisture transfer model for a standard food package system, indentifying key processes and properties, and specifying valid assumptions allowing the system to be appropriately simplified.

- Formulate a mathematical model based on identified processes and assumptions using relevant theory. A transient model will be required.

- Solve the formulated model using an appropriate method, and ensure the solution is free of errors.

- Validate model predictions against experimental observations to ensure accurate representation of real-world systems.

4.2 CONCEPTUAL MODEL DEVELOPMENT

4.2.1 Outline of Conceptualised System

A schematic diagram of the conceptualised food package system to be modelled is shown in Figure 4-1, and a more detailed diagram of the packaging material is shown in Figure 4-2. The system consists of a food product within an enclosed package. Moisture transfer occurs into or out of the food package through the packaging material. The package can be of various size and shape, and the packaging material or film may consist of multiple layers with different properties. It should be noted that all packaging layers are in direct contact (such as with laminated films), thus the system contains only a single individual packaging layer. The size and shape of the package will determine the surface area through which permeation can occur, and the barrier properties (the permeability, which is the product of the solubility and diffusivity) of each layer will govern the rate of permeation. The barrier properties of each layer will be dependent on the temperature, and may also be affected by the water vapour pressure (Robertson, 2006).

The food package may also contain perforations and/or unsealed edges. This will allow moisture diffusion through the air in these perforations, which will be in parallel to permeation through the packaging material. The rate of diffusion will be affected by the size and shape of the perforations, including the total area of perforations, and the diameter and length of each pore.

Various food products may need to be modelled for the intended application, thus allowance will need to be made for a range of food characteristics. Of most importance will be the moisture sorption isotherm, initial and critical moisture contents, and mass of dry solids in the food product. Multiple mathematical expressions of moisture sorption

isotherms have been used for different foods and therefore will likely need to be utilised. The food package will also experience variations in ambient temperature and/or RH (thus water vapour pressure), and as such these variables may change with time.

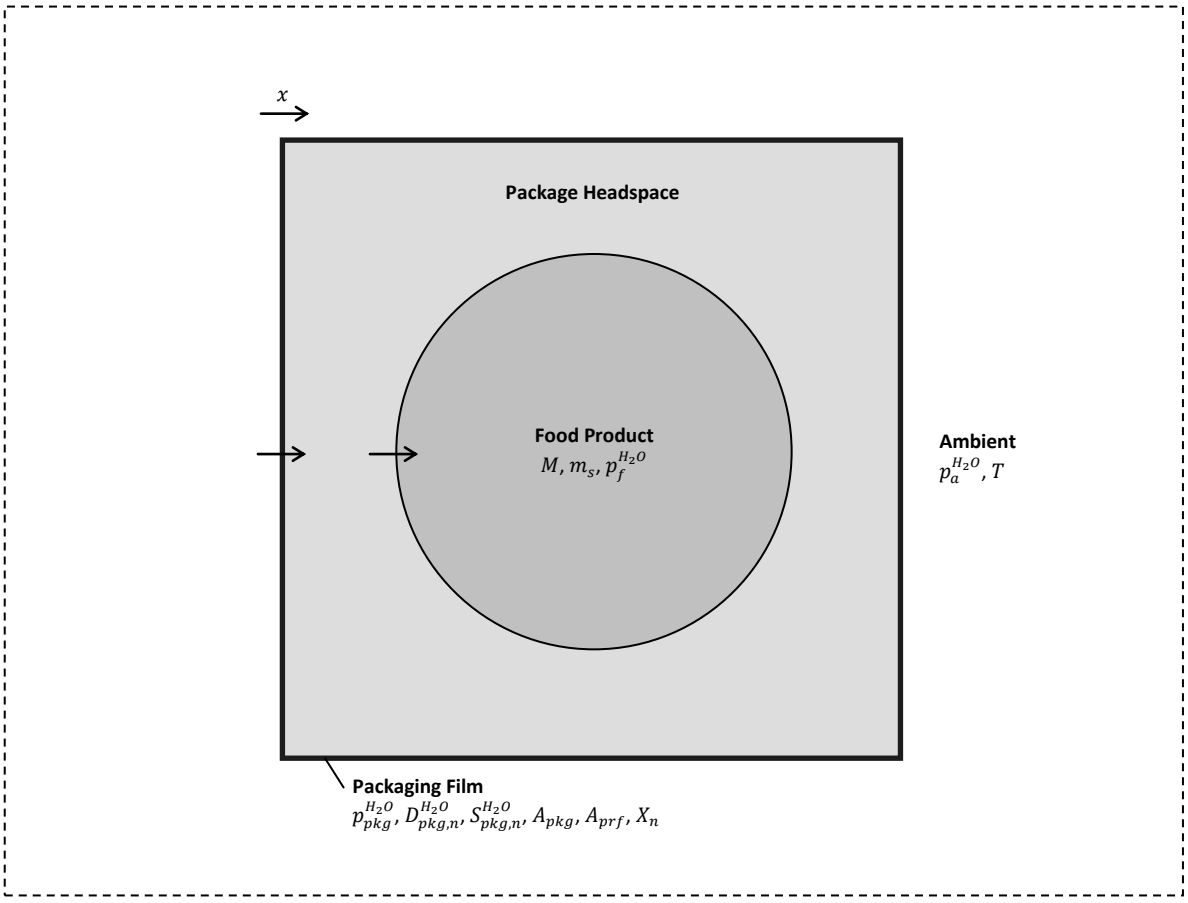

Figure 4-1: Schematic diagram of conceptualised food package system.

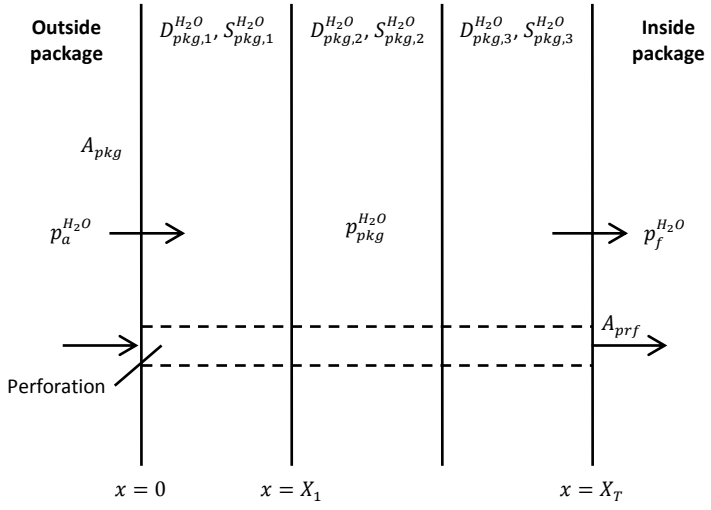

Figure 4-2: Schematic diagram of packaging cross-section.

4.2.2 Assumptions

To simplify the mathematical modelling process as well as produce a model that can practically be solved and utilised, it is necessary to make several assumptions. Assumptions made for the standard food package moisture transfer model and justifications for the validity of these will be discussed in detail.

4.2.2.1 Packaging is the Largest Resistance to Moisture Transfer

The underlying assumption of the standard food package moisture transfer model is that the packaging is the largest resistance to moisture transfer in the system. This assumption is linked to three key assumptions: instantaneous moisture diffusion through air, instantaneous moisture transfer in the food product, and instantaneous moisture transfer at the surface of the food product and packaging. These assumptions have been fairly common in similar studies (Utto, 2008; Genkawa et al, 2008; Azanha & Faria, 2005), although such work have generally focussed on a single food package and product type. Each assumption will be investigated in more detail.

4.2.2.1.1 Instantaneous Moisture Diffusion through Air

For most packaged food systems involving low moisture foods, the diffusivity of water vapour in the packaging material will be several orders of magnitude lower than the diffusivity of water vapour in air. Therefore it can generally be expected that permeation through the packaging will be the rate determining process, and diffusion through air can be considered instantaneous. Situations where this assumption may be invalid are in systems where the water vapour transfer rate through packaging is relatively high, such as for paperboard packaging without a barrier material, packaging with a large area of perforations, or very thin permeable films. Such packaged food systems will generally not be applicable to this study, and the assumption should therefore be valid.

To gain an indication of the point where the rate of moisture diffusion through air becomes significant, dimensional analysis was carried out. For this purpose, a variation of the Biot number was used, which is a dimensionless number expressing the ratio of external to internal resistances to gas transfer:

$$Bi = \frac{P_{pkg}^{H_2O} LRT}{XD_{air}^{H_2O}} \quad \textbf{(4-1)}$$

where:

Bi = Biot number (-)

$P_{pkg}^{H_2O}$ = Permeability of water vapour in packaging film (mol.m.m^{-2}.s^{-1}.Pa^{-1})

L = Length of diffusion through air inside the package (m)

R = Ideal gas constant (m^3.Pa.K^{-1}.mol^{-1})

T = Absolute temperature (K)

X = Packaging film thickness (m)

$D_{air}^{H_2O}$ = Diffusivity of water vapour in air (m^2.s^{-1})

The Biot number for various food package systems are shown in Figure 4-3.

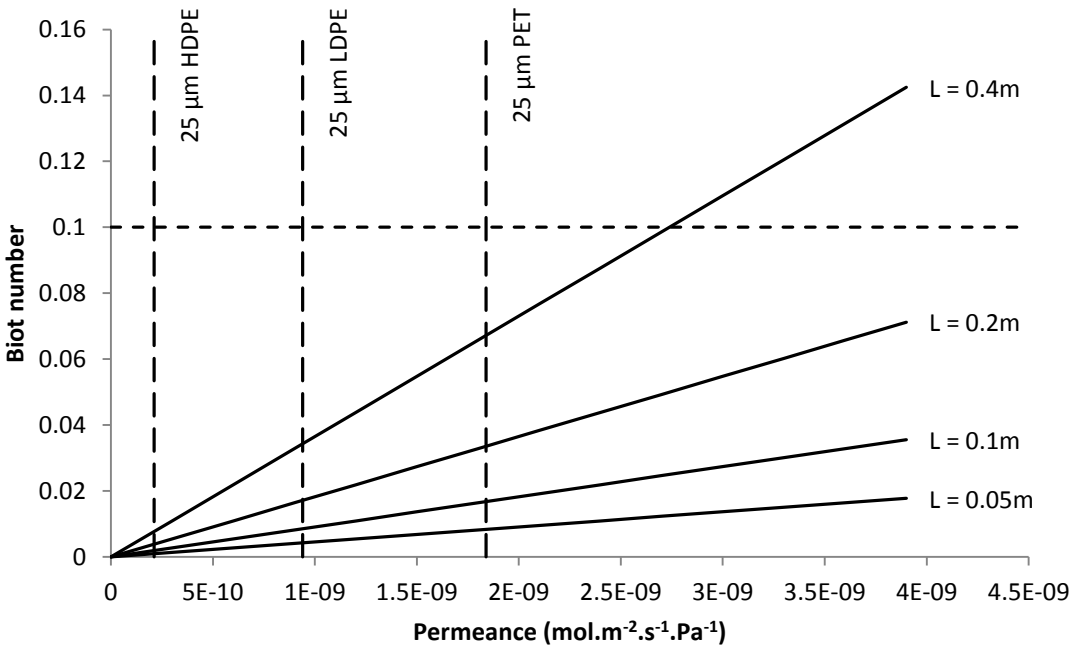

Figure 4-3: Plot of Biot number for food packages of various size (expressed as length of diffusion through air inside package, *L* (m)) and permeance (mol. m^{-2}.s^{-1}.Pa^{-1}) at 0°C. Approximate values of permeance for various polymer films are also indicated (refer to Section 3.2).

The dimensional analysis was carried out for a "worst case" scenario of extreme parameters leading to the highest Biot number, including a temperature of 40°C. A Biot number above 0.1 was taken as the point above which the rate of moisture diffusion through air became significant (Geankoplis, 1993). Under these conditions, for a very large food package with a diffusion length of 0.4 m inside the package, the diffusion through air only became significant for a high permeance of greater than about 2.7×10^{-9} mol. $m^{-2}.s^{-1}.Pa^{-1}$. For a very thin packaging film of 20 µm this corresponds to a relatively high permeability of 5.4×10^{-14} $mol.m^{-2}.s^{-1}.Pa^{-1}$. It is expected that most food package systems of interest will be significantly smaller, and as such this assumption should be reasonable. Where very large food package systems with low barrier properties are required to be simulated, further dimensional analysis will have to be carried out and changes to the mathematical model may need to be considered.

4.2.2.1.2 Instantaneous Moisture Transfer in Food

For the standard food package model it was assumed that moisture transfer in the food is instantaneous. For many food products this is a reasonable assumption since moisture transfer through the packaging film is considerably slower. However scenarios where this does not apply will also be covered in a later chapter.

4.2.2.1.3 Instantaneous Moisture Transfer at Surface of Packaging Film

For most food packaging systems, the rate of moisture transfer through the packaging will be considerably lower than the rate of moisture transfer at the surface of the packaging. Therefore it is very common practice to assume that moisture transfer at the surface of the packaging film will be instantaneous (Genkawa et al., 2008; Azanha & Faria, 2005; Dury-Brun et al., 2006). To confirm the validity of this assumption, dimensional analysis was again used for this purpose:

$$Bi = \frac{P_{pkg}^{H_2O} RT}{Xk} \quad \textbf{(4-2)}$$

where:

k = Mass transfer coefficient (m.s^{-1})

Due to the extensive use of the above assumption, the mass transfer coefficient for packaging films is very difficult to obtain from literature. However, Treybal (1980) suggested that for air-water vapour systems, the Lewis number is generally approximately equal to 1. The Lewis number is a dimensionless number defined as the ratio of thermal diffusivity to mass diffusivity, or expressed mathematically as:

$$Le = \frac{\lambda}{\rho c_p D} = \frac{h}{\rho c_p k} \quad \textbf{(4-3)}$$

where:

Le = Lewis number (-)

λ = Thermal conductivity (W.m^{-1}.K^{-1})

ρ = Density of air (kg.m^{-3})

c_p = Specific heat capacity (J.kg^{-1}.K^{-1})

D = Diffusivity (m^2.s^{-1})

h = Heat transfer coefficient (W.m^{-2}.K^{-1})

Assuming that the Lewis number is equal to 1, the following expression can be derived to estimate the mass transfer coefficient for packaging films:

$$k = \frac{h}{\rho c_p} \quad \textbf{(4-4)}$$

Singh & Heldman (2009) suggested the heat transfer coefficient for a surface exposed to air with free convection is commonly in the range of 5 to 25 W.m^{-2}.K^{-1}. Assuming a "worst case" scenario of extreme parameters resulting in the slowest rate of moisture transfer at the surface of the packaging film and fastest rate of moisture transfer through the packaging, including a heat transfer coefficient of 1 W.m^{-2}.K^{-1}, a temperature of 40°C, and a permeance of 1×10^{-8} mol.m^{-2}.s^{-1}.Pa^{-1}, the Biot number was found to be 0.0295. This is still much less than 0.1 (refer to Section 4.2.2.1.1), suggesting that this assumption should be valid for all packaging systems of interest.

4.2.2.2 Mass of Water in Package Headspace is Negligible

It is expected that the solubility of water vapour in a food product and packaging will be much greater than in air. Therefore it should be safe to assume the mass of water in the package headspace will be negligible (Robertson, 2006). This is not the case for oxygen, and as a result changes would need to be made to the formulated model if oxygen transfer is also to be considered. To ensure the assumption is valid for water vapour, dimensional analysis was carried out for two food products with different characteristic moisture sorption isotherms. GAB moisture sorption isotherm parameters for corn flakes and crystalline α-lactose were obtained from literature (Farroni et al., 2008; Bronlund & Paterson, 2003), and resulting moisture sorption isotherms are shown in Figure 4-4. Note that the moisture sorption isotherm for crystalline α-lactose has a typical curve similar to that of the corn flakes, but the slope is considerably lower making it appear flat relative to the isotherm for corn flakes. For simplicity the temperature dependence of the moisture sorption isotherm parameters were ignored. For the dimensional analysis, the ratio of mass of water in air to mass of water in the food product was calculated as follows:

$$\frac{m_{air}^{H_2O}}{m_f^{H_2O}} = \frac{V_R M_{r,H_2O} p_i^{H_2O}}{RT\rho_b m_f^{H_2O}} \quad \textbf{(4-5)}$$

where:

$m_{air}^{H_2O}/m_f^{H_2O}$ = Ratio of mass of water in air to mass of water in food (kg.kg^{-1})

$p_i^{H_2O}$ = Water vapour pressure (Pa)

V_R = Ratio of volume of air to volume of food (-)

M_{r,H_2O} = Molecular mass of water (kg.m^{-3})

R = Ideal gas constant (m^3.Pa.K^{-1}.mol^{-1})

T = Absolute temperature (K)

ρ_b = Bulk density of food (kg.m^{-3})

$m_f^{H_2O}$ = Mass of water in food (kg), which is a function of water vapour pressure as defined by the moisture sorption isotherm

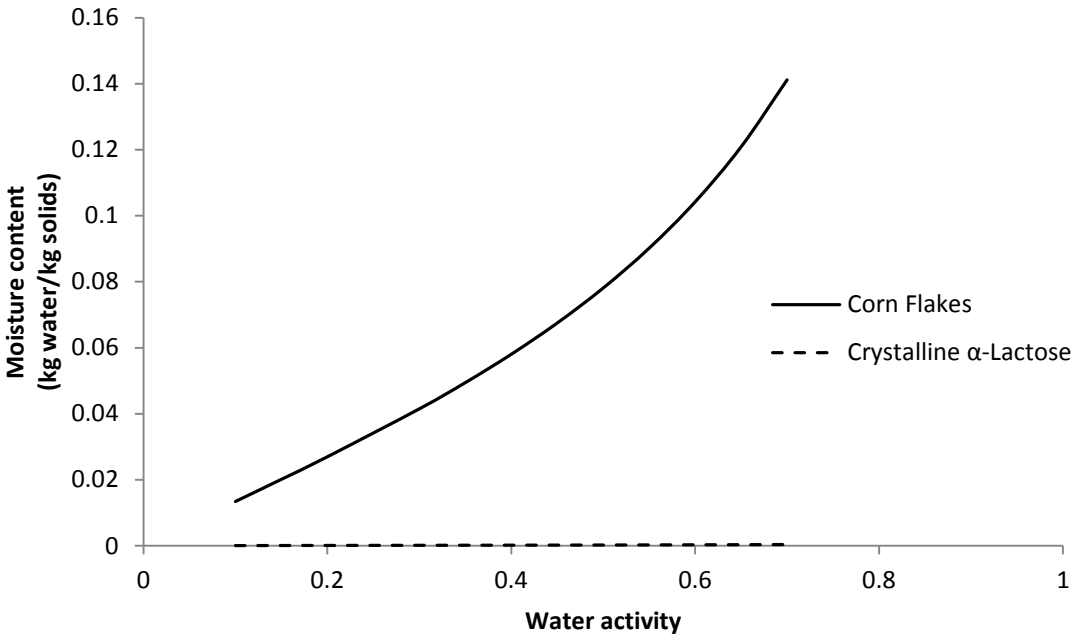

Figure 4-4: Plot of moisture sorption isotherms of corn flakes and crystalline α-lactose obtained from literature.

The ratio of mass of water in air inside the food package to mass of water in the food product for various sized packages of corn flakes and crystalline α-lactose are shown in Figure 4-5 and Figure 4-6.

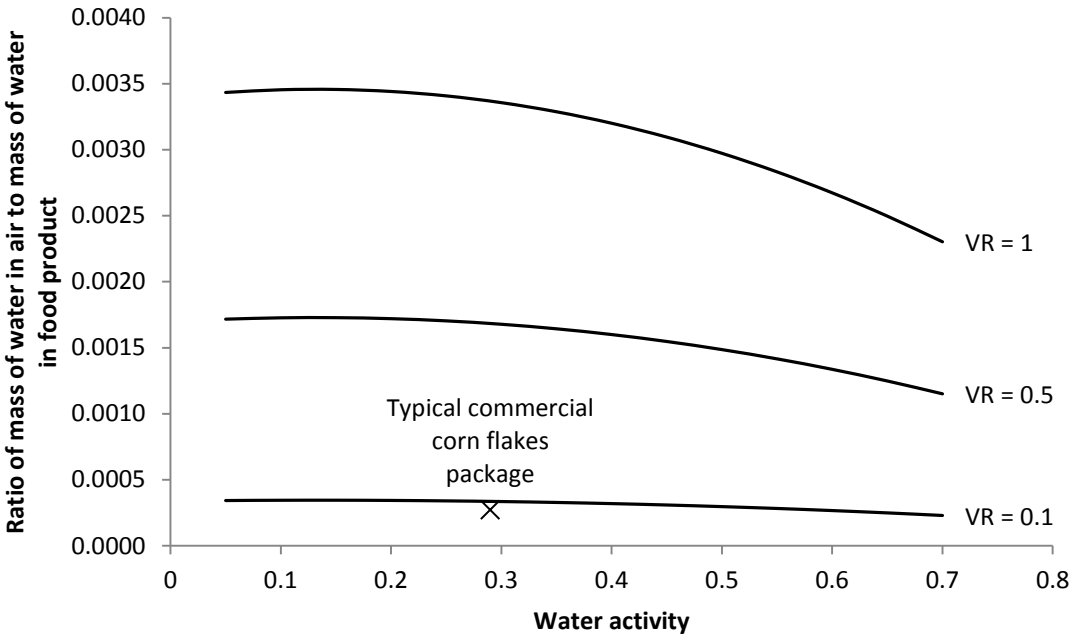

Figure 4-5: Plot of ratio of mass of water in air (inside package) to mass of water in food for corn flake packages of various size and a range of water activities at 40°C (V_R = ratio of volume of air inside package to volume of food product).

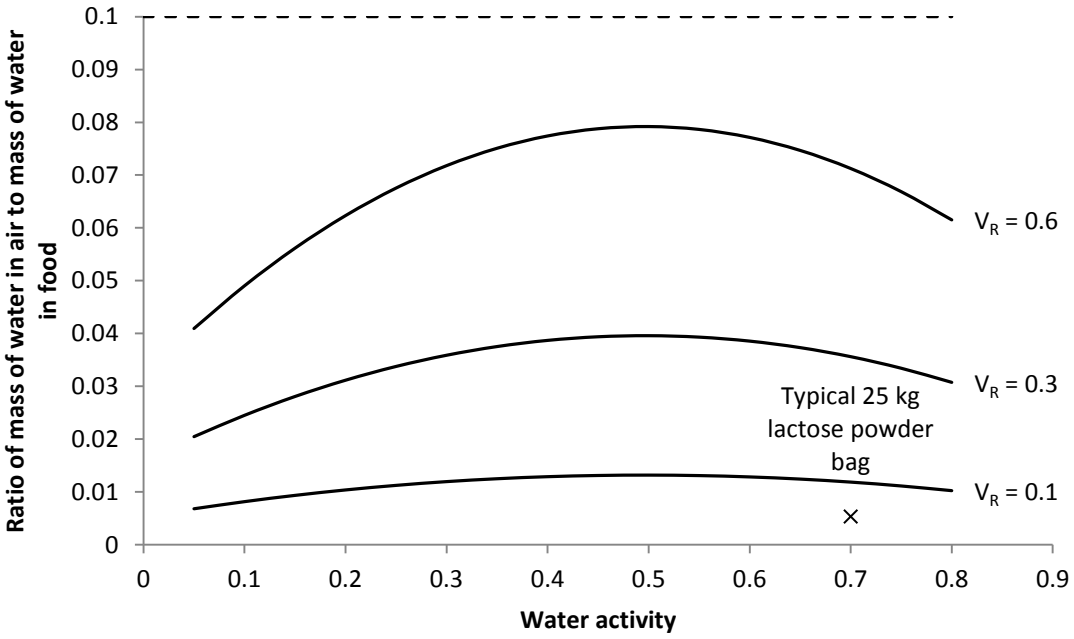

Figure 4-6: Plot of ratio of mass of water in air (inside package) to mass of water in food for crystalline α-lactose packages of various size and a range of water activities at 40°C (V_R = ratio of volume of air inside package to volume of food product). Dotted line represents point above which mass of water in air is considered significant.

Again the dimensional analysis was carried out for a "worst case" scenario of extreme parameters leading to the highest ratio of mass of water in air to mass of water in the food, including a temperature of 40°C. A mass ratio of above 0.1 was considered to indicate significant mass of water in air relative to the mass of water in the food product. The dimensional analysis for packages of corn flakes clearly suggested that the mass of water vapour in air would be negligible for any realistic package size, which is expected to be the case for all systems of interest for this investigation. For crystalline α-lactose (a product with a very flat moisture sorption isotherm) mass ratios were much higher, although still below 0.1. Regardless, it should be noted that crystalline α-lactose is very much an extreme case, and is unlikely to be encountered when simulating a standard food package. Therefore the assumption of negligible mass of water in air is valid.

4.2.2.3 Permeation is in One-Dimension Only

To greatly simplify the mathematical model and increase the range of applications, it was assumed that the food packaging system can be represented by one-dimension. This assumption requires that each packaging material layer has a constant thickness, and that the effect of package corners and folds are negligible. These assumptions are considered in turn below. It is also required that the package is fully sealed, which was specified in the conceptual model and will generally be the case for moisture sensitive foods. Furthermore, in most cases the surface area of a food package will be significantly greater than the thickness of the packaging materials.

The assumption of one-dimensional permeation greatly reduces the number of calculations required by a mathematical model thus decreasing time required for computation. Similarly, it decreases the number of system inputs required, thereby increasing the practical usefulness of the model and the likelihood for practical utilisation. Similar assumptions have been common in related studies (Dury-Brun et al., 2006; Azanha & Faria, 2005; Utto, 2008; del Nobile et al., 2003).

4.2.2.3.1 Each Packaging Material Layer has a Constant Thickness

It is common knowledge that the thickness of a polymer film is not constant across its entire surface (Piringer & Baner, 1999), although the degree of variation is largely dependent on the specific film. It can therefore also be expected that the thickness of individual layers within a film will also vary, and a similar situation is no doubt true for other packaging materials such as paperboard. However it is expected that such variations would have a negligible effect on model predictions provided a reasonable estimate of the average thickness is used. In fact, it is very common practice to assume a constant film thickness in studies which consider moisture and gas permeation (Dury-Brun et al., 2006; Azanha & Faria, 2005; Utto, 2008; del Nobile et al., 2003).

4.2.2.3.2 Effect of Package Corners and Folds are Negligible

For many food packages of interest to this investigation, particularly for large food packages, the surface area affected by folds and corners is relatively small compared with the surface area of the total package surface. Where this is not the case, folds and corners will generally increase the resistance to moisture transfer. Therefore not considering folds and corners will give a “worst case” analysis of the food package system. Similar assumptions are common in investigations of moisture and gas permeation (Dury-Brun et al., 2006; Azanha & Faria, 2005; Utto, 2008; del Nobile et al., 2003).

4.2.2.4 Temperature Changes are Instantaneous throughout the System

Due to the very thin thickness of food packaging and the relatively slow rate of mass transfer in most food package systems of interest, it is expected that the rate of temperature changes would be several orders of magnitude greater than changes in mass. Thus the assumption of instantaneous temperature changes is believed to be reasonable, which avoids the need to model temperature changes. Where this assumption may become questionable is in very large food packages where heat transfer into the food product is

slow; however in such systems the validity of the assumption of uniform water vapour pressure in the food product may also need to be examined.

4.2.2.5 Package Headspace and Ambient are at Atmospheric Pressure

The absolute pressure of the headspace of a food package and ambient environment will affect key model parameters, including saturated water vapour pressure. Also, an absolute pressure gradient across a packaging film containing perforations will facilitate moisture transfer by mechanisms not in the scope of this study. Therefore for simplicity it will be assumed that both the package interior and ambient environment are at atmospheric pressure. In some situations changes in absolute pressure inside the package may result from temperature changes. These may need to be considered in future studies if found to be significant.

4.2.2.6 Other Assumptions

It is assumed that water vapour exhibits ideal gas behaviour. Such practice is fairly common for water vapour at atmospheric pressure, and has been validated experimentally in several studies (Banks et al., 1995; Geankoplis, 2003; del Nobile, 2003). The ideal gas law will therefore be assumed to be valid for water vapour in all food package systems of interest to this study.

The surface area of the packaging is assumed to be much greater than the total area of perforations. This should be true for all food package systems of interest since other assumptions (such as that the packaging is the largest resistance to mass transfer) would become questionable in systems containing a large perforated area.

For this model respiring food products such as horticultural produce were not considered. If such food packaging systems are to be covered, extensions to the model will be required.

It was also assumed that perforations consist of a perfect cylindrical geometry. This will not be the case for many perforations, particularly large perforations produced with a needle or similar. However the diameter of perforations will generally be significantly larger than the length (total thickness of packaging), therefore this assumption is expected to be reasonable.

4.3 MATHEMATICAL MODEL FORMULATION

4.3.1 Variables

Variables defined in the model formulation are summarised in Table 4-1.

Table 4-1: List of model variables.

Symbol	Description	Unit	Class *
$\Delta H_{S,pkg,n}^{H_2O}$	Partial molar enthalpy of sorption of water vapour in nth layer of packaging	J.mol^{-1}	SI
$\Delta x_{pkg,n}$	Width of node in nth layer of packaging	m	SI
A_{pkg}	Package surface area	m^2	SI
A_{prf}	Total area of perforation(s) in packaging	m^2	SI
C_{BET}	Guggenheim constant for BET isotherm of food	-	SI
C_{GAB}	Guggenheim constant for GAB isotherm of food	-	SI
$D_{0,pkg,n}^{H_2O}$	Pre-exponential factor of diffusivity of water vapour in nth layer of packaging	m^2.s^{-1}	SI
$D_{air}^{H_2O}$	Diffusivity of water vapour in air	m^2.s^{-1}	CV
$D_{pkg,n}^{H_2O}$	Diffusivity of water vapour in nth layer of packaging	m^2.s^{-1}	CV
$D_{ref,pkg,n}^{H_2O}$	Reference diffusivity of water vapour in nth layer of packaging	m^2.s^{-1}	SI
$E_{D,pkg,n}^{H_2O}$	Activation energy of diffusion of water vapour in nth layer of packaging	J.mol^{-1}	SI
$E_{P,pkg,n}^{H_2O}$	Activation energy of permeation of water vapour in nth layer of packaging	J.mol^{-1}	SI

$J_{prf}^{H_2O}$	Diffusive flux of water vapour through perforation(s) in packaging	mol.m^{-2}.s^{-1}	CV
$M_{0,GAB}$	Moisture content of monolayer for GAB isotherm of food	(kg water).(kg solids)$^{-1}$	SI
$M_{1,BET}$	Moisture content of monolayer for BET isotherm of food	(kg water).(kg solids)$^{-1}$	SI
M_i	Initial moisture content of food	(kg water).(kg solids)$^{-1}$	SI
M_{r,H_2O}	Molecular mass of water	kg.mol^{-1}	SI
$P_{0,pkg,n}^{H_2O}$	Pre−exponential factor of permeability of water vapour in nth layer of packaging	mol.m.m^{-2}.s^{-1}.Pa^{-1}	SI
$P_{pkg,n}^{H_2O}$	Permeability of water vapour in nth layer of packaging	mol.m.m^{-2}.s^{-1}.Pa^{-1}	CV
RH_a	Ambient relative humidity	%	CV
$S_{0,pkg,n}^{H_2O}$	Pre−exponential factor of solubility of water vapour in nth layer of packaging	mol.m^{-3}.Pa^{-1}	SI
$S_{pkg,n}^{H_2O}$	Solubility of water vapour in nth layer of packaging	mol.m^{-3}.Pa^{-1}	CV
$S_{ref,pkg,n}^{H_2O}$	Reference solubility of water vapour in nth layer of packaging	mol.m^{-3}.Pa^{-1}	SI
$T_{ref,D_{pkg}^{H_2O},n}$	Temperature of reference diffusivity of water vapour in nth layer of packaging	K	SI
$T_{ref,S_{pkg}^{H_2O},n}$	Temperature of reference solubility of water vapour in nth layer of packaging	K	SI
$X_{T,pkg}$	Total thickness of packaging	m	SI
X_n	Thickness of nth layer of packaging	m	SI
b_{lin}	Slope of linear isotherm of food	-	SI
c_{lin}	Constant for linear isotherm of food	(kg water).(kg solids)$^{-1}$	SI
d_{prf}	Average diameter of perforations	m	SI
k_{GAB}	Constant for GAB isotherm of food	-	SI
m_s	Mass of solids in food product	kg	SI
$p_0^{H_2O}$	Saturated water vapour pressure	Pa	CV
$p_a^{H_2O}$	Water vapour pressure in ambient air	Pa	CV
$p_f^{H_2O}$	Water vapour pressure in food	Pa	CV
$p_{pkg}^{H_2O}$	Water vapour pressure in packaging	Pa	D

$p_{pkg,i}^{H_2O}$	Initial water vapour pressure in packaging	Pa	SI
J	Total number of nodes per layer	-	SI
M	Moisture content of food	(kg water).(kg solids)$^{-1}$	D
N	Total number of packaging layers	-	SI
R	Ideal gas constant (8.314)	m^3.Pa.K^{-1}.mol^{-1} or J.K^{-1}.mol^{-1}	SI
T	Temperature	K	CV
j	Node number	-	SI
t	Time	s	I
x	Spatial position in packaging	m	I

* I = independent variable, D = dependent variable, CV = consequential variable, SI = system input

Variables defined in the model formulation consist of one of four classes: independent (I), dependent (D), consequential (CV), or system input (SI) (Bronlund & Davey, 2007). An independent variable has a value that is independent of any other variable. A dependent variable changes as a function of the independent variable, but cannot be determined directly (most often it is affected by the history of the system). A consequential variable changes with other variables, but can be determined directly. A system input has a value that is either constant or predetermined.

The conceptualised system consists of two dependent variables: the moisture content of the food and the water vapour pressure in the packaging. The moisture content of the food can be expressed as an ordinary differential equation (ODE). Since the barrier properties of the packaging may be dependent on the water vapour pressure itself, the water vapour pressure in the packaging will need to be solved as a partial differential equation (PDE). Only one dimension will be considered, thus two boundary conditions will need to be defined. Two initial conditions are also required, one for the moisture content of the food and one for the water vapour pressure across the entire thickness of the packaging.

4.3.2 Word Balances and Equations

4.3.2.1 ODE for Moisture Content of Food Product

The packaged food system to be modelled consists of a food fully enclosed in a packaging film, as illustrated in Figure 4-1. Thus any changes in the amount of moisture contained in the food will be dependent on moisture transfer through the packaging film and/or perforations in the packaging. As a result the following unsteady-state mass balance of moisture in the food product can be derived:

$$\begin{pmatrix} \textit{rate of} \\ \textit{accumulation} \\ \textit{of moisture} \\ \textit{in food} \end{pmatrix} = \begin{pmatrix} \textit{rate of moisture} \\ \textit{permeating through} \\ \textit{inside surface of} \\ \textit{packaging} \end{pmatrix} + \begin{pmatrix} \textit{rate of moisture} \\ \textit{diffusing through} \\ \textit{perforation(s)} \\ \textit{in packaging} \end{pmatrix} \quad \textbf{(4-6)}$$

This word balance can be expressed as an ODE for use in the mathematical model as follows (derivation shown in Appendix C.1.1.1):

$$\frac{dM}{dt} = \frac{M_{r,H_2O}}{m_s}\left[P^{H_2O}_{pkg,n=N} A_{pkg} \left(\frac{dp^{H_2O}_{pkg}}{dx}\right)_{x=X_{T,pkg}} + J^{H_2O}_{prf} A_{prf}\right] \quad \textbf{(4-7)}$$

$for\ t \geq 0$

where:

M = Moisture content of food ((kg water).(kg solids)$^{-1}$)

t = Time (s)

M_{r,H_2O} = Molecular mass of water (kg.mol^{-1})

m_s = Mass of solids in food (kg)

$P^{H_2O}_{pkg,n}$ = Permeability of water vapour in nth layer of packaging (mol.m.m^{-2}.s^{-1}.Pa^{-1})

A_{pkg} = Surface area of packaging (m^2)

$p^{H_2O}_{pkg}$ = Water vapour pressure in packaging (Pa)

x = Spatial position in packaging (m)

$X_{T,pkg}$ = Total thickness of packaging (m)

$J^{H_2O}_{prf}$ = Diffusive flux of water vapour through perforation(s) in packaging (mol.m^{-2}.s^{-1})

A_{prf} = Total area of perforation(s) in packaging (m^2)

4.3.2.2 PDE for Water Vapour Pressure in Packaging

As covered in Section 2.5.2.1, the PDE for one-dimensional unsteady-state moisture permeation through a packaging material has the following form expressed in terms of equilibrium partial pressures:

$$S_{pkg}^{H_2O}\frac{\partial p_{pkg}^{H_2O}}{\partial t}=\frac{\partial}{\partial x}\left(P_{pkg}^{H_2O}\frac{\partial p_{pkg}^{H_2O}}{\partial x}\right) \qquad \textbf{(4-8)}$$

$$for\ t \geq 0,\ 0 < x < X_{T,pkg}$$

where:

$S_{pkg}^{H_2O}$ = Solubility of water vapour in packaging (mol.m^{-3}.Pa^{-1})

$X_{T,pkg}$ = Total thickness of packaging (m)

4.3.2.3 Equation for Water Vapour Pressure in Food Product

As discussed in Section 2.4.2.2, the water vapour pressure in the food product is related to its moisture content by the moisture sorption isotherm of the food. Consequently this is also equal to the water vapour pressure in the package headspace due to assumptions made in the modelling process (Section 4.2.2).

Three common moisture sorption isotherms will be included in the model: the Guggenheim, Anderson and de Boer (GAB) equation, Brunauer, Emmett and Teller (BET) equation, and linear isotherm. However it should be noted the same procedure should be applicable for any isotherm equation.

4.3.2.3.1 GAB Isotherm

To obtain an expression for the water vapour pressure in the food product, the GAB isotherm equation (Equation 2-4) can be rearranged to give Equation 4-9. The derivation of Equation 4-9 is shown in Appendix C.1.1.2.1.

$$p_f^{H_2O} = p_0^{H_2O}\left[\frac{-B_2 - \sqrt{{B_2}^2 - 4B_1}}{2B_1}\right] \quad \textbf{(4-9)}$$

where:

$$B_1 = {k_{GAB}}^2(1 - C_{GAB}) \quad \textbf{(4-10)}$$

$$B_2 = k_{GAB}\left(C_{GAB} - C_{GAB}\frac{M_{0,GAB}}{M} - 2\right) \quad \textbf{(4-11)}$$

$p_f^{H_2O}$ = Water vapour pressure in food (Pa)

$p_0^{H_2O}$ = Saturated water vapour pressure (Pa)

k_{GAB} = Constant for GAB isotherm of food (-)

C_{GAB} = Guggenheim constant for GAB isotherm of food (-)

$M_{0,GAB}$ = Moisture content of monolayer for GAB isotherm of food ((kg water).(kg solids)$^{-1}$)

4.3.2.3.2 BET Isotherm

The derivation of an expression for the water vapour pressure based on the BET isotherm equation (Equation 2-3) is very similar to the procedure for the GAB isotherm equation. The resulting expression is as follows (derivation in Appendix C.1.1.2.2):

$$p_f^{H_2O} = p_0^{H_2O}\left[\frac{-B_2 - \sqrt{{B_2}^2 - 4B_1}}{2B_1}\right] \quad \textbf{(4-12)}$$

where:

$$B_1 = 1 - C_{BET} \quad \textbf{(4-13)}$$

$$B_2 = C_{BET} - C_{BET}\frac{M_{1,BET}}{M} - 2 \quad \textbf{(4-14)}$$

C_{BET} = Guggenheim constant for BET isotherm of food (-)

$M_{1,BET}$ = Moisture content of monolayer for BET isotherm of food ((kg water).(kg solids)$^{-1}$)

4.3.2.3.3 Linear Isotherm

An expression for the water vapour pressure based on the linear isotherm equation (Equation 2-2) has the following form:

$$p_f^{H_2O} = p_0^{H_2O}\left(\frac{M - c_{lin}}{b_{lin}}\right) \quad \textbf{(4-15)}$$

where:

c_{lin} = Constant for linear isotherm of food (-)

b_{lin} = Slope of linear isotherm of food (-)

4.3.2.4 Equation for Diffusivity of Water Vapour in Packaging Material

Depending on the specific application for the mathematical model, various expressions for temperature and/or concentration dependence of the diffusivity may need to be utilised. It is also possible that different expressions would be required for different packaging layers. Some temperature and concentration dependence expressions for diffusivity were discussed in Sections 2.4.3.3 and 2.5.2.3. Due to the large range and possible combinations, allowance will be made in the model to enter any equation for the diffusivity of water vapour in the packaging material for each layer. However since concentration dependence of diffusivity is not expected to be encountered in this investigation, only temperature dependence will be included.

As covered in Section 2.5.2.3, the temperature dependence of the diffusivity is generally expressed in the form of an Arrhenius relationship (Equation 2-22). For the purpose of the model it may be more useful to state this relative to a reference diffusivity at a given temperature as follows:

$$D_{pkg,n}^{H_2O} = D_{ref,pkg,n}^{H_2O} exp\left[\frac{E_{D,pkg,n}^{H_2O}}{R}\left(\frac{1}{T_{ref,D_{pkg}^{H_2O},n}} - \frac{1}{T}\right)\right] \quad \textbf{(4-16)}$$

where:

$D_{pkg,n}^{H_2O}$ = Diffusivity of water vapour in nth layer of packaging (m^2.s^{-1})

$D^{H_2O}_{ref,pkg,n}$ = Reference diffusivity of water vapour in nth layer of packaging (m^2.s^{-1})

$E^{H_2O}_{D,pkg,n}$ = Activation energy of diffusion of water vapour in nth layer of packaging (J.mol^{-1})

$T_{ref,D^{H_2O}_{pkg},n}$ = Temperature of reference diffusivity of water vapour in nth layer of packaging (K)

4.3.2.5 Equation for Solubility of Water Vapour in Packaging Material

Similar to diffusivity, expressions for solubility of water vapour in the packaging material and combinations of these are numerous. Therefore it would not be practical to attempt to include all such combinations. For this investigation, temperature dependence of solubility will be included, as well as an expression for concentration dependence based on the GAB isotherm equation.

Due to the similarity of the solubility and diffusivity temperature dependence equations (Equations 2-23 and 2-22 respectively), the solubility can also be expressed relative to a reference solubility at a given temperature:

$$S^{H_2O}_{pkg,n} = S^{H_2O}_{ref,pkg,n} exp\left[\frac{\Delta H^{H_2O}_{S,pkg,n}}{R}\left(\frac{1}{T_{ref,S^{H_2O}_{pkg},n}} - \frac{1}{T}\right)\right] \quad \textbf{(4-17)}$$

where:

$S^{H_2O}_{pkg,n}$ = Solubility of water vapour in nth layer of packaging (mol.m^{-3}.Pa^{-1})

$S^{H_2O}_{ref,pkg,n}$ = Reference solubility of water vapour in nth layer of packaging (mol.m^{-3}.Pa^{-1})

$\Delta H^{H_2O}_{S,pkg,n}$ = Partial molar enthalpy of sorption of water vapour in nth layer of packaging (J.mol^{-1})

$T_{ref,S^{H_2O}_{pkg},n}$ = Temperature of reference solubility of water vapour in nth layer of packaging (K)

Moisture content is essentially a concentration of water (expressed as mass of water per mass of solids), and water activity is a measure of relative water vapour pressure;

therefore the derivative of the moisture sorption isotherm for a material will be proportional to the solubility of water vapour in that material. As a result, given a GAB moisture sorption isotherm for the packaging material, an expression for the solubility of water vapour in the packaging can be derived (Equation 4-18). The derivation of Equation 4-18 is shown in Appendix C.1.1.3. A similar procedure can be used for other sorption isotherm equations.

$$S_{pkg,n}^{H_2O} = \frac{\rho_{s,pkg,n}}{M_{r,H_2O}} \left[\frac{M_{0,pkg,n} k_{pkg,n}{}^2 C_{pkg,n} p_{pkg}^{H_2O}}{\left(p_0^{H_2O}\right)^2 \left(1 - k_{pkg,n} \frac{p_{pkg}^{H_2O}}{p_0^{H_2O}}\right)^2 \left(1 + k_{pkg,n} \frac{p_{pkg}^{H_2O}}{p_0^{H_2O}} \left(C_{pkg,n} - 1\right)\right)} + \frac{M_{0,pkg,n} k_{pkg,n} C_{pkg,n}}{p_0^{H_2O} \left(1 - k_{pkg,n} \frac{p_{pkg}^{H_2O}}{p_0^{H_2O}}\right) \left(1 + k_{pkg,n} \frac{p_{pkg}^{H_2O}}{p_0^{H_2O}} \left(C_{pkg,n} - 1\right)\right)} - \frac{M_{0,pkg,n} k_{pkg,n}{}^2 C_{pkg,n} \left(C_{pkg,n} - 1\right) p_{pkg}^{H_2O}}{\left(p_0^{H_2O}\right)^2 \left(1 - k_{pkg,n} \frac{p_{pkg}^{H_2O}}{p_0^{H_2O}}\right) \left(1 + k_{pkg,n} \frac{p_{pkg}^{H_2O}}{p_0^{H_2O}} \left(C_{pkg,n} - 1\right)\right)^2} \right] \quad \textbf{(4-18)}$$

where:

$\rho_{s,pkg,n}$ = Density of solids in food (kg.m^{-3})

$M_{0,pkg,n}$ = Moisture content of monolayer for GAB isotherm of packaging ((kg water).(kg solids)$^{-1}$)

$C_{pkg,n}$ = Guggenheim constant for GAB isotherm of packaging (-)

$k_{pkg,n}$ = Constant for GAB isotherm of packaging (-)

4.3.2.6 Equation for Saturated Water vapour pressure

ASHRAE (1997) proposed the following empirical expression for the saturated water vapour pressure:

$$p_0^{H_2O} = exp\left(23.4795 - \frac{3990.56}{T - 39.317}\right) \quad \textbf{(4-19)}$$

4.3.2.7 Equation for Diffusivity of Water Vapour in Air

The diffusivity of water vapour in air was reported to be a function of temperature by Shah et al. (1984) as follows:

$$D_{air}^{H_2O} = 1.7255 \times 10^{-7} T - 2.552 \times 10^{-5} \quad \textbf{(4-20)}$$

4.3.2.8 Equation for Solubility of Water Vapour in Air

The solubility of water vapour in air can be derived from the ideal gas law as shown in Appendix C.1.2. The resulting expression has the following form:

$$S_{air}^{H_2O} = \frac{1}{RT} \quad \textbf{(4-21)}$$

where:

$S_{air}^{H_2O}$ = Solubility of water vapour in air (mol.m^{-3}.Pa^{-1})

4.3.2.9 Equation for Diffusive Flux through Perforations

As discussed in Section 2.5.2.2, when the diameter of perforations is greater than 1 × 10^{-5} m, mass transfer through the perforations can be treated as diffusion in a cylindrical pathway filled with air. Thus (Fishman et al., 1996):

$$J_{prf}^{H_2O} = \frac{D_{air}^{H_2O} S_{air}^{H_2O}}{X_{T,pkg}} \left(p_a^{H_2O} - p_f^{H_2O}\right) \quad \textbf{(4-22)}$$

$for\ d_{prf} \geq 1 \times 10^{-5}$ m

where:

$p_a^{H_2O}$ = Water vapour pressure in ambient air (Pa)

$p_f^{H_2O}$ = Water vapour pressure in food (Pa)

d_{prf} = Average diameter of perforations in packaging (m)

For a situation where the diameter of perforations is less than 1×10^{-5} m but greater or equal to 1×10^{-7} m, the following expression was proposed (Fishman et al., 1996):

$$J_{prf}^{H_2O} = \frac{D_{air}^{H_2O} S_{air}^{H_2O}}{\left(X_{T,pkg} + \frac{d_{prf}}{2}\right)} \left(p_a^{H_2O} - p_f^{H_2O}\right) \quad \textbf{(4-23)}$$

$$for\ 1 \times 10^{-7} \leq d_{prf} < 1 \times 10^{-5}\ \text{m}$$

It should be noted that this is only valid if the distance between perforations is much greater than d_{prf}.

Finally, if the diameter of perforations is less than 1×10^{-7} m, mass transfer through the perforations was suggested to follow Knudsen's law (Equation 2-21). Therefore:

$$J_{prf}^{H_2O} = \frac{48.5 d_{prf}}{RTX_{T,pkg}} \left(\frac{T}{1000 M_{r,H_2O}}\right)^{0.5} \left(p_a^{H_2O} - p_f^{H_2O}\right) \quad \textbf{(4-24)}$$

$$for\ d_{prf} < 1 \times 10^{-7}\ \text{m}$$

4.3.3 Boundary Conditions

It was assumed that the packaging is the largest resistance to mass transfer in the system and that as a result mass transfer at the surface of the packaging will be negligible (Section 4.2.2.1.3). Therefore the first kind of boundary condition will apply at both packaging surfaces (Cleland, 2000). At the exterior packaging surface (the surface exposed to the ambient environment), the water vapour pressure will be equal to water vapour pressure in the ambient air. This can be expressed mathematically as follows:

$$p_{pkg}^{H_2O} = p_a^{H_2O} \quad \textbf{(4-25)}$$

$$for\ t \geq 0,\ at\ x = 0$$

At the interior surface (the surface closest to the food), the water vapour pressure will be equal to water vapour pressure in the package headspace and as a result that of the food:

$$p_{pkg}^{H_2O} = p_f^{H_2O} \quad for\ t \geq 0,\ at\ x = X_{T,pkg} \tag{4-26}$$

4.3.4 Initial Conditions

For simplicity, the initial water vapour pressure in the packaging will be assumed to be uniform. Therefore the following initial conditions apply:

$$p_{pkg}^{H_2O} = p_{pkg,i}^{H_2O} \quad at\ t = 0 \tag{4-27}$$

$$M = M_i \quad at\ t = 0 \tag{4-28}$$

where:

$p_{pkg,i}^{H_2O}$ = Initial water vapour pressure in packaging (Pa)

M_i = Initial moisture content of food product ((kg water).(kg solids)$^{-1}$)

4.4 SOLUTION

Due to complexities in the developed mathematical model such as non-linear expressions for moisture sorption isotherms and concentration/temperature dependence of water vapour diffusivity/solubility, an analytical solution would not have been feasible. Therefore the developed mathematical model was solved numerically. For this purpose MATLAB® software was utilised (The MathWorks Inc., 2008) using the ode23s solver function.

To solve the PDE for water vapour pressure in the packaging, a finite difference method was implemented. This method involves approximating the PDE by a series of ODEs which can be solved simultaneously. A similar method has commonly been utilised for many systems involving unsteady-state mass transfer by diffusion in infinite slabs (Cleland, 2000; Utto, 2008; Nevins, 2008).

4.4.1 Finite Difference Grid

The finite difference grid used for the packaging material is illustrated in Figure 4-9. Each packaging layer was divided into J space steps, and space steps of the nth layer had a thickness of Δx_n, for a total of N layers. Thus:

$$\Delta x_{pkg,n} = \frac{X_{pkg,n}}{J} \quad \textbf{(4-29)}$$

where:

$\Delta x_{pkg,n}$ = Width of node in nth layer of packaging (m)

$X_{pkg,n}$ = Thickness of nth layer of packaging (m)

J = Number of nodes (-)

The area of packaging contained within each space step was designated a node number from $j = 1$ at the exterior packaging surface (the surface exposed to the ambient environment) to $j = NJ + 1$ at the interior surface (the surface closest to the food), and the water vapour pressure within each node considered uniform.

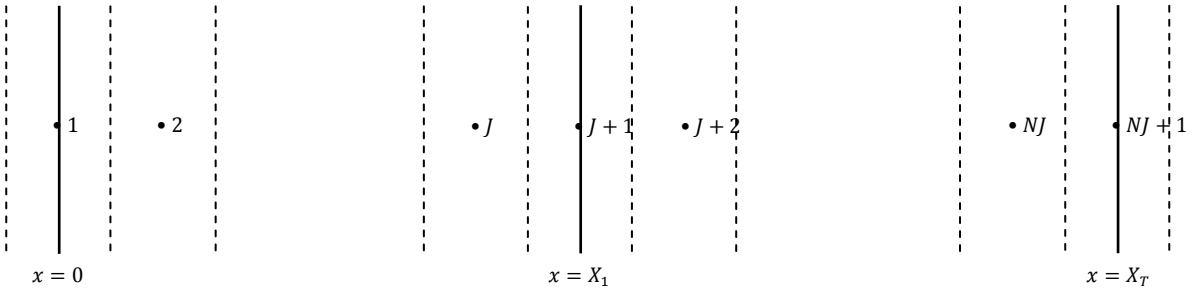

Figure 4-7: Finite difference grid for packaging material.

4.4.2 Finite Difference Approximations

The derivation of finite difference approximations are shown in Appendix C.2.1.

4.4.2.1 Case 1

Nodes:

$$n = 1, j = 1$$

$$n = N, j = nJ + 1$$

Case 1 refers to nodes at the external and internal surfaces of the packaging. Schematic diagrams of case 1 nodes are shown in Figure 4-8, and the finite difference approximations are given in Equation 4-30. The first kind of boundary condition applies to both surfaces, suggesting a fixed surface water vapour pressure. However since the water vapour pressure of the ambient air and food product may be changing with time, so too the water vapour pressure in these nodes may not actually be constant. It should be noted that, to simplify the numbering scheme that was used to allow any number of packaging layers, Case 2 and Case 5 also account for the boundary condition. Case 1 is therefore essentially only included for completeness and to avoid confusion.

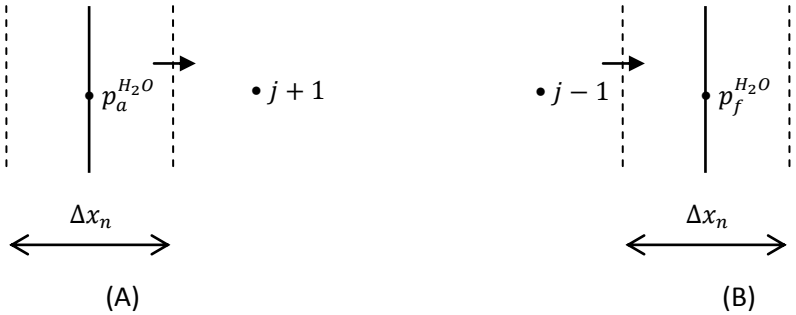

Figure 4-8: Diagram of finite difference approximations for case 1, including the external (A) and internal (B) packaging surfaces.

$$p_{pkg,j}^{H_2O} = p_a^{H_2O}$$
$$p_{pkg,j}^{H_2O} = p_f^{H_2O} \quad \textbf{(4-30)}$$
$$for\ t \geq 0$$

4.4.2.2 Case 2

Node:

$$n = 1, j = 2$$

Case 2 refers to the node immediately adjacent to the external packaging surface. A schematic diagram of the Case 2 node is shown in Figure 4-9, and the finite difference approximation is given in Equation 4-31. As noted for Case 1, this node also accounts for the boundary condition due to the numbering scheme that was adopted. As such this node essentially has the same form as the internal nodes (Case 3), except that the water vapour pressure in the previous node is specified as the water vapour pressure in the ambient air.

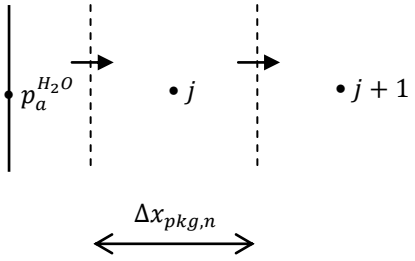

Figure 4-9: Diagram of finite difference approximation for case 2.

$$\frac{dp_{pkg,j}^{H_2O}}{dt} = \frac{P_{pkg,n}^{H_2O}}{S_{pkg,n}^{H_2O}\Delta x_{pkg,n}{}^2}\left(p_a^{H_2O} - 2p_{pkg,j}^{H_2O} + p_{pkg,j+1}^{H_2O}\right) \quad \textbf{(4-31)}$$

$$for\ t \geq 0$$

4.4.2.3 Case 3

Nodes:

$$n = 1, j = (n-1)J + 3 : nJ$$

$$n = 2 : N-1, j = (n-1)J + 2 : nJ$$

$$n = N, j = (n-1)J + 2 : nJ - 1$$

Case 3 consists of internal nodes that make up the bulk of the packaging system. A schematic diagram of Case 3 nodes is shown in Figure 4-10, and the finite difference approximation is given in Equation 4-32.

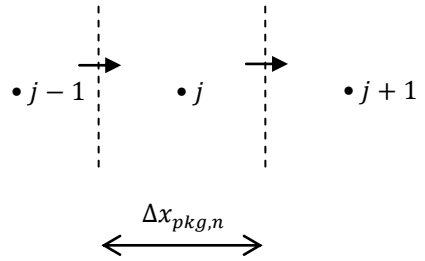

Figure 4-10: Diagram of finite difference approximation for case 3.

$$\frac{dp_{pkg,j}^{H_2O}}{dt} = \frac{P_{pkg,n}^{H_2O}}{S_{pkg,n}^{H_2O}\Delta x_{pkg,n}{}^2}\left(p_{pkg,j-1}^{H_2O} - 2p_{pkg,j}^{H_2O} + p_{pkg,j+1}^{H_2O}\right) \quad \textbf{(4-32)}$$

$$for\ t \geq 0$$

4.4.2.4 Case 4

Nodes:

$$n = 1{:}N-1, j = nJ + 1$$

Case 4 refers to nodes on the boundary of two packaging layers. For a single layer packaging system Case 4 will not be required. A schematic diagram of Case 4 nodes is shown in Figure 4-11, and the finite difference approximation is given in Equation 4-33.

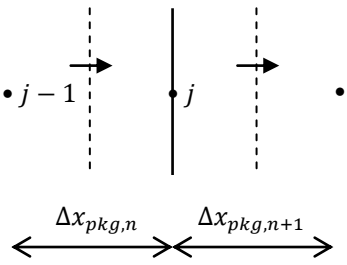

Figure 4-11: Diagram of finite difference approximation for case 4.

$$\frac{dp_{pkg,j}^{H_2O}}{dt} = \frac{2}{\Delta x_{pkg,n} S_{pkg,n}^{H_2O} + \Delta x_{pkg,n+1} S_{pkg,n+1}^{H_2O}} \left[\frac{P_{pkg,n}^{H_2O}}{\Delta x_{bag,n}} \left(p_{pkg,j-1}^{H_2O} - p_{pkg,j}^{H_2O} \right) - \frac{P_{pkg,n+1}^{H_2O}}{\Delta x_{pkg,n+1}} \left(p_{pkg,j}^{H_2O} - p_{pkg,j+1}^{H_2O} \right) \right] \quad \textbf{(4-33)}$$

$for\ t \geq 0$

4.4.2.5 Case 5

Node:

$n = N, j = nJ$

The Case 5 node is similar to Case 2, except immediately adjacent to the internal packaging surface. A schematic diagram of the Case 5 node is shown in Figure 4-12, and the finite difference approximation is given in Equation 4-34. Again it is necessary to specify the water vapour pressure in the food product to account for the boundary condition.

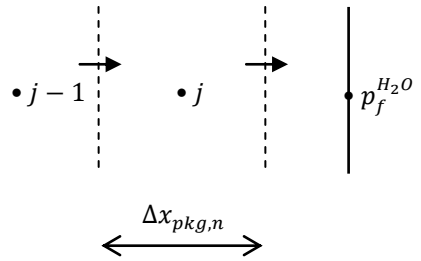

Figure 4-12: Diagram of finite difference approximation for case 5.

$$\frac{dp_{pkg,j}^{H_2O}}{dt} = \frac{P_{pkg,n}^{H_2O}}{S_{pkg,n}^{H_2O} \Delta x_{pkg,n}^{\ 2}} \left(p_{pkg,j-1}^{H_2O} - 2p_{pkg,j}^{H_2O} + p_f^{H_2O} \right) \quad \textbf{(4-34)}$$

$for\ t \geq 0$

4.4.3 MATLAB® Solution

The formulated ODEs for moisture content of the food product and finite difference approximations for water vapour pressure in the packaging were converted to MATLAB® code. The resulting script and function files are shown in Appendix C.2.2.

4.4.4 Example Simulations

A series of preliminary simulations were carried out for moisture transfer in various packaged food systems to gain a general indication of whether the model was working correctly. The following systems were considered: corn flakes in a standard consumer polymer bag consisting of 5 layers, milk powder in an industrial paperboard bag with a polymer liner, cheese in a consumer polymer bag, and bread in a consumer polymer bag with perforations. It should be noted that system inputs used for these simulations were approximate only, and will not be presented here.

4.4.4.1 Corn Flakes in a Consumer-Size Package

Model predictions for moisture transfer in a consumer-size (310g) package of corn flakes consisting of a multiple layer polymer liner are shown in Figure 4-13. For this simulation the exterior fibreboard box was not considered. A polymer liner consisting of 5 layers was assumed, with a relatively high moisture barrier in the centre. As expected for a low moisture food, the moisture content of the corn flakes rose, roughly reaching the critical moisture content after 183 days. Predictions of the water vapour pressure profile in the packaging film were also as expected, with the different layers clearly visible, and a relatively steep decline in the centre.

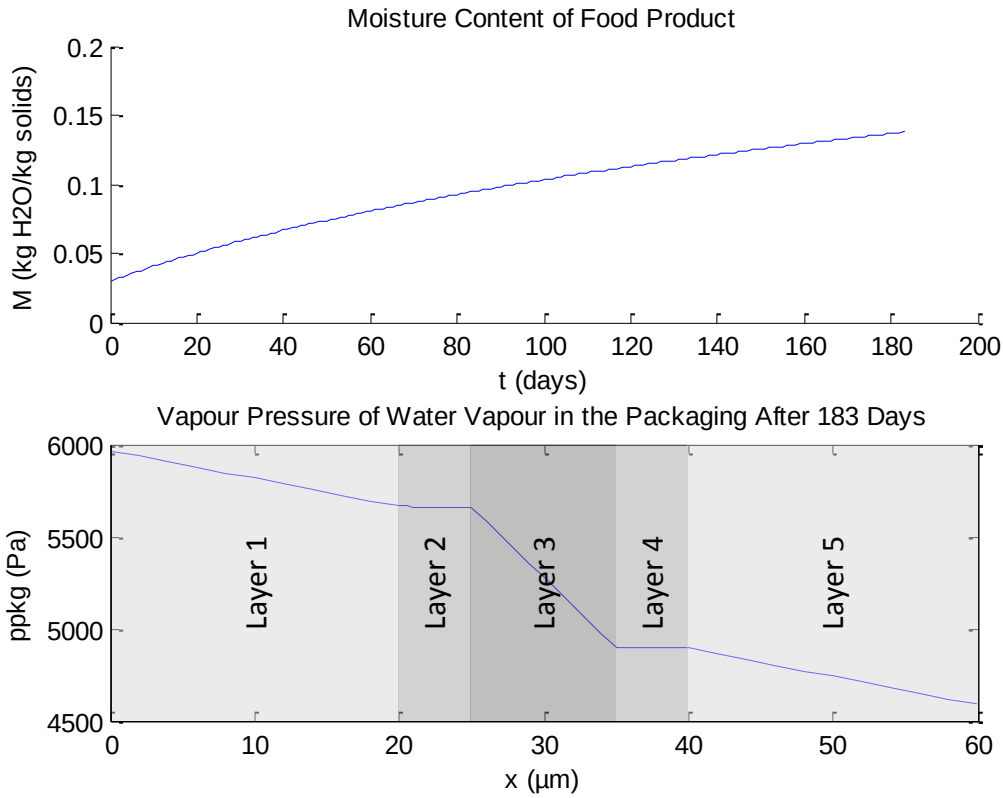

Figure 4-13: Model predictions of moisture content of corn flakes and water vapour pressure profile in polymer liner after 183 days at 38°C and 90% RH.

4.4.4.2 Skim Milk Powder in an Industrial-Size Bag

Model predictions for moisture transfer in an industrial-size (25 kg) bag of skim milk powder consisting of a paperboard bag with a polymer liner are shown in Figure 4-14. The system was modelled such that the paperboard bag and polymer liner were considered a single packaging film consisting of two layers, which is reasonable due to the lack of perforations. Again, as expected for a low moisture food, the moisture content of the skim milk powder increased over time. The relatively constant water vapour pressure in the paperboard bag and steep gradient in the polymer liner were also as expected.

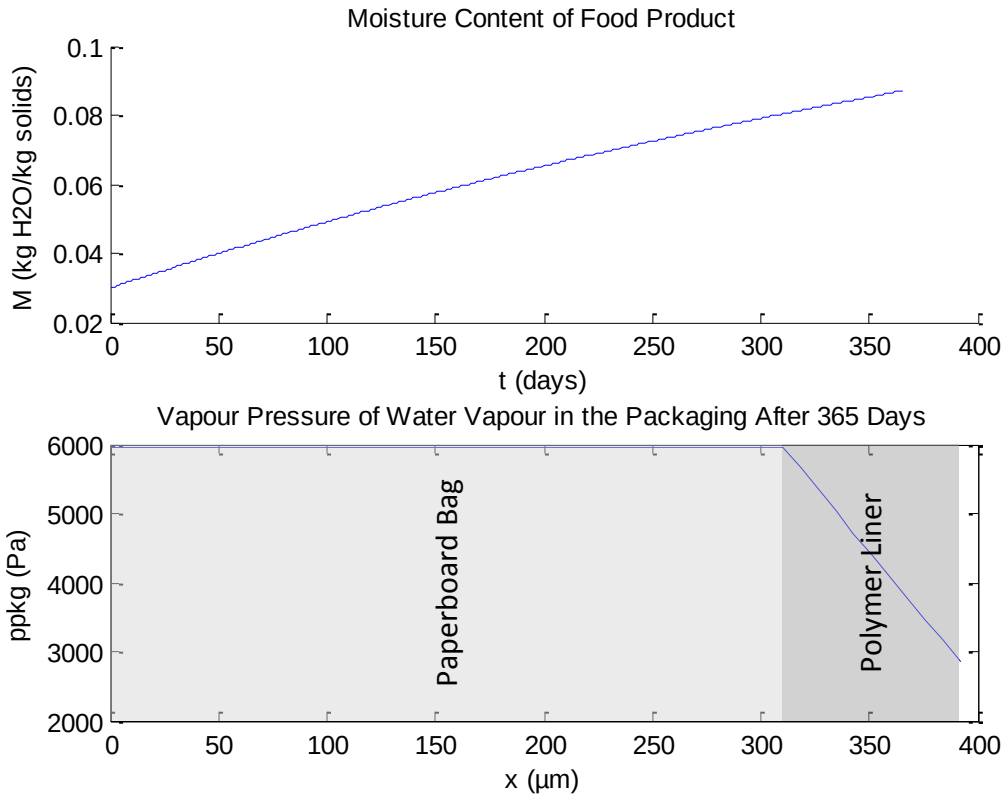

Figure 4-14: Model predictions of moisture content of skim milk powder and water vapour pressure profile in paperboard bag and polymer liner after 365 days at 38°C and 90% RH.

4.4.4.3 Edam Cheese in an Industrial-Size Polymer Bag

Model predictions for moisture transfer in a block of Edam cheese in an industrial-size (20 kg) polymer bag are shown in Figure 4-15. As expected for a high moisture food, the moisture content of the cheese decreased over time, although relatively slowly due to the large amount of water present. This is also consistent with the linear change in moisture content, since the water vapour pressure gradient would essentially remain constant.

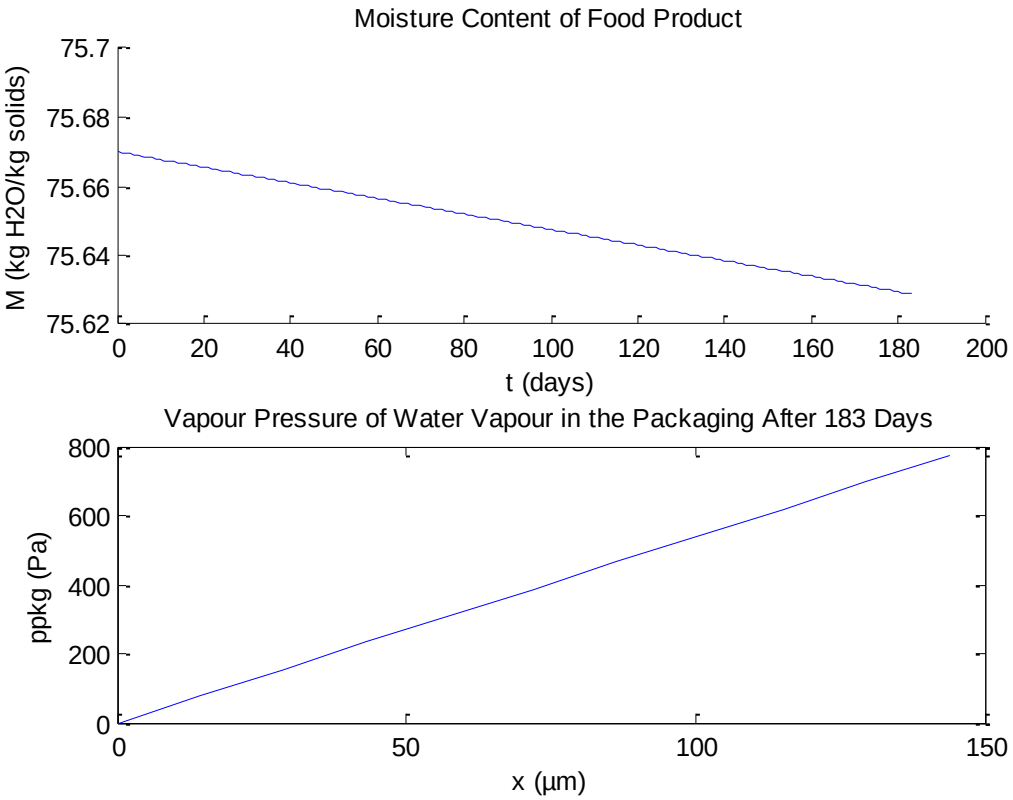

Figure 4-15: Model predictions of moisture content of Edam cheese and water vapour pressure profile in polymer bag after 270 days at 4°C and 0% RH.

4.4.5 Error Checks

To ensure the mathematical model was formulated correctly and that the solution method was appropriate, error checks were carried out. Both numerical and mathematical error checks were performed, which are summarised in Appendix C.3.

A numerical solution of the formulated model involves dividing continuous dimensions of time and space into a series of discrete intervals. Generally as the number of intervals tend to infinity, the accuracy of the numerical solution increases. However this also increases computational time, to a point where a numerical solution may no longer be practical. Therefore the ideal number of time and space intervals consists of the lowest number for which predictions are practically similar. To determine an appropriate time step, the relative error tolerance of the MATLAB® ODE23s solver function was varied and model predictions compared. A similar approach was used for the space step, where the number of

nodes per packaging layer was varied. Only predictions of moisture content of the food were considered to allow direct comparison for a different number of nodes. Results of numerical error checks are shown in Appendix C.3.1, which suggested a default relative error tolerance value of 1×10^{-3} and 10 nodes per packaging layer should be appropriate. Nevins (2008) reported the use of 40 nodes for a similar finite difference solution, which is in a similar range (dependent on the number of packaging layers).

To ensure the model is free of mathematical errors, model predictions using the numerical solution can be compared with predictions of a different solution method. As mentioned previously, solving the model analytically was not feasible. However to allow an analytical solution it is possible to simulate a simplified system by adjusting system inputs as required. Using this technique, various scenarios were simulated and predictions compared with analytical solutions as shown in Appendix C.3.2. It was found that numerical predictions agreed closely with analytical results, suggesting that the formulated model is free of mathematical errors.

4.5 MODEL VALIDATION

This section outlines the methods used to validate the developed mathematical model. The purpose of model validation is to gain an indication of the performance of the model in terms of predicting real life observations. A series of experiments were conducted covering various aspects of the model, and the results compared with model predictions to determine the level of agreement. Aspects that were validated include moisture permeation through the packaging, moisture diffusion through perforations, and the overall food package system.

4.5.1 Experimental Methodology

4.5.1.1 Moisture Permeation through Packaging

The permeation component of the model was validated by conducting various water vapour transfer rate (WVTR) tests. The ASTM E96 standard test consisting of the desiccant cup method was used for all water vapour permeability tests, which is outlined in Section 3.3.1.5.

For model validation an external RH of approximately 75% was used, which was produced using a 57.8% (by weight) glycerol in water solution (Forney & Brandl, 1992). A polymer liner consisting of mostly LDPE and paperboard bag samples were tested. The polymer liner sample was also tested at various temperatures of approximately 20°C, 30°C and 40°C to obtain temperature dependence data for use as model system inputs. Replicates of test samples varied between 4 and 6 depending on availability and practical limitations. Test conditions for validating model predictions of permeation are summarised in Table 4-2. Custom made aluminium permeability dishes were used due to the relatively low transfer rates through the test samples; these are shown with test samples in Figure 4-16. The inside diameter of the dishes was 70 mm, resulting in an exposed packaging surface area of 3.85×10^{-3} m^2. Sufficient silica gel beads were used to cover the bottom of each dish.

To ensure the test method was appropriate and produced dependable results, permeability tests were also carried out using a Mocon© Permatran® water vapour permeation testing instrument.

Table 4-2: Summary of samples and test conditions for validation of water vapour permeation through packaging.

Sample *	**Approximate Temperature † (°C)**	**RH Gradient ¶ (% RH - % RH)**
Polymer liner	20	$0 - 75$
Polymer liner	20	$75 - 0$
Polymer liner	30	$0 - 75$
Polymer liner	40	$0 - 75$
Paperboard bag	20	$0 - 75$
Polymer liner and two-ply paperboard bag	20	$0 - 75$
Two-ply paperboard bag and polymer liner	20	$75 - 0$

***** Multiple samples are in order of sample in contact with interior of permeability dish to sample exposed to ambient environment.

† The actual temperature was determined by the average of temperature readings logged at 15 minute intervals for the duration of each test.

¶ RH gradients are expressed as % RH at interior surface (surface closest to food product) to % RH at exterior surface (surface closest to ambient environment) as positioned in original packaging system. The actual ambient RH was determined by the average of RH readings logged at 15 minute intervals for the duration of each test.

(A)

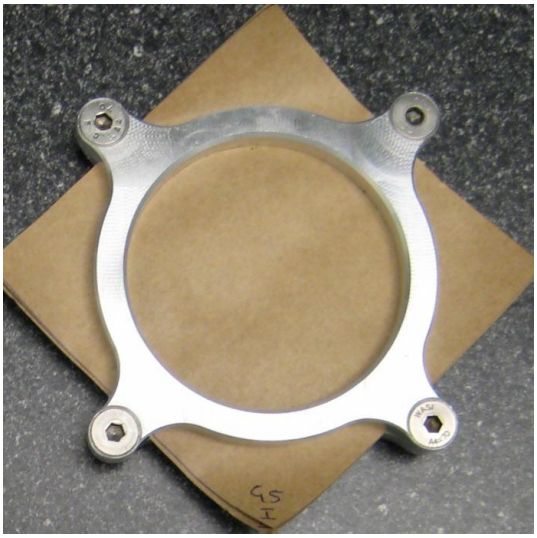

(B)

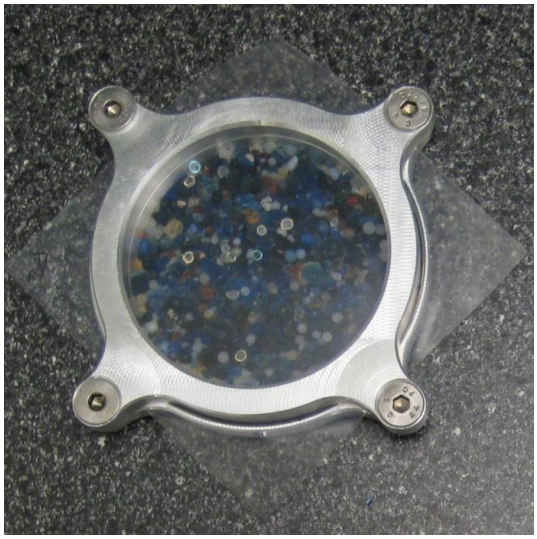

(C)

Figure 4-16: Aluminium foil blank (A), two-ply paperboard bag (B) and polymer liner (C) test samples in aluminium permeability dishes containing desiccant (silica beads).

4.5.1.2 Moisture Diffusion through Perforations

To validate model predictions of moisture diffusion through perforations, the same method used to validate water vapour permeation was utilised (Section 4.5.1.1). Perforations were created in test samples using a syringe needle with a 0.33 mm diameter. Both one and two perforations in a polymer liner were tested. An external RH of

approximately 75% produced using a 57.8% (by weight) glycerol in water solution was again used. Test conditions are outlined in Table 4-3, and samples are shown in Figure 4-17.

Table 4-3: Summary of samples and test conditions for validation of water vapour diffusion through perforations in packaging.

Sample	Approximate Temperature * (°C)	Approximate RH Gradient † (% RH - % RH)
Polymer liner with 1 perforation	20	$0 - 75$
Polymer liner with 2 perforations	20	$0 - 75$

* The actual temperature was determined by the average of temperature readings logged at 15 minute intervals for the duration of each test.

† RH gradients are expressed as % RH at interior surface (surface closest to food product) to % RH at exterior surface (surface closest to ambient environment) as positioned in original packaging system. The actual ambient RH was determined by the average of RH readings logged at 15 minute intervals for the duration of each test.

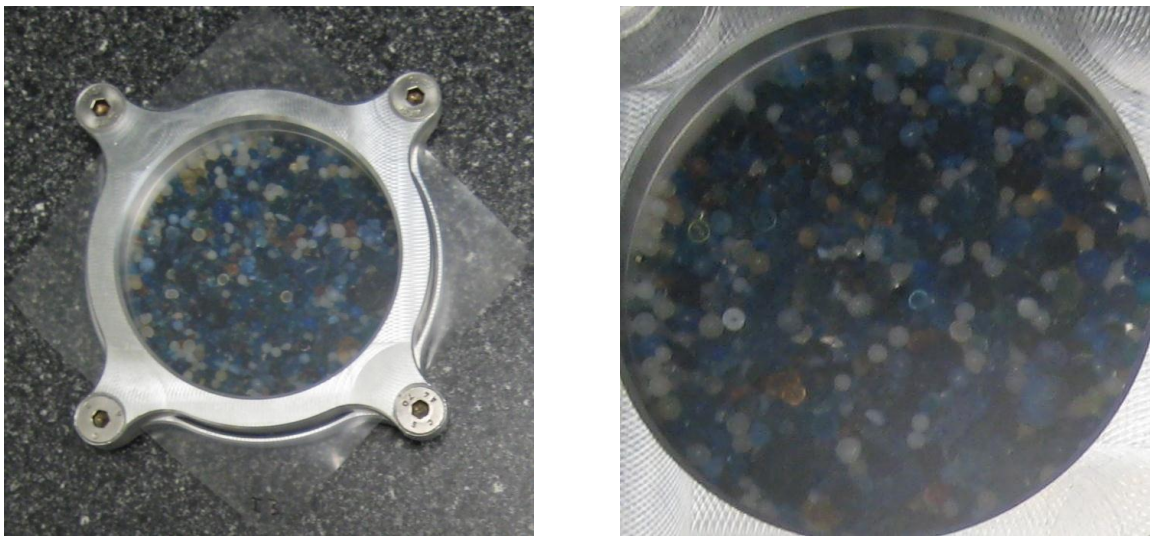

(A) (B)

Figure 4-17: Polymer liner test sample with 1 (A) and 2 (B) perforations in aluminium permeability dishes containing desiccant (silica beads).

4.5.1.3 Overall Food Package System

Permeability tests similar to those used to validate water vapour permeation through packaging (Section 4.5.1.1) were carried out to validate model predictions for an

overall food package system including water vapour pressure in the package headspace. However instead of using silica beads to maintain a constant RH gradient across the packaging samples, skim milk powder (SMP) was used, producing a variable driving force due to the effect of the moisture sorption isotherm. To gain an indication of the accuracy of model predictions for systems exhibiting larger driving force variability, as well as overall food package systems containing perforations, perforated test samples were also tested. Samples with 1 and 20 perforations were tested, again created using a syringe needle with a diameter of 0.33 mm, as well as a non-perforated sample. All samples were tested at approximately 30°C and an external RH of approximately 75%. Test conditions are summarised in Table 4-4, and samples are shown in Figure 4-18.

Table 4-4: Summary of samples and test conditions for validation of overall food package system.

Sample	**Approximate Temperature * (°C)**	**Approximate Ambient RH † (%)**
Polymer liner	30	75
Polymer liner with 1 perforation	30	75
Polymer liner with 20 perforations	30	75

* The actual temperature was determined by the average of temperature readings logged at 15 minute intervals for the duration of each test.

† The actual ambient RH was determined by the average of RH readings logged at 15 minute intervals for the duration of each test.

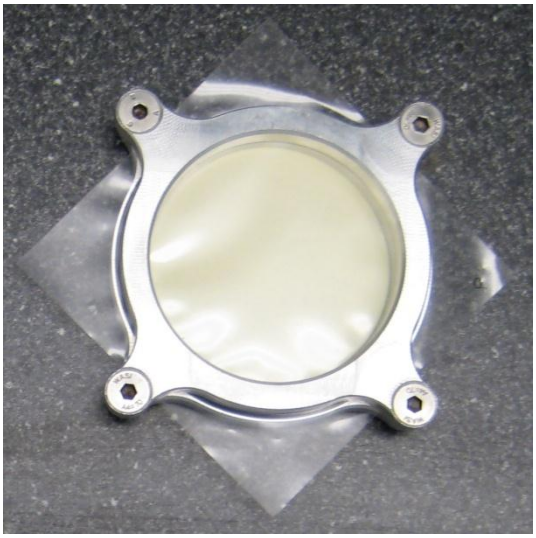

(A)

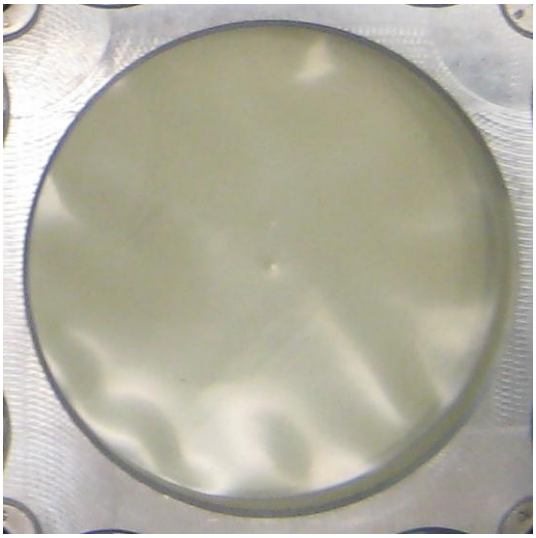

(B)

(C)

Figure 4-18: Polymer liner test samples with 0 (A), 1 (B) and 20 (C) perforations in aluminium permeability dishes containing SMP.

4.5.1.4 Initial Water Activity

To determine the initial water activity of SMP used to validate the overall food package system, a Decagon© CX-2 water activity meter was used. Water activity measurements were repeated until three consecutive readings agreed within 0.003, and an average value was reported.

4.5.2 Model Input Parameters and Data Analysis

4.5.2.1 Temperature and Relative Humidity

To determine actual conditions of the WVTR tests, temperature and RH readings were logged at 15 minute intervals for the duration of each test. Readings were plotted to ensure conditions remained relatively constant over each test period, and average values and 95% confidence intervals (CIs) calculated.

4.5.2.2 Packaging Material Thickness

The thickness of each packaging sample was determined using micrometer measurements. Three measurements were taken at random locations for each sample, from which the average thickness and 95% CI could be calculated. Where available, experimental thickness measurements were generally in reasonable agreement with commercially reported values.

4.5.2.3 Water Vapour Transfer Rate

WVTRs were determined for all samples from experimental data of change in mass versus time using regression analysis. Due to the nature of the data collected, each individual sample was analysed separately, and an average value calculated. Similar analysis was carried out for blank samples, and the resulting WVTRs subtracted from those of the test samples. 95% CIs were calculated for each value based on the standard error (SE) determined by the regression analysis, and combined as necessary for corrected WVTRs. Experimental change in mass versus time data for a polymer liner sample at 20.1 ± 0.5 °C and a 0% to 74 ± 3 % RH gradient is shown in Figure 4-19. WVTRs were converted to $g.m^{-2}.day^{-1}$ using the known surface area in the permeability dishes to allow comparison with other permeability data.

It was observed that for all experimental test samples there was a higher initial increase in mass over the first 24 hours, which is shown in Figure 4-19 for both the polymer liner and blank samples. Since determination of WVTRs is only concerned with the steady state change in mass, this period was ignored. However this will potentially be significant for model validation experiments, which will be discussed further in Section 4.5.3.1.1.

It was observed that some samples appeared to remain consistently higher or lower than others when compared directly (for example sample 1 and 4 in Figure 4-19). This effect was particularly notable at low temperatures and therefore low WVTRs. It is expected that this error is the result of using the sample mass at 0 hours as the initial condition, which itself contains significant error due to mass balance inaccuracies. Since WVTRs are only dependent on the slope of the data, this error will not affect calculations of permeability. However when comparing model predictions with experimental measurements, such error will be significant. One option was to use the intercept value as the initial condition for model comparisons, however this is only possible for steady-state scenarios. Therefore to remain consistent, the initial error was estimated by calculating a 95% CI for blank sample intercepts based on regression analysis, and presented visually as an error bar at 0 hours. This is shown in Figure 4-19.

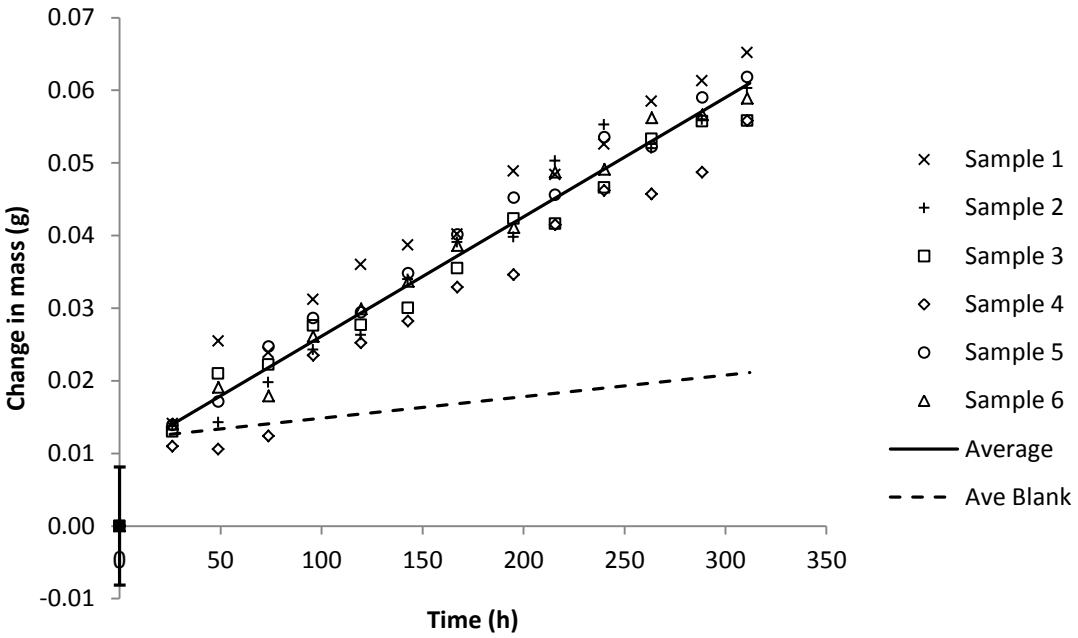

Figure 4-19: Experimental data of change in mass (g) versus time (hours) due to water vapour transfer through a polymer liner at 20.1°C and 0% to 74% RH gradient. Dashed-line represents average blank based on regression analysis. Error bar at 0 hours represents 95% CI of initial mass.

4.5.2.4 Water Vapour Permeability

To calculate the water vapour permeability of test samples, the following expression based on Equation 2-5 was used:

$$P_{pkg}^{H_2O} = \frac{WVTR.X_{T,pkg}}{36M_{r,H_2O}.RH_a.p_0^{H_2O}} \quad \textbf{(4-35)}$$

where:

$P_{pkg}^{H_2O}$ = Permeability of water vapour in packaging (mol.m.m^{-2}.s^{-1}.Pa^{-1})

$WVTR$ = Water vapour transfer rate (g.m^{-2}.day^{-1})

$X_{T,pkg}$ = Sample thickness (m)

M_{r,H_2O} = molecular mass of water (18.02 g.mol^{-1})

RH_a = Ambient relative humidity (%)

$p_0^{H_2O}$ = Saturated water vapour pressure (Pa)

To calculate the saturated water vapour pressure, the expression proposed by Shah et al. (1984) was used (Equation 4-19), and 95% CIs converted as required. 95% CIs for each parameter were combined as appropriate and reported with the calculated permeability.

To determine the activation energy of permeation, the natural logarithm of permeability values determined at a range of temperatures were plotted versus the reciprocal of absolute temperature, according to the following equation derived from the Arrhenius equation:

$$ln\left(P_{pkg}^{H_2O}\right) = ln\left(P_{0,pkg}^{H_2O}\right) - \frac{E_{P,pkg}^{H_2O}}{R}\frac{1}{T} \quad \textbf{(4-36)}$$

where:

$P_{0,pkg}^{H_2O}$ = Pre-exponential factor of permeability of water vapour in packaging (mol.m.m^{-2}.s^{-1}.Pa^{-1})

$E_{P,pkg}^{H_2O}$ = Activation energy of permeation of water vapour in packaging (J.mol^{-1})

R = Ideal gas constant (8.314 J.K^{-1}.mol^{-1})

T = Absolute temperature (K)

The resulting plot is shown in Figure 4-20. The activation energy of permeation was calculated from the slope based on regression analysis, and found to be (2.4 ± 0.5) × 10^4 J.mol^{-1}. This is in somewhat reasonable agreement with 3.35 × 10^4 J.mol^{-1} proposed by Doty et al. (1946).

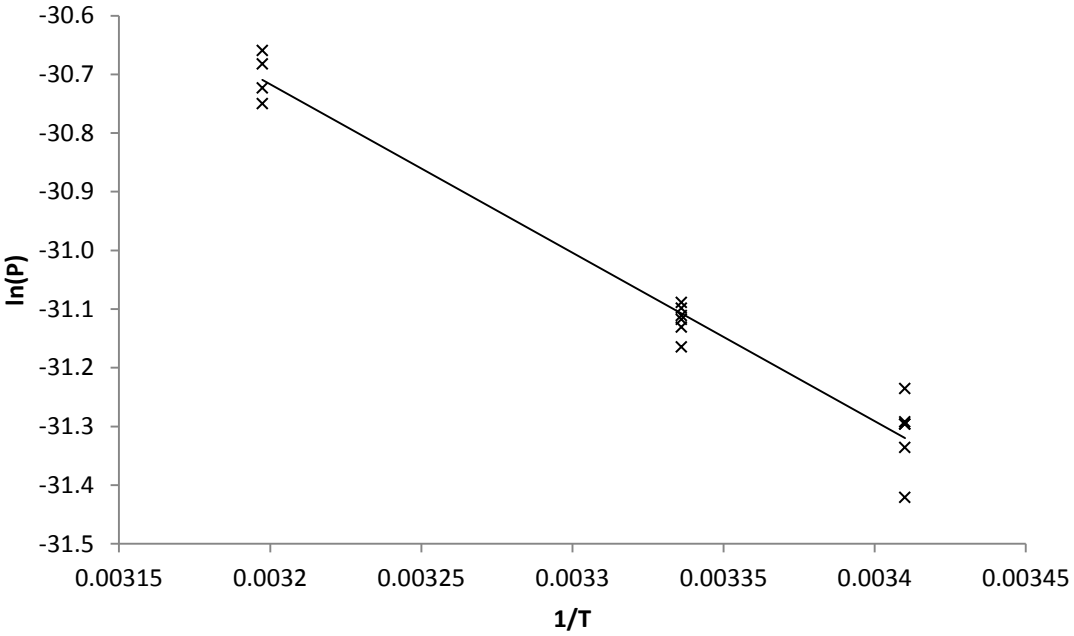

Figure 4-20: Plot of ln(P) (where P is the permeability of water vapour in the packaging (mol.m.m^{-2}.s^{-1}.Pa^{-1})) versus 1/T (where T is the absolute temperature (K)).

Experimentally determined WVTR and permeability values are shown in Table 4-5. As shown, Mocon® Permatran® permeability measurements were all within the calculated 95% CI of those determined using the desiccant cup method. This suggests that the desiccant cup method produces reliable results.

Table 4-5: Summary of WVTR and permeability data based on experimental measurements of polymer liner.

Method	Temperature (°C)	RH Gradient * (% RH - % RH)	WVTR ($g.m^{-2}.day^{-1}$)	Permeability † ($mol.m.m^{-2}.s^{-1}.Pa^{-1}$)
Mocon®	20.2	$0 - 75.1$	0.724	2.13×10^{-14}
Mocon®	26.6	$0 - 75.5$	1.31	2.62×10^{-14}
Mocon®	39.5	$0 - 74.2$	4.48	4.41×10^{-14}
Mocon®	39.6	$74.1 - 0$	4.50	4.41×10^{-14}
Desiccant cup	20.1	$0 - (74 \pm 3)$	0.84	$(2.5 \pm 0.4) \times 10^{-14}$
Desiccant cup	20.1	$(76.5 \pm 0.8) - 0$	0.83	$(2.4 \pm 0.4) \times 10^{-14}$
Desiccant cup	26.6	$0 - (76.5 \pm 0.9)$	1.53	$(3.0 \pm 0.5) \times 10^{-14}$
Desiccant cup	39.6	$0 - (78.0 \pm 1.0)$	4.98	$(4.6 \pm 0.7) \times 10^{-14}$

* RH gradients are expressed as % RH at the interior surface (surface closest to food product) to % RH at the exterior surface (surface closest to ambient environment) as positioned in original packaging system.

† Error values represent a 95% CI relative to the mean. 95% CIs were not estimated for Mocon® measurements.

4.5.2.5 Moisture Sorption Isotherm

To simulate desiccant (silica beads) inside a food package (permeability dish), a linear isotherm with a very large slope of 1×10^{10} and a constant of 0 (kg water).(kg solids)$^{-1}$ was used in the mathematical model. This has the effect of maintaining the water vapour pressure at 0 for any practical increase in moisture content of the food product. Whilst a moisture sorption isotherm for silica beads could be obtained from literature, this was not considered practically necessary in this instance.

For validating the moisture sorption isotherm component of the model, GAB moisture sorption isotherm parameters for SMP were obtained from literature. Joupila & Roos (1994) suggested values for $M_{0,GAB}$, C_{GAB} and k_{GAB} of 0.051 (kg water).(kg solids)$^{-1}$, 12.11 and 1.08 respectively. These parameters were determined at 24 °C, however it was suggested by Foster et al. (2005) that temperature has a negligible influence on moisture sorption isotherm parameters of milk powders over the temperature range of 4-37 °C. Since

the error in these parameters was not indicated, such error was not included in model sensitivity analysis.

4.5.2.6 Size of Perforations

As mentioned previously, perforations were created in test samples using a syringe needle with a 0.33 mm diameter. It was therefore expected that the area of the perforation could be estimated directly. However initial model predictions of WVTRs using this assumption were much higher than experimental measurements. To gain a more accurate indication of the size of the perforations, microscope images were taken. The length of each perforation was measured using an ocular scale, allowing the scale of the images to be calculated. The perforation was then approximated by a basic geometric shape, from which the area to be calculated. An example microscope image of a perforation created by a syringe needle is shown in Figure 4-21. Using this method the size of perforations created by the syringe was found to be $(5.2 \pm 1.3) \times 10^{-9}$ m^2, much lower than the 8.6×10^{-8} m^2 initially expected based on the size of the syringe. It is believed this significant difference is likely due to stretching during penetration of the syringe needle.

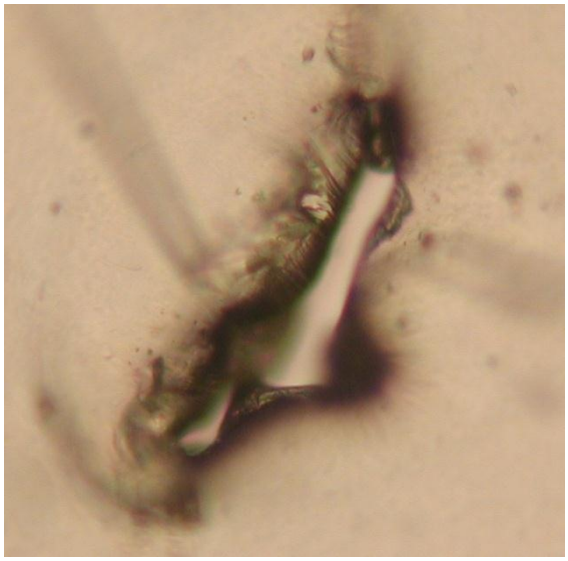

Figure 4-21: Example microscope image of a perforation created using a syringe needle.

4.5.3 Results and Discussion

4.5.3.1 Moisture Permeation through Packaging

The permeation component of the model was the first to be validated as it forms a basis for most systems of interest. Two scenarios were considered: permeation through a single layer of packaging, and permeation through two layers.

4.5.3.1.1 Single Layer Packaging System

To validate permeation through a single layer system, the WVTR test of a polymer liner sample was simulated as a food package consisting of a sealed polymer liner containing desiccant. Values of system inputs for the simulation are summarised in Table 4-6. System inputs with no bearing on predictions and universal parameters (such as the ideal gas constant) were not included in the summary.

Table 4-6: Summary of system inputs used for validation of water vapour permeation through a single layer packaging system.

Parameter Description	Symbol	Units	Value*
General system inputs			
Initial moisture content of silica beads	M_i	(kg water).(kg solids)$^{-1}$	0
Ambient temperature	T	K	$(20.1 \pm 0.5) + 273.15$
Ambient relative humidity	RH_a	%	(74 ± 3)
Surface area of packaging	A_{pkg}	m^2	$\pi\left(\frac{0.07}{2}\right)^2$
Number of layers	N	-	1
Linear isotherm parameters			
Slope of linear isotherm	b_{lin}	-	1×10^{10}
Constant for linear isotherm	c_{lin}	-	0
Properties of layer 1 of packaging film			
Thickness of layer 1 of packaging film	$X_{pkg,1}$	m	$(8.2 \pm 1.2) \times 10^{-5}$
Solubility of water vapour in layer 1 of packaging at reference temperature	$S^{H_2O}_{ref,pkg,1}$	mol.m^{-3}.Pa^{-1}	0.001
Permeability of water vapour in layer 1 of packaging at reference temperature	$P^{H_2O}_{ref,pkg,1}$	mol.m.m^{-2}.s^{-1}.Pa^{-1}	$(2.5 \pm 0.4) \times 10^{-14}$

*Error values represent a 95% CI relative to the mean.

To allow direct comparison with experimental results, model predictions were converted from a moisture content to an increase in mass. As noted in Section 4.5.2.3, a higher initial increase in mass over the first 24 hours was observed for all samples. This initial period was partly due to moisture sorption in the test samples. It was therefore attempted to simulate this period with the developed mathematical model; however predictions were significantly different to experimental measurements (not shown). It is believed this difference was a result of other significant effects, such as condensation on the exterior surfaces of the samples and permeability dishes. Although these effects should have been partly accounted for by the blank samples, the variability between samples over this period was very high (much greater than the error in individual measurements).

Therefore to reduce error and greatly simplify data analysis, the first set of measurements were ignored.

An error bar was again included to indicate the error in the initial value, in this case consisting of the combined errors of blank and test samples. Similarly, to gain an indication of the sensitivity of model predictions on system inputs, extreme system input values based on calculated 95% CIs resulting in the fastest and slowest changing model predictions were also simulated. A comparison of model predictions and experimental results for the single layer system is shown in Figure 4-22.

Due to the experimental method used to determine water vapour barrier properties, only the permeability of the polymer liner could be obtained. Since the mathematical model required both the solubility and diffusivity of water vapour in the packaging as system inputs, it was necessary to estimate the solubility. To test the sensitivity of model predictions to the value of solubility, brief sensitivity analysis was carried out. This showed that the solubility only affected the rate with which steady-state was reached provided that the product of the diffusivity and solubility was equal to the permeability (not shown), which is consistent with what is expected mathematically. Therefore, so that steady-state is practically reached instantly, a very low value of 0.001 $mol.m^{-3}.Pa^{-1}$ was used for the solubility of water vapour in the polymer liner. As a result the unsteady-state period of model predictions could be ignored allowing model predictions to be compared directly with experimental results without using the steady-state vapour pressure profile as an initial condition.

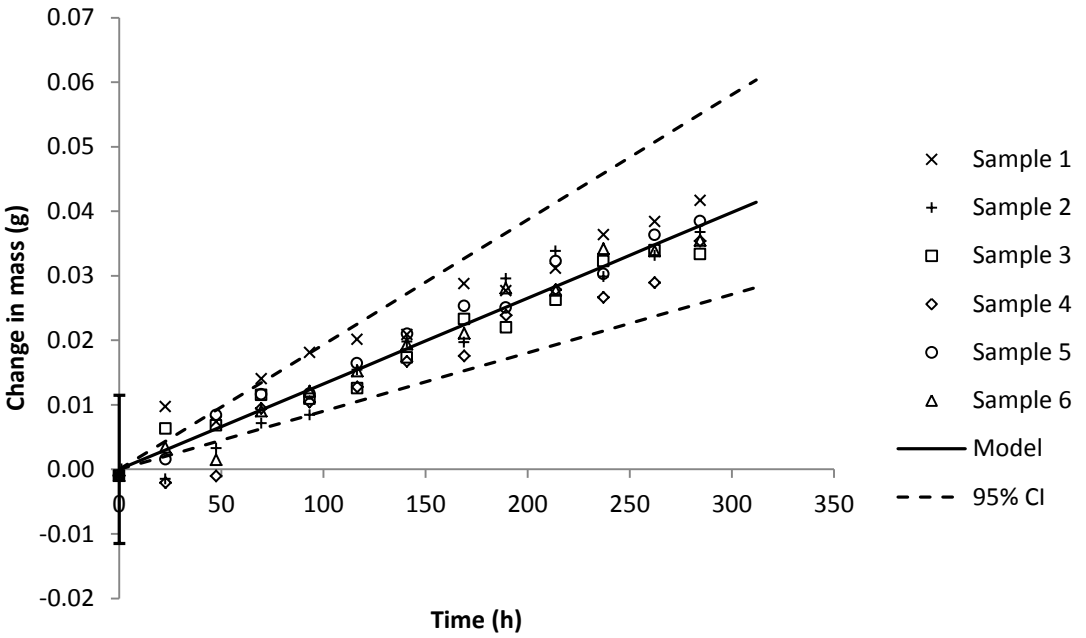

Figure 4-22: Comparison of change in mass (g) versus time (hours) due to water vapour transfer through a polymer liner at 20.1°C and 0% to 74% RH gradient as predicted by the standard food package model and measured experimentally. Error bar at 0 hours represents 95% CI of initial experimental mass. Model 95% CI limits represent extreme predictions based on 95% CIs of system inputs.

As expected, there was excellent agreement between model predictions and experimental measurements of water vapour transfer through the polymer liner. Some early experimental measurements were outside model 95% CI limits, however error bar representing the 95% CI of initial experimental mass suggests this is within experimental error. It should be noted that for this test the same experimental data used to calculate the permeability of water vapour in the polymer liner sample was used to compare model predictions. Therefore it is not a true model validation test as the model predictions would be expected to agree with the experimental results simply because the same data is essentially being analysed using two different methods. However this test does further confirm the mathematical error checks carrier out earlier (Section 4.4.5), as well as verify that the analysis method used to calculate the water vapour permeability from experimental data is appropriate. Similar simulations of water vapour transfer through a polymer liner at 26.6°C and 39.6°C also agreed with experimental results as expected (not shown).

A further point to note is that the polymer liner sample actually consisted of multiple layers (each layer consisting mostly of various blends of LDPE); however since it was not possible to test each layer individually, only the overall water vapour barrier properties of the film were considered. This means the dynamics of the water vapour transfer within the packaging could not be considered for model validation. Furthermore, individual layers were configured in an asymmetrical configuration. Therefore any significant concentration dependence of barrier properties would lead to results that are dependent on the RH gradient (both the absolute gradient and its direction). To ensure that no significant concentration dependence of individual layers existed within the film, the polymer liner sample was also tested with a reversed RH gradient (Table 4-5). The polymer liner was found to have a W.V.T.R. of 0.84 ± 0.06 $g.m^{-2}.day^{-1}$ at 20.1°C and a 0% to 74% RH gradient in a standard configuration (low water vapour pressure at the interior surface of the film), and 0.83 ± 0.06 $g.m^{-2}.day^{-1}$ at 20.1°C and a 0% to 76.5% RH gradient in the reversed direction, suggesting that any concentration dependence is fairly insignificant. Although this does not confirm a lack of concentration dependence (this agreement could be purely coincidental and/or may not reflect barrier properties at other temperatures), since all layers consist mainly of LDPE it is believed that concentration dependence should be negligible (Morillon et al., 2000).

4.5.3.1.2 Two Layer Packaging System

To validate permeation through a system with multiple layers, the WVTR test of paperboard bag and polymer liner samples was simulated as a food package consisting of a sealed polymer liner containing desiccant with a fully enclosed exterior paperboard bag. Values of system inputs for the simulation are summarised in Table 4-7.

Table 4-7: Summary of system inputs used for validation of water vapour permeation through a two layer packaging system.

Parameter Description	Symbol	Units	Value *
General system inputs			
Initial moisture content of silica beads	M_i	(kg water).(kg solids)$^{-1}$	0
Ambient temperature	T	K	$(20.1 \pm 0.5) + 273.15$
Ambient relative humidity	RH_a	%	(74 ± 3)
Surface area of packaging	A_{pkg}	m^2	$\pi\left(\frac{0.07}{2}\right)^2$
Number of layers	N	-	2
Linear isotherm parameters			
Slope of linear isotherm	b_{lin}	-	1×10^{10}
Constant for linear isotherm	c_{lin}	-	0
Properties of layer 1 of packaging film			
Thickness of layer 1 of packaging film	$X_{pkg,1}$	m	$(3.1 \pm 0.5) \times 10^{-4}$
Solubility of water vapour in layer 1 of packaging at reference temperature	$S^{H_2O}_{ref,pkg,1}$	mol.m^{-3}.Pa^{-1}	0.001
Permeability of water vapour in layer 1 of packaging at reference temperature	$P^{H_2O}_{ref,pkg,1}$	mol.m.m^{-2}.s^{-1}.Pa^{-1}	1.6×10^{-11} †
Properties of layer 2 of packaging film			
Thickness of layer 2 of packaging film	$X_{pkg,2}$	m	$(8.2 \pm 1.2) \times 10^{-5}$
Solubility of water vapour in layer 2 of packaging at reference temperature	$S^{H_2O}_{ref,pkg,2}$	mol.m^{-3}.Pa^{-1}	0.001
Permeability of water vapour in layer 2 of packaging at reference temperature	$P^{H_2O}_{ref,pkg,2}$	mol.m.m^{-2}.s^{-1}.Pa^{-1}	$(2.5 \pm 0.4) \times 10^{-14}$

* Error values represent a 95% CI relative to the mean.

† The 95% CI was not considered due to approximations made for the simulation.

It is believed that, due to the very high water vapour transfer rates through the paperboard bag, the experimental test method used to determine its permeability was actually limited by the rate of adsorption onto the silica beads. This is indicated by the non-linear increase in mass as shown in Figure 4-23. Therefore the initial slope after the transient period was used to estimate the permeability of water vapour in the paperboard

bag (as indicated) which was found to be 1.6×10^{-11} mol.m.m^{-2}.s^{-1}.Pa^{-1} at 20.1°C and a 0% to 74.4% RH gradient, although it is expected that the actual permeability would be higher. It is also believed the permeability of the paperboard bag may exhibit significant concentration dependence due to the concentration dependence of the solubility (as determined from the moisture sorption isotherm). Since the permeability of the polymer liner was much lower than that of the paperboard bag (even relative to the low estimated value), it was predicted that the specific barrier properties of the paperboard bag would not have a significant effect on model predictions, and further investigation was not considered worthwhile. Therefore constant values were used for both the diffusivity and solubility of water vapour in the paperboard bag in the model. A brief sensitivity analysis confirmed increasing the permeability of the paperboard bag had no significant effect on model predictions (not shown).

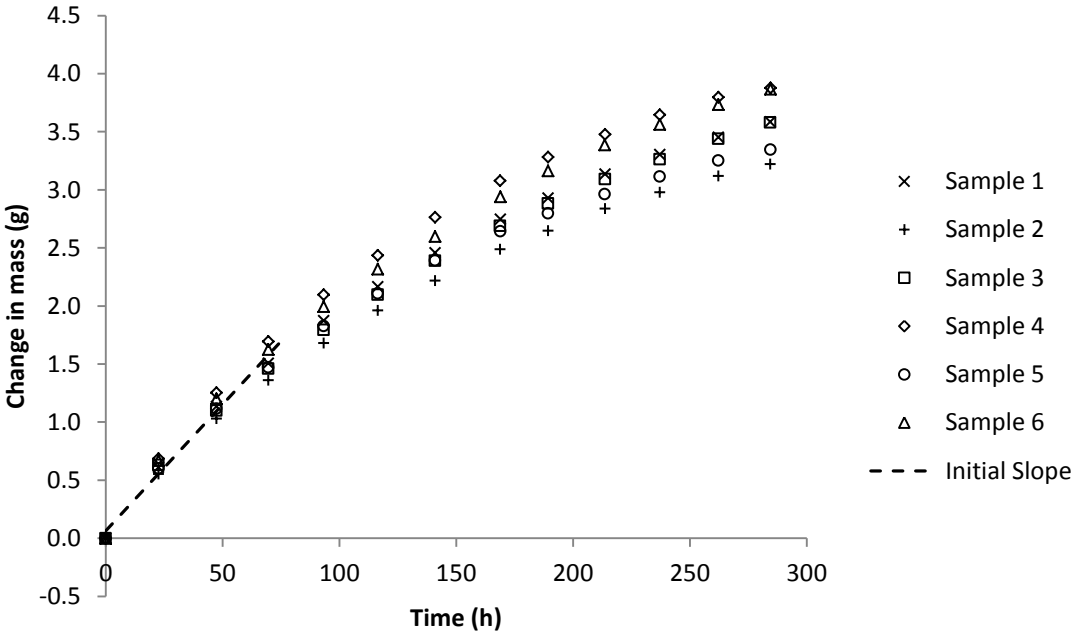

Figure 4-23: Change in mass (g) versus time (hours) due to water vapour transfer through a paperboard bag test sample at 20.1°C and 0% to 74% RH gradient as measured experimentally (unsteady-state period not included).

As for the single layer system, the unsteady-state period of the experimental results was again ignored, and a very low solubility used. In this case, since the system had two layers, it is mathematically possible that the solubility could also affect the water vapour

profile in the packaging in addition to the rate with which the steady-state is reached. However given that the permeability of the polymer liner was much lower than that of the paperboard bag, this effect was expected to be insignificant.

A comparison of model predictions and experimental results for the two layer system is shown in Figure 4-24.

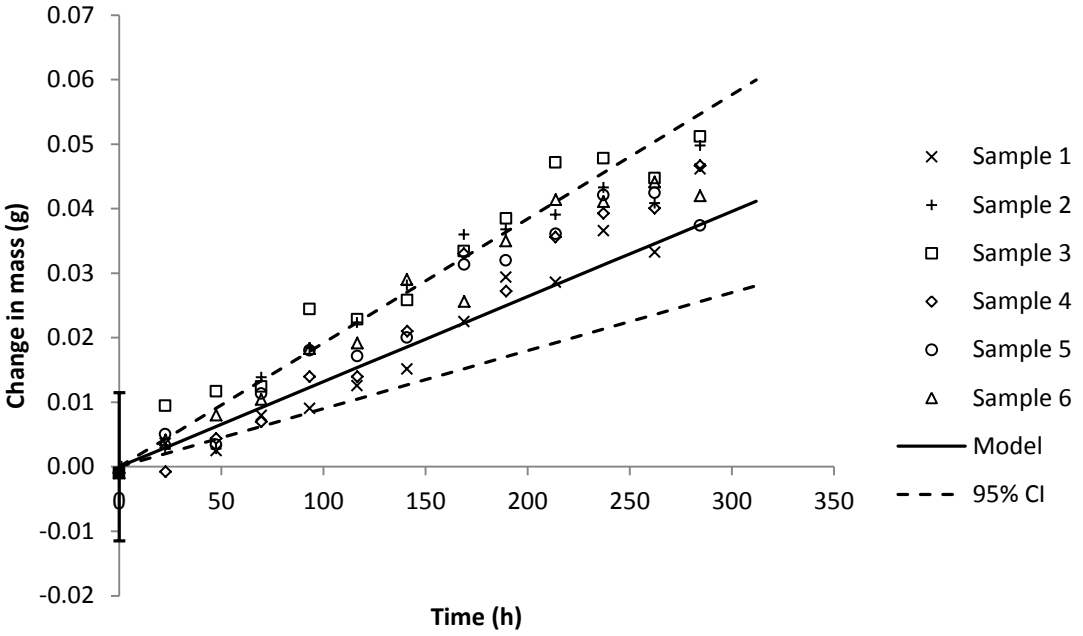

Figure 4-24: Comparison of change in mass (g) versus time (hours) due to water vapour transfer through a polymer liner and paperboard bag at 20.1°C and 0% to 74% RH gradient as predicted by the standard food package model and measured experimentally. Error bar at 0 hours represents 95% CI of initial experimental mass. Model 95% CI limits represent extreme predictions based on 95% CIs of system inputs.

As shown, there was reasonably good agreement between model predictions and experimental measurements of water vapour transfer through the polymer liner and paperboard bag. Again, experimental measurements outside the model 95% CI limits are most likely explained by the error in the initial experimental mass. Somewhat unexpectedly, the increase in mass of the test samples for the two layer system (0.84 ± 0.06 $g.m^{-2}.day^{-1}$ at 20.1°C and a 0% to 74.4% RH gradient) was slightly higher than for the single layer system (1.06 ± 0.07 $g.m^{-2}.day^{-1}$ at 20.1°C and a 0% to 74.4% RH gradient). This could be related to a

lower degree of sealing in the two layer test samples, which would also explain why the model predictions are at the lower end of the experimental measurement error range.

4.5.3.2 Moisture Diffusion through Perforations

Diffusion of water vapour through perforations in packaging was validated with systems in which permeation also occurred (validated in Section 4.5.3.1). Systems with one and two perforations in a single layer of packaging were considered.

4.5.3.2.1 Single Perforation in a Single Layer Packaging System

To validate diffusion through a single perforation in a single layer of packaging, the WVTR test of a polymer liner with one perforation was simulated as a food package containing desiccant. Values of system inputs for the simulation are summarised in Table 4-8.

Table 4-8: Summary of system inputs used for validation of diffusion of water vapour through a single perforation.

Parameter Description	Symbol	Units	Value *
General system inputs			
Initial moisture content of silica beads	M_i	(kg water).(kg solids)$^{-1}$	0
Ambient temperature	T	K	$(20.1 \pm 0.5) + 273.15$
Ambient relative humidity	RH_a	%	(74 ± 3)
Surface area of packaging	A_{pkg}	m^2	$\pi\left(\frac{0.07}{2}\right)^2$
Number of layers	N	-	1
Total area of perforations	A_{prf}	m^2	$(5.2 \pm 1.3) \times 10^{-9}$
Diameter of perforation	d_{prf}	m	1×10^{-4}
Linear isotherm parameters			
Slope of linear isotherm	b_{lin}	-	1×10^{10}
Constant for linear isotherm	c_{lin}	-	0
Properties of layer 1 of packaging film			
Thickness of layer 1 of packaging film	$X_{pkg,1}$	m	$(8.2 \pm 1.2) \times 10^{-5}$
Solubility of water vapour in layer 1 of packaging at reference temperature	$S_{ref,pkg,1}^{H_2O}$	mol.m^{-3}.Pa^{-1}	0.001
Permeability of water vapour in layer 1 of packaging at reference temperature	$P_{ref,pkg,1}^{H_2O}$	mol.m.m^{-2}.s^{-1}.Pa^{-1}	$(2.5 \pm 0.4) \times 10^{-14}$

* Error values represent a 95% CI relative to the mean.

An approximate value of 1×10^{-4} m was used for the perforation diameter in the model. In this case the specific value was not significant, as long as it was greater or equal to 1×10^{-5} m, as this parameter only determines which expression to use for diffusive flux through perforations (below 1×10^{-5} m the perforation diameter is used as a parameter in the diffusive flux expression). It should be noted that, due to the very small size of perforations below 1×10^{-5} m in diameter, it was not practical to create such perforations with the available equipment. As a result it was not possible to validate the other expressions, and these can only be included in the model for reference. Since no applications for perforations smaller than 1×10^{-5} m in diameter were encountered in this

investigation, it was decided that to pursue its validation further was not worthwhile. However it is suggested that the model be independently validated for such a scenario if its application is required.

Again, as for validation of permeation, the initial 24 hour unsteady-state period was not considered in the simulation, and the solubility of water vapour in the polymer liner was assumed to be 1 $mol.m^{-3}.Pa^{-1}$. A comparison of model predictions and experimental results for the single perforation system is shown in Figure 4-25.

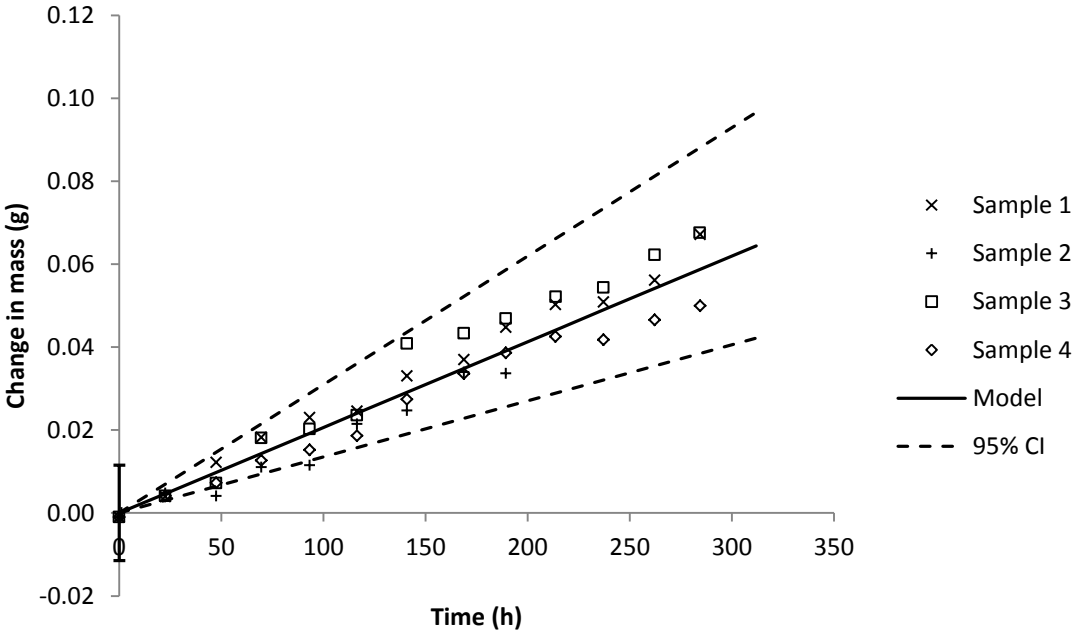

Figure 4-25: Comparison of change in mass (g) versus time (hours) due to water vapour transfer through a polymer liner with 1 perforation at 20.1°C and 0% to 74% RH gradient as predicted by the standard food package model and measured experimentally. Error bar at 0 hours represents 95% CI of initial experimental mass. Model 95% CI limits represent extreme predictions based on 95% CIs of system inputs.

As can be seen, model predictions and experimental measurements of water vapour transfer through the polymer liner with 1 perforation matched very closely. The rate of moisture transfer for the perforated sample is slightly higher than the non-perforated sample (as shown in Figure 4-22), as expected. This test suggests that water vapour diffusion through a single perforation with a diameter greater or equal to 1×10^{-5} m in parallel to permeation through a single layer of packaging can accurately be simulated by the model.

Since permeation occurs in parallel to diffusion through perforations, this test also further validates permeation through a single layer of packaging.

4.5.3.2.2 Two Perforations in a Single Layer Packaging System

To ensure water vapour diffusion through multiple perforations was also correctly predicted by the model, a polymer liner with 2 perforations was also validated. Assumptions and values of system inputs for the simulation were the same as for the single perforation system (Table 4-8), except the total area of perforations was doubled ($(1.04 \pm 0.14) \times 10^{-8}$ m^2). A comparison of model predictions and experimental results for the 2 perforation system is shown in Figure 4-26.

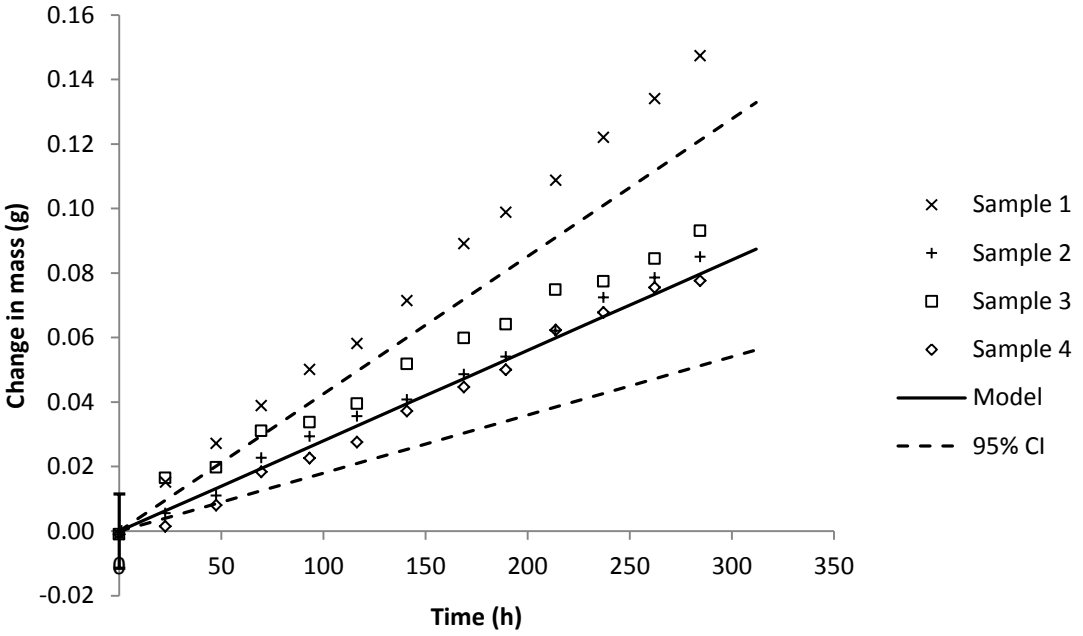

Figure 4-26: Comparison of change in mass (g) versus time (hours) due to water vapour transfer through a polymer liner with 2 perforations at 20.1°C and 0% to 74% RH gradient as predicted by the standard food package model and measured experimentally. Error bar at 0 hours represents 95% CI of initial experimental mass. Model 95% CI limits represent extreme predictions based on 95% CIs of system inputs.

The comparison of model predictions and experimental measurements showed reasonable agreement for water vapour transfer through the polymer liner with two perforations. It was noted that experimental measurements for sample 1 were unusually

high, both relative to the other experimental samples and to model predictions. It is possible that this difference was due to a less perfect seal in the permeability dish. If sample 1 is not considered, the agreement between model predictions and experimental measurements becomes very good.

4.5.3.3 Overall Food Package System

The water vapour pressure in the package headspace for an actual food package will be dependent on the moisture sorption isotherm of the food product in the package. Therefore to validate model predictions for an overall food package system, water vapour transfer in systems containing SMP were simulated. Three scenarios were considered: a single layer packaging system without perforations, as well as systems containing 1 and 20 perforations respectively.

4.5.3.3.1 Single Layer Packaging System

To validate the overall model for a single layer unperforated packaging system, the polymer liner test sample in a permeability dish containing SMP was simulated as a sealed food package. Values of system inputs for the simulation are summarised in Table 4-9.

Table 4-9: Summary of system inputs used for validation of the moisture isotherm component of the model for a single layer system.

Parameter Description	Symbol	Units	Value *
General system inputs			
Mass of solids in SMP	m_s	kg	0.0094
Initial moisture content of SMP	M_i	(kg water).(kg solids)$^{-1}$	0.0623 ± 0.0009
Ambient temperature	T	K	$(26.8 \pm 1.0) + 273.15$
Ambient relative humidity	RH_a	%	(76.5 ± 0.9)
Surface area of packaging	A_{pkg}	m^2	$\pi\left(\frac{0.07}{2}\right)^2$
Number of layers	N	-	1
GAB isotherm parameters			
Moisture content of monolayer for GAB isotherm	$M_{0,GAB}$	(kg water).(kg solids)$^{-1}$	0.051
Guggenheim constant for GAB isotherm	C_{GAB}	-	12.11
Constant for GAB isotherm	k_{GAB}	-	1.08
Properties of layer 1 of packaging film			
Thickness of layer 1 of packaging film	$X_{pkg,1}$	m	$(8.2 \pm 1.2) \times 10^{-5}$
Solubility of water vapour in layer 1 of packaging at reference temperature	$S_{ref,pkg,1}^{H_2O}$	mol.m^{-3}.Pa^{-1}	0.001
Reference temperature of solubility of water vapour in layer 1 of packaging	$T_{ref,S_{pkg}^{H_2O},1}$	K	$(26.6 \pm 0.9) + 273.15$
Partial molar enthalpy of sorption of water vapour in layer 1 of packaging material	$\Delta H_{S,pkg,1}^{H_2O}$	J.mol^{-1}	0
Permeability of water vapour in layer 1 of packaging at reference temperature	$P_{ref,pkg,1}^{H_2O}$	mol.m.m^{-2}.s^{-1}.Pa^{-1}	$(3.1 \pm 0.5) \times 10^{-14}$
Activation energy of permeation of water vapour in layer 1 of packaging material	$E_{P,pkg,1}^{H_2O}$	J.mol^{-1}	$(2.4 \pm 0.5) \times 10^4$
Reference temperature of diffusivity of water vapour in layer 1 of packaging	$T_{ref,D_{pkg}^{H_2O},1}$	K	$(26.6 \pm 0.9) + 273.15$

* Error values represent a 95% CI relative to the mean.

To allow direct comparison with model predictions, experimental results were converted from an increase in mass to a moisture content. As for the samples tested at a constant RH gradient using silica beads, the experimental test samples containing SMP also experienced a higher initial increase in mass over the first 24 hours, associated with the initial moisture sorption as well as other effects. However unlike the constant RH gradient samples, the SMP samples did not reach steady-state since the water vapour pressure in the package headspace was not constant. Therefore it was not possible to use a steady-state profile as the initial condition for the simulation. To overcome this problem, the first set of experimental measurements were again ignored, as well as model predictions corresponding to the same initial time period. Similarly, since steady-state was not reached, model predictions were no longer independent of the solubility. As was carried out earlier (Section 4.5.3.1.1), a brief sensitivity analysis was used to determine the sensitivity of model predictions on the solubility. This showed that, for the system of interest, below approximately 1 $mol.m^{-3}.Pa^{-1}$ model predictions were independent of the value of solubility (Figure 4-27). To gain a general indication of the solubility of water vapour in the polymer liner, samples were stored at 0% RH (using silica beads) and weighed, followed by 75% RH (57.8% (by weight) glycerol in water solution) and 100% RH (pure water). It was found that the mass of samples remained relatively unchanged (not shown), suggesting that the solubility value is very low. Therefore a very low solubility value of 0.001 $mol.m^{-3}.Pa^{-1}$ was used in the model.

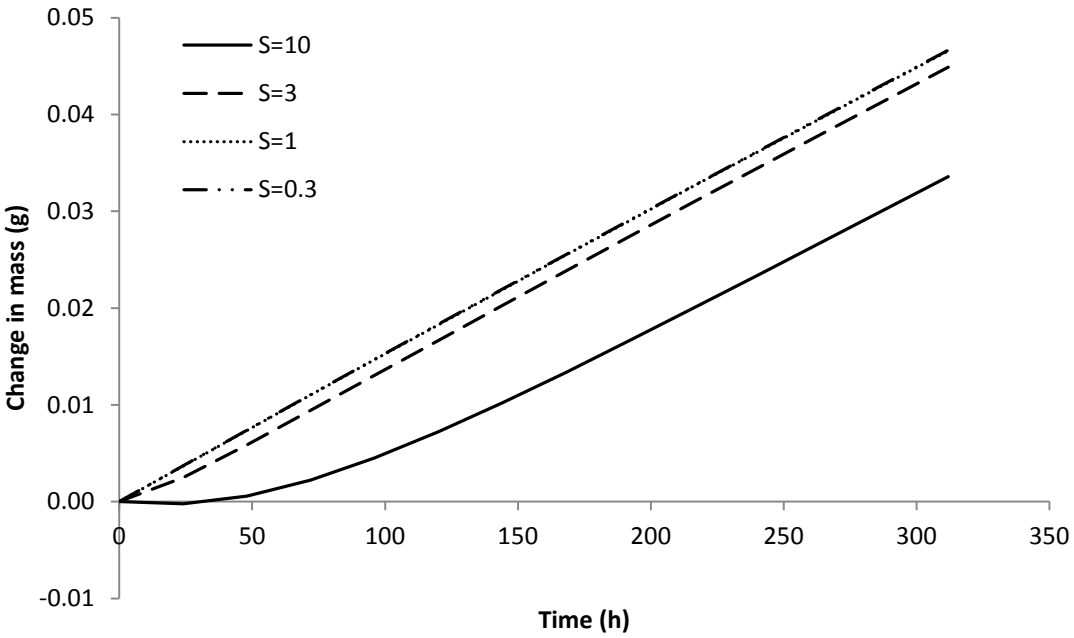

Figure 4-27: Sensitivity of model predictions on solubility (S = 0.3, 1, 3 and 10 mol.m^{-3}.Pa^{-1}) for a single layer polymer liner system containing SMP at 26.6°C and 76.5% ambient RH.

A comparison of model predictions and experimental results for the single layer non-perforated system is shown in Figure 4-28.

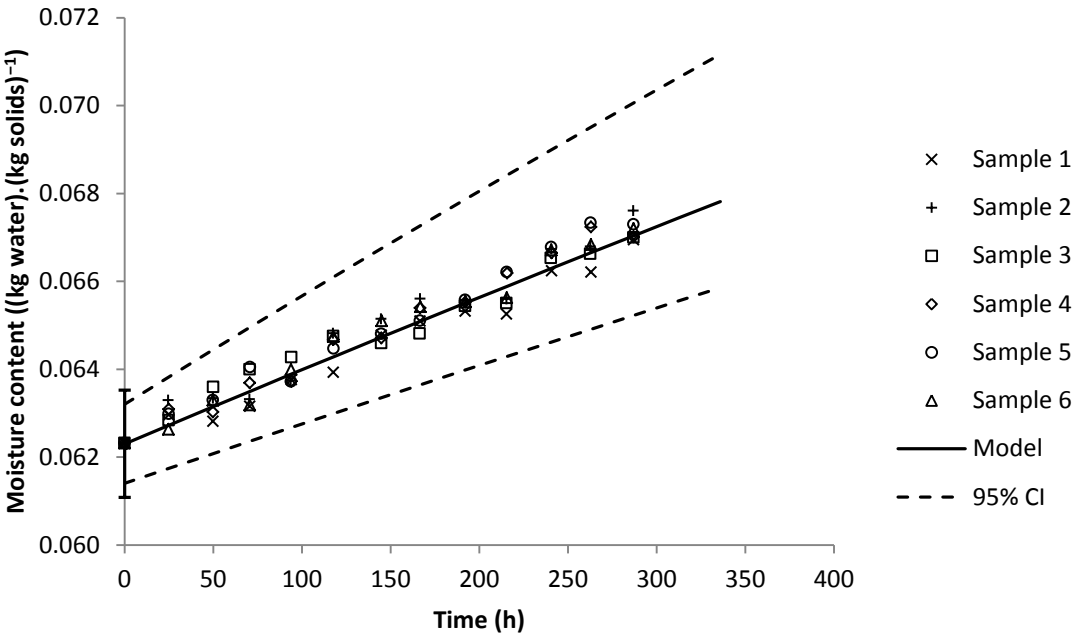

Figure 4-28: Comparison of moisture content of SMP ((kg water).(kg solids)$^{-1}$) versus time (hours) for a polymer liner at 26.6°C and 76.5% ambient RH as predicted by the standard food package model and measured experimentally. Error bar at 0 hours represents 95% CI of initial experimental mass. Model 95% CI limits represent extreme predictions based on 95% CIs of system inputs.

The comparison of model predictions and experimental measurements for the single layer non-perforated system showed excellent agreement, with all experimental measurements well within model 95% CI limits. This suggests that the model is correctly predicting the water vapour pressure in the package headspace, as well as permeation through the packaging material. However since the water vapour transfer rate was essentially linear it is evident that the water vapour pressure in the package headspace remained relatively constant during the trial period (as a result of the relatively high slope of the moisture sorption isotherm at this point). Thus the system was practically at steady-state, and the moisture isotherm component of the model could not be truly validated. Therefore perforated polymer liner systems which have a higher water vapour transfer rate were also considered.

4.5.3.3.2 Single Perforation in a Single Layer Packaging System

A package system consisting of a polymer liner with a single perforation containing SMP was simulated. Values of system inputs for the simulation are summarised in Table 4-10.

Table 4-10: Summary of system inputs used for validation of the moisture isotherm component of the model for a single layer system with a single perforation.

Parameter Description	Symbol	Units	Value *
General system inputs			
Mass of solids in SMP	m_s	kg	0.0094
Initial moisture content of SMP	M_i	(kg water).(kg solids)$^{-1}$	0.0623 ± 0.0009
Ambient temperature	T	K	$(26.8 \pm 1.0) + 273.15$
Ambient relative humidity	RH_a	%	(72.7 ± 0.9)
Surface area of packaging	A_{pkg}	m^2	$\pi\left(\frac{0.07}{2}\right)^2$
Number of layers	N	-	1
Total area of perforation(s)	A_{prf}	m^2	$(5.2 \pm 1.3) \times 10^{-9}$
Diameter of perforation	d_{prf}	m	1×10^{-4}
GAB isotherm parameters			
Moisture content of monolayer for GAB isotherm	$M_{0,GAB}$	(kg water).(kg solids)$^{-1}$	0.051
Guggenheim constant for GAB isotherm	C_{GAB}	-	12.11
Constant for GAB isotherm	k_{GAB}	-	1.08
Properties of layer 1 of packaging film			
Thickness of layer 1 of packaging film	$X_{pkg,1}$	m	$(8.2 \pm 1.2) \times 10^{-5}$
Solubility of water vapour in layer 1 of packaging at reference temperature	$S_{ref,pkg,1}^{H_2O}$	mol.m^{-3}.Pa^{-1}	0.001
Reference temperature of solubility of water vapour in layer 1 of packaging	$T_{ref,S_{pkg}^{H_2O},1}$	K	$(26.6 \pm 0.9) + 273.15$
Partial molar enthalpy of sorption of	$\Delta H_{S,pkg,1}^{H_2O}$	J.mol^{-1}	0

water vapour in layer 1 of packaging material			
Permeability of water vapour in layer 1 of packaging at reference temperature	$P_{ref,pkg,1}^{H_2O}$	mol.m.m^{-2}.s^{-1}.Pa^{-1}	$(3.1 \pm 0.5) \times 10^{-14}$
Activation energy of permeation of water vapour in layer 1 of packaging material	$E_{P,pkg,1}^{H_2O}$	J.mol^{-1}	$(2.4 \pm 0.5) \times 10^{4}$
Reference temperature of diffusivity of water vapour in layer 1 of packaging	$T_{ref,D_{pkg}^{H_2O},1}$	K	$(26.6 \pm 0.9) + 273.15$

* Error values represent a 95% CI relative to the mean.

A comparison of model predictions and experimental results for the single layer non-perforated system is shown in Figure 4-29.

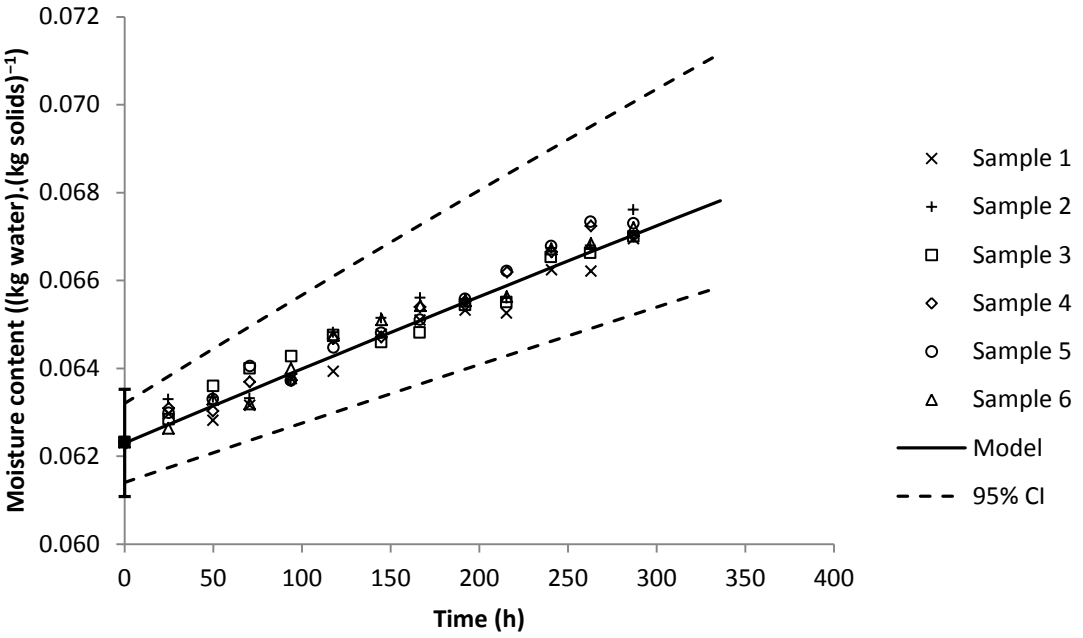

Figure 4-29: Comparison of moisture content of SMP ((kg water).(kg solids)$^{-1}$) versus time (hours) for a polymer liner with 1 perforation at 26.6°C and 76.5% ambient RH as predicted by the standard food package model and measured experimentally. Error bar at 0 hours represents 95% CI of initial experimental mass. Model 95% CI limits represent extreme predictions based on 95% CIs of system inputs.

As can be seen, there was excellent agreement between model predictions and experimental measurements for the single polymer liner containing a single perforation. Like the non-perforated system (Section 4.5.3.3.1), the water vapour transfer rate also remained relatively linear, suggesting a relatively constant water vapour pressure in the package headspace during the trial period. Therefore a polymer liner containing 20 perforations was also considered for validation.

4.5.3.3.3 Multiple Perforations in a Single Layer Packaging System

A polymer liner with 20 perforations containing SMP was simulated. Values of system inputs for the simulation were the same as for the single perforation system (Table 4-10), except the total area of perforations was increased 20-fold ($(1.04 \pm 0.14) \times 10^{-7}$ m^2). A comparison of model predictions and experimental results is shown in Figure 4-30.

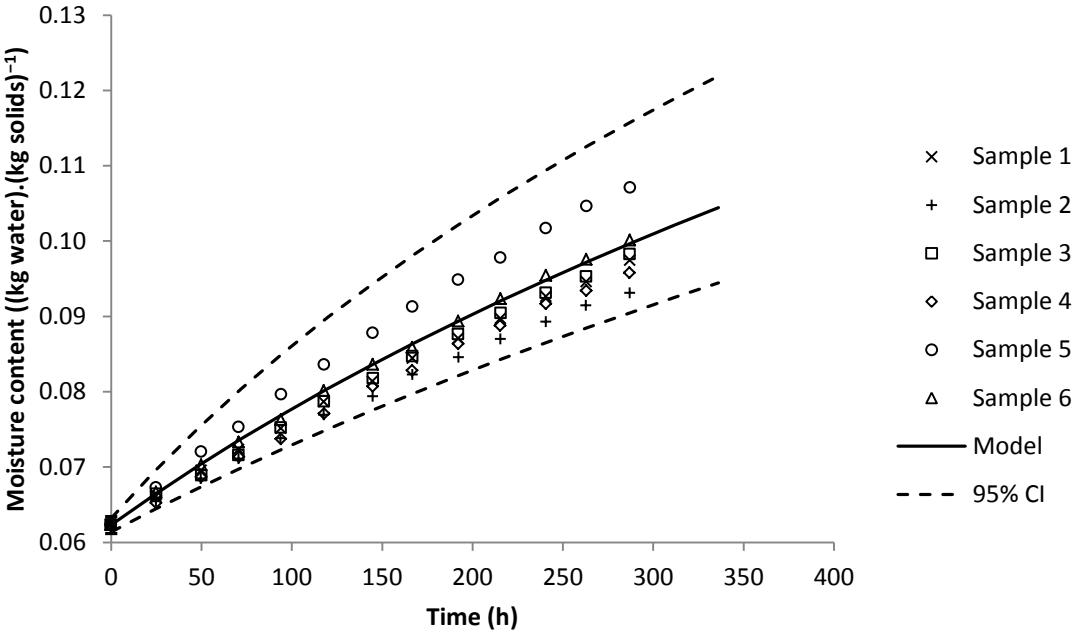

Figure 4-30: Comparison of moisture content of SMP ((kg water).(kg solids)$^{-1}$) versus time (hours) for a polymer liner with 20 perforations at 26.6°C and 76.5% ambient RH as predicted by the standard food package model and measured experimentally. Error bar at 0 hours represents 95% CI of initial experimental mass. Model 95% CI limits represent extreme predictions based on 95% CIs of system inputs.

Again there was excellent agreement of model predictions with experimental results. In this case the water vapour transfer rate was clearly not linear, suggesting a change in the water vapour pressure in the package headspace. The experimentally measured increase in mass of sample 5 appears somewhat high relative to the other samples, however this was well within the 95% confidence interval of model predictions.

Based on the predicted moisture content of the SMP, it was calculated using the moisture sorption isotherm that the water activity of the SMP increased from 0.286 to 0.490 over the simulated period. This water activity range covers a relatively large proportion of the applicable range reported by the source of 0.115 to 0.538 (Joupila & Roos, 1994), suggesting that the model is correctly predicting the water vapour pressure in the package headspace.

4.6 SUMMARY

In this chapter, the development of a standard food package moisture transfer model was presented. The standard food package system contains a single individual packaging layer that may consist of multiple layers with different properties in direct contact. Moisture transfer occurs by permeation through the packaging, as well as diffusion through perforations. Key underlying assumptions for the standard system include instantaneous water vapour transfer in air, in the food product, and at the surface of the food product and packaging, negligible mass of water in the package headspace, and that the system can accurately be represented by one-dimension. A mathematical model was formulated and solved numerically using MATLAB® software. Error checks and validation against experimental observations were carried out, which suggested the model can accurately predict real-world observations for food packaging systems of interest.

Chapter 5

EXTENDING THE STANDARD FOOD PACKAGE MOISTURE TRANSFER MODEL

5.1 INTRODUCTION

This chapter outlines work carried out to extend the standard food package moisture transfer model covered in Chapter 4, allowing representation of a larger range of food packaging systems. Of particular relevance to this study are systems containing multiple individual packaging layers with an air gap in between. These layers can have various configurations of perforations in the separate layers. There is also the scenario in which the food product itself also causes significant resistance to moisture transfer, in which case the moisture gradient in the food needs to be considered with the food packaging system. Such systems are fairly common for exported food products, including food powders and horticultural produce.

The standard food package moisture transfer model (Chapter 4) formed a basis for the models presented in this chapter. As a result work covered in this chapter follows the same format, and work previously covered is referred to the appropriate sections.

5.2 TWO SEPARATE PACKAGING LAYERS WITH PERFORATIONS

For systems containing perforations, the standard food package moisture transfer model applies where there is no air gap between layers and therefore perforations have a length equal to the total thickness of the packaging. However systems consisting of two packaging layers with an air gap are fairly common, such as a polymer liner inside a paperboard bag. Generally moisture transfer through a paperboard bag can be considered instantaneous in a system containing a polymer liner (refer to Section 4.5.3.1.2); however if a barrier coating is to be applied to the paperboard bag it will be necessary to consider both layers.

5.2.1 Conceptual Model Development

5.2.1.1 Outline of Conceptualised System

A schematic diagram of the conceptualised food package system to be modelled is shown in Figure 5-1, and more detailed diagrams of the paperboard bag and polymer liner are shown in Figure 5-2 and Figure 5-3 respectively. The system is similar to the standard food package system defined in Section 4.2.1. However in this case there is a headspace between two separate packaging layers. Each separate packaging layer may each contain different perforations, and may consist of multiple layers in direct contact.

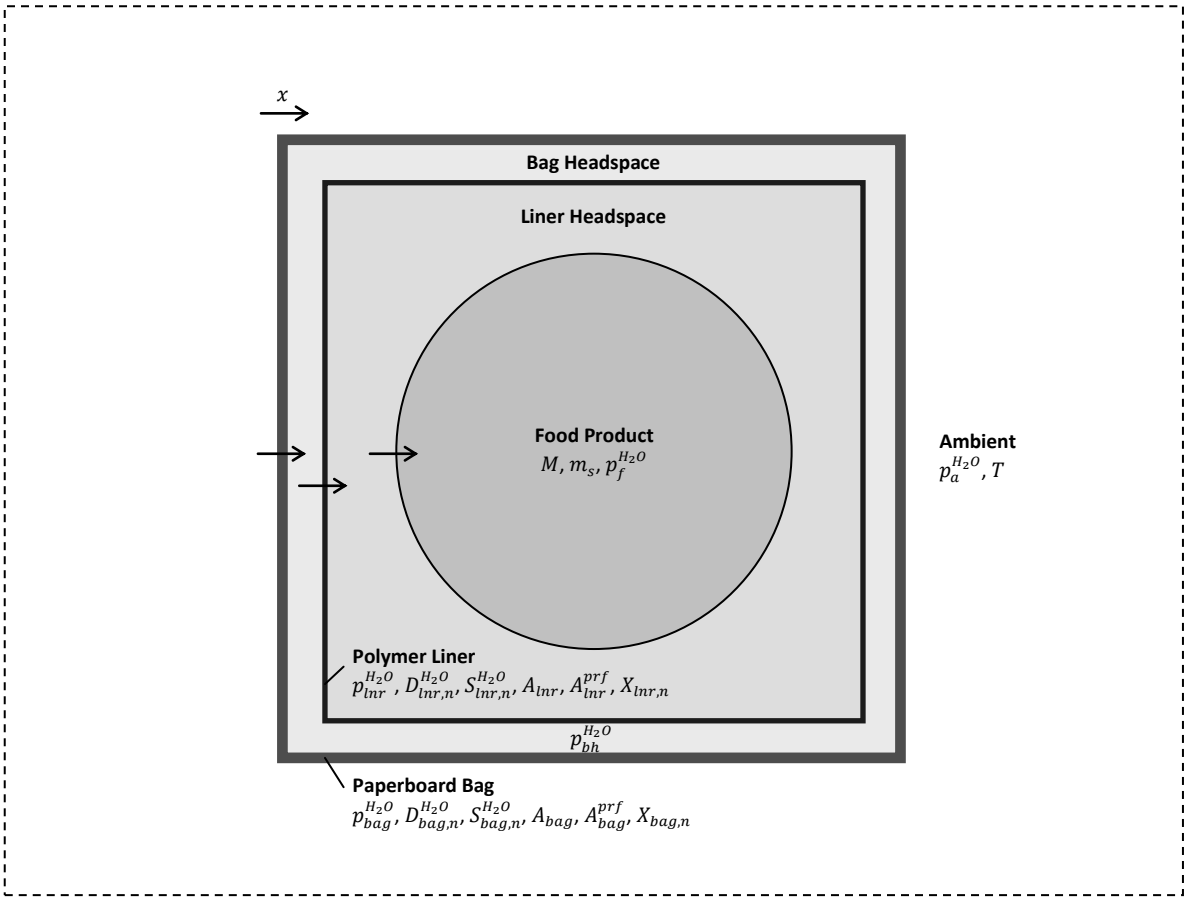

Figure 5-1: Schematic diagram of conceptualised food package system.

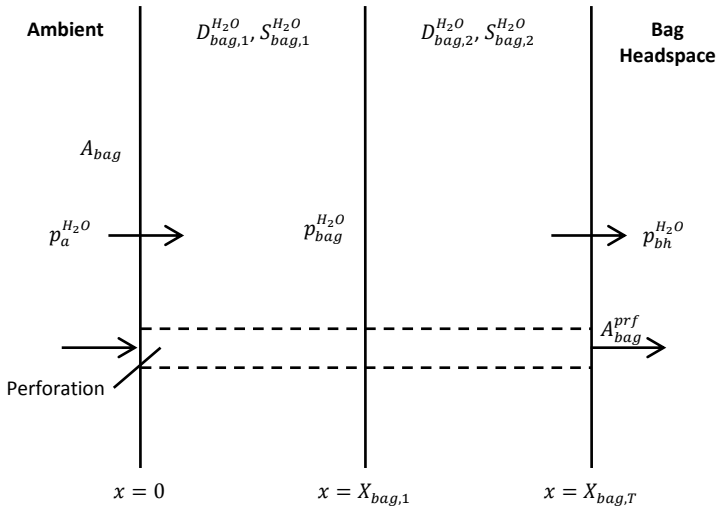

Figure 5-2: Schematic diagram of paperboard bag cross-section.

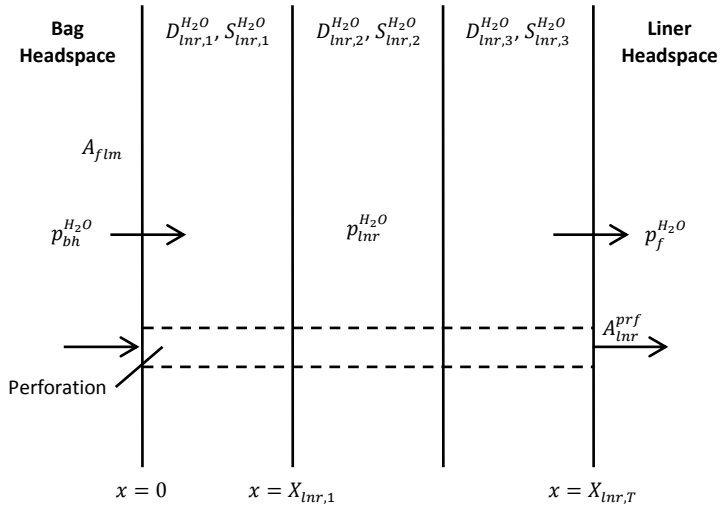

Figure 5-3: Schematic diagram of polymer liner cross-section.

5.2.1.2 Assumptions

The same assumptions outlined in Section 4.2.2 apply to the extended food package moisture transfer model, which include:

- Packaging is the largest resistance to moisture transfer, therefore:
  - moisture transfer in the food product is instantaneous,

  - moisture transfer at surface of the food product and packaging is instantaneous, and
  - moisture diffusion through air is instantaneous.
- Permeation is in one-dimension only, which includes:
  - each packaging material layer has a constant thickness, and
  - the effect of package corners and folds are negligible.
- Temperature changes are instantaneous throughout the system.
- The bag headspace, liner headspace and ambient air are at atmospheric pressure.
- Water vapour exhibits ideal gas behaviour.
- The surface area of the packaging is much greater than the total surface area of perforations.
- The food does not respire.
- Perforations consist of a perfect cylindrical geometry.

5.2.2 Mathematical Model Formulation

5.2.2.1 Variables

Variables defined in the model formulation are summarised in Table 5-1.

Table 5-1: List of model variables.

Symbol	Description	Unit	Class*
$\Delta H_{S,bag,n}^{H_2O}$	Partial molar enthalpy of sorption of water vapour in nth layer of paperboard bag	J.mol^{-1}	SI
$\Delta H_{S,lnr,n}^{H_2O}$	Partial molar enthalpy of sorption of water vapour in nth layer of polymer liner	J.mol^{-1}	SI
$\Delta x_{bag,n}$	Width of node in nth layer of paperboard bag	m	SI
$\Delta x_{lnr,n}$	Width of node in nth layer of polymer liner	m	SI
A_{bag}	Surface area of paperboard bag	m^2	SI
A_{lnr}	Surface area of polymer liner	m^2	SI

$A_{prf,bag}$	Total area of perforation(s) in paperboard bag	m^2	SI
$A_{prf,lnr}$	Total area of perforation(s) in polymer liner	m^2	SI
C_{BET}	Guggenheim constant for BET isotherm of food	-	SI
C_{GAB}	Guggenheim constant for GAB isotherm of food	-	SI
$D_{0,bag,n}^{H_2O}$	Pre-exponential factor of diffusivity of water vapour in nth layer of paperboard bag	$m^2.s^{-1}$	SI
$D_{0,lnr,n}^{H_2O}$	Pre-exponential factor of diffusivity of water vapour in nth layer of polymer liner	$m^2.s^{-1}$	SI
$D_{air}^{H_2O}$	Diffusivity of water vapour in air	$m^2.s^{-1}$	CV
$D_{bag,n}^{H_2O}$	Diffusivity of water vapour in n^{th} layer of paperboard bag	$m^2.s^{-1}$	CV
$D_{lnr,n}^{H_2O}$	Diffusivity of water vapour in n^{th} layer of polymer liner	$m^2.s^{-1}$	CV
$D_{ref,bag,n}^{H_2O}$	Reference diffusivity of water vapour in n^{th} layer of paperboard bag	$m^2.s^{-1}$	SI
$D_{ref,lnr,n}^{H_2O}$	Reference diffusivity of water vapour in n^{th} layer of polymer liner	$m^2.s^{-1}$	SI
$E_{D,bag,n}^{H_2O}$	Activation energy of diffusion of water vapour in n^{th} layer of paperboard bag	$J.mol^{-1}$	SI
$E_{D,lnr,n}^{H_2O}$	Activation energy of diffusion of water vapour in n^{th} layer of polymer liner	$J.mol^{-1}$	SI
$E_{P,bag,n}^{H_2O}$	Activation energy of permeation of water vapour in n^{th} layer of paperboard bag	$J.mol^{-1}$	SI
$E_{P,lnr,n}^{H_2O}$	Activation energy of permeation of water vapour in n^{th} layer of polymer liner	$J.mol^{-1}$	SI
$J_{prf,bag}^{H_2O}$	Diffusive flux of water vapour through perforation(s) in paperboard bag	$mol.m^{-2}.s^{-1}$	CV
$J_{prf,lnr}^{H_2O}$	Diffusive flux of water vapour through perforation(s) in polymer liner	$mol.m^{-2}.s^{-1}$	CV
$M_{0,GAB}$	Moisture content of monolayer for GAB isotherm of food	$(kg\ water).(kg\ solids)^{-1}$	SI
$M_{1,BET}$	Moisture content of monolayer for BET isotherm of food	$(kg\ water).(kg\ solids)^{-1}$	SI
M_i	Initial moisture content of food	$(kg\ water).(kg\ solids)^{-1}$	SI

M_{r,H_2O}	Molecular mass of water	kg.mol^{-1}	SI
N_{bag}	Total number of layers in paperboard bag	-	SI
N_{lnr}	Total number of layers in polymer liner	-	SI
$P_{0,bag,n}^{H_2O}$	Pre-exponential factor of permeability of water vapour in nth layer of paperboard bag	mol.m.m^{-2}.s^{-1}.Pa^{-1}	SI
$P_{0,lnr,n}^{H_2O}$	Pre-exponential factor of permeability of water vapour in nth layer of polymer liner	mol.m.m^{-2}.s^{-1}.Pa^{-1}	SI
$P_{bag,n}^{H_2O}$	Permeability of water vapour in nth layer of paperboard bag	mol.m.m^{-2}.s^{-1}.Pa^{-1}	CV
$P_{lnr,n}^{H_2O}$	Permeability of water vapour in nth layer of polymer liner	mol.m.m^{-2}.s^{-1}.Pa^{-1}	CV
RH_a	Ambient relative humidity	%	CV
$S_{0,bag,n}^{H_2O}$	Pre-exponential factor of solubility of water vapour in nth layer of paperboard bag	mol.m^{-3}.Pa^{-1}	SI
$S_{0,lnr,n}^{H_2O}$	Pre-exponential factor of solubility of water vapour in nth layer of polymer liner	mol.m^{-3}.Pa^{-1}	SI
$S_{bag,n}^{H_2O}$	Solubility of water vapour in nth layer of paperboard bag	mol.m^{-3}.Pa^{-1}	CV
$S_{lnr,n}^{H_2O}$	Solubility of water vapour in nth layer of polymer liner	mol.m^{-3}.Pa^{-1}	CV
$S_{ref,bag,n}^{H_2O}$	Reference solubility of water vapour in nth layer of paperboard bag	mol.m^{-3}.Pa^{-1}	SI
$S_{ref,lnr,n}^{H_2O}$	Reference solubility of water vapour in nth layer of polymer liner	mol.m^{-3}.Pa^{-1}	SI
$T_{ref,D_{bag}^{H_2O},n}$	Temperature of reference diffusivity of water vapour in nth layer of paperboard bag	K	SI
$T_{ref,D_{lnr}^{H_2O},n}$	Temperature of reference diffusivity of water vapour in nth layer of polymer liner	K	SI
$T_{ref,S_{bag}^{H_2O},n}$	Temperature of reference solubility of water vapour in nth layer of paperboard bag	K	SI
$T_{ref,S_{lnr}^{H_2O},n}$	Temperature of reference solubility of water vapour in nth layer of polymer liner	K	SI
$X_{T,bag}$	Total thickness of paperboard bag	m	SI
$X_{T,lnr}$	Total thickness of polymer liner	m	SI

$X_{bag,n}$	Thickness of nth layer of paperboard bag	m	SI
$X_{lnr,n}$	Thickness of nth layer of polymer liner	m	SI
b_{lin}	Slope of linear isotherm of food	-	SI
c_{lin}	Constant for linear isotherm of food	(kg water).(kg solids)$^{-1}$	SI
$d_{prf,bag}$	Average diameter of perforation(s) in paperboard bag	m	SI
$d_{prf,lnr}$	Average diameter of perforation(s) in polymer liner	m	SI
k_{GAB}	Constant for GAB isotherm of food	-	SI
m_s	Mass of solids in food product	kg	SI
$p_0^{H_2O}$	Saturated water vapour pressure	Pa	CV
$p_a^{H_2O}$	Water vapour pressure in ambient air	Pa	CV
$p_{bh}^{H_2O}$	Water vapour pressure in bag headspace	Pa	D
$p_{bag,i}^{H_2O}$	Initial water vapour pressure in paperboard bag	Pa	SI
$p_{bag}^{H_2O}$	Water vapour pressure in paperboard bag	Pa	D
$p_f^{H_2O}$	Water vapour pressure in food	Pa	CV
$p_{lnr,i}^{H_2O}$	Initial water vapour pressure in polymer liner	Pa	SI
$p_{lnr,j}^{H_2O}$	Water vapour pressure in jth node of polymer liner	Pa	D
J	Total number of nodes per layer of polymer liner and paperboard bag	-	SI
M	Moisture content of food	(kg water).(kg solids)$^{-1}$	D
R	Ideal gas constant (8.314)	m^3.Pa.K^{-1}.mol^{-1}	SI
T	Temperature	K	CV
j	Node number	-	SI
t	Time	s	I
x	Spatial position in packaging	m	I

*I = independent variable, D = dependent variable, CV = consequential variable, SI = system input

For this extended system an additional ordinary differential equation (ODE) was required for the water vapour pressure in the bag headspace. Furthermore the water vapour pressure in the two separate packaging layers must be solved as separate partial differential equations (PDEs). Therefore four boundary conditions were defined and four initial conditions were required.

5.2.2.2 Word Balances and Equations

5.2.2.2.1 ODE for Moisture Content of Food Product

Similar to the standard food package model, changes in the amount of moisture contained in the food product are dependent on moisture transfer by permeation through the packaging or diffusion through perforations. However since the water vapour pressure in the bag headspace requires a separate ODE, only the polymer liner needs to be included. Therefore an unsteady-state mass balance of moisture in the food product for the extended system yields a similar result to the standard food package model:

$$\begin{pmatrix} \textit{rate of accumulation of moisture in food product} \end{pmatrix} = \begin{pmatrix} \textit{rate of moisture permeating through inside surface of liner} \end{pmatrix} + \begin{pmatrix} \textit{rate of moisture diffusing through perforation(s) in liner} \end{pmatrix} \quad \textbf{(5-1)}$$

This word balance can be expressed as an ODE for use in the mathematical model as follows (derivation shown in Appendix D.1.1.1.1):

$$\frac{dM}{dt} = \frac{M_{r,H_2O}}{m_s}\left[P^{H_2O}_{lnr,n=N_{lnr}} A_{lnr} \left(\frac{dp^{H_2O}_{lnr}}{dx}\right)_{x=X_{T,lnr}} + J^{H_2O}_{prf,lnr} A_{prf,lnr}\right] \quad \textbf{(5-2)}$$

for $t \geq 0$

where:

M = Moisture content of food ((kg water).(kg solids)$^{-1}$)

t = Time (s)

M_{r,H_2O} = Molecular mass of water (kg.mol^{-1})

m_s = Mass of solids in food (kg)

$P^{H_2O}_{lnr,n}$ = Permeability of water vapour in nth layer of polymer liner (mol.m.m^{-2}.s^{-1}.Pa^{-1})

A_{lnr} = Surface area of polymer liner (m^2)

$p^{H_2O}_{lnr}$ = Water vapour pressure in polymer liner (Pa)

x = Spatial position in packaging (m)

$J^{H_2O}_{prf,lnr}$ = Diffusive flux of water vapour through perforation(s) in polymer liner (mol.m^{-2}.s^{-1})

$A_{prf,lnr}$ = Total area of perforation(s) in polymer liner (m^2)

5.2.2.2.2 ODE for Water Vapour Pressure in Bag Headspace

The water vapour pressure in the bag headspace will be dependent on moisture transfer by permeation or diffusion through perforations in both the paperboard bag and polymer liner. Since it was assumed that the mass of water in the bag headspace is negligible, a steady-state mass balance of water vapour in the bag headspace yields the following:

$$\begin{pmatrix} \textit{rate of} \\ \textit{accumulation} \\ \textit{of moisture in} \\ \textit{bag headspace} \end{pmatrix} = 0$$

$$= \begin{pmatrix} \textit{rate of moisture} \\ \textit{permeating through} \\ \textit{inside surface of} \\ \textit{bag} \end{pmatrix} + \begin{pmatrix} \textit{rate of moisture} \\ \textit{diffusing through} \\ \textit{perforation(s)} \\ \textit{in bag} \end{pmatrix} \quad \textbf{(5-3)}$$

$$- \begin{pmatrix} \textit{rate of moisture} \\ \textit{permeating through} \\ \textit{outside surface of} \\ \textit{liner} \end{pmatrix} - \begin{pmatrix} \textit{rate of moisture} \\ \textit{diffusing through} \\ \textit{perforation(s)} \\ \textit{in liner} \end{pmatrix}$$

This word balance can be used to derive an ODE expression for use in the mathematical model as follows (derivation shown in Appendix D.1.1.1.2):

$$\frac{dp_{bh}^{H_2O}}{dt} = 0 = P_{bag,n=N_{bag}}^{H_2O} A_{bag} \left(\frac{dp_{bag}^{H_2O}}{dx} \right)_{x=X_{T,bag}} + J_{prf,bag}^{H_2O} A_{prf,bag}$$

$$- P_{lnr,n=1}^{H_2O} A_{lnr} \left(\frac{dp_{lnr}^{H_2O}}{dx} \right)_{x=1} - J_{prf,lnr}^{H_2O} A_{prf,lnr} \quad \textbf{(5-4)}$$

for $t \geq 0$

where:

$p_{bh}^{H_2O}$ = Water vapour pressure in bag headspace (Pa)

A_{bag} = Surface area of paperboard bag (m^2)

$P_{bag,n}^{H_2O}$ = Permeability of water vapour in n^{th} layer of paperboard bag ($m^2.s^{-1}$)

$J_{prf,bag}^{H_2O}$ = Diffusive flux of water vapour through perforation(s) in paperboard bag ($mol.m^{-2}.s^{-1}$)

$A_{prf,bag}$ = Total area of perforation(s) in paperboard bag (m^2)

This equation can then be solved after substituting the appropriate expressions for the diffusive flux of water vapour through perforation(s) in the paperboard bag and polymer liner (Sections 5.2.2.2.9 and 5.2.2.2.10).

5.2.2.2.3 PDE for Water Vapour Pressure in Paperboard Bag

The PDE for one-dimensional unsteady-state moisture permeation through the paperboard bag is identical to the PDE previously derived for packaging (Equation 4-5). However new variables were defined to distinguish between the paperboard bag and polymer liner.

$$S_{bag}^{H_2O}\frac{\partial p_{bag}^{H_2O}}{\partial t}=\frac{\partial}{\partial x}\left(P_{bag}^{H_2O}\frac{\partial p_{bag}^{H_2O}}{\partial x}\right) \qquad \textbf{(5-5)}$$

$$for\ t \geq 0,\ 0 < x < X_{T,bag}$$

where:

$S_{bag}^{H_2O}$ = Solubility of water vapour in paperboard bag (mol.m^{-3}.Pa^{-1})

$X_{T,bag}$ = Total thickness of paperboard bag (m)

5.2.2.2.4 PDE for Water Vapour Pressure in Polymer Liner

The PDE for one-dimensional unsteady-state moisture permeation through packaging (Equation 4-5) expressed specifically for the polymer liner is as follows:

$$S_{lnr}^{H_2O}\frac{\partial p_{lnr}^{H_2O}}{\partial t}=\frac{\partial}{\partial x}\left(P_{lnr}^{H_2O}\frac{\partial p_{lnr}^{H_2O}}{\partial x}\right) \qquad \textbf{(5-6)}$$

$$for\ t \geq 0,\ 0 < x < X_{T,lnr}$$

where:

$S_{lnr}^{H_2O}$ = Solubility of water vapour in polymer liner (mol.m^{-3}.Pa^{-1})

5.2.2.2.5 Equation for Diffusivity of Water Vapour in Paperboard Bag

The temperature dependence of the diffusivity of water vapour in packaging (Equation 4-13) expressed specifically for the paperboard bag is as follows:

$$D_{bag,n}^{H_2O} = D_{ref,bag,n}^{H_2O} exp\left[\frac{E_{D,bag,n}^{H_2O}}{R}\left(\frac{1}{T_{ref,D_{bag}^{H_2O},n}} - \frac{1}{T}\right)\right] \quad \textbf{(5-7)}$$

where:

$D_{bag,n}^{H_2O}$ = Diffusivity of water vapour in nth layer of paperboard bag (m^2.s^{-1})

$D_{ref,bag,n}^{H_2O}$ = Reference diffusivity of water vapour in nth layer of paperboard bag (m^2.s^{-1})

$E_{D,bag,n}^{H_2O}$ = Activation energy of diffusion of water vapour in nth layer of paperboard bag (J.mol^{-1})

$T_{ref,D_{bag}^{H_2O},n}$ = Temperature of reference diffusivity of water vapour in nth layer of paperboard bag (K)

T = Absolute temperature (K)

5.2.2.2.6 Equation for Diffusivity of Water Vapour in Polymer Liner

The temperature dependence of the diffusivity of water vapour in packaging (Equation 4-13) expressed specifically for the polymer liner is as follows:

$$D_{lnr,n}^{H_2O} = D_{ref,lnr,n}^{H_2O} exp\left[\frac{E_{D,lnr,n}^{H_2O}}{R}\left(\frac{1}{T_{ref,D_{lnr}^{H_2O},n}} - \frac{1}{T}\right)\right] \quad \textbf{(5-8)}$$

where:

$D_{lnr,n}^{H_2O}$ = Diffusivity of water vapour in nth layer of polymer liner (m^2.s^{-1})

$D_{ref,lnr,n}^{H_2O}$ = Reference diffusivity of water vapour in nth layer of polymer liner (m^2.s^{-1})

$E_{D,lnr,n}^{H_2O}$ = Activation energy of diffusion of water vapour in nth layer of polymer liner (J.mol^{-1})

$T_{ref,D_{lnr}^{H_2O},n}$ = Temperature of reference diffusivity of water vapour in nth layer of polymer liner (K)

5.2.2.2.7 Equation for Solubility of Water Vapour in Paperboard Bag

The temperature dependence of the solubility of water vapour in packaging (Equation 4-14) expressed specifically for the paperboard bag is as follows:

$$S_{bag,n}^{H_2O} = S_{ref,bag,n}^{H_2O} exp\left[\frac{\Delta H_{S,bag,n}^{H_2O}}{R}\left(\frac{1}{T_{ref,S_{bag}^{H_2O},n}} - \frac{1}{T}\right)\right] \quad \textbf{(5-9)}$$

where:

$S_{bag,n}^{H_2O}$ = Solubility of water vapour in nth layer of paperboard bag (mol.m^{-3}.Pa^{-1})

$S_{ref,bag,n}^{H_2O}$ = Reference solubility of water vapour in nth layer of paperboard bag (mol.m^{-3}.Pa^{-1})

$\Delta H_{S,bag,n}^{H_2O}$ = Partial molar enthalpy of sorption of water vapour in nth layer of paperboard bag (J.mol^{-1})

$T_{ref,S_{bag}^{H_2O},n}$ = Temperature of reference solubility of water vapour in nth layer of paperboard bag (K)

The concentration dependence of the solubility of water vapour in packaging based on the GAB isotherm (Equation 4-15) expressed specifically for the paperboard bag is as follows:

$$S_{bag,n}^{H_2O} = \frac{\rho_{s,bag,n}}{M_{r,H_2O}}\left[\frac{M_{0,bag,n}{k_{bag,n}}^2 C_{bag,n} p_{bag}^{H_2O}}{{p_0^{H_2O}}^2\left(1 - k_{bag,n}\frac{p_{bag}^{H_2O}}{p_0^{H_2O}}\right)^2\left(1 + k_{bag,n}\frac{p_{bag}^{H_2O}}{p_0^{H_2O}}(C_{bag,n} - 1)\right)}\right.$$
$$+ \frac{M_{0,bag,n}k_{bag,n}C_{bag,n}}{p_0^{H_2O}\left(1 - k_{bag,n}\frac{p_{bag}^{H_2O}}{p_0^{H_2O}}\right)\left(1 + k_{bag,n}\frac{p_{bag}^{H_2O}}{p_0^{H_2O}}(C_{bag,n} - 1)\right)} \quad \textbf{(5-10)}$$
$$\left. - \frac{M_{0,bag,n}{k_{bag,n}}^2 C_{bag,n}(C_{bag,n} - 1) p_{bag}^{H_2O}}{{p_0^{H_2O}}^2\left(1 - k_{bag,n}\frac{p_{bag}^{H_2O}}{p_0^{H_2O}}\right)\left(1 + k_{bag,n}\frac{p_{bag}^{H_2O}}{p_0^{H_2O}}(C_{bag,n} - 1)\right)^2}\right]$$

where:

$\rho_{s,bag,n}$ = Density of solids in food (kg.m^{-3})

$M_{0,bag,n}$ = Moisture content of monolayer for GAB isotherm of paperboard bag ((kg water).(kg solids)$^{-1}$)

$C_{bag,n}$ = Guggenheim constant for GAB isotherm of paperboard bag (-)

$k_{bag,n}$ = Constant for GAB isotherm of paperboard bag (-)

5.2.2.2.8 Equation for Solubility of Water Vapour in Polymer Liner

The temperature dependence of the solubility of water vapour in packaging (Equation 4-14) expressed specifically for the polymer liner is as follows:

$$S_{lnr,n}^{H_2O} = S_{ref,lnr,n}^{H_2O} exp\left[\frac{\Delta H_{S,lnr,n}^{H_2O}}{R}\left(\frac{1}{T_{ref,S_{lnr}^{H_2O},n}} - \frac{1}{T}\right)\right] \quad \textbf{(5-11)}$$

where:

$S_{lnr,n}^{H_2O}$ = Solubility of water vapour in nth layer of polymer liner (mol.m^{-3}.Pa^{-1}), which is dependent on water vapour pressure

$S_{ref,lnr,n}^{H_2O}$ = Reference solubility of water vapour in nth layer of polymer liner (mol.m^{-3}.Pa^{-1})

$\Delta H_{S,lnr,n}^{H_2O}$ = Partial molar enthalpy of sorption of water vapour in nth layer of polymer liner (J.mol^{-1})

$T_{ref,S_{lnr}^{H_2O},n}$ = Temperature of reference solubility of water vapour in nth layer of polymer liner (K)

Concentration dependence of solubility of water vapour in the polymer liner is not expected to be encountered in this investigation, and was therefore not included in the mathematical model. However should it be required, Equation 4-15 can be used for a GAB sorption isotherm, or a similar equation derived for other sorption isotherm equations (Appendix C.1.1.3).

5.2.2.2.9 Equation for Diffusive Flux of Water Vapour through Perforation(s) in Paperboard Bag

Equations for diffusive flux of water vapour through perforation(s) in the packaging (Equations 4-19 to 4-21) expressed specifically for the paperboard bag are as follows:

$$J_{prf,bag}^{H_2O} = \frac{D_{air}^{H_2O} S_{air}^{H_2O}}{X_{T,bag}} \left(p_a^{H_2O} - p_{bh}^{H_2O}\right) \quad \textbf{(5-12)}$$

for $d_{prf,bag} \geq 1 \times 10^{-5}$ m

$$J_{prf,bag}^{H_2O} = \frac{D_{air}^{H_2O} S_{air}^{H_2O}}{\left(X_{T,bag} + \frac{d_{prf,bag}}{2}\right)} \left(p_a^{H_2O} - p_{bh}^{H_2O}\right) \quad \textbf{(5-13)}$$

for $1 \times 10^{-7} \leq d_{prf,bag} < 1 \times 10^{-5}$ m

$$J_{prf,bag}^{H_2O} = \frac{48.5 d_{prf,bag}}{RTX_{T,bag}} \left(\frac{T}{1000 M_{r,H_2O}}\right)^{0.5} \left(p_a^{H_2O} - p_{bh}^{H_2O}\right) \quad \textbf{(5-14)}$$

for $d_{prf,bag} < 1 \times 10^{-7}$ m

where:

$X_{T,bag}$ = Total thickness of paperboard bag (m)

$D_{air}^{H_2O}$ = Diffusivity of water vapour in air ($m^2.s^{-1}$)

$S_{air}^{H_2O}$ = Solubility of water vapour in air ($mol.m^{-3}.Pa^{-1}$)

$p_a^{H_2O}$ = Water vapour pressure in ambient air (Pa)

$d_{prf,bag}$ = Average diameter of perforations in paperboard bag (m)

5.2.2.2.10 Equation for Diffusive Flux of Water Vapour through Perforation(s) in Polymer Liner

Equations for diffusive flux of water vapour through perforation(s) in the packaging (Equations 4-19 to 4-21) expressed specifically for the polymer liner are as follows:

$$J_{prf,lnr}^{H_2O} = \frac{D_{air}^{H_2O} S_{air}^{H_2O}}{X_{T,lnr}} \left(p_{bh}^{H_2O} - p_f^{H_2O}\right) \quad \textbf{(5-15)}$$

for $d_{prf,lnr} \geq 1 \times 10^{-5}$ m

$$J_{prf,lnr}^{H_2O} = \frac{D_{air}^{H_2O} S_{air}^{H_2O}}{\left(X_{T,lnr} + \frac{d_{prf,lnr}}{2}\right)} \left(p_{bh}^{H_2O} - p_f^{H_2O}\right) \quad \textbf{(5-16)}$$

for $1 \times 10^{-7} \leq d_{prf,lnr} < 1 \times 10^{-5}$ m

$$J_{prf,lnr}^{H_2O} = \frac{48.5 d_{prf,lnr}}{RTX_{T,lnr}} \left(\frac{T}{1000 M_{r,H_2O}}\right)^{0.5} \left(p_{bh}^{H_2O} - p_f^{H_2O}\right) \quad \textbf{(5-17)}$$

for $d_{prf,lnr} < 1 \times 10^{-7}$ m

where:

$X_{T,lnr}$ = Total thickness of polymer liner (m)

$d_{prf,lnr}$ = Average diameter of perforations in polymer liner (m)

$p_f^{H_2O}$ = Water vapour pressure in food (Pa)

5.2.2.3 Boundary Conditions

Boundary conditions for the extended model will be similar to the standard food package model, except that two addition boundary conditions are required at the bag headspace. At these surfaces the water vapour pressure will be equal to the water vapour pressure in the bag headspace. This can be expressed mathematically as follows:

$$p_{bag}^{H_2O} = p_a^{H_2O} \quad \textbf{(5-18)}$$

for $t \geq 0, x = 0$

$$p_{lnr}^{H_2O} = p_{bh}^{H_2O} \quad \textbf{(5-19)}$$

for $t \geq 0, x = 0$

$$p_{bag}^{H_2O} = p_{bh}^{H_2O} \quad \textbf{(5-20)}$$

for $t \geq 0, x = X_{T,bag}$

$$p_{lnr}^{H_2O} = p_f^{H_2O} \quad \textbf{(5-21)}$$

for $t \geq 0, x = X_{T,lnr}$

5.2.2.4 Initial Conditions

For simplicity, the initial water vapour pressure in all packaging layers was assumed to be equal and uniform. Consequently this will also be equal to the initial water vapour pressure in the bag headspace. The initial moisture content of the food product will remain unchanged.

$$p_{bag}^{H_2O} = p_{lnr}^{H_2O} = p_{bh}^{H_2O} = p_{pkg,i}^{H_2O} \quad at\ t = 0 \tag{5-22}$$

where:

$p_{pkg,i}^{H_2O}$ = Initial water vapour pressure in packaging (Pa)

5.2.3 Solution

5.2.3.1 Finite Difference Grid

The finite difference grids used for the paperboard bag and polymer liner are illustrated in Figure 5-4 and Figure 5-5 respectively. Each layer was divided into J space steps, thus space steps of the nth layer of the paperboard bag had a thickness of $\Delta x_{bag,n}$, for a total of N_{bag} layers, and space steps of the nth layer of the polymer film had a thickness of $\Delta x_{lnr,n}$, for a total of N_{lnr} layers. Thus:

$$\Delta x_{bag,n} = \frac{X_{bag,n}}{J} \tag{5-23}$$

$$\Delta x_{lnr,n} = \frac{X_{lnr,n}}{J} \tag{5-24}$$

where:

$\Delta x_{bag,n}$ = Width of node in nth layer of paperboard bag (m)

$X_{pkg,n}$ = Thickness of nth layer of paperboard bag (m)

J = Number of nodes (-)

$\Delta x_{lnr,n}$ = Width of node in nth layer of polymer liner (m)

$X_{lnr,n}$ = Thickness of nth layer of polymer liner (m)

The section of the paperboard bag contained within each space step was designated a node number from $j = 1$ at the exterior packaging surface (the surface exposed to the ambient environment) to $j = N_{bag}J + 1$ at the interior surface (the surface closest to the polymer liner); similarly, the section of the polymer liner contained within each space step was designated a node number from $j = 1$ at the exterior packaging surface (the surface closest to the polymer liner) to $j = N_{bag}J + 1$ at the interior surface (the surface closest to the food product). The water vapour pressure within each node was considered to be uniform.

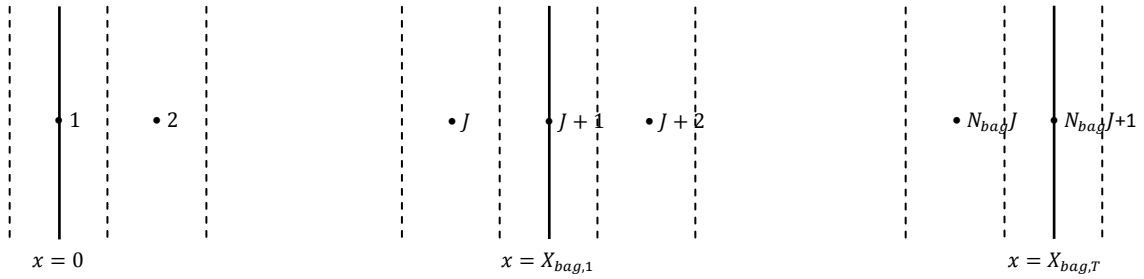

Figure 5-4: Finite difference grid for paperboard bag.

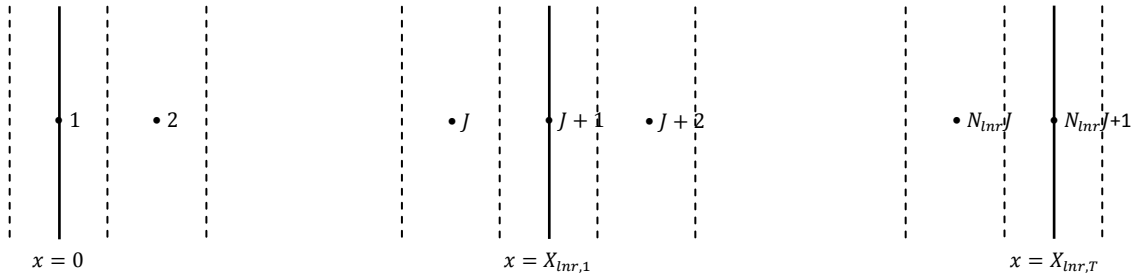

Figure 5-5: Finite difference grid for polymer liner.

5.2.3.2 Finite Difference Approximations

Finite difference approximations were similar to those previously derived for the standard food package model (Section 4.4.2). These are summarised here for completeness.

5.2.3.2.1 Case 1

Nodes:

$$n = 1, j = 1$$

$$n = N_{bag}, j = nJ + 1$$

(A) (B)

Figure 5-6: Diagram of finite difference approximations for case 1, including the external (A) and internal (B) paperboard bag surfaces.

$$p_{bag,j}^{H_2O} = p_a^{H_2O}$$
$$for\ t \geq 0,\ x = 0$$
$$p_{bag,j}^{H_2O} = p_{bh}^{H_2O} \quad \textbf{(5-25)}$$
$$for\ t \geq 0,\ x = X_{T,bag}$$

5.2.3.2.2 Case 2

Node:

$$n = 1, j = 2$$

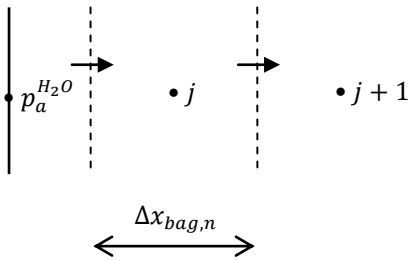

Figure 5-7: Diagram of finite difference approximation for case 2.

$$\frac{dp_{bag,j}^{H_2O}}{dt} = \frac{P_{bag,n}^{H_2O}}{S_{bag,n}^{H_2O}\Delta x_{bag,n}{}^2}\left(p_a^{H_2O} - 2p_{bag,j}^{H_2O} + p_{bag,j+1}^{H_2O}\right) \quad \textbf{(5-26)}$$

$for\ t \geq 0$

5.2.3.2.3 Case 3

Nodes:

$n = 1, j = (n-1)J + 3 : nJ$

$n = 2 : N_{bag} - 1, j = (n-1)J + 2 : nJ$

$n = N_{bag}, j = (n-1)J + 2 : nJ - 1$

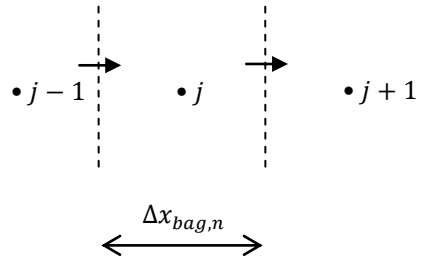

Figure 5-8: Diagram of finite difference approximation for case 3.

$$\frac{dp_{bag,j}^{H_2O}}{dt} = \frac{P_{bag,n}^{H_2O}}{S_{bag,n}^{H_2O}\Delta x_{bag,n}{}^2}\left(p_{bag,j-1}^{H_2O} - 2p_{bag,j}^{H_2O} + p_{bag,j+1}^{H_2O}\right) \quad \textbf{(5-27)}$$

$for\ t \geq 0$

5.2.3.2.4 Case 4

Nodes:

$n = 1 : N_{bag} - 1, j = nJ + 1$

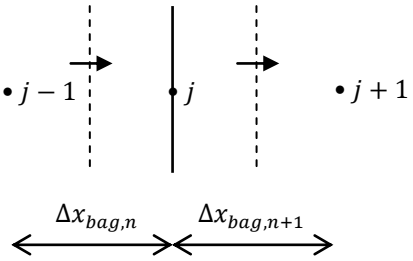

Figure 5-9: Diagram of finite difference approximation for case 4.

$$\frac{dp_{bag,j}^{H_2O}}{dt} = \frac{2}{\Delta x_{bag,n} S_{bag,n}^{H_2O} + \Delta x_{bag,n+1} S_{bag,n+1}^{H_2O}} \left[\frac{P_{bag,n}^{H_2O}}{\Delta x_{bag,n}} \left(p_{bag,j-1}^{H_2O} - p_{bag,j}^{H_2O} \right) - \frac{P_{bag,n+1}^{H_2O}}{\Delta x_{bag,n+1}} \left(p_{bag,j}^{H_2O} - p_{bag,j+1}^{H_2O} \right) \right] \quad \textbf{(5-28)}$$

for $t \geq 0$

5.2.3.2.5 Case 5

Node:

$n = N_{bag}, j = nJ$

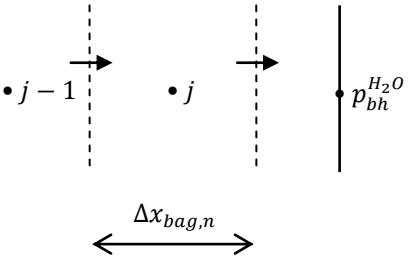

Figure 5-10: Diagram of finite difference approximation for case 5.

$$\frac{dp_{bag,j}^{H_2O}}{dt} = \frac{P_{bag,n}^{H_2O}}{S_{bag,n}^{H_2O} \Delta x_{bag,n}{}^2} \left(p_{bag,j-1}^{H_2O} - 2p_{bag,j}^{H_2O} + p_{bh}^{H_2O} \right) \quad \textbf{(5-29)}$$

for $t \geq 0$

5.2.3.2.6 Case 6

Nodes:

$$n = 1, j = 1$$

$$n = N_{lnr}, j = nJ + 1$$

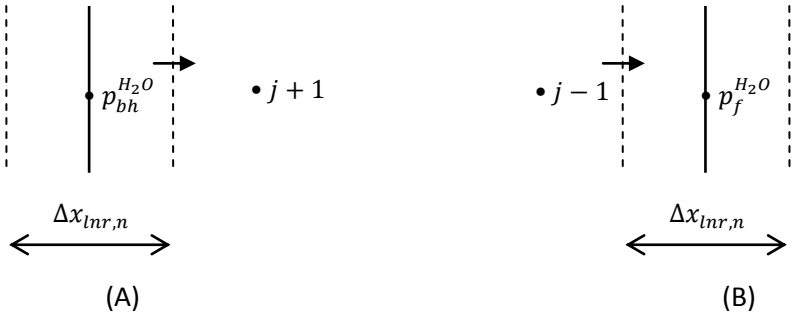

Figure 5-11: Diagram of finite difference approximations for case 6, including the external (A) and internal (B) polymer liner surfaces.

$$p_{lnr,j}^{H_2O} = p_{bh}^{H_2O} \quad for\ t \geq 0,\ x = 0$$
$$p_{lnr,j}^{H_2O} = p_f^{H_2O} \quad for\ t \geq 0,\ x = X_{T,lnr} \qquad \textbf{(5-30)}$$

5.2.3.2.7 Case 7

Node:

$$n = 1, j = 2$$

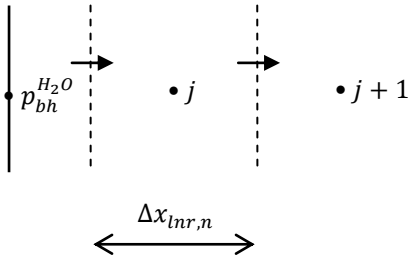

Figure 5-12: Diagram of finite difference approximation for case 7.

$$\frac{dp_{lnr,j}^{H_2O}}{dt} = \frac{P_{lnr,n}^{H_2O}}{S_{lnr,n}^{H_2O}\Delta x_{lnr,n}{}^2}\left(p_{bh}^{H_2O} - 2p_{lnr,j}^{H_2O} + p_{lnr,j+1}^{H_2O}\right) \quad \textbf{(5-31)}$$

$$for\ t \geq 0$$

5.2.3.2.8 Case 8

Nodes:

$$n = 1, j = (n-1)J + 3 : nJ$$

$$n = 2 : N_{lnr} - 1, j = (n-1)J + 2 : nJ$$

$$n = N_{lnr}, j = (n-1)J + 2 : nJ - 1$$

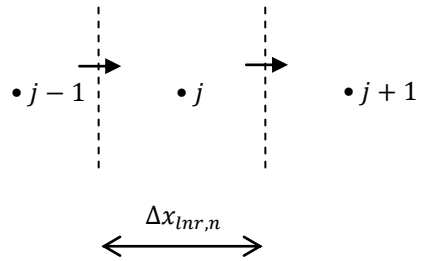

Figure 5-13: Diagram of finite difference approximation for case 8.

$$\frac{dp_{lnr,j}^{H_2O}}{dt} = \frac{P_{lnr,n}^{H_2O}}{S_{lnr,n}^{H_2O}\Delta x_{lnr,n}{}^2}\left(p_{lnr,j-1}^{H_2O} - 2p_{lnr,j}^{H_2O} + p_{lnr,j+1}^{H_2O}\right) \quad \textbf{(5-32)}$$

$$for\ t \geq 0$$

5.2.3.2.9 Case 9

Nodes:

$$n = 1 : N_{lnr} - 1, j = nJ + 1$$

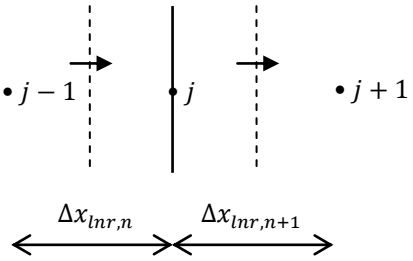

Figure 5-14: Diagram of finite difference approximation for case 9.

$$\frac{dp_{lnr,j}^{H_2O}}{dt} = \frac{2}{\Delta x_{lnr,n} S_{lnr,n}^{H_2O} + \Delta x_{lnr,n+1} S_{lnr,n+1}^{H_2O}} \left[\frac{P_{lnr,n}^{H_2O}}{\Delta x_{lnr,n}} \left(p_{lnr,j-1}^{H_2O} - p_{lnr,j}^{H_2O} \right) - \frac{P_{lnr,n+1}^{H_2O}}{\Delta x_{lnr,n+1}} \left(p_{lnr,j}^{H_2O} - p_{lnr,j+1}^{H_2O} \right) \right] \quad \textbf{(5-33)}$$

$for\ t \geq 0$

5.2.3.2.10 Case 10

Node:

$$n = N_{lnr}, j = nJ$$

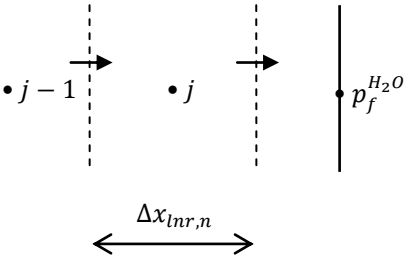

Figure 5-15: Diagram of finite difference approximation for case 10.

$$\frac{dp_{lnr,j}^{H_2O}}{dt} = \frac{P_{lnr,n}^{H_2O}}{S_{lnr,n}^{H_2O} \Delta x_{lnr,n}^{\ 2}} \left(p_{lnr,j-1}^{H_2O} - 2p_{lnr,j}^{H_2O} + p_f^{H_2O} \right) \quad \textbf{(5-34)}$$

$for\ t \geq 0$

5.2.3.3 MATLAB® Solution

The formulated ODEs for moisture content of the food product and finite difference approximations for water vapour pressure in the paperboard bag and polymer liner were converted to MATLAB® code. The resulting script and function files are shown in Appendix D.1.2.2.

5.2.3.4 Example Simulation

A preliminary simulation was carried out for a 25 kg skim milk powder bag system to gain a general indication of whether the model was working correctly. Where possible, model parameters were based on known or literature values to simulate the actual system fairly closely, although several values were approximate only. A polymer liner consisting of 5 layers was assumed, with a relatively high moisture barrier in the centre. The paperboard bag was simulated as having 2 layers, consisting of the paperboard itself (which could be multiple layers with equal properties) and a barrier coating. Model predictions are shown in Figure 5-16 and Figure 5-17. As expected for a low moisture food product, the moisture content of the skim milk powder rises, and as a result so too does the water vapour pressure in the bag headspace. Predictions of the water vapour pressure profile in the paperboard bag and polymer liner were also as expected, with the different layers clearly visible, and a relatively steep decline for the barrier material in the centre.

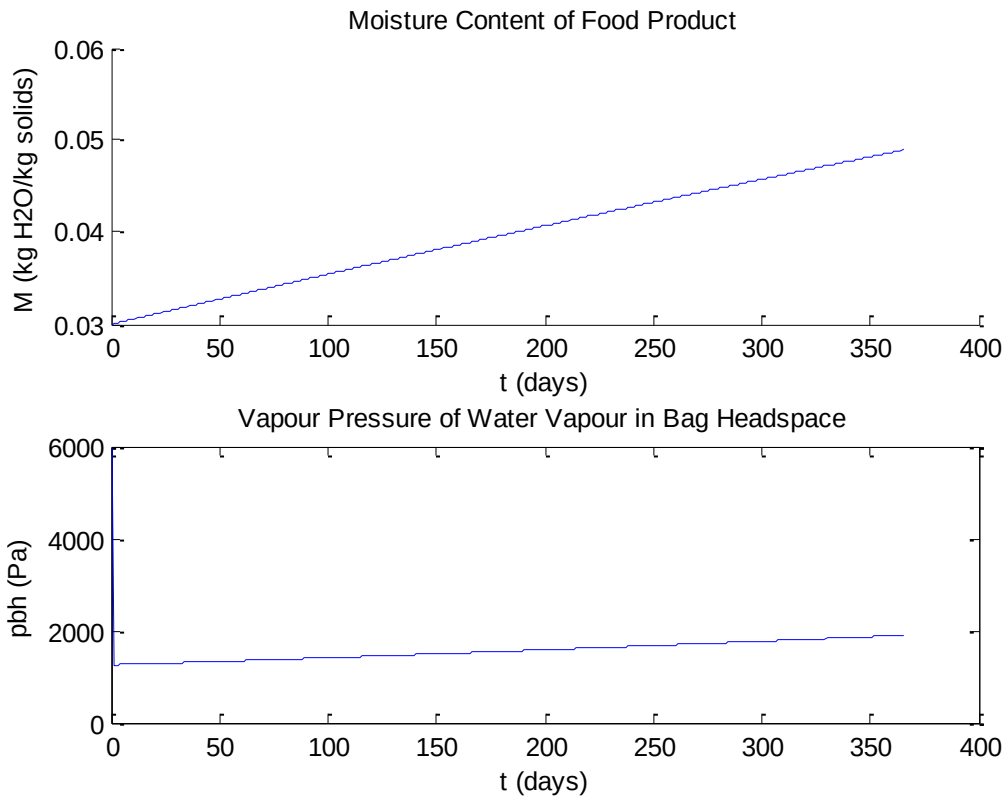

Figure 5-16: Model predictions of moisture content of skim milk powder and water vapour pressure in bag headspace over 365 days at 38°C and 90% RH.

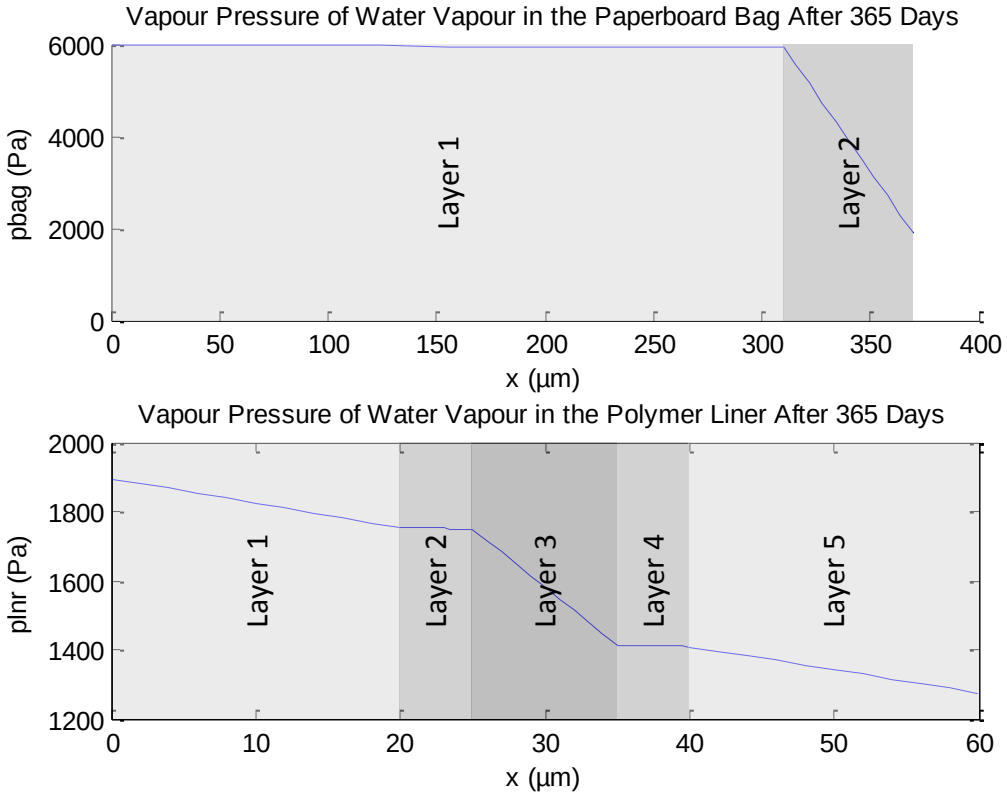

Figure 5-17: Model predictions of water vapour pressure profile in paperboard bag and polymer liner after 365 days at 38°C and 90% RH.

5.2.3.5 Error Checks

Error checks were carried out as was done previously for the standard food package model (Section 4.4.5). These are summarised in Appendix D.1.3. Numerical error checks suggested a default relative error tolerance value of 1×10^{-3} and 10 nodes per packaging layer should be appropriate. Also, there was good agreement between numerical predictions and analytical results in simplified scenarios, suggesting that the formulated model is free of mathematical errors.

5.3 NON-INSTANTANEOUS MASS TRANSFER IN FOOD PRODUCT

For a system where moisture transfer in the food product is slow, the assumption of instantaneous mass transfer in the food may no longer be valid. In this situation it will be necessary to model mass transfer in the food product. Therefore as a further extension to the standard food package model, diffusion in the food product was also included in a separate mathematical model. Mass transfer in a food is largely dependent on the type of food product; for this investigation a food powder was considered.

5.3.1 Conceptual Model Development

5.3.1.1 Outline of Conceptualised System

The extended food package system was defined in Section 5.2.1.1. In this case the system is essentially the same, except that mass transfer in the food product will also be significant. As a consequence the water vapour pressure in the liner headspace will also need to be considered.

Mass transfer in a food powder involves two phases: a solid phase consisting of the food powder particles and a vapour phase of air between these particles. This is illustrated in Figure 5-18.

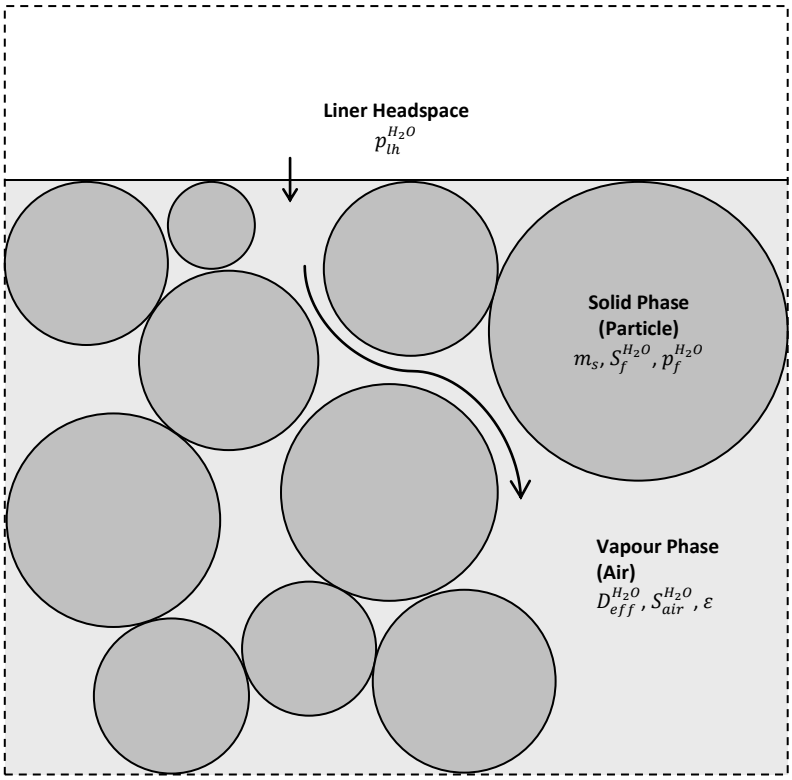

Figure 5-18: Schematic diagram of food powder system.

5.3.1.2 Assumptions

The same assumptions outlined in Section 5.2.1.2 also apply to this extension of the standard food package model, except that the food powder also causes significant resistance to mass transfer. Mass transfer at the surface of the food product and packaging, and diffusion of water vapour through air were still assumed to be instantaneous. In addition, to simplify the mathematical modelling of mass transfer in the food powder, further assumptions were required.

5.3.1.2.1 Moisture Transfer in Food Powder Occurs Only by Diffusion in the Vapour Phase

In a food powder moisture transfer may occur by diffusion in the vapour phase, surface diffusion, capillary action and diffusion within particles. The significant mode(s) of moisture transfer is(are) expected to be somewhat dependent on the type of food powder,

therefore formulating a generalised model would be difficult. However Bronlund & Paterson (2008) proposed diffusion in the vapour to be the only significant mode of moisture transfer in their study of moisture migration in crystalline lactose powder. Since similar food powders were encountered in this study, a similar assumption was made for this mathematical model. The validity of this assumption will need to be analysed independently for individual applications.

5.3.1.2.2 Vapour and Solid Phases in the Food Powder are in Local Equilibrium

If surface diffusion, capillary action and diffusion within particles is assumed to be negligible, or if diffusion through the powder bed is assumed slow compared with moisture uptake by the particle, it should also be valid to assume the vapour and solid phases will be in equilibrium locally. A similar assumption was made by Bronlund & Paterson (2008).

5.3.1.2.3 Permeation is in One-Dimension Only

For this scenario the primary focus is on “worst case” conditions of moisture transfer, as this will determine the overall shelf life of the food product. Whilst in reality the moisture gradients in most food powder systems will have a three dimensional structure, in this case only a single dimension of the food powder with the minimum thickness to the centre of the package will be considered as this will have the lowest resistance to moisture transfer. This assumes that the food powder is homogenous, which is reasonable.

5.3.1.2.4 Other Assumptions

It was assumed that the physical properties of the food powder are constant throughout the system, including porosity and density. This is expected to be reasonable for most food powders.

5.3.2 Mathematical Model Formulation

5.3.2.1 Variables

Additional variables defined in the model formulation not included in Table 5-1 are summarised in Table 5-2.

Table 5-2: List of model variables.

Symbol	Description	Unit	Class*
Δx_f	Width of node in food powder	m	SI
A_f	Surface area of food powder	m^2	SI
$D_{eff}^{H_2O}$	Effective diffusivity of water vapour in food powder	$m^2.s^{-1}$	CV
$S_f^{H_2O}$	Solubility of water vapour in food powder	$mol.m^{-3}.Pa^{-1}$	CV
X_f	Thickness of food powder	m	I
$p_f^{H_2O}$	Water vapour pressure in food powder	Pa	D
$p_{lh}^{H_2O}$	Water vapour pressure in liner headspace	Pa	D
x	Spatial position in packaging or food powder	m	I
ε	Porosity of food powder	-	SI

*I = independent variable, D = dependent variable, CV = consequential variable, SI = system input

In addition to the requirements of the extended food package moisture transfer model outlined earlier (Section 5.2.2.1), an additional ODE is required for the water vapour pressure in the liner headspace. Furthermore, instead of a single ODE for the moisture content of the food product, a PDE will be required. For simplicity this will be expressed in terms of the water vapour pressure in the food powder. As a result an additional two boundary conditions are required for the food powder. Again the initial water vapour pressure in the food product will be considered uniform, thus two additional initial conditions are required.

5.3.2.2 Word Balances and Equations

5.3.2.2.1 ODE for Water Vapour Pressure in Liner Headspace

The water vapour pressure in the liner headspace will be dependent of permeation and diffusion through perforations in the polymer liner as well as diffusion into the food powder. Since it was assumed that the mass of water in the liner headspace is negligible, a steady-state mass balance of water vapour in the liner headspace yields the following:

$$\begin{pmatrix} \textit{rate of} \\ \textit{accumulation of} \\ \textit{water vapour in} \\ \textit{liner headspace} \end{pmatrix} = 0$$

$$= \begin{pmatrix} \textit{rate of water vapour} \\ \textit{permeating through} \\ \textit{inside surface of} \\ \textit{liner} \end{pmatrix} + \begin{pmatrix} \textit{rate of water} \\ \textit{vapour diffusing} \\ \textit{through perforation(s)} \\ \textit{in liner} \end{pmatrix} \qquad \textbf{(5-35)}$$

$$- \begin{pmatrix} \textit{rate of water} \\ \textit{vapour diffusing} \\ \textit{into food} \\ \textit{powder} \end{pmatrix}$$

This word balance can be expressed as an ODE for use in the mathematical model as follows (derivation shown in Appendix D.2.1.1.1):

$$\frac{dp_{lh}^{H_2O}}{dt} = 0 = P_{lnr,n=N_{lnr}}^{H_2O} A_{lnr} \left(\frac{dp_{lnr}^{H_2O}}{dx} \right)_{x=X_{lnr,n}} + J_{prf,lnr}^{H_2O} A_{prf,lnr}$$

$$- D_{eff}^{H_2O} S_{air}^{H_2O} A_f \left(\frac{dp_f^{H_2O}}{dx} \right)_{x=0} \qquad \textbf{(5-36)}$$

for $t \geq 0$

where:

$p_{lh}^{H_2O}$ = Water vapour pressure in liner headspace (Pa)

A_f = Surface area of food powder (m^2)

x = Spatial position in packaging or food powder (m)

This equation can then be solved after substituting the appropriate expression for the diffusive flux of water vapour through perforation(s) in the polymer liner (Section 5.2.2.2.10).

5.3.2.2.2 PDE for Water Vapour Pressure in Food Powder

A PDE for one-dimensional unsteady-state diffusion of water vapour in the food powder is very similar to that previously derived for the permeation of water vapour in the paperboard bag (Section 5.2.2.2.1). Since moisture transfer was assumed to occur only by diffusion in the vapour phase, all moisture transfer involves diffusion through air. To account for the increased diffusion length and reduced volume due to particles in the system, the diffusivity of water vapour in air is adjusted to an effective diffusivity of water vapour in the food product. Sorption capacity consists of water vapour in the vapour phase as well as moisture sorption in the food particles. The resulting PDE is as follows (derivation shown in Appendix D.2.1.1.2):

$$\left(\varepsilon S_{air}^{H_2O} + (1-\varepsilon) S_f^{H_2O}\right) \frac{\partial p_f^{H_2O}}{\partial t} = D_{eff}^{H_2O} S_{air}^{H_2O} \frac{\partial^2 p_f^{H_2O}}{\partial x^2} \quad \textbf{(5-37)}$$

$$for\ t \geq 0,\ 0 < x < X_f$$

where:

ε = Porosity of food powder (-)

$S_f^{H_2O}$ = Solubility of water vapour in food powder (mol.m^{-3}.Pa^{-1})

$D_{eff}^{H_2O}$ = Effective diffusivity of water vapour in food powder (m^2.s^{-1})

X_f = Thickness of food powder (m)

5.3.2.2.3 Equation for Effective Diffusivity of Water Vapour in Food Powder

Bronlund & Paterson (2008) suggested the following equation to estimate the effective diffusivity of water vapour in the food powder:

$$D_{eff}^{H_2O} = (\delta/\tau)\varepsilon D_{air}^{H_2O} \quad \textbf{(5-38)}$$

where:

δ/τ = Constructivity-tortuosity ratio (-)

$D_{air}^{H_2O}$ = Diffusivity of water vapour in air ($m^2.s^{-1}$)

5.3.2.2.4 Equation for Solubility of Water Vapour in Food Powder

An expression for the solubility of water vapour in the food powder can be derived from the moisture sorption isotherm equation using the same procedure as outlined in Section 4.3.2.5 for the solubility of water vapour in the packaging. For a GAB moisture isotherm equation, the resulting equation is as follows:

$$S_f^{H_2O} = \frac{\rho_s}{M_{r,H_2O}}\left[\frac{M_{0,GAB}{k_{GAB}}^2 C_{GAB} p_f^{H_2O}}{\left(p_0^{H_2O}\right)^2\left(1-k_{GAB}\frac{p_f^{H_2O}}{p_0^{H_2O}}\right)^2\left(1+k_{GAB}\frac{p_f^{H_2O}}{p_0^{H_2O}}(C_{GAB}-1)\right)}\right.$$
$$+\frac{M_{0,GAB}k_{GAB}C_{GAB}}{p_0^{H_2O}\left(1-k_{GAB}\frac{p_f^{H_2O}}{p_0^{H_2O}}\right)\left(1+k_{GAB}\frac{p_f^{H_2O}}{p_0^{H_2O}}(C_{GAB}-1)\right)} \quad \textbf{(5-39)}$$
$$\left.-\frac{M_{0,GAB}{k_{GAB}}^2 C_{GAB}(C_{GAB}-1)p_f^{H_2O}}{\left(p_0^{H_2O}\right)^2\left(1-k_{GAB}\frac{p_f^{H_2O}}{p_0^{H_2O}}\right)\left(1+k_{GAB}\frac{p_f^{H_2O}}{p_0^{H_2O}}(C_{GAB}-1)\right)^2}\right]$$

where:

ρ_s = Density of solids in food powder ($kg.m^{-3}$)

$M_{0,GAB}$ = Moisture content of monolayer for GAB isotherm of food powder ((kg water).(kg solids)$^{-1}$)

C_{GAB} = Guggenheim constant for GAB isotherm of food powder (-)

k_{GAB} = Constant for GAB isotherm of food powder (-)

Similar expressions can be derived based on other moisture sorption isotherm equations. For this investigation, BET and linear isotherm equations may also be encountered; therefore expressions for the solubility of water vapour in the food powder based on these equations were also derived (derivation shown in Appendix C.1.1.3).

$$S_f^{H_2O} = \frac{\rho_s}{M_{r,H_2O}} \left[\frac{M_{1,BET} C_{BET} p_f^{H_2O}}{\left(p_0^{H_2O}\right)^2 \left(1 - \frac{p_f^{H_2O}}{p_0}\right)^2 \left(1 + \frac{p_f^{H_2O}}{p_0}(C_{BET} - 1)\right)} + \frac{M_{1,BET} C_{BET}}{p_0 \left(1 - \frac{p_f^{H_2O}}{p_0}\right)\left(1 + \frac{p_f^{H_2O}}{p_0}(C_{BET} - 1)\right)} - \frac{M_{1,BET} C_{BET} (C_{BET} - 1) p_f^{H_2O}}{\left(p_0^{H_2O}\right)^2 \left(1 - \frac{p_f^{H_2O}}{p_0}\right)\left(1 + \frac{p_f^{H_2O}}{p_0}(C_{BET} - 1)\right)^2} \right] \quad \textbf{(5-40)}$$

where:

$M_{1,BET}$ = Moisture content of monolayer for BET isotherm of food powder ((kg water).(kg solids)$^{-1}$)

C_{BET} = Guggenheim constant for BET isotherm of food powder (-)

$$S_f^{H_2O} = \frac{\rho_s b_{lin}}{M_{r,H_2O} p_0^{H_2O}} \quad \textbf{(5-41)}$$

where:

b_{lin} = Slope of linear isotherm for food powder (-)

5.3.2.2.5 Equation for Density of Solids in the Food Powder

An equation for the density of solids in the food powder can be derived from the definition of moisture content based on the particle density at a specified moisture content:

$$\rho_s = \frac{\rho_p}{(1+M)} \quad \textbf{(5-42)}$$

where:

ρ_p = Particle density of food powder (kg.m^{-3}) at specified moisture content

M = Moisture content of food powder ((kg water).(kg solids)$^{-1}$)

5.3.2.2.6 Equation for Porosity of Food Powder

Muramatsu et al. (2005) indicated the following expression for the porosity of a food powder:

$$\varepsilon = 1 - \frac{\rho_b}{\rho_p} \quad \textbf{(5-43)}$$

where:

ρ_b = Bulk density of food powder (kg.m^{-3})

5.3.2.3 Boundary Conditions

Similar to previous models, a first kind of boundary condition was assumed for the food powder surface bordering the liner headspace. At the other end of the food powder a symmetry boundary was assumed, which may represent a depth at which the water vapour pressure is practically uniform, or the centre of a food package.

$$p_f^{H_2O} = p_{lh}^{H_2O} \quad \textbf{(5-44)}$$

$$for\ t \geq 0,\ at\ x = 0$$

$$\frac{dp_f^{H_2O}}{dx} = 0 \quad \textbf{(5-45)}$$

$$for\ t \geq 0,\ at\ x = X_f$$

5.3.2.4 Initial Conditions

The initial water vapour pressure in the food powder was assumed to be uniform. It is also expected that the food powder will dictate the water vapour pressure in the liner headspace, thus:

$$p_f^{H_2O} = p_{lh}^{H_2O} = p_{f,i}^{H_2O} \quad at\ t = 0,\ 0 < x < X_f \tag{5-46}$$

where:

$p_{f,i}^{H_2O}$ = Initial water vapour pressure in food powder (Pa)

5.3.3 Solution

5.3.3.1 Finite Difference Grid

The finite difference grid used for the food powder is illustrated in Figure 5-19. The food powder divided into J space steps each with a thickness of Δx_f. Thus:

$$\Delta x_f = \frac{X_f}{J} \tag{5-47}$$

where:

Δx_f = Width of node in food powder (m)

X_f = Thickness of food powder (m)

The section of the food powder contained within each space step was designated a node number from $j = 1$ at the powder surface to $j = J + 1$ at the symmetry boundary. The water vapour pressure within each node was considered to be uniform.

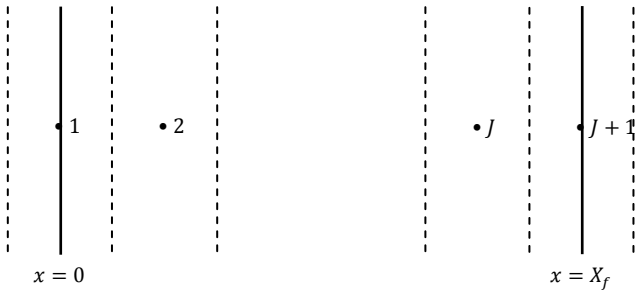

Figure 5-19: Finite difference grid for food powder.

5.3.3.2 Finite Difference Approximations

Additional finite difference approximations were derived as previously for the packaging. However in this case, since the food powder consisted of only one layer, no boundary between layers was required. Also, the boundary opposite the food powder surface consisted of a symmetry boundary condition.

5.3.3.2.1 Case 11

Node:

$j = 1$

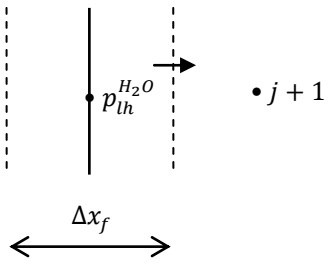

Figure 5-20: Diagram of finite difference approximations for case 11.

$$p_{f,j}^{H_2O} = p_{lh}^{H_2O} \quad \text{for } t \geq 0,\ x = 0 \qquad \textbf{(5-48)}$$

5.3.3.2.2 Case 12

Node:

$$j = 2$$

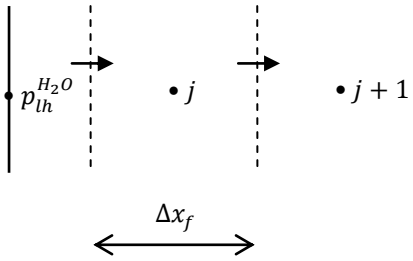

Figure 5-21: Diagram of finite difference approximation for case 12.

$$\frac{dp_{f,j}^{H_2O}}{dt} = \frac{D_{eff}^{H_2O} S_{air}^{H_2O} \left(p_{lh}^{H_2O} - 2p_{f,j}^{H_2O} + p_{f,j+1}^{H_2O}\right)}{\Delta x_f{}^2 \left[\varepsilon S_{air}^{H_2O} + (1-\varepsilon) S_f^{H_2O}\right]} \qquad \textbf{(5-49)}$$

$$for\ t \geq 0$$

5.3.3.2.3 Case 13

Nodes:

$$j = 3{:}J$$

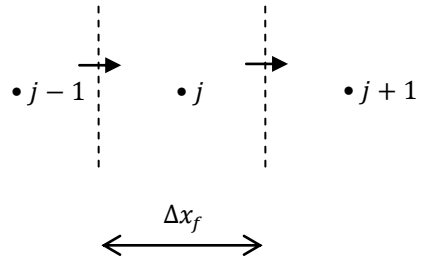

Figure 5-22: Diagram of finite difference approximation for case 13.

$$\frac{dp_{f,j}^{H_2O}}{dt} = \frac{D_{eff}^{H_2O} S_{air}^{H_2O} \left(p_{f,j-1}^{H_2O} - 2p_{f,j}^{H_2O} + p_{f,j+1}^{H_2O}\right)}{\Delta x_f{}^2 \left[\varepsilon S_{air}^{H_2O} + (1-\varepsilon) S_f^{H_2O}\right]} \qquad \textbf{(5-50)}$$

$$for\ t \geq 0$$

5.3.3.2.4 Case 14

Node:

$$j = J + 1$$

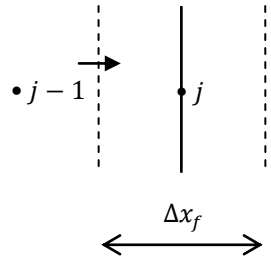

Figure 5-23: Diagram of finite difference approximations for case 14.

$$\frac{dp_{f,j}^{H_2O}}{dt} = \frac{2D_{eff}^{H_2O} S_{air}^{H_2O} \left(p_{f,j-1}^{H_2O} - p_{f,j}^{H_2O}\right)}{\Delta x_f{}^2 \left[\varepsilon S_{air}^{H_2O} + (1-\varepsilon) S_f^{H_2O}\right]} \quad \textbf{(5-51)}$$

$$for\ t \geq 0$$

5.3.3.3 MATLAB® Solution

The formulated ODEs for water vapour pressure in the liner headspace and finite difference approximations for water vapour pressure in the paperboard bag, polymer liner and food powder were converted to MATLAB® code. The resulting script and function files are shown in Appendix D.2.2.2.

5.3.3.4 Example Simulation

As a preliminary simulation, the same skim milk powder system previously considered for the extended food package model with instantaneous mass transfer in the food product (Section 5.2.3.4) was used. Model predictions are shown in Figure 5-24 to Figure 5-27. As expected, the water vapour pressure profiles in the paperboard bag and polymer liner agree closely with predictions for the extended food package model. The water vapour pressure profile in the milk powder appeared realistic, decreasing and

eventually reaching a constant value. Similarly, the water vapour pressure in the food product and liner headspace rose as expected for a low moisture food product.

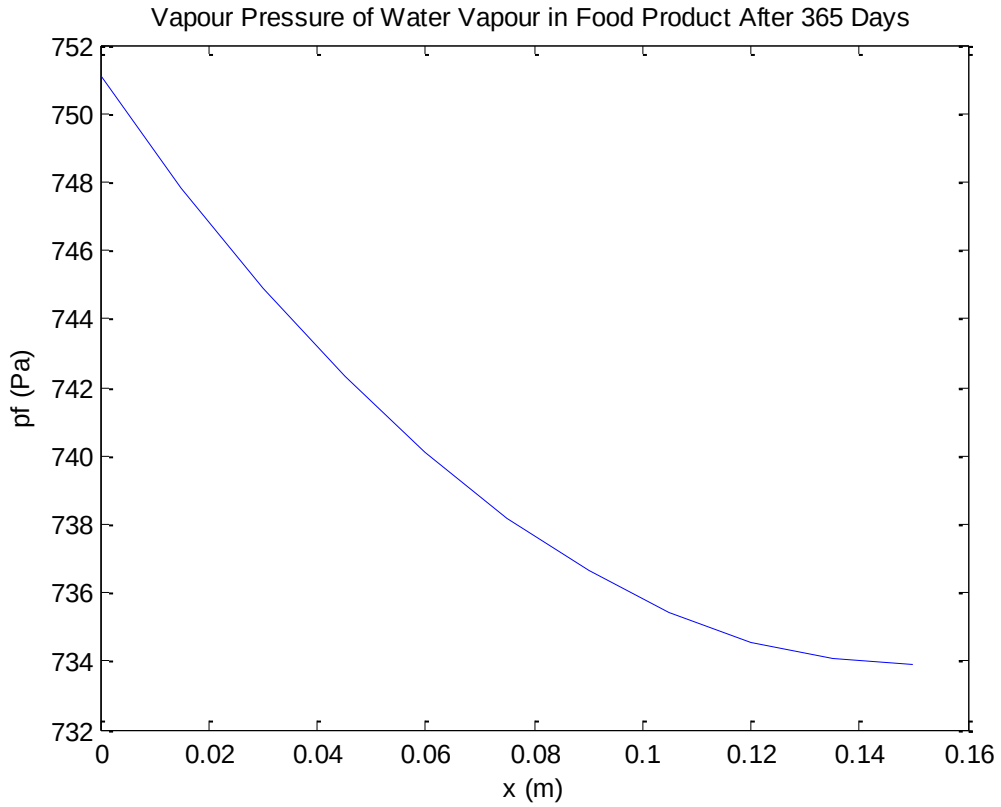

Figure 5-24: Model predictions of water vapour pressure profile in skim milk powder after 365 days at 38°C and 90% RH.

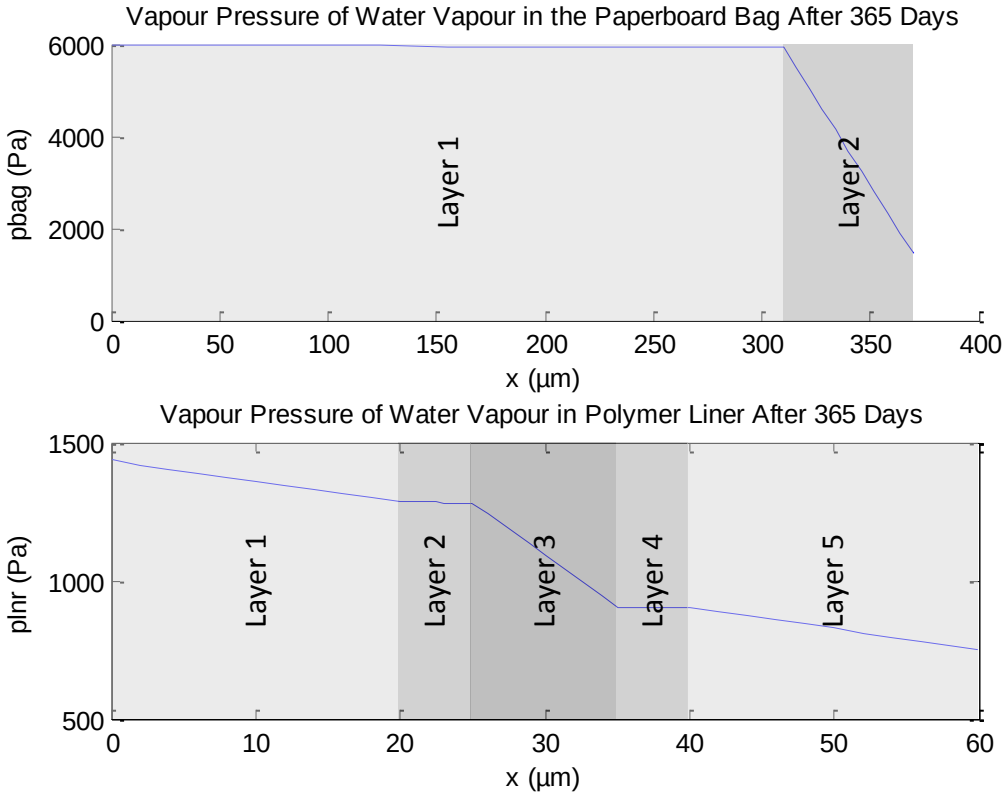

Figure 5-25: Model predictions of water vapour pressure profile in paperboard bag and polymer liner after 365 days at 38°C and 90% RH.

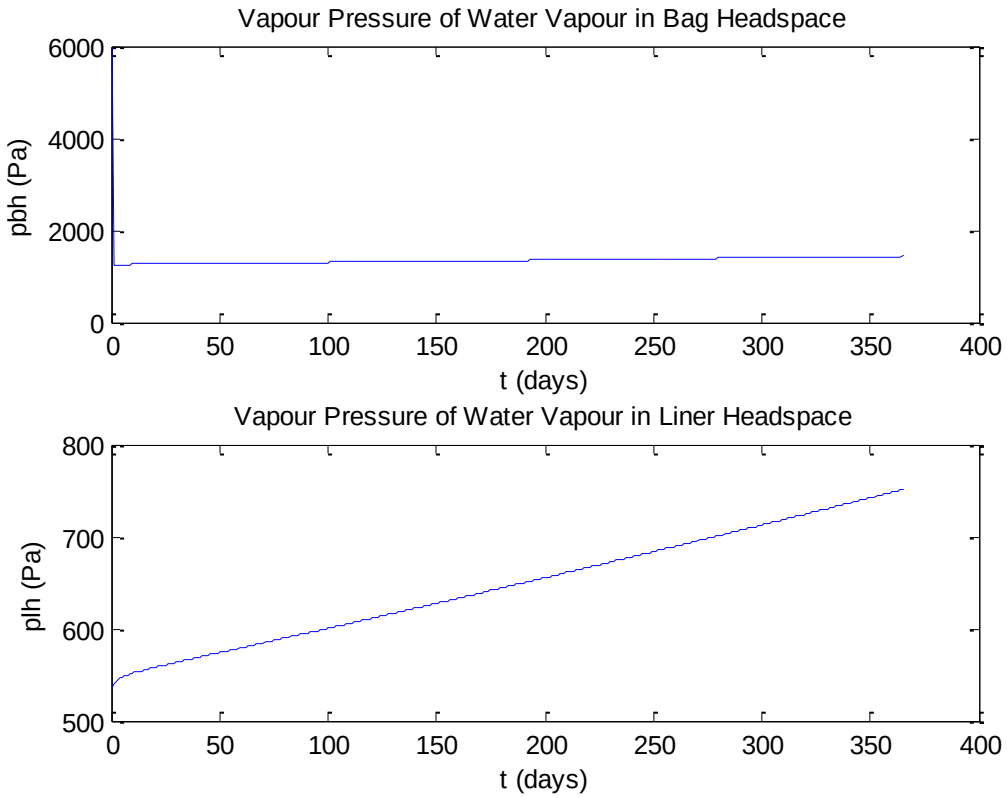

Figure 5-26: Model predictions of water vapour pressure in bag headspace and liner headspace over 365 days at 38°C and 90% RH.

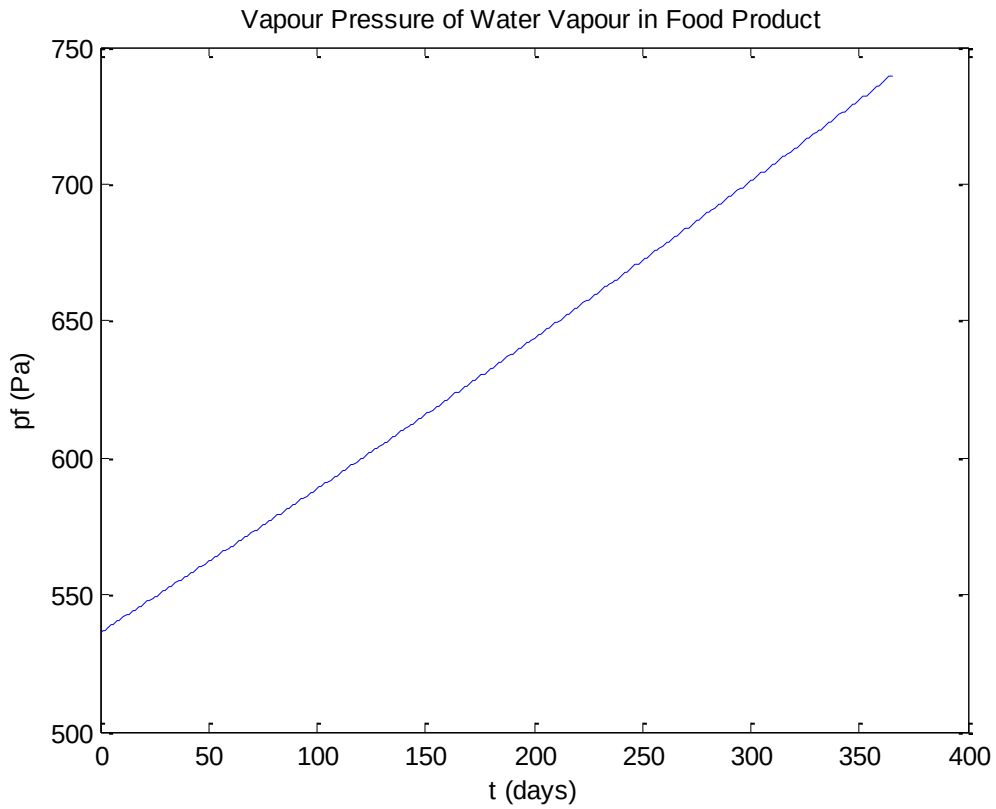

Figure 5-27: Model predictions of average water vapour pressure in skim milk powder over 365 days at 38°C and 90% RH.

5.3.3.5 Error Checks

Again, error checks were carried out as was done previously for the standard food package model (Section 4.4.5). These are summarised in Appendix D.2.3. Numerical error checks suggested a default relative error tolerance value of 1×10^{-3} and 10 nodes per packaging layer and for the food powder is appropriate. Also, there was excellent agreement between numerical predictions and analytical results, suggesting that the formulated model is free of mathematical errors.

5.4 MODEL VALIDATION

Validation for the extended models followed closely with that previously carried out for the standard food package model (Section 4.5). Much of the experimental data considered previously was also compared with predictions of the extended models to ensure similar agreement.

5.4.1 Experimental Methodology

Experimental methodology for model validation was previously covered in Section 4.5.1 for the standard food package model. Where changes or additions to the methodology were made for validating the extended models, these are outlined below.

5.4.1.1 Diffusion of Water Vapour through Perforations

In addition to the experimental methodology used for the standard food package model, a polymer liner and paperboard bag with one perforation through both samples was also considered. Test conditions are outlined in Table 5-3.

Table 5-3: Summary of samples and test conditions for validation of water vapour diffusion through perforations in packaging.

Sample[1]	**Approximate Temperature**[2] **(°C)**	**Approximate RH Gradient**[3] **(%)**
Polymer liner and paperboard bag with 1 perforation in each	20	$0 - 75$

[1] Multiple samples are in order of sample in contact with interior of permeability dish to sample exposed to ambient environment.

[2] The actual temperature was determined by the average of temperature readings logged at 15 minute intervals for the duration of each test.

[3] RH gradients are expressed as interior surface (surface closest to food product) to exterior surface (surface closest to ambient environment) as positioned in original packaging system. The actual ambient RH was determined by the average of RH readings logged at 15 minute intervals for the duration of each test.

5.4.2 Model Input Parameters and Data Analysis

Model input parameters and data analysis used for model were previously covered in Section 4.5.2 for the standard food package model. Additional input parameters required for the extended food package models are discussed below.

5.4.2.1 Physical Properties of the Food Powder

To allow previously considered food package systems to be simulated by the extended food package model with non-instantaneous mass transfer in the food powder, additional properties of the SMP were obtained from literature.

Muramatsu et al. (2005) measured several physical properties of SMP at various conditions, including bulk density and particle density. It was found that these parameters did not significantly affect model predictions, which is attributed to the fact that the solubility of water vapour in the food powder, porosity and volume of food powder all depended on these parameters in a somewhat opposing manner. Similarly, it was expected that only the water vapour pressure gradient in the food powder would be significantly affected, which remained practically uniform anyway. Therefore only a “worst case” scenario resulting in the slowest mass transfer was considered, for which a particle density of 1493 $kg.m^{-3}$ and bulk density of 850 $kg.m^{-3}$ were used. For this reason the error in these parameters were not included in model sensitivity analysis.

Bronlund and Paterson (2008) suggested a constructivity-tortuosity ratio of 0.7 for lactose powders. Since the rate of mass transfer in the food powder was expected to be much higher than through the packaging, the specific value of this parameter was not expected to have a significant impact on model predictions, which was supported by subsequent simulations. Therefore a constructivity-tortuosity ratio of 0.7 was also used for simulations of mass transfer in SMP.

5.4.3 Results and Discussion

All food package systems previously considered for model validation of the standard food package model were also simulated by the extended models where possible. These were covered in Section 4.5.3. To allow single layer packaging systems to be simulated by the extended models very large perforation surface areas were used for the external layer, resulting in a bag headspace water vapour pressure that is equal to that of the ambient air.

5.4.3.1 Permeation of Water Vapour through Packaging

A comparison of model predictions and experimental results for validating the permeation component of the extended food package model showed identical results to similar analysis carried out for the standard food package model (Section 4.5.3.1), which was as expected. The extended food package model with non-instantaneous mass transfer in the food could not be used to simulate the same system due to a lack of data for the silica beads; however similar agreement was expected since the same base model was used.

5.4.3.2 Diffusion of Water Vapour through Perforations

Again, a comparison of model predictions and experimental results for validating the prediction of diffusion through perforations of the extended food package model were identical to similar analysis carried out for the standard food package model (Section 4.5.3.2). In addition to the scenarios involving single and multiple perforations in a single packaging layer system, perforations in multiple separate layers was also considered. This scenario could not previously be simulated by the standard food package model due to the air gap between the layers. Again this system could not be simulated by the extended food package model with non-instantaneous mass transfer in the food due to a lack of data.

5.4.3.2.1 Single Perforation in a Two Layer System

The WVTR test carried out with a paperboard bag and polymer liner with a single perforation through both layers was simulated as a food package containing desiccator. System inputs for the simulation are summarised in Table 5-4.

Table 5-4: Summary of system inputs used for validation of diffusion of water vapour through multiple perforations.

Parameter Description	Symbol	Units	Value [a]
General system inputs			
Initial moisture content of silica beads	M_i	(kg water).(kg solids)$^{-1}$	0
Ambient temperature	T	K	$(20.1 \pm 0.5) + 273.15$
Ambient relative humidity	RH_a	%	(76.5 ± 0.8)
Surface area of packaging	A_{pkg}	m^2	$\pi\left(\frac{0.07}{2}\right)^2$
Number of layers	N	-	2
Total area of perforations	A_{prf}	m^2	$(5.2 \pm 1.3) \times 10^{-9}$
Diameter of perforation	d_{prf}	m	1×10^{-4}
Linear isotherm parameters			
Slope of linear isotherm	b_{lin}	-	1×10^{10}
Constant for linear isotherm	c_{lin}	-	0
Properties of layer 1 of packaging film			
Thickness of layer 1 of packaging film	X_1	m	$(3.1 \pm 0.5) \times 10^{-4}$
Solubility of water vapour in layer 1 of packaging at reference temperature	$S^{H_2O}_{ref,pkg,1}$	mol.m^{-3}.Pa^{-1}	0.001
Permeability of water vapour in layer 1 of packaging at reference temperature	$P^{H_2O}_{ref,pkg,1}$	mol.m.m^{-2}.s^{-1}.Pa^{-1}	1.6×10^{-11} [b]
Diffusivity of water vapour in layer 1 of packaging at reference temperature	$D^{H_2O}_{ref,pkg,1}$	m^2.s^{-1}	$\frac{P^{H_2O}_{ref,pkg,1}}{S^{H_2O}_{ref,pkg,1}}$
Properties of layer 2 of packaging film			
Thickness of layer 2 of packaging film	X_2	m	$(8.2 \pm 1.2) \times 10^{-5}$
Solubility of water vapour in layer 2 of packaging at reference temperature	$S^{H_2O}_{ref,pkg,2}$	mol.m^{-3}.Pa^{-1}	0.001

Permeability of water vapour in layer 2 of packaging at reference temperature	$P^{H_2O}_{ref,pkg,2}$	mol.m.m^{-2}.s^{-1}.Pa^{-1}	$(2.5 \pm 0.4) \times 10^{-14}$
Diffusivity of water vapour in layer 2 of packaging at reference temperature	$D^{H_2O}_{ref,pkg,2}$	m^2.s^{-1}	$\frac{P^{H_2O}_{ref,pkg,2}}{S^{H_2O}_{ref,pkg,2}}$

[a] Error values represent a 95% CI relative to the mean.

[b] A 95% CI was not considered due to approximations made for the simulation.

A comparison of model predictions and experimental results for the two layer perforated system is shown in Figure 5-28.

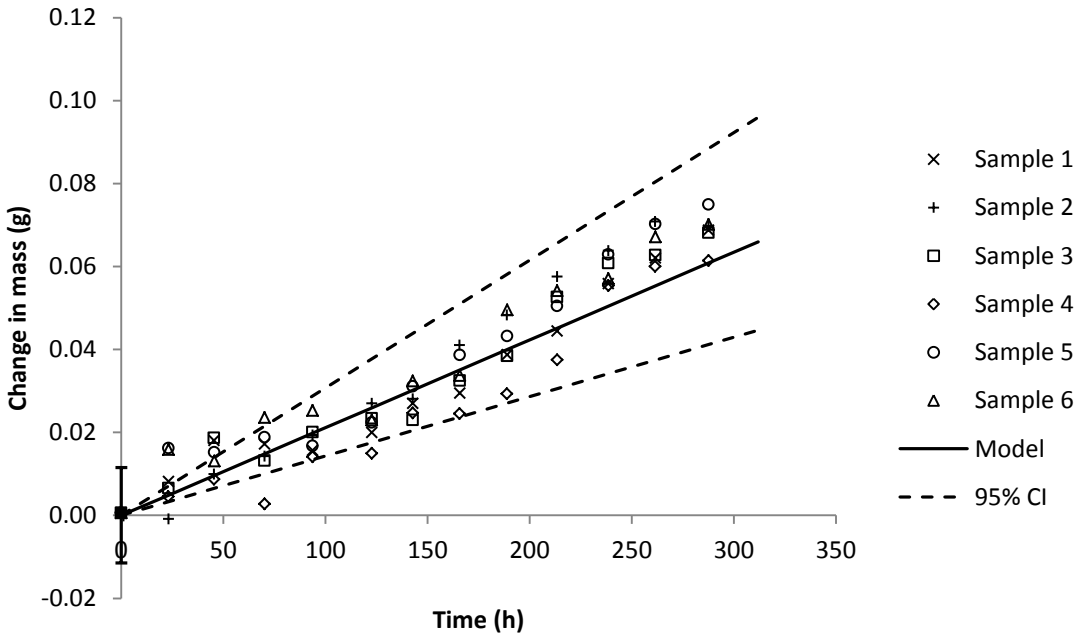

Figure 5-28: Comparison of change in mass (g) versus time (hours) due to moisture transfer through a polymer liner and paperboard bag with a single perforation at 20.1°C and 0% to 76.5% RH gradient as predicted by the model and measured experimentally. Error bar at 0 hours represents 95% CI of initial experimental mass. Model 95% CI limits represent extreme predictions based on 95% CIs of system inputs.

There was quite good agreement between experimental measurements and model predictions. Experimental measurements outside model 95% CI limits can realistically be explained by the error of initial experimental mass values. It should be noted that due to the very high permeability of the paperboard bag relative to the perforated polymer liner, it can be expected that the paperboard bag would not have had a practical influence on moisture transfer. In fact, this was confirmed by comparing the experimental water vapour transfer

rate to that of the single perforation system (Section 4.5.3.2.1), which were 1.33 ± 0.08 $g.m^{-2}.day^{-1}$ (at 20.1°C and a 0% to 74.4% RH gradient) and 1.48 ± 0.11 $g.m^{-2}.day^{-1}$ (at 20.1°C and a 0% to 76.5% RH gradient) respectively. Therefore the system could realistically also have been treated as a single layer packaging system. However due to the mathematical nature of the model, similar agreement is expected for other perforated two layer packaging systems, and will not be investigated further.

5.4.3.3 Overall Food Package System

To validate the moisture isotherm component of the extended food package models, similar analysis to that previously carried out for the standard food package model were used, which is covered in Section 4.5.3.3. In this case both extended models could be considered since literature data of the physical properties of SMP could be obtained.

5.4.3.3.1 Single Layer Packaging System

To validate the moisture sorption isotherm component of the models in a single layer non-perforated packaging system, the polymer liner test sample in a permeability dish containing SMP was simulated as a sealed food package. Values of system inputs for the simulation were previously outlined in Table 4-8. Additional system inputs required for the extended model with non-instantaneous mass transfer in the food powder are summarised in Table 5-5.

Table 5-5: Summary of system inputs used for validation of the moisture isotherm component of the model for a single layer system.

Parameter Description	Symbol	Units	Value*
General system inputs			
Mass of food powder	m_f	kg	0.01
Surface area of food powder	A_f	m^2	$\pi\left(\frac{0.07}{2}\right)^2$
Bulk density of food powder	ρ_b	$kg.m^{-3}$	850
Particle density of food powder	ρ_p	$kg.m^{-3}$	1493
Thickness of food powder	X_f	m	$\frac{m_f}{\rho_b A_f}$
Constructivity-tortuosity ratio	δ/τ	-	0.7

Comparisons of model predictions and experimental results for the single layer non-perforated system are shown in Figure 5-29 for the extended model and Figure 5-30 for the extended model with non-instantaneous mass transfer in the food product.

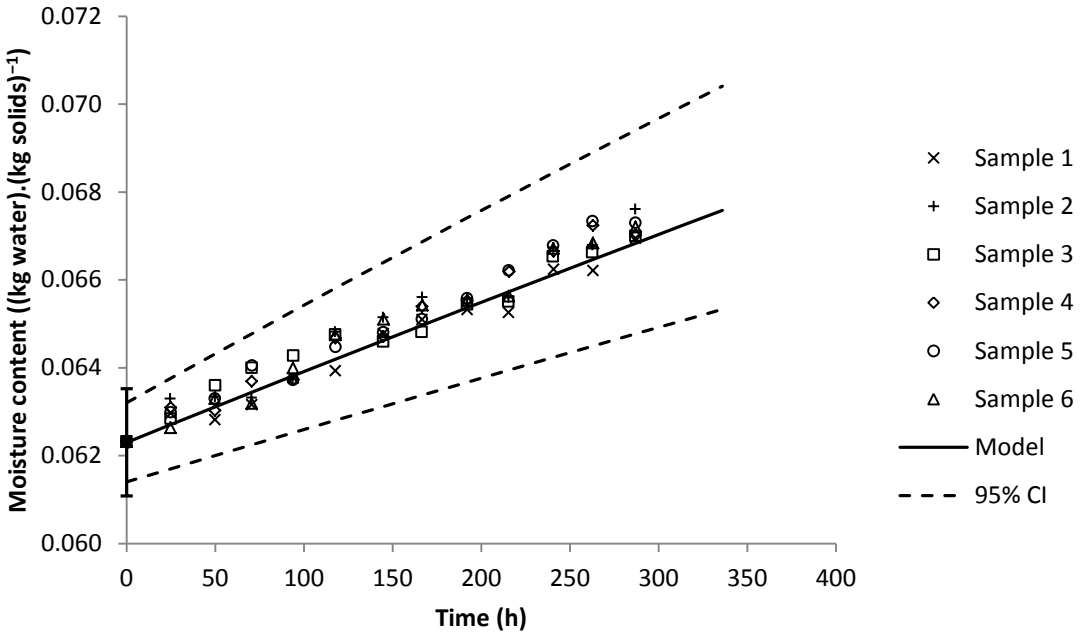

Figure 5-29: Comparison of moisture content of SMP ((kg water).(kg solids)$^{-1}$) versus time (hours) for a polymer liner at 26.6°C and 76.5% ambient RH as predicted by the extended food package model and measured experimentally. Error bar at 0 hours represents 95% CI of initial experimental mass. Model 95% CI limits represent extreme predictions based on 95% CIs of system inputs.

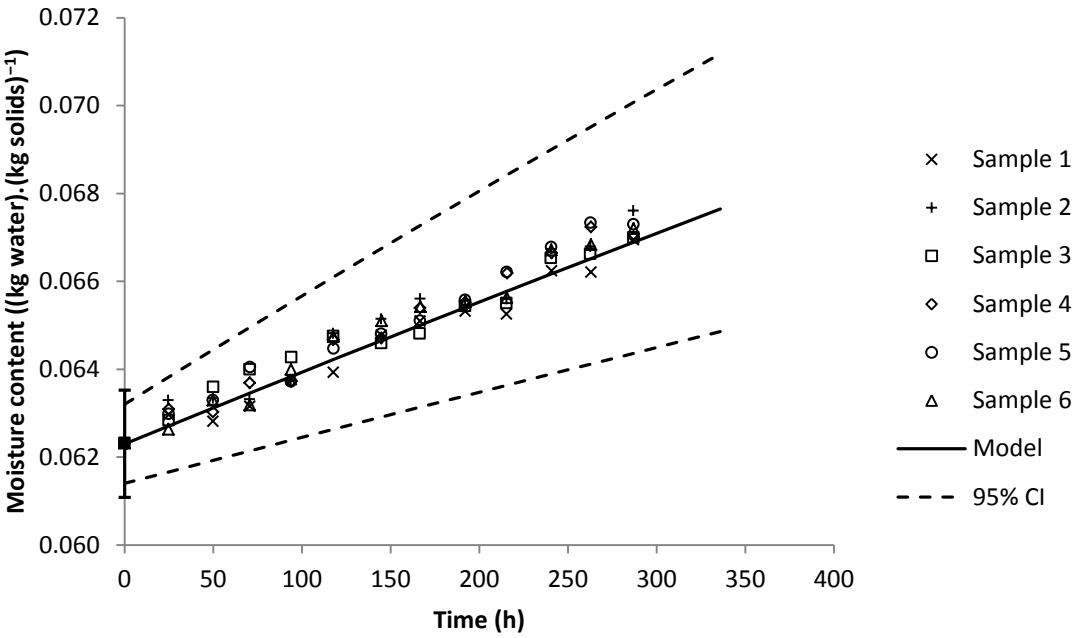

Figure 5-30: Comparison of moisture content of SMP ((kg water).(kg solids)$^{-1}$) versus time (hours) for a polymer liner at 26.6°C and 76.5% ambient RH as predicted by the extended food package model with non-instantaneous mass transfer in the food powder and measured experimentally. Error bar at 0 hours represents 95% CI of initial experimental mass. Model 95% CI limits represent extreme predictions based on 95% CIs of system inputs.

As can be seen, predictions of both models showed excellent agreement with experimental measurements. As expected the two models produced very similar predictions, although 95% CI limits for the extended model with non-instantaneous mass transfer in the food product appeared to cover a larger area. This may be due to using the derivative of the moisture sorption isotherm which could have the effect of exaggerating error between the actual system and literature data. Model predictions of the extended model with non-instantaneous mass transfer in the food product also showed that the water vapour pressure in the food product was practically uniform, thus for this particular system the assumption of instantaneous mass transfer in the food powder is justified.

5.4.3.3.2 Single Perforation in a Single Layer Packaging System

A package system consisting of a polymer liner with a single perforation containing SMP was simulated. Values of system inputs for the simulation were previously outlined in Table 4-9, and additional system inputs required for the extended model with non-instantaneous mass were summarised in Table 5-5.

Comparisons of model predictions and experimental results for the single layer system with one perforation are shown in Figure 5-31 for the extended model and Figure 5-32 for the extended model with non-instantaneous mass transfer in the food product.

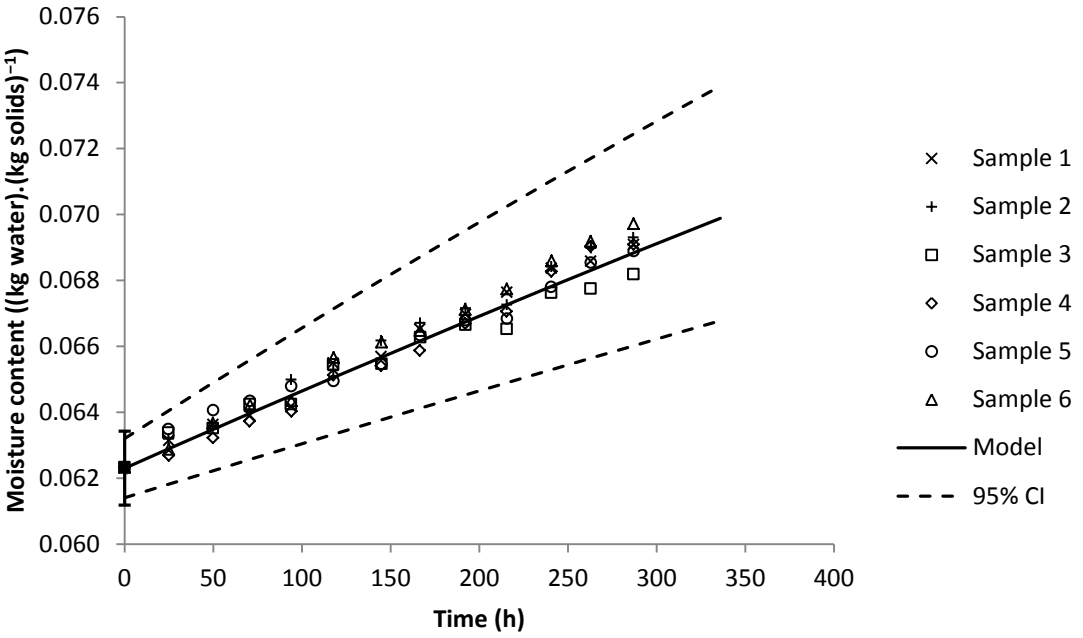

Figure 5-31: Comparison of moisture content of SMP ((kg water).(kg solids)$^{-1}$) versus time (hours) for a polymer liner with 1 perforation at 26.6°C and 76.5% ambient RH as predicted by the extended food package model and measured experimentally. Error bar at 0 hours represents 95% CI of initial experimental mass. Model 95% CI limits represent extreme predictions based on 95% CIs of system inputs.

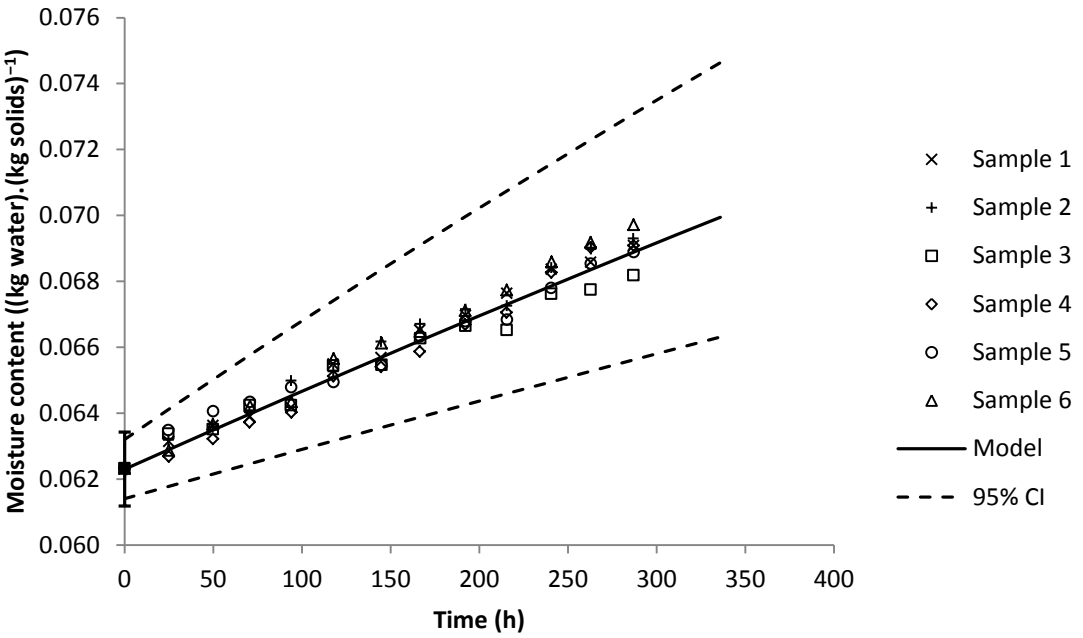

Figure 5-32: Comparison of moisture content of SMP ((kg water).(kg solids)$^{-1}$) versus time (hours) for a polymer liner with 1 perforation at 26.6°C and 76.5% ambient RH as predicted by the extended food package model with non-instantaneous mass transfer in the food powder and measured experimentally. Error bar at 0 hours represents 95% CI of initial experimental mass. Model 95% CI limits represent extreme predictions based on 95% CIs of system inputs.

Again there was very good agreement between model predictions and experimental measurements. Similarly, the effect of a larger 95% CI area for the extended model with non-instantaneous mass transfer in the food product was again noted, although predictions were generally very similar.

5.4.3.3.3 Multiple Perforations in a Single Layer Packaging System

A polymer liner with 20 perforations containing SMP was simulated. Values of system inputs for the simulation were the same as for the single perforation system (Table 4-9), except the total surface area of perforations was increased 20-fold ($(1.04 \pm 0.14) \times 10^{-7}$ m^2). Additional system inputs required for the extended model with non-instantaneous mass were summarised in Table 5-5.

Comparisons of model predictions and experimental results for the single layer system with one perforation are shown in Figure 5-33 for the extended model and Figure 5-34 for the extended model with non-instantaneous mass transfer in the food product.

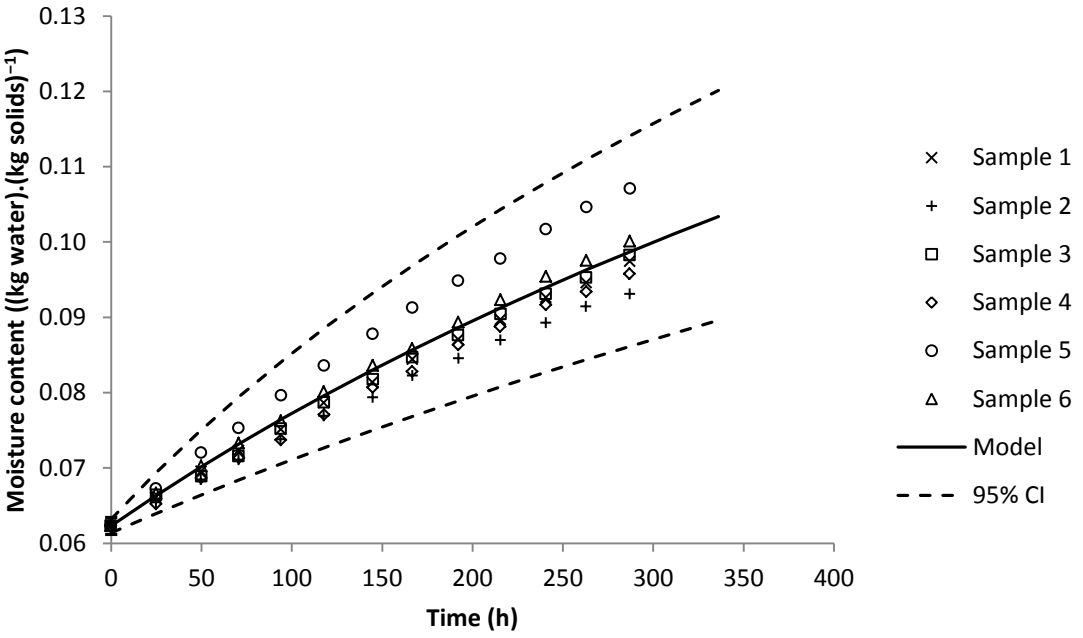

Figure 5-33: Comparison of moisture content of SMP ((kg water).(kg solids)$^{-1}$) versus time (hours) for a polymer liner with 20 perforations at 26.6°C and 76.5% ambient RH as predicted by the extended food package model and measured experimentally. Error bar at 0 hours represents 95% CI of initial experimental mass. Model 95% CI limits represent extreme predictions based on 95% CIs of system inputs.

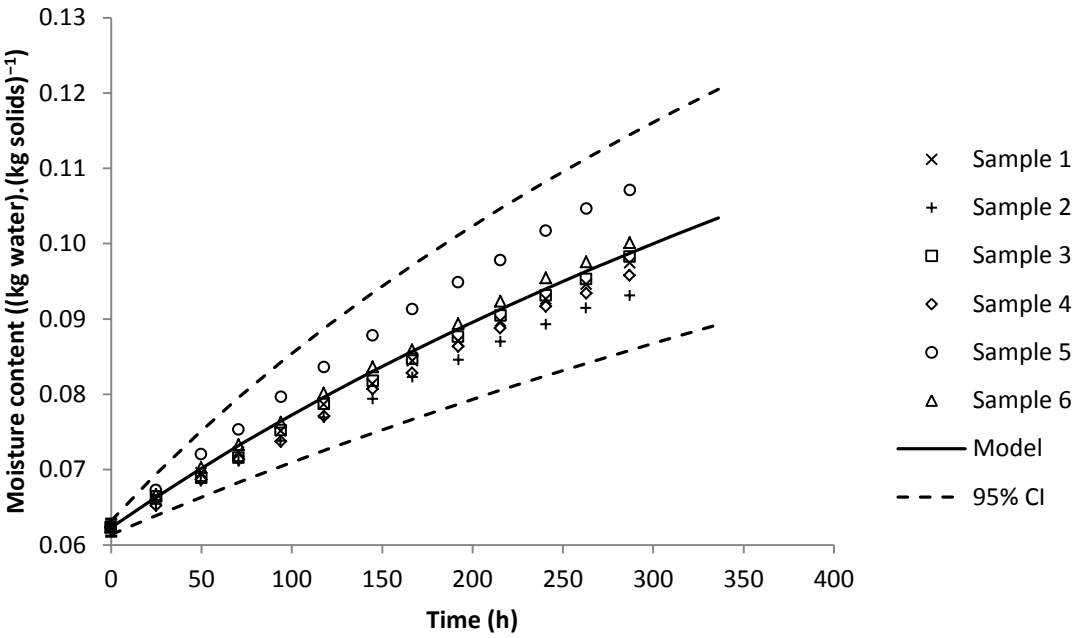

Figure 5-34: Comparison of moisture content of SMP ((kg water).(kg solids)$^{-1}$) versus time (hours) for a polymer liner with 20 perforations at 26.6°C and 76.5% ambient RH as predicted by the extended food package model with non-instantaneous mass transfer in the food powder and measured experimentally. Error bar at 0 hours represents 95% CI of initial experimental mass. Model 95% CI limits represent extreme predictions based on 95% CIs of system inputs.

As for the previous systems containing SMP, there was again excellent agreement of model predictions with experimental measurements.

Again there was very good agreement between model predictions and experimental measurements. Similarly, the effect of a larger 95% CI area for the extended model with non-instantaneous mass transfer in the food product was again noted, although predictions were generally very similar. These results suggest that model predictions are valid.

5.5 SUMMARY

In this chapter, extensions to the standard food package moisture transfer model were presented. Scenarios considered include systems with multiple individual packaging layers containing perforations, and/or systems where mass transfer in the food product is

significant. In terms of modelling moisture transfer in a food product, only a food powder was considered, for which additional assumptions were required. Mathematical models were formulated for the extended scenarios and solved numerically using MATLAB® software. Error checks and validation against experimental observations were again carried out, which suggested the models can accurately predict real-world observations for food packaging systems of interest.

Chapter 6

DEVELOPMENT OF TWO-DIMENSIONAL PERFORATION MOISTURE TRANSFER MODELS

6.1 INTRODUCTION

In this chapter, the development of two-dimensional perforation moisture transfer models are presented. Previously modelled systems have assumed that moisture transfer in the food product is instantaneous, or that perforations border on the package headspace resulting in a one-dimensional moisture profile in the food product. Where perforations border directly on the food product, or on a relatively small isolated air pocket, a localised two-dimensional moisture profile may result due to the relatively high water vapour transfer rate. In this case the localised region may become out of specification before the bulk of the food product. To investigate this process, it was necessary to model a two-dimensional system. Due to differences between systems with and without an isolated air pocket bordering the perforation such as different boundary conditions, these were modelled separately.

Work presented in this chapter again follows the same format as the standard food package moisture transfer model covered in Chapter 4. Some work has also previously been covered, therefore where repetition exists it is referred to the appropriate sections.

6.2 PERFORATION DIRECTLY BORDERING THE FOOD POWDER

6.2.1 Conceptual Model Development

6.2.1.1 Outline of Conceptualised System

A schematic diagram of the conceptualised food powder perforation system is shown in Figure 6-1. The system consists of a section of food powder directly bordering the

position of a perforation. There is no isolated pocket of air between the food powder and packaging at the position of the perforation. Due to symmetry about the axis which extends from the perforation perpendicular to the packaging, the system can be treated as two-dimensional. Moisture transfer occurs radially and axially to/from the perforation within the food powder. Provided the total thickness of the food powder in the axial and radial directions are sufficiently large, the moisture gradient in these respective directions will be approximately zero.

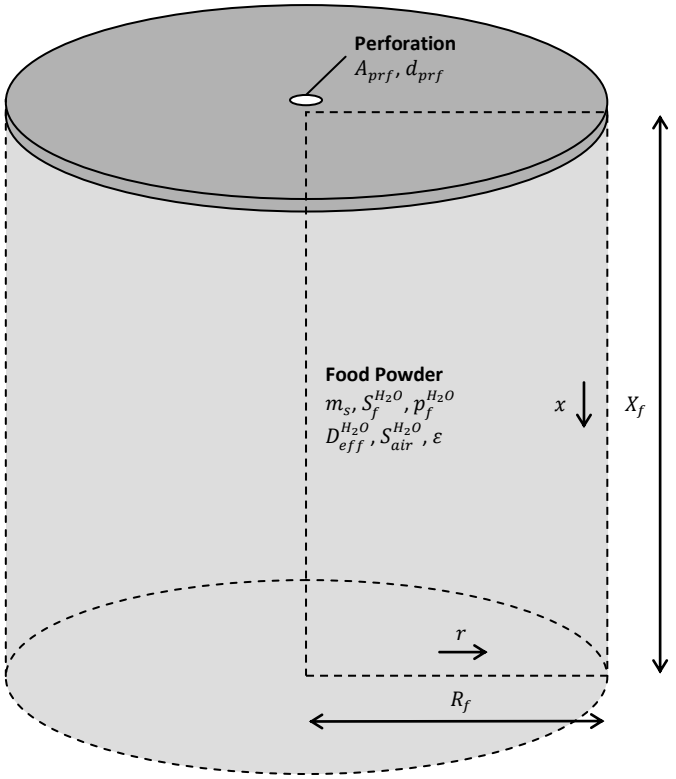

Figure 6-1: Schematic diagram of conceptualised food package system consisting of a perforation directly bordering a food powder.

6.2.1.2 Assumptions

Assumptions made for the two-dimensional perforation moisture transfer model with no air pocket bordering the perforation include many assumptions made previously (Sections 4.2.2 and 5.3.1.2). These include:

- Mass transfer at the surface of the food product and packaging is instantaneous.

- Temperature changes are instantaneous throughout the system.
- The package headspace and ambient are at atmospheric pressure.
- Water vapour exhibits ideal gas behaviour.
- The food does not respire.
- Moisture transfer in the food powder occurs only by diffusion in the vapour phase.
- Vapour and solid phases in the food powder are in local equilibrium.
- Physical properties of the food powder such as porosity and density of the food powder are constant throughout the system.
- Perforations consist of a perfect cylindrical geometry.

In addition, several other assumptions were required to simplify the modelling process for a two-dimensional system, which will be discussed in more detail.

6.2.1.2.1 Water Vapour Permeation through Packaging is Negligible

For a moisture gradient to form in a localised area of the food powder, it is expected that the water vapour transfer rate through the packaging will have to be relatively high. Therefore the perforation will likely be of a sufficient size so that permeation through the packaging relative to diffusion through the perforation will be negligible. This avoids the need to model permeation through the packaging, thereby greatly simplifying the model.

6.2.1.2.2 The System has a Regular Geometry

It was assumed that the packaging around the perforation is perfectly level. As a result the geometry of the system will be a perfect cylinder, thereby greatly simplifying the formulation of two-dimensional finite difference approximations. In practice the packaging will rarely be perfectly level, and the validity of this assumption will need to be analysed for individual applications. However it is believed a regular geometry model should give reasonable estimates of most real life systems.

6.2.1.2.3 Multiple Perforations are Independent

This assumption implies that moisture transfer in one section of the food powder due to one perforation is not affected by moisture transfer due to other perforations. For this assumption to be valid, the spacing between perforations will need to be greater or equal to $2R_f$, and the distance between perforations on oppose sides of a food package will have to be at least $2X_f$ (refer to Figure 6-1).

6.2.1.2.4 Diffusion is in Two-Dimensions Only

The assumption of a two-dimensional system is related to the assumptions of a regular system geometry and independent perforations. Where these assumptions are reasonable, a model consisting of two spatial dimensions should provide an appropriate representation of the system.

6.2.2 Mathematical Model Formulation

6.2.2.1 Variables

Variables defined in the model formulation are summarised in Table 6-1.

Table 6-1: List of model variables.

Symbol	Description	Unit	Class*
Δr_f	Width of node in radial direction of food powder	m	CV
Δx_f	Width of node in axial direction of food powder	m	CV
$A_{f,r}$	Area of node in radial direction	m^2	CV
$A_{f,x}$	Area of node in axial direction	m^2	CV
A_{prf}	Area of perforation in packaging	m^2	SI
C_{BET}	Guggenheim constant for BET isotherm of food	-	SI
C_{GAB}	Guggenheim constant for GAB isotherm of food	-	SI
$D_{air}^{H_2O}$	Diffusivity of water vapour in air	$m^2.s^{-1}$	CV

$D_{eff}^{H_2O}$	Effective diffusivity of water vapour in food powder	$m^2.s^{-1}$	CV
$J_{prf}^{H_2O}$	Diffusive flux of water vapour through perforation(s) in packaging	$mol.m^{-2}.s^{-1}$	CV
$M_{0,GAB}$	Moisture content of monolayer for GAB isotherm of food	(kg water).(kg solids)$^{-1}$	SI
$M_{1,BET}$	Moisture content of monolayer for BET isotherm of food	(kg water).(kg solids)$^{-1}$	SI
M_i	Initial moisture content of food	(kg water).(kg solids)$^{-1}$	SI
M_{r,H_2O}	Molecular mass of water	$kg.mol^{-1}$	SI
RH_a	Ambient relative humidity	%	CV
R_f	Thickness of food powder in radial direction	m	SI
$S_{air}^{H_2O}$	Solubility of water vapour in air	$mol.m^{-3}.Pa^{-1}$	CV
$S_f^{H_2O}$	Solubility of water vapour in food powder	$mol.m^{-3}.Pa^{-1}$	CV
X_T	Total thickness of packaging	m	SI
X_f	Thickness of food powder in axial direction	m	SI
b_{lin}	Slope of linear isotherm of food	–	SI
c_{lin}	Constant for linear isotherm of food	(kg water).(kg solids)$^{-1}$	SI
d_{prf}	Average diameter of perforations	m	SI
k_{GAB}	Constant for GAB isotherm of food	–	SI
m_s	Mass of solids in food product	kg	SI
$p_0^{H_2O}$	Saturated water vapour pressure	Pa	CV
$p_a^{H_2O}$	Water vapour pressure in ambient air	Pa	CV
$p_f^{H_2O}$	Water vapour pressure in food powder	Pa	D
$p_{f,i}^{H_2O}$	Initial water vapour pressure in food powder	Pa	SI
J	Total number of nodes in axial direction of food powder	–	SI
K	Total number of nodes in radial direction of food powder	–	SI
M	Moisture content of food	(kg water).(kg solids)$^{-1}$	CV
R	Ideal gas constant (8.314)	$m^3.Pa.K^{-1}.mol^{-1}$ or $J.K^{-1}.mol^{-1}$	SI
T	Temperature	K	CV

j	Node number in axial direction	–	SI
k	Node number in radial direction	–	SI
r	Spatial position in food powder in radial direction	m	I
t	Time	s	I
x	Spatial position in food powder in axial direction	m	I
ε	Porosity of food powder	-	SI

*I = independent variable, D = dependent variable, CV = consequential variable, SI = system input

The conceptualised system requires three independent variables, time and spatial position in the food powder in two-dimensions. One dependent variable, the water vapour pressure in the food powder, is to be modelled, therefore one partial differential equation (PDE) will be required consisting of two spatial dimensions. As a result, at least four boundary conditions are needed, as well as one initial condition assuming a uniform initial water vapour pressure.

6.2.2.2 Word Balances and Equations

6.2.2.2.1 PDE for Water Vapour Pressure in Food Powder

The PDE for one-dimensional unsteady-state diffusion of water vapour in the food powder was previously derived in Section 5.3.2.2.2. Extending this model to two-dimensional unsteady-state diffusion in a finite cylinder configuration is a relatively simple process (Cleland, 2000). The resulting PDE is as follows:

$$\left(\varepsilon S_{air}^{H_2O} + (1-\varepsilon) S_f^{H_2O}\right) \frac{\partial p_f^{H_2O}}{\partial t} = \frac{\partial}{\partial x}\left(D_{eff}^{H_2O} S_{air}^{H_2O} \frac{\partial p_f^{H_2O}}{\partial x}\right) + \frac{\partial}{\partial r}\left(D_{eff}^{H_2O} S_{air}^{H_2O} \frac{\partial p_f^{H_2O}}{\partial r}\right) + \frac{D_{eff}^{H_2O} S_{air}^{H_2O}}{r} \frac{\partial p_f^{H_2O}}{\partial r} \quad \textbf{(6-1)}$$

$$for\ t \geq 0,\ 0 < x < X_f,\ 0 < r < R_f$$

where:

ε = Porosity of food powder (-)

$S_{air}^{H_2O}$ = Solubility of water vapour in air (mol.m^{-3}.Pa^{-1})

$S_{f}^{H_2O}$ = Solubility of water vapour in food powder (mol.m^{-3}.Pa^{-1})

$p_{f}^{H_2O}$ = Water vapour pressure in food powder (Pa)

$D_{eff}^{H_2O}$ = Effective diffusivity of water vapour in food powder (m^2.s^{-1})

t = Time (s)

x = Spatial position in food powder in axial direction (m^2.s^{-1})

r = Spatial position in food powder in radial direction (m^2.s^{-1})

X_f = Thickness of food powder in axial direction (m^2.s^{-1})

R_f = Thickness of food powder in radial direction (m^2.s^{-1})

6.2.2.2.2 Equation for Diffusive Flux of Water Vapour through Perforation(s) in Polymer Liner

Equations for diffusive flux of water vapour through perforation(s) were previously derived for the standard food package model (Section 4.3.2.9). Expressing these specifically for this model, the internal water vapour pressure will be equal to that of the food directly bordering the perforation. Therefore:

$$J_{prf}^{H_2O} = \frac{D_{air}^{H_2O} S_{air}^{H_2O}}{X_T}\left(p_a^{H_2O} - p_{f,x=0,r=0}^{H_2O}\right) \quad \textbf{(6-2)}$$

for $d_{prf} \geq 1 \times 10^{-5}$ m

$$J_{prf}^{H_2O} = \frac{D_{air}^{H_2O} S_{air}^{H_2O}}{\left(X_T + \frac{d_{prf}}{2}\right)}\left(p_a^{H_2O} - p_{f,x=0,r=0}^{H_2O}\right) \quad \textbf{(6-3)}$$

for $1 \times 10^{-7} \leq d_{prf} < 1 \times 10^{-5}$ m

$$J_{prf}^{H_2O} = \frac{48.5 d_{prf}}{RTX_T}\left(\frac{T}{1000 M_{r,H_2O}}\right)^{0.5}\left(p_a^{H_2O} - p_{f,x=0,r=0}^{H_2O}\right) \quad \textbf{(6-4)}$$

for $d_{prf} < 1 \times 10^{-7}$ m

where:

X_T = Total thickness of packaging (m)

$p_a^{H_2O}$ = Water vapour pressure in ambient air (Pa)

d_{prf} = Average diameter of perforations in packaging (m)

6.2.2.3 Boundary Conditions

As mentioned previously, at least four boundary conditions are required for the two-dimensional system. In fact, an additional boundary condition is needed for the node directly bordering the perforation. Therefore:

$$w = J_{prf}^{H_2O} A_{prf}$$
$$\text{for } t \geq 0,\ x = 0,\ 0 \leq r \leq \frac{d_{prf}}{2} \quad \textbf{(6-5)}$$

$$\frac{dp_f^{H_2O}}{dx} = 0$$
$$\text{for } t \geq 0,\ x = 0,\ \frac{d_{prf}}{2} < r \leq R_f \quad \textbf{(6-6)}$$

$$\frac{dp_f^{H_2O}}{dx} = 0$$
$$\text{for } t \geq 0,\ x = X_f \quad \textbf{(6-7)}$$

$$\frac{dp_f^{H_2O}}{dr} = 0$$
$$\text{for } t \geq 0,\ r = 0 \text{ and } r = R_f \quad \textbf{(6-8)}$$

where:

A_{prf} = Total area of perforation(s) in packaging (m^2)

6.2.2.4 Initial Conditions

As mentioned previously, the initial water vapour pressure in the food powder will be considered uniform. Therefore:

$$p_f^{H_2O} = p_{f,i}^{H_2O}$$
$$at\ t = 0 \quad \textbf{(6-9)}$$

where:

$p_{f,i}^{H_2O}$ = Initial water vapour pressure in food powder (Pa)

6.2.3 Solution

6.2.3.1 Finite Difference Grid

The finite difference grid used for the food powder system is illustrated in Figure 6-2. As described earlier (Section 6.2.1.1), the three-dimensional cylindrical system could be represented by a two-dimensional plane due to symmetry about the axis. The food powder was divided into J space steps in the axial direction each with a thickness of Δx_f, and K space steps in the radial direction each with a thickness of Δr_f. Thus:

$$\Delta x_f = \frac{X_f}{J} \quad \textbf{(6-10)}$$

$$\Delta r_f = \frac{R_f}{K} \quad \textbf{(6-11)}$$

where:

Δx_f = Width of node in axial direction of food powder (m)

J = Number of nodes in axial direction (-)

Δr_f = Width of node in radial direction of food powder (m)

K = Number of nodes in radial direction (-)

The section of the food powder contained within each node was designated a node number from $j = 1, k = 1$ at the powder surface bordering the axis of symmetry (directly adjacent to the perforation), to $j = J + 1, k = K + 1$ at a depth X_f into the food powder and length R_f from the axis of symmetry (the furthest point from the perforation). As usual the water vapour pressure within each node was treated as uniform.

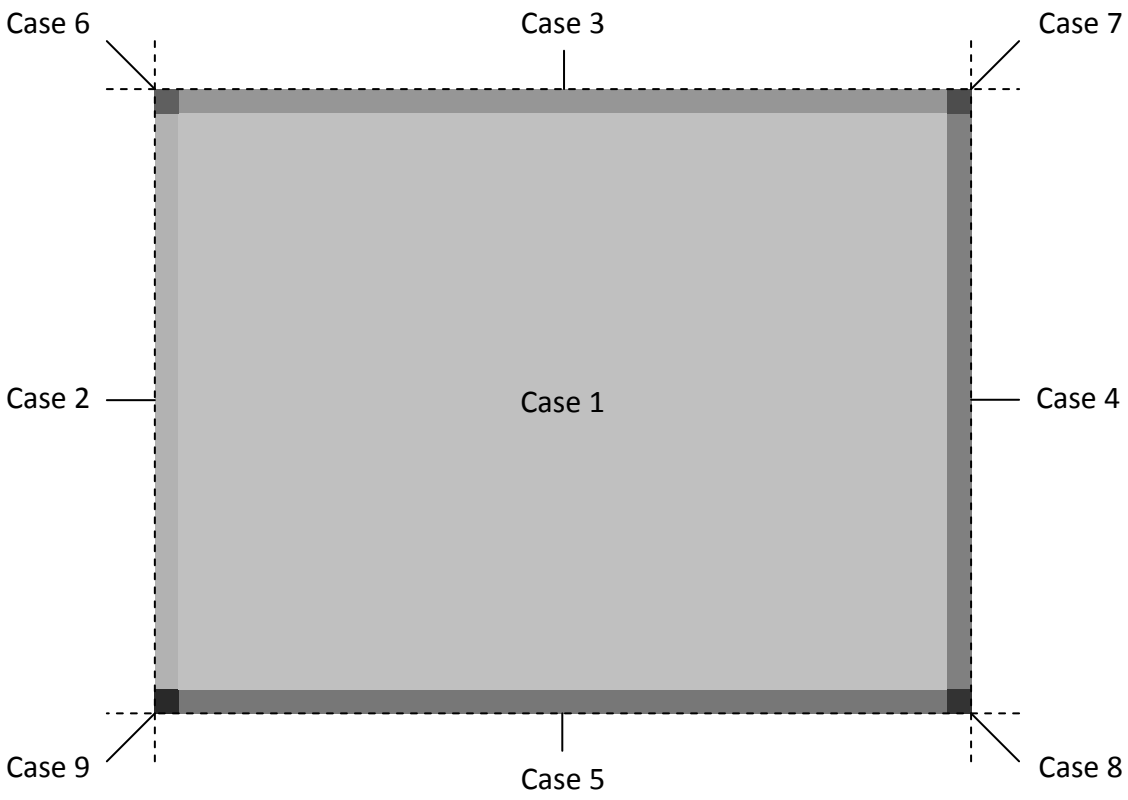

Figure 6-2: Finite difference grid for two-dimensional food powder system.

6.2.3.2 Finite Difference Approximations

6.2.3.2.1 Case 1

Nodes:

$$j = 2{:}J, k = 2{:}K$$

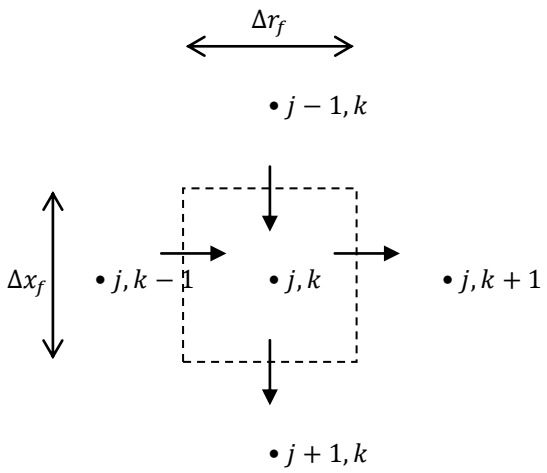

Figure 6-3: Diagram of finite difference approximations for case 1.

$$\frac{dp_{f,j,k}^{H_2O}}{dt} = \frac{D_{eff}^{H_2O} S_{air}^{H_2O}}{V_f \left[\varepsilon S_{air}^{H_2O} + (1-\varepsilon) S_f^{H_2O}\right]} \left[A_{f,x} \frac{\left(p_{f,j-1,k}^{H_2O} - p_{f,j,k}^{H_2O}\right)}{\Delta x_f} - A_{f,x} \frac{\left(p_{f,j,k}^{H_2O} - p_{f,j+1,k}^{H_2O}\right)}{\Delta x_f} + \left(A_{f,r}\right)_{k-\frac{1}{2}} \frac{\left(p_{f,j,k-1}^{H_2O} - p_{f,j,k}^{H_2O}\right)}{\Delta r_f} - \left(A_{f,r}\right)_{k+\frac{1}{2}} \frac{\left(p_{f,j,k}^{H_2O} - p_{f,j,k+1}^{H_2O}\right)}{\Delta r_f} \right] \quad \textbf{(6-12)}$$

for $t \geq 0$

where:

$$V_f = 2\pi(k-1)\Delta {r_f}^2 \Delta x_f \quad \textbf{(6-13)}$$

$$A_{f,x} = 2\pi(k-1)\Delta {r_f}^2 \quad \textbf{(6-14)}$$

$$\left(A_{f,r}\right)_{k-\frac{1}{2}} = 2\pi\left(k-\frac{3}{2}\right)\Delta r_f \Delta x_f \quad \textbf{(6-15)}$$

$$\left(A_{f,r}\right)_{k+\frac{1}{2}} = 2\pi\left(k-\frac{1}{2}\right)\Delta r_f \Delta x_f \quad \textbf{(6-16)}$$

6.2.3.2.2 Case 2

Nodes:

$$j = 2{:}J,\ k = 1$$

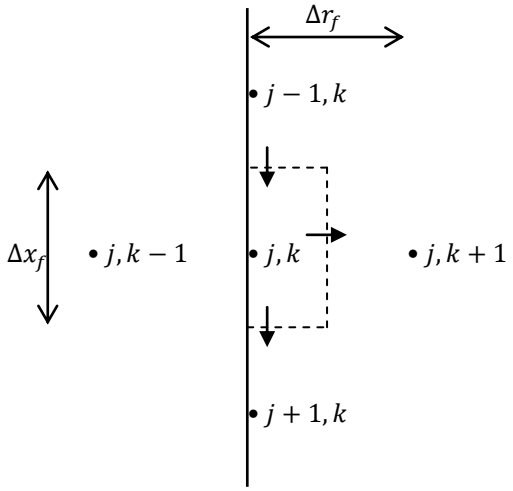

Figure 6-4: Diagram of finite difference approximation for case 2.

$$\frac{dp_{f,j,k}^{H_2O}}{dt} = \frac{D_{eff}^{H_2O} S_{air}^{H_2O}}{V_f \left[\varepsilon S_{air}^{H_2O} + (1-\varepsilon) S_f^{H_2O}\right]} \left[A_{f,x} \frac{\left(p_{f,j-1,k}^{H_2O} - p_{f,j,k}^{H_2O}\right)}{\Delta x_f} - A_{f,x} \frac{\left(p_{f,j,k}^{H_2O} - p_{f,j+1,k}^{H_2O}\right)}{\Delta x_f} - \left(A_{f,r}\right)_{k+\frac{1}{2}} \frac{\left(p_{f,j,k}^{H_2O} - p_{f,j,k+1}^{H_2O}\right)}{\Delta r_f} \right] \quad \textbf{(6-17)}$$

for $t \geq 0$

where:

$$V_f = \frac{\pi}{4} {\Delta r_f}^2 \Delta x_f \quad \textbf{(6-18)}$$

$$A_{f,x} = \frac{\pi}{4} {\Delta r_f}^2 \quad \textbf{(6-19)}$$

$$\left(A_{f,r}\right)_{k+\frac{1}{2}} = \pi \Delta r_f \Delta x_f \quad \textbf{(6-20)}$$

6.2.3.2.3 Case 3

Nodes:

$$j = 1, k = 2{:}K$$

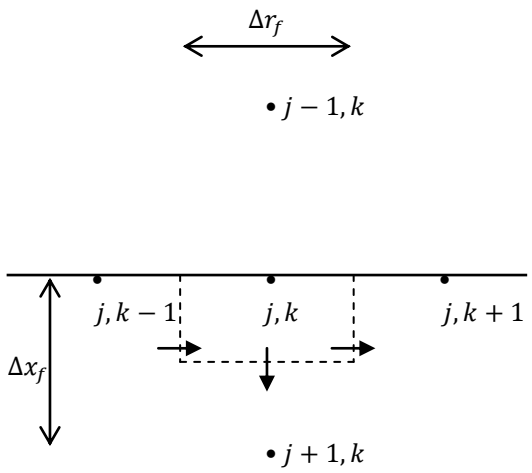

Figure 6-5: Diagram of finite difference approximation for case 3.

$$\frac{dp_{f,j,k}^{H_2O}}{dt} = \frac{D_{eff}^{H_2O} S_{air}^{H_2O}}{V_f \left[\varepsilon S_{air}^{H_2O} + (1-\varepsilon) S_f^{H_2O}\right]} \left[-A_{f,x} \frac{\left(p_{f,j,k}^{H_2O} - p_{f,j+1,k}^{H_2O}\right)}{\Delta x_f} + \left(A_{f,r}\right)_{k-\frac{1}{2}} \frac{\left(p_{f,j,k-1}^{H_2O} - p_{f,j,k}^{H_2O}\right)}{\Delta r_f} - \left(A_{f,r}\right)_{k+\frac{1}{2}} \frac{\left(p_{f,j,k}^{H_2O} - p_{f,j,k+1}^{H_2O}\right)}{\Delta r_f} \right] \quad \textbf{(6-21)}$$

for $t \geq 0$

where:

$$V_f = \pi(k-1)\Delta {r_f}^2 \Delta x_f \quad \textbf{(6-22)}$$

$$A_{f,x} = 2\pi(k-1)\Delta {r_f}^2 \quad \textbf{(6-23)}$$

$$\left(A_{f,r}\right)_{k-\frac{1}{2}} = \pi\left(k-\frac{3}{2}\right)\Delta r_f \Delta x_f \quad \textbf{(6-24)}$$

$$\left(A_{f,r}\right)_{k+\frac{1}{2}} = \pi\left(k-\frac{1}{2}\right)\Delta r_f \Delta x_f \quad \textbf{(6-25)}$$

6.2.3.2.4 Case 4

Nodes:

$$j = 2{:}J, k = K+1$$

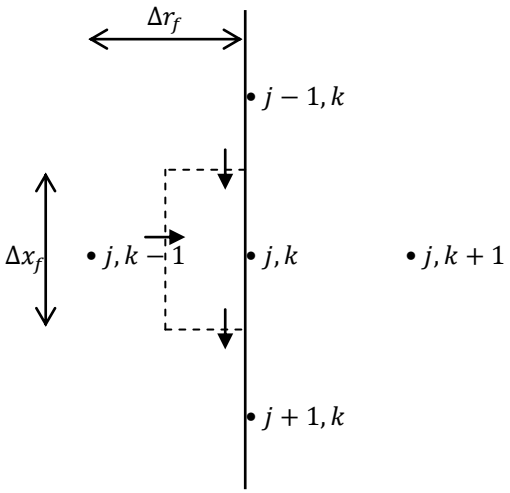

Figure 6-6: Diagram of finite difference approximation for case 4.

$$\frac{dp_{f,j,k}^{H_2O}}{dt} = \frac{D_{eff}^{H_2O} S_{air}^{H_2O}}{V_f \left[\varepsilon S_{air}^{H_2O} + (1-\varepsilon) S_f^{H_2O}\right]} \left[A_{f,x} \frac{\left(p_{f,j-1,k}^{H_2O} - p_{f,j,k}^{H_2O}\right)}{\Delta x_f} - A_{f,x} \frac{\left(p_{f,j,k}^{H_2O} - p_{f,j+1,k}^{H_2O}\right)}{\Delta x_f} + \left(A_{f,r}\right)_{k-\frac{1}{2}} \frac{\left(p_{f,j,k-1}^{H_2O} - p_{f,j,k}^{H_2O}\right)}{\Delta r_f} \right] \quad \textbf{(6-26)}$$

for $t \geq 0$

where:

$$V_f = \pi \left(k - \frac{5}{4}\right) {\Delta r_f}^2 \Delta x_f \quad \textbf{(6-27)}$$

$$A_{f,x} = \pi \left(k - \frac{5}{4}\right) {\Delta r_f}^2 \quad \textbf{(6-28)}$$

$$\left(A_{f,r}\right)_{k-\frac{1}{2}} = 2\pi \left(k - \frac{3}{2}\right) \Delta r_f \Delta x_f \quad \textbf{(6-29)}$$

6.2.3.2.5 Case 5

Node:

$$j = J+1,\ k = 2{:}K$$

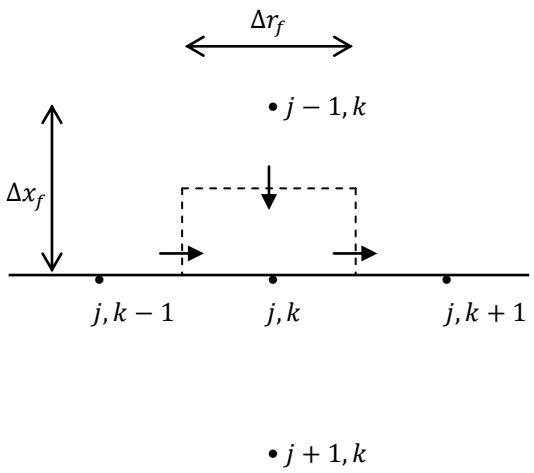

Figure 6-7: Diagram of finite difference approximation for case 5.

$$\frac{dp_{f,j,k}^{H_2O}}{dt} = \frac{D_{eff}^{H_2O} S_{air}^{H_2O}}{V_f \left[\varepsilon S_{air}^{H_2O} + (1-\varepsilon) S_f^{H_2O}\right]} \left[A_{f,x} \frac{\left(p_{f,j-1,k}^{H_2O} - p_{f,j,k}^{H_2O}\right)}{\Delta x_f} + \left(A_{f,r}\right)_{k-\frac{1}{2}} \frac{\left(p_{f,j,k-1}^{H_2O} - p_{f,j,k}^{H_2O}\right)}{\Delta r_f} - \left(A_{f,r}\right)_{k+\frac{1}{2}} \frac{\left(p_{f,j,k}^{H_2O} - p_{f,j,k+1}^{H_2O}\right)}{\Delta r_f} \right] \quad \textbf{(6-30)}$$

for $t \geq 0$

where:

$$V_f = \pi(k-1)\Delta {r_f}^2 \Delta x_f \quad \textbf{(6-31)}$$

$$A_{f,x} = 2\pi(k-1)\Delta {r_f}^2 \quad \textbf{(6-32)}$$

$$\left(A_{f,r}\right)_{k-\frac{1}{2}} = \pi\left(k-\frac{3}{2}\right)\Delta r_f \Delta x_f \quad \textbf{(6-33)}$$

$$\left(A_{f,r}\right)_{k+\frac{1}{2}} = \pi\left(k-\frac{1}{2}\right)\Delta r_f \Delta x_f \quad \textbf{(6-34)}$$

6.2.3.2.6 Case 6

Node:

$j = 1, k = 1$

Case 6 refers to the node directly adjacent to the perforation. Note that for most realistic simulations of a system with no isolated pocket bordering the perforation, the

diameter of the perforation should be much smaller than the diameter of the node. Therefore case 6 will be the only node with a moisture flux across the boundary. In the unlikely situation where the perforation is larger than the size of the node, the model for a system with an isolated air pocket adjacent to the perforation (Section 6.3) can be used.

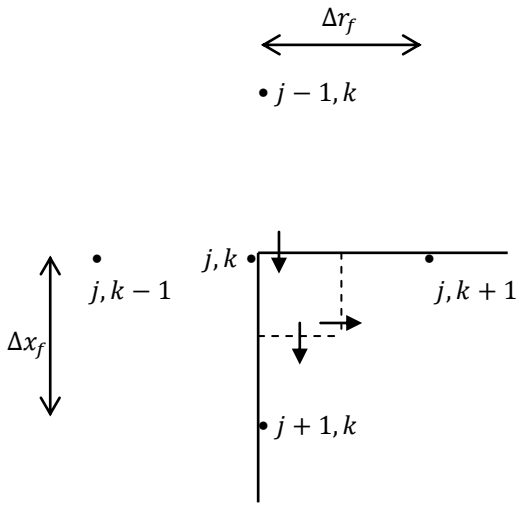

Figure 6-8: Diagram of finite difference approximations for case 6.

$$\frac{dp_{f,j,k}^{H_2O}}{dt} = \frac{1}{V_f\left[\varepsilon S_{air}^{H_2O} + (1-\varepsilon)S_f^{H_2O}\right]}\left[J_{prf,lnr}^{H_2O} A_{prf,lnr} + D_{eff}^{H_2O} S_{air}^{H_2O}\left(-A_{f,x}\frac{\left(p_{f,j,k}^{H_2O} - p_{f,j+1,k}^{H_2O}\right)}{\Delta x_f} - \left(A_{f,r}\right)_{k+\frac{1}{2}}\frac{\left(p_{f,j,k}^{H_2O} - p_{f,j,k+1}^{H_2O}\right)}{\Delta r_f}\right)\right] \quad \textbf{(6-35)}$$

for $t \geq 0$

where:

$$V_f = \frac{\pi}{8}\Delta {r_f}^2 \Delta x_f \quad \textbf{(6-36)}$$

$$A_{f,x} = \frac{\pi}{4}\Delta {r_f}^2 \quad \textbf{(6-37)}$$

$$\left(A_{f,r}\right)_{k+\frac{1}{2}} = \frac{\pi}{2}\Delta r_f \Delta x_f \quad \textbf{(6-38)}$$

6.2.3.2.7 Case 7

Node:

$$j = 1, k = K + 1$$

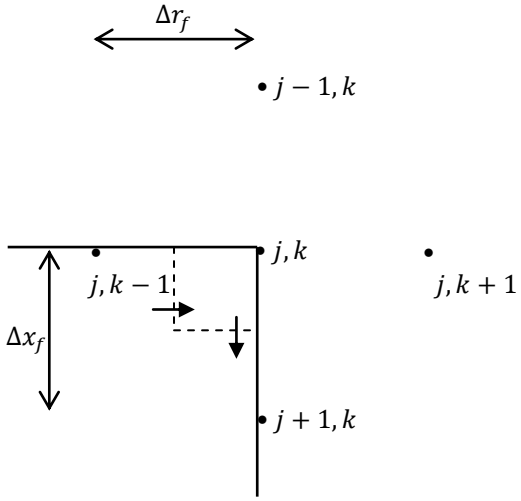

Figure 6-9: Diagram of finite difference approximation for case 7.

$$\frac{dp_{f,j,k}^{H_2O}}{dt} = \frac{D_{eff}^{H_2O} S_{air}^{H_2O}}{V_f \left[\varepsilon S_{air}^{H_2O} + (1-\varepsilon) S_f^{H_2O}\right]} \left[-A_{f,x} \frac{\left(p_{f,j,k}^{H_2O} - p_{f,j+1,k}^{H_2O}\right)}{\Delta x_f} + \left(A_{f,r}\right)_{k-\frac{1}{2}} \frac{\left(p_{f,j,k-1}^{H_2O} - p_{f,j,k}^{H_2O}\right)}{\Delta r_f} \right] \quad \textbf{(6-39)}$$

for $t \geq 0$

where:

$$V_f = \frac{\pi}{2}\left(k - \frac{5}{4}\right) {\Delta r_f}^2 \Delta x_f \quad \textbf{(6-40)}$$

$$A_{f,x} = \pi \left(k - \frac{5}{4}\right) {\Delta r_f}^2 \quad \textbf{(6-41)}$$

$$\left(A_{f,r}\right)_{k-\frac{1}{2}} = \pi \left(k - \frac{3}{2}\right) \Delta r_f \Delta x_f \quad \textbf{(6-42)}$$

6.2.3.2.8 Case 8

Node:

$$j = J + 1, k = K + 1$$

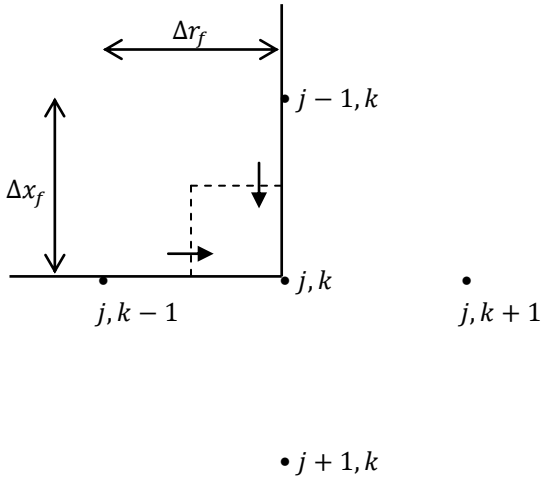

Figure 6-10: Diagram of finite difference approximation for case 8.

$$\frac{dp_{f,j,k}^{H_2O}}{dt} = \frac{D_{eff}^{H_2O} S_{air}^{H_2O}}{V_f \left[\varepsilon S_{air}^{H_2O} + (1-\varepsilon) S_f^{H_2O}\right]} \left[A_{f,x} \frac{\left(p_{f,j-1,k}^{H_2O} - p_{f,j,k}^{H_2O}\right)}{\Delta x_f} + \left(A_{f,r}\right)_{k-\frac{1}{2}} \frac{\left(p_{f,j,k-1}^{H_2O} - p_{f,j,k}^{H_2O}\right)}{\Delta r_f} \right] \quad \textbf{(6-43)}$$

for $t \geq 0$

where:

$$V_f = \frac{\pi}{2}\left(k - \frac{5}{4}\right) {\Delta r_f}^2 \Delta x_f \quad \textbf{(6-44)}$$

$$A_{f,x} = \pi \left(k - \frac{5}{4}\right) {\Delta r_f}^2 \quad \textbf{(6-45)}$$

$$\left(A_{f,r}\right)_{k-\frac{1}{2}} = \pi \left(k - \frac{3}{2}\right) \Delta r_f \Delta x_f \quad \textbf{(6-46)}$$

6.2.3.2.9 Case 9

Node:

$j = J + 1, k = 1$

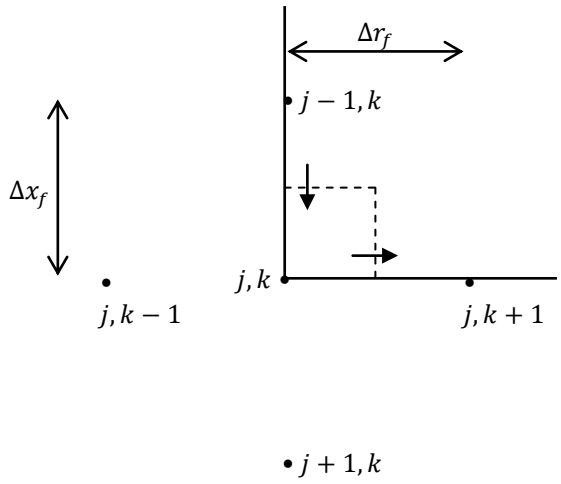

Figure 6-11: Diagram of finite difference approximation for case 9.

$$\frac{dp_{f,j,k}^{H_2O}}{dt} = \frac{D_{eff}^{H_2O} S_{air}^{H_2O}}{V_f \left[\varepsilon S_{air}^{H_2O} + (1-\varepsilon) S_f^{H_2O}\right]} \left[A_{f,x} \frac{\left(p_{f,j-1,k}^{H_2O} - p_{f,j,k}^{H_2O}\right)}{\Delta x_f} - \left(A_{f,r}\right)_{k+\frac{1}{2}} \frac{\left(p_{f,j,k}^{H_2O} - p_{f,j,k+1}^{H_2O}\right)}{\Delta r_f} \right] \quad \textbf{(6-47)}$$

for $t \geq 0$

where:

$$V_f = \frac{\pi}{8} \Delta {r_f}^2 \Delta x_f \quad \textbf{(6-48)}$$

$$A_{f,x} = \frac{\pi}{4} \Delta {r_f}^2 \quad \textbf{(6-49)}$$

$$\left(A_{f,r}\right)_{k+\frac{1}{2}} = \frac{\pi}{2} \Delta r_f \Delta x_f \quad \textbf{(6-50)}$$

6.2.3.3 MATLAB® Solution

The formulated finite difference approximations for the water vapour pressure in the food powder were converted to MATLAB® code. The resulting script and function files are shown in Appendix E.1.2.2.

6.2.3.4 Example Simulation

A preliminary simulation was carried out for a skim milk powder bag with a perforation. Where possible, model parameters were based on known or literature values, although several values were approximate only. The thickness of skim milk powder in the radial and axial directions were based on a distance at which the water vapour pressure remained practically unchanged over the simulation period. Model predictions are shown in Figure 6-12 and Figure 6-13. As expected for a food powder, after 365 days the water vapour pressure is highest next to the perforation, decreasing further into the skim milk powder until a constant value equal to the initial water vapour pressure is reached. The average water vapour pressure in the section of powder considered also rises relatively linearly over the simulation period, which appears reasonable.

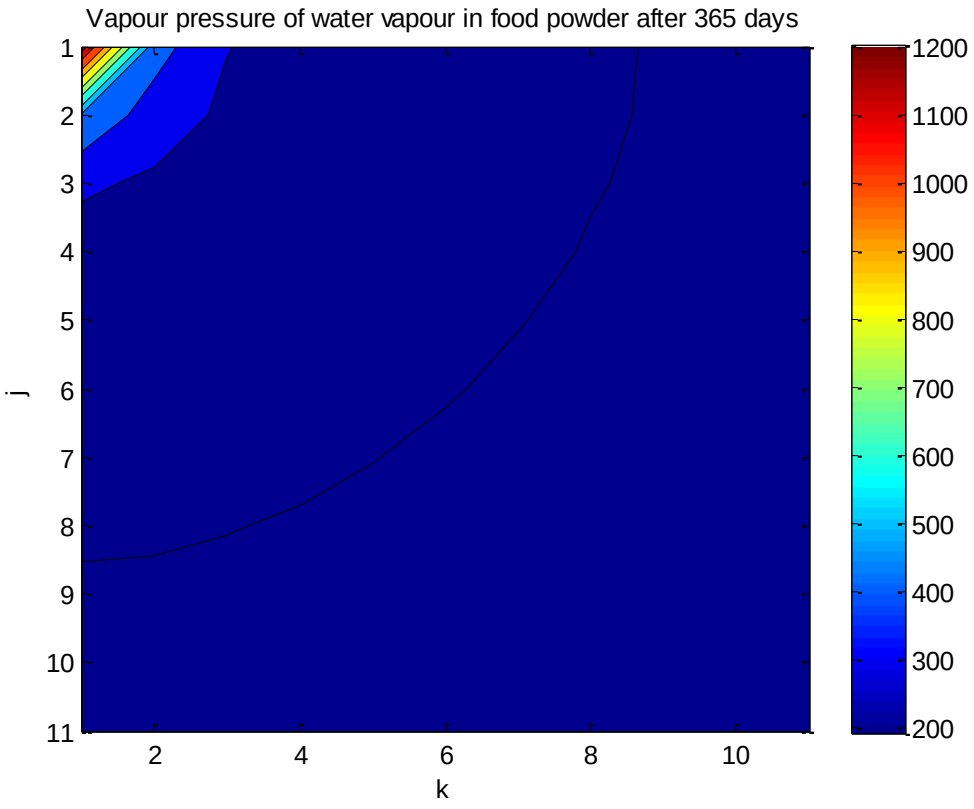

Figure 6-12: Model predictions of water vapour pressure profile in skim milk powder after 365 days at 20°C and 75% RH.

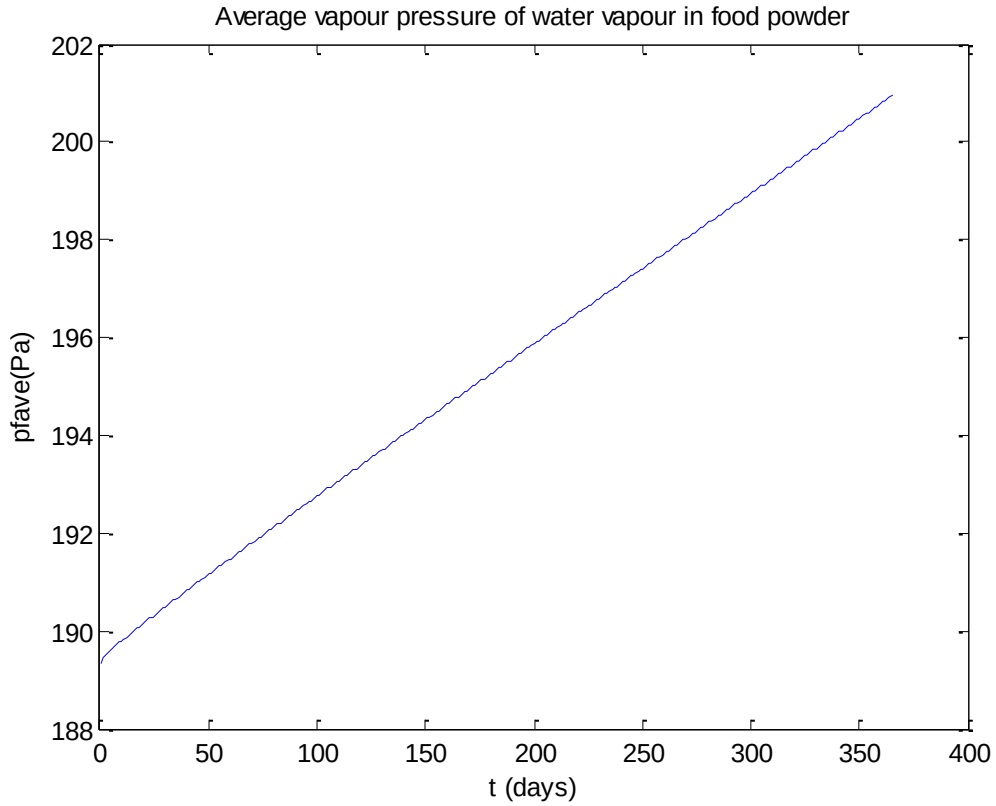

Figure 6-13: Model predictions of average water vapour pressure in skim milk powder over 365 days at 20°C and 75% RH.

6.2.3.5 Error Checks

As usual, error checks were carried out as for previous models (Section 4.4.5). These are summarised in Appendix E.1.3. Numerical error checks suggested a default relative error tolerance value of 1×10^{-3} and 10 nodes in both axial and radial directions were numerically accurate and allowed for a reasonable solving time. Mathematical error checks against analytical solutions were not possible due to the nature of boundary conditions.

6.3 ISOLATED AIR POCKET ADJACENT TO THE PERFORATION

6.3.1 Conceptual Model Development

6.3.1.1 Outline of Conceptualised System

A schematic diagram of the conceptualised food powder perforation system with an air pocket adjacent to the perforation is shown in Figure 6-14. The system is very similar to the system with no air pocket outlined previously (Section 6.2.1.1), although in this case moisture transfer through the perforation is distributed over a larger food powder surface area due to the isolated pocket of air between the food powder and packaging at the position of the perforation. The system will again be treated as two-dimensional; however the axis of symmetry will be positioned at the centre of the air pocket rather than the perforation.

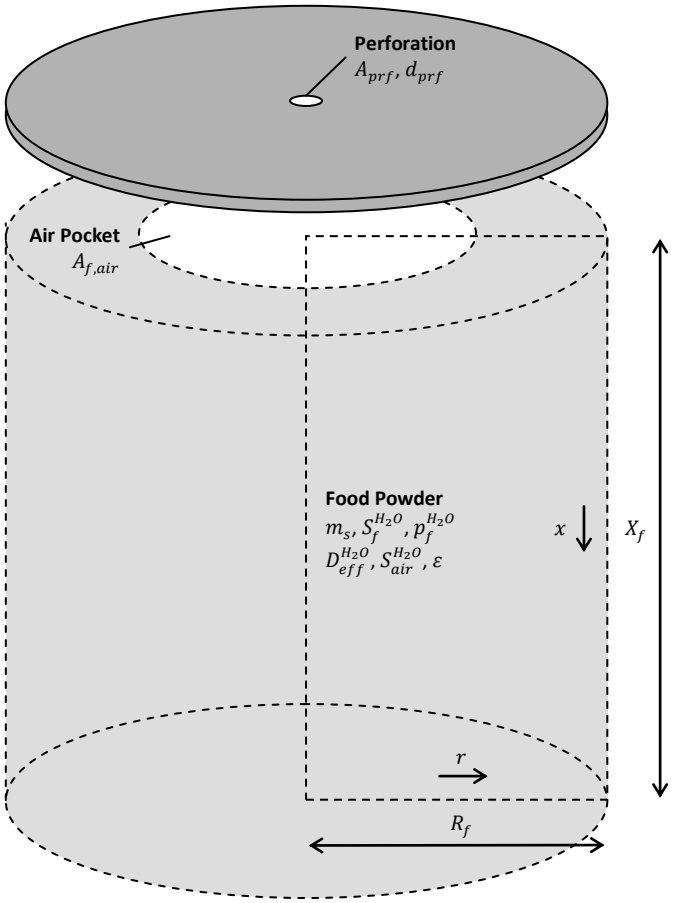

Figure 6-14: Schematic diagram of conceptualised food package system consisting of a perforation adjacent to an isolated air pocket and food powder.

6.3.1.2 Assumptions

All assumptions made for the system with no air pocket remain valid. These are as follows:

- Mass transfer at the surface of the food product and packaging is instantaneous.
- Temperature changes are instantaneous throughout the system.
- The package headspace and ambient are at atmospheric pressure.
- Water vapour exhibits ideal gas behaviour.
- Moisture transfer in the food powder occurs only by diffusion in the vapour phase.
- Vapour and solid phases in the food powder are in local equilibrium.
- Water vapour permeation through the packaging is negligible.
- Moisture transfer in one section of the food powder due to one perforation is not affected by moisture transfer due to other perforations.
- Physical properties of the food powder such as porosity and density are constant throughout the system.
- Instantaneous moisture transfer through air in the air pocket.

The assumption of a regular geometry is also expected to remain reasonable. To maintain a cylindrical geometry, it was assumed that the food powder has a level surface, and that the isolated air pocket is circular with no depth into the powder. Such assumptions are fairly approximate, however it is believed the formulated model should give useful predictions.

6.3.2 Mathematical Model Formulation

6.3.2.1 Variables

Variables for the two-dimensional perforation model with an isolated air pocket adjacent to the perforation include those previously defined for the system with no air

pocket (Section 6.2.2.1). Additional variables required to account for the isolated air pocket are summarised in Table 6-2.

Table 6-2: List of model variables.

Symbol	Description	Unit	Class*
$A_{f,air}$	Area of air pocket in contact with food powder	m^2	SI
$A_{f,x,air}$	Area of node in axial direction in contact with air pocket	m^2	CV
K_{air}	Node number in radial direction positioned at edge of air pocket	-	CV
$p_{ap}^{H_2O}$	Water vapour pressure in air pocket	Pa	CV

*I = independent variable, D = dependent variable, CV = consequential variable, SI = system input

No additional independent or dependent variables were introduced to account for the isolated air pocket, therefore the model will still consist of a single PDE. At least four boundary conditions will still be needed, as well as a single initial condition.

6.3.2.2 Equations

6.3.2.2.1 Equation for Diffusive Flux of Water Vapour through Perforation(s) in Polymer Liner

Using the water vapour pressure in the air pocket, equations for the diffusive flux of water vapour through the perforation (Equations 6-2 to 6-4) can be expressed specifically for the system with an air pocket as follows:

$$J_{prf}^{H_2O} = \frac{D_{air}^{H_2O} S_{air}^{H_2O}}{X_T}\left(p_a^{H_2O} - p_{ap}^{H_2O}\right) \quad \textbf{(6-51)}$$

for $d_{prf} \geq 1 \times 10^{-5}$ m

$$J_{prf}^{H_2O} = \frac{D_{air}^{H_2O} S_{air}^{H_2O}}{\left(X_T + \frac{d_{prf}}{2}\right)}\left(p_a^{H_2O} - p_{ap}^{H_2O}\right) \quad \textbf{(6-52)}$$

for $1 \times 10^{-7} \leq d_{prf} < 1 \times 10^{-5}$ m

$$J_{prf}^{H_2O} = \frac{48.5 d_{prf}}{RTX_T}\left(\frac{T}{1000 M_{r,H_2O}}\right)^{0.5}\left(p_a^{H_2O} - p_{ap}^{H_2O}\right) \quad \textbf{(6-53)}$$

$$for\ d_{prf} < 1 \times 10^{-7}\ \text{m}$$

6.3.2.3 Boundary Conditions

Similar to previously, the diffusive flux through the perforation was assumed to be distributed evenly over the surface area of food powder in contact with the air pocket, taking into account the different areas of contact for each node. Therefore the following changes were made to the previously derived boundary conditions (Section 6.2.2.3):

$$w = J_{prf}^{H_2O} A_{prf} \frac{A_{f,x}}{A_{f,air}} \quad \textbf{(6-54)}$$

$$for\ t \geq 0,\ x = 0,\ 0 \leq r < R_{air}$$

$$w = J_{prf}^{H_2O} A_{prf} \frac{A_{f,x,air}}{A_{f,air}} \quad \textbf{(6-55)}$$

$$for\ t \geq 0,\ x = 0,\ r = R_{air}$$

$$\frac{dp_f^{H_2O}}{dx} = 0 \quad \textbf{(6-56)}$$

$$for\ t \geq 0,\ x = 0,\ R_{air} < r \leq R_f$$

6.3.3 Solution

6.3.3.1 Equation for Water Vapour Pressure in Air Pocket

In the case of an isolated air pocket adjacent to the perforation, the internal water vapour pressure will be influenced by multiple nodes in the food powder rather than a single node bordering the perforation. Therefore, to allow the diffusive flux through perforations to be determined, the water vapour pressure in the air pocket needs to be modelled. To avoid the need for an additional ODE as well as complexities associated with the air pocket not aligning perfectly with designated nodes, the water vapour pressure in the air pocket was assumed to be the average of the nodes in contact with the air pocket,

taking into account the different areas of contact for each node. As a result, the following expression was derived:

$$p_{ap}^{H_2O} = \left[\sum_{k=1}^{K_{air}-1} p_{f,j=1,k}^{H_2O} A_{f,x} + p_{f,j=1,k=K_{air}}^{H_2O} A_{f,x,air} \right] \Big/ A_{air} \quad \textbf{(6-57)}$$

where:

$$A_{f,x} = \frac{\pi}{4} \Delta {r_f}^2 \quad for\ k = 1 \quad \textbf{(6-58)}$$

$$A_{f,x} = 2\pi(k-1) \Delta {r_f}^2 \quad for\ k = 2 : K_{air} - 1 \quad \textbf{(6-59)}$$

$$A_{f,x,air} = A_{f,air} - \pi \left(k - \frac{3}{2}\right)^2 \Delta {r_f}^2 \quad \textbf{(6-60)}$$

6.3.3.2 Finite Difference Grid

The finite difference grid used for the food powder system is illustrated in Figure 6-15. This is very similar to that previously developed for the system with no air pocket, with the same nodes designations. However, two additional finite difference approximations were required for the food powder boundary condition as a result of the air pocket.

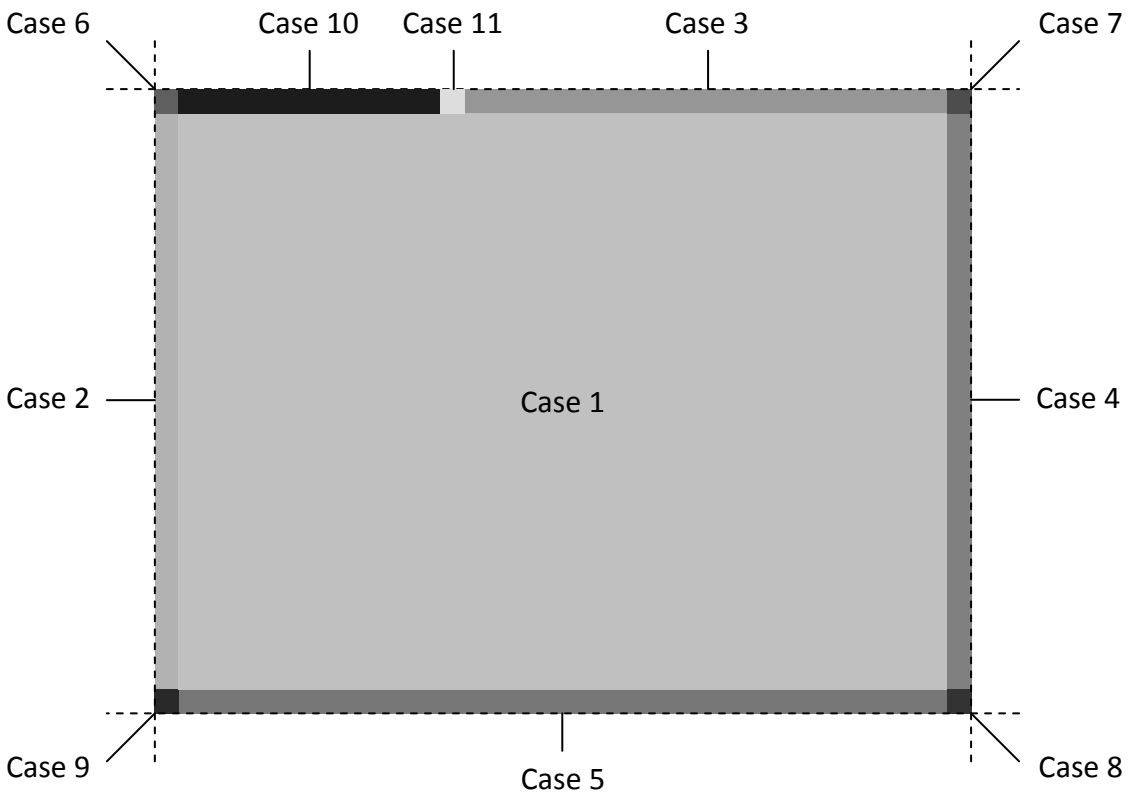

Figure 6-15: Finite difference grid for food product.

6.3.3.3 Finite Difference Approximations

Finite difference approximations for the perforation model with no air pocket were previously covered in Section 6.2.3.2. Changes made to case 6, as well as the two additional finite difference approximations required for the air pocket, case 10 and 11, are summarised below. For this model case 3 applies to nodes $j = 1, k = K_{air} + 1 : K$.

6.3.3.3.1 Case 6

Node:

$j = 1, k = 1$

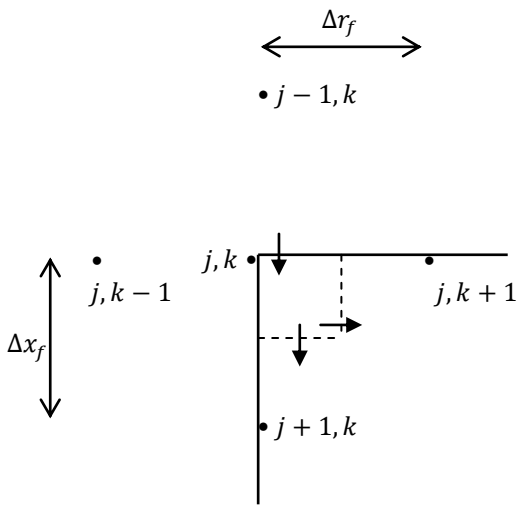

Figure 6-16: Diagram of finite difference approximations for case 6.

$$\frac{dp_{f,j,k}^{H_2O}}{dt} = \frac{1}{V_f\left[\varepsilon S_{air}^{H_2O} + (1-\varepsilon)S_f^{H_2O}\right]}\left[J_{prf,lnr}^{H_2O} A_{prf,lnr}\frac{A_{f,x}}{A_{f,air}} + D_{eff}^{H_2O} S_{air}^{H_2O}\left(-A_{f,x}\frac{\left(p_{f,j,k}^{H_2O} - p_{f,j+1,k}^{H_2O}\right)}{\Delta x_f} - \left(A_{f,r}\right)_{m+\frac{1}{2}}\frac{\left(p_{f,j,k}^{H_2O} - p_{f,j,k+1}^{H_2O}\right)}{\Delta r_f}\right)\right] \quad \textbf{(6-61)}$$

for $t \geq 0$

where:

$$V_f = \frac{\pi}{8}\Delta {r_f}^2 \Delta x_f \quad \textbf{(6-62)}$$

$$A_{f,x} = \frac{\pi}{4}\Delta {r_f}^2 \quad \textbf{(6-63)}$$

$$\left(A_{f,r}\right)_{k+\frac{1}{2}} = \frac{\pi}{2}\Delta r_f \Delta x_f \quad \textbf{(6-64)}$$

6.3.3.3.2 Case 10

Nodes:

$$j = 1,\ k = 2{:}\,K_{air} - 1$$

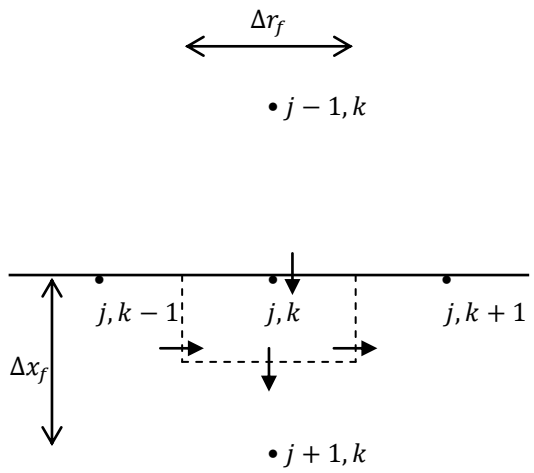

Figure 6-17: Diagram of finite difference approximation for case 10.

$$\frac{dp_{f,j,k}^{H_2O}}{dt} = \frac{1}{V_f\left[\varepsilon S_{air}^{H_2O} + (1-\varepsilon)S_f^{H_2O}\right]}\left[J_{prf,lnr}^{H_2O} A_{prf,lnr}\frac{A_{f,x}}{A_{f,air}}\right.$$
$$+ D_{eff}^{H_2O} S_{air}^{H_2O}\left(-A_{f,x}\frac{\left(p_{f,j,k}^{H_2O} - p_{f,j+1,k}^{H_2O}\right)}{\Delta x_f}\right. \quad \textbf{(6-65)}$$
$$\left.\left. + \left(A_{f,r}\right)_{k-\frac{1}{2}}\frac{\left(p_{f,j,k-1}^{H_2O} - p_{f,j,k}^{H_2O}\right)}{\Delta r_f} - \left(A_{f,r}\right)_{k+\frac{1}{2}}\frac{\left(p_{f,j,k}^{H_2O} - p_{f,j,k+1}^{H_2O}\right)}{\Delta r_f}\right)\right]$$

for $t \geq 0$

where:

$$V_f = \pi(k-1)\Delta {r_f}^2 \Delta x_f \quad \textbf{(6-66)}$$

$$A_{f,x} = 2\pi(k-1)\Delta {r_f}^2 \quad \textbf{(6-67)}$$

$$\left(A_{f,r}\right)_{k-\frac{1}{2}} = \pi\left(k-\frac{3}{2}\right)\Delta r_f \Delta x_f \quad \textbf{(6-68)}$$

$$\left(A_{f,r}\right)_{k+\frac{1}{2}} = \pi\left(k-\frac{1}{2}\right)\Delta r_f \Delta x_f \quad \textbf{(6-69)}$$

6.3.3.3.3 Case 11

Node:

$$j = 1, k = K_{air}$$

Case 11 consists of the node at the edge of the air pocket. As a result the surface area in contact with the air pocket is not equal to the area of the node in the axial direction, but rather some proportion of this.

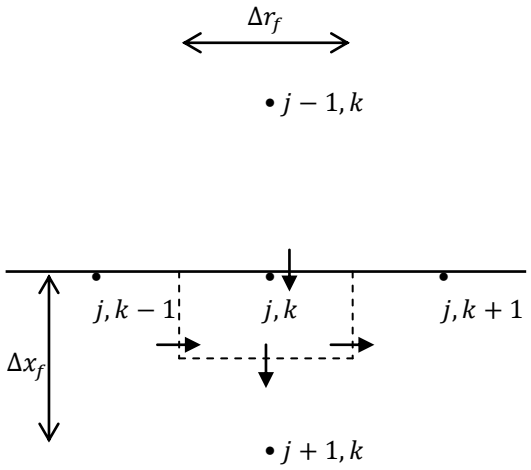

Figure 6-18: Diagram of finite difference approximation for case 11.

$$\frac{dp_{f,j,k}^{H_2O}}{dt} = \frac{1}{V_f\left[\varepsilon S_{air}^{H_2O} + (1-\varepsilon)S_f^{H_2O}\right]}\left[J_{prf,lnr}^{H_2O} A_{prf,lnr}\frac{A_{f,x,air}}{A_{air}}\right.$$
$$+ D_{eff}^{H_2O} S_{air}^{H_2O}\left(-A_{f,x}\frac{\left(p_{f,j,k}^{H_2O} - p_{f,j+1,k}^{H_2O}\right)}{\Delta x_f}\right. \quad \textbf{(6-70)}$$
$$\left.\left. + \left(A_{f,r}\right)_{k-\frac{1}{2}}\frac{\left(p_{f,j,k-1}^{H_2O} - p_{f,j,k}^{H_2O}\right)}{\Delta r_f} - \left(A_{f,r}\right)_{k+\frac{1}{2}}\frac{\left(p_{f,j,k}^{H_2O} - p_{f,j,k+1}^{H_2O}\right)}{\Delta r_f}\right)\right]$$

for $t \geq 0$

where:

$$V_f = \pi(k-1)\Delta {r_f}^2 \Delta x_f \quad \textbf{(6-71)}$$

$$A_{f,x} = 2\pi(k-1)\Delta {r_f}^2 \quad \textbf{(6-72)}$$

$$A_{f,x,air} = A_{air} - \pi\left(k-\frac{3}{2}\right)^2 \Delta {r_f}^2 \quad \textbf{(6-73)}$$

$$\left(A_{f,r}\right)_{k-\frac{1}{2}} = \pi\left(k-\frac{3}{2}\right)\Delta r_f \Delta x_f \quad \textbf{(6-74)}$$

$$\left(A_{f,r}\right)_{k+\frac{1}{2}} = \pi\left(k-\frac{1}{2}\right)\Delta r_f \Delta x_f \quad \textbf{(6-75)}$$

6.3.3.4 MATLAB® Solution

The formulated finite difference approximations for the water vapour pressure in the food powder were converted to MATLAB® code. The resulting script and function files are shown in Appendix E2.1.2.

6.3.3.5 Example Simulation

A preliminary simulation was carried out for a skim milk powder bag with an isolated air pocket adjacent to a perforation. Where possible, model parameters were based on known or literature values, although several values were approximate only. The thickness of skim milk powder in the radial and axial directions were based on a distance at which the water vapour pressure remained practically unchanged over the simulation period. Model predictions are shown in Figure 6-19 and Figure 6-20. As expected for a food powder, after 365 days the water vapour pressure is highest next to the perforation, decreasing further into the skim milk powder until a constant value equal to the initial water vapour pressure is reached. The average water vapour pressure in the section of powder considered also rises relatively linearly over the simulation period, which again appears reasonable.

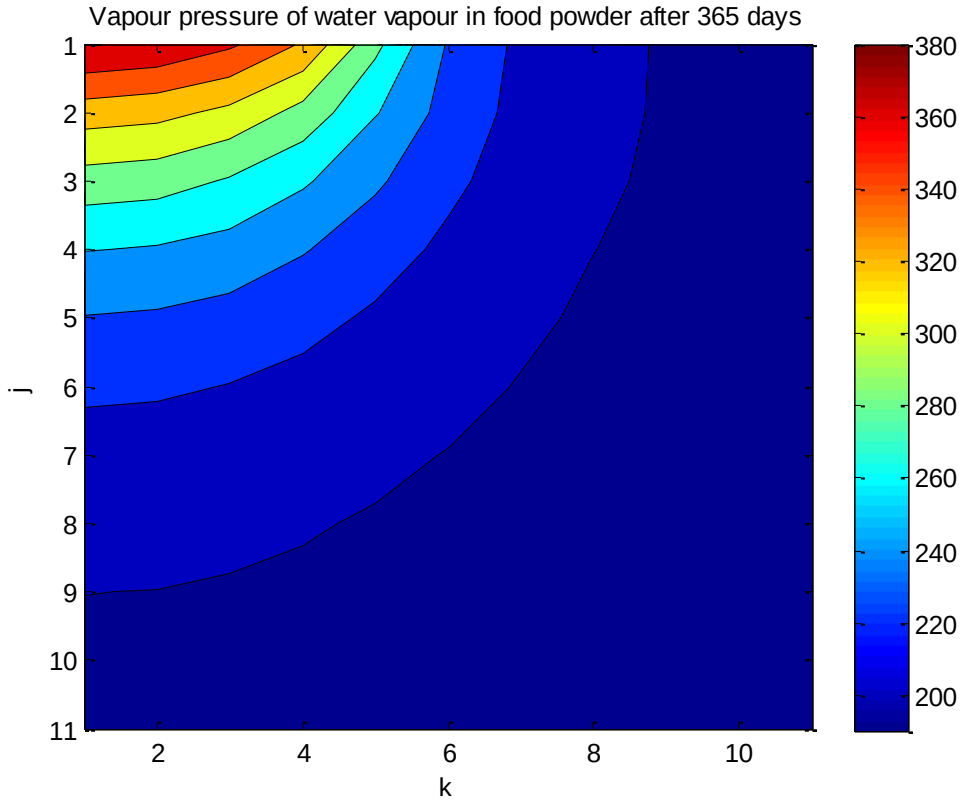

Figure 6-19: Model predictions of water vapour pressure profile in skim milk powder after 365 days at 20°C and 75% RH.

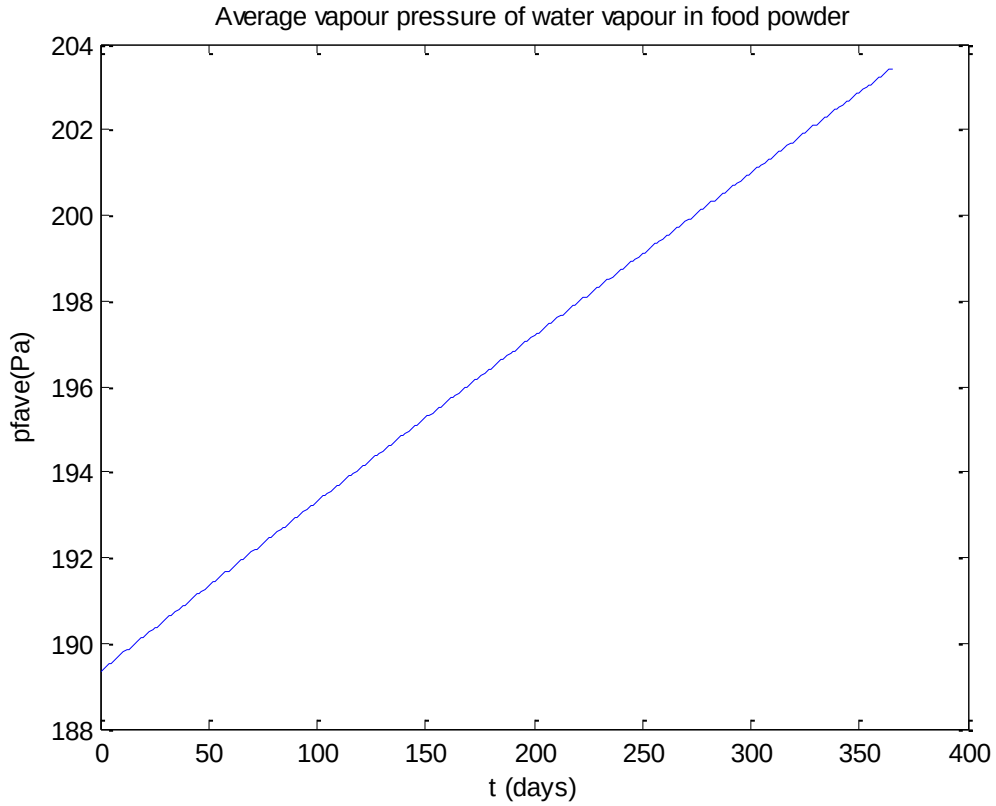

Figure 6-20: Model predictions of average water vapour pressure in skim milk powder over 365 days at 20°C and 75% RH.

6.3.4 Error Checks

Error checks were carried out as for previous models (Section 4.4.5). These are summarised in Appendix E.2.2. Numerical error checks suggested a default relative error tolerance value of 1×10^{-3} and 10 nodes in both axial and radial directions was numerically accurate and allowed for a reasonable solving time. Mathematical error checks against analytical solutions were not possible due to the nature of boundary conditions.

6.4 MODEL VALIDATION

6.4.1 Experimental Methodology

6.4.1.1 Diffusion of Water Vapour in Food Powder

To validate the two-dimensional perforation moisture transfer models, the same equipment previously used for water vapour permeability tests (Section 4.5.1.1) were used, including aluminium permeability dishes and relative humidity chambers. iButton® Hygrochron data loggers (Maxim Integrated Products, model DS1923, ± 0.5°C and ± 5% RH) were used to measure temperature and relative humidity at two positions within the dish: one at the centre (x=9 mm and r=0 mm) and one at the edge of the dish (x=9 mm and r=25 mm). To prevent data loggers from obstructing moisture transfer, the aluminium permeability dishes were modified so that the data loggers could be positioned flush with the bottom surface. A nylon mesh was placed over each data logger to prevent powder from obstructing the sensor area. A modified permeability dish with iButton® data loggers is shown in Figure 6-21, and an iButton® data logger is shown separately in Figure 6-22.

Figure 6-21: Modified permeability dish with iButton® hygrochron temperature and RH data loggers.

Figure 6-22: iButton® Hygrochron temperature and RH data logger.

Skim milk powder (SMP) was again used for the trial. An impermeable laminated aluminium foil packaging sample was used to ensure moisture permeation through the packaging did not affect moisture transfer in the SMP. Test conditions consisted of approximately 40°C and 75% relative humidity (RH). A relatively large needle with a 0.9 mm diameter was used to produce perforations to ensure a measurable change in water vapour pressure over the trial period. Both scenarios without and with an isolated air pocket were considered. To produce an air pocket, a small o-ring with a 25 mm inside diameter was inserted into the surface of the SMP, and a layer of about 1 mm of SMP removed from the inner section. Open permeability dishes without and with an isolated air pocket respectively, and a permeability dish with a perforated film are shown in Figure 6-23.

(A)

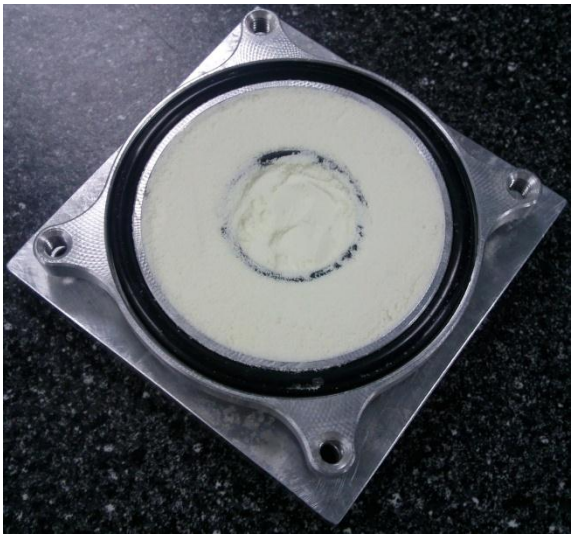

(B)

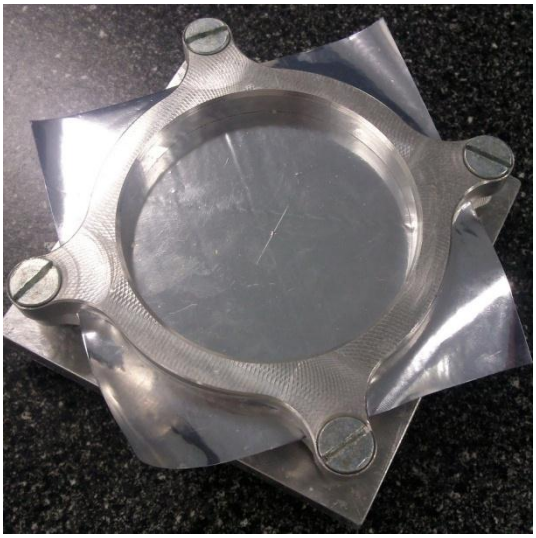

(C)

Figure 6-23: Modified permeability dishes containing SMP open without (A) and with (B) an isolated air pocket, and sealed with a perforated film (C).

6.4.2 Results and Discussion

Relative humidity readings obtained experimentally using the iButton® data loggers were converted to water vapour pressures to allow direct comparison with model predictions. Model parameters used for the validation simulation are summarised in Table 6-3. Experimental methods and literature references for these values were previously outlined in Sections 4.5.1, 4.5.2, 5.4.1 and 5.4.2.

Table 6-3: Summary of system inputs used for validation of the two-dimensional perforation models.

Parameter Description	Symbol	Units	Value
General system inputs			
Ambient temperature	T	K	$39.9 + 273.15$
Ambient relative humidity	RH_a	%	73.3
Area of perforation	A_{prf}	m^2	1.9×10^{-7}
Area of air pocket in contact with SMP (model with air pocket only)	$A_{f,air}$	m^2	$\pi \times 0.015^2$
SMP properties			
Initial moisture content of SMP	M_i	(kg water).(kg solids)$^{-1}$	0.0532
Bulk density of SMP	ρ_b	kg.m^{-3}	850
Particle density of SMP	ρ_p	kg.m^{-3}	1493
Thickness of SMP in axial direction	X_f	m	0.009
Thickness of SMP in radial direction	R_f	m	0.035
Constructivity-tortuosity ratio	δ/τ	-	0.7
GAB isotherm parameters			
Moisture content of monolayer for GAB isotherm	$M_{0,GAB}$	(kg water).(kg solids)$^{-1}$	0.051
Guggenheim constant for GAB isotherm	C_{GAB}	-	12.11
Constant for GAB isotherm	k_{GAB}	-	1.08

Water vapour pressure profiles after 14 days as predicted by the mathematical models are shown in Figure 6-24 and Figure 6-26, and comparisons of model predictions and experimental results in Figure 6-25 and Figure 6-27 for systems without and with an air pocket respectively. Note that the absolute dimensions in the radial and axial directions of the cross-sectional area of SMP modelled are not as shown. This section was in fact rectangular rather than square as shown.

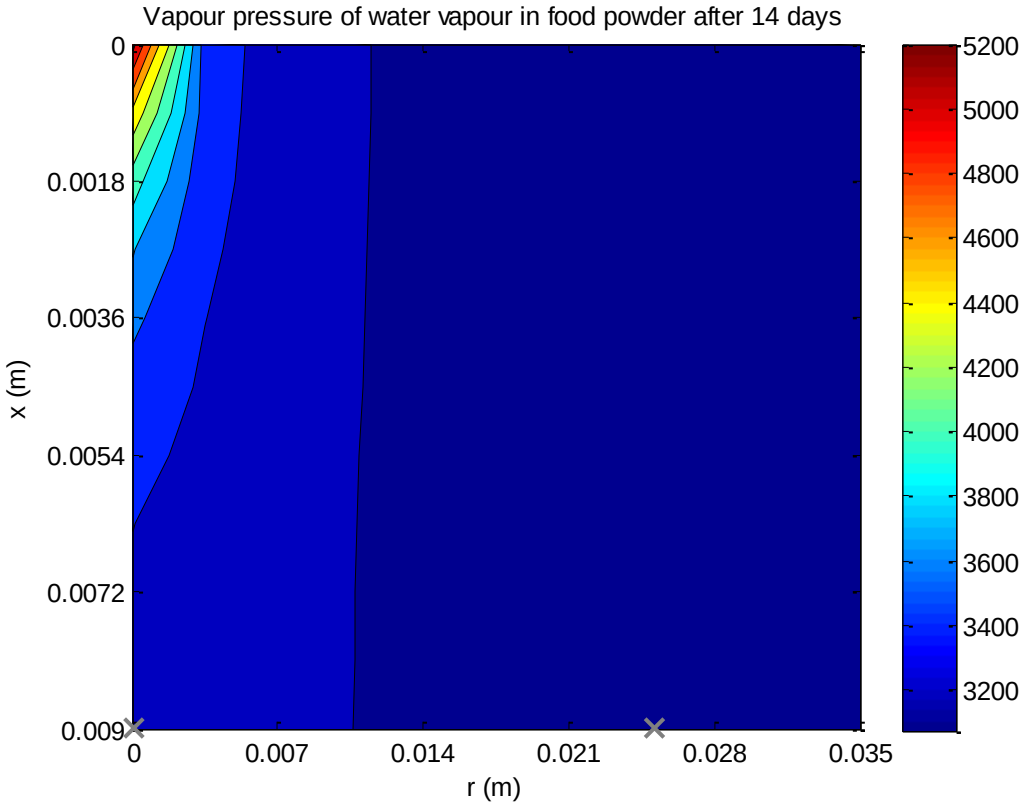

Figure 6-24: Water vapour pressure profile (Pa) of SMP in a permeability dish after 14 days as predicted by the model for a system without an air pocket adjacent to a perforation. Positions of data loggers are shown with an x.

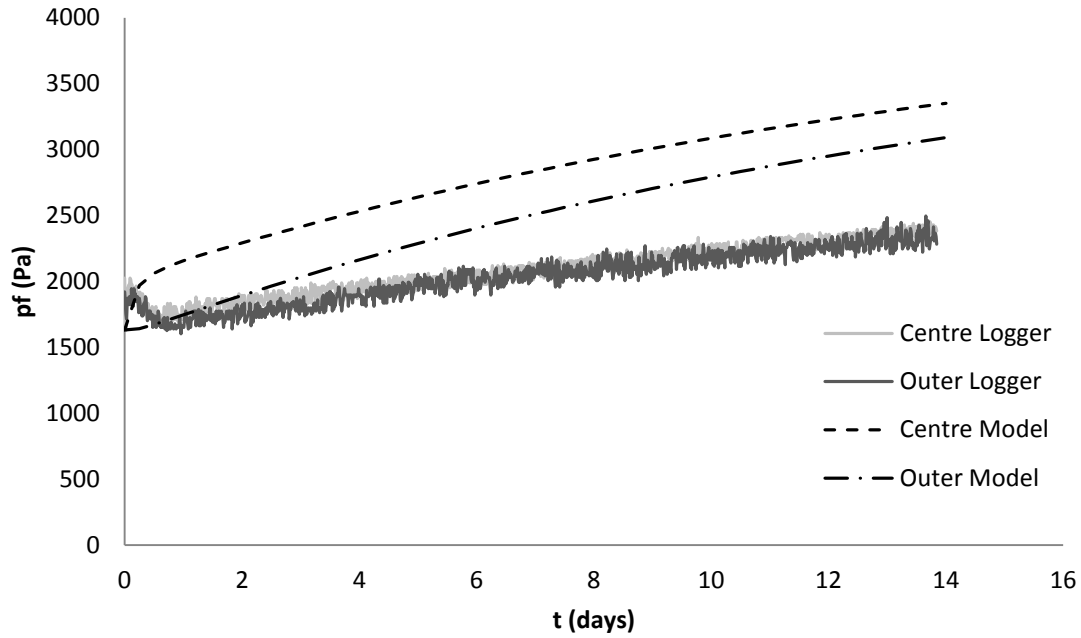

Figure 6-25: Plot of water vapour pressure (Pa) at centre (x=9 mm and r=0 mm) and outer (x=9 mm and r=25 mm) positions in the SMP versus time (days) as measured experimentally and predicted by the model for a system with no air pocket adjacent to the perforation.

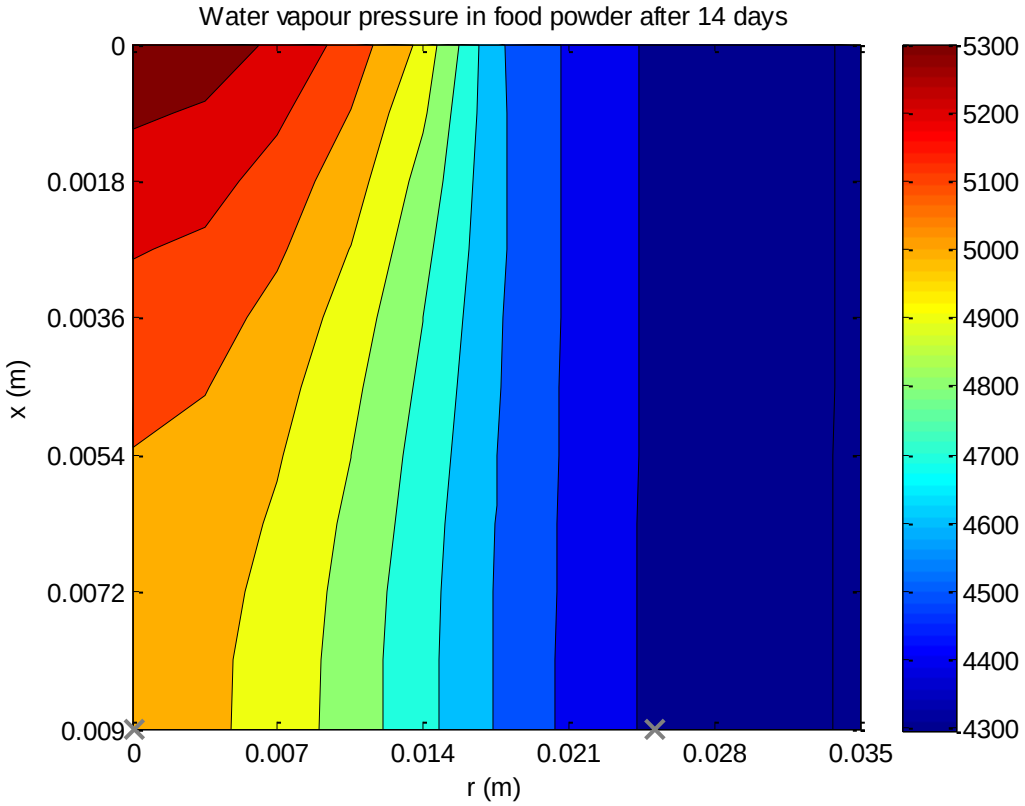

Figure 6-26: Water vapour pressure profile (Pa) of SMP in a permeability dish after 14 days as predicted by the model for a system with an isolated air pocket adjacent to a perforation. Positions of data loggers are shown with an x.

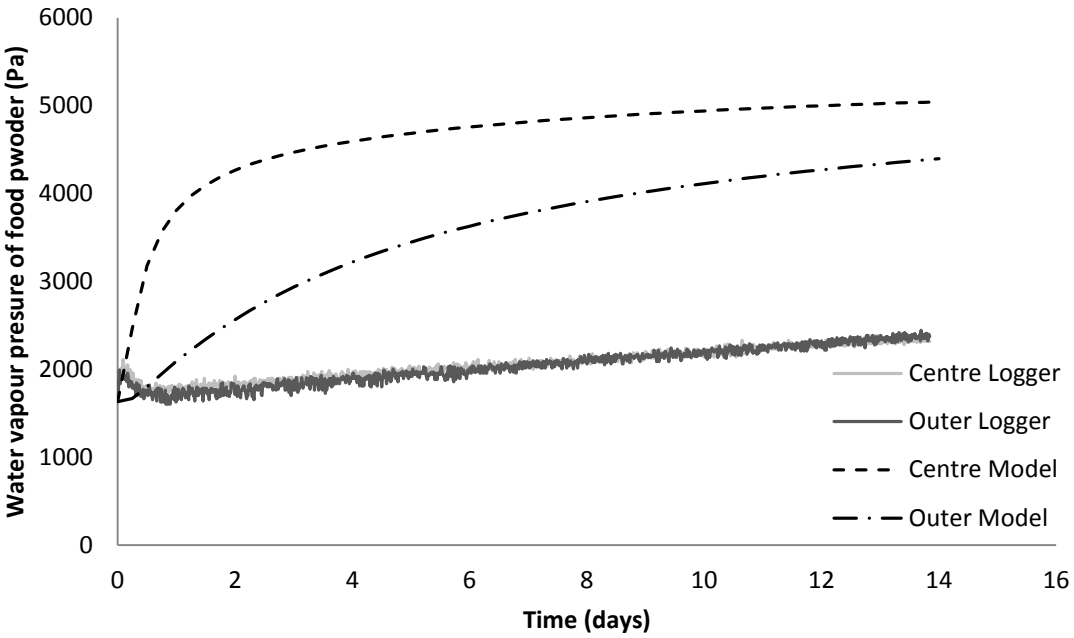

Figure 6-27: Plot of water vapour pressure (Pa) at centre (x=9 mm and r=0 mm) and outer (x=9 mm and r=25 mm) positions in the SMP versus time (days) as measured experimentally and predicted by the model for a system with an isolated air pocket adjacent to the perforation.

It was observed that the rates of moisture increase for experimental measurements were significantly lower than model predictions. A possible explanation is the partial blockage of perforations by SMP particles, despite careful attempts to avoid this occurring. Also, as noted previously (Section 4.5.2.6) and covered in more detail in Section 7.5.2.1, the perforation can have an irregular structure with “flaps” that can obstruct moisture transfer, particularly for large perforations such as those used for this trial. The error resulting from these potential factors are expected to be particularly significant for this trial since practically all moisture transfer occurred through the perforation. Although earlier findings suggest otherwise, this difference may also be a result of an inappropriate model for predicting moisture transfer through perforations. More complex models may therefore need to be considered in future studies.

Another aspect of the experimental method that may have affected findings is the time that was required to create a level SMP surface and to seal the permeability dish, during which the SMP was exposed to ambient air conditions. The resulting change in moisture content could be particularly significant for such a shallow permeability dish.

Similarly, the SMP removed for the system with an isolated air pocket could also have been significant based on the relatively small total volume of SMP.

Based on these difficulties with the experimental method used it is not believed that the determined values of perforation area were accurate real-world representations. Unfortunately due to time constraints it was not possible to carry out other methods for determining the perforation area. To attempt to gain better agreement of model predictions with experimental measurements, the size of the perforations were adjusted. Adjusted values are summarised in Table 6-4, and resulting comparisons are shown in Figure 6-28 and Figure 6-29.

Table 6-4: Summary of adjusted values of perforation area to improve agreement of model predictions with experimental measurements.

Model	Original value (m^2)	Adjusted value (m^2)
No air pocket	$(1.9 \pm 0.7) \times 10^{-7}$	5.1×10^{-9} m^2
With isolated air pocket	$(1.9 \pm 0.7) \times 10^{-7}$	4.0×10^{-9} m^2

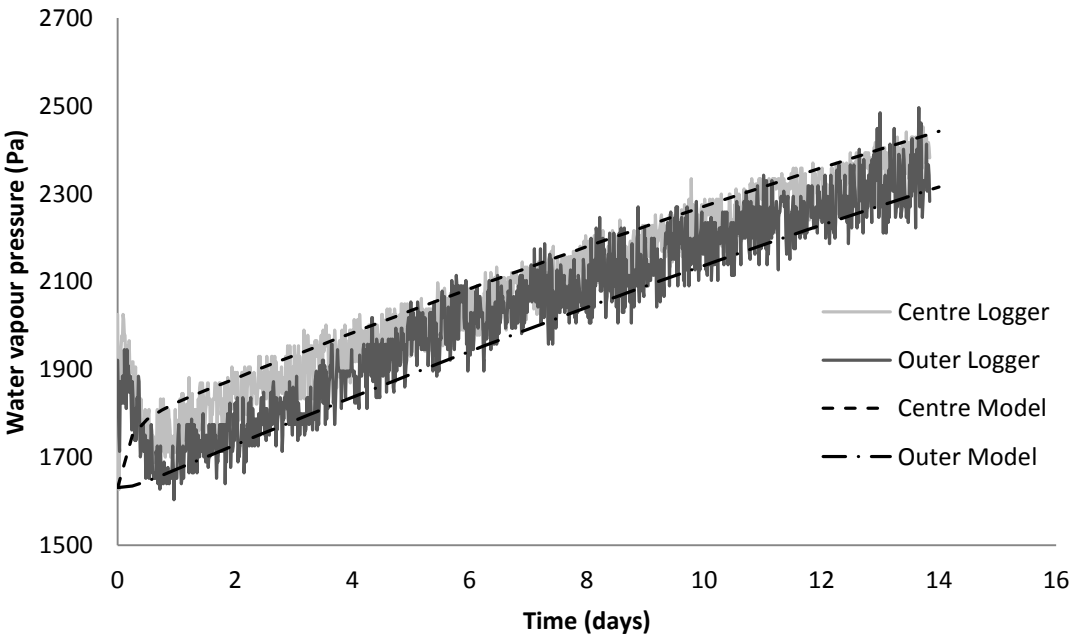

Figure 6-28: Plot of water vapour pressure (Pa) at centre (x=9 mm and r=0 mm) and outer (x=9 mm and r=25 mm) positions in the SMP versus time (days) as measured experimentally and predicted by the model with adjusted parameters for a system with no air pocket adjacent to the perforation.

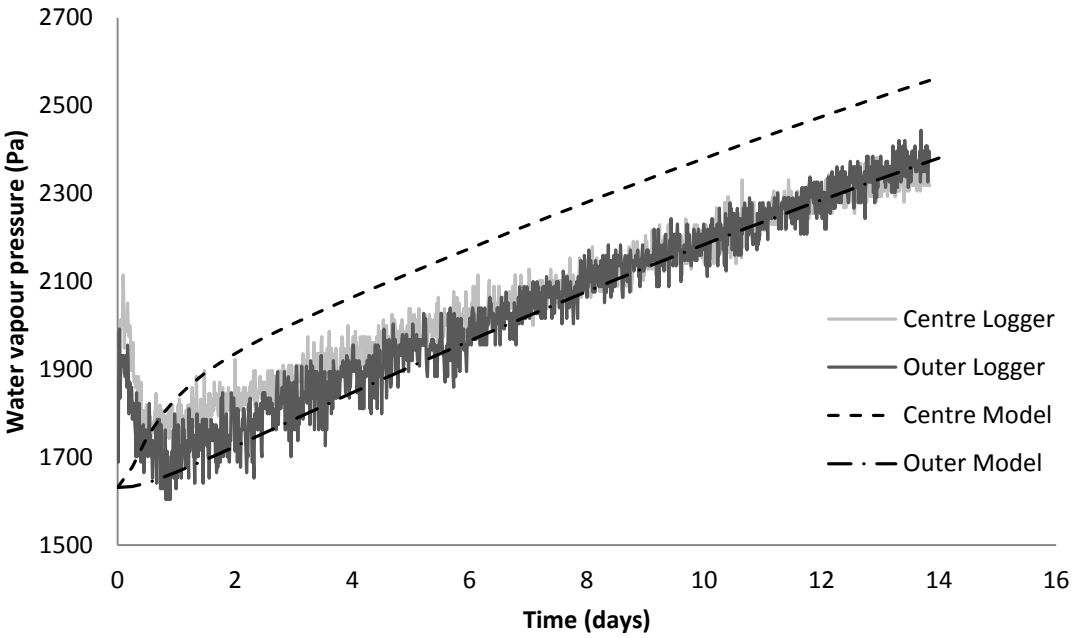

Figure 6-29: Plot of water vapour pressure (Pa) at centre (x=9 mm and r=0 mm) and outer (x=9 mm and r=25 mm) positions in the SMP versus time (days) as measured experimentally and predicted by the model with adjusted parameters for a system with an isolated air pocket adjacent to the perforation.

As shown, agreement was significantly improved by adjusting the perforation area, particularly for the system with no air pocket. These adjusted values were in the practical range expected.

For the system with an isolated air pocket, the difference between water vapour pressures at the centre and outer positions as predicted by the model (Figure 6-29) was not evident in the experimental data. This may be associated with the experimental difficulties encountered while attempting to prevent an air gap between the top surface of the food powder and the packaging film, as mentioned earlier. Some systematic error resulting from incorrectly calibrated measuring equipment may also have affected results. It is therefore suggested that these data loggers be calibrated before any future experiments.

Clearly model predictions are very sensitive to the area of the perforation, as can be expected. More accurate estimation of the perforation area may therefore be required for accurate model validation, which could involve alternative methods of producing perforations. Laser cut perforations is one such method that could be particularly effective if

the appropriate equipment can be obtained. Alternatively a heated needle may give a more regular perforation if the action of perforating the film as well as heating of the needle can be mechanically controlled. In terms of determining the perforation area, a potential method could be testing a perforated impermeable film using the Mocon permeability test equipment and back-calculating the perforation area using the appropriate equation from Section 2.5.2.2. A series of such tests should give useful estimation of the degree of variability of perforation size. Such procedures were not in the scope of this investigation, but would be useful for future studies.

To gain more reliable experimental results, it is suggested that further model validation trials be carried out. In particular, a much larger test container would reduce effects of exposure of the sample food powder to ambient air during set up, as well as that of removing some powder to produce an air pocket. This may also allow the use of multiple data loggers in several locations to give better indication of the actual water vapour profile. Such tests would need to be long term, which unfortunately were not possible for this investigation due to time constraints.

6.5 SUMMARY

This chapter outlined the development of two-dimensional perforation moisture transfer models. These models apply to scenarios where the position of a perforation in the food packaging is in direct contact with the food powder, or a relatively small isolated air pocket between the packaging and food powder, resulting in a localised two-dimensional moisture profile in the food powder. Key assumptions included negligible moisture transfer by permeation through the packaging, and that the system can be approximated by two-dimensions. Such assumptions are fairly approximate relative to real-world scenarios, however in this case only indicative predictions were required. Mathematical models were formulated and solved numerically using MATLAB® software. Error checks and validation against experimental observations were carried out, which suggested reasonable model

predictions of real-world scenarios. It was suggested that further model validation be carried out in future studies for more confidence in model predictions.

Chapter 7

DEVELOPMENT OF A FOOD PACKAGE CONSOLIDATION MODEL

7.1 INTRODUCTION

This chapter outlines the development of a food package consolidation model. A common factor limiting the optimisation of food export packaging in terms of moisture transfer is the need to consolidate the package. Perforations may be required to allow expulsion of air initially in the package headspace after filling; however these perforations also facilitate a high rate of moisture transfer through the packaging. Thus the optimal food package design is one where consolidation is achieved in the required timeframe, whilst providing the highest barrier to moisture transfer obtainable. To investigate such a scenario, a food package consolidation model was formulated to allow prediction of the time required for consolidation.

The objectives of work covered in this chapter were to:

- Develop a conceptual food package consolidation system, indentifying key processes and properties, and specifying valid assumptions allowing the system to be appropriately simplified.

- Formulate a mathematical model based on identified processes and assumptions using relevant theory.

- Solve the formulated model using an appropriate method, and ensure the solution is free of errors.

- Validate model predictions against experimental observations to ensure accurate representation of real-world systems.

- Discuss applications of the developed mathematical model and demonstrate how it can be used in combination with the moisture transfer models developed earlier for food packaging optimisation.

7.2 CONCEPTUAL MODEL DEVELOPMENT

7.2.1 Outline of Conceptualised System

A schematic diagram of the conceptualised food package consolidation system is shown in Figure 7-1. The system consists of an enclosed package containing perforation(s) and an air headspace. As other food packages are stacked on top, the pressure of air in the package headspace increases creating a driving force for air flow through the perforation(s) and allowing consolidation of the package.

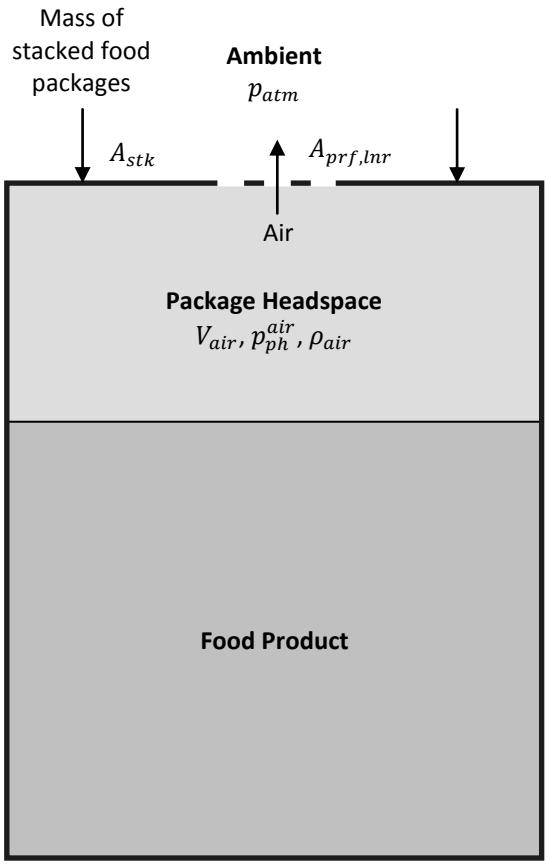

Figure 7-1: Schematic diagram of conceptualised food package consolidation system.

7.2.2 Assumptions

7.2.2.1 Bernoulli's Equation Applies

Several models can be applied to fluid flow through perforations, including Poiseuille's law (González-Buesa et al., 2009), Bernoulli's equation for incompressible fluids (Geankoplis, 2003) and other more complex models (Geankoplis, 2003). For this scenario the system resembles fluid flow through an orifice, where the diameter of the perforations will be greater than the thickness of the packaging film. Therefore Bernoulli's equation will be used (Geankoplis, 2003). Other assumptions relating to the use of Bernoulli's equation are covered below. It should be noted that this mathematical model is mainly intended as a general indication for which accuracy is not critical. Therefore Bernoulli's equation is expected to give an adequate estimation of the rate of air flow.

7.2.2.1.1 Air is an Incompressible Fluid

For Bernoulli's equation to be applicable to fluid flow, it is required that the fluid of interest is incompressible. To test the validity of this assumption, the Mach number was considered, which is defined as follows (Geankoplis, 2003):

$$N_{Ma} = \frac{v}{v_{max}} \quad \textbf{(7-1)}$$

where:

N_{Ma} = Mach number (-)

v = Velocity of fluid (m.s^{-1})

v_{max} = Speed of sound in fluid at flow conditions (m.s^{-1})

The speed of sound in the fluid can be calculated by the following equation (Geankoplis, 2003):

$$v_{max} = \sqrt{\frac{\gamma RT}{M}} \quad \textbf{(7-2)}$$

where:

γ = Ratio of heat capacity at constant pressure to heat capacity at constant volume (-)

R = Ideal gas constant (8.314 $m^3.Pa.K^{-1}.mol^{-1}$)

T = Absolute temperature (K)

M = Molecular mass of fluid ($kg.mol^{-1}$)

For dry air, the ratio of heat capacities is equal to 1.4 and the molecular mass is equal to 0.02897 $kg.mol^{-1}$ (Geankoplis, 2003). A plot of Mach number for air flow at 18°C over a range of pressure drops is shown in Figure 7-2.

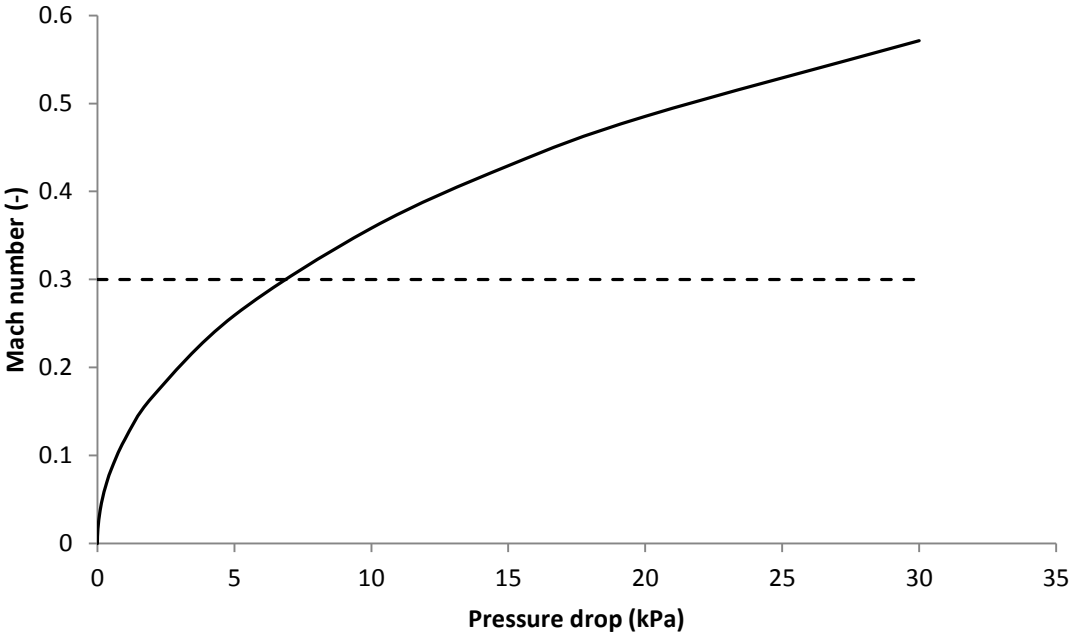

Figure 7-2: Plot of Mach number for air flow through perforations at 18°C over a range of pressure drops.

Geankoplis (2003) suggested that when the Mach number is less than 0.3, the fluid can practically be considered incompressible. As shown, a pressure drop of above about 7 kPa results in a Mach number above 0.3. However, it is expected that most applications of the consolidation model would involve pressure drops at the lower end of the 30 kPa range, particularly for "worst case" scenarios resulting in the slowest consolidation. It is expected that error from other sources such as the size of perforations would be much more significant. Therefore this should be a reasonable assumption.

7.2.2.1.2 Pressure Drop Due to Friction is Negligible

Since the diameter of perforations is generally significantly larger than the thickness of polymer packaging, it is expected that the pressure drop due to friction will be negligible.

7.2.2.2 Air Flow through a Single Individual Packaging Layer is the Largest Resistance to Air Flow

This assumption implies that perforations in the individual packaging layer being considered (which may consist of multiple layers in direct contact) are much smaller than perforations and unsealed edges in other individual layers. For example, a paperboard bag with a polymer liner where the paperboard bag does not have a perfect seal, or a polymer liner in a paperboard box. As a result resistance to air flow through other individual layers can be assumed to be negligible. Similarly, it was also assumed that air flow through perforations is not affected by other layers, such as creating a tortuous path between packaging layers and/or obstructing air flow. Again, for a general indication of consolidation of a food package, these assumptions are expected to be reasonable.

7.2.2.3 Constant Temperature

To apply Bernoulli's equation, the process is required to be isothermal to neglect changes in density. In practice the temperature will not be constant. However, it is expected that temperature variations over the consolidation period will be relatively insignificant. Also, the density of air remains relatively constant over the temperature range relevant to food packages of interest. Therefore this should be a reasonable assumption.

7.2.2.4 Other Assumptions

It was assumed that air exhibits ideal gas behaviour. This is a fairly common assumption (Geankoplis, 2003), and is therefore considered reasonable. It was also assumed that the food package contains dry air. In reality there will be water vapour in the air, particularly for high moisture content food. However it is expected that any affect on the density of the air resulting from water vapour will be negligible relative to error from other approximations.

It is also assumed that the shape of the food product will have no bearing on the package consolidation, and the food package will simply consolidate until all headspace air has been expelled. In reality the food product may deform during consolidation, resulting in a changing load and therefore changing pressure in the package headspace. However as a guide of the relative rates of consolidation, it is believed that this assumption should be reasonable for the required model application.

7.3 MATHEMATICAL MODEL FORMULATION

7.3.1 Variables

Table 7-1: List of model variables.

Symbol	Description	Unit	Class*
A_{prf}	Total area of perforation(s) in packaging	m^2	SI
A_{stk}	Contact area of mass stacked on top of food package	m^2	SI
$M_{r,air}$	Molecular mass of dry air	$kg.mol^{-1}$	SI
V_{air}	Volume of air in package headspace	m^3	D
m_{stk}	Mass stacked on top of food package	kg	SI
p_{atm}	Atmospheric pressure	Pa	SI
p_{ph}^{air}	Pressure of air in package headspace	Pa	CV
ρ_{air}	Density of air	$kg.m^3$	CV
R	Ideal gas constant (8.314)	$m^3.Pa.K^{-1}.mol^{-1}$	SI
T	Absolute temperature	K	SI
g	Acceleration due to gravity	$m.s^{-1}$	SI
t	Time	s	I

*I = independent variable, D = dependent variable, CV = consequential variable, SI = system input

The mathematical model consists of one independent and one dependent variable; therefore a single ordinary differential equation (ODE) will be required for the volume of air in the package headspace, as well as one initial condition.

7.3.2 Word Balances and Equations

7.3.2.1 ODE for Volume of Air in Package Headspace

The food package system to be modelled consists of a fully sealed polymer liner (or other packaging material), apart from perforation(s) in the liner. Therefore any changes in the amount of air contained in the liner headspace will be dependent on air flow through

the perforations. As a result the following unsteady-state mass balance of air in the food package can be derived:

$$\begin{pmatrix} \textit{rate of} \\ \textit{accumulation} \\ \textit{of air in bag} \\ \textit{headspace} \end{pmatrix} = -\begin{pmatrix} \textit{rate of air} \\ \textit{leaving} \\ \textit{through} \\ \textit{perforations} \end{pmatrix} \quad \textbf{(7-3)}$$

This word balance can be expressed as an ODE using Bernoulli's principle as follows (derivation shown in Appendix F.1.1.1):

$$\frac{dV_{air}}{dt} = -A_{prf}\sqrt{\frac{2}{\rho_{air}}\left(p_{ph}^{air} - p_{atm}\right)} \quad \textbf{(7-4)}$$

$$for\ t \geq 0$$

where:

V_{air} = Volume of air in package headspace (m^3)

t = Time (s)

A_{prf} = Total area of perforation(s) in packaging (m^2)

ρ_{air} = Density of air ($kg.m^{-3}$)

p_{ph}^{air} = Pressure of air in package headspace (Pa)

p_{atm} = Atmospheric pressure (Pa)

7.3.2.2 Equation for Pressure of Air in Package Headspace

An equation for the pressure of air in the package headspace can be derived based on food product stacked on the food package using the definition of pressure. It should be noted that this is somewhat approximate since the mass of stacked food product may be spread across multiple packages, and the area of contact may change during consolidation. However, it is useful as a general indication. The resulting expression is as follows:

$$p_{ph}^{air} = \frac{m_{stk}g}{A_{stk}} + p_{atm} \quad \textbf{(7-5)}$$

where:

m_{stk} = Mass of food product stacked on food package (kg)

g = Acceleration due to gravity ($m.s^{-1}$)

A_{stk} = Area of contact of food product stacked on food package (m^2)

7.3.2.3 Equation for Density of Air

An expression for the density of air can be derived based on the ideal gas law:

$$\rho_{air} = \frac{M_{r,air} p_{ph}^{air}}{RT} \quad \textbf{(7-6)}$$

where:

$M_{r,air}$ = Molecular mass of dry air ($kg.mol^{-1}$)

R = Ideal gas constant (8.314 $m^3.Pa.K^{-1}.mol^{-1}$)

T = Absolute temperature (K)

7.3.3 Initial Conditions

$$V_{air} = V_{air,i} \quad at\ t = 0 \quad \textbf{(7-7)}$$

7.4 SOLUTION

Due to the simplicity of the formulated model an analytical solution was very straight forward. Since previous models were solved using MATLAB® software (Sections 4.4.3), it was convenient to create a similar MATLAB® script file for the consolidation model.

7.4.1 Analytical Solution

The analytical solution for Equation 7-4 is as follows (derivation shown in Appendix F.2.1):

$$V_{air} = V_{air,i} - A_{prf} t \sqrt{\frac{2}{\rho_{air}} \left(p_{ph}^{air} - p_{atm} \right)} \quad \textbf{(7-8)}$$

$$for\ t \geq 0$$

7.4.2 MATLAB® Solution

The MATLAB® script file for the consolidation model is shown in Appendix F.2.2.

7.4.3 Example Simulation

A preliminary simulation was carried out for a large bag of sugar typical of exported food powder products. Model predictions are shown in Figure 7-3. As expected, the volume of air in the bag headspace decreases linearly.

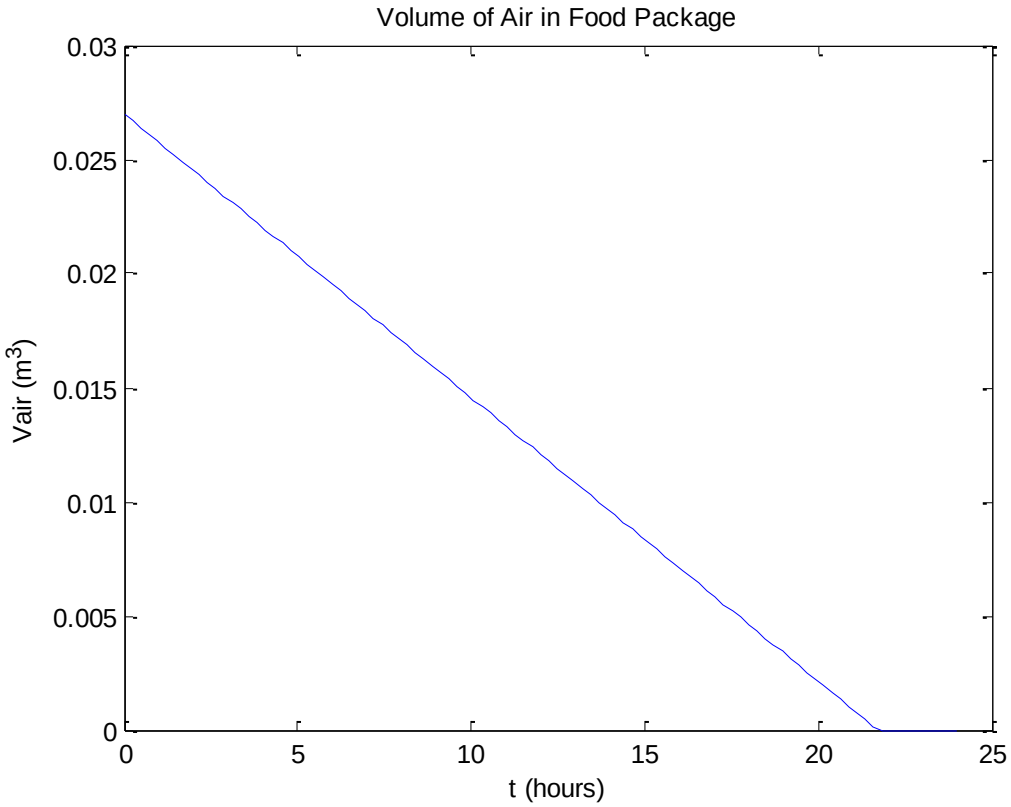

Figure 7-3: Preliminary model predictions of volume of air in food package (m^3) over 24 hours for a large bag of sugar.

7.4.4 Error Checks

To ensure the mathematical model was formulated correctly and that the solution method was appropriate, the model was also solved numerically (not shown). This produced identical results to the analytical solution, suggesting that the model is free of mathematical errors.

7.5 MODEL VALIDATION

7.5.1 Experimental Methodology

The rate of air flow through perforations as predicted by the consolidation model was validated by conducting air flow measurements for various pressure drops. Perforated polymer liner samples were placed in a permeability cell, and air pressure applied to one side of the sample (the other side was maintained at atmospheric pressure). Pressure was adjusted to the desired level using a pneumatic valve as measured by a pressure gauge, and air flow rate measurements taken using an AALBORG® mass flow controller (used as a flow meter). Flow rate measurements were taken at 5 kPa increments increasing from 0 to 30 kPa, followed by the reverse. Perforations of two sizes were considered. To ensure flow rate measurements were reasonably accurate, the mass flow meter was calibrated by measuring the volume of air in an inverted measuring cylinder filled with water over a specified time period for a range of flow rates. A schematic diagram of the experimental system is illustrated in Figure 7-4, and the test equipment is shown in Figure 7-5.

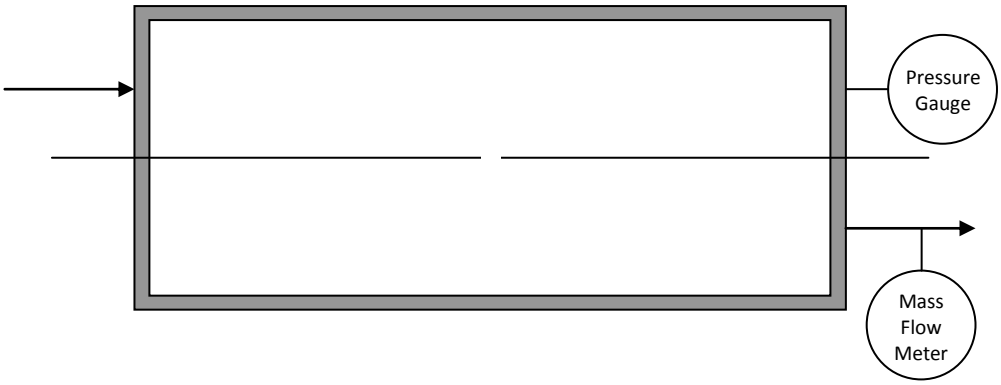

Figure 7-4: Schematic diagram of experimental system used for validation of the consolidation model.

(A)

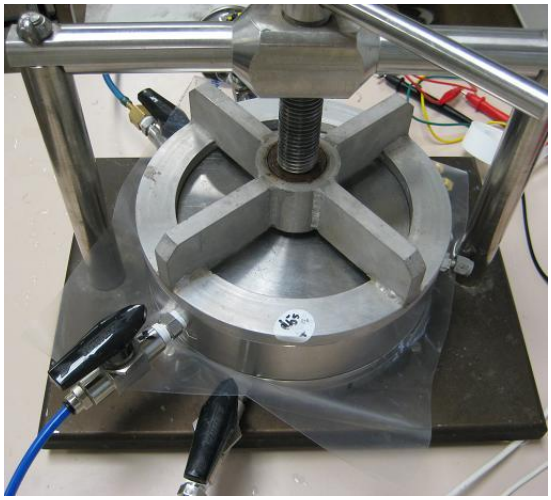

(B)

(C)

Figure 7-5: Mass flow controller (A), permeability cell (B) and pressure gauge (C) used for validation of the consolidation model.

7.5.2 Model Input Parameters and Data Analysis

7.5.2.1 Size of Perforations

For validating the consolidation model, two different sized perforations were considered, produced with 0.33 mm and 0.9 mm diameter syringe needles. The microscope method for determining the size of perforations was previously discussed in Section 4.5.2.6, and it was found the size of perforations produced with the 0.33 mm diameter syringe needle were $(5.2 \pm 1.3) \times 10^{-9}$ m^2. Using the same method, the size of perforations created with the 0.9 mm diameter syringe needle were found to be $(1.9 \pm 0.7) \times 10^{-7}$ m^2. A microscope image of the larger perforation is shown in Figure 7-6.

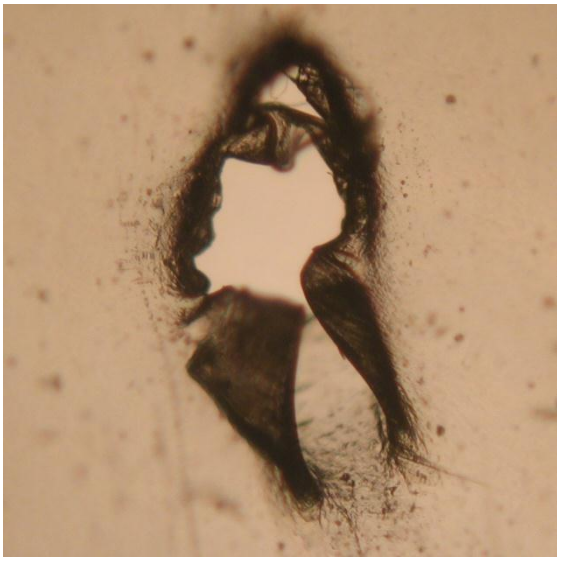

Figure 7-6: Microscope image of a perforation created using a syringe needle with a 0.9 mm diameter.

It should be noted that due to the irregular shape of the perforations an accurate estimation of the size was difficult. Also, particularly for the larger perforations, a 3-dimensional structure was common, making it difficult to focus on the actual area of interest and obscuring sections of the perforation. Calculated values are therefore approximate.

7.5.3 Results and Discussion

To validate the consolidation model, consolidation of a perforated polymer liner system was simulated. Predicted values of headspace volume were converted to a change in volume which is equal to the flow rate through all perforations. A summary of system inputs used for the simulation is shown in Table 7-2.

Table 7-2: Summary of system inputs used for validation of the consolidation model.

Parameter Description	Symbol	Units	Value
Molecular mass of air	$M_{r,air}$	kg.mol^{-1}	0.02897
Temperature	T	K	$18 + 273.15$
Total area of perforations	A_{prf}	m^2	$3 \times (1.6 \pm 1.2) \times 10^{-8}$ and $3 \times (2.4 \pm 1.9) \times 10^{-7}$
Pressure of air in package headspace	p_{ph}^{air}	Pa	0, 5×10^3, 1×10^4, 1.5×10^4, 2×10^4, 2.5×10^4 and 3×10^4

As shown in Figure 7-7, significant hysteresis of experimental measurements was observed when the pressure drop was first increased then decreased. This suggests significant stretching of the perforations occurred during the pressure drop test. To confirm this hypothesis, microscope images were taken of the perforations after the test. A microscope image of one of the perforations after the pressure drop test is shown in Figure 7-8. From these images the area of the perforations was estimated to be (1.6± 1.4) × 10^{-8} m^2, notably larger than the original area of (5.2 ± 1.3) × 10^{-9} m^2, confirming the hypothesis. As a result only data during the decreasing pressure drop section were considered.

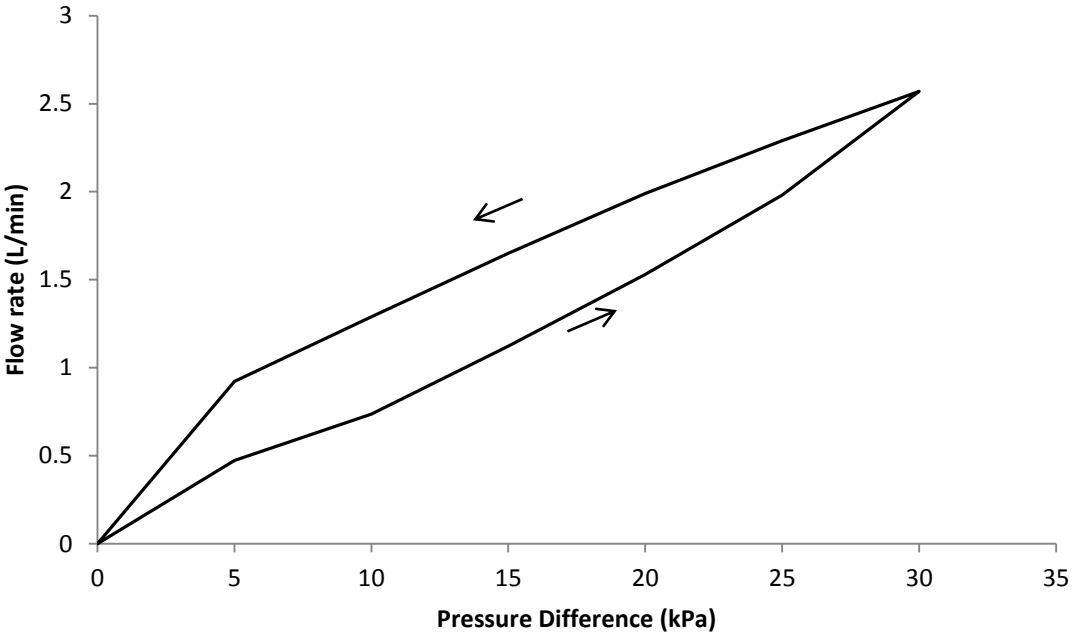

Figure 7-7: Plot of flow rate (L.min^{-1}) versus pressure drop (kPa) for air flow through perforations as measured experimentally. Pressure drops were increased incrementally from 0 to 30 kPa and back down to 0 kPa.

Figure 7-8: Microscope image of perforation created using a 0.33 mm diameter syringe needle after applying a 30 kPa pressure drop.

A comparison of model predictions and experimental results of air flow rates through perforations produced by the 0.33 mm diameter syringe needle for a range of pressure drops is shown in Figure 7-9. As can be seen, model predictions were significantly lower than experimental measurements, even when the estimated variation in size of the

perforations was considered. However the microscope image of a perforation after the pressure drop test (Figure 7-8) seemed to indicate creasing over a much larger area than the actual perforation. It is therefore believed that while the pressure drop is applied, the perforation stretches significantly, possibly by more than 400% of the estimated area (in addition to the increase observed before and after the pressure drop test). Estimating the actual area of the perforation during the pressure drop test would therefore be difficult. To gain an indication of the increase required to achieve model predictions that agree with the experimental measurements, the total area of perforations was varied. This showed that an enlargement of 240% accounted for the lack of agreement (Figure 7-9), much lower than the potential 400% enlargement.

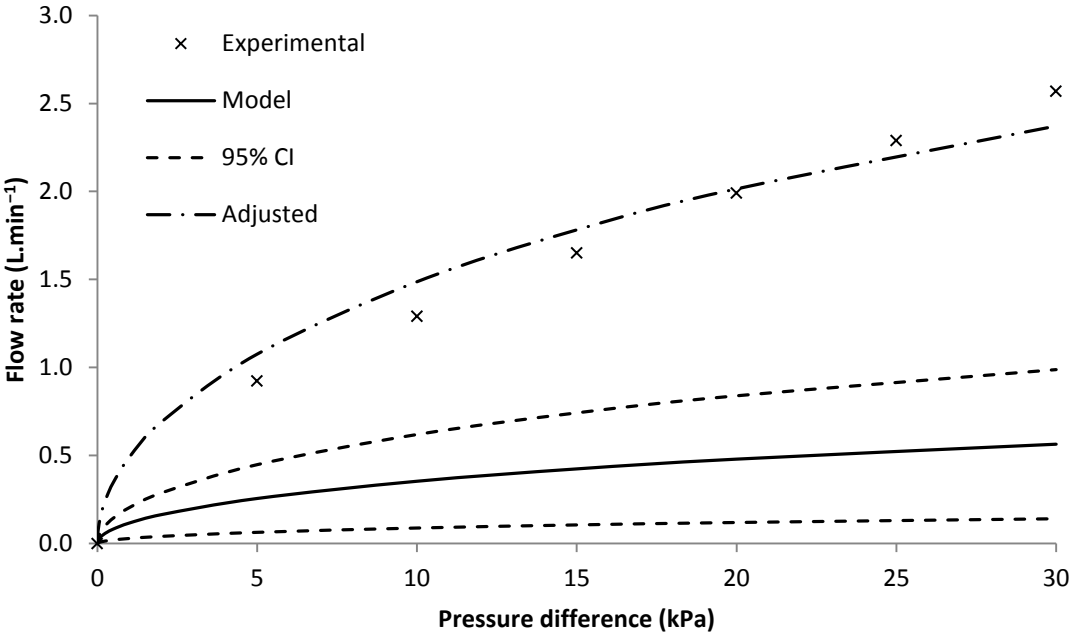

Figure 7-9: Comparison of flow rate (L.min^{-1}) versus pressure drop (kPa) for air flow through perforations produced with a 0.33 mm diameter syringe needle as predicted by the model and measured experimentally, as well as adjusted model predictions.

A similar comparison was carried out for the larger perforation created with a needle, for which results are shown in Figure 7-10. In this case there was much closer agreement between model predictions and experimental measurements, however experimental measurements were still constantly above mean predictions. This is most likely also due to stretching, although the effect is much less significant due to the larger

size of the perforations. It is therefore believed that the consolidation model will be valid if the actual size of perforations for a given pressure drop can be estimated. Because the model was only required to provide a guide to how consolidation is effected by perforation size, further validation was not pursued.

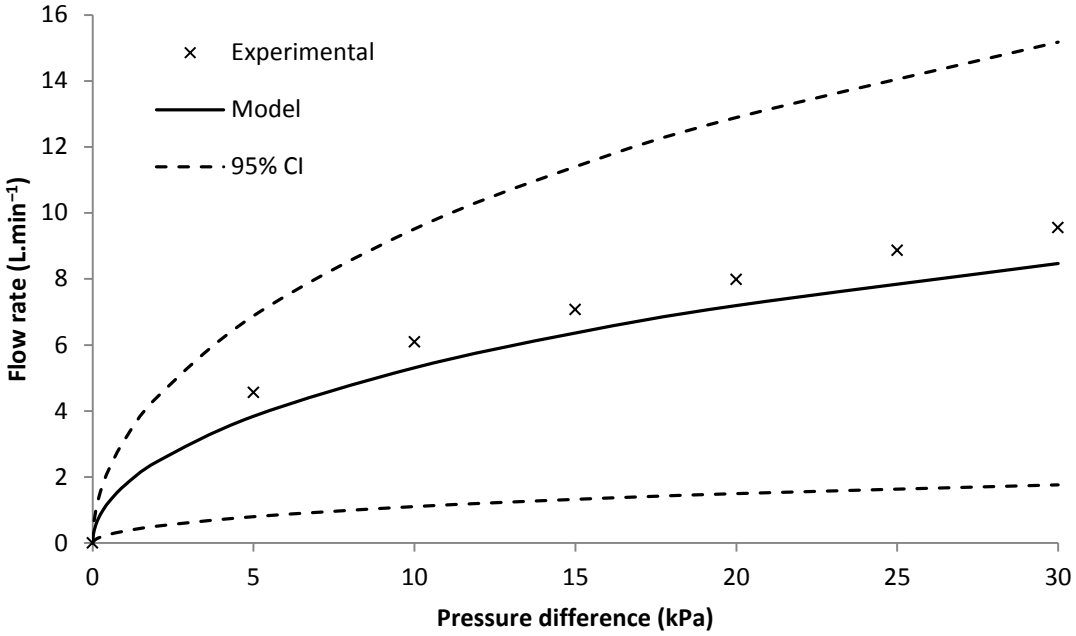

Figure 7-10: Comparison of flow rate (L.min^{-1}) versus pressure drop (kPa) for air flow through perforations created with a 0.9 mm diameter syringe needle as predicted by the model and measured experimentally.

7.6 MODEL APPLICATIONS

Potential applications for the developed mathematical models were previously discussed in Section 3.5. It was suggested that the mathematical models would be useful tools for optimising current food packaging systems, particularly in cases where packaging was selected either qualitatively or based on a “worst case” design approach. Applying the models for such scenarios is fairly straight forward, and simply requires selection of the model most representative of the system and reasonable estimation of model parameters. However with the extension of the models for more complex systems, and particularly in the development of the consolidation model, a particular focus was placed on the scenario

of dense phase filled or similar food packages. In these systems perforations are commonly required to allow consolidation of air in the package after filling. Perforations can significantly increase moisture transfer into (or out of) the package, resulting in a reduced product shelf life or quality concerns. Therefore in such systems an optimised design involves consideration of both time required for consolidation as well as resistance to moisture transfer, which are conflicting aspects.

7.6.1 Wheat Flour Bags for Export

To demonstrate application of the mathematical models for a dense phase filled food powder bag, wheat flour was used as a specific example. The wheat flour system consisted of a large paperboard bag with a polymer liner containing 20 kg of wheat flour for industrial markets. The polymer liner contained 10 perforations to allow consolidation of the bag after filling.

It should be noted that practical applications require detailed data of system specific properties and conditions, much of which is highly commercially sensitive. Therefore the aim was not to provide an example of an actual system, but rather to indicate how the models can be applied. As a result data from various sources were used for the simulation, which are summarised in Table 7-3.

Table 7-3: Summary of system properties for a wheat flour bag for export.

Parameter Description	Symbol	Units	Value
Ambient conditions			
Ambient temperature	T	K	$25 + 273.15$
Ambient relative humidity	RH_a	%	75
Food product properties			
Initial mass	m_i	kg	20
Initial moisture content	M_i	(kg water).(kg solids)$^{-1}$	0.101 [a]

Mass of solids	m_s	kg	22.7 [b]
Bulk density	ρ_b	kg.m^{-3}	630 [c]
Particle density	ρ_p	kg.m^{-3}	1475 [d]
Porosity	ε	-	0.573 [e]
Critical moisture content	M_c	(kg water).(kg solids)$^{-1}$	
GAB isotherm parameters			
Moisture content of monolayer for GAB isotherm	$M_{0,GAB}$	(kg water).(kg solids)$^{-1}$	0.0644 [f]
Guggenheim constant for GAB isotherm	C_{GAB}	-	22.23 [f]
Constant for GAB isotherm	k_{GAB}	-	0.91 [f]
Packaging properties			
Surface area of packaging	A_{pkg}	m^2	1.04 [g]
Volume of air in package headspace	V_{air}	m^3	
Average diameter of perforations	d_{prf}	m	1×10^{-4} [g]
Number of perforations	N_{prf}	-	10 [g]
Number of layers	N	-	1
Layer thickness	X_1	m	5×10^{-5} [h]
Solubility of water vapour in layer 1 of packaging at ambient temperature	$S^{H_2O}_{ref,pkg,1}$	mol.m^{-3}.Pa^{-1}	0.001 [i]
Permeability of water vapour in layer 1 of packaging at ambient temperature	$P^{H_2O}_{ref,pkg,1}$	mol.m.m^{-2}.s^{-1}.Pa^{-1}	2.5×10^{-14} [j]

[a] Obtained from literature (Leung et al., 2006). [b] Calculated using initial moisture content and initial mass. [c] Obtained from literature (Okaka & Potter, 1977). [d] Obtained from literature (Kamath et al., 1994). [e] Calculated from bulk density and particle density. [f] Obtained from literature (Lewicki, 2009). [g] Estimated based on bulk density and relative dimensions of similar food packaging systems. [h] Estimated based on packaging for similar food powders. [i] A low solubility was assumed. [j] Estimated based on compiled permeability data for LDPE (Section 3.2).

A comparison of shelf life as predicted by the extended model with non-instantaneous mass transfer in the food powder (Section 5.3) and consolidation time as predicted by the consolidation model based on the total perforated area is shown in Figure 7-11.

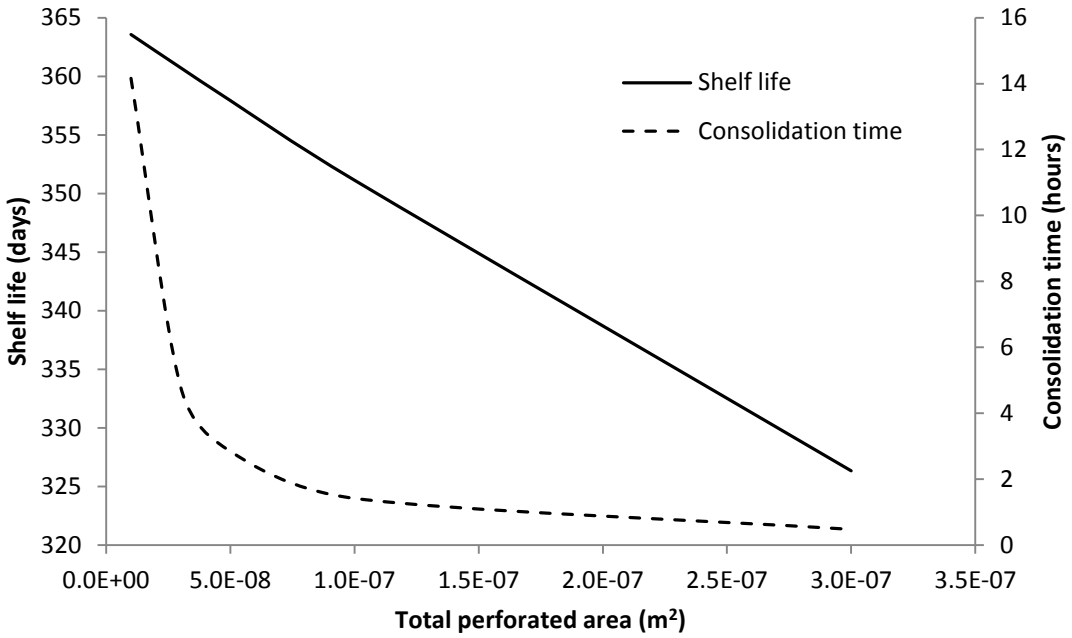

Figure 7-11: Comparison of shelf life (days) and consolidation time (hours) for a bag of wheat flour for varying total perforated area (m^2).

As shown, a total perforated area of below about 1×10^{-7} m^2 resulted in only a relatively small change in consolidation time. Therefore a perforated area of about 1×10^{-7} m^2 may be most optimal for this system provided a shelf life of 351 days is adequate. If a higher shelf life is required, a smaller perforated area resulting in a longer consolidation time may need to be considered, or a higher barrier film could be used. For this particular scenario the change in shelf life due to the perforated area was relatively linear. It is expected that for other food systems with different moisture sorption isotherms the resulting change in shelf life may be more non-linear, in which case the effect of the perforated area may be more complex.

The developed mathematical models should be equally applicable to other similar food systems, including sugar, rice flour, soy powders, dairy powders, and other food ingredients, particularly those for industrial markets. Some high moisture food products may also similarly be optimised using the models, including fresh produce (apples and kiwifruit), dairy products (butter and cheese), meat products (beef, lamb, mutton and pork), and seafood. However it should be noted that for some of these systems other aspects may also need to be considered, such as respiration and below freezing temperatures. Extending

the models for such scenarios should be fairly straight forward, and future studies undertaking such work would be useful.

7.6.2 Consolidation of Palletised Food Powder Bags

In terms of package consolidation, up to this point only a single food powder bag has been considered. A situation that may be more common in real world applications is the consolidation of multiple bags stacked vertically such as in a pallet. In this case the change in total headspace volume or total height of the stacked bags will be more dynamic. To demonstrate this effect, the scenario of five wheat flour bags stacked vertically was considered. To simulate this system, the five bags were simulated separately and the total headspace volume calculated as the sum of the individual volumes. Model parameters for these simulations are summarised in Table 7-4, and predictions are shown in Figure 7-12.

Table 7-4: Summary of system inputs used for validation of the consolidation model.

Parameter Description	Symbol	Units	Value
Temperature	T	K	$20 + 273.15$
Total perforated area	A_{prf}	m^2	5×10^{-8}
Mass stacked on top of food package	m_{stk}	kg	0, 20, 40, 60 and 80
Contact area of mass stacked on top of food package	A_{stk}	m^2	0.343

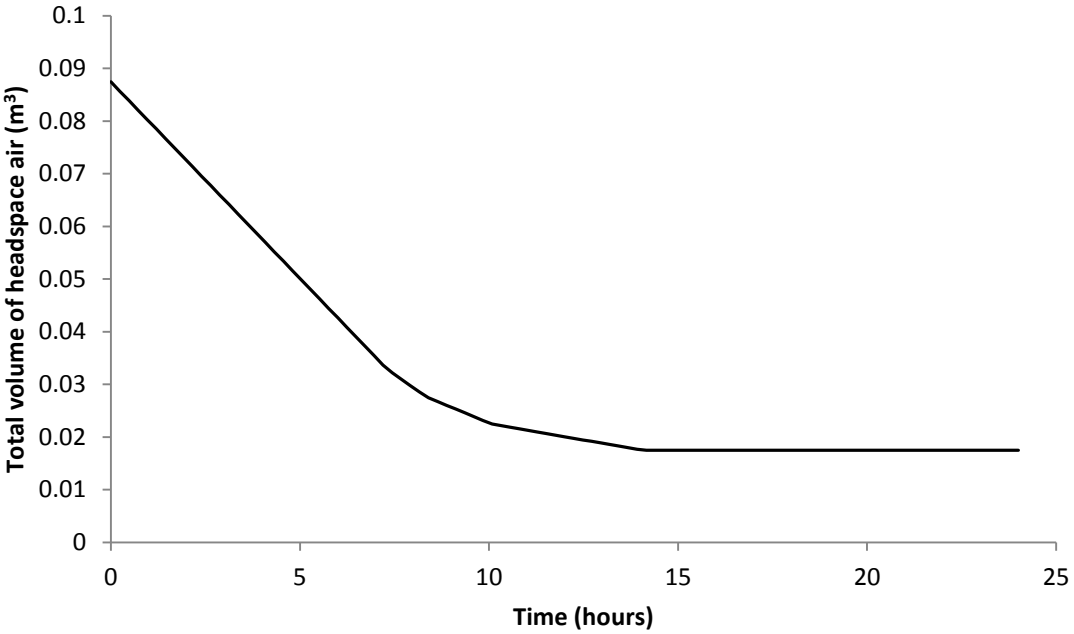

Figure 7-12: Plot of changing total volume of headspace air (m^3) due to air expulsion in five bags of wheat flour stacked vertically versus time (hours) as predicted by the model.

As shown, the change in total volume of headspace air in the wheat flour bags, and thus the total height of the pallet, was non-linear. This affect is due to the different rates of air expulsion of the individual bags based on the different headspace air pressures. Based on this simulation the bags would never fully consolidate since the top bag has no mass on top of it, and therefore no driving force for air expulsion. In reality the weight of the packaging may cause a very slow rate of air expulsion.

7.7 SUMMARY

In this chapter, the development of a food package consolidation model was presented. The system consists of an enclosed package containing perforations, through which air in the package headspace is expelled. Key assumptions included that air is an incompressible fluid, pressure drop due to friction is negligible, and the process occurs at a constant temperature. A mathematical model was formulated and solved analytically, for which a MATLAB® script file was created. As usual, error checks and model validation were carried out, confirming that the model was correctly formulated.

Potential applications of the developed mathematical models were discussed, including dense phase filled food products. The specific example of wheat flour was used to demonstrate the use of the package consolidation model together with the moisture transfer models to optimise perforated area.

Chapter 8

CONCLUSIONS AND RECOMMENDATIONS

8.1 CONCLUSIONS

The processes and considerations involved in food packaging selection were investigated. Several considerations in addition to mass transfer were identified, and it was noted that some of these considerations are generally conflicting. In terms of barrier requirements, detailed theory allowing quantitative packaging design was reviewed. However it was found that industry practice often involves a qualitative approach to packaging design, or a focus on “worst case” ambient conditions. As a result it was suggested that many current food packaging systems may either be under- or over-designed.

Review of literature revealed significant gaps regarding data of food packaging barrier properties. Therefore to aid this investigation a summary of the barrier property requirements of various food products was produced using literature and experimental data. As part of this work a table of the barrier properties of food packaging materials presented in a standard format was compiled.

A series of mathematical models were formulated allowing the prediction of moisture transfer in various food packaging systems, and the effect on product shelf life and quality. Firstly a standard food package system was considered, consisting of a food product enclosed in a single individual packaging layer which may contain perforations. Further models were developed extending the standard system to include systems with two individual packaging layers containing perforations, as well as packages containing food powders where mass transfer in the food powder is also significant. Systems with perforations in contact with food powder or centred on a relatively small isolated air pocket were also considered, where a localised two-dimensional moisture profile results.

Several potential applications for the developed mathematical models were identified. A particular focus was placed on food powder systems with perforated packaging, such as those for which dense phase filling is used. This may include flours, sugar, soy powders, dairy powders, and other industrial or commercial food ingredients. To allow optimisation of these packaging systems, a mathematical model was also formulated to allow prediction of package headspace consolidation. Many high moisture content food products were also identified as having conceptually similar packaging systems, such as fresh produce, dairy products, meat products, and seafood. However it was noted that some extensions to the mathematical models may be required in some cases.

8.2 RECOMMENDATIONS

Some phenomena that may be encountered in food packaging systems were not included in the mathematical models as they were not relevant to this investigation. These include respiration, below freezing temperatures, temperature profiles, and other more complex aspects. Other gases such as oxygen and interaction of multiple permeating species were also not considered. It was suggested that if simulation of such systems is required, appropriate extensions to the mathematical models should be possible and in most cases relatively straight forward. Therefore such work is recommended for future studies.

Note that the work presented here was completed over the course of 1 year as required for a masters thesis. Unfortunately this significantly constrained the scope of model validation experiments, particularly since some aspects of the mathematical models only manifest over a relatively long term period. It is therefore suggested that further validation be carried out if the developed mathematical models are to be adopted for real-world applications.

Chapter 9

REFERENCES

Akbari, Z., Ghomashchi, T. & Moghadam, S. (2007). Improvement in food packaging industry with biobased nanocomposites. *International Journal of Food Engineering, 3*(4).

Allen, L., Nelson, A. I., Steinberg, M. P. & McGill, J. N. (1963). Edible corn-carbohydrate food coatings. 1. Development and physical testing of a starch-algin coating. *Food Technology, 17*(11), 1437.

Al-Muhtaseb, A. H., McMinn, W. A. M. & Magee, T. R. A. (2002). Moisture sorption isotherm characteristics of food products: a review. *Food and Bioproducts Processing, 80*(2), 118-128.

Ashley, R. J. (1985). Permeability and plastics packaging. In J. Comyn (Ed.), *Polymer and Permeability* (pp. 269-307). London: Elsevier.

ASHRAE. (1997). *ASHRAE Handbook−Fundamentals*. Atlanta: American Society of Heating, Refrigerating and Air−Conditioning Engineers.

Automation Creations. (2009). *MatWeb: Material Property Data.* Retrieved September 16, 2009, from http://www.matweb.com

Azanha, A. B. & Faria, J. A. F. (2005). Use of mathematical models for estimating the shelf life of cornflakes in flexible packaging. *Packaging Technology and Science, 18*(4), 171-178.

Banks, N. H., Cleland, D. J., Cameron, A. C., Beaudry, R. M. & Kader, A. A. (1995). Proposal for a Rationalized System of Units for Postharvest Research in Gas Exchange. *HortScience, 30*(6), 1129-1131.

Barront, F. H., Harte, B., Giacin, J. & Hernandez, R. (1993). Modelling of oxygen diffusion through a model permeable package and simultaneous degradation of vitamin C in apple juice. *Packaging Technology and Science, 6*(6), 301-309.

Brody, A. L. & Marsh, K. S. (Eds.). (1997). *The Wiley Encyclopedia of Packaging Technology.* New York: John Wiley & Sons.

Brody, A. L. (2000). Packaging, food. In *Kirk-Othmer Encyclopedia of Chemical Technology* (3rd ed.). New York: John Wiley & Sons.

Bronlund, J. E. & Davey, L. (2007). *140391 Process Operations and Modelling: An introduction to mathematical modelling.* School of Engineering and Advanced Technology, Massey University, Palmerston North.

Bronlund, J. E. & Paterson, A. H. J. (2004). Moisture sorption isotherms for crystalline, amorphous and predominantly crystalline lactose powders. *International Dairy Journal, 14*(3), 247-254.

Buekens, A. & Huang, H. (1998). Comparative evaluation of techniques for controlling the formation and emission of chlorinated dioxins/furans in municipal waste incineration. *Journal of Hazardous Materials, 62*(1), 1-33.

Cleland, D. J. (2008). *140403 Advanced Modelling and Simulation: Process simulations with more than one independent variable.* School of Engineering and Advanced Technology, Massey University, Palmerston North.

Coles, R., McDowell, D. & Kirwan, M. J. (Eds.). (2003). *Food Packaging Technology.* Oxford: Blackwell.

Commonwealth of Australia. (2007). *Australia New Zealand Food Standards Code*. Melbourne: Anstat.

Comyn, J. (Ed.). (1985). *Polymer Permeability.* London: Elsevier Applied Science.

Conte, A., Scrocco, C., Brescia, I. & Del Nobile, M. A. (2009). Packaging strategies to prolong the shelf life of minimally processed lampascioni (Muscari comosum). *Journal of Food Engineering, 90*(2), 199-206.

del Nobile, M. A., Buonocore, G. G., La Notte, E. & Nicolais, L. (2003). Modeling the Oxygen Barrier Properties of Nylon Film Intended for Food Packaging Applications. *Journal of Food Science, 6*(68), 2017-2021.

del Nobile, M. A., Buonocore, G. G., Limbo, S. & Fava, P. (2003). Shelf life prediction of cereal-based dry foods packed in moisture-sensitive films. *Journal of Food Science, 68*(4), 1292-1300.

del Pilar Noriega, M., Estrada, O. & Vargas, C. A. (2003, May 4-8). *Design of plastic multi-layer structure that fit the requirements of a specific food or beverage.* Paper presented at the 2003 ANTEC Plastics Annual Technical Conference, Nashville, Tennessee.

Doty, P. M., Aiken, W. H. & Mark, H. (1946). Temperature dependence of water vapor permeability. *Industrial and Engineering Chemistry, 38*(8), 788-791.

Dury-Brun, C., Jury, V., Guillard, V., Desobry, S., Voilley, A., et al. (2006). Water barrier properties of treated-papers and application to sponge cake storage. *Food Research International, 39*(9), 1002-1011.

Eckert, W. (2003, May 12-14). *Improvement of adhesion on polymer film, foil and paperboard by flame treatment.* Paper presented at the TAPPI 9th European PLACE Conference, Rome, Italy.

Eskin, N. A. M. & Robinson, D. S. (Eds.). (2001). *Food Shelf Life Stability: Chemical, Biochemical, and Microbiological Changes.* Boca Raton, Florida: CRC Press.

Euromonitor International. (2005). *Sustainability: Its impact on global consumption to 2010.* Retrieved July 27, 2009, from Global Market Information Database.

Euromonitor International. (2009). *Euromonitor International: Global market research on industries, countries and consumers.* Retrieved September 24, 2009, from http://www.euromonitor.com/

EVAL Americas. (2009). *Gas Barrier Properties of Resins.* Retrieved September 24, 2009, from http://www.eval.be/upl/1/default/doc/EA%20-%20Technical%20Bulletin%20No%20110.pdf

Farroni, A. E., Matiacevich, S. B., Guerrero, S., Alzamora, S. & Buera, M. (2008). Multi-level approach for the analysis of water effects in corn flakes. *Journal of Agricultural and Food Chemistry, 56*(15), 6447-6453.

Fennema, O. R. (Ed.). (1996). *Food Chemistry* (3rd ed.). New York: Marcel Dekker.

Fishman, S., Rodov, V. & Ben-Yehoshua, S. (1996). Mathematical model for perforation effect on oxygen and water vapour dynamics in modified-atmosphere packages. *Journal of Food Science, 61*(5), 956-961.

Fishman, S., Rodov, V., Peretz, J. & Ben-Yehoshua, S. (1995). Model for gas exchange dynamics in modified-atmosphere packages of fruits and vegetables. *Journal of Food Science, 60*(5), 1078-1083.

Fonseca, S. C., Oliveira, F. A. R. & Brecht, J. K. (2002). Modelling respiration rate of fresh fruits and vegetables for modified atmosphere packages: a review. *Journal of Food Engineering, 52*(2), 99-119.

Forney, C. F. & Brandl, D. G. (1992). Control of humidity in small controlled-environment chambers using glycerol-water solutions. *HortTechnology, 2*, 52-54.

Foster, K. D., Bronlund, J. E. & Paterson, A. H. J. (2005). The prediction of moisture sorption isotherms for dairy powders. *International Dairy Journal, 15*(4), 411-418.

Geankoplis, C. J. (1993). Principles of unsteady−state heat transfer. In *Transport Processes and Unit Operations* (pp. 330−380). New Jersey: Prentice Hall.

Geankoplis, C. J. (2003). Principles of Unsteady−State and Convective Mass Transfer. In *Transport Processes and Separation Process Principles (Includes Unit Operations)* (4^{th} ed.) (pp. 456−507). New Jersey: Prentice Hall.

Genkawa, T., Uchino, T., Miyamoto, S., Inoue, A., Ide, Y. et al. (2008). Development of mathematical model for simulating moisture content during the re-wetting of brown rice stored in film packaging. *Biosystems Engineering, 101*(4), 445-451.

Ghosal, K. & Freeman, B. D. (1994). Gas separation using polymer membranes: an overview. *Polymers for Advanced Technologies, 5*(11), 673-697.

Gontard, N., Thibault, R., Cuq J. L. & Guilbert, S. (1996). Influence of relative humidity and film composition on oxygen and carbon dioxide permeabilities of edible films. *Journal of Agricultural and Food Chemistry, 44*(4), 1064-1069.

González-Buesa, J., Ferrer-Mairal, A. Oria, R. & Salvador, M. L. (2009). A mathematical model for packaging with microperforated films of fresh-cut fruits and vegetables. *Journal of Food Engineering*, 95(1), 158-165.

Greener, I. K. & Fennema, O. (1989). Barrier properties and surface characteristics of edible, bilayer films. *Journal of Food Science, 54*(6), 1393-1399.

Guilbert, S., Gontard, N. & Gorris, L. G. (1996). Prolongation of the shelf-life of perishable food products using biodegradable films and coatings. *Food Science and Technology, 29*(1-2), 10-17.

Guillard, V., Broyart, B., Bonazzi, C., Guilbert, S. & Gontard, N. (2003). Evolution of moisture distribution during storage in a composite food modelling and simulation. *Journal of Food Science, 68*(3), 958-966.

Guillard, V., Broyart, B., Guilbert, S., Bonazzi, C. & Gontard, N. (2004). Moisture diffusivity and transfer modelling in dry biscuit. *Journal of Food Engineering, 64*(1), 81-87.

Horticulture & Food Research Institute of New Zealand. (2007). *Fresh Facts: New Zealand Horticulture 2007*. Retrieved January 19, 2010 from http://www.hortresearch.co.nz/files/aboutus/factsandfigs/ff2007.pdf

Iglesias, H. A. & Chirife, J. (1982). *Handbook of Food Isotherms: Water Sorption Parameters for Food and Food Components.* New York: Academic Press.

Jahromi, S. & Moosheimer, U. (2000). Oxygen Barrier Coatings Based on Supramolecular Assembly of Melamine. *Macromolecules, 33*(20), 7582-7587.

Jay, J. M., Loessner, M. J. & Golden, D. A. (2005). *Modern Food Microbiology* (7th ed.). New York: Springer.

Joupila, K. & Roos, Y. H. (1994). Water sorption and time-dependent phenomena of milk powders. *Journal of Dairy Science, 77*(7), 1798-1808.

Kamath, S., Puri, V. M. & Manback, H. B. (1994). Flow property measurement using the Jenike cell for wheat flour at various moisture contents and consolidation times. *Powder Technology, 81*(3), 293-297.

Kesting, R. E. & Fritzsche, A. K. (1993). *Polymeric gas separation membranes.* New York: John Wiley & Sons.

Labuza, T. P. & Hyman, C. R. (1998). Moisture migration and control in multi-domain foods. *Trends in Food Science & Technology, 9*(2), 47-55.

Lange, J. & Wyser, Y. (2003). Recent innovations in barrier technologies for plastic packaging - a review. *Packaging Technology and Science, 16*(4), 149-158.

Lee, D. S., Hagger, P. E., Lee, J. & Yam, K. L. (1991). Model for fresh produce respiration in modified atmospheres based on principles of enzyme kinetics. *Journal of Food Science, 56*(6), 1580-1585.

Leung, H. K., Magnuson, J. A. & Bruinsma, B. L. (1983). Water binding of wheat flour doughs and breads as studied by deuteron relaxation. *Journal of Food Science, 48*(1), 95-99.

Lewicki, P. P. (2009). Data and models of water activity. II: Solid foods. In S. Rahman (Ed.), *Food Properties Handbook* (2nd ed.). Boca Raton, Florida: CRC Press.

Lohwasser, W. & Frei, O. (1999). *Breakthrough in commercially produced SiO_x-films in Europe – It will happen.* Paper presented at Flex-Pak Europe '99, Amsterdam, The Netherlands.

Lord, T. (2003). Packaging materials as a source of taints. In B. Baigrie (Ed.), *Taints and Off-Flavours in Foods* (pp. 64-111). Cambridge, England: Woodhead Publishing.

Lukens, R. P. (2000). Units and conversion factors. In *Kirk-Othmer Encyclopedia of Chemical Technology* (3rd ed.). New York: John Wiley & Sons.

Lyijynen, T., Hurme, E. & Ahvenainen, R. (2003). Optimizing packaging. In R. Ahvenainen (Ed.), *Novel food packaging techniques* (pp. 441-458). Cambridge, England: Woodhead Publishing.

Massey, L. K. (2003). *Permeability Properties of Plastics and Elastomers: A Guide to Packaging and Barrier Materials* (2nd ed.). New York: William Andrew Publishing/Plastics Design Library.

Meat Industry Association of New Zealand. (2010). *Industry Statistics.* Retrieved January 19, 2010 from http://www.mia.co.nz/statistics/

Ministry of Agriculture and Forestry. (2007). *Horticulture and Arable Monitoring Report.* Retrieved January 19, 2010 from http://www.maf.govt.nz/mafnet/rural-nz/statistics-and-forecasts/farm-monitoring/2007/horticulture-and-arable/2007-horticulture-monitoring-report.pdf

Morillon, V., Debeaufort, F., Capelle, M., Blond, G. & Voilley, A. (2000). Influence of the physical state of water on the barrier properties of hydrophilic and hydrophobic films. *Journal of Agricultural Food Chemistry, 48*(1), 11-16.

Muramatsu, Y., Tagawa, A. & Kasai, T. (2005). Effective thermal conductivity of rice flour and whole and skim milk powder. *Journal of Food Science, 70*(4), E279-E287.

Nevins, A. L. (2008). *Significant factors affecting horticultural corrugated fibreboard strength.* PhD Thesis. Massey University. Retrieved 15 June, 2010, from Massey Research Online.

New Zealand Trade and Enterprise. (2007a). *Dairy industry in New Zealand*. Retrieved January 20, 2010 from http://marketnewzealand.com/common/files/Dairy-industry-in-New-Zealand.pdf

New Zealand Trade and Enterprise. (2007b). *Meat industry in New Zealand*. Retrieved January 19, 2010 from http://www.marketnewzealand.com/common/files/Meat-industry-in-New-Zealand.pdf

New Zealand Trade and Enterprise. (2009). *Seafood industry in New Zealand*. Retrieved January 20, 2010 from http://marketnewzealand.com/common/files/Seafood-industry-in-New-Zealand.pdf

Okaka, J. C. & Potter, N. N. (). Functional and storage properties of cowpea powder-wheat flour blends in breadmaking. *Journal of Food Science, 42*(3), 828-833.

Packaging Council of New Zealand. (2009). *Mass Balance: Consumption and Collection*. Retrieved September 16, 2009, from http://www.packaging.org.nz/packaging_info/packaging_consum.php

Park, H. J. (1990). *Properties of edible coatings for fruits and vegetables.* Paper presented at the 1990 American Society of Agricultural Engineers, St. Joseph, MI.

Parris, N., Sykes, M., Dickey, L. C., Wiles, J. L., Urbanik, T. J., et al. (2002). Recyclable Zein-Coated Kraft Paper and Linerboard. *Progress in Paper Recycling, 11*(3), 24-29.

Pavlath, A. E., Wong, D. S. W. & Kumosinski, T. F. (1993). New coatings for cut fruits and vegetables. *Chemtech, 23*(2), 36-40.

Petersen, K., Nielsen, P. V., Bertelsen, G., Lawther, M., Olsen, M. B., et al. (1999). Potential of biobased materials for food packaging. *Trends in Food Science & Technology, 10*(2), 52-68.

Piringer, O. G. & Baner, A. L. (Eds.). (1999). *Plastic Packaging Materials for Food: Barrier Function, Mass Transport, Quality Assurance, and Legislation*. Weinheim: Wiley-VCH.

Plastics Design Library. (1995). *Permeability and other properties of plastics and elastomers.* Norwich, New York: William Andrews Publishing.

Poyet, J. (1993, April 1-2). *Les polyme`res "barrie`res".* Paper presented at the 1993 Congre`s S.A.G.E., "L'alimentarite´ dans les matie`res plastiques et les caoutchoucs", Paris, France.

Quast, D. G., Karel, M. & Rand, W. M. (2006). Development of a mathematical model for the oxidation of potato chips as a function of oxygen pressure, extent of oxidation and equilibrium relative humidity. *Journal of Food Science, 37*(5), 673-678.

Rahman, S. (Ed.). (1995). *Food Properties Handbook.* Boca Raton, Florida: CRC Press.

Rico-Pena, D. C. & Torres, J. A. (1990). Oxygen transmission rate of an edible ethylcellulose-palmitic acid film. *Journal of Food Process Engineering, 13*(2), 125-133.

Rigg, W. J. (1979). Measurement of the permeability of chilled meat packaging film under conditions of high humidity. *Journal of Food Technology, 14*(2), 149-155.

Robertson, G. L. (2006). *Food Packaging: Principles and Practice* (2nd ed.). Boca Raton, Florida: Taylor & Francis.

Roca, A., Broyart, B., Guillard, V., Guilbert, S. & Gontard, N. (2008). Predicting moisture transfer and shelf-life of multidomain food products. *Journal of Food Engineering 86*(1), 74-83.

Salame, M. (1986). Barrier polymers. In Bakker, M. (Ed.), *The Wiley Encyclopedia of Packaging Technology* (pp. 48-54). New York: John Wiley & Sons.

Shah, D. J., Ramsey, J. W. & Wang, M. (1984). An experimental determination of the heat and mass transfer coefficients in moist unsaturated soils. *International Journal of Heat and Mass Transfer, 27*(7), 1075−1085.

Sidel SA. (1999). *Amorphous Carbon Treatment on Internal Surface* [Brochure]. Havre, France: Author.

Singh, R. P. & Heldman, D. R. (2009). *Introduction to food engineering.* Amsterdam, Netherlands: Academic Press.

Singh, R. & Oliveira, F. A. R. (Eds.). (1994). *Minimal Processing of Foods and Process Optimization: An Interface.* Boca Raton, Florida: CRC Press.

Sirpatrawan, U. (2009). Shelf-life simulation of packaged rice crackers. *Journal of Food Quality, 32*(2), 224-239.

Song, Y. S., Begley, T., Paquette, K. & Komolprasert, V. (2003). Effectiveness of polypropylene film as a barrier to migration from recycled paperboard packaging to fatty and high-moisture food. *Food Additives and Contaminants, 20*(9), 875-883.

Sorrentino, A., Gorrasi, G. & Vittoria, V. (2007). Potential perspectives of bio-nanocomposites for food packaging applications. *Trends in Food Science & Technology, 18*(2), 84-95.

Stringleman, H. & Scrimgeour, F. (2009). Dairying and dairy products. *Te Ara - the Encyclopedia of New Zealand.* Retrieved January 19, 2010 from http://www.TeAra.govt.nz/en/dairying-and-dairy-products/11/2

Tanner, D. J., Cleland, A C. & Robertson, T. R. (2002). A generalised mathematical modelling methodology for design of horticultural food packages exposed to refrigerated conditions: Part 3, mass transfer modelling and testing. *International Journal of Refrigeration 25*(1), 54-65.

Taylor, C. C. (1986). Cellophane. In M. Bakker (Ed.), *The Wiley Encyclopedia of Packaging Technology* (pp. 159-163). New York: John Wiley & Sons.

Techavises, N. & Hikida, Y. (2008). Development of a mathematical model for simulating gas and water vapour exchanges in modified atmosphere packaging with macroscopic perforations. *Journal of Food Engineering, 85*(1), 94-104.

The MathWorks Inc (2008). MATLAB® (Version R2008a) [Computer Software]. Natick, MA: The MathWorks Inc.

Treybal, R. E. (1980). *Mass transfer operations* (3rd ed.). Tokyo, Japan: McGraw-Hill.

Utto, W. (2008). *Mathematical modelling of active packaging systems for horticultural products.* PhD Thesis. Massey University. Retrieved 14 May, 2010, from Massey Research Online.

Vahdat, N. & Sullivan, V. D. (2001). Estimation of Permeation Rate of Chemicals Through Elastometric Materials. *Journal of Applied Polymer Science, 79*(7), 1265-1272.

Wolf, R. & Ellwanger, R. E. (2003, August 3-7). *Inline functional coatings of surfaces via plasma CVD at atmospheric pressure*. Paper presented at the 2003 PLACE Conference and the Global Hot Melt Symposium, Orlando, Florida.

Appendix A

BARRIER PROPERTIES OF PACKAGING MATERIALS

A table of the barrier properties of various food packaging materials can be found in a digital format on the attached compact disk.

Appendix B

DIGITAL COPIES OF NUMERICAL SOLUTIONS FOR MATHEMATICAL MODELS

Numerical solutions for the mathematical models developed for this study can be found in a digital format on the attached compact disk. An index to the files and folders on the compact disk is outlined below. These numerical solutions are also included in the respective model chapter appendices.

- Appendix B – Food Package Moisture Transfer Models
    - Standard Model
        - Package.m (Script File)
        - PackageFun.m (Model Function File)
        - DpkgFun.m
        - SpkgFun.m
    - Extended Models
        - Two Separate Packaging Layers
            - PackageExtended.m (Script File)
            - PackageExtendedFun.m (Model Function File)
            - DbagFun.m
            - DlnrFun.m
            - SbagFun.m
            - SlnrFun.m
        - Non-Instantaneous Mass Transfer in Food
            - PackageExtended2.m (Script File)
            - PackageExtended2Fun.m (Model Function File)
            - DbagFun.m
            - DlnrFun.m
            - SbagFun.m
            - SlnrFun.m

        - IsothermFun.m
- 2D Perforation Models
    - No Air Pocket
        - Perforation.m (Script File)
        - PerforationFun.m (Model Function File)
        - IsothermFun.m
    - With Isolated Air Pocket
        - Perforation.m (Script File)
        - PerforationFun.m (Model Function File)
        - IsothermFun.m
- Consolidation Model
    - Consolidation.m (Script File)

Appendix C

STANDARD FOOD PACKAGE MOISTURE TRANSFER MODEL

C.1 MATHEMATICAL MODEL FORMULATION

C.1.1 Word Balances and Equations

C.1.1.1 ODE for Moisture Content of Food Product

Unsteady-state mass balance of water in food

$$\frac{dn_f^{H_2O}}{dt} = P_{pkg,n=N}^{H_2O} A_{pkg} \left(\frac{dp_{pkg}^{H_2O}}{dx}\right)_{x=X_{T,pkg}} + J_{prf}^{H_2O} A_{prf}$$

$$n_f^{H_2O} = \frac{m_f^{H_2O}}{M_{r,H_2O}} = \frac{M m_s}{M_{r,H_2O}}$$

$$\therefore \frac{dn_f^{H_2O}}{dt} = \frac{m_s}{M_{r,H_2O}} \frac{dM}{dt} = P_{pkg,n=N}^{H_2O}(p_{pkg}^{H_2O}) A_{pkg} \left(\frac{dp_{pkg}^{H_2O}}{dx}\right)_{x=X_{T,pkg}} + J_{prf}^{H_2O} A_{prf}$$

$$\frac{dM}{dt} = \frac{M_{r,H_2O}}{m_s} \left[P_{pkg,n=N}^{H_2O}(p_{pkg}^{H_2O}) A_{pkg} \left(\frac{dp_{pkg}^{H_2O}}{dx}\right)_{x=X_{T,pkg}} + J_{prf}^{H_2O} A_{prf} \right]$$

$$\left[\frac{kg}{kg.s}\right] = \left[\frac{kg}{mol}\right] \frac{1}{[kg]} \left(\left[\frac{mol.m}{m^2.s.Pa}\right] [m^2] \frac{[Pa]}{[m]} + \left[\frac{mol}{m^2.s}\right] [m^2] \right)$$

C.1.1.2 Equation for Water Vapour Pressure in the Food Product

C.1.1.2.1 GAB Isotherm

$$\frac{M}{M_{0,GAB}} = \frac{C_{GAB} k_{GAB} a_w}{(1 - k_{GAB} a_w)(1 - k_{GAB} a_w + C_{GAB} k_{GAB} a_w)}$$

$$\left[{k_{GAB}}^2(1-C_{GAB})\right]{a_w}^2+\left[k_{GAB}\left(C_{GAB}-C_{GAB}\frac{M_{0,GAB}}{M}-2\right)\right]a_w+1=0$$

$$B_1{a_w}^2+B_2a_w+B_3=0$$

where:

$$B_1={k_{GAB}}^2(1-C_{GAB})$$

$$B_2=k_{GAB}\left(C_{GAB}-C_{GAB}\frac{M_{0,GAB}}{M}-2\right)$$

$$B_3=1$$

$$a_w=\frac{-B_2-\sqrt{{B_2}^2-B_1B_3}}{2B_1}$$

$$p_f^{H_2O}=p_0^{H_2O}\left[\frac{-B_2-\sqrt{{B_2}^2-4B_1}}{2B_1}\right]$$

C.1.1.2.2 BET Isotherm

$$\frac{M}{M_{1,BET}}=\frac{C_{BET}a_w}{(1-a_w)(1-a_w+C_{BET}a_w)}$$

$$(1-C_{BET}){a_w}^2+\left(C_{BET}-C_{BET}\frac{M_{1,BET}}{M}-2\right)a_w+1=0$$

$$B_1{a_w}^2+B_2a_w+B_3=0$$

where:

$$B_1=1-C_{BET}$$

$$B_2=C_{BET}-C_{BET}\frac{M_{1,BET}}{M}-2$$

$$B_3=1$$

$$a_w=\frac{-B_2-\sqrt{{B_2}^2-B_1B_3}}{2B_1}$$

$$p_f^{H_2O} = p_0^{H_2O}\left[\frac{-B_2 - \sqrt{{B_2}^2 - 4B_1}}{2B_1}\right]$$

C.1.1.2.3 Linear Isotherm

$$M = b_{lin}a_w + c_{lin}$$

$$a_w = \frac{M - c_{lin}}{b_{lin}}$$

$$p_f^{H_2O} = p_0^{H_2O}\left(\frac{M - c_{lin}}{b_{lin}}\right)$$

C.1.1.3 Equation for Solubility of Water Vapour in the Packaging Material

$$M = \frac{M_{0,pkg,n}k_{pkg,n}C_{pkg,n}p_{pkg}^{H_2O}}{{p_0}^2\left(1 - k_{pkg,n}\frac{p_{pkg}^{H_2O}}{p_0}\right)^2\left(1 - k_{pkg,n}\frac{p_{pkg}^{H_2O}}{p_0} + k_{pkg,n}C_{pkg,n}\frac{p_{pkg}^{H_2O}}{p_0}\right)}$$

$$\frac{dM}{dp_{pkg}^{H_2O}} = \frac{M_{0,pkg,n}{k_{pkg,n}}^2C_{pkg,n}p_{pkg}^{H_2O}}{{p_0}^2\left(1 - k_{pkg,n}\frac{p_{pkg}^{H_2O}}{p_0}\right)^2\left(1 + k_{pkg,n}\frac{p_{pkg}^{H_2O}}{p_0}(C_{pkg,n} - 1)\right)} + \frac{M_{0,bag,n}k_{bag,n}C_{bag,n}}{p_0\left(1 - k_{pkg,n}\frac{p_{pkg}^{H_2O}}{p_0}\right)\left(1 + k_{pkg,n}\frac{p_{pkg}^{H_2O}}{p_0}(C_{pkg,n} - 1)\right)} - \frac{M_{0,bag,n}{k_{bag,n}}^2C_{bag,n}(C_{bag,n} - 1)p_{bag}^{H_2O}}{{p_0}^2\left(1 - k_{pkg,n}\frac{p_{pkg}^{H_2O}}{p_0}\right)\left(1 + k_{pkg,n}\frac{p_{pkg}^{H_2O}}{p_0}(C_{pkg,n} - 1)\right)^2}$$

$$M = \frac{m_w}{m_s}$$

$$C_{pkg}^{H_2O} = \frac{\rho_{s,pkg,n} M}{M_{r,H_2O}}$$

$$S_{pkg,n}^{H_2O} = \frac{C_{pkg}^{H_2O}}{p_{pkg}^{H_2O}} = \frac{\rho_{s,pkg,n}}{M_{r,H_2O}} \frac{dM}{dp_{pkg}^{H_2O}}$$

$$S_{pkg,n}^{H_2O} = \frac{\rho_{s,pkg,n}}{M_{r,H_2O}} \left[\frac{M_{0,pkg,n} k_{pkg,n}{}^2 C_{pkg,n} p_{pkg}^{H_2O}}{p_0{}^2 \left(1 - k_{pkg,n} \frac{p_{pkg}^{H_2O}}{p_0}\right)^2 \left(1 + k_{pkg,n} \frac{p_{pkg}^{H_2O}}{p_0} (C_{pkg,n} - 1)\right)} + \frac{M_{0,bag,n} k_{bag,n} C_{bag,n}}{p_0 \left(1 - k_{pkg,n} \frac{p_{pkg}^{H_2O}}{p_0}\right) \left(1 + k_{pkg,n} \frac{p_{pkg}^{H_2O}}{p_0} (C_{pkg,n} - 1)\right)} - \frac{M_{0,bag,n} k_{bag,n}{}^2 C_{bag,n} (C_{bag,n} - 1) p_{bag}^{H_2O}}{p_0{}^2 \left(1 - k_{pkg,n} \frac{p_{pkg}^{H_2O}}{p_0}\right) \left(1 + k_{pkg,n} \frac{p_{pkg}^{H_2O}}{p_0} (C_{pkg,n} - 1)\right)^2} \right]$$

C.1.2 Equation for Solubility of Water Vapour in Air

$$C = \frac{n}{V} = \frac{p}{RT}$$

$$S_{air}^{H_2O} = \frac{C}{p_{air}^{H_2O}} = \frac{1}{RT}$$

C.2 SOLUTION

C.2.1 Finite Difference Approximations

C.2.1.1 Case 1

$$\frac{dp_{pkg,j}^{H_2O}}{dt} = 0$$

C.2.1.2 Case 2

$$A_{pkg}\Delta x_{pkg,n} S_{pkg,n}^{H_2O} \frac{dp_{pkg,j}^{H_2O}}{dt} = P_{pkg,n}^{H_2O} A_{pkg} \frac{\left(p_a^{H_2O} - p_{pkg,j}^{H_2O}\right)}{\Delta x_{pkg,n}} - P_{pkg,n}^{H_2O} A_{pkg} \frac{\left(p_{pkg,j}^{H_2O} - p_{pkg,j+1}^{H_2O}\right)}{\Delta x_{pkg,n}}$$

$$[m^2][m]\left[\frac{mol}{m^3.Pa}\right]\left[\frac{Pa}{s}\right] = \left[\frac{m^2}{s}\right]\left[\frac{mol}{m^3.Pa}\right][m^2]\frac{[Pa]}{[m]} - \left[\frac{m^2}{s}\right]\left[\frac{mol}{m^3.Pa}\right][m^2]\frac{[Pa]}{[m]}$$

$$\Delta x_{pkg,n}\frac{dp_{pkg,j}^{H_2O}}{dt} = \frac{P_{pkg,n}^{H_2O}}{S_{pkg,n}^{H_2O}}\frac{\left(p_a^{H_2O} - p_{pkg,j}^{H_2O}\right)}{\Delta x_{pkg,n}} - \frac{P_{pkg,n}^{H_2O}}{S_{pkg,n}^{H_2O}}\frac{\left(p_{pkg,j}^{H_2O} - p_{pkg,j+1}^{H_2O}\right)}{\Delta x_{pkg,n}}$$

$$\frac{dp_{pkg,j}^{H_2O}}{dt} = \frac{P_{pkg,n}^{H_2O}}{S_{pkg,n}^{H_2O}\Delta x_{pkg,n}^{\ 2}}\left(p_a^{H_2O} - 2p_{pkg,j}^{H_2O} + p_{pkg,j+1}^{H_2O}\right)$$

C.2.1.3 Case 3

$$A_{pkg}\Delta x_{pkg,n} S_{pkg,n}^{H_2O} \frac{dp_{pkg,j}^{H_2O}}{dt} = P_{pkg,n}^{H_2O} A_{pkg} \frac{\left(p_{pkg,j-1}^{H_2O} - p_{pkg,j}^{H_2O}\right)}{\Delta x_{pkg,n}} - P_{pkg,n}^{H_2O} A_{pkg} \frac{\left(p_{pkg,j}^{H_2O} - p_{pkg,j+1}^{H_2O}\right)}{\Delta x_{pkg,n}}$$

$$[m^2][m]\left[\frac{mol}{m^3.Pa}\right]\left[\frac{Pa}{s}\right] = \left[\frac{m^2}{s}\right]\left[\frac{mol}{m^3.Pa}\right][m^2]\frac{[Pa]}{[m]} - \left[\frac{m^2}{s}\right]\left[\frac{mol}{m^3.Pa}\right][m^2]\frac{[Pa]}{[m]}$$

$$\Delta x_{pkg,n}\frac{dp_{pkg,j}^{H_2O}}{dt}=\frac{P_{pkg,n}^{H_2O}}{S_{pkg,n}^{H_2O}}\frac{\left(p_{pkg,j-1}^{H_2O}-p_{pkg,j}^{H_2O}\right)}{\Delta x_{pkg,n}}-\frac{P_{pkg,n}^{H_2O}}{S_{pkg,n}^{H_2O}}\frac{\left(p_{pkg,j}^{H_2O}-p_{pkg,j+1}^{H_2O}\right)}{\Delta x_{pkg,n}}$$

$$\frac{dp_{pkg,j}^{H_2O}}{dt}=\frac{P_{pkg,n}^{H_2O}}{S_{pkg,n}^{H_2O}\Delta x_{pkg,n}{}^2}\left(p_{pkg,j-1}^{H_2O}-2p_{pkg,j}^{H_2O}+p_{pkg,j+1}^{H_2O}\right)$$

C.2.1.4 Case 4

$$A_{pkg}\left[\frac{\Delta x_{pkg,n}}{2}S_{pkg,n}^{H_2O}+\frac{\Delta x_{pkg,n+1}}{2}S_{pkg,n+1}^{H_2O}\right]\frac{dp_{pkg,j}^{H_2O}}{dt}$$
$$=P_{pkg,n}^{H_2O}A_{pkg}\frac{\left(p_{pkg,j-1}^{H_2O}-p_{pkg,j}^{H_2O}\right)}{\Delta x_{pkg,n}}-P_{pkg,n+1}^{H_2O}A_{pkg}\frac{\left(p_{pkg,j}^{H_2O}-p_{pkg,j+1}^{H_2O}\right)}{\Delta x_{pkg,n+1}}$$

$$[m^2]\left([m]\left[\frac{mol}{m^3.Pa}\right]+[m]\left[\frac{mol}{m^3.Pa}\right]\right)\left[\frac{Pa}{s}\right]$$
$$=\left[\frac{m^2}{s}\right]\left[\frac{mol}{m^3.Pa}\right][m^2]\frac{[Pa]}{[m]}-\left[\frac{m^2}{s}\right]\left[\frac{mol}{m^3.Pa}\right][m^2]\frac{[Pa]}{[m]}$$

$$\left[\frac{\Delta x_{pkg,n}}{2}S_{pkg,n}^{H_2O}+\frac{\Delta x_{pkg,n+1}}{2}S_{pkg,n+1}^{H_2O}\right]\frac{dp_{pkg,j}^{H_2O}}{dt}$$
$$=P_{pkg,n}^{H_2O}\frac{\left(p_{pkg,j-1}^{H_2O}-p_{pkg,j}^{H_2O}\right)}{\Delta x_{pkg,n}}-P_{pkg,n+1}^{H_2O}\frac{\left(p_{pkg,j}^{H_2O}-p_{pkg,j+1}^{H_2O}\right)}{\Delta x_{pkg,n+1}}$$

$$\frac{dp_{pkg,j}^{H_2O}}{dt}=\frac{2}{\Delta x_{pkg,n}S_{pkg,n}^{H_2O}+\Delta x_{pkg,n+1}S_{pkg,n+1}^{H_2O}}$$
$$\left[P_{pkg,n}^{H_2O}\frac{\left(p_{pkg,j-1}^{H_2O}-p_{pkg,j}^{H_2O}\right)}{\Delta x_{pkg,n}}-P_{pkg,n+1}^{H_2O}\frac{\left(p_{pkg,j}^{H_2O}-p_{pkg,j+1}^{H_2O}\right)}{\Delta x_{pkg,n+1}}\right]$$

C.2.1.5 Case 5

$$A_{pkg}\Delta x_{pkg,n}S_{pkg,n}^{H_2O}\frac{dp_{pkg,j}^{H_2O}}{dt}=P_{pkg,n}^{H_2O}A_{pkg}\frac{\left(p_{pkg,j-1}^{H_2O}-p_{pkg,j}^{H_2O}\right)}{\Delta x_{pkg,n}}-P_{pkg,n}^{H_2O}A_{pkg}\frac{\left(p_{pkg,j}^{H_2O}-p_f^{H_2O}\right)}{\Delta x_{pkg,n}}$$

$$[m^2][m]\left[\frac{mol}{m^3.Pa}\right]\left[\frac{Pa}{s}\right]=\left[\frac{m^2}{s}\right]\left[\frac{mol}{m^3.Pa}\right][m^2]\frac{[Pa]}{[m]}-\left[\frac{m^2}{s}\right]\left[\frac{mol}{m^3.Pa}\right][m^2]\frac{[Pa]}{[m]}$$

$$\Delta x_{pkg,n}\frac{dp_{pkg,j}^{H_2O}}{dt}=\frac{P_{pkg,n}^{H_2O}}{S_{pkg,n}^{H_2O}}\frac{\left(p_{pkg,j-1}^{H_2O}-p_{pkg,j}^{H_2O}\right)}{\Delta x_{pkg,n}}-\frac{P_{pkg,n}^{H_2O}}{S_{pkg,n}^{H_2O}}\frac{\left(p_{pkg,j}^{H_2O}-p_f^{H_2O}\right)}{\Delta x_{pkg,n}}$$

$$\frac{dp_{pkg,j}^{H_2O}}{dt}=\frac{P_{pkg,n}^{H_2O}}{S_{pkg,n}^{H_2O}\Delta x_{pkg,n}{}^2}\left(p_{pkg,j-1}^{H_2O}-2p_{pkg,j}^{H_2O}+p_f^{H_2O}\right)$$

C.2.2 Matlab Solution

Refer to Appendix B for a digital copy of this numerical solution.

C.2.2.1 Script File (Package.m)

```
%Script File

clear all

global MrH2O ms R J;
global kGAB CGAB M0GAB CBET M1BET blin clin;
global Apkg Aprf XT N dx dprf Drefpkg TrefDpkg EDpkg Srefpkg TrefSpkg dHSpkg;
global isotherm pa pf;


%System Inputs
%General SIs
MrH2O=(1.01*2+16.00)*10^-3;          %Molecular mass of water (kg/mol)
R=8.314;                             %Ideal gas constant (m^3.Pa/K/mol)


%Food Product SIs
ms=0.31/(1+0.0357);                  %Mass of dry solids in food (kg)
isotherm='GAB';                      %Type of moisture (GAB, BET, lin)
if lower(isotherm)=='gab'        %GAB isotherm
    kGAB=0.897;                      %A constant for GAB isotherm
    CGAB=2.31;                       %Guggenheim constant for GAB isotherm
    M0GAB=0.066;                     %Moisture content of monolayer for GAB isotherm (kg
water/kg solids)
elseif lower(isotherm)=='bet'    %BET isotherm
    CBET=0;                          %Guggenheim constant for BET isotherm
    M1BET=0;                         %Moisture content of monolayer for BET isotherm (kg
water/kg solids)
elseif lower(isotherm)=='lin'    %Linear isotherm
    blin=0;                          %Slope of linear isotherm
    clin=0;                          %Constant for linear isotherm (kg water/kg solids)
end


%Packaging SIs
Apkg=0.1403;                         %Surface area of packaging (m^2)
N=5;                                 %Number of layers in packaging (-)
Aprf=0;                              %Total surface area of perforation(s) in packaging (m^2)
dprf=1e-4;                           %Average diameter of perforation(s) in packaging (m)
```

```
%Layer 1
n=1;
X(n)=20e-6;                         %Thickness of layer 1 of packaging (m)
Srefpkg(n)=0.001;                   %Reference solubility of water vapour in layer 1 of
packaging (mol/m^3/Pa)
TrefSpkg(n)=273.15+38;              %Temperature of reference solubility of water vapour in
layer 1 of packaging (K)
dHSpkg(n)=-3.5e4;                   %Partial molar enthalpy of sorption of water vapour in
layer 1 of packaging (J/mol)
Drefpkg(n)=1e-14/Srefpkg(n);        %Reference diffusivity of water vapour in layer 1 of
packaging (m^2/s)
TrefDpkg(n)=273.15+38;              %Temperature of reference diffusivity of water vapour in
layer 1 of packaging (K)
EDpkg(n)=2.5e4-dHSpkg(n);           %Activation energy of diffusion of water vapour in layer 1
of packaging (J/mol)

%Layer 2
if N>=2
    n=2;
    X(n)=5e-6;                      %Thickness of layer 2 of packaging (m)
    Srefpkg(n)=0.001;               %Reference solubility of water vapour in layer 2 of
packaging (mol/m^3/Pa)
    TrefSpkg(n)=273.15+38;          %Temperature of reference solubility of water vapour in
layer 2 of packaging (K)
    dHSpkg(n)=-3.5e4;               %Partial molar enthalpy of sorption of water vapour in
layer 2 of packaging (J/mol)
    Drefpkg(n)=1e-13/Srefpkg(n);    %Reference diffusivity of water vapour in layer 2 of
packaging (m^2/s)
    TrefDpkg(n)=273.15+38;          %Temperature of reference diffusivity of water vapour in
layer 2 of packaging (K)
    EDpkg(n)=2.5e4-dHSpkg(n);       %Activation energy of diffusion of water vapour in layer 2
of packaging (J/mol)
end

%Layer 3
if N>=3
    n=3;
    X(n)=10e-6;                     %Thickness of layer 3 of packaging (m)
    Srefpkg(n)=0.001;               %Reference solubility of water vapour in layer 3 of
packaging (mol/m^3/Pa)
    TrefSpkg(n)=273.15+38;          %Temperature of reference solubility of water vapour in
layer 3 of packaging (K)
    dHSpkg(n)=-3.5e4;               %Partial molar enthalpy of sorption of water vapour in
layer 3 of packaging (J/mol)
    Drefpkg(n)=1e-15/Srefpkg(n);    %Reference diffusivity of water vapour in layer 3 of
packaging (m^2/s)
    TrefDpkg(n)=273.15+38;          %Temperature of reference diffusivity of water vapour in
layer 3 of packaging (K)
    EDpkg(n)=2.5e4-dHSpkg(n);       %Activation energy of diffusion of water vapour in layer 3
of packaging (J/mol)
end

%Layer 4
if N>=4
    n=4;
    X(n)=5e-6;                      %Thickness of layer 4 of packaging (m)
    Srefpkg(n)=0.001;               %Reference solubility of water vapour in layer 4 of
packaging (mol/m^3/Pa)
    TrefSpkg(n)=273.15+38;          %Temperature of reference solubility of water vapour in
layer 4 of packaging (K)
    dHSpkg(n)=-3.5e4;               %Partial molar enthalpy of sorption of water vapour in
layer 4 of packaging (J/mol)
    Drefpkg(n)=1e-13/Srefpkg(n);    %Reference diffusivity of water vapour in layer 4 of
packaging (m^2/s)
    TrefDpkg(n)=273.15+38;          %Temperature of reference diffusivity of water vapour in
layer 4 of packaging (K)
    EDpkg(n)= 2.5e4-dHSpkg(n);      %Activation energy of diffusion of water vapour in layer 4
of packaging (J/mol)
end

%Layer 5
if N>=5
    n=5;
    X(n)=20e-6;                     %Thickness of layer 5 of packaging (m)
    Srefpkg(n)=0.001;               %Reference solubility of water vapour in layer 5 of
packaging (mol/m^3/Pa)
```

```
    TrefSpkg(n)=273.15+38;          %Temperature of reference solubility of water vapour in
layer 5 of packaging (K)
    dHSpkg(n)=-3.5e4;               %Partial molar enthalpy of sorption of water vapour in
layer 5 of packaging (J/mol)
    Drefpkg(n)=1e-14/Srefpkg(n);    %Reference diffusivity of water vapour in layer 5 of
packaging (m^2/s)
    TrefDpkg(n)=273.15+38;          %Temperature of reference diffusivity of water vapour in
layer 5 of packaging (K)
    EDpkg(n)= 2.5e4-dHSpkg(n);      %Activation energy of diffusion of water vapour in layer 5
of packaging (J/mol)
end

%Layer 6
if N>=6
    n=6;
    X(n)=0;                         %Thickness of layer 6 of packaging (m)
    Srefpkg(n)=0;                   %Reference solubility of water vapour in layer 6 of
packaging (mol/m^3/Pa)
    TrefSpkg(n)=273.15+0;           %Temperature of reference solubility of water vapour in
layer 6 of packaging (K)
    dHSpkg(n)=0;                    %Partial molar enthalpy of sorption of water vapour in
layer 6 of packaging (J/mol)
    Drefpkg(n)=0;                   %Reference diffusivity of water vapour in layer 6 of
packaging (m^2/s)
    TrefDpkg(n)=273.15+0;           %Temperature of reference diffusivity of water vapour in
layer 6 of packaging (K)
    EDpkg(n)=0;                     %Activation energy of diffusion of water vapour in layer 6
of packaging (J/mol)
end

%Layer 7
if N>=7
    n=7;
    X(n)=0;                         %Thickness of layer 7 of packaging (m)
    Srefpkg(n)=0;                   %Reference solubility of water vapour in layer 7 of
packaging (mol/m^3/Pa)
    TrefSpkg(n)=273.15+0;           %Temperature of reference solubility of water vapour in
layer 7 of packaging (K)
    dHSpkg(n)=0;                    %Partial molar enthalpy of sorption of water vapour in
layer 7 of packaging (J/mol)
    Drefpkg(n)=0;                   %Reference diffusivity of water vapour in layer 7 of
packaging (m^2/s)
    TrefDpkg(n)=273.15+0;           %Temperature of reference diffusivity of water vapour in
layer 7 of packaging (K)
    EDpkg(n)=0;                     %Activation energy of diffusion of water vapour in layer 7
of packaging (J/mol)
end

%Layer 8
if N>=8
    n=8;
    X(n)=0;                         %Thickness of layer 8 of packaging (m)
    Srefpkg(n)=0;                   %Reference solubility of water vapour in layer 8 of
packaging (mol/m^3/Pa)
    TrefSpkg(n)=273.15+0;           %Temperature of reference solubility of water vapour in
layer 8 of packaging (K)
    dHSpkg(n)=0;                    %Partial molar enthalpy of sorption of water vapour in
layer 8 of packaging (J/mol)
    Drefpkg(n)=0;                   %Reference diffusivity of water vapour in layer 8 of
packaging (m^2/s)
    TrefDpkg(n)=273.15+0;           %Temperature of reference diffusivity of water vapour in
layer 8 of packaging (K)
    EDpkg(n)=0;                     %Activation energy of diffusion of water vapour in layer 8
of packaging (J/mol)
end

%Layer 9
if N>=9
    n=9;
    X(n)=0;                         %Thickness of layer 9 of packaging (m)
    Srefpkg(n)=0;                   %Reference solubility of water vapour in layer 9 of
packaging (mol/m^3/Pa)
    TrefSpkg(n)=273.15+0;           %Temperature of reference solubility of water vapour in
layer 9 of packaging (K)
    dHSpkg(n)=0;                    %Partial molar enthalpy of sorption of water vapour in
layer 9 of packaging (J/mol)
```

```
    Drefpkg(n)=0;                   %Reference diffusivity of water vapour in layer 9 of
packaging (m^2/s)
    TrefDpkg(n)=273.15+0;           %Temperature of reference diffusivity of water vapour in
layer 9 of packaging (K)
    EDpkg(n)=0;                     %Activation energy of diffusion of water vapour in layer 9
of packaging (J/mol)
end

XT=sum(X);                          %Total thickness of packaging (m)


%Model Node SIs
J=10;                               %Number of nodes (-)
dx=X/J;                             %Node width of layer n of packaging (m)


%Initial Conditions
RHi=90;
Ti=273.15+38;
p0i=exp(23.4795-3990.56/(Ti-273.15+233.833));

ppkgi=zeros(1,N*J-1)+RHi/100*p0i;   %Initial water vapour pressure in packaging (Pa)
Mi=0.0357;                          %Initial moisture content of food product (kg water/kg
solids)

pai=RHi/100*p0i;
if lower(isotherm)=='gab'
    pfi=p0i*(-(kGAB*(CGAB-CGAB*M0GAB/Mi-2))-sqrt((kGAB*(CGAB-CGAB*M0GAB/Mi-2))^2-4*kGAB^2*(1-
CGAB)))/(2*kGAB^2*(1-CGAB));
elseif lower(isotherm)=='bet'
    pfi=p0i*(-(CBET-CBET*M1BET/Mi-2)-sqrt((CBET-CBET*M1BET/Mi-2)^2-4*(1-CBET)))/(2*(1-CBET));
elseif lower(isotherm)=='lin'
    pfi=p0i*(Mi-clin)/blin;
end

ICs=[pai ppkgi pfi Mi];
stime=183;                          %Simulation time (days)


%Solver
options=odeset('RelTol', 1e-3);
[t,D]=ode23s('PackageFun',[0:24*60^2:stime*24*60^2],ICs,options);


%Plots
%Plot of moisture content of food product
M=D(:,N*J+2);

figure
subplot(2,1,1);
hold on
plot(t/(24*60^2),M,'b-');
title('Moisture Content of Food Product');
xlabel('t (days)');
ylabel('M (kg H2O/kg solids)');

%Plot of water vapour pressure in packaging
x1(1)=0;
for n=1:N
    for i=(n-1)*J+2:n*J+1
        x1(i,1)=dx(n)+x1(i-1);
    end
end
ppkgend=[pa D(end,2:N*J) pf]';

subplot(2,1,2);
plot(x1*1e6,ppkgend,'b-');
title(['Water vapour Pressure in the Packaging After ',num2str(stime),' Days']);
xlabel('x (µm)');
ylabel('ppkg (Pa)');


%Output data to Excel spreadsheet
outputtitle={'t (s)','M (kg water/kg solids)'};
outputdata=[t,M];
xlswrite('PackageOutput.xls',outputtitle,'M');
xlswrite('PackageOutput.xls',outputdata,'M','A2');
```

```
outputtitle={'x (m)','ppkg (Pa)'};
outputdata=[x1 ppkgend];
xlswrite('PackageOutput.xls',outputtitle,'ppkg');
xlswrite('PackageOutput.xls',outputdata,'ppkg','A2');
```

C.2.2.2 Model Function File (PackageFun.m)

```
%Model Function File

function dD=PackageFun(t,D)

global MrH2O ms R J;
global kGAB CGAB M0GAB CBET M1BET blin clin;
global Apkg Aprf XT N dx dprf Drefpkg TrefDpkg EDpkg Srefpkg TrefSpkg dHSpkg;
global isotherm pa pf;


M=D(N*J+2);


%General CVs
T=273.15+38;                                %Ambient temperature (K)
RHa=90;                                     %Relative humidity of ambient air (%RH)
p0=exp(23.4795-3990.56/(T-273.15+233.833)); %Saturated vapour pressure of pure water at T (Pa)
pa=RHa*p0/100;                              %Partial pressure of water vapour in ambient air
(Pa)
Dair=1.7255e-7*T-2.552e-5;                  %Diffusivity of water vapour in air (m^2/s)
Sair=1/R/T;                                 %Solubility of water vapour in air (mol/m^3/Pa)


%Food Isotherm
if lower(isotherm)=='gab'               %GAB isotherm
    %B1*aw^2+B2*aw+B3=0
    %B1=k^2*(1-C)
    %B2=k*(C-C*M0/M-2)
    %B3=1
    pf=p0*(-(kGAB*(CGAB-CGAB*M0GAB/M-2))-sqrt((kGAB*(CGAB-CGAB*M0GAB/M-2))^2-4*kGAB^2*(1-
CGAB)))/(2*kGAB^2*(1-CGAB));
elseif lower(isotherm)=='bet'           %BET isotherm
    %B1*aw^2+B2*aw+B3=0
    %B1=1-C
    %B2=C-C*M1/M-2
    %B3=1
    pf=p0*(-(CBET-CBET*M1BET/M-2)-sqrt((CBET-CBET*M1BET/M-2)^2-4*(1-CBET)))/(2*(1-CBET));
elseif lower(isotherm)=='lin'           %Linear isotherm
    pf=p0*(M-clin)/blin;
end


ppkg(1)=pa;
ppkg(2:N*J)=D(2:N*J);
ppkg(N*J+1)=pf;

dD=zeros(1,N*J+2);


%Perforation Equations
if dprf<(1e-7)
    Jprf=48.5*dprf/R/T/XT*(T/1000/MrH2O)^0.5*(pa-pf);
elseif dprf>=(1e-7) && dprf<(1e-5)
    Jprf=Dair*Sair*(pa-pf)/(XT+dprf/2);     %Only valid if distance between perforations >>
pore radius
elseif dprf>=(1e-5)
    Jprf=Dair*Sair*(pa-pf)/XT;
end


%Finite Difference Approximations
%Case 1
n=1;
j=1;
dppkg(j)=0;
```

```
n=N;
j=n*J+1;
dppkg(j)=0;

%Case 2
n=1;
j=2;
Dpkg=DpkgFun(n,j,ppkg,T);
dppkg(j)=Dpkg/dx(n)^2*(pa-2*ppkg(j)+ppkg(j+1));

%Case 3
if N==1
    n=1;
    for j=(n-1)*J+3:n*J-1
        Dpkg=DpkgFun(n,j,ppkg,T);
        dppkg(j)=Dpkg/dx(n)^2*(ppkg(j-1)-2*ppkg(j)+ppkg(j+1));
    end
else
    n=1;
    for j=(n-1)*J+3:n*J
        Dpkg=DpkgFun(n,j,ppkg,T);
        dppkg(j)=Dpkg/dx(n)^2*(ppkg(j-1)-2*ppkg(j)+ppkg(j+1));
    end
    for n=2:N-1
        for j=(n-1)*J+2:n*J
            Dpkg=DpkgFun(n,j,ppkg,T);
            dppkg(j)=Dpkg/dx(n)^2*(ppkg(j-1)-2*ppkg(j)+ppkg(j+1));
        end
    end
    n=N;
    for j=(n-1)*J+2:n*J-1
        Dpkg=DpkgFun(n,j,ppkg,T);
        dppkg(j)=Dpkg/dx(n)^2*(ppkg(j-1)-2*ppkg(j)+ppkg(j+1));
    end
end

%Case 4
for n=1:N-1
    j=n*J+1;
    Dpkg(1)=DpkgFun(n,j,ppkg,T);
    Spkg(1)=SpkgFun(n,j,ppkg,T);
    n=n+1;
    Dpkg(2)=DpkgFun(n,j,ppkg,T);
    Spkg(2)=SpkgFun(n,j,ppkg,T);
    n=n-1;
    dppkg(j)=2/(dx(n)*Spkg(1)+dx(n+1)*Spkg(2))*(Dpkg(1)*Spkg(1)/dx(n)*(ppkg(j-1)-ppkg(j))-
Dpkg(2)*Spkg(2)/dx(n+1)*(ppkg(j)-ppkg(j+1)));
end

%Case 5
n=N;
j=n*J;
Dpkg=DpkgFun(n,j,ppkg,T);
dppkg(j)=Dpkg/dx(n)^2*(ppkg(j-1)-2*ppkg(j)+pf);


%Moisture Content of Food Product
n=N;
j=n*J;
Dpkg=DpkgFun(n,j,ppkg,T);
Spkg=SpkgFun(n,j,ppkg,T);
dM=MrH2O/ms*(Dpkg*Spkg*Apkg/dx(n)*(ppkg(j)-pf)+Aprf*Jprf);


dD=[dppkg dM]';
```

C.2.2.3 Diffusivity of Water Vapour in Packaging Function File (DpkgFun.m)

```
%Diffusivity of Water Vapour in Packaging Function File

function Dpkg=DpkgFun(n,j,ppkg,T)
```

```
global MrH2O ms R J;
global kGAB CGAB M0GAB CBET M1BET blin clin;
global Apkg Aprf XT N dx dprf Drefpkg TrefDpkg EDpkg Srefpkg TrefSpkg dHSpkg;
global isotherm pa pf;


switch n
    case 1
        Dpkg=Drefpkg(n)*exp(EDpkg(n)/R*(1/TrefDpkg(n)-1/T));
    case 2
        Dpkg=Drefpkg(n)*exp(EDpkg(n)/R*(1/TrefDpkg(n)-1/T));
    case 3
        Dpkg=Drefpkg(n)*exp(EDpkg(n)/R*(1/TrefDpkg(n)-1/T));
    case 4
        Dpkg=Drefpkg(n)*exp(EDpkg(n)/R*(1/TrefDpkg(n)-1/T));
    case 5
        Dpkg=Drefpkg(n)*exp(EDpkg(n)/R*(1/TrefDpkg(n)-1/T));
    case 6
        Dpkg=Drefpkg(n)*exp(EDpkg(n)/R*(1/TrefDpkg(n)-1/T));
    case 7
        Dpkg=Drefpkg(n)*exp(EDpkg(n)/R*(1/TrefDpkg(n)-1/T));
    case 8
        Dpkg=Drefpkg(n)*exp(EDpkg(n)/R*(1/TrefDpkg(n)-1/T));
    case 9
        Dpkg=Drefpkg(n)*exp(EDpkg(n)/R*(1/TrefDpkg(n)-1/T));
end
```

C.2.2.4 Solubility of Water Vapour in Packaging Function File (SpkgFun.m)

```
%Solubility of Water Vapour in Packaging Function File

function Spkg=SpkgFun(n,j,ppkg,T)

global MrH2O ms R J;
global kGAB CGAB M0GAB CBET M1BET blin clin;
global Apkg Aprf XT N dx dprf Drefpkg TrefDpkg EDpkg Srefpkg TrefSpkg dHSpkg;
global isotherm pa pf;


switch n
    case 1
        Spkg=Srefpkg(n)*exp(dHSpkg(n)/R*(1/TrefSpkg(n)-1/T));
    case 2
        Spkg=Srefpkg(n)*exp(dHSpkg(n)/R*(1/TrefSpkg(n)-1/T));
    case 3
        Spkg=Srefpkg(n)*exp(dHSpkg(n)/R*(1/TrefSpkg(n)-1/T));
    case 4
        Spkg=Srefpkg(n)*exp(dHSpkg(n)/R*(1/TrefSpkg(n)-1/T));
    case 5
        Spkg=Srefpkg(n)*exp(dHSpkg(n)/R*(1/TrefSpkg(n)-1/T));
    case 6
        Spkg=Srefpkg(n)*exp(dHSpkg(n)/R*(1/TrefSpkg(n)-1/T));
    case 7
        Spkg=Srefpkg(n)*exp(dHSpkg(n)/R*(1/TrefSpkg(n)-1/T));
    case 8
        Spkg=Srefpkg(n)*exp(dHSpkg(n)/R*(1/TrefSpkg(n)-1/T));
    case 9
        Spkg=Srefpkg(n)*exp(dHSpkg(n)/R*(1/TrefSpkg(n)-1/T));
end
```

C.3 ERROR CHECKS

C.3.1 Numerical Error Checks

C.3.1.1 Time Step

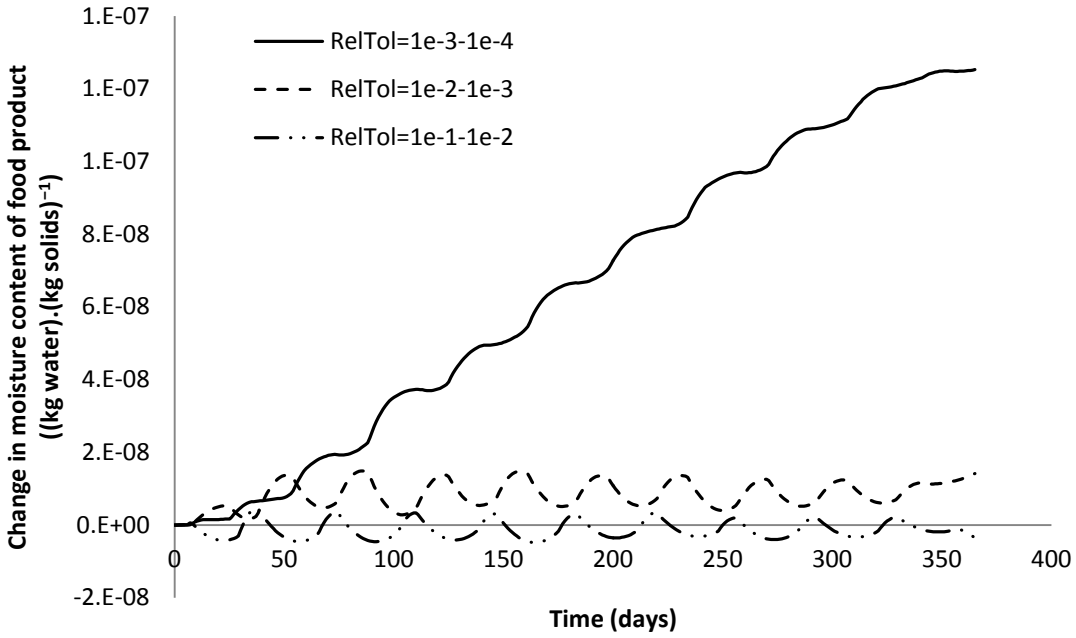

Figure C-1: Plot of change in predicted values of moisture content of food product ((kg water).(kg solids)$^{-1}$), with changes to relative error tolerance of MATLAB® solver (RelTol).

As shown in Figure C-1, all changes to relative error tolerance of the MATLAB® solver (RelTol) had relatively insignificant effects on predicted values of moisture content of the food, with no differences greater than 1.3×10^{-7} (kg water).(kg solids)$^{-1}$ over the period $0 \leq t \leq 365$ days. Therefore the default RelTol of 1×10^{-3} should be suitable for use in the model. However it should be noted that, although a similar case is expected for other simulated scenarios, this is somewhat application specific.

C.3.1.2 Space Step

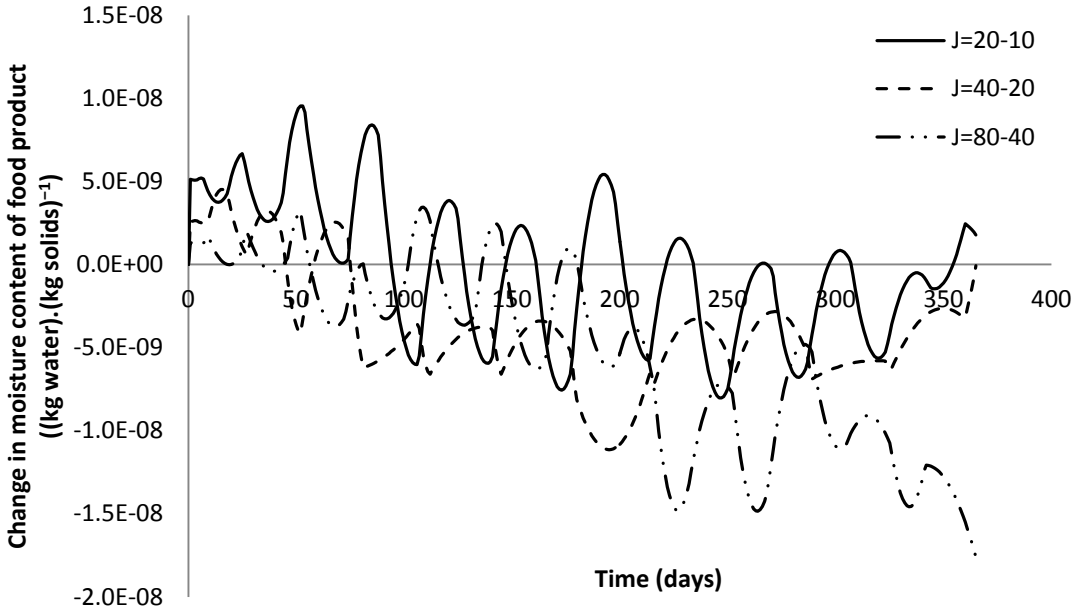

Figure C-2: Plot of change in predicted values of moisture content of food product ((kg water).(kg solids)$^{-1}$) with changes to number of nodes per layer of packaging (J).

As shown in Figure C-2, all changes to the number of nodes per layer of packaging had relatively insignificant effects on predicted values of moisture content of the food, with no differences greater than 1.8×10^{-8} (kg water).(kg solids)$^{-1}$ over the period $0 \leq t \leq 365$ days. Therefore a standard number of 10 nodes per layer of packaging should be suitable for use in the model. Again this is somewhat application specific, although 10 nodes per layer is expected to be suitable for most systems of interest.

C.3.2 Mathematical Error Checks

C.3.2.1 Water Vapour Pressure in Packaging

To allow an analytical solution for the water vapour pressure in the packaging, the following model conditions were used:

- The properties of all packaging layers were set the same. A two layer system was simulated to ensure all finite difference approximations were correct.
- A linear isotherm with a very high slope was used to ensure the water vapour pressure in the food product remained constant. The linear isotherm constant was adjusted to obtain the desired water vapour pressure.
- The concentration dependence of the diffusivity and solubility of water vapour in the packaging were disabled.
- Only the water vapour pressure profile after 24 hours was considered.

Formulated problem:

$$S_{pkg}^{H_2O}\frac{\partial p_{pkg}^{H_2O}}{\partial t} = S_{pkg}^{H_2O}D_{pkg}^{H_2O}\frac{\partial^2 p_{pkg}^{H_2O}}{\partial x^2}$$

for $t \geq 0,\ 0 < x < X_T$

$$p_{pkg}^{H_2O} = p_a^{H_2O}$$

for $t \geq 0$, *at* $x = 0$ *and* $x = X_T$

$$p_{pkg}^{H_2O} = p_{pkg,i}^{H_2O}$$

for $t = 0,\ 0 < x < X_T$

Analytical solution:

$$R = \frac{X_T}{2} = \frac{5 \times 10^{-5}}{2} = 2.5 \times 10^{-5}$$

$$Fo = \frac{D_{pkg}^{H_2O}t}{R^2} = \frac{1 \times 10^{-15} \times 24 \times 60^2}{(2.5 \times 10^{-5})^2} = 0.1382$$

$$Y = \frac{4}{\pi}\sum_{m=0}^{\infty}\frac{(-1)^m}{2m+1}cos\left[(2m+1)\frac{\pi}{2}\frac{x}{R}\right]exp\left[-(2m+1)^2\frac{\pi^2}{4}Fo\right]$$

m	$\boldsymbol{\frac{(-1)^m}{2m+1}cos\left[(2m+1)\frac{\pi}{2}\frac{x}{R}\right]exp\left[-(2m+1)^2\frac{\pi^2}{4}Fo\right]}$
0	0.7110

1	−0.01548
2	3.960×10^{-5}
Total	0.6956

$$Y = \frac{4}{\pi} 0.6956 = 0.8856$$

$$Y = \frac{C - C_\infty}{C_i - C_\infty} = \frac{S_{pkg}^{H_2O}\left(p_{pkg}^{H_2O} - p_a^{H_2O}\right)}{S_{pkg}^{H_2O}\left(p_{pkg,i}^{H_2O} - p_a^{H_2O}\right)} = \frac{p_{pkg}^{H_2O} - p_a^{H_2O}}{p_{pkg,i}^{H_2O} - p_a^{H_2O}}$$

$$Y\left(p_{pkg,i}^{H_2O} - p_a^{H_2O}\right) = p_{pkg}^{H_2O} - p_a^{H_2O}$$

$$p_{pkg}^{H_2O} = Y\left(p_{pkg,i}^{H_2O} - p_a^{H_2O}\right) + p_a^{H_2O} = 0.8856(585 - 1756) + 1756 = 719.1 \text{ Pa}$$

This procedure was repeated to calculate the water vapour pressure after 24 hours for various positions within the packaging.

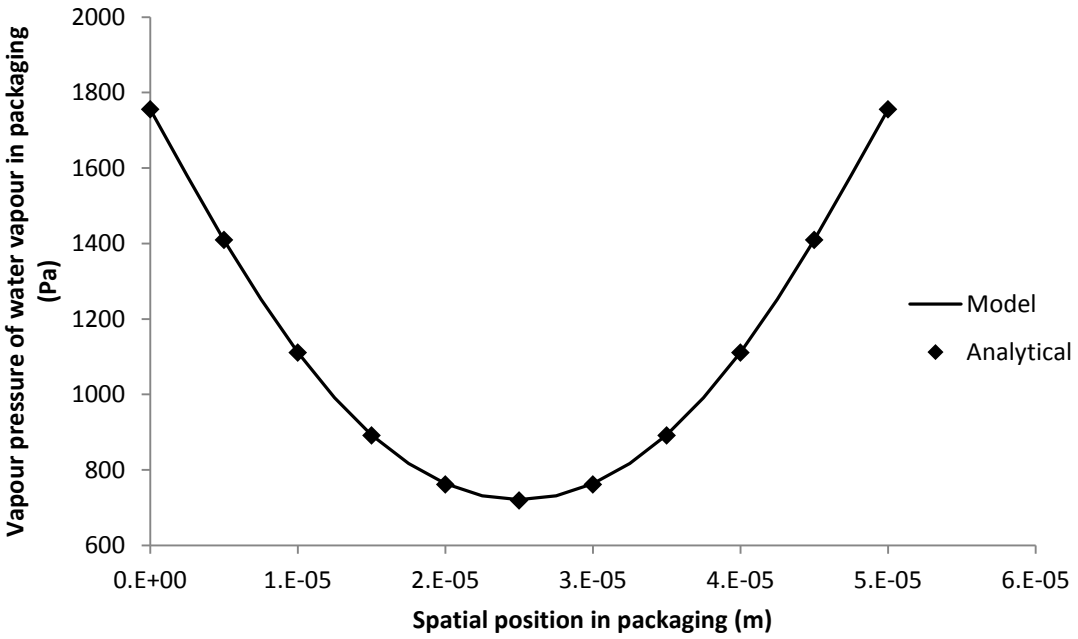

Figure C-3: Comparison of water vapour pressure profile in packaging after 24 hours as predicted analytically and by the model.

As shown in Figure C-3, the values predicted by the model agree very closely with those calculated analytically, suggesting the model is correctly calculating the water vapour pressure in the packaging.

C.3.2.2 Moisture Content of Food Product

To allow an analytical solution for the moisture content of the food product, the following changes were made:

- A linear isotherm was used for the food product.
- The concentration dependence of the diffusivity and solubility of water vapour in the packaging were disabled.
- A perforation with a large diameter was used.

Formulated problem:

$$\frac{dM}{dt} = \frac{M_{r,H_2O}}{m_s}\left[P_{pkg,n=N}^{H_2O} A_{pkg} \left(\frac{dp_{pkg}^{H_2O}}{dx}\right)_{x=X_{T,pkg}} + J_{prf}^{H_2O} A_{prf}\right]$$

$$for\ t \geq 0$$

Analytical solution:

$$\frac{dM}{dt} = \frac{M_{r,H_2O}}{m_s X_T}\left(P_{pkg}^{H_2O} A_{pkg} + D_{air}^{H_2O} S_{air}^{H_2O} A_{prf}\right)\left(p_a^{H_2O} - p_0^{H_2O}\left(\frac{M - c_{lin}}{b_{lin}}\right)\right)$$

$$\frac{dM}{dt} = aM + b$$

where:

$$a = -\frac{M_{r,H_2O} p_0^{H_2O}}{m_s X_T b_{lin}}\left(P_{pkg}^{H_2O} A_{pkg} + D_{air}^{H_2O} S_{air}^{H_2O} A_{prf}\right)$$

$$b = \frac{M_{r,H_2O}}{m_s X_T}\left(p_a^{H_2O} + p_0^{H_2O}\frac{c_{lin}}{b_{lin}}\right)\left(P_{pkg}^{H_2O} A_{pkg} + D_{air}^{H_2O} S_{air}^{H_2O} A_{prf}\right)$$

$$\int_{M_i}^{M} \frac{1}{aM+b}\partial M = \int_0^t \partial t$$

$$M = \left(M_i + \frac{b}{a}\right) exp(at) - \frac{b}{a}$$

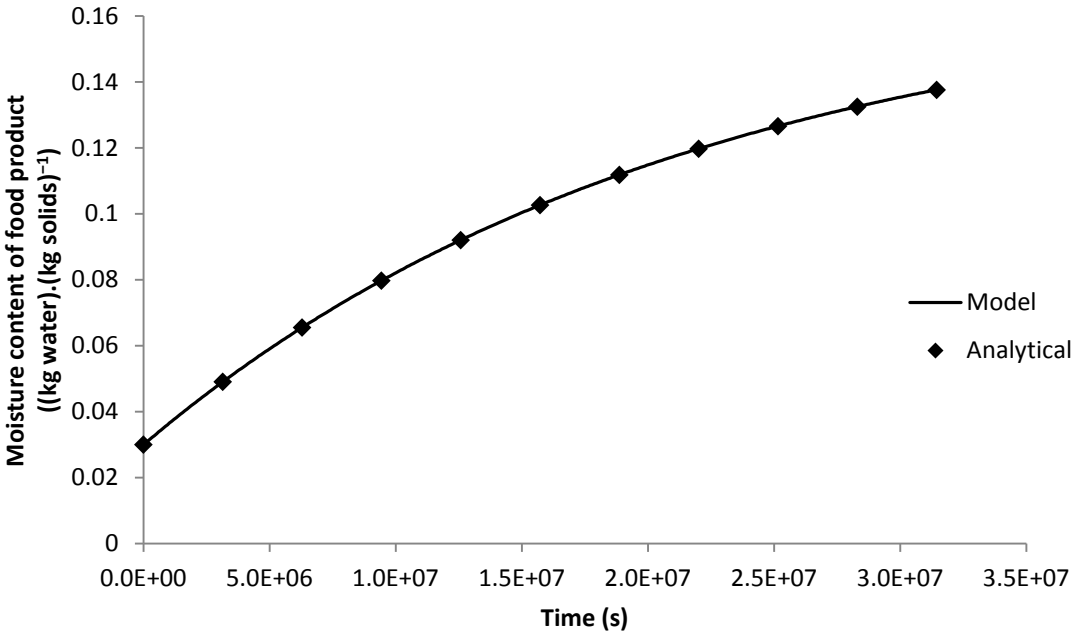

Figure C-4: Comparison of moisture content of food product as predicted analytically and by the model.

As shown in Figure C-4, the values predicted by the model agree relatively closely with those calculated analytically, suggesting the model is correctly calculating the moisture content of the food product.

Appendix D

EXTENDED FOOD PACKAGE MOISTURE TRANSFER MODELS

D.1 TWO SEPARATE PACKAGING LAYERS WITH PERFORATIONS

D.1.1 Conceptual Model Development

D.1.1.1 Word Balances and Equations

D.1.1.1.1 ODE for Moisture Content of Food Product

Unsteady-state mass balance of water in food product

$$\frac{dn_f^{H_2O}}{dt} = P_{lnr,n=N_{lnr}}^{H_2O} A_{lnr} \left(\frac{dp_{lnr}^{H_2O}}{dx}\right)_{x=X_{T,lnr}} + J_{prf,lnr}^{H_2O} A_{prf,lnr}$$

$$n_f^{H_2O} = \frac{m_f^{H_2O}}{M_{r,H_2O}} = \frac{Mm_s}{M_{r,H_2O}}$$

$$\therefore \frac{dn_f^{H_2O}}{dt} = \frac{m_s}{M_{r,H_2O}} \frac{dM}{dt} = P_{lnr,n=N_{lnr}}^{H_2O} A_{lnr} \left(\frac{dp_{lnr}^{H_2O}}{dx}\right)_{x=X_{T,lnr}} + J_{prf,lnr}^{H_2O} A_{prf,lnr}$$

$$\frac{dM}{dt} = \frac{M_{r,H_2O}}{m_s} \left[P_{lnr,n=N_{lnr}}^{H_2O} A_{lnr} \left(\frac{dp_{lnr}^{H_2O}}{dx}\right)_{x=X_{T,lnr}} + J_{prf,lnr}^{H_2O} A_{prf,lnr} \right]$$

$$\left[\frac{kg}{kg.s}\right] = \left[\frac{kg}{mol}\right] \frac{1}{[kg]} \left(\left[\frac{mol.m}{m^2.s.Pa}\right] [m^2] \frac{[Pa]}{[m]} + \left[\frac{mol}{m^2.s}\right] [m^2] \right)$$

D.1.1.1.2 ODE for Water Vapour Pressure in Bag Headspace

Steady-state mass balance of water vapour in paperboard bag headspace

$$\frac{dp_{bh}^{H_2O}}{dt} = 0 = P_{bag,n=N_{bag}}^{H_2O} A_{bag} \left(\frac{dp_{bag}^{H_2O}}{dx}\right)_{x=X_{T,bag}} + J_{prf,bag}^{H_2O} A_{prf,bag} - P_{lnr,n=1}^{H_2O} A_{lnr} \left(\frac{dp_{lnr}^{H_2O}}{dx}\right)_{x=1} - J_{prf,lnr}^{H_2O} A_{prf,lnr}$$

$$\left[\frac{mol.m}{m^2.s.Pa}\right][m^2]\frac{[Pa]}{[m]} + \left[\frac{mol}{m^2.s}\right][m^2] - \left[\frac{mol.m}{m^2.s.Pa}\right][m^2]\frac{[Pa]}{[m]} - \left[\frac{mol}{m^2.s}\right][m^2]$$

D.1.2 Solution

D.1.2.1 Finite Difference Approximations

D.1.2.1.1 Case 2

$$A_{bag}\Delta x_{bag,n} S_{bag,n}^{H_2O} \frac{dp_{bag,j}^{H_2O}}{dt} = P_{bag,n}^{H_2O} A_{bag} \frac{(p_a^{H_2O} - p_{bag,j}^{H_2O})}{\Delta x_{bag,n}} - P_{bag,n}^{H_2O} A_{bag} \frac{(p_{bag,j}^{H_2O} - p_{bag,j+1}^{H_2O})}{\Delta x_{bag,n}}$$

$$[m^2][m]\left[\frac{mol}{m^3.Pa}\right]\left[\frac{Pa}{s}\right] = \left[\frac{m^2}{s}\right]\left[\frac{mol}{m^3.Pa}\right][m^2]\frac{[Pa]}{[m]} - \left[\frac{m^2}{s}\right]\left[\frac{mol}{m^3.Pa}\right][m^2]\frac{[Pa]}{[m]}$$

$$\Delta x_{bag,n}\frac{dp_{bag,j}^{H_2O}}{dt} = \frac{P_{bag,n}^{H_2O}}{S_{bag,n}^{H_2O}}\frac{(p_a^{H_2O} - p_{bag,j}^{H_2O})}{\Delta x_{bag,n}} - \frac{P_{bag,n}^{H_2O}}{S_{bag,n}^{H_2O}}\frac{(p_{bag,j}^{H_2O} - p_{bag,j+1}^{H_2O})}{\Delta x_{bag,n}}$$

$$\frac{dp_{bag,j}^{H_2O}}{dt} = \frac{P_{bag,n}^{H_2O}}{S_{bag,n}^{H_2O}\Delta x_{bag,n}^{\ 2}}(p_a^{H_2O} - 2p_{bag,j}^{H_2O} + p_{bag,j+1}^{H_2O})$$

D.1.2.1.2 Case 3

$$A_{bag}\Delta x_{bag,n} S_{bag,n}^{H_2O} \frac{dp_{bag,j}^{H_2O}}{dt} = P_{bag,n}^{H_2O} A_{bag} \frac{(p_{bag,j-1}^{H_2O} - p_{bag,j}^{H_2O})}{\Delta x_{bag,n}} - P_{bag,n}^{H_2O} A_{bag} \frac{(p_{bag,j}^{H_2O} - p_{bag,j+1}^{H_2O})}{\Delta x_{bag,n}}$$

$$[m^2][m]\left[\frac{mol}{m^3.Pa}\right]\left[\frac{Pa}{s}\right] = \left[\frac{m^2}{s}\right]\left[\frac{mol}{m^3.Pa}\right][m^2]\frac{[Pa]}{[m]} - \left[\frac{m^2}{s}\right]\left[\frac{mol}{m^3.Pa}\right][m^2]\frac{[Pa]}{[m]}$$

$$\Delta x_{bag,n}\frac{dp_{bag,j}^{H_2O}}{dt} = \frac{P_{bag,n}^{H_2O}}{S_{bag,n}^{H_2O}}\frac{\left(p_{bag,j-1}^{H_2O} - p_{bag,j}^{H_2O}\right)}{\Delta x_{bag,n}} - \frac{P_{bag,n}^{H_2O}}{S_{bag,n}^{H_2O}}\frac{\left(p_{bag,j}^{H_2O} - p_{bag,j+1}^{H_2O}\right)}{\Delta x_{bag,n}}$$

$$\frac{dp_{bag,j}^{H_2O}}{dt} = \frac{P_{bag,n}^{H_2O}}{S_{bag,n}^{H_2O}\Delta x_{bag,n}^{\ 2}}\left(p_{bag,j-1}^{H_2O} - 2p_{bag,j}^{H_2O} + p_{bag,j+1}^{H_2O}\right)$$

D.1.2.1.3 Case 4

$$A_{bag}\left[\frac{\Delta x_{bag,n}}{2}S_{bag,n}^{H_2O} + \frac{\Delta x_{bag,n+1}}{2}S_{bag,n+1}^{H_2O}\right]\frac{dp_{bag,j}^{H_2O}}{dt} = P_{bag,n}^{H_2O}A_{bag}\frac{\left(p_{bag,j-1}^{H_2O} - p_{bag,j}^{H_2O}\right)}{\Delta x_{bag,n}} - P_{bag,n+1}^{H_2O}A_{bag}\frac{\left(p_{bag,j}^{H_2O} - p_{bag,j+1}^{H_2O}\right)}{\Delta x_{bag,n+1}}$$

$$[m^2]\left([m]\left[\frac{mol}{m^3.Pa}\right] + [m]\left[\frac{mol}{m^3.Pa}\right]\right)\left[\frac{Pa}{s}\right] = \left[\frac{m^2}{s}\right]\left[\frac{mol}{m^3.Pa}\right][m^2]\frac{[Pa]}{[m]} - \left[\frac{m^2}{s}\right]\left[\frac{mol}{m^3.Pa}\right][m^2]\frac{[Pa]}{[m]}$$

$$\left[\frac{\Delta x_{bag,n}}{2}S_{bag,n}^{H_2O} + \frac{\Delta x_{bag,n+1}}{2}S_{bag,n+1}^{H_2O}\right]\frac{dp_{bag,j}^{H_2O}}{dt} = P_{bag,n}^{H_2O}\frac{\left(p_{bag,j-1}^{H_2O} - p_{bag,j}^{H_2O}\right)}{\Delta x_{bag,n}} - P_{bag,n+1}^{H_2O}\frac{\left(p_{bag,j}^{H_2O} - p_{bag,j+1}^{H_2O}\right)}{\Delta x_{bag,n+1}}$$

$$\frac{dp_{bag,j}^{H_2O}}{dt} = \frac{2}{\Delta x_{bag,n}S_{bag,n}^{H_2O} + \Delta x_{bag,n+1}S_{bag,n+1}^{H_2O}}\left[\frac{P_{bag,n}^{H_2O}}{\Delta x_{bag,n}}\left(p_{bag,j-1}^{H_2O} - p_{bag,j}^{H_2O}\right) - \frac{P_{bag,n+1}^{H_2O}}{\Delta x_{bag,n+1}}\left(p_{bag,j}^{H_2O} - p_{bag,j+1}^{H_2O}\right)\right]$$

D.1.2.1.4 Case 5

$$A_{bag}\Delta x_{bag,n}S_{bag,n}^{H_2O}\frac{dp_{bag,j}^{H_2O}}{dt}=P_{bag,n}^{H_2O}A_{bag}\frac{\left(p_{bag,j-1}^{H_2O}-p_{bag,j}^{H_2O}\right)}{\Delta x_{bag,n}}-P_{bag,n}^{H_2O}A_{bag}\frac{\left(p_{bag,j}^{H_2O}-p_{bh}^{H_2O}\right)}{\Delta x_{bag,n}}$$

$$[m^2][m]\left[\frac{mol}{m^3.Pa}\right]\left[\frac{Pa}{s}\right]=\left[\frac{m^2}{s}\right]\left[\frac{mol}{m^3.Pa}\right][m^2]\frac{[Pa]}{[m]}-\left[\frac{m^2}{s}\right]\left[\frac{mol}{m^3.Pa}\right][m^2]\frac{[Pa]}{[m]}$$

$$\Delta x_{bag,n}\frac{dp_{bag,j}^{H_2O}}{dt}=\frac{P_{bag,n}^{H_2O}}{S_{bag,n}^{H_2O}}\frac{\left(p_{bag,j-1}^{H_2O}-p_{bag,j}^{H_2O}\right)}{\Delta x_{bag,n}}-\frac{P_{bag,n}^{H_2O}}{S_{bag,n}^{H_2O}}\frac{\left(p_{bag,j}^{H_2O}-p_{bh}^{H_2O}\right)}{\Delta x_{bag,n}}$$

$$\frac{dp_{bag,j}^{H_2O}}{dt}=\frac{P_{bag,n}^{H_2O}}{S_{bag,n}^{H_2O}\Delta x_{bag,n}{}^2}\left(p_{bag,j-1}^{H_2O}-2p_{bag,j}^{H_2O}+p_{bh}^{H_2O}\right)$$

D.1.2.1.5 Case 7

$$A_{lnr}\Delta x_{lnr,n}S_{lnr,n}^{H_2O}\frac{dp_{lnr,j}^{H_2O}}{dt}=P_{lnr,n}^{H_2O}A_{lnr}\frac{\left(p_{bh}^{H_2O}-p_{lnr,j}^{H_2O}\right)}{\Delta x_{lnr,n}}-P_{lnr,n}^{H_2O}A_{lnr}\frac{\left(p_{lnr,j}^{H_2O}-p_{lnr,j+1}^{H_2O}\right)}{\Delta x_{lnr,n}}$$

$$[m^2][m]\left[\frac{mol}{m^3.Pa}\right]\left[\frac{Pa}{s}\right]=\left[\frac{m^2}{s}\right]\left[\frac{mol}{m^3.Pa}\right][m^2]\frac{[Pa]}{[m]}-\left[\frac{m^2}{s}\right]\left[\frac{mol}{m^3.Pa}\right][m^2]\frac{[Pa]}{[m]}$$

$$\Delta x_{lnr,n}\frac{dp_{lnr,j}^{H_2O}}{dt}=\frac{P_{lnr,n}^{H_2O}}{S_{lnr,n}^{H_2O}}\frac{\left(p_{bh}^{H_2O}-p_{lnr,j}^{H_2O}\right)}{\Delta x_{lnr,n}}-\frac{P_{lnr,n}^{H_2O}}{S_{lnr,n}^{H_2O}}\frac{\left(p_{lnr,j}^{H_2O}-p_{lnr,j+1}^{H_2O}\right)}{\Delta x_{lnr,n}}$$

$$\frac{dp_{lnr,j}^{H_2O}}{dt}=\frac{P_{lnr,n}^{H_2O}}{S_{lnr,n}^{H_2O}\Delta x_{lnr,n}{}^2}\left(p_{bh}^{H_2O}-2p_{lnr,j}^{H_2O}+p_{lnr,j+1}^{H_2O}\right)$$

D.1.2.1.6 Case 8

$$A_{lnr}\Delta x_{lnr,n}S_{lnr,n}^{H_2O}\frac{dp_{lnr,j}^{H_2O}}{dt}=P_{lnr,n}^{H_2O}A_{lnr}\frac{\left(p_{lnr,j-1}^{H_2O}-p_{lnr,j}^{H_2O}\right)}{\Delta x_{lnr,n}}-P_{lnr,n}^{H_2O}A_{lnr}\frac{\left(p_{lnr,j}^{H_2O}-p_{lnr,j+1}^{H_2O}\right)}{\Delta x_{lnr,n}}$$

$$[m^2][m]\left[\frac{mol}{m^3.Pa}\right]\left[\frac{Pa}{s}\right] = \left[\frac{m^2}{s}\right]\left[\frac{mol}{m^3.Pa}\right][m^2]\frac{[Pa]}{[m]} - \left[\frac{m^2}{s}\right]\left[\frac{mol}{m^3.Pa}\right][m^2]\frac{[Pa]}{[m]}$$

$$\Delta x_{lnr,n}\frac{dp_{lnr,j}^{H_2O}}{dt} = \frac{P_{lnr,n}^{H_2O}}{S_{lnr,n}^{H_2O}}\frac{\left(p_{lnr,j-1}^{H_2O} - p_{lnr,j}^{H_2O}\right)}{\Delta x_{lnr,n}} - \frac{P_{lnr,n}^{H_2O}}{S_{lnr,n}^{H_2O}}\frac{\left(p_{lnr,j}^{H_2O} - p_{lnr,j+1}^{H_2O}\right)}{\Delta x_{lnr,n}}$$

$$\frac{dp_{lnr,j}^{H_2O}}{dt} = \frac{P_{lnr,n}^{H_2O}}{S_{lnr,n}^{H_2O}\Delta x_{lnr,n}^{\ 2}}\left(p_{lnr,j-1}^{H_2O} - 2p_{lnr,j}^{H_2O} + p_{lnr,j+1}^{H_2O}\right)$$

D.1.2.1.7 Case 9

$$A_{lnr}\left[\frac{\Delta x_{lnr,n}}{2}S_{lnr,n}^{H_2O} + \frac{\Delta x_{lnr,n+1}}{2}S_{lnr,n+1}^{H_2O}\right]\frac{dp_{lnr,j}^{H_2O}}{dt}$$
$$= P_{lnr,n}^{H_2O}A_{lnr}\frac{\left(p_{lnr,j-1}^{H_2O} - p_{lnr,j}^{H_2O}\right)}{\Delta x_{lnr,n}} - P_{lnr,n+1}^{H_2O}A_{lnr}\frac{\left(p_{lnr,j}^{H_2O} - p_{lnr,j+1}^{H_2O}\right)}{\Delta x_{lnr,n+1}}$$

$$[m^2]\left([m]\left[\frac{mol}{m^3.Pa}\right] + [m]\left[\frac{mol}{m^3.Pa}\right]\right)\left[\frac{Pa}{s}\right]$$
$$= \left[\frac{m^2}{s}\right]\left[\frac{mol}{m^3.Pa}\right][m^2]\frac{[Pa]}{[m]} - \left[\frac{m^2}{s}\right]\left[\frac{mol}{m^3.Pa}\right][m^2]\frac{[Pa]}{[m]}$$

$$\left[\frac{\Delta x_{lnr,n}}{2}S_{lnr,n}^{H_2O} + \frac{\Delta x_{lnr,n+1}}{2}S_{lnr,n+1}^{H_2O}\right]\frac{dp_{lnr,j}^{H_2O}}{dt}$$
$$= P_{lnr,n}^{H_2O}\frac{\left(p_{lnr,j-1}^{H_2O} - p_{lnr,j}^{H_2O}\right)}{\Delta x_{lnr,n}} - P_{lnr,n+1}^{H_2O}\frac{\left(p_{lnr,j}^{H_2O} - p_{lnr,j+1}^{H_2O}\right)}{\Delta x_{lnr,n+1}}$$

$$\frac{dp_{lnr,j}^{H_2O}}{dt} = \frac{2}{\Delta x_{lnr,n}S_{lnr,n}^{H_2O} + \Delta x_{lnr,n+1}S_{lnr,n+1}^{H_2O}}$$
$$\left[\frac{P_{lnr,n}^{H_2O}}{\Delta x_{lnr,n}}\left(p_{lnr,j-1}^{H_2O} - p_{lnr,j}^{H_2O}\right) - \frac{P_{lnr,n+1}^{H_2O}}{\Delta x_{lnr,n+1}}\left(p_{lnr,j}^{H_2O} - p_{lnr,j+1}^{H_2O}\right)\right]$$

D.1.2.1.8 Case 10

$$A_{lnr}\Delta x_{lnr,n}S_{lnr,n}^{H_2O}\frac{dp_{lnr,j}^{H_2O}}{dt}=P_{lnr,n}^{H_2O}A_{lnr}\frac{\left(p_{lnr,j-1}^{H_2O}-p_{lnr,j}^{H_2O}\right)}{\Delta x_{lnr,n}}-P_{lnr,n}^{H_2O}A_{lnr}\frac{\left(p_{lnr,j}^{H_2O}-p_{f}^{H_2O}\right)}{\Delta x_{lnr,n}}$$

$$[m^2][m]\left[\frac{mol}{m^3.Pa}\right]\left[\frac{Pa}{s}\right]=\left[\frac{m^2}{s}\right]\left[\frac{mol}{m^3.Pa}\right][m^2]\frac{[Pa]}{[m]}-\left[\frac{m^2}{s}\right]\left[\frac{mol}{m^3.Pa}\right][m^2]\frac{[Pa]}{[m]}$$

$$\Delta x_{lnr,n}\frac{dp_{lnr,j}^{H_2O}}{dt}=\frac{P_{lnr,n}^{H_2O}}{S_{lnr,n}^{H_2O}}\frac{\left(p_{lnr,j-1}^{H_2O}-p_{lnr,j}^{H_2O}\right)}{\Delta x_{lnr,n}}-\frac{P_{lnr,n}^{H_2O}}{S_{lnr,n}^{H_2O}}\frac{\left(p_{lnr,j}^{H_2O}-p_{f}^{H_2O}\right)}{\Delta x_{lnr,n}}$$

$$\frac{dp_{lnr,j}^{H_2O}}{dt}=\frac{P_{lnr,n}^{H_2O}}{S_{lnr,n}^{H_2O}\Delta x_{lnr,n}{}^2}\left(p_{lnr,j-1}^{H_2O}-2p_{lnr,j}^{H_2O}+p_{f}^{H_2O}\right)$$

D.1.2.2 MATLAB® Solution

Refer to Appendix B for a digital copy of this numerical solution.

D.1.2.2.1 Script File (PackageExtended.m)

```
%Script File

clear all

global MrH2O ms R J;
global kGAB CGAB M0GAB CBET M1BET blin clin;
global Abag Aprfbag XTbag Nbag dxbag dprfbag Drefbag TrefDbag EDbag Srefbag TrefSbag dHSbag;
global Alnr Aprflnr XTlnr Nlnr dxlnr dprflnr Dreflnr TrefDlnr EDlnr Sreflnr TrefSlnr dHSlnr;
global isotherm pa pf;


%System Inputs
%General SIs
MrH2O=(1.01*2+16.00)*10^-3;             %Molecular mass of water (kg/mol)
R=8.314;                                %Ideal gas constant (m^3.Pa/K/mol)


%Food Product SIs
ms=0.31/(1+0.0357);                     %Mass of dry solids in food product (kg)
isotherm='gab';                         %Type of moisture (GAB, BET, lin)
if lower(isotherm)=='gab'           %GAB isotherm
    kGAB=0.897;                         %GAB isotherm constant (correcting factor)
    CGAB=2.31;                          %GAB isotherm constant (Guggenheim constant)
    M0GAB=0.066;                        %GAB isotherm constant (monolayer) (kg water/kg
solids)
elseif lower(isotherm)=='bet'       %BET isotherm
    CBET=0;                             %BET isotherm constant
```

```
    M1BET=0;                            %BET isotherm constant (monolayer) (kg water/kg
solids)
elseif lower(isotherm)=='lin'       %Linear isotherm
    blin=0;                             %Linear isotherm slope
    clin=0;                             %Linear isotherm intercept
end


%Packaging Material SIs
%Paperboard bag
Abag=0.1403;                            %Surface area of paperboard bag (m^2)
Nbag=1;                                 %Number of layers in paperboard bag (-)
Aprfbag=0;                              %Total surface area of perforation(s) in paperboard
bag (m^2)
dprfbag=1e-4;                           %Average diameter of perforation(s) in paperboard bag
(m)

%Layer 1
n=1;
Xbag(n)=310e-6;                         %Thickness of layer 1 of paperboard bag (m)
Srefbag(n)=0.001;                       %Reference solubility of water vapour in layer 1 of
paperboard bag (mol/m^3/Pa)
TrefSbag(n)=273.15+38;                  %Temperature of reference solubility of water vapour
in layer 1 of paperboard bag (K)
dHSbag(n)=0;                            %Partial molar enthalpy of sorption of water vapour in
layer 1 of paperboard bag (J/mol)
Drefbag(n)=1e-8/Srefbag(n);             %Reference diffusivity of water vapour in layer 1 of
paperboard bag (m^2/s)
TrefDbag(n)=273.15+38;                  %Temperature of reference diffusivity of water vapour
in layer 1 of paperboard bag (K)
EDbag(n)=26500-dHSbag(n);               %Activation energy of diffusion of water vapour in
layer 1 of paperboard bag (J/mol)

%Layer 2
if Nbag>=2
    n=2;
    Xbag(n)=0;                          %Thickness of layer 2 of paperboard bag (m)
    Srefbag(n)=0;                       %Reference solubility of water vapour in layer 2 of
paperboard bag (mol/m^3/Pa)
    TrefSbag(n)=273.15+0;               %Temperature of reference solubility of water vapour
in layer 2 of paperboard bag (K)
    dHSbag(n)=0;                        %Partial molar enthalpy of sorption of water vapour in
layer 2 of paperboard bag (J/mol)
    Drefbag(n)=0;                       %Reference diffusivity of water vapour in layer 2 of
paperboard bag (m^2/s)
    TrefDbag(n)=273.15+0;               %Temperature of reference diffusivity of water vapour
in layer 2 of paperboard bag (K)
    EDbag(n)=0;                         %Activation energy of diffusion of water vapour in
layer 2 of paperboard bag (J/mol)
end

XTbag=sum(Xbag);                        %Total thickness of paperboard bag (m)


%Polymer liner
Alnr=Abag;                              %Surface area of polymer liner (m^2)
Nlnr=5;                                 %Number of layers in polymer liner (-)
Aprflnr=0;                              %Total surface area of perforation(s) in polymer liner
(m^2)
dprflnr=1e-4;                           %Average diameter of perforation(s) in polymer liner
(m)

%Layer 1
n=1;
Xlnr(n)=20e-6;                          %Thickness of layer 1 of polymer liner (m)
Sreflnr(n)=0.001;                       %Reference solubility of water vapour in layer 1 of
polymer liner (mol/m^3/Pa)
TrefSlnr(n)=273.15+38;                  %Temperature of reference solubility of water vapour
in layer 1 of polymer liner (K)
dHSlnr(n)=0;                            %Partial molar enthalpy of sorption of water vapour in
layer 1 of polymer liner (J/mol)
Dreflnr(n)=1e-14/Sreflnr(n);            %Reference diffusivity of water vapour in layer 1 of
polymer liner (m^2/s)
TrefDlnr(n)=273.15+38;                  %Temperature of reference diffusivity of water vapour
in layer 1 of polymer liner (K)
EDlnr(n)=2.5e4-dHSlnr(n);               %Activation energy of diffusion of water vapour in
layer 1 of polymer liner (J/mol)
```

```
%Layer 2
if Nlnr>=2
    n=2;
    Xlnr(n)=5e-6;                       %Thickness of layer 2 of polymer liner (m)
    Sreflnr(n)=0.001;                   %Reference solubility of water vapour in layer 2 of
polymer liner (mol/m^3/Pa)
    TrefSlnr(n)=273.15+38;              %Temperature of reference solubility of water vapour
in layer 2 of polymer liner (K)
    dHSlnr(n)=0;                        %Partial molar enthalpy of sorption of water vapour in
layer 2 of polymer liner (J/mol)
    Dreflnr(n)=1e-13/Sreflnr(n);        %Reference diffusivity of water vapour in layer 2 of
polymer liner (m^2/s)
    TrefDlnr(n)=273.15+38;              %Temperature of reference diffusivity of water vapour
in layer 2 of polymer liner (K)
    EDlnr(n)=2.5e4-dHSlnr(n);           %Activation energy of diffusion of water vapour in
layer 2 of polymer liner (J/mol)
end

%Layer 3
if Nlnr>=3
    n=3;
    Xlnr(n)=10e-6;                      %Thickness of layer 3 of polymer liner (m)
    Sreflnr(n)=0.001;                   %Reference solubility of water vapour in layer 3 of
polymer liner (mol/m^3/Pa)
    TrefSlnr(n)=273.15+38;              %Temperature of reference solubility of water vapour
in layer 3 of polymer liner (K)
    dHSlnr(n)=0;                        %Partial molar enthalpy of sorption of water vapour in
layer 3 of polymer liner (J/mol)
    Dreflnr(n)=1e-15/Sreflnr(n);        %Reference diffusivity of water vapour in layer 3 of
polymer liner (m^2/s)
    TrefDlnr(n)=273.15+38;              %Temperature of reference diffusivity of water vapour
in layer 3 of polymer liner (K)
    EDlnr(n)=2.5e4-dHSlnr(n);           %Activation energy of diffusion of water vapour in
layer 3 of polymer liner (J/mol)
end

%Layer 4
if Nlnr>=4
    n=4;
    Xlnr(n)=5e-6;                       %Thickness of layer 4 of polymer liner (m)
    Sreflnr(n)=0.001;                   %Reference solubility of water vapour in layer 4 of
polymer liner (mol/m^3/Pa)
    TrefSlnr(n)=273.15+38;              %Temperature of reference solubility of water vapour
in layer 4 of polymer liner (K)
    dHSlnr(n)=0;                        %Partial molar enthalpy of sorption of water vapour in
layer 4 of polymer liner (J/mol)
    Dreflnr(n)=1e-13/Sreflnr(n);        %Reference diffusivity of water vapour in layer 4 of
polymer liner (m^2/s)
    TrefDlnr(n)=273.15+38;              %Temperature of reference diffusivity of water vapour
in layer 4 of polymer liner (K)
    EDlnr(n)=2.5e4-dHSlnr(n);           %Activation energy of diffusion of water vapour in
layer 4 of polymer liner (J/mol)
end

%Layer 5
if Nlnr>=5
    n=5;
    Xlnr(n)=20e-6;                      %Thickness of layer 5 of polymer liner (m)
    Sreflnr(n)=0.001;                   %Reference solubility of water vapour in layer 5 of
polymer liner (mol/m^3/Pa)
    TrefSlnr(n)=273.15+38;              %Temperature of reference solubility of water vapour
in layer 5 of polymer liner (K)
    dHSlnr(n)=0;                        %Partial molar enthalpy of sorption of water vapour in
layer 5 of polymer liner (J/mol)
    Dreflnr(n)=1e-14/Sreflnr(n);        %Reference diffusivity of water vapour in layer 5 of
polymer liner (m^2/s)
    TrefDlnr(n)=273.15+38;              %Temperature of reference diffusivity of water vapour
in layer 5 of polymer liner (K)
    EDlnr(n)=2.5e4-dHSlnr(n);           %Activation energy of diffusion of water vapour in
layer 5 of polymer liner (J/mol)
end

%Layer 6
if Nlnr>=6
    n=6;
    Xlnr(n)=0;                          %Thickness of layer 6 of polymer liner (m)
```

```
    Sreflnr(n)=0;                       %Reference solubility of water vapour in layer 6 of
polymer liner (mol/m^3/Pa)
    TrefSlnr(n)=273.15+0;               %Temperature of reference solubility of water vapour
in layer 6 of polymer liner (K)
    dHSlnr(n)=0;                        %Partial molar enthalpy of sorption of water vapour in
layer 6 of polymer liner (J/mol)
    Dreflnr(n)=0;                       %Reference diffusivity of water vapour in layer 6 of
polymer liner (m^2/s)
    TrefDlnr(n)=273.15+0;               %Temperature of reference diffusivity of water vapour
in layer 6 of polymer liner (K)
    EDlnr(n)=0;                         %Activation energy of diffusion of water vapour in
layer 6 of polymer liner (J/mol)
end

%Layer 7
if Nlnr>=7
    n=7;
    Xlnr(n)=0;                          %Thickness of layer 7 of polymer liner (m)
    Sreflnr(n)=0;                       %Reference solubility of water vapour in layer 7 of
polymer liner (mol/m^3/Pa)
    TrefSlnr(n)=273.15+0;               %Temperature of reference solubility of water vapour
in layer 7 of polymer liner (K)
    dHSlnr(n)=0;                        %Partial molar enthalpy of sorption of water vapour in
layer 7 of polymer liner (J/mol)
    Dreflnr(n)=0;                       %Reference diffusivity of water vapour in layer 7 of
polymer liner (m^2/s)
    TrefDlnr(n)=273.15+0;               %Temperature of reference diffusivity of water vapour
in layer 7 of polymer liner (K)
    EDlnr(n)=0;                         %Activation energy of diffusion of water vapour in
layer 7 of polymer liner (J/mol)
end

%Layer 8
if Nlnr>8
    n=8;
    Xlnr(n)=0;                          %Thickness of layer 8 of polymer liner (m)
    Sreflnr(n)=0;                       %Reference solubility of water vapour in layer 8 of
polymer liner (mol/m^3/Pa)
    TrefSlnr(n)=273.15+0;               %Temperature of reference solubility of water vapour
in layer 8 of polymer liner (K)
    dHSlnr(n)=0;                        %Partial molar enthalpy of sorption of water vapour in
layer 8 of polymer liner (J/mol)
    Dreflnr(n)=0;                       %Reference diffusivity of water vapour in layer 8 of
polymer liner (m^2/s)
    TrefDlnr(n)=273.15+0;               %Temperature of reference diffusivity of water vapour
in layer 8 of polymer liner (K)
    EDlnr(n)=0;                         %Activation energy of diffusion of water vapour in
layer 8 of polymer liner (J/mol)
end

%Layer 9
if Nlnr>=9
    n=9;
    Xlnr(n)=0;                          %Thickness of layer 9 of polymer liner (m)
    Sreflnr(n)=0;                       %Reference solubility of water vapour in layer 9 of
polymer liner (mol/m^3/Pa)
    TrefSlnr(n)=273.15+0;               %Temperature of reference solubility of water vapour
in layer 9 of polymer liner (K)
    dHSlnr(n)=0;                        %Partial molar enthalpy of sorption of water vapour in
layer 9 of polymer liner (J/mol)
    Dreflnr(n)=0;                       %Reference diffusivity of water vapour in layer 9 of
polymer liner (m^2/s)
    TrefDlnr(n)=273.15+0;               %Temperature of reference diffusivity of water vapour
in layer 9 of polymer liner (K)
    EDlnr(n)=0;                         %Activation energy of diffusion of water vapour in
layer 9 of polymer liner (J/mol)
end

XTlnr=sum(Xlnr);                        %Total thickness of polymer liner (m)


%Model Node SIs
J=10;                                   %Number of nodes (-)
dxbag=Xbag/J;                           %Node width of layer n of paperboard bag (m)
dxlnr=Xlnr/J;                           %Node width of layer n of polymer liner (m)
```

```
%Initial Conditions
RHi=90;
Ti=273.15+38;
p0i=exp(23.4795-3990.56/(Ti-273.15+233.833));

pbagi=zeros(1,Nbag*J-1)+RHi/100*p0i;     %Initial water vapour pressure in paperboard bag (Pa)
plnri=zeros(1,Nlnr*J-1)+RHi/100*p0i;     %Initial water vapour pressure in polymer liner (Pa)
Mi=0.03;                                 %Initial moisture content of food product (kg water/kg
solids)
pbhi=RHi/100*p0i;                        %Initial water vapour pressure in bag headspace (Pa)

pai=RHi/100*p0i;
if lower(isotherm)=='gab'
    pfi=p0i*(-(kGAB*(CGAB-CGAB*M0GAB/Mi-2))-sqrt((kGAB*(CGAB-CGAB*M0GAB/Mi-2))^2-4*kGAB^2*(1-
CGAB)))/(2*kGAB^2*(1-CGAB));
elseif lower(isotherm)=='bet'
    pfi=p0i*(-(CBET-CBET*M1BET/Mi-2)-sqrt((CBET-CBET*M1BET/Mi-2)^2-4*(1-CBET)))/(2*(1-CBET));
elseif lower(isotherm)=='lin'
    pfi=p0i*(Mi-clin)/blin;
end

ICs=[pai pbagi pbhi pbhi plnri pfi Mi pbhi];
stime=183;                               %Simulation time (days)


%Solver
options=odeset('RelTol', 1e-3);
[t,D]=ode23s('PackageExtendedFun',[0:24*60^2:stime*24*60^2],ICs,options);


%Plots
%Plot of moisture content of food product
M=D(:,Nbag*J+Nlnr*J+3);

figure
subplot(2,1,1);
hold on
plot(t/(24*60^2),M,'b-');
title('Moisture Content of Food Product');
xlabel('t (days)');
ylabel('M (kg H2O/kg solids)');

%Plot of water vapour pressure in bag headspace
pbh=D(:,Nbag*J+Nlnr*J+4);

subplot(2,1,2);
plot(t/(24*60^2),pbh,'b-');
title('Water Vapour Pressure in Bag Headspace');
xlabel('t (days)');
ylabel('pbh (Pa)');

%Plot of water vapour pressure in paperboard bag
x1(1)=0;
for n=1:Nbag
    for i=(n-1)*J+2:n*J+1
        x1(i,1)=dxbag(n)+x1(i-1);
    end
end
pbagend=[pa D(end,2:Nbag*J) D(end,Nbag*J+Nlnr*J+4)]';

figure
subplot(2,1,1);
hold on
plot(x1*1e6,pbagend,'b-');
title(['Water Vapour Pressure in the Paperboard Bag After ',num2str(stime),' Days']);
xlabel('x (µm)');
ylabel('pbag (Pa)');

%Plot of water vapour pressure in polymer liner
x2(1)=0;
for n=1:Nlnr
    for i=(n-1)*J+2:n*J+1
        x2(i,1)=dxlnr(n)+x2(i-1);
    end
end
plnrend=[D(end,Nbag*J+Nlnr*J+4) D(end,Nbag*J+3:Nbag*J+Nlnr*J+1) pf]';
```

```
subplot(2,1,2);
plot(x2*1e6,plnrend,'b-');
title(['Water Vapour Pressure in the Polymer Liner After ',num2str(stime),' Days']);
xlabel('x (µm)');
ylabel('plnr (Pa)');


%Output data to Excel spreadsheet
outputtitle1={'t (s)','M (kg water/kg solids)'};
outputdata1=[t,M];
xlswrite('PackageExtendedOutput.xls',outputtitle1,'M');
xlswrite('PackageExtendedOutput.xls',outputdata1,'M','A2');

outputtitle2={'t (s)','pbh (Pa)'};
outputdata2=[t,pbh];
xlswrite('PackageExtendedOutput.xls',outputtitle2,'pbh');
xlswrite('PackageExtendedOutput.xls',outputdata2,'pbh','A2');

outputtitle3={'x (m)','pbag (Pa)'};
outputdata3=[x1 pbagend];
xlswrite('PackageExtendedOutput.xls',outputtitle3,'pbag');
xlswrite('PackageExtendedOutput.xls',outputdata3,'pbag','A2');

outputtitle4={'x (m)','plnr (Pa)'};
outputdata4=[x2 plnrend];
xlswrite('PackageExtendedOutput.xls',outputtitle4,'plnr');
xlswrite('PackageExtendedOutput.xls',outputdata4,'plnr','A2');
```

D.1.2.2.2 Model Function File (PackageExtendedFun.m)

```
%Model Function File

function dD=PackageExtendedFun(t,D)

global MrH2O ms R J;
global kGAB CGAB M0GAB CBET M1BET blin clin;
global Abag Aprfbag XTbag Nbag dxbag dprfbag Drefbag TrefDbag EDbag Srefbag TrefSbag dHSbag;
global Alnr Aprflnr XTlnr Nlnr dxlnr dprflnr Dreflnr TrefDlnr EDlnr Sreflnr TrefSlnr dHSlnr;
global isotherm pa pf;


M=D(Nbag*J+Nlnr*J+3);
pbh=D(Nbag*J+Nlnr*J+4);


%General CVs
T=273.15+38;                                    %Ambient temperature (K)
RHa=90;                                         %Relative humidity of ambient air (%RH)
p0=exp(23.4795-3990.56/(T-273.15+233.833));     %Saturated vapour pressure of pure water at T
(Pa)
pa=RHa*p0/100;                                  %Partial pressure of water vapour in ambient
air (Pa)
Dair=1.7255e-7*T-2.552e-5;                      %Diffusivity of water vapour in air (m^2/s)
Sair=1/R/T;                                     %Solubility of water vapour in air
(mol/m^3/Pa)


%Food Isotherm
if lower(isotherm)=='gab'                       %GAB isotherm
    %B1*aw^2+B2*aw+B3=0
    %B1=k^2*(1-C)
    %B2=k*(C-C*M0/M-2)
    %B3=1
    pf=p0*(-(kGAB*(CGAB-CGAB*M0GAB/M-2))-sqrt((kGAB*(CGAB-CGAB*M0GAB/M-2))^2-4*kGAB^2*(1-
CGAB)))/(2*kGAB^2*(1-CGAB));
elseif lower(isotherm)=='bet'                   %BET isotherm
    %B1*aw^2+B2*aw+B3=0
    %B1=1-C
    %B2=C-C*M1/M-2
    %B3=1
    pf=p0*(-(CBET-CBET*M1BET/M-2)-sqrt((CBET-CBET*M1BET/M-2)^2-4*(1-CBET)))/(2*(1-CBET));
```

```
elseif lower(isotherm)=='lin'                   %Linear isotherm
    pf=p0*(M-clin)/blin;
end


pbag(1)=pa;
pbag(2:Nbag*J)=D(2:Nbag*J);
pbag(Nbag*J+1)=pbh;
plnr(1)=pbh;
plnr(2:Nlnr*J)=D(Nbag*J+3:Nbag*J+Nlnr*J+1);
plnr(Nlnr*J+1)=pf;

dD=zeros(1,Nbag*J+Nlnr*J+4);


%Perforation Equations
%Perforation(s) in paperboard bag
if dprfbag<(1e-7)
    Jprfbag=48.5*dprfbag/R/T/XTbag*(T/1000/MrH2O)^0.5*(pa-pbh);
elseif dprfbag>=(1e-7) && dprfbag<(1e-5)
    Jprfbag=Dair*Sair*(pa-pbh)/(XTbag+dprfbag/2);   %Only valid if distance between
perforations >> pore radius
elseif dprfbag>=(1e-5)
    Jprfbag=Dair*Sair*(pa-pbh)/XTbag;               %Only valid if no total pressure
difference across packaging
end

%Perforation(s) in polymer liner
if dprflnr<(1e-7)
    Jprflnr=48.5*dprflnr/R/T/XTlnr*(T/1000/MrH2O)^0.5*(pbh-pf);
elseif dprflnr>=(1e-7) && dprflnr<(1e-5)
    Jprflnr=Dair*Sair*(pbh-pf)/(XTlnr+dprflnr/2);   %Only valid if distance between
perforations >> pore radius
elseif dprflnr>=(1e-5)
    Jprflnr=Dair*Sair*(pbh-pf)/XTlnr;               %Only valid if no total pressure
difference across packaging
end


%Finite Difference Approximations
%Paperboard bag
%Case 1
n=1;
j=1;
dpbag(j)=0;
n=Nbag;
j=n*J+1;
dpbag(j)=0;

%Case 2
n=1;
j=2;
Dbag=DbagFun(n,j,pbag,T);
dpbag(j)=Dbag/dxbag(n)^2*(pa-2*pbag(j)+pbag(j+1));

%Case 3
if Nbag==1
    n=1;
    for j=(n-1)*J+3:n*J-1
        Dbag=DbagFun(n,j,pbag,T);
        dpbag(j)=Dbag/dxbag(n)^2*(pbag(j-1)-2*pbag(j)+pbag(j+1));
    end
else
    n=1;
    for j=(n-1)*J+3:n*J
        Dbag=DbagFun(n,j,pbag,T);
        dpbag(j)=Dbag/dxbag(n)^2*(pbag(j-1)-2*pbag(j)+pbag(j+1));
    end
    for n=2:Nbag-1
        for j=(n-1)*J+2:n*J
            Dbag=DbagFun(n,j,pbag,T);
            dpbag(j)=Dbag/dxbag(n)^2*(pbag(j-1)-2*pbag(j)+pbag(j+1));
        end
    end
    n=Nbag;
    for j=(n-1)*J+2:n*J-1
        Dbag=DbagFun(n,j,pbag,T);
```

```
        dpbag(j)=Dbag/dxbag(n)^2*(pbag(j-1)-2*pbag(j)+pbag(j+1));
    end
end

%Case 4
for n=1:Nbag-1
    j=n*J+1;
    Dbag(1)=DbagFun(n,j,pbag,T);
    Sbag(1)=SbagFun(n,j,pbag,T);
    n=n+1;
    Dbag(2)=DbagFun(n,j,pbag,T);
    Sbag(2)=SbagFun(n,j,pbag,T);
    n=n-1;
    dpbag(j)=2/(dxbag(n)*Sbag(1)+dxbag(n+1)*Sbag(2))*(Dbag(1)*Sbag(1)/dxbag(n)*(pbag(j-1)-
pbag(j))-Dbag(2)*Sbag(2)/dxbag(n+1)*(pbag(j)-pbag(j+1)));
end

%Case 5
n=Nbag;
j=n*J;
Dbag=DbagFun(n,j,pbag,T);
dpbag(j)=Dbag/dxbag(n)^2*(pbag(j-1)-2*pbag(j)+pbh);


%Polymer liner
%Case 6
n=1;
j=1;
dplnr(j)=0;
n=Nlnr;
j=n*J+1;
dplnr(j)=0;

%Case 7
n=1;
j=2;
Dlnr=DlnrFun(n,j,plnr,T);
dplnr(j)=Dlnr/dxlnr(n)^2*(pbh-2*plnr(j)+plnr(j+1));

%Case 8
if Nlnr==1
    n=1;
    for j=(n-1)*J+3:n*J-1
        Dlnr=DlnrFun(n,j,plnr,T);
        dplnr(j)=Dlnr/dxlnr(n)^2*(plnr(j-1)-2*plnr(j)+plnr(j+1));
    end
else
    n=1;
    for j=(n-1)*J+3:n*J
        Dlnr=DlnrFun(n,j,plnr,T);
        dplnr(j)=Dlnr/dxlnr(n)^2*(plnr(j-1)-2*plnr(j)+plnr(j+1));
    end
    for n=2:Nlnr-1
        for j=(n-1)*J+2:n*J
            Dlnr=DlnrFun(n,j,plnr,T);
            dplnr(j)=Dlnr/dxlnr(n)^2*(plnr(j-1)-2*plnr(j)+plnr(j+1));
        end
    end
    n=Nlnr;
    for j=(n-1)*J+2:n*J-1
        Dlnr=DlnrFun(n,j,plnr,T);
        dplnr(j)=Dlnr/dxlnr(n)^2*(plnr(j-1)-2*plnr(j)+plnr(j+1));
    end
end

%Case 9
for n=1:Nlnr-1
    j=n*J+1;
    Dlnr(1)=DlnrFun(n,j,plnr,T);
    Slnr(1)=SlnrFun(n,j,plnr,T);
    n=n+1;
    Dlnr(2)=DlnrFun(n,j,plnr,T);
    Slnr(2)=SlnrFun(n,j,plnr,T);
    n=n-1;
    dplnr(j)=2/(dxlnr(n)*Slnr(1)+dxlnr(n+1)*Slnr(2))*(Dlnr(1)*Slnr(1)/dxlnr(n)*(plnr(j-1)-
plnr(j))-Dlnr(2)*Slnr(2)/dxlnr(n+1)*(plnr(j)-plnr(j+1)));
end
```

```
%Case 10
n=Nlnr;
j=n*J;
Dlnr=DlnrFun(n,j,plnr,T);
dplnr(j)=Dlnr(1)/dxlnr(n)^2*(plnr(j-1)-2*plnr(j)+pf);


%Moisture content of food product
n=Nlnr;
j=n*J;
Dlnr=DlnrFun(n,j,plnr,T);
Slnr=SlnrFun(n,j,plnr,T);
dM=MrH2O/ms*(Dlnr*Slnr*Alnr/dxlnr(n)*(plnr(j)-pf)+Aprflnr*Jprflnr);


%Bag headspace water vapour pressure
n=Nbag;
j=n*J;
Dbag=DbagFun(n,j,pbag,T);
Sbag=SbagFun(n,j,pbag,T);
n=1;
j=2;
Dlnr=DlnrFun(n,j,plnr,T);
Slnr=SlnrFun(n,j,plnr,T);
n1=Nbag;
j1=n1*J;
n2=1;
j2=2;
dpbh=2/(Abag*dxbag(n1)*Sbag+Alnr*dxlnr(n2)*Slnr)*(Dbag*Sbag*Abag/dxbag(n1)*(pbag(j1)-pbh)-
Dlnr*Slnr*Alnr/dxlnr(n2)*(pbh-plnr(j2))+Jprfbag*Aprfbag-Jprflnr*Aprflnr);


dD=[dpbag dplnr dM dpbh]';
```

D.1.2.2.3 Diffusivity of Water Vapour in Paperboard Bag Function File (DbagFun.m)

```
%Diffusivity of Water Vapour in Paperboard Bag Function File

function Dbag=DbagFun(n,j,pbag,T)

global MrH2O ms R J;
global kGAB CGAB M0GAB CBET M1BET blin clin;
global Abag Aprfbag XTbag Nbag dxbag dprfbag Drefbag TrefDbag EDbag Srefbag TrefSbag dHSbag;
global Alnr Aprflnr XTlnr Nlnr dxlnr dprflnr Dreflnr TrefDlnr EDlnr Sreflnr TrefSlnr dHSlnr;
global isotherm pa pf;


switch n
    case 1
        Dbag=Drefbag(n)*exp(EDbag(n)/R*(1/TrefDbag(n)-1/T));
    case 2
        Dbag=Drefbag(n)*exp(EDbag(n)/R*(1/TrefDbag(n)-1/T));
    case 3
        Dbag=Drefbag(n)*exp(EDbag(n)/R*(1/TrefDbag(n)-1/T));
end
```

D.1.2.2.4 Diffusivity of Water Vapour in Polymer Liner Function File (DlnrFun.m)

```
%Diffusivity of Water Vapour in Polymer Liner Function File

function Dlnr=DlnrFun(n,j,plnr,T)

global MrH2O ms R J;
global kGAB CGAB M0GAB CBET M1BET blin clin;
global Abag Aprfbag XTbag Nbag dxbag dprfbag Drefbag TrefDbag EDbag Srefbag TrefSbag dHSbag;
global Alnr Aprflnr XTlnr Nlnr dxlnr dprflnr Dreflnr TrefDlnr EDlnr Sreflnr TrefSlnr dHSlnr;
global isotherm pa pf;


switch n
    case 1
        Dlnr=Dreflnr(n)*exp(EDlnr(n)/R*(1/TrefDlnr(n)-1/T));
    case 2
        Dlnr=Dreflnr(n)*exp(EDlnr(n)/R*(1/TrefDlnr(n)-1/T));
    case 3
        Dlnr=Dreflnr(n)*exp(EDlnr(n)/R*(1/TrefDlnr(n)-1/T));
    case 4
        Dlnr=Dreflnr(n)*exp(EDlnr(n)/R*(1/TrefDlnr(n)-1/T));
    case 5
        Dlnr=Dreflnr(n)*exp(EDlnr(n)/R*(1/TrefDlnr(n)-1/T));
    case 6
        Dlnr=Dreflnr(n)*exp(EDlnr(n)/R*(1/TrefDlnr(n)-1/T));
    case 7
        Dlnr=Dreflnr(n)*exp(EDlnr(n)/R*(1/TrefDlnr(n)-1/T));
    case 8
        Dlnr=Dreflnr(n)*exp(EDlnr(n)/R*(1/TrefDlnr(n)-1/T));
    case 9
        Dlnr=Dreflnr(n)*exp(EDlnr(n)/R*(1/TrefDlnr(n)-1/T));
end
```

D.1.2.2.5 Solubility of Water Vapour in Paperboard Bag Function File (SbagFun.m)

```
%Solubility of Water Vapour in Paperboard Bag Function File

function Sbag=SbagFun(n,j,pbag,T)

global MrH2O ms R J;
global kGAB CGAB M0GAB CBET M1BET blin clin;
global Abag Aprfbag XTbag Nbag dxbag dprfbag Drefbag TrefDbag EDbag Srefbag TrefSbag dHSbag;
global Alnr Aprflnr XTlnr Nlnr dxlnr dprflnr Dreflnr TrefDlnr EDlnr Sreflnr TrefSlnr dHSlnr;
global isotherm pa pf;


switch n
    case 1
        Sbag=Srefbag(n)*exp(dHSbag(n)/R*(1/TrefSbag(n)-1/T));
    case 2
        Sbag=Srefbag(n)*exp(dHSbag(n)/R*(1/TrefSbag(n)-1/T));
    case 3
        Sbag=Srefbag(n)*exp(dHSbag(n)/R*(1/TrefSbag(n)-1/T));
end
```

D.1.2.2.6 Solubility of Water Vapour in Polymer Liner Function File (SlnrFun.m)

```
%Solubility of Water Vapour in Polymer Liner Function File

function Slnr=SlnrFun(n,j,plnr,T)

global MrH2O ms R J;
global kGAB CGAB M0GAB CBET M1BET blin clin;
global Abag Aprfbag XTbag Nbag dxbag dprfbag Drefbag TrefDbag EDbag Srefbag TrefSbag dHSbag;
global Alnr Aprflnr XTlnr Nlnr dxlnr dprflnr Dreflnr TrefDlnr EDlnr Sreflnr TrefSlnr dHSlnr;
global isotherm pa pf;


switch n
    case 1
        Slnr=Sreflnr(n)*exp(dHSlnr(n)/R*(1/T-1/TrefSlnr(n)));
    case 2
        Slnr=Sreflnr(n)*exp(dHSlnr(n)/R*(1/T-1/TrefSlnr(n)));
    case 3
        Slnr=Sreflnr(n)*exp(dHSlnr(n)/R*(1/T-1/TrefSlnr(n)));
    case 4
        Slnr=Sreflnr(n)*exp(dHSlnr(n)/R*(1/T-1/TrefSlnr(n)));
    case 5
        Slnr=Sreflnr(n)*exp(dHSlnr(n)/R*(1/T-1/TrefSlnr(n)));
    case 6
        Slnr=Sreflnr(n)*exp(dHSlnr(n)/R*(1/T-1/TrefSlnr(n)));
    case 7
        Slnr=Sreflnr(n)*exp(dHSlnr(n)/R*(1/T-1/TrefSlnr(n)));
    case 8
        Slnr=Sreflnr(n)*exp(dHSlnr(n)/R*(1/T-1/TrefSlnr(n)));
    case 9
        Slnr=Sreflnr(n)*exp(dHSlnr(n)/R*(1/T-1/TrefSlnr(n)));
end
```

D.1.3 Error checks

D.1.3.1 Numerical Error Checks

D.1.3.1.1 Time Step

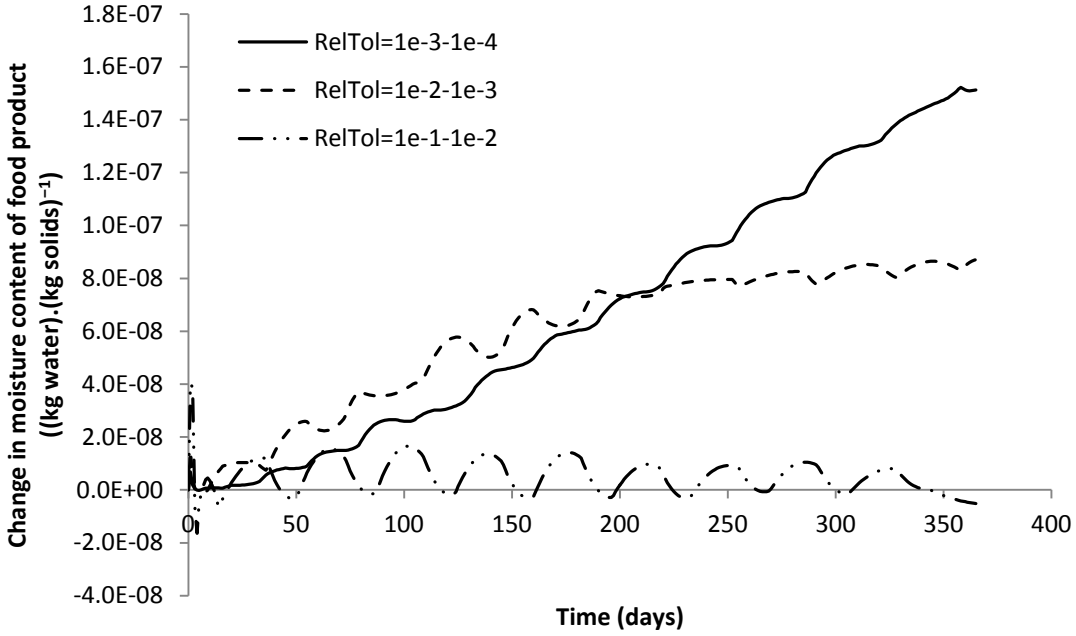

Figure D-1: Plot of change in predicted values of moisture content of food product ((kg water).(kg solids)$^{-1}$), with changes to relative error tolerance of MATLAB® solver (RelTol).

As shown in Figure D-1, all changes to relative error tolerance of the MATLAB® solver (RelTol) had relatively insignificant effects on predicted values of moisture content of the food product, with no differences greater than 1.5×10^{-7} (kg water).(kg solids)$^{-1}$ over the period $0 \leq t \leq 365$ days. Therefore the default RelTol value of 1×10^{-3} should be suitable for use in the model.

D.1.3.1.2 Space Step

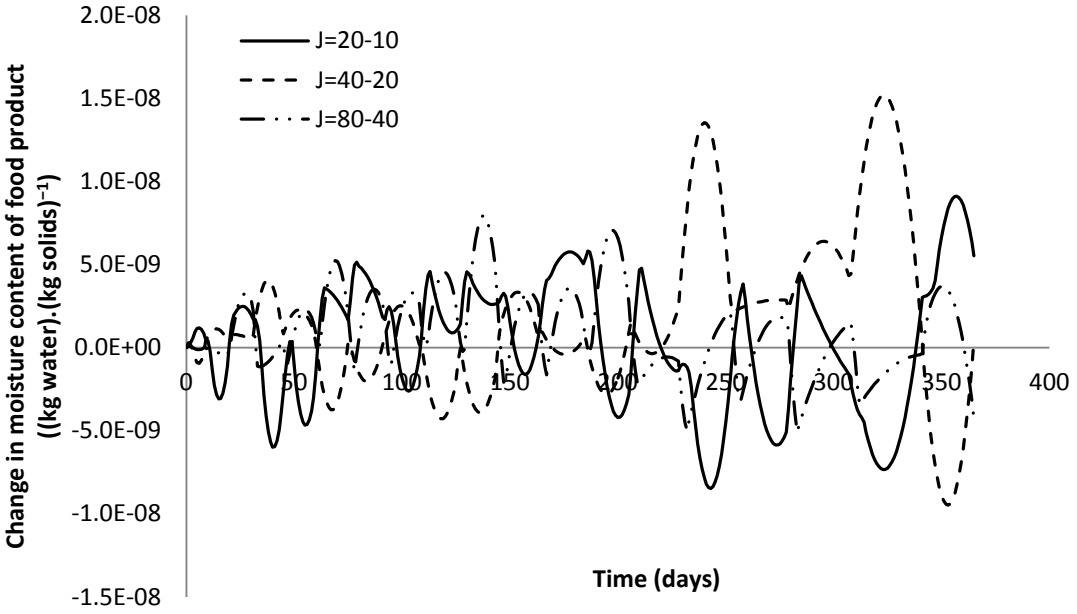

Figure D-2: Plot of change in predicted values of moisture content of food product ((kg water).(kg solids)$^{-1}$) with changes to number of nodes per layer of packaging (J).

As shown in Figure D-2, all changes to the number of nodes per layer of packaging had relatively insignificant effects on predicted values of moisture content of the food, with no differences greater than 1.6×10^{-8} (kg water).(kg solids)$^{-1}$ over the period $0 \leq t \leq 365$ days. Therefore a standard number of 10 nodes per layer of packaging should be suitable for use in the model.

D.1.3.2 Mathematical Error Checks

D.1.3.2.1 Water Vapour Pressure in Paperboard Bag

To allow an analytical solution for the water vapour pressure in the paperboard bag, the following changes were made:

- The properties of all paperboard bag layers were set the same. A two layer system was simulated to ensure all finite difference approximations were correct.

- A linear isotherm with a very high slope was used to ensure the water vapour pressure in the food product remained constant. The linear isotherm constant was adjusted to obtain the desired water vapour pressure.
- The concentration dependence of the diffusivity and solubility of water vapour in the paperboard bag were disabled.
- Only the water vapour pressure profile after 24 hours was considered.
- The surface area of perforations in the polymer liner was set to a very high value to ensure the water vapour pressure in the bag headspace remained equal to the water vapour pressure in the food product.

Formulated problem:

$$S_{bag}^{H_2O}\frac{\partial p_{bag}^{H_2O}}{\partial t} = D_{bag}^{H_2O}S_{bag}^{H_2O}\frac{\partial^2 p_{bag}^{H_2O}}{\partial x^2}$$

$$\textit{for } t \geq 0,\ 0 < x < X_{T,bag}$$

$$p_{bag}^{H_2O} = p_a^{H_2O}$$

$$\textit{for } t \geq 0, \textit{ at } x = 0 \textit{ and } x = X_{T,bag}$$

$$p_{bag}^{H_2O} = p_{bag,i}^{H_2O}$$

$$\textit{for } t = 0,\ 0 < x < X_{T,bag}$$

Analytical solution:

$$R = \frac{X_{T,bag}}{2} = \frac{5 \times 10^{-5}}{2} = 2.5 \times 10^{-5}$$

$$Fo = \frac{D_{bag}^{H_2O}t}{R^2} = \frac{1 \times 10^{-15} \times 24 \times 60^2}{(2.5 \times 10^{-5})^2} = 0.1382$$

$$Y = \frac{4}{\pi}\sum_{m=0}^{\infty}\frac{(-1)^m}{2m+1}cos\left[(2m+1)\frac{\pi}{2}\frac{x}{R}\right]exp\left[-(2m+1)^2\frac{\pi^2}{4}Fo\right]$$

m	$\frac{(-1)^m}{2m+1} cos\left[(2m+1)\frac{\pi}{2}\frac{x}{R}\right] exp\left[-(2m+1)^2\frac{\pi^2}{4}Fo\right]$
0	0.7110
1	−0.01548
2	3.960×10^{-5}
Total	0.6956

$$Y = \frac{4}{\pi}0.6956 = 0.8856$$

$$p_{bag}^{H_2O} = Y\left(p_{bag,i}^{H_2O} - p_a^{H_2O}\right) + p_a^{H_2O} = 0.8856(585 - 1756) + 1756 = 719.1 \text{ Pa}$$

This procedure was repeated to calculate the water vapour pressure after 24 hours for various positions within the paperboard bag.

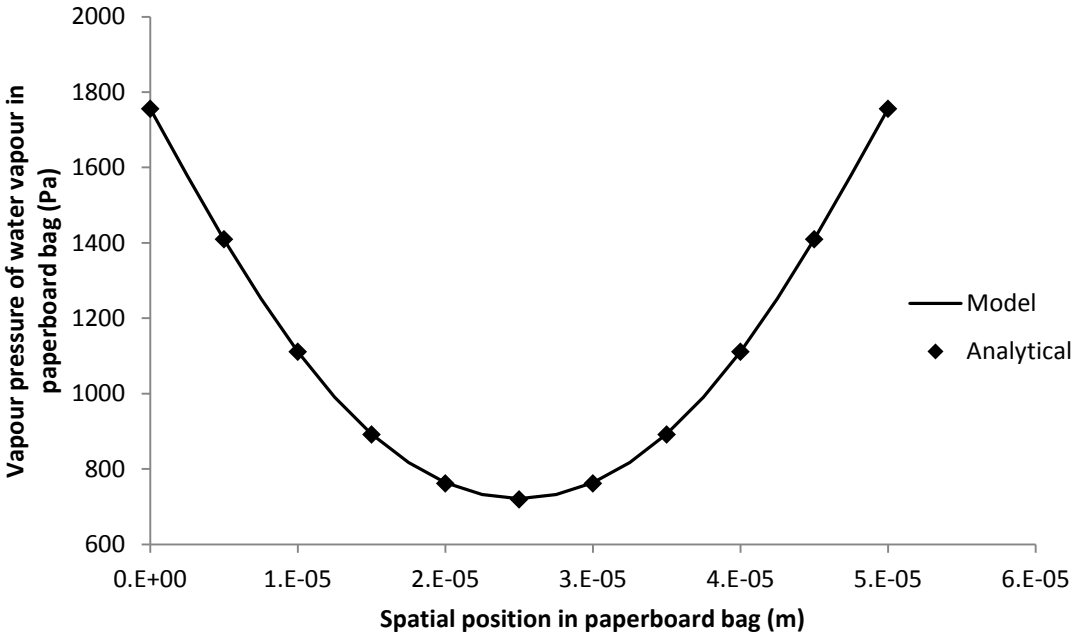

Figure D-3: Comparison of water vapour pressure profile in paperboard bag after 24 hours as predicted analytically and by the model.

As shown in Figure D-3, the values predicted by the model agree very closely with those calculated analytically, suggesting the model is correctly calculating the water vapour pressure in the paperboard bag.

D.1.3.2.2 Water Vapour Pressure in Polymer Liner

To allow an analytical solution for the water vapour pressure in the polymer liner, the following changes were made:

- The properties of all polymer liner layers were set the same. A two layer system was simulated to ensure all finite difference approximations were correct.
- A linear isotherm with a very high slope was used to ensure the water vapour pressure in the food product remained constant. The linear isotherm constant was adjusted to obtain the desired water vapour pressure.
- The concentration dependence of the diffusivity and solubility of water vapour in the polymer liner were disabled.
- Only the water vapour pressure profile after 24 hours was considered.
- The area of perforations in the paperboard bag was set to a very high value to ensure the water vapour pressure in the bag headspace remained equal to the water vapour pressure in the ambient air.

Formulated problem:

$$S_{lnr}^{H_2O}\frac{\partial p_{lnr}^{H_2O}}{\partial t} = D_{lnr}^{H_2O}S_{lnr}^{H_2O}\frac{\partial^2 p_{lnr}^{H_2O}}{\partial x^2}$$

for $t \geq 0,\ 0 < x < X_{T,lnr}$

$$p_{lnr}^{H_2O} = p_a^{H_2O}$$

for $t \geq 0$, *at* $x = 0$ *and* $x = X_{T,lnr}$

$$p_{lnr}^{H_2O} = p_{lnr,i}^{H_2O}$$

for $t = 0,\ 0 < x < X_{T,lnr}$

Analytical solution:

$$R = \frac{X_{T,lnr}}{2} = \frac{5 \times 10^{-5}}{2} = 2.5 \times 10^{-5}$$

$$Fo = \frac{D_{lnr}^{H_2O} t}{R^2} = \frac{1 \times 10^{-15} \times 24 \times 60^2}{(2.5 \times 10^{-5})^2} = 0.1382$$

$$Y = \frac{4}{\pi} \sum_{m=0}^{\infty} \frac{(-1)^m}{2m+1} cos\left[(2m+1)\frac{\pi}{2}\frac{x}{R}\right] exp\left[-(2m+1)^2 \frac{\pi^2}{4} Fo\right]$$

m	$\boldsymbol{\frac{(-1)^m}{2m+1} cos\left[(2m+1)\frac{\pi}{2}\frac{x}{R}\right] exp\left[-(2m+1)^2 \frac{\pi^2}{4} Fo\right]}$
0	0.7110
1	−0.01548
2	3.960×10^{-5}
Total	0.6956

$$Y = \frac{4}{\pi} 0.6956 = 0.8856$$

$$p_{lnr}^{H_2O} = Y\left(p_{lnr,i}^{H_2O} - p_a^{H_2O}\right) + p_a^{H_2O} = 0.8856(585 - 1756) + 1756 = 719.1 \text{ Pa}$$

This procedure was repeated to calculate the water vapour pressure after 24 hours for various positions within the polymer liner.

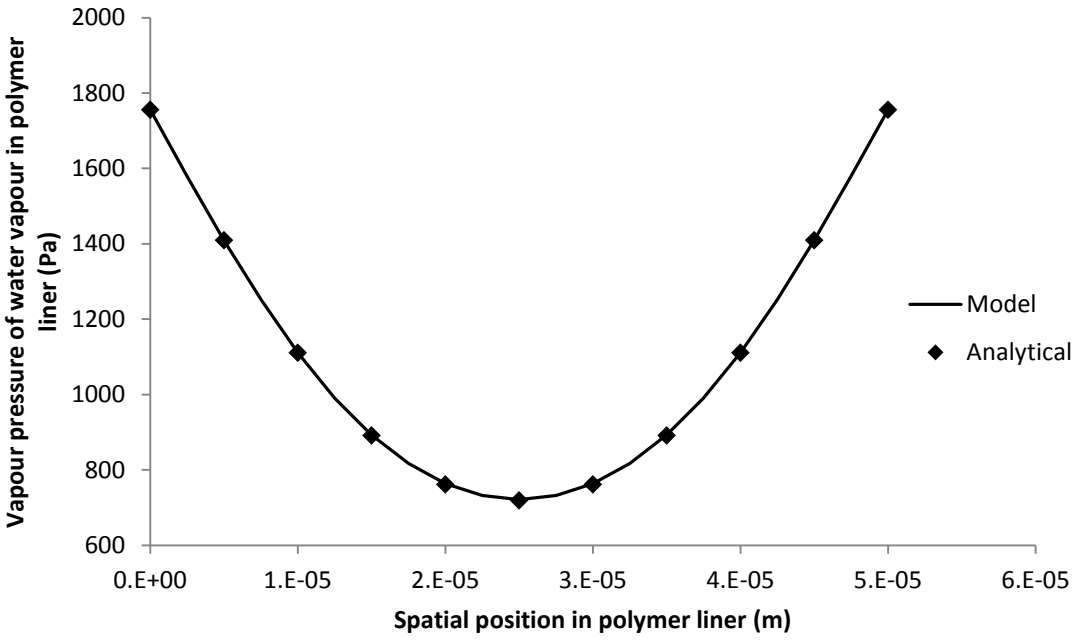

Figure D-4: Comparison of water vapour pressure profile in polymer liner after 24 hours as predicted analytically and by the model.

As shown in Figure D-3, the values predicted by the model agree very closely with those calculated analytically, suggesting the model is correctly calculating the water vapour pressure in the polymer liner.

D.1.3.2.3 Moisture Content of Food Product

To allow an analytical solution for the moisture content of the food product, the following changes were made:

- A linear isotherm was used for the food product.
- The concentration dependence of the diffusivity and solubility of water vapour in the polymer liner were disabled.
- The area of perforations in the paperboard bag was set to a very high value to ensure the water vapour pressure in the bag headspace remained equal to the water vapour pressure in the ambient air.
- A perforation with a large diameter was used.

Formulated problem:

$$\frac{dM}{dt} = \frac{M_{r,H_2O}}{m_s}\left[P^{H_2O}_{lnr,n=N_{lnr}}\left(\frac{dp^{H_2O}_{lnr}}{dx}\right)_{x=X_{T,lnr}} + J^{H_2O}_{prf,lnr}A_{prf,lnr}\right]$$

$$for\ t \geq 0$$

Analytical solution:

$$\frac{dM}{dt} = \frac{M_{r,H_2O}}{m_s X_T}\left(P^{H_2O}_{lnr}A_{lnr} + D^{H_2O}_{air}S^{H_2O}_{air}A_{prf,lnr}\right)\left(p^{H_2O}_{a} - p^{H_2O}_{0}\left(\frac{M - c_{lin}}{b_{lin}}\right)\right)$$

$$\frac{dM}{dt} = aM + b$$

where:

$$a = -\frac{M_{r,H_2O}p^{H_2O}_{0}}{m_s X_T b_{lin}}\left(P^{H_2O}_{lnr}A_{lnr} + D^{H_2O}_{air}S^{H_2O}_{air}A_{prf,lnr}\right)$$

$$b = \frac{M_{r,H_2O}}{m_s X_T}\left(p^{H_2O}_{a} + p^{H_2O}_{0}\frac{c_{lin}}{b_{lin}}\right)\left(P^{H_2O}_{lnr}A_{lnr} + D^{H_2O}_{air}S^{H_2O}_{air}A_{prf,lnr}\right)$$

$$\int_{M_i}^{M}\frac{1}{aM+b}\partial M = \int_{0}^{t}\partial t$$

$$M = \left(M_i + \frac{b}{a}\right)exp(at) - \frac{b}{a}$$

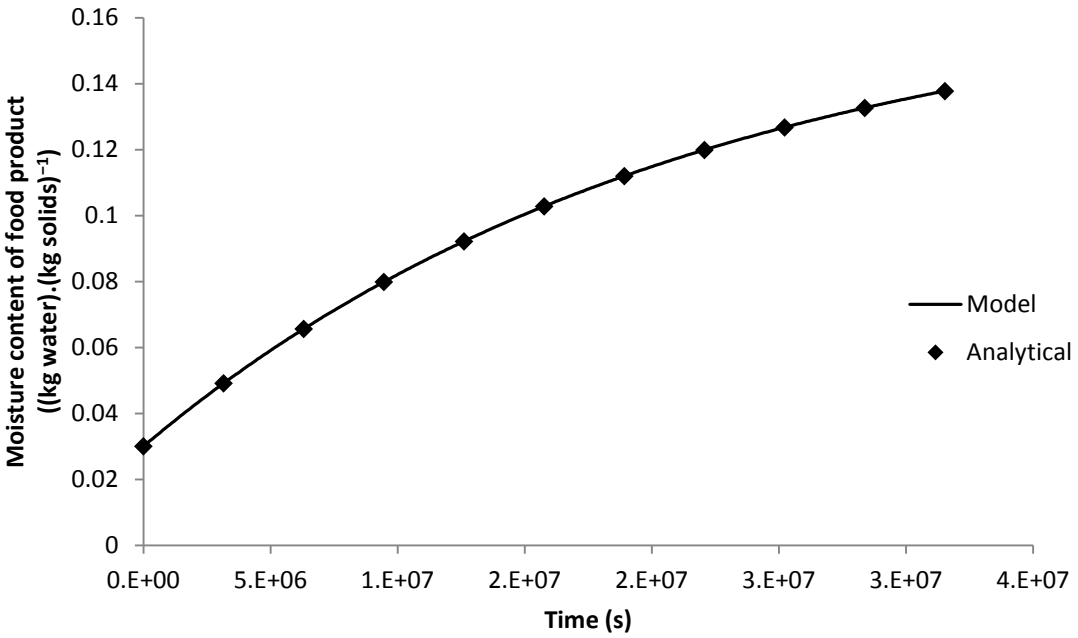

Figure D-5: Comparison of moisture content of food product as predicted analytically and by the model.

As shown in Figure D-5, the values predicted by the model agree very closely with those calculated analytically, suggesting the model is correctly calculating the moisture content of the food product.

D.1.3.2.4 Water Vapour Pressure in Bag Headspace

Since the mass of water in air in the bag headspace was assumed to be negligible, the bag headspace is essentially a node on the boundary of two packaging layers with additional mositure transfer due to perforations. To verify the permeation component of the bag headspace, the paperboard bag and polymer liner were treated as a single packaging layer, for which an analytical solution is possible. Other changes included the following:

- The area of perforations in the paperboard bag and polymer liner were set to zero.
- The properties of all paperboard bag and polymer liner layers were set the same. A two layer system in both was simulated to further verify all finite difference approximations.
- A linear isotherm with a very high slope was used to ensure the water vapour pressure in the food product remained constant. The linear isotherm constant was adjusted to obtain the desired water vapour pressure.
- The concentration dependence of the diffusivity and solubility of water vapour in the paperboard bag and polymer liner were disabled.

Formulated problem:

$$S_{bag}^{H_2O}\frac{\partial p_{bag}^{H_2O}}{\partial t} = D_{bag}^{H_2O}S_{bag}^{H_2O}\frac{\partial^2 p_{bag}^{H_2O}}{\partial x^2}$$

$$\textit{for } t \geq 0,\ 0 < x < X_{T,bag}$$

$$S_{lnr}^{H_2O}\frac{\partial p_{lnr}^{H_2O}}{\partial t} = D_{lnr}^{H_2O}S_{lnr}^{H_2O}\frac{\partial^2 p_{lnr}^{H_2O}}{\partial x^2}$$

$$\textit{for } t \geq 0,\ 0 < x < X_{T,lnr}$$

$$p_{bag}^{H_2O} = p_a^{H_2O}$$

$$\textit{for } t \geq 0, \textit{ at } x = 0$$

$$p_{lnr}^{H_2O} = p_a^{H_2O}$$

$$\textit{for } t \geq 0, \textit{ at } x = X_{T,lnr}$$

$$p_{bag}^{H_2O} = p_{lnr}^{H_2O} = p_{bag,i}^{H_2O} = p_{lnr,i}^{H_2O}$$

$$for\ t = 0,\ 0 < x < X_{T,bag}\ and\ 0 < x < X_{T,lnr}$$

Analytical solution:

$$R = \frac{X_{T,bag} + X_{T,lnr}}{2} = \frac{2 \times 10^{-5} + 3 \times 10^{-5}}{2} = 2.5 \times 10^{-5}$$

$$Fo = \frac{D_{pkg}^{H_2O} t}{R^2} = \frac{1 \times 10^{-15} \times 24 \times 60^2}{(2.5 \times 10^{-5})^2} = 0.1382$$

$$Y = \frac{4}{\pi} \sum_{m=0}^{\infty} \frac{(-1)^m}{2m+1} cos\left[(2m+1)\frac{\pi}{2}\frac{x}{R}\right] exp\left[-(2m+1)^2 \frac{\pi^2}{4} Fo\right]$$

m	$\boldsymbol{\frac{(-1)^m}{2m+1} cos\left[(2m+1)\frac{\pi}{2}\frac{x}{R}\right] exp\left[-(2m+1)^2\frac{\pi^2}{4}Fo\right]}$
0	0.6762
1	-0.009097
2	-6.367×10^{-21}
Total	0.6671

$$Y = \frac{4}{\pi} 0.6671 = 0.8494$$

$$p_{bh}^{H_2O} = Y\left(p_{lnr,i}^{H_2O} - p_a^{H_2O}\right) + p_a^{H_2O} = 0.8494(585 - 1756) + 1756 = 761.5 \text{ Pa}$$

This procedure was repeated to calculate the water vapour pressure in the package headspace at 2 hour intervals up to 24 hours.

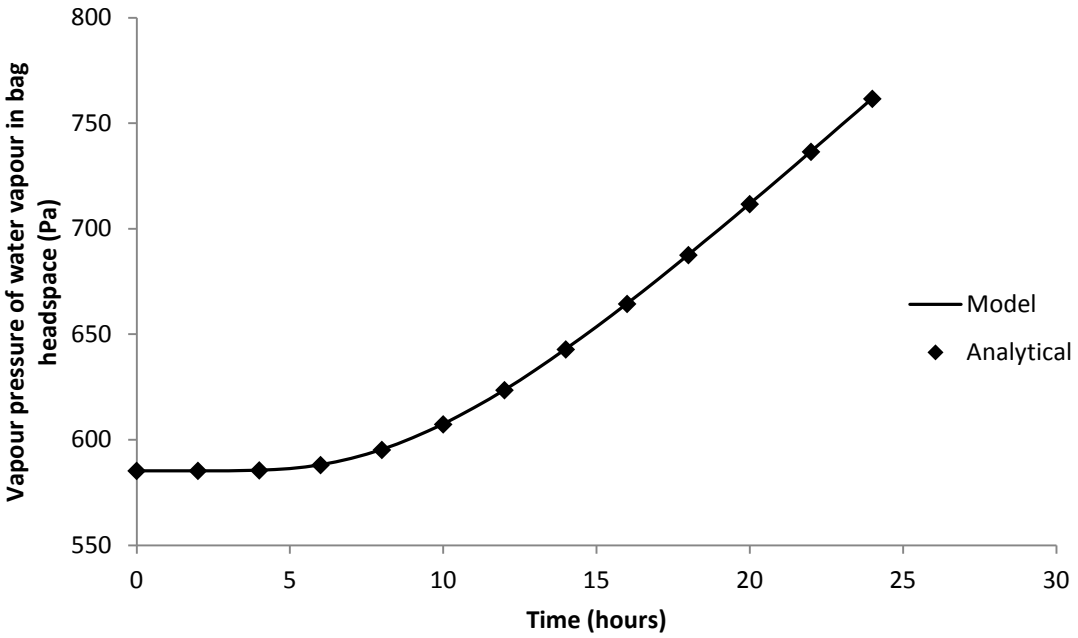

Figure D-6: Comparison of water vapour pressure in bag headspace as predicted analytically and by the model.

As shown in Figure D-6, the values predicted by the model agree very closely with those calculated analytically, suggesting the model is correctly calculating the water vapour pressure in the bag headspace due to permeation. Since the perforation component of the bag headspace only consists of inward and outward water vapour fluxes, these were not verified separately.

D.2 NON-INSTANTANEOUS MASS TRANSFER IN FOOD PRODUCT

D.2.1 Conceptual Model Development

D.2.1.1 Word Balances and Equations

D.2.1.1.1 ODE for Water Vapour Pressure in Liner Headspace

Steady-state mass balance of water vapour in polymer liner headspace

$$\frac{dp_{lh}^{H_2O}}{dt} = 0 = P_{lnr,n=N_{lnr}}^{H_2O} A_{lnr} \left(\frac{dp_{lnr}^{H_2O}}{dx}\right)_{x=X_{lnr,n}} + J_{prf,lnr}^{H_2O} A_{prf,lnr} - D_{eff}^{H_2O} S_{air}^{H_2O} A_f \left(\frac{dp_f^{H_2O}}{dx}\right)_{x=0}$$

$$\left[\frac{mol.m}{m^2.s.Pa}\right][m^2]\frac{[Pa]}{[m]} + \left[\frac{mol}{m^2.s}\right][m^2] + \left[\frac{mol}{m^2.s}\right][m^2] - \left[\frac{m^2}{s}\right]\left[\frac{mol}{m^3.Pa}\right][m^2]\frac{[Pa]}{[m]}$$

D.2.1.1.2 PDE for Water Vapour Pressure in Food Powder

$$\frac{\partial}{\partial t}(\varepsilon S_v p_v + (1-\varepsilon)C_s) = \frac{\partial}{\partial x}\left(D_v S_v \frac{\partial p_v}{\partial x}\right)$$

$$\varepsilon S_v \frac{\partial p_v}{\partial t} + (1-\varepsilon)\frac{\partial C_s}{\partial t} = \frac{\partial}{\partial x}\left(D_v S_v \frac{\partial p_v}{\partial x}\right)$$

$$\varepsilon S_v \frac{\partial p_v}{\partial t} + (1-\varepsilon)\frac{\partial C_s}{\partial p_v}\frac{\partial p_v}{\partial t} = \frac{\partial}{\partial x}\left(D_v S_v \frac{\partial p_v}{\partial x}\right)$$

$$\frac{\partial C_s}{\partial p_v} = S_s$$

$$(\varepsilon S_v + (1-\varepsilon)S_s)\frac{\partial p_v}{\partial t} = \frac{\partial}{\partial x}\left(D_v S_v \frac{\partial p_v}{\partial x}\right)$$

$$\left(\varepsilon S_{air}^{H_2O} + (1-\varepsilon)S_f^{H_2O}\right)\frac{\partial p_f^{H_2O}}{\partial t} = D_{eff}^{H_2O} S_{air}^{H_2O} \frac{\partial^2 p_f^{H_2O}}{\partial x^2}$$

D.2.2 Solution

D.2.2.1 Finite Difference Approximations

$$\Delta x_f = \frac{X_f}{J}$$

D.2.2.1.1 Case 12

$$A_f \Delta x_f \left[\varepsilon S_{air}^{H_2O} + (1-\varepsilon) S_f^{H_2O}\right] \frac{dp_{f,j}^{H_2O}}{dt} = D_{eff}^{H_2O} S_{air}^{H_2O} A_f \frac{\left(p_{lh}^{H_2O} - p_{f,j}^{H_2O}\right)}{\Delta x_f} - D_{eff}^{H_2O} S_{air}^{H_2O} A_f \frac{\left(p_{f,j}^{H_2O} - p_{f,j+1}^{H_2O}\right)}{\Delta x_f}$$

$$[m^2][m]\left(\left[\frac{mol}{m^3.Pa}\right] + \left[\frac{mol}{m^3.Pa}\right]\right)\left[\frac{Pa}{s}\right] = \left[\frac{m^2}{s}\right]\left[\frac{mol}{m^3.Pa}\right][m^2]\frac{[Pa]}{[m]} - \left[\frac{m^2}{s}\right]\left[\frac{mol}{m^3.Pa}\right][m^2]\frac{[Pa]}{[m]}$$

$$\Delta x_f \left[\varepsilon S_{air}^{H_2O} + (1-\varepsilon) S_f^{H_2O}\right] \frac{dp_{f,j}^{H_2O}}{dt} = D_{eff}^{H_2O} S_{air}^{H_2O} \frac{\left(p_{lh}^{H_2O} - p_{f,j}^{H_2O}\right)}{\Delta x_f} - D_{eff}^{H_2O} S_{air}^{H_2O} \frac{\left(p_{f,j}^{H_2O} - p_{f,j+1}^{H_2O}\right)}{\Delta x_f}$$

$$\frac{dp_{f,j}^{H_2O}}{dt} = \frac{D_{eff}^{H_2O} S_{air}^{H_2O}\left(p_{lh}^{H_2O} - 2p_{f,j}^{H_2O} + p_{f,j+1}^{H_2O}\right)}{\Delta x_f{}^2 \left[\varepsilon S_{air}^{H_2O} + (1-\varepsilon) S_f^{H_2O}\right]}$$

D.2.2.1.2 Case 13

$$A_f \Delta x_f \left[\varepsilon S_{air}^{H_2O} + (1-\varepsilon) S_f^{H_2O}\right] \frac{dp_{f,j}^{H_2O}}{dt} = D_{eff}^{H_2O} S_{air}^{H_2O} A_f \frac{\left(p_{f,j-1}^{H_2O} - p_{f,j}^{H_2O}\right)}{\Delta x_f} - D_{eff}^{H_2O} S_{air}^{H_2O} A_f \frac{\left(p_{f,j}^{H_2O} - p_{f,j+1}^{H_2O}\right)}{\Delta x_f}$$

$$[m^2][m]\left(\left[\frac{mol}{m^3.Pa}\right]+\left[\frac{mol}{m^3.Pa}\right]\right)\left[\frac{Pa}{s}\right]$$
$$=\left[\frac{m^2}{s}\right]\left[\frac{mol}{m^3.Pa}\right][m^2]\frac{[Pa]}{[m]}-\left[\frac{m^2}{s}\right]\left[\frac{mol}{m^3.Pa}\right][m^2]\frac{[Pa]}{[m]}$$

$$\Delta x_f\left[\varepsilon S_{air}^{H_2O}+(1-\varepsilon)S_f^{H_2O}\right]\frac{dp_{f,j}^{H_2O}}{dt}$$
$$=D_{eff}^{H_2O}S_{air}^{H_2O}\frac{\left(p_{f,j-1}^{H_2O}-p_{f,j}^{H_2O}\right)}{\Delta x_f}-D_{eff}^{H_2O}S_{air}^{H_2O}\frac{\left(p_{f,j}^{H_2O}-p_{f,j+1}^{H_2O}\right)}{\Delta x_f}$$
$$\frac{dp_{f,j}^{H_2O}}{dt}=\frac{D_{eff}^{H_2O}S_{air}^{H_2O}\left(p_{f,j-1}^{H_2O}-2p_{f,j}^{H_2O}+p_{f,j+1}^{H_2O}\right)}{{\Delta x_f}^2\left[\varepsilon S_{air}^{H_2O}+(1-\varepsilon)S_f^{H_2O}\right]}$$

D.2.2.1.3 Case 14

$$\frac{A_f\Delta x_f}{2}\left[\varepsilon S_{air}^{H_2O}+(1-\varepsilon)S_f^{H_2O}\right]\frac{dp_{f,j}^{H_2O}}{dt}=D_{eff}^{H_2O}S_{air}^{H_2O}A_f\frac{\left(p_{f,j-1}^{H_2O}-p_{f,j}^{H_2O}\right)}{\Delta x_f}$$

$$[m^2][m]\left(\left[\frac{mol}{m^3.Pa}\right]+\left[\frac{mol}{m^3.Pa}\right]\right)\left[\frac{Pa}{s}\right]$$
$$=\left[\frac{m^2}{s}\right]\left[\frac{mol}{m^3.Pa}\right][m^2]\frac{[Pa]}{[m]}-\left[\frac{m^2}{s}\right]\left[\frac{mol}{m^3.Pa}\right][m^2]\frac{[Pa]}{[m]}$$

$$\frac{\Delta x_f}{2}\left[\varepsilon S_{air}^{H_2O}+(1-\varepsilon)S_f^{H_2O}\right]\frac{dp_{f,j}^{H_2O}}{dt}=D_{eff}^{H_2O}S_{air}^{H_2O}\frac{\left(p_{f,j-1}^{H_2O}-p_{f,j}^{H_2O}\right)}{\Delta x_f}$$
$$\frac{dp_{f,j}^{H_2O}}{dt}=\frac{2D_{eff}^{H_2O}S_{air}^{H_2O}\left(p_{f,j-1}^{H_2O}-p_{f,j}^{H_2O}\right)}{{\Delta x_f}^2\left[\varepsilon S_{air}^{H_2O}+(1-\varepsilon)S_f^{H_2O}\right]}$$

D.2.2.2 MATLAB® Solution

Refer to Appendix B for a digital copy of this numerical solution.

D.2.2.2.1 Script File (PackageExtended2.m)

```
%Script File

clear all

global MrH2O ms R J;
global kGAB CGAB M0GAB CBET M1BET blin clin;
global Abag Aprfbag XTbag Nbag dxbag dprfbag Drefbag TrefDbag EDbag Srefbag TrefSbag dHSbag;
global Alnr Aprflnr XTlnr Nlnr dxlnr dprflnr Dreflnr TrefDlnr EDlnr Sreflnr TrefSlnr dHSlnr;
global E rhos dxf Af;
global isotherm pa;


%System Inputs
%General SIs
MrH2O=(1.01*2+16.00)*10^-3;                 %Molecular mass of water (kg/mol)
R=8.314;                                    %Ideal gas constant (m^3.Pa/K/mol)

%Food Powder SIs
rhob=850;                                   %Bulk density
rhop=1493;                                  %Particle density
mf=25;                                      %Mass of food product (kg)
ms=mf/(1+0.03);                             %Mass of dry solids in food product (kg)
Af=1.12;                                    %Surface area of food product (m^2)
rhos=rhop/(1+0.03);                         %Density of solids in the food product (kg/m^3)
Xf=mf/rhob/Af;                              %Distance of water vapour diffusion into food
product (m)
E=1-rhob/rhop;                              %Porosity of food product (-)
isotherm='GAB';                             %Type of moisture (GAB, BET, or lin)

%Isotherm SIs
if lower(isotherm)=='gab'       %GAB Isotherm
    kGAB=1.08;                              %GAB isotherm constant (correcting factor)
    CGAB=12.11;                             %GAB isotherm constant (Guggenheim constant)
    M0GAB=0.051;                            %GAB isotherm constant (monolayer) (kg water/kg
solids)
elseif lower(isotherm)=='bet'   %BET isotherm
    CBET=0;                                 %BET isotherm constant
    M1BET=0;                                %BET isotherm constant (monolayer) (kg water/kg
solids)
elseif lower(isotherm)=='lin'   %Linear isotherm
    blin=0;                                 %Linear isotherm slope
    clin=0;                                 %Linear isotherm intercept
end


%Packaging Material SIs
%Paperboard bag
Abag=1.12;                                  %Surface area of paperboard bag (m^2)
Nbag=2;                                     %Number of layers in paperboard bag (-)
Aprfbag=0;                                  %Total surface area of perforation(s) in
paperboard bag (m^2)
dprfbag=1e-4;                               %Average diameter of perforation(s) in paperboard
bag (m)

%Layer 1
n=1;
Xbag(n)=310e-6;                             %Thickness of layer 1 of paperboard bag (m)
Srefbag(n)=0.001;                           %Reference solubility of water vapour in layer 1
of paperboard bag (mol/m^3/Pa)
TrefSbag(n)=273.15+38;                      %Temperature of reference solubility of water
vapour in layer 1 of paperboard bag (K)
dHSbag(n)=0;                                %Partial molar enthalpy of sorption of water
vapour in layer 1 of paperboard bag (J/mol)
Drefbag(n)=1e-11/Srefbag(n);                %Reference diffusivity of water vapour in layer 1
of paperboard bag (m^2/s)
TrefDbag(n)=273.15+38;                      %Temperature of reference diffusivity of water
vapour in layer 1 of paperboard bag (K)
EDbag(n)=26500-dHSbag(n);                   %Activation energy of diffusion of water vapour in
layer 1 of paperboard bag (J/mol)

%Layer 2 (Biopolymer Barrier Coating)
if Nbag>=2;
```

```
    n=2;
    Xbag(n)=60e-6;                          %Thickness of layer 2 of paperboard bag (m)
    Srefbag(n)=0.001;                       %Reference solubility of water vapour in layer 2
of paperboard bag (mol/m^3/Pa)
    TrefSbag(n)=273.15+26.8;                %Temperature of reference solubility of water
vapour in layer 2 of paperboard bag (K)
    dHSbag(n)=0;                            %Partial molar enthalpy of sorption of water
vapour in layer 2 of paperboard bag (J/mol)
    Drefbag(n)=1e-14/Srefbag(n);            %Reference diffusivity of water vapour in layer 2
of paperboard bag (m^2/s)
    TrefDbag(n)=273.15+38;                  %Temperature of reference diffusivity of water
vapour in layer 2 of paperboard bag (K)
    EDbag(n)=26500-dHSbag(n);               %Activation energy of diffusion of water vapour in
layer 2 of paperboard bag (J/mol)
end

XTbag=sum(Xbag);                            %Total thickness of paperboard bag (m)


%Polymer liner
Alnr=Abag;                                  %Surface area of polymer liner (m^2)
Nlnr=5;                                     %Number of layers in polymer liner (-)
Aprflnr=0;                                  %Total surface area of perforation(s) in polymer
liner (m^2)
dprflnr=1e-4;                               %Average diameter of perforation(s) in polymer
liner (m)

%Layer 1
n=1;
Xlnr(n)=20e-6;                              %Thickness of layer 1 of polymer liner (m)
Sreflnr(n)=0.001;                           %Reference solubility of water vapour in layer 1
of polymer liner (mol/m^3/Pa)
TrefSlnr(n)=273.15+38;                      %Temperature of reference solubility of water
vapour in layer 1 of polymer liner (K)
dHSlnr(n)=0;                                %Partial molar enthalpy of sorption of water
vapour in layer 1 of polymer liner (J/mol)
Dreflnr(n)=1e-13/Sreflnr(n);                %Reference diffusivity of water vapour in layer 1
of polymer liner (m^2/s)
TrefDlnr(n)=273.15+38;                      %Temperature of reference diffusivity of water
vapour in layer 1 of polymer liner (K)
EDlnr(n)=26500-dHSlnr(n);                   %Activation energy of diffusion of water vapour in
layer 1 of polymer liner (J/mol)

%Layer 2
if Nlnr>=2;
    n=2;
    Xlnr(n)=5e-6;                           %Thickness of layer 2 of polymer liner (m)
    Sreflnr(n)=0.001;                       %Reference solubility of water vapour in layer 2
of polymer liner (mol/m^3/Pa)
    TrefSlnr(n)=273.15+38;                  %Temperature of reference solubility of water
vapour in layer 2 of polymer liner (K)
    dHSlnr(n)=0;                            %Partial molar enthalpy of sorption of water
vapour in layer 2 of polymer liner (J/mol)
    Dreflnr(n)=1e-12/Sreflnr(n);            %Reference diffusivity of water vapour in layer 2
of polymer liner (m^2/s)
    TrefDlnr(n)=273.15+38;                  %Temperature of reference diffusivity of water
vapour in layer 2 of polymer liner (K)
    EDlnr(n)=26500-dHSlnr(n);               %Activation energy of diffusion of water vapour in
layer 2 of polymer liner (J/mol)
end

%Layer 3
if Nlnr>=3;
    n=3;
    Xlnr(n)=10e-6;                          %Thickness of layer 3 of polymer liner (m)
    Sreflnr(n)=0.001;                       %Reference solubility of water vapour in layer 3
of polymer liner (mol/m^3/Pa)
    TrefSlnr(n)=273.15+38;                  %Temperature of reference solubility of water
vapour in layer 3 of polymer liner (K)
    dHSlnr(n)=0;                            %Partial molar enthalpy of sorption of water
vapour in layer 3 of polymer liner (J/mol)
    Dreflnr(n)=2e-14/Sreflnr(n);            %Reference diffusivity of water vapour in layer 3
of polymer liner (m^2/s)
    TrefDlnr(n)=273.15+38;                  %Temperature of reference diffusivity of water
vapour in layer 3 of polymer liner (K)
    EDlnr(n)=26500-dHSlnr(n);               %Activation energy of diffusion of water vapour in
layer 3 of polymer liner (J/mol)
```

```
end

%Layer 4
if Nlnr>=4;
    n=4;
    Xlnr(n)=5e-6;                          %Thickness of layer 4 of polymer liner (m)
    Sreflnr(n)=0.001;                      %Reference solubility of water vapour in layer 4
of polymer liner (mol/m^3/Pa)
    TrefSlnr(n)=273.15+38;                 %Temperature of reference solubility of water
vapour in layer 4 of polymer liner (K)
    dHSlnr(n)=0;                           %Partial molar enthalpy of sorption of water
vapour in layer 4 of polymer liner (J/mol)
    Dreflnr(n)=1e-12/Sreflnr(n);           %Reference diffusivity of water vapour in layer 4
of polymer liner (m^2/s)
    TrefDlnr(n)=273.15+38;                 %Temperature of reference diffusivity of water
vapour in layer 4 of polymer liner (K)
    EDlnr(n)=26500-dHSlnr(n);              %Activation energy of diffusion of water vapour in
layer 4 of polymer liner (J/mol)
end

%Layer 5
if Nlnr>=5;
    n=5;
    Xlnr(n)=20e-6;                         %Thickness of layer 5 of polymer liner (m)
    Sreflnr(n)=0.001;                      %Reference solubility of water vapour in layer 5
of polymer liner (mol/m^3/Pa)
    TrefSlnr(n)=273.15+38;                 %Temperature of reference solubility of water
vapour in layer 5 of polymer liner (K)
    dHSlnr(n)=0;                           %Partial molar enthalpy of sorption of water
vapour in layer 5 of polymer liner (J/mol)
    Dreflnr(n)=1e-13/Sreflnr(n);           %Reference diffusivity of water vapour in layer 5
of polymer liner (m^2/s)
    TrefDlnr(n)=273.15+38;                 %Temperature of reference diffusivity of water
vapour in layer 5 of polymer liner (K)
    EDlnr(n)=26500-dHSlnr(n);              %Activation energy of diffusion of water vapour in
layer 5 of polymer liner (J/mol)
end

%Layer 6
if Nlnr>=6;
    n=6;
    Xlnr(n)=0;                             %Thickness of layer 6 of polymer liner (m)
    Sreflnr(n)=0;                          %Reference solubility of water vapour in layer 6
of polymer liner (mol/m^3/Pa)
    TrefSlnr(n)=273.15+0;                  %Temperature of reference solubility of water
vapour in layer 6 of polymer liner (K)
    dHSlnr(n)=0;                           %Partial molar enthalpy of sorption of water
vapour in layer 6 of polymer liner (J/mol)
    Dreflnr(n)=0;                          %Reference diffusivity of water vapour in layer 6
of polymer liner (m^2/s)
    TrefDlnr(n)=273.15+0;                  %Temperature of reference diffusivity of water
vapour in layer 6 of polymer liner (K)
    EDlnr(n)=0;                            %Activation energy of diffusion of water vapour in
layer 6 of polymer liner (J/mol)
end

%Layer 7
if Nlnr>=7;
    n=7;
    Xlnr(n)=0;                             %Thickness of layer 7 of polymer liner (m)
    Sreflnr(n)=0;                          %Reference solubility of water vapour in layer 7
of polymer liner (mol/m^3/Pa)
    TrefSlnr(n)=273.15+0;                  %Temperature of reference solubility of water
vapour in layer 7 of polymer liner (K)
    dHSlnr(n)=0;                           %Partial molar enthalpy of sorption of water
vapour in layer 7 of polymer liner (J/mol)
    Dreflnr(n)=0;                          %Reference diffusivity of water vapour in layer 7
of polymer liner (m^2/s)
    TrefDlnr(n)=273.15+0;                  %Temperature of reference diffusivity of water
vapour in layer 7 of polymer liner (K)
    EDlnr(n)=0;                            %Activation energy of diffusion of water vapour in
layer 7 of polymer liner (J/mol)
end

%Layer 8
if Nlnr>=8;
    n=8;
```

```
    Xlnr(n)=0;                                  %Thickness of layer 8 of polymer liner (m)
    Sreflnr(n)=0;                               %Reference solubility of water vapour in layer 8
of polymer liner (mol/m^3/Pa)
    TrefSlnr(n)=273.15+0;                       %Temperature of reference solubility of water
vapour in layer 8 of polymer liner (K)
    dHSlnr(n)=0;                                %Partial molar enthalpy of sorption of water
vapour in layer 8 of polymer liner (J/mol)
    Dreflnr(n)=0;                               %Reference diffusivity of water vapour in layer 8
of polymer liner (m^2/s)
    TrefDlnr(n)=273.15+0;                       %Temperature of reference diffusivity of water
vapour in layer 8 of polymer liner (K)
    EDlnr(n)=0;                                 %Activation energy of diffusion of water vapour in
layer 8 of polymer liner (J/mol)
end

%Layer 9
if Nlnr>=9;
    n=9;
    Xlnr(n)=0;                                  %Thickness of layer 9 of polymer liner (m)
    Sreflnr(n)=0;                               %Reference solubility of water vapour in layer 9
of polymer liner (mol/m^3/Pa)
    TrefSlnr(n)=273.15+0;                       %Temperature of reference solubility of water
vapour in layer 9 of polymer liner (K)
    dHSlnr(n)=0;                                %Partial molar enthalpy of sorption of water
vapour in layer 9 of polymer liner (J/mol)
    Dreflnr(n)=0;                               %Reference diffusivity of water vapour in layer 9
of polymer liner (m^2/s)
    TrefDlnr(n)=273.15+0;                       %Temperature of reference diffusivity of water
vapour in layer 9 of polymer liner (K)
    EDlnr(n)=0;                                 %Activation energy of diffusion of water vapour in
layer 9 of polymer liner (J/mol)
end

XTlnr=sum(Xlnr);                                %Total thickness of polymer liner (m)


%Model Node SIs
J=10;                                           %Number of nodes (-)
dxbag=Xbag/J;                                   %Node width of layer n of paperboard bag (m)
dxlnr=Xlnr/J;                                   %Node width of layer n of polymer liner (m)
dxf=Xf/J;                                       %Node width of food product (m)


%Initial Conditions
Mi=0.03;                                        %Initial moisture content of food product (kg
water/kg solids)
RHi=90;                                         %Initial ambient relative humidity (%)
Ti=273.15+38;                                   %Initial ambient tempearture (*C)

p0i=exp(23.4795-3990.56/(Ti-273.15+233.833));
pai=RHi/100*p0i;

pbagi=zeros(1,Nbag*J-1)+RHi/100*p0i;            %Initial water vapour pressure in paperboard bag
(Pa)
pbhi=RHi/100*p0i;                               %Initial water vapour pressure in bag headspace
(Pa)
plnri=zeros(1,Nlnr*J-1)+RHi/100*p0i;            %Initial water vapour pressure in polymer liner
(Pa)

if lower(isotherm)=='gab'
    pfi=zeros(1,J)+p0i*(-(kGAB*(CGAB-CGAB*M0GAB/Mi-2))-sqrt((kGAB*(CGAB-CGAB*M0GAB/Mi-2))^2-
4*kGAB^2*(1-CGAB)))/(2*kGAB^2*(1-CGAB));
elseif lower(isotherm)=='bet'
    pfi=zeros(1,J)+p0i*(-(CBET-CBET*M1BET/Mi-2)-sqrt((CBET-CBET*M1BET/Mi-2)^2-4*(1-
CBET)))/(2*(1-CBET));
elseif lower(isotherm)=='lin'
    pfi=zeros(1,J)+p0i*(Mi-clin)/blin;
end
plhi=pfi(1);                                    %Initial water vapour pressure in liner headspace
(Pa)

ICs=[pai pbagi pbhi pbhi plnri plhi plhi pfi pbhi plhi];

stime=365;                                      %Simulation time (days)


%Solver
```

```
options=odeset('RelTol', 1e-3);
[t,D]=ode23s('PackageExtended2Fun',[0:24*60^2:stime*24*60^2],ICs,options);


%Plots
%Plot of water vapour pressure in paperboard bag
x1(1)=0;
for n=1:Nbag
    for i=(n-1)*J+2:n*J+1
        x1(i,1)=dxbag(n)+x1(i-1);
    end
end
pbagend=[pa D(end,2:Nbag*J) D(end,Nbag*J+Nlnr*J+J+4)]';

figure
subplot(2,1,1);
hold on
plot(x1*1e6,pbagend,'b-');
title(['Water Vapour Pressure in the Paperboard Bag After ',num2str(stime),' Days']);
xlabel('x (µm)');
ylabel('pbag (Pa)');

%Plot of water vapour pressure in polymer liner
x2(1)=0;
for n=1:Nlnr
    for i=(n-1)*J+2:n*J+1
        x2(i,1)=dxlnr(n)+x2(i-1);
    end
end
plnrend=[D(end,Nbag*J+Nlnr*J+J+4) D(end,Nbag*J+3:Nbag*J+Nlnr*J+1) D(end,Nbag*J+Nlnr*J+J+5)]';

subplot(2,1,2);
plot(x2*1e6,plnrend,'b-');
title(['Water Vapour Pressure in Polymer Liner After ',num2str(stime),' Days']);
xlabel('x (µm)');
ylabel('plnr (Pa)');

%Plot of water vapour pressure in food powder
x3(1)=0;
for i=2:J+1
    x3(i,1)=dxf+x3(i-1);
end
pfend=[D(end,Nbag*J+Nlnr*J+J+5) D(end,Nbag*J+Nlnr*J+4:Nbag*J+Nlnr*J+J+3)]';

figure
subplot(1,1,1);
plot(x3,pfend,'b-');
title(['Water Vapour Pressure in the Food Powder After ',num2str(stime),' Days']);
xlabel('x (m)');
ylabel('pf (Pa)');

%Plot of water vapour pressure in bag headspace
pbh=D(:,Nbag*J+Nlnr*J+J+4);

figure
subplot(2,1,1);
plot(t/(24*60^2),pbh,'b-');
title('Water Vapour Pressure in the Bag Headspace');
xlabel('t (days)');
ylabel('pbh (Pa)');

%Plot of water vapour pressure in liner headspace
plh=D(:,Nbag*J+Nlnr*J+J+5);

subplot(2,1,2);
plot(t/(24*60^2),plh,'b-');
title('Water Vapour Pressure in the Liner Headspace');
xlabel('t (days)');
ylabel('plh (Pa)');

%Plot of average water vapour pressure in food powder vs time
for i=1:size(D,1)

pfave(i,1)=(D(i,Nbag*J+Nlnr*J+J+5)/2+sum(D(i,Nbag*J+Nlnr*J+4:Nbag*J+Nlnr*J+J+2))+D(i,Nbag*J+Nl
nr*J+J+3)/2)/J;
```

```
    Mave(i,1)=M0GAB*kGAB*CGAB*pfave(i)/p0i/(1-kGAB*pfave(i)/p0i)/(1-
kGAB*pfave(i)/p0i+CGAB*kGAB*pfave(i)/p0i); %Only valid for GAB isotherm and constant
temperature
end

figure
subplot(1,1,1);
plot(t/(24*60^2),pfave,'b-');
title('Average Water Vapour Pressure in the Food Powder');
xlabel('t (days)');
ylabel('pf (Pa)');


%Output data to Excel spreadsheet
outputtitle={'x (m)','pbag (Pa)'};
outputdata=[x1 pbagend];
xlswrite('FoodPackageOutput.xls',outputtitle,'pbag');
xlswrite('FoodPackageOutput.xls',outputdata,'pbag','A2');

outputtitle={'x (m)','plnr (Pa)','M (kg water/kg solids)'};
outputdata=[x2 plnrend];
xlswrite('FoodPackageOutput.xls',outputtitle,'plnr');
xlswrite('FoodPackageOutput.xls',outputdata,'plnr','A2');

outputtitle={'x (m)','pf (Pa)'};
outputdata=[x3 pfend];
xlswrite('FoodPackageOutput.xls',outputtitle,'pf');
xlswrite('FoodPackageOutput.xls',outputdata,'pf','A2');

outputtitle={'t (s)','pbh (Pa)'};
outputdata=[t pbh];
xlswrite('FoodPackageOutput.xls',outputtitle,'pbh');
xlswrite('FoodPackageOutput.xls',outputdata,'pbh','A2');

outputtitle={'t (s)','plh (Pa)'};
outputdata=[t plh];
xlswrite('FoodPackageOutput.xls',outputtitle,'pbh');
xlswrite('FoodPackageOutput.xls',outputdata,'pbh','A2');

outputtitle={'t (s)','pfave (Pa)','Mave (kg water/kg solids)'};
outputdata=[t pfave Mave];
xlswrite('FoodPackageOutput.xls',outputtitle,'pfave');
xlswrite('FoodPackageOutput.xls',outputdata,'pfave','A2');
```

D.2.2.2.2 Model Function File (PackageExtended2Fun.m)

```
%Model Function File

function dD=PackageWaterTransferFun(t,D)

global MrH2O ms R J;
global kGAB CGAB M0GAB CBET M1BET blin clin;
global Abag Aprfbag XTbag Nbag dxbag dprfbag Drefbag TrefDbag EDbag Srefbag TrefSbag dHSbag;
global Alnr Aprflnr XTlnr Nlnr dxlnr dprflnr Dreflnr TrefDlnr EDlnr Sreflnr TrefSlnr dHSlnr;
global E rhos dxf Af;
global isotherm pa;


pbh=D(Nbag*J+Nlnr*J+J+4);
plh=D(Nbag*J+Nlnr*J+J+5);


%General CVs
T=273.15+38;                                        %Ambient temperature (K)
RHa=90;                                             %Relative humidity of ambient air (%RH)
p0=exp(23.4795-3990.56/(T-273.15+233.833));         %Saturated vapour pressure of pure water
at T (Pa)
pa=RHa*p0/100;                                      %Partial pressure of water vapour in
ambient air (Pa)
Dair=1.7255e-7*T-2.552e-5;                          %Diffusivity of water vapour in air
(m^2/s)
```

```
Sair=1/R/T;                                          %Solubility of water vapour in air
(mol/m^3/Pa)
Deff=0.7*E*Dair;                                     %Diffusivity of water vapour in vapour
phase of food product (m^2/s)


pbag(1)=pa;                                          %pbag(1:Nbag*J+1)=D(1:Nbag*J+1)
pbag(2:Nbag*J)=D(2:Nbag*J);
pbag(Nbag*J+1)=pbh;
plnr(1)=pbh;
%plnr(1:Nlnr*J+1)=D(Nbag*J+1+1:Nbag*J+1+Nlnr*J+1)
plnr(2:Nlnr*J)=D(Nbag*J+3:Nbag*J+Nlnr*J+1);
plnr(Nlnr*J+1)=plh;
pf(1)=plh;
%pf(1:J+1)=D(Nbag*J+1+Nlnr*J+1+1:Nbag*J+1+Nlnr*J+1+J+1)
pf(2:J+1)=D(Nbag*J+Nlnr*J+4:Nbag*J+Nlnr*J+J+3);

dD=zeros(1,Nbag*J+Nlnr*J+J+5);


%Perforation Equations
%Perforation(s) in paperboard bag
if dprfbag<(1e-7)
    Jprfbag=48.5*dprfbag/R/T/XTbag*(T/1000/MrH2O)^0.5*(pa-pbh);
elseif dprfbag>=(1e-7) && dprfbag<(1e-5)
    Jprfbag=Dair*Sair*(pa-pbh)/(XTbag+dprfbag/2);    %Only valid if distance between
perforations >> pore radius
elseif dprfbag>=(1e-5)
    Jprfbag=Dair*Sair*(pa-pbh)/XTbag;                %Only valid if no total pressure
difference across packaging
end

%Perforation(s) in polymer liner
if dprflnr<(1e-7)
    Jprflnr=48.5*dprflnr/R/T/XTlnr*(T/1000/MrH2O)^0.5*(pbh-plh);
elseif dprflnr>=(1e-7) && dprflnr<(1e-5)
    Jprflnr=Dair*Sair*(pbh-plh)/(XTlnr+dprflnr/2);   %Only valid if distance between
perforations >> pore radius
elseif dprflnr>=(1e-5)
    Jprflnr=Dair*Sair*(pbh-plh)/XTlnr;               %Only valid if no total pressure
difference across packaging
end


%Finite Difference Approximations
%Paperboard bag
%Case 1
n=1;
j=1;
dpbag(j)=0;
n=Nbag;
j=n*J+1;
dpbag(j)=0;

%Case 2
n=1;
j=2;
Dbag=DbagFun(n,j,pbag,T);
dpbag(j)=Dbag/dxbag(n)^2*(pa-2*pbag(j)+pbag(j+1));

%Case 3
if Nbag==1
    n=1;
    for j=(n-1)*J+3:n*J-1
        Dbag=DbagFun(n,j,pbag,T);
        dpbag(j)=Dbag/dxbag(n)^2*(pbag(j-1)-2*pbag(j)+pbag(j+1));
    end
else
    n=1;
    for j=(n-1)*J+3:n*J
        Dbag=DbagFun(n,j,pbag,T);
        dpbag(j)=Dbag/dxbag(n)^2*(pbag(j-1)-2*pbag(j)+pbag(j+1));
    end
    for n=2:Nbag-1
        for j=(n-1)*J+2:n*J
            Dbag=DbagFun(n,j,pbag,T);
            dpbag(j)=Dbag/dxbag(n)^2*(pbag(j-1)-2*pbag(j)+pbag(j+1));
```

```
        end
    end
    n=Nbag;
    for j=(n-1)*J+2:n*J-1
        Dbag=DbagFun(n,j,pbag,T);
        dpbag(j)=Dbag/dxbag(n)^2*(pbag(j-1)-2*pbag(j)+pbag(j+1));
    end
end

%Case 4
for n=1:Nbag-1
    j=n*J+1;
    Dbag(1)=DbagFun(n,j,pbag,T);
    Sbag(1)=SbagFun(n,j,pbag,T);
    n=n+1;
    Dbag(2)=DbagFun(n,j,pbag,T);
    Sbag(2)=SbagFun(n,j,pbag,T);
    n=n-1;
    dpbag(j)=2/(dxbag(n)*Sbag(1)+dxbag(n+1)*Sbag(2))*(Dbag(1)*Sbag(1)/dxbag(n)*(pbag(j-1)-
pbag(j))-Dbag(2)*Sbag(2)/dxbag(n+1)*(pbag(j)-pbag(j+1)));
end

%Case 5
n=Nbag;
j=n*J;
Dbag=DbagFun(n,j,pbag,T);
dpbag(j)=Dbag/dxbag(n)^2*(pbag(j-1)-2*pbag(j)+pbh);


%Polymer liner
%Case 6
n=1;
j=1;
dplnr(j)=0;
n=Nlnr;
j=n*J+1;
dplnr(j)=0;

%Case 7
n=1;
j=2;
Dlnr=DlnrFun(n,j,plnr,T);
dplnr(j)=Dlnr/dxlnr(n)^2*(pbh-2*plnr(j)+plnr(j+1));

%Case 8
if Nlnr==1
    n=1;
    for j=(n-1)*J+3:n*J-1
        Dlnr=DlnrFun(n,j,plnr,T);
        dplnr(j)=Dlnr/dxlnr(n)^2*(plnr(j-1)-2*plnr(j)+plnr(j+1));
    end
else
    n=1;
    for j=(n-1)*J+3:n*J
        Dlnr=DlnrFun(n,j,plnr,T);
        dplnr(j)=Dlnr/dxlnr(n)^2*(plnr(j-1)-2*plnr(j)+plnr(j+1));
    end
    for n=2:Nlnr-1
        for j=(n-1)*J+2:n*J
            Dlnr=DlnrFun(n,j,plnr,T);
            dplnr(j)=Dlnr/dxlnr(n)^2*(plnr(j-1)-2*plnr(j)+plnr(j+1));
        end
    end
    n=Nlnr;
    for j=(n-1)*J+2:n*J-1
        Dlnr=DlnrFun(n,j,plnr,T);
        dplnr(j)=Dlnr/dxlnr(n)^2*(plnr(j-1)-2*plnr(j)+plnr(j+1));
    end
end

%Case 9
for n=1:Nlnr-1
    j=n*J+1;
    Dlnr(1)=DlnrFun(n,j,plnr,T);
    Slnr(1)=SlnrFun(n,j,plnr,T);
    n=n+1;
    Dlnr(2)=DlnrFun(n,j,plnr,T);
```

```
    Slnr(2)=SlnrFun(n,j,plnr,T);
    n=n-1;
    dplnr(j)=2/(dxlnr(n)*Slnr(1)+dxlnr(n+1)*Slnr(2))*(Dlnr(1)*Slnr(1)/dxlnr(n)*(plnr(j-1)-
plnr(j))-Dlnr(2)*Slnr(2)/dxlnr(n+1)*(plnr(j)-plnr(j+1)));
end

%Case 10
n=Nlnr;
j=n*J;
Dlnr=DlnrFun(n,j,plnr,T);
dplnr(j)=Dlnr(1)/dxlnr(n)^2*(plnr(j-1)-2*plnr(j)+plh);


%Food powder
%Case 11
j=1;
dpf(j)=0;

%Case 12
j=2;
Sf=IsothermFun(j,pf,p0);
dpf(j)=1/dxf^2/(E*Sair+(1-E)*Sf)*Deff*Sair*(plh-2*pf(j)+pf(j+1));

%Case 13
for j=3:J
    Sf=IsothermFun(j,pf,p0);
    dpf(j)=1/dxf^2/(E*Sair+(1-E)*Sf)*Deff*Sair*(pf(j-1)-2*pf(j)+pf(j+1));
end

%Case 14
j=J+1;
Sf=IsothermFun(j,pf,p0);
dpf(j)=2/dxf^2/(E*Sair+(1-E)*Sf)*Deff*Sair*(pf(j-1)-pf(j));


%Bag headspace water vapour pressure
n=Nbag;
j=n*J+1;
Dbag=DbagFun(n,j,pbag,T);
Sbag=SbagFun(n,j,pbag,T);
n=1;
j=1;
Dlnr=DlnrFun(n,j,plnr,T);
Slnr=SlnrFun(n,j,plnr,T);
n1=Nbag;
j1=n1*J;
n2=1;
j2=2;
dpbh=2/(Abag*dxbag(n1)*Sbag+Alnr*dxlnr(n2)*Slnr)*(Dbag*Sbag*Abag/dxbag(n1)*(pbag(j1)-pbh)-
Dlnr*Slnr*Alnr/dxlnr(n2)*(pbh-plnr(j2))+Jprfbag*Aprfbag-Jprflnr*Aprflnr);


%Liner headspace water vapour pressure
n=Nlnr;
j=n*J+1;
Dlnr=DlnrFun(n,j,plnr,T);
Slnr=SlnrFun(n,j,plnr,T);
j=1;
Sf=IsothermFun(j,pf,p0);
j1=n*J;
j2=2;
dplh=2/(Alnr*dxlnr(n)*Slnr+Af*dxf*(E*Sair+(1-E)*Sf))*(Dlnr*Slnr*Alnr/dxlnr(n)*(plnr(j1)-
plh)+Jprflnr*Aprflnr-Deff*Sair*Af/dxf*(plh-pf(j2)));


dD=[dpbag dplnr dpf dpbh dplh]';
```

D.2.2.2.3 Diffusivity of Water Vapour in Paperboard Bag Function File (DbagFun.m)

```
%Diffusivity of Water Vapour in Paperboard Bag Function File

function Dbag=DbagFun(n,j,pbag,T)

global MrH2O ms R J;
global kGAB CGAB M0GAB CBET M1BET blin clin;
global Abag Aprfbag XTbag Nbag dxbag dprfbag Drefbag TrefDbag EDbag Srefbag TrefSbag dHSbag;
global Alnr Aprflnr XTlnr Nlnr dxlnr dprflnr Dreflnr TrefDlnr EDlnr Sreflnr TrefSlnr dHSlnr;
global E rhos dxf Af;
global isotherm pa pbh plh;


switch n
    case 1
        Dbag=Drefbag(n)*exp(EDbag(n)/R*(1/TrefDbag(n)-1/T));
    case 2
        Dbag=Drefbag(n)*exp(EDbag(n)/R*(1/TrefDbag(n)-1/T));
    case 3
        Dbag=Drefbag(n)*exp(EDbag(n)/R*(1/TrefDbag(n)-1/T));
end
```

D.2.2.2.4 Diffusivity of Water Vapour in Polymer Liner Function File (DlnrFun.m)

```
%Diffusivity of Water Vapour in Polymer Liner Function File

function Dlnr=DlnrFun(n,j,plnr,T)

global MrH2O ms R J;
global kGAB CGAB M0GAB CBET M1BET blin clin;
global Abag Aprfbag XTbag Nbag dxbag dprfbag Drefbag TrefDbag EDbag Srefbag TrefSbag dHSbag;
global Alnr Aprflnr XTlnr Nlnr dxlnr dprflnr Dreflnr TrefDlnr EDlnr Sreflnr TrefSlnr dHSlnr;
global E rhos dxf Af;
global isotherm pa pbh plh;


switch n
    case 1
        Dlnr=Dreflnr(n)*exp(EDlnr(n)/R*(1/TrefDlnr(n)-1/T));
    case 2
        Dlnr=Dreflnr(n)*exp(EDlnr(n)/R*(1/TrefDlnr(n)-1/T));
    case 3
        Dlnr=Dreflnr(n)*exp(EDlnr(n)/R*(1/TrefDlnr(n)-1/T));
    case 4
        Dlnr=Dreflnr(n)*exp(EDlnr(n)/R*(1/TrefDlnr(n)-1/T));
    case 5
        Dlnr=Dreflnr(n)*exp(EDlnr(n)/R*(1/TrefDlnr(n)-1/T));
    case 6
        Dlnr=Dreflnr(n)*exp(EDlnr(n)/R*(1/TrefDlnr(n)-1/T));
    case 7
        Dlnr=Dreflnr(n)*exp(EDlnr(n)/R*(1/TrefDlnr(n)-1/T));
    case 8
        Dlnr=Dreflnr(n)*exp(EDlnr(n)/R*(1/TrefDlnr(n)-1/T));
    case 9
        Dlnr=Dreflnr(n)*exp(EDlnr(n)/R*(1/TrefDlnr(n)-1/T));
end
```

D.2.2.2.5 Solubility of Water Vapour in Paperboard Bag Function File (SbagFun.m)

```
%Solubility of Water Vapour in Paperboard Bag Function File

function Sbag=SbagFun(n,j,pbag,T)

global MrH2O ms R J;
global kGAB CGAB M0GAB CBET M1BET blin clin;
global Abag Aprfbag XTbag Nbag dxbag dprfbag Drefbag TrefDbag EDbag Srefbag TrefSbag dHSbag;
global Alnr Aprflnr XTlnr Nlnr dxlnr dprflnr Dreflnr TrefDlnr EDlnr Sreflnr TrefSlnr dHSlnr;
global E rhos dxf Af;
global isotherm pa pbh plh;


switch n
    case 1
        Sbag=Srefbag(n)*exp(dHSbag(n)/R*(1/TrefSbag(n)-1/T));
    case 2
        Sbag=Srefbag(n)*exp(dHSbag(n)/R*(1/TrefSbag(n)-1/T));
    case 3
        Sbag=Srefbag(n)*exp(dHSbag(n)/R*(1/TrefSbag(n)-1/T));
end
```

D.2.2.2.6 Solubility of Water Vapour in Polymer Liner Function File (SlnrFun.m)

```
%Solubility of Water Vapour in Polymer Liner Function File

function Slnr=SlnrFun(n,j,plnr,T)

global MrH2O ms R J;
global kGAB CGAB M0GAB CBET M1BET blin clin;
global Abag Aprfbag XTbag Nbag dxbag dprfbag Drefbag TrefDbag EDbag Srefbag TrefSbag dHSbag;
global Alnr Aprflnr XTlnr Nlnr dxlnr dprflnr Dreflnr TrefDlnr EDlnr Sreflnr TrefSlnr dHSlnr;
global E rhos dxf Af;
global isotherm pa pbh plh;


switch n
    case 1
        Slnr=Sreflnr(n)*exp(dHSlnr(n)/R*(1/TrefSlnr(n)-1/T));
    case 2
        Slnr=Sreflnr(n)*exp(dHSlnr(n)/R*(1/TrefSlnr(n)-1/T));
    case 3
        Slnr=Sreflnr(n)*exp(dHSlnr(n)/R*(1/TrefSlnr(n)-1/T));
    case 4
        Slnr=Sreflnr(n)*exp(dHSlnr(n)/R*(1/TrefSlnr(n)-1/T));
    case 5
        Slnr=Sreflnr(n)*exp(dHSlnr(n)/R*(1/TrefSlnr(n)-1/T));
    case 6
        Slnr=Sreflnr(n)*exp(dHSlnr(n)/R*(1/TrefSlnr(n)-1/T));
    case 7
        Slnr=Sreflnr(n)*exp(dHSlnr(n)/R*(1/TrefSlnr(n)-1/T));
    case 8
        Slnr=Sreflnr(n)*exp(dHSlnr(n)/R*(1/TrefSlnr(n)-1/T));
    case 9
        Slnr=Sreflnr(n)*exp(dHSlnr(n)/R*(1/TrefSlnr(n)-1/T));
end
```

D.2.2.2.7 Solubility of Water Vapour in Food Powder Function File (IsothermFun)

```
%Food Product Isotherm Function File

function dCsdpf=IsothermFun(j,pf,p0)

global MrH2O ms R J;
global kGAB CGAB M0GAB CBET M1BET blin clin;
global Abag Aprfbag XTbag Nbag dxbag dprfbag Drefbag TrefDbag EDbag Srefbag TrefSbag dHSbag;
global Alnr Aprflnr XTlnr Nlnr dxlnr dprflnr Dreflnr TrefDlnr EDlnr Sreflnr TrefSlnr dHSlnr;
global E rhos dxf Af;
global isotherm pa pbh plh;


if isotherm=='gab'                          %GAB isotherm
    dCsdpf=rhos/MrH2O*(M0GAB*kGAB^2*CGAB*pf(j)/p0^2/(1-kGAB*pf(j)/p0)^2/(1-
kGAB*pf(j)/p0+kGAB*CGAB*pf(j)/p0)+M0GAB*kGAB*CGAB/p0/(1-kGAB*pf(j)/p0)/(1-
kGAB*pf(j)/p0+kGAB*CGAB*pf(j)/p0)-M0GAB*kGAB^2*CGAB*(CGAB-1)*pf(j)/p0^2/(1-kGAB*pf(j)/p0)/(1-
kGAB*pf(j)/p0+kGAB*CGAB*pf(j)/p0)^2);
elseif isotherm=='bet'                      %BET isotherm
    dCsdpf=rhos/MrH2O*(M1BET*CBET/p0/(1-pf(j)/p0)/(1-pf(j)/p0+CBET*pf(j)/p0)-M1BET*CBET*(CBET-
1)*pf(j)/p0^2/(1-pf(j)/p0)/(1-pf(j)/p0+CBET*pf(j)/p0)^2-M1BET*CBET*pf(j)/p0^2/(1-
pf(j)/p0)^2/(1-pf(j)/p0+CBET*pf(j)/p0));
elseif isotherm=='lin'                      %Linear isotherm
    dCsdpf=rhos/MrH2O*blin/p0;
end
```

D.2.3 Error checks

D.2.3.1 Numerical Error Checks

D.2.3.1.1 Time Step

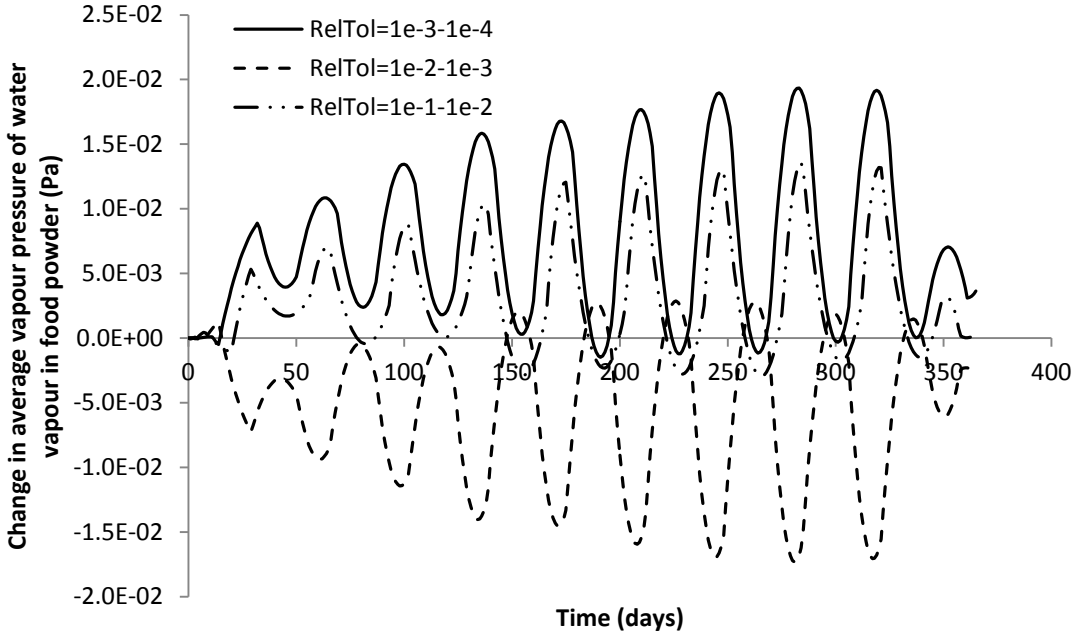

Figure D-7: Plot of change in predicted values of average water vapour pressure in food powder (Pa), with changes to relative error tolerance of MATLAB® solver (RelTol).

As shown in Figure D-7, all changes to relative error tolerance of the MATLAB® solver (RelTol) had relatively insignificant effects on predicted values of average water vapour pressure in the food powder, with no differences greater than 0.019 Pa over the period $0 \leq t \leq 365$ days. Therefore the default RelTol value of 1×10^{-3} should be suitable for use in the model.

D.2.3.1.2 Space Step

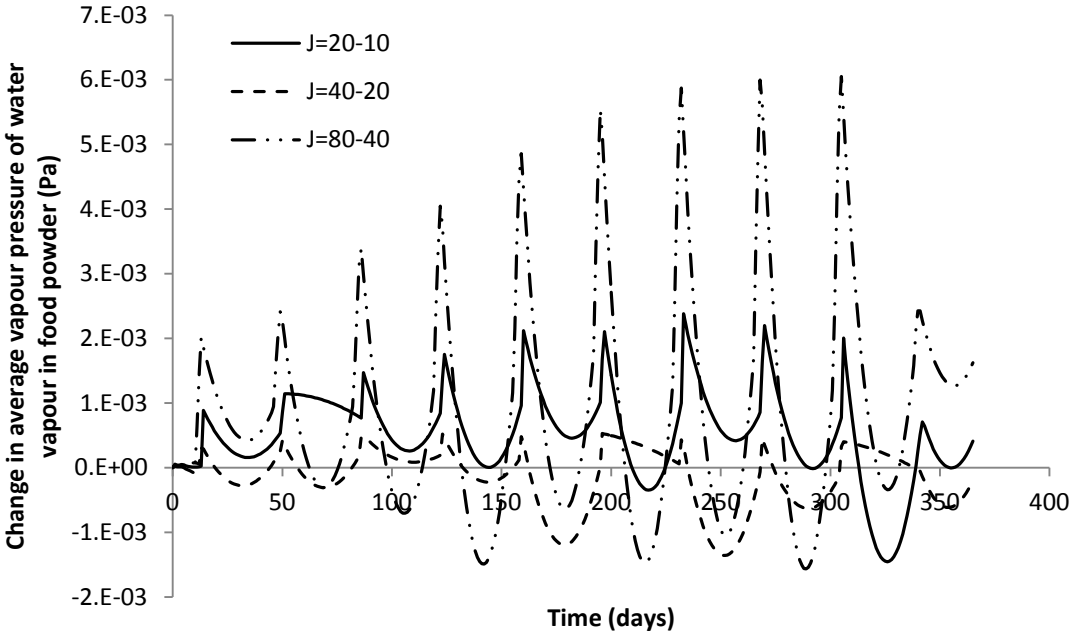

Figure D-8: Plot of change in predicted values of average water vapour pressure in food powder (Pa) with changes to number of nodes per layer of packaging and food powder (J).

As shown in Figure D-8, all changes to the number of nodes per layer of packaging and for the food powder had relatively insignificant effects on the predicted values of average water vapour pressure in the food powder, with no differences greater than 6.1×10^{-3} Pa over the period $0 \leq t \leq 365$ days. Therefore a standard number of 10 nodes per layer of packaging and for the food powder should be suitable for use in the model.

D.2.3.2 Mathematical Error Checks

D.2.3.2.1 Water Vapour Pressure in Paperboard Bag

To allow an analytical solution for the water vapour pressure in the paperboard bag, the following changes were made:

- The properties of all paperboard bag layers were set the same. A two layer system was simulated to ensure all finite difference approximations were correct.

- A linear isotherm with a very high slope was used to ensure the water vapour pressure in the food product remained constant. The linear isotherm constant was adjusted to obtain the desired water vapour pressure.
- A very high diffusivity of water vapour in the food powder was used to ensure the water vapour pressure remained uniform.
- The concentration dependence of the diffusivity and solubility of water vapour in the paperboard bag were disabled.
- Only the water vapour pressure profile after 24 hours was considered.
- The surface area of perforations in the polymer liner was set to a very high value to ensure the water vapour pressure in the bag headspace remained equal to the water vapour pressure in the food product.

Formulated problem:

$$S_{bag}^{H_2O}\frac{\partial p_{bag}^{H_2O}}{\partial t} = D_{bag}^{H_2O}S_{bag}^{H_2O}\frac{\partial^2 p_{bag}^{H_2O}}{\partial x^2}$$

for $t \geq 0,\ 0 < x < X_{T,bag}$

$$p_{bag}^{H_2O} = p_a^{H_2O}$$

for $t \geq 0$, *at* $x = 0$ *and* $x = X_{T,bag}$

$$p_{bag}^{H_2O} = p_{bag,i}^{H_2O}$$

for $t = 0,\ 0 < x < X_{T,bag}$

Analytical solution:

$$R = \frac{X_{T,bag}}{2} = \frac{5 \times 10^{-5}}{2} = 2.5 \times 10^{-5}$$

$$Fo = \frac{D_{bag}^{H_2O}t}{R^2} = \frac{5 \times 10^{-18} \times 365 \times 24 \times 60^2}{(2.5 \times 10^{-5})^2} = 0.2523$$

$$Y = \frac{4}{\pi}\sum_{m=0}^{\infty}\frac{(-1)^m}{2m+1}cos\left[(2m+1)\frac{\pi}{2}\frac{x}{R}\right]exp\left[-(2m+1)^2\frac{\pi^2}{4}Fo\right]$$

m	$\frac{(-1)^m}{2m+1} cos\left[(2m+1)\frac{\pi}{2}\frac{x}{R}\right] exp\left[-(2m+1)^2\frac{\pi^2}{4}Fo\right]$
0	0.5366
1	-1.2296×10^{-3}
2	3.4863×10^{-8}
Total	0.5354

$$Y = \frac{4}{\pi}0.5354 = 0.6817$$

$$p_{bag}^{H_2O} = Y\left(p_{bag,i}^{H_2O} - p_a^{H_2O}\right) + p_a^{H_2O} = 0.6817(585.2 - 1755.7) + 1755.7 = 957.8 \text{ Pa}$$

This procedure was repeated to calculate the water vapour pressure after 24 hours for various positions within the paperboard bag.

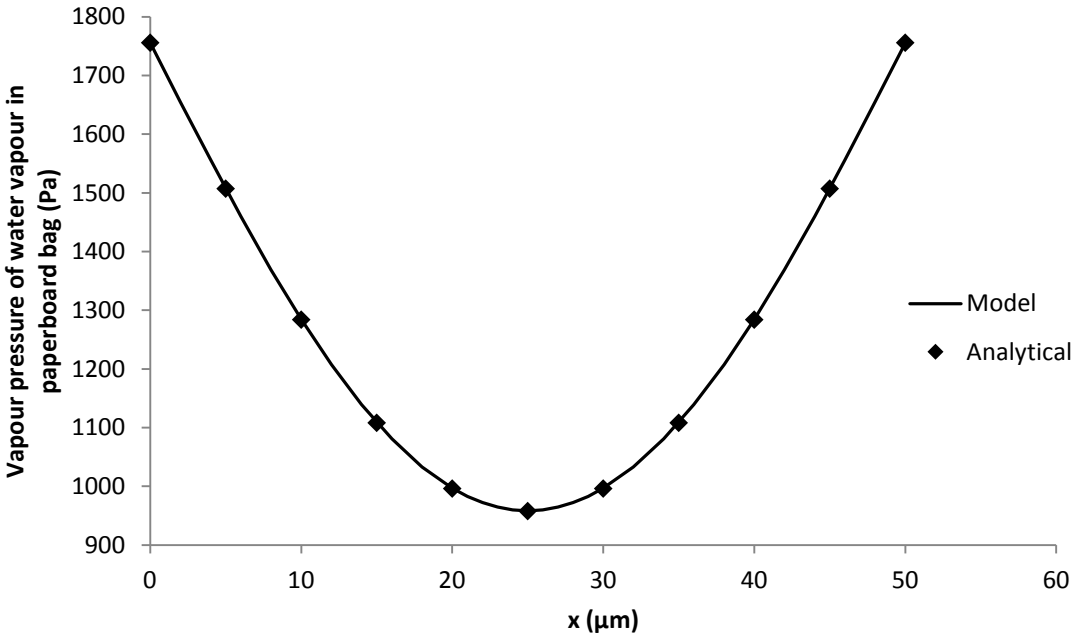

Figure D-9: Comparison of water vapour pressure profile in paperboard bag after 24 hours as predicted analytically and by the model.

As shown in Figure D-3, the values predicted by the model agree relatively closely with those calculated analytically, suggesting the model is correctly calculating the water vapour pressure in the paperboard bag.

D.2.3.2.2 Water Vapour Pressure in Polymer Liner

To allow an analytical solution for the water vapour pressure in the polymer liner, the following changes were made:

- The properties of all polymer liner layers were set the same. A two layer system was simulated to ensure all finite difference approximations were correct.
- A linear isotherm with a very high slope was used to ensure the water vapour pressure in the food product remained constant. The linear isotherm constant was adjusted to obtain the desired water vapour pressure.
- A very high diffusivity of water vapour in the food powder was used to ensure the water vapour pressure remained uniform.
- The concentration dependence of the diffusivity and solubility of water vapour in the polymer liner were disabled.
- Only the water vapour pressure profile after 24 hours was considered.
- The surface area of perforations in the paperboard bag was set to a very high value to ensure the water vapour pressure in the bag headspace remained equal to the water vapour pressure in the ambient air.

Formulated problem:

$$S_{lnr}^{H_2O}\frac{\partial p_{lnr}^{H_2O}}{\partial t} = D_{lnr}^{H_2O}S_{lnr}^{H_2O}\frac{\partial^2 p_{lnr}^{H_2O}}{\partial x^2}$$

for $t \geq 0$, $0 < x < X_{T,lnr}$

$$p_{lnr}^{H_2O} = p_a^{H_2O}$$

for $t \geq 0$, *at* $x = 0$ *and* $x = X_{T,lnr}$

$$p_{lnr}^{H_2O} = p_{lnr,i}^{H_2O}$$

for $t = 0$, $0 < x < X_{T,lnr}$

Analytical solution:

$$R = \frac{X_{T,lnr}}{2} = \frac{5 \times 10^{-5}}{2} = 2.5 \times 10^{-5}$$

$$Fo = \frac{D_{lnr}^{H_2O} t}{R^2} = \frac{1 \times 10^{-17} \times 365 \times 24 \times 60^2}{(2.5 \times 10^{-5})^2} = 0.5046$$

$$Y = \frac{4}{\pi} \sum_{m=0}^{\infty} \frac{(-1)^m}{2m+1} cos\left[(2m+1)\frac{\pi}{2}\frac{x}{R}\right] exp\left[-(2m+1)^2 \frac{\pi^2}{4} Fo\right]$$

m	$\frac{(-\mathbf{1})^{\boldsymbol{m}}}{\mathbf{2m+1}} \boldsymbol{cos}\left[(\mathbf{2m+1})\frac{\boldsymbol{\pi}}{\mathbf{2}}\frac{\boldsymbol{x}}{\boldsymbol{R}}\right] \boldsymbol{exp}\left[-(\mathbf{2m+1})^2 \frac{\boldsymbol{\pi^2}}{\mathbf{4}} \boldsymbol{Fo}\right]$
0	0.5366
1	-1.2296×10^{-3}
2	3.4863×10^{-8}
Total	0.5354

$$Y = \frac{4}{\pi} 0.5354 = 0.6817$$

$$p_{lnr}^{H_2O} = Y\left(p_{lnr,i}^{H_2O} - p_a^{H_2O}\right) + p_a^{H_2O} = 0.6817(585.2 - 1755.7) + 1755.7 = 957.8 \text{ Pa}$$

This procedure was repeated to calculate the water vapour pressure after 24 hours for various positions within the polymer liner.

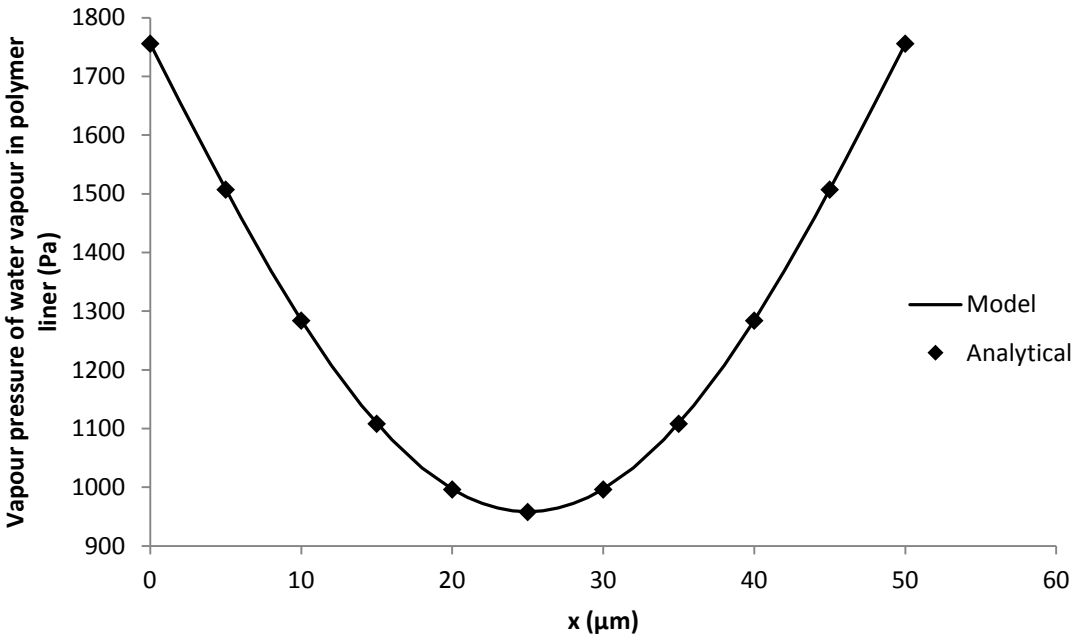

Figure D-10: Comparison of water vapour pressure profile in polymer liner after 24 hours as predicted analytically and by the model.

As shown in Figure D-3, the values predicted by the model agree relatively closely with those calculated analytically, suggesting the model is correctly calculating the water vapour pressure in the packaging.

D.2.3.2.3 Water Vapour Pressure in Food Powder

To allow an analytical solution for the water vapour pressure in the food powder, the following changes were made:

- The porosity of the food powder was set to 1 to disable water sorption in the solid phase.
- Only the water vapour pressure profile after 1 minute was considered.
- The area of perforations in the paperboard bag and polymer liner were set to very high values to ensure the water vapour pressure in the liner headspace remained equal to the water vapour pressure in the ambient air.

Formulated problem:

$$\left(\varepsilon S_{air}^{H_2O} + (1-\varepsilon) S_f^{H_2O}\left(p_f^{H_2O}\right)\right)\frac{\partial p_f^{H_2O}}{\partial t} = D_{eff}^{H_2O} S_{air}^{H_2O}\frac{\partial^2 p_f^{H_2O}}{\partial x^2}$$

for $t \geq 0$, $0 < x < X_f$

$$p_f^{H_2O} = p_a^{H_2O}$$

for $t \geq 0$, *at* $x = 0$

$$\frac{dp_f^{H_2O}}{dx} = 0$$

for $t \geq 0$, *at* $x = X_f$

$$p_f^{H_2O} = p_{f,i}^{H_2O}$$

for $t = 0$, $0 < x < X_f$

Analytical solution:

$$Fo = \frac{D_{eff}^{H_2O} t}{{X_f}^2} = \frac{1.754 \times 10^{-5} \times 60}{0.1^2} = 0.1053$$

$$Y = \frac{4}{\pi}\sum_{m=0}^{\infty}\frac{(-1)^m}{2m+1} cos\left[(2m+1)\frac{\pi}{2}\frac{x}{X_f}\right] exp\left[-(2m+1)^2\frac{\pi^2}{4}Fo\right]$$

m	$\boldsymbol{\frac{(-1)^m}{2m+1} cos\left[(2m+1)\frac{\pi}{2}\frac{x}{X_f}\right] exp\left[-(2m+1)^2\frac{\pi^2}{4}Fo\right]}$
0	0.7713
1	-0.03219
2	3.027×10^{-4}
Total	0.7394

$$Y = \frac{4}{\pi}0.7394 = 0.9414$$

$$p_{lnr}^{H_2O} = Y\left(p_{lnr,i}^{H_2O} - p_a^{H_2O}\right) + p_a^{H_2O} = 0.9414(585.2 - 1755.7) + 1755.7 = 653.8 \text{ Pa}$$

This procedure was repeated to calculate the water vapour pressure after 60 seconds for various positions within the food powder.

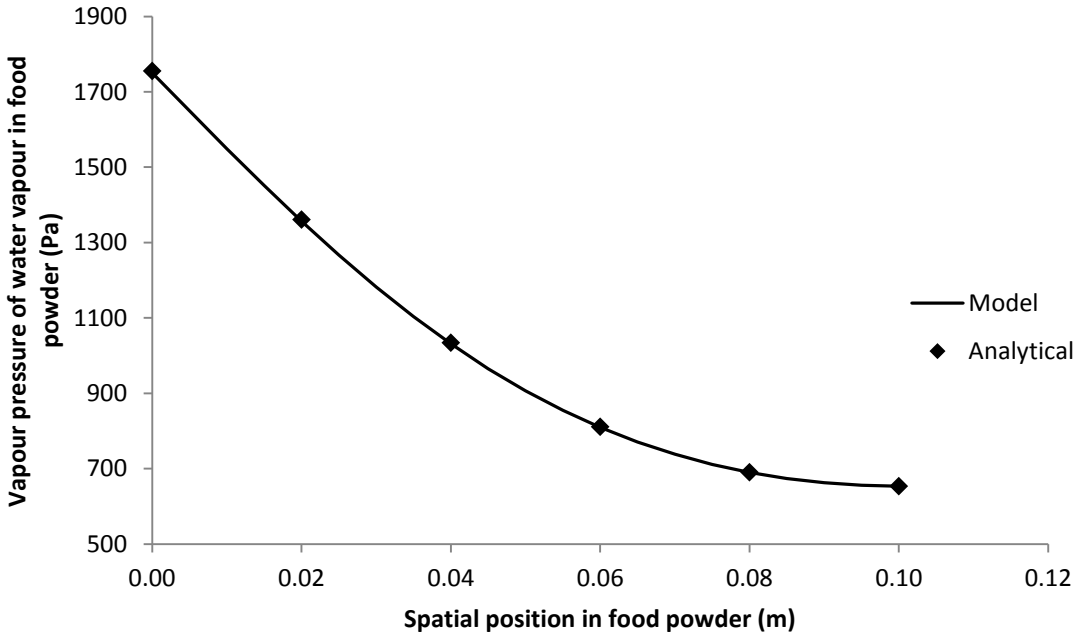

Figure D-11: Comparison of water vapour pressure profile in food powder after 60 seconds as predicted analytically and by the model.

As shown in Figure D-3, the values predicted by the model agree relatively closely with those calculated analytically, suggesting the model is correctly calculating the water vapour pressure in the food powder.

D.2.3.2.4 Water Vapour Pressure in Bag Headspace

Since the mass of water in air in the bag headspace was assumed to be negligible, the bag headspace is essentially a node on the boundary of two packaging layers with additional mositure transfer due to perforations. To verify the permeation component of the bag headspace, the paperboard bag and polymer liner were treated as a single packaging layer, for which an analytical solution is possible. Other changes included the following:

- The area of perforations in the paperboard bag and polymer liner were set to zero.
- The properties of all paperboard bag and polymer liner layers were set the same. A two layer system in both was simulated to further verify all finite difference approximations.
- A linear isotherm with a very high slope was used to ensure the water vapour pressure in the food product remained constant. The linear isotherm constant was adjusted to obtain the desired water vapour pressure.
- The concentration dependence of the diffusivity and solubility of water vapour in the paperboard bag and polymer liner were disabled.

Formulated problem:

$$S_{bag}^{H_2O}\frac{\partial p_{bag}^{H_2O}}{\partial t} = D_{bag}^{H_2O}S_{bag}^{H_2O}\frac{\partial^2 p_{bag}^{H_2O}}{\partial x^2}$$

for $t \geq 0,\ 0 < x < X_{T,bag}$

$$S_{lnr}^{H_2O}\frac{\partial p_{lnr}^{H_2O}}{\partial t} = D_{lnr}^{H_2O}S_{lnr}^{H_2O}\frac{\partial^2 p_{lnr}^{H_2O}}{\partial x^2}$$

for $t \geq 0,\ 0 < x < X_{T,lnr}$

$$p_{bag}^{H_2O} = p_a^{H_2O}$$

for $t \geq 0$, *at* $x = 0$

$$p_{lnr}^{H_2O} = p_a^{H_2O}$$

for $t \geq 0$, *at* $x = X_{T,lnr}$

$$p_{bag}^{H_2O} = p_{lnr}^{H_2O} = p_{bag,i}^{H_2O} = p_{lnr,i}^{H_2O}$$

for $t = 0,\ 0 < x < X_{T,bag}$ *and* $0 < x < X_{T,lnr}$

Analytical solution:

$$R = \frac{X_{T,bag} + X_{T,lnr}}{2} = \frac{2 \times 10^{-5} + 3 \times 10^{-5}}{2} = 2.5 \times 10^{-5}$$

$$Fo = \frac{D_{pkg}^{H_2O} t}{R^2} = \frac{1 \times 10^{-15} \times 24 \times 60^2}{(2.5 \times 10^{-5})^2} = 0.1382$$

$$Y = \frac{4}{\pi}\sum_{m=0}^{\infty}\frac{(-1)^m}{2m+1}cos\left[(2m+1)\frac{\pi}{2}\frac{x}{R}\right]exp\left[-(2m+1)^2\frac{\pi^2}{4}Fo\right]$$

m	$\frac{(-1)^m}{2m+1}cos\left[(2m+1)\frac{\pi}{2}\frac{x}{R}\right]exp\left[-(2m+1)^2\frac{\pi^2}{4}Fo\right]$
0	0.6762
1	-0.009097
2	-6.367×10^{-21}
Total	0.6671

$$Y = \frac{4}{\pi}0.6671 = 0.8494$$

$$p_{bh}^{H_2O} = Y\left(p_{lnr,i}^{H_2O} - p_a^{H_2O}\right) + p_a^{H_2O} = 0.8494(585 - 1756) + 1756 = 761.5 \text{ Pa}$$

This procedure was repeated to calculate the water vapour pressure in the bag headspace at 2 hour intervals up to 24 hours.

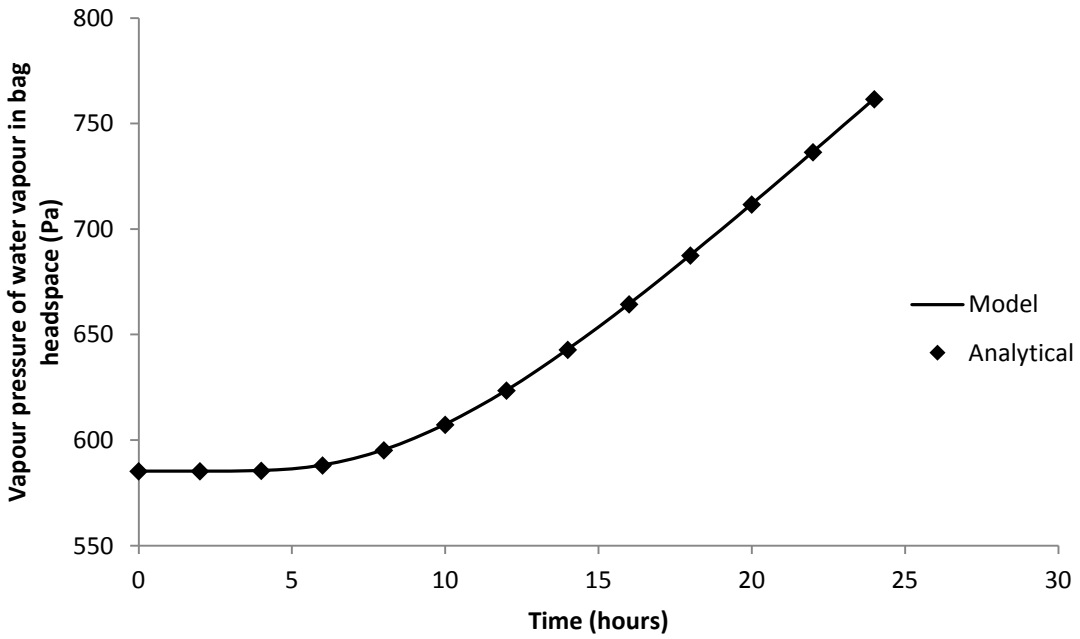

Figure D-12: Comparison of water vapour pressure in bag headspace as predicted analytically and by the model.

As shown in Figure D-12, the values predicted by the model agree very closely with those calculated analytically, suggesting the model is correctly calculating the water vapour pressure in the bag headspace due to permeation.

D.2.3.2.5 Water Vapour Pressure in Liner Headspace

Similar to the bag headspace, since the mass of water in air in the bag headspace was assumed to be negligible, the liner headspace can be treated as a node on the boundary of two packaging layers. To verify the permeation component of the liner headspace, the polymer liner and food powder were treated as a single packaging layer, for which an analytical solution is possible. Other changes included the following:

- The area of perforations in the paperboard bag was set to a very high value to ensure the water vapour pressure in the bag headspace remained equal to the water vapour pressure in the ambient air.
- The area of perforations in the polymer liner was set to zero.
- The properties of the polymer liner and food powder were set the same.
- The concentration dependence of the diffusivity and solubility of water vapour in the polymer liner was disabled.

Formulated problem:

$$S_{lnr}^{H_2O}\frac{\partial p_{lnr}^{H_2O}}{\partial t} = D_{lnr}^{H_2O}S_{lnr}^{H_2O}\frac{\partial^2 p_{lnr}^{H_2O}}{\partial x^2}$$

$$\text{for } t \geq 0,\ 0 < x < X_{T,lnr}$$

$$\left(\varepsilon S_{air}^{H_2O} + (1-\varepsilon)S_f^{H_2O}\left(p_f^{H_2O}\right)\right)\frac{\partial p_f^{H_2O}}{\partial t} = D_{eff}^{H_2O}S_{air}^{H_2O}\frac{\partial^2 p_f^{H_2O}}{\partial x^2}$$

$$\text{for } t \geq 0,\ 0 < x < X_f$$

$$p_{lnr}^{H_2O} = p_a^{H_2O}$$

$$\text{for } t \geq 0, \text{ at } x = 0$$

$$\frac{dp_f^{H_2O}}{dx} = 0$$

for $t \geq 0$, *at* $x = X_f$

$$p_{lnr}^{H_2O} = p_{bag}^{H_2O} = p_{lnr,i}^{H_2O} = p_{f,i}^{H_2O}$$

for $t = 0$, $0 < x < X_{T,lnr}$ *and* $0 < x < X_f$

Analytical solution:

$$R = X_{T,lnr} + X_f = 0.04 + 0.06 = 0.1$$

$$Fo = \frac{D_{eff}^{H_2O} t}{R^2} = \frac{1.745 \times 10^{-5} \times 60}{0.1^2} = 0.1053$$

$$Y = \frac{4}{\pi} \sum_{m=0}^{\infty} \frac{(-1)^m}{2m+1} cos\left[(2m+1)\frac{\pi}{2}\frac{x}{R}\right] exp\left[-(2m+1)^2 \frac{\pi^2}{4} Fo\right]$$

m	$\boldsymbol{\frac{(-1)^m}{2m+1} cos\left[(2m+1)\frac{\pi}{2}\frac{x}{R}\right] exp\left[-(2m+1)^2 \frac{\pi^2}{4} Fo\right]}$
0	0.4533
1	0.03061
2	-5.563×10^{-20}
Total	0.4839

$$Y = \frac{4}{\pi} 0.4839 = 0.6162$$

$$p_{bh}^{H_2O} = Y\left(p_{lnr,i}^{H_2O} - p_a^{H_2O}\right) + p_a^{H_2O} = 0.6162(585 - 1756) + 1756 = 1034 \text{ Pa}$$

This procedure was repeated to calculate the water vapour pressure in the liner headspace at 5 second intervals up to 60 seconds.

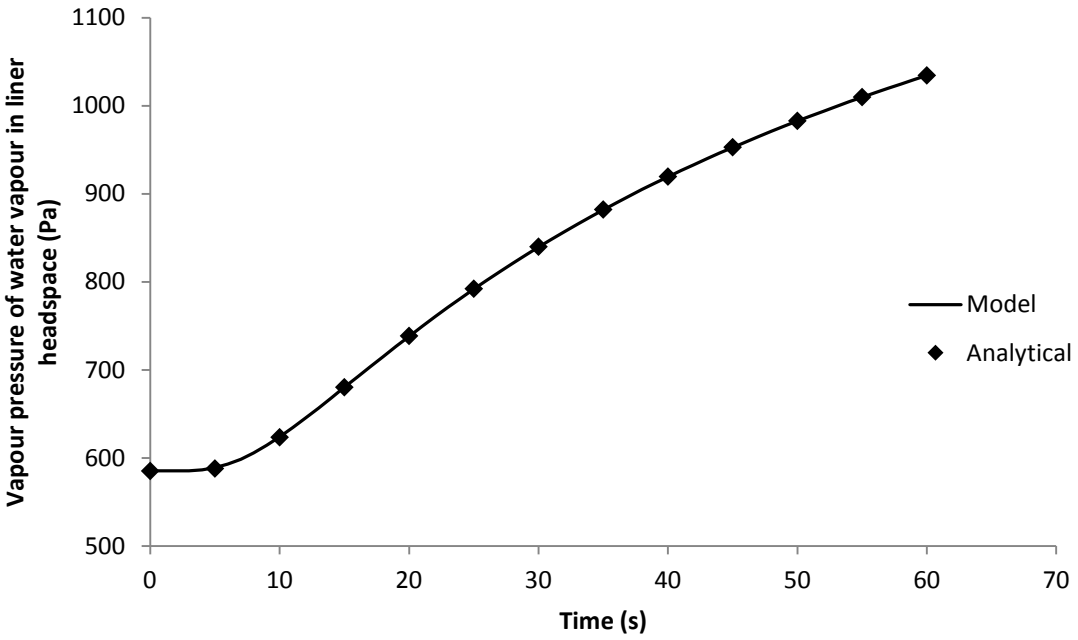

Figure D-13: Comparison of water vapour pressure in liner headspace as predicted analytically and by the model.

As shown in Figure D-13, the values predicted by the model agree very closely with those calculated analytically, suggesting the model is correctly calculating the water vapour pressure in the linear headspace due to permeation. Since the perforation component of the liner headspace only consists of an inward water vapour flux, these were not verified separately.

Appendix E

TWO-DIMENSIONAL PERFORATION MOISTURE TRANSFER MODELS

E.1 NO ISOLATED AIR POCKET AROUND PERFORATION

E.1.1 Mathematical Model Formulation

E.1.1.1 Word Balances and Equations

E.1.1.1.1 ODE for Water Vapour Pressure in Food Powder

$$\frac{\partial}{\partial t}(\varepsilon S_v(p_v)p_v + (1-\varepsilon)C_s) = \frac{\partial}{\partial x}\left(D_v(p_v)S_v(p_v)\frac{\partial p_v}{\partial x}\right) + \frac{\partial}{\partial r}\left(D_v(p_v)S_v(p_v)\frac{\partial p_v}{\partial r}\right) + \frac{D_v(p_v)S_v(p_v)}{r}\frac{\partial p_v}{\partial r}$$

$$\varepsilon S_v(p_v)\frac{\partial p_v}{\partial t} + (1-\varepsilon)\frac{\partial C_s}{\partial t} = \frac{\partial}{\partial x}\left(D_v(p_v)S_v(p_v)\frac{\partial p_v}{\partial x}\right) + \frac{\partial}{\partial r}\left(D_v(p_v)S_v(p_v)\frac{\partial p_v}{\partial r}\right) + \frac{D_v(p_v)S_v(p_v)}{r}\frac{\partial p_v}{\partial r}$$

$$\varepsilon S_v(p_v)\frac{\partial p_v}{\partial t} + (1-\varepsilon)\frac{\partial C_s}{\partial p_v}\frac{\partial p_v}{\partial t} = \frac{\partial}{\partial x}\left(D_v(p_v)S_v(p_v)\frac{\partial p_v}{\partial x}\right) + \frac{\partial}{\partial r}\left(D_v(p_v)S_v(p_v)\frac{\partial p_v}{\partial r}\right) + \frac{D_v(p_v)S_v(p_v)}{r}\frac{\partial p_v}{\partial r}$$

$$\frac{\partial C_s}{\partial p_v} = S_s(p_v)$$

$$\left(\varepsilon S_v(p_v) + (1-\varepsilon)S_s(p_v)\right)\frac{\partial p_v}{\partial t} = \frac{\partial}{\partial x}\left(D_v(p_v)S_v(p_v)\frac{\partial p_v}{\partial x}\right) + \frac{\partial}{\partial r}\left(D_v(p_v)S_v(p_v)\frac{\partial p_v}{\partial r}\right) + \frac{D_v(p_v)S_v(p_v)}{r}\frac{\partial p_v}{\partial r}$$

$$\left(\varepsilon S_{air}^{H_2O} + (1-\varepsilon)S_f^{H_2O}\left(p_f^{H_2O}\right)\right)\frac{\partial p_f^{H_2O}}{\partial t} = \frac{\partial}{\partial x}\left(D_{eff}^{H_2O}S_{air}^{H_2O}\frac{\partial p_f^{H_2O}}{\partial x}\right) + \frac{\partial}{\partial r}\left(D_{eff}^{H_2O}S_{air}^{H_2O}\frac{\partial p_f^{H_2O}}{\partial r}\right) + \frac{D_{eff}^{H_2O}S_{air}^{H_2O}}{r}\frac{\partial p_f^{H_2O}}{\partial r}$$

E.1.2 Solution

E.1.2.1 Finite Difference Approximations

$$r_k = (k-1)\Delta r$$

$$r_{k-\frac{1}{2}} = \left(k-\frac{3}{2}\right)\Delta r$$

$$r_{k+\frac{1}{2}} = \left(k-\frac{1}{2}\right)\Delta r$$

E.1.2.1.1 Case 1

$$V_f = \pi\left[\left(\left(k-\frac{1}{2}\right)\Delta r\right)^2 - \left(\left(k-\frac{3}{2}\right)\Delta r\right)^2\right]\Delta x = 2\pi(k-1)\Delta r^2\Delta x$$

$$A_{f,x} = \pi\left[\left(\left(k-\frac{1}{2}\right)\Delta r\right)^2 - \left(\left(k-\frac{3}{2}\right)\Delta r\right)^2\right] = 2\pi(k-1)\Delta r^2$$

$$\left(A_{f,r}\right)_{k-\frac{1}{2}} = 2\pi\left(k-\frac{3}{2}\right)\Delta r\Delta x$$

$$\left(A_{f,r}\right)_{k+\frac{1}{2}} = 2\pi\left(k-\frac{1}{2}\right)\Delta r\Delta x$$

$$V_f\left[\varepsilon S_{air}^{H_2O} + (1-\varepsilon)S_f^{H_2O}\right]\frac{dp_{f,j,k}^{H_2O}}{dt}$$
$$= D_{eff}^{H_2O} S_{air}^{H_2O} A_{f,x}\frac{\left(p_{f,j-1,k}^{H_2O} - p_{f,j,k}^{H_2O}\right)}{\Delta x} - D_{eff}^{H_2O} S_{air}^{H_2O} A_{f,x}\frac{\left(p_{f,j,k}^{H_2O} - p_{f,j+1,k}^{H_2O}\right)}{\Delta x}$$
$$+ D_{eff}^{H_2O} S_{air}^{H_2O}\left(A_{f,r}\right)_{k-\frac{1}{2}}\frac{\left(p_{f,j,k-1}^{H_2O} - p_{f,j,k}^{H_2O}\right)}{\Delta r}$$
$$- D_{eff}^{H_2O} S_{air}^{H_2O}\left(A_{f,r}\right)_{k+\frac{1}{2}}\frac{\left(p_{f,j,k}^{H_2O} - p_{f,j,k+1}^{H_2O}\right)}{\Delta r}$$

$$\frac{dp_{f,j,k}^{H_2O}}{dt} = \frac{D_{eff}^{H_2O} S_{air}^{H_2O}}{V_f\left[\varepsilon S_{air}^{H_2O} + (1-\varepsilon)S_f^{H_2O}\right]}\left[A_{f,x}\frac{\left(p_{f,j-1,k}^{H_2O} - p_{f,j,k}^{H_2O}\right)}{\Delta x} - A_{f,x}\frac{\left(p_{f,j,k}^{H_2O} - p_{f,j+1,k}^{H_2O}\right)}{\Delta x}\right.$$
$$\left. + \left(A_{f,r}\right)_{k-\frac{1}{2}}\frac{\left(p_{f,j,k-1}^{H_2O} - p_{f,j,k}^{H_2O}\right)}{\Delta r} - \left(A_{f,r}\right)_{k+\frac{1}{2}}\frac{\left(p_{f,j,k}^{H_2O} - p_{f,j,k+1}^{H_2O}\right)}{\Delta r}\right]$$

E.1.2.1.2 Case 2

$$V_f = \frac{\pi}{4}\Delta r^2 \Delta x$$

$$A_{f,x} = \frac{\pi}{4}\Delta r^2$$

$$\left(A_{f,r}\right)_{k+\frac{1}{2}} = 2\pi\left(k-\frac{1}{2}\right)\Delta r\Delta x = \pi\Delta r\Delta x$$

$$V_f\left[\varepsilon S_{air}^{H_2O} + (1-\varepsilon)S_f^{H_2O}\right]\frac{dp_{f,j,k}^{H_2O}}{dt}$$
$$= D_{eff}^{H_2O} S_{air}^{H_2O} A_{f,x}\frac{\left(p_{f,j-1,k}^{H_2O} - p_{f,j,k}^{H_2O}\right)}{\Delta x} - D_{eff}^{H_2O} S_{air}^{H_2O} A_{f,x}\frac{\left(p_{f,j,k}^{H_2O} - p_{f,j+1,k}^{H_2O}\right)}{\Delta x}$$
$$- D_{eff}^{H_2O} S_{air}^{H_2O}\left(A_{f,r}\right)_{k+\frac{1}{2}}\frac{\left(p_{f,j,k}^{H_2O} - p_{f,j,k+1}^{H_2O}\right)}{\Delta r}$$

$$\frac{dp_{f,j,k}^{H_2O}}{dt} = \frac{D_{eff}^{H_2O} S_{air}^{H_2O}}{V_f\left[\varepsilon S_{air}^{H_2O} + (1-\varepsilon)S_f^{H_2O}\right]}\left[A_{f,x}\frac{\left(p_{f,j-1,k}^{H_2O} - p_{f,j,k}^{H_2O}\right)}{\Delta x} - A_{f,x}\frac{\left(p_{f,j,k}^{H_2O} - p_{f,j+1,k}^{H_2O}\right)}{\Delta x}\right.$$
$$\left. - \left(A_{f,r}\right)_{k+\frac{1}{2}}\frac{\left(p_{f,j,k}^{H_2O} - p_{f,j,k+1}^{H_2O}\right)}{\Delta r}\right]$$

E.1.2.1.3 Case 3

$$V_f = \frac{\pi}{2}(k-1)\Delta r^2 \Delta x$$

$$A_{f,x} = 2\pi(k-1)\Delta r^2$$

$$\left(A_{f,r}\right)_{k-\frac{1}{2}} = 2\pi\left(k-\frac{3}{2}\right)\Delta r\frac{\Delta x}{2} = \pi\left(k-\frac{3}{2}\right)\Delta r\Delta x$$

$$\left(A_{f,r}\right)_{k+\frac{1}{2}} = 2\pi\left(k-\frac{1}{2}\right)\Delta r\frac{\Delta x}{2} = \pi\left(k-\frac{1}{2}\right)\Delta r\Delta x$$

$$V_f\left[\varepsilon S_{air}^{H_2O} + (1-\varepsilon)S_f^{H_2O}\right]\frac{dp_{f,j,k}^{H_2O}}{dt}$$
$$= -D_{eff}^{H_2O} S_{air}^{H_2O} A_{f,x}\frac{\left(p_{f,j,k}^{H_2O} - p_{f,j+1,k}^{H_2O}\right)}{\Delta x} + D_{eff}^{H_2O} S_{air}^{H_2O}\left(A_{f,r}\right)_{k-\frac{1}{2}}\frac{\left(p_{f,j,k-1}^{H_2O} - p_{f,j,k}^{H_2O}\right)}{\Delta r}$$
$$- D_{eff}^{H_2O} S_{air}^{H_2O}\left(A_{f,r}\right)_{k+\frac{1}{2}}\frac{\left(p_{f,j,k}^{H_2O} - p_{f,j,k+1}^{H_2O}\right)}{\Delta r}$$
$$\frac{dp_{f,j,k}^{H_2O}}{dt} = \frac{D_{eff}^{H_2O} S_{air}^{H_2O}}{V_f\left[\varepsilon S_{air}^{H_2O} + (1-\varepsilon)S_f^{H_2O}\right]}\left[-A_{f,x}\frac{\left(p_{f,j,k}^{H_2O} - p_{f,j+1,k}^{H_2O}\right)}{\Delta x} + \left(A_{f,r}\right)_{k-\frac{1}{2}}\frac{\left(p_{f,j,k-1}^{H_2O} - p_{f,j,k}^{H_2O}\right)}{\Delta r}\right.$$
$$\left. - \left(A_{f,r}\right)_{k+\frac{1}{2}}\frac{\left(p_{f,j,k}^{H_2O} - p_{f,j,k+1}^{H_2O}\right)}{\Delta r}\right]$$

E.1.2.1.4 Case 4

$$V_f = \pi\left[\left((k-1)\Delta r\right)^2 - \left(\left(k-\frac{3}{2}\right)\Delta r\right)^2\right]\Delta x = \pi\left(k-\frac{5}{4}\right)\Delta r^2\Delta x$$
$$A_{f,x} = \pi\left[\left((k-1)\Delta r\right)^2 - \left(\left(k-\frac{3}{2}\right)\Delta r\right)^2\right] = \pi\left(k-\frac{5}{4}\right)\Delta r^2$$
$$\left(A_{f,r}\right)_{k-\frac{1}{2}} = \pi\left(k-\frac{3}{2}\right)\Delta r\Delta x$$

$$V_f\left[\varepsilon S_{air}^{H_2O} + (1-\varepsilon)S_f^{H_2O}\right]\frac{dp_{f,j,k}^{H_2O}}{dt}$$
$$= D_{eff}^{H_2O} S_{air}^{H_2O} A_{f,x}\frac{\left(p_{f,j-1,k}^{H_2O} - p_{f,j,k}^{H_2O}\right)}{\Delta x} - D_{eff}^{H_2O} S_{air}^{H_2O} A_{f,x}\frac{\left(p_{f,j,k}^{H_2O} - p_{f,j+1,k}^{H_2O}\right)}{\Delta x}$$
$$+ D_{eff}^{H_2O} S_{air}^{H_2O}\left(A_{f,r}\right)_{k-\frac{1}{2}}\frac{\left(p_{f,j,k-1}^{H_2O} - p_{f,j,k}^{H_2O}\right)}{\Delta r}$$
$$\frac{dp_{f,j,k}^{H_2O}}{dt} = \frac{D_{eff}^{H_2O} S_{air}^{H_2O}}{V_f\left[\varepsilon S_{air}^{H_2O} + (1-\varepsilon)S_f^{H_2O}\right]}\left[A_{f,x}\frac{\left(p_{f,j-1,k}^{H_2O} - p_{f,j,k}^{H_2O}\right)}{\Delta x} - A_{f,x}\frac{\left(p_{f,j,k}^{H_2O} - p_{f,j+1,k}^{H_2O}\right)}{\Delta x}\right.$$
$$\left. + \left(A_{f,r}\right)_{k-\frac{1}{2}}\frac{\left(p_{f,j,k-1}^{H_2O} - p_{f,j,k}^{H_2O}\right)}{\Delta r}\right]$$

E.1.2.1.5 Case 5

$$V_f = \frac{\pi}{2}(k-1)\Delta r^2 \Delta x$$

$$A_{f,x} = 2\pi(k-1)\Delta r^2$$

$$\left(A_{f,r}\right)_{k-\frac{1}{2}} = \pi\left(k-\frac{3}{2}\right)\Delta r \Delta x$$

$$\left(A_{f,r}\right)_{k+\frac{1}{2}} = \pi\left(k-\frac{1}{2}\right)\Delta r \Delta x$$

$$V_f\left[\varepsilon S_{air}^{H_2O} + (1-\varepsilon)S_f^{H_2O}\right]\frac{dp_{f,j,k}^{H_2O}}{dt}$$

$$= D_{eff}^{H_2O} S_{air}^{H_2O} A_{f,x} \frac{\left(p_{f,j-1,k}^{H_2O} - p_{f,j,k}^{H_2O}\right)}{\Delta x} + D_{eff}^{H_2O} S_{air}^{H_2O}\left(A_{f,r}\right)_{k-\frac{1}{2}} \frac{\left(p_{f,j,k-1}^{H_2O} - p_{f,j,k}^{H_2O}\right)}{\Delta r}$$

$$- D_{eff}^{H_2O} S_{air}^{H_2O}\left(A_{f,r}\right)_{k+\frac{1}{2}} \frac{\left(p_{f,j,k}^{H_2O} - p_{f,j,k+1}^{H_2O}\right)}{\Delta r}$$

$$\frac{dp_{f,j,k}^{H_2O}}{dt} = \frac{D_{eff}^{H_2O} S_{air}^{H_2O}}{V_f\left[\varepsilon S_{air}^{H_2O} + (1-\varepsilon)S_f^{H_2O}\right]}\left[A_{f,x}\frac{\left(p_{f,j-1,k}^{H_2O} - p_{f,j,k}^{H_2O}\right)}{\Delta x} + \left(A_{f,r}\right)_{k-\frac{1}{2}}\frac{\left(p_{f,j,k-1}^{H_2O} - p_{f,j,k}^{H_2O}\right)}{\Delta r}\right.$$

$$\left. - \left(A_{f,r}\right)_{k+\frac{1}{2}}\frac{\left(p_{f,j,k}^{H_2O} - p_{f,j,k+1}^{H_2O}\right)}{\Delta r}\right]$$

E.1.2.1.6 Case 6

$$V_f = \frac{\pi}{8}\Delta r^2 \Delta x$$

$$A_{f,x} = \frac{\pi}{4}\Delta r^2$$

$$\left(A_{f,r}\right)_{k+\frac{1}{2}} = \frac{\pi}{2}\Delta r \Delta x$$

$$V_f\left[\varepsilon S_{air}^{H_2O} + (1-\varepsilon)S_f^{H_2O}\right]\frac{dp_{f,j,k}^{H_2O}}{dt}$$
$$= J_{prf,lnr}^{H_2O} A_{prf,lnr} - D_{eff}^{H_2O} S_{air}^{H_2O} A_{f,x}\frac{\left(p_{f,j,k}^{H_2O} - p_{f,j+1,k}^{H_2O}\right)}{\Delta x}$$
$$- D_{eff}^{H_2O} S_{air}^{H_2O}\left(A_{f,r}\right)_{m+\frac{1}{2}}\frac{\left(p_{f,j,k}^{H_2O} - p_{f,j,k+1}^{H_2O}\right)}{\Delta r}$$

$$\frac{dp_{f,j,k}^{H_2O}}{dt} = \frac{1}{V_f\left[\varepsilon S_{air}^{H_2O} + (1-\varepsilon)S_f^{H_2O}\right]}\left[J_{prf,lnr}^{H_2O} A_{prf,lnr}\right.$$
$$\left. + D_{eff}^{H_2O} S_{air}^{H_2O}\left(-A_{f,x}\frac{\left(p_{f,j,k}^{H_2O} - p_{f,j+1,k}^{H_2O}\right)}{\Delta x} - \left(A_{f,r}\right)_{m+\frac{1}{2}}\frac{\left(p_{f,j,k}^{H_2O} - p_{f,j,k+1}^{H_2O}\right)}{\Delta r}\right)\right]$$

E.1.2.1.7 Case 7

$$V_f = \frac{\pi}{4}\left(k - \frac{5}{4}\right)\Delta r^2 \Delta x$$
$$A_{f,x} = \pi\left(k - \frac{5}{4}\right)\Delta r^2$$
$$\left(A_{f,r}\right)_{k-\frac{1}{2}} = \pi\left(k - \frac{3}{2}\right)\Delta r \Delta x$$

$$V_f\left[\varepsilon S_{air}^{H_2O} + (1-\varepsilon)S_f^{H_2O}\right]\frac{dp_{f,j,k}^{H_2O}}{dt}$$
$$= -D_{eff}^{H_2O} S_{air}^{H_2O} A_{f,x}\frac{\left(p_{f,j,k}^{H_2O} - p_{f,j+1,k}^{H_2O}\right)}{\Delta x} + D_{eff}^{H_2O} S_{air}^{H_2O}\left(A_{f,r}\right)_{k-\frac{1}{2}}\frac{\left(p_{f,j,k-1}^{H_2O} - p_{f,j,k}^{H_2O}\right)}{\Delta r}$$

$$\frac{dp_{f,j,k}^{H_2O}}{dt} = \frac{D_{eff}^{H_2O} S_{air}^{H_2O}}{V_f\left[\varepsilon S_{air}^{H_2O} + (1-\varepsilon)S_f^{H_2O}\right]}\left[-A_{f,x}\frac{\left(p_{f,j,k}^{H_2O} - p_{f,j+1,k}^{H_2O}\right)}{\Delta x}\right.$$
$$\left. + \left(A_{f,r}\right)_{k-\frac{1}{2}}\frac{\left(p_{f,j,k-1}^{H_2O} - p_{f,j,k}^{H_2O}\right)}{\Delta r}\right]$$

E.1.2.1.8 Case 8

$$V_f = \frac{\pi}{4}\left(k - \frac{5}{4}\right)\Delta r^2 \Delta x$$

$$A_{f,x} = \pi\left(k - \frac{5}{4}\right)\Delta r^2$$

$$\left(A_{f,r}\right)_{k-\frac{1}{2}} = \pi\left(k - \frac{3}{2}\right)\Delta r \Delta x$$

$$V_f\left[\varepsilon S_{air}^{H_2O} + (1-\varepsilon)S_f^{H_2O}\right]\frac{dp_{f,j,k}^{H_2O}}{dt} = D_{eff}^{H_2O} S_{air}^{H_2O} A_{f,x}\frac{\left(p_{f,j-1,k}^{H_2O} - p_{f,j,k}^{H_2O}\right)}{\Delta x} + D_{eff}^{H_2O} S_{air}^{H_2O}\left(A_{f,r}\right)_{k-\frac{1}{2}}\frac{\left(p_{f,j,k-1}^{H_2O} - p_{f,j,k}^{H_2O}\right)}{\Delta r}$$

$$\frac{dp_{f,j,k}^{H_2O}}{dt} = \frac{D_{eff}^{H_2O} S_{air}^{H_2O}}{V_f\left[\varepsilon S_{air}^{H_2O} + (1-\varepsilon)S_f^{H_2O}\right]}\left[A_{f,x}\frac{\left(p_{f,j-1,k}^{H_2O} - p_{f,j,k}^{H_2O}\right)}{\Delta x} + \left(A_{f,r}\right)_{k-\frac{1}{2}}\frac{\left(p_{f,j,k-1}^{H_2O} - p_{f,j,k}^{H_2O}\right)}{\Delta r}\right]$$

E.1.2.1.9 Case 9

$$V_f = \frac{\pi}{8}\Delta r^2 \Delta x$$

$$A_{f,x} = \frac{\pi}{4}\Delta r^2$$

$$\left(A_{f,r}\right)_{k+\frac{1}{2}} = \frac{\pi}{2}\Delta r \Delta x$$

$$V_f\left[\varepsilon S_{air}^{H_2O} + (1-\varepsilon)S_f^{H_2O}\right]\frac{dp_{f,j,k}^{H_2O}}{dt} = D_{eff}^{H_2O} S_{air}^{H_2O} A_{f,x}\frac{\left(p_{f,j-1,k}^{H_2O} - p_{f,j,k}^{H_2O}\right)}{\Delta x} - D_{eff}^{H_2O} S_{air}^{H_2O}\left(A_{f,r}\right)_{k+\frac{1}{2}}\frac{\left(p_{f,j,k}^{H_2O} - p_{f,j,k+1}^{H_2O}\right)}{\Delta r}$$

$$\frac{dp_{f,j,k}^{H_2O}}{dt} = \frac{D_{eff}^{H_2O} S_{air}^{H_2O}}{V_f\left[\varepsilon S_{air}^{H_2O} + (1-\varepsilon)S_f^{H_2O}\right]}\left[A_{f,x}\frac{\left(p_{f,j-1,k}^{H_2O} - p_{f,j,k}^{H_2O}\right)}{\Delta x} - \left(A_{f,r}\right)_{k+\frac{1}{2}}\frac{\left(p_{f,j,k}^{H_2O} - p_{f,j,k+1}^{H_2O}\right)}{\Delta r}\right]$$

E.1.2.2 MATLAB® Solution

Refer to Appendix B for a digital copy of this numerical solution.

E.1.2.2.1 Script File (Perforation.m)

```
%Script File

clear all

global J K dxf drf;
global MrH2O R;
global rhos E isotherm;
global XTlnr Aprflnr dprflnr;
global kGAB CGAB M0GAB CBET M1BET blin clin;


%System Inputs
%General SIs
MrH2O=0.01802;                          %Molecular mass of water (kg/mol)
R=8.314;                                %Ideal gas constant (m^3.Pa/K/mol)

%Food Powder SIs
rhob=850;                               %Bulk density
rhop=1493;                              %Particle density
rhos=rhop/(1+0.03);                     %Density of solids in the food product (kg/m^3)
E=1-rhob/rhop;                          %Porosity of food product (-)
Xf=0.35;                                %Distance of water vapour diffusion into food
product in x-direction (m)
Rf=0.35;                                %Distance of water vapour diffusion into food
product in r-direction (m)

isotherm='gab';                         %Type of moisture (GAB, BET, or lin)

%Isotherm SIs
if lower(isotherm)=='gab'           %GAB Isotherm
    kGAB=1.08;                          %GAB isotherm constant (correcting factor)
    CGAB=12.11;                         %GAB isotherm constant (Guggenheim constant)
    M0GAB=0.051;                        %GAB isotherm constant (monolayer) (kg water/kg
solids)
elseif lower(isotherm)=='bet'       %BET isotherm
    CBET=0;                             %BET isotherm constant
    M1BET=0;                            %BET isotherm constant (monolayer) (kg water/kg
solids)
elseif lower(isotherm)=='lin'       %Linear isotherm
    blin=0;                             %Linear isotherm slope
    clin=0;                             %Linear isotherm intercept
end

%Packaging SIs
XTlnr=82e-6;                            %Total thickness of polymer liner (m)
Aprflnr=pi*(2e-3/2)^2;                  %Surface area of perforation in polymer liner
(m^2)
dprflnr=1e-4;                           %Diameter of perforation in polymer liner (m)

%Model Node SIs
J=10;                                   %Number of nodes in x-direction (-)
dxf=Xf/J;                               %Node width of food product in x-direction (m)

K=10;                                   %Number of nodes in r-direction (-)
drf=Rf/K;                               %Node width of food product in r-direction (m)


%Initial Conditions
Mi=0.03;                                %Initial moisture content of food product (kg
water/kg solids)
Ti=273.15+20;                           %Initial ambient tempearture (*C)
```

```
p0i=exp(23.4795-3990.56/(Ti-273.15+233.833));

if lower(isotherm)=='gab'
    pfi=zeros(1,(J+1)*(K+1))+p0i*(-(kGAB*(CGAB-CGAB*M0GAB/Mi-2))-sqrt((kGAB*(CGAB-
CGAB*M0GAB/Mi-2))^2-4*kGAB^2*(1-CGAB)))/(2*kGAB^2*(1-CGAB));
elseif lower(isotherm)=='bet'
    pfi=zeros(1,(J+1)*(K+1))+p0i*(-(CBET-CBET*M1BET/Mi-2)-sqrt((CBET-CBET*M1BET/Mi-2)^2-4*(1-
CBET)))/(2*(1-CBET));
elseif lower(isotherm)=='lin'
    pfi=zeros(1,(J+1)*(K+1))+p0i*(Mi-clin)/blin;
end

ICs=pfi;

stime=365;                                  %Simulation time (days)


%Solver
options=odeset('RelTol', 1e-3);
[t,D]=ode23s('PerforationFun',[0:24*60^2:stime*24*60^2],ICs,options);


%Plots
%Plot of water vapour pressure in food powder
figure
pfend=D(end,1:(J+1)*(K+1));
pfend=reshape(pfend,J+1,K+1);
contourf(pfend(1:J+1,1:K+1));
axis ij
colorbar;
title(['Water Vapour Pressure in the Food Powder after ',num2str(stime),' Days']);
xlabel('k');
ylabel('j');

%Plot of average water vapour pressure in food powder vs time
VfT=pi*Rf^2*Xf;
for i=1:size(D,1)
    pf=reshape(D(i,:),J+1,K+1);
    for j=[1,J+1]
        k=1;
        Vf=pi/8*drf^2*dxf;
        pfVf(j,k)=pf(j,k)*Vf;
        for k=2:K
            Vf=pi*(k-1)*drf^2*dxf;
            pfVf(j,k)=pf(j,k)*Vf;
        end
        k=K+1;
        Vf=pi/2*(k-5/4)*drf^2*dxf;
        pfVf(j,k)=pf(j,k)*Vf;
    end
    for j=2:J
        k=1;
        Vf=pi/4*drf^2*dxf;
        pfVf(j,k)=pf(j,k)*Vf;
        for k=2:K
            Vf=2*pi*(k-1)*drf^2*dxf;
            pfVf(j,k)=pf(j,k)*Vf;
        end
        k=K+1;
        Vf=pi*(k-5/4)*drf^2*dxf;
        pfVf(j,k)=pf(j,k)*Vf;
    end
    pfave(i,1)=sum(sum(pfVf))/VfT;
end
figure
plot(t/(24*60^2),pfave,'b-');
title('Average Water Vapour Pressure in Food Powder');
xlabel('t (days)');
ylabel('pfave(Pa)');


%Output data to Excel spreadsheet
outputtitle={'t(s)','pfave (Pa)'};
outputdata=[t pfave];
xlswrite('PerforationOutput',outputtitle,'pfave');
xlswrite('PerforationOutput',outputdata,'pfave','A2');
```

E.1.2.2.2 Model Function File (PerforationFun.m)

```
%Model Function File

function dD=PerforationFun(t,D)

global J K dxf drf;
global MrH2O R;
global rhos E isotherm;
global XTlnr Aprflnr dprflnr;
global kGAB CGAB M0GAB CBET M1BET blin clin;


D=reshape(D,J+1,K+1);
pf=D;

dD=zeros(J+1,K+1);


%General CVs
T=273.15+20;                                        %Ambient temperature (K)
RHa=75;                                             %Relative humidity of ambient air (%RH)
p0=exp(23.4795-3990.56/(T-273.15+233.833));         %Saturated vapour pressure of pure water
at T (Pa)
pa=RHa*p0/100;                                      %Partial pressure of water vapour in
ambient air (Pa)
Dair=1.7255e-7*T-2.552e-5;                          %Diffusivity of water vapour in air
(m^2/s)
Sair=1/R/T;                                         %Solubility of water vapour in air
(mol/m^3/Pa)
Deff=0.7*E*Dair;                                    %Effective diffusivity of water vapour in
vapour phase of food product (m^2/s)


%Perforation Equations
%Perforation(s) in polymer liner
j=1;
k=1;
if dprflnr<(1e-7)
    Jprflnr=48.5*dprflnr/R/T/XTlnr*(T/1000/MrH2O)^0.5*(pa-pf(j,k));
elseif dprflnr>=(1e-7) && dprflnr<(1e-5)
    Jprflnr=Dair*Sair*(pa-pf(j,k))/(XTlnr+dprflnr/2);   %Only valid if distance between
perforations >> pore radius
elseif dprflnr>=(1e-5)
    Jprflnr=Dair*Sair*(pa-pf(j,k))/XTlnr;           %Only valid if no total pressure
difference across packaging
end


%Finite Difference Approximations for Food powder
%Case 1
for j=2:J
    for k=2:K
        Vf=2*pi*(k-1)*drf^2*dxf;
        Afx=2*pi*(k-1)*drf^2;
        Afr(1)=2*pi*(k-3/2)*drf*dxf;
        Afr(2)=2*pi*(k-1/2)*drf*dxf;
        Sf=IsothermFun(j,k,pf,p0);
        dpf(j,k)=Deff*Sair/Vf/(E*Sair+(1-E)*Sf)*(Afx*(pf(j-1,k)-pf(j,k))/dxf-Afx*(pf(j,k)-
pf(j+1,k))/dxf+Afr(1)*(pf(j,k-1)-pf(j,k))/drf-Afr(2)*(pf(j,k)-pf(j,k+1))/drf);
    end
end

%Case 2
for j=2:J
    k=1;
    Vf=pi/4*drf^2*dxf;
    Afx=pi/4*drf^2;
    Afr(2)=pi*drf*dxf;
    Sf=IsothermFun(j,k,pf,p0);
    dpf(j,k)=Deff*Sair/Vf/(E*Sair+(1-E)*Sf)*(Afx*(pf(j-1,k)-pf(j,k))/dxf-Afx*(pf(j,k)-
pf(j+1,k))/dxf-Afr(2)*(pf(j,k)-pf(j,k+1))/drf);
end
```

```
%Case 3
j=1;
for k=2:K
    Vf=pi*(k-1)*drf^2*dxf;
    Afx=2*pi*(k-1)*drf^2;
    Afr(1)=pi*(k-3/2)*drf*dxf;
    Afr(2)=pi*(k-1/2)*drf*dxf;
    Sf=IsothermFun(j,k,pf,p0);
    dpf(j,k)=Deff*Sair/Vf/(E*Sair+(1-E)*Sf)*(-Afx*(pf(j,k)-pf(j+1,k))/dxf+Afr(1)*(pf(j,k-1)-
pf(j,k))/drf-Afr(2)*(pf(j,k)-pf(j,k+1))/drf);
end

%Case 4
for j=2:J
    k=K+1;
    Vf=pi*(k-5/4)*drf^2*dxf;
    Afx=pi*(k-5/4)*drf^2;
    Afr(1)=2*pi*(k-3/2)*drf*dxf;
    Sf=IsothermFun(j,k,pf,p0);
    dpf(j,k)=Deff*Sair/Vf/(E*Sair+(1-E)*Sf)*(Afx*(pf(j-1,k)-pf(j,k))/dxf-Afx*(pf(j,k)-
pf(j+1,k))/dxf+Afr(1)*(pf(j,k-1)-pf(j,k))/drf);
end

%Case 5
j=J+1;
for k=2:K
    Vf=pi*(k-1)*drf^2*dxf;
    Afx=2*pi*(k-1)*drf^2;
    Afr(1)=pi*(k-3/2)*drf*dxf;
    Afr(2)=pi*(k-1/2)*drf*dxf;
    Sf=IsothermFun(j,k,pf,p0);
    dpf(j,k)=Deff*Sair/Vf/(E*Sair+(1-E)*Sf)*(Afx*(pf(j-1,k)-pf(j,k))/dxf+Afr(1)*(pf(j,k-1)-
pf(j,k))/drf-Afr(2)*(pf(j,k)-pf(j,k+1))/drf);
end

%Case 6
j=1;
k=1;
Vf=pi/8*drf^2*dxf;
Afx=pi/4*drf^2;
Afr(2)=pi/2*drf*dxf;
Sf=IsothermFun(j,k,pf,p0);
dpf(j,k)=1/Vf/(E*Sair+(1-E)*Sf)*(Jprflnr*Aprflnr+Deff*Sair*(-Afx*(pf(j,k)-pf(j+1,k))/dxf-
Afr(2)*(pf(j,k)-pf(j,k+1))/drf));

%Case 7
j=1;
k=K+1;
Vf=pi/2*(k-5/4)*drf^2*dxf;
Afx=pi*(k-5/4)*drf^2;
Afr(1)=pi*(k-3/2)*drf*dxf;
Sf=IsothermFun(j,k,pf,p0);
dpf(j,k)=Deff*Sair/Vf/(E*Sair+(1-E)*Sf)*(-Afx*(pf(j,k)-pf(j+1,k))/dxf+Afr(1)*(pf(j,k-1)-
pf(j,k))/drf);

%Case 8
j=J+1;
k=K+1;
Vf=pi/2*(k-5/4)*drf^2*dxf;
Afx=pi*(k-5/4)*drf^2;
Afr(1)=pi*(k-3/2)*drf*dxf;
Sf=IsothermFun(j,k,pf,p0);
dpf(j,k)=Deff*Sair/Vf/(E*Sair+(1-E)*Sf)*(Afx*(pf(j-1,k)-pf(j,k))/dxf+Afr(1)*(pf(j,k-1)-
pf(j,k))/drf);

%Case 9
j=J+1;
k=1;
Vf=pi/8*drf^2*dxf;
Afx=pi/4*drf^2;
Afr(2)=pi/2*drf*dxf;
Sf=IsothermFun(j,k,pf,p0);
dpf(j,k)=Deff*Sair/Vf/(E*Sair+(1-E)*Sf)*(Afx*(pf(j-1,k)-pf(j,k))/dxf-Afr(2)*(pf(j,k)-
pf(j,k+1))/drf);


dD=reshape(dpf,(J+1)*(K+1),1);
```

E.1.2.2.3 Solubility of Water Vapour in Food Powder Function File (IsothermFun.m)

```
%Food Product Isotherm Function File

function Sf=IsothermFun(j,k,pf,p0)

global J K dxf drf Kair;
global MrH2O R;
global rhos E isotherm Afair;
global XTlnr Aprflnr dprflnr;
global kGAB CGAB M0GAB CBET M1BET blin clin;


if lower(isotherm)=='gab'           %GAB isotherm
    Sf=rhos/MrH2O*(M0GAB*kGAB^2*CGAB*pf(j,k)/p0^2/(1-kGAB*pf(j,k)/p0)^2/(1-
kGAB*pf(j,k)/p0+kGAB*CGAB*pf(j,k)/p0)+M0GAB*kGAB*CGAB/p0/(1-kGAB*pf(j,k)/p0)/(1-
kGAB*pf(j,k)/p0+kGAB*CGAB*pf(j,k)/p0)-M0GAB*kGAB^2*CGAB*(CGAB-1)*pf(j,k)/p0^2/(1-
kGAB*pf(j,k)/p0)/(1-kGAB*pf(j,k)/p0+kGAB*CGAB*pf(j,k)/p0)^2);
elseif lower(isotherm)=='bet'       %BET isotherm
    Sf=rhos/MrH2O*(M1BET*CBET/p0/(1-pf(j,k)/p0)/(1-pf(j,k)/p0+CBET*pf(j,k)/p0)-
M1BET*CBET*(CBET-1)*pf(j,k)/p0^2/(1-pf(j,k)/p0)/(1-pf(j,k)/p0+CBET*pf(j,k)/p0)^2-
M1BET*CBET*pf(j,k)/p0^2/(1-pf(j,k)/p0)^2/(1-pf(j,k)/p0+CBET*pf(j,k)/p0));
elseif lower(isotherm)=='lin'       %Linear isotherm
    Sf=rhos/MrH2O*blin/p0;
end
```

E.1.3 Error Checks

E.1.3.1 Numerical Error Checks

E.1.3.1.1 Time Step

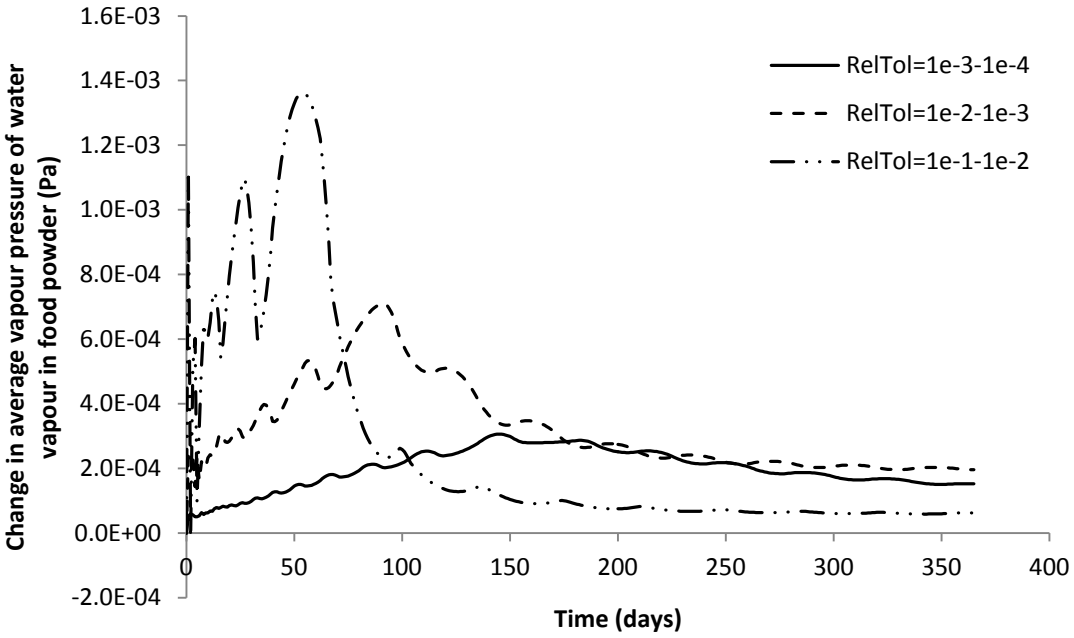

Figure E-1: Plot of change in predicted values of average water vapour pressure in food powder (Pa), with changes to relative error tolerance of MATLAB® solver (RelTol).

As shown in Figure E-1, all changes to relative error tolerance of the MATLAB® solver (RelTol) had a relatively insignificant effect on predicted values of average water vapour pressure in the food powder, with no differences greater than 1.4×10^{-3} Pa over the period $0 \leq t \leq 365$ days. Therefore the default RelTol value of 1×10^{-3} should be suitable for use in the model.

E.1.3.1.2 Space Step

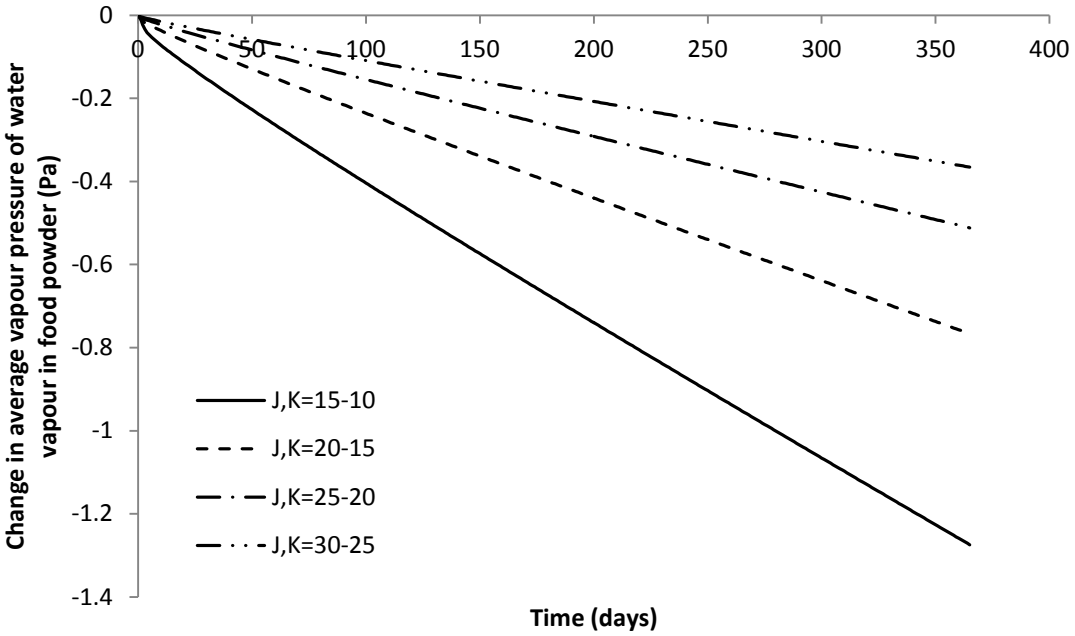

Figure E-2: Plot of change in predicted values of average water vapour pressure in food powder (Pa) with changes to number of nodes in axial (J) and radial (K) directions.

As shown in Figure E-2, changes to the number of nodes in axial and radial directions had a somewhat significant effect on model predictions of average water vapour pressure in the food powder. This is believed to be a result of water vapour only entering the system in a single node, causing a relatively small moisture profile most significant in only a very few nodes. Unfortunately increasing the number of nodes increased solving time exponentially, significantly affecting the practical usefulness of the model, and not largely increasing the number of nodes in the area of interest. The most appropriate solution would be to use non-constant node widths, with relatively small nodes near the perforation, increasing in size further away. However this would greatly complicate the numerical solution method. Due to other approximations made during model formulation, such changes were not deemed worthwhile for this investigation, and the standard 10 nodes in both axial and radial directions resulting in a reasonable solving time were used. However if more accurate predictions are required, these changes should certainly be considered.

E.1.3.2 Mathematical Error Checks

Due to the nature of boundary conditions (all symmetry except for the node bordering the perforation), an analytical solution was not possible. However, model validation is expected to provide further verification of the mathematical correctness of the developed model.

E.2 ISOLATED AIR POCKET AROUND PERFORATION

5.1.1 Solution

5.1.1.1 Finite Difference Approximations

$$K_{air} = ceil\left(\sqrt{\frac{A_{air}}{\pi}}\frac{1}{\Delta r} + 1\right)$$

Where ceil is the MATLAB® function for rounding up to the nearest integer.

E.2.1.1.1 Case 6

$$V_f = \frac{\pi}{8}\Delta r^2 \Delta x$$

$$A_{f,x} = \frac{\pi}{4}\Delta r^2$$

$$\left(A_{f,r}\right)_{k+\frac{1}{2}} = \frac{\pi}{2}\Delta r \Delta x$$

$$V_f\left[\varepsilon S_{air}^{H_2O} + (1-\varepsilon)S_f^{H_2O}\right]\frac{dp_{f,j,k}^{H_2O}}{dt}$$
$$= J_{prf,lnr}^{H_2O} A_{prf,lnr}\frac{A_{f,x}}{A_{f,air}} - D_{eff}^{H_2O} S_{air}^{H_2O} A_{f,x}\frac{\left(p_{f,j,k}^{H_2O} - p_{f,j+1,k}^{H_2O}\right)}{\Delta x}$$
$$- D_{eff}^{H_2O} S_{air}^{H_2O}\left(A_{f,r}\right)_{m+\frac{1}{2}}\frac{\left(p_{f,j,k}^{H_2O} - p_{f,j,k+1}^{H_2O}\right)}{\Delta r}$$

$$\frac{dp_{f,j,k}^{H_2O}}{dt} = \frac{1}{V_f\left[\varepsilon S_{air}^{H_2O} + (1-\varepsilon)S_f^{H_2O}\right]}\left[J_{prf,lnr}^{H_2O} A_{prf,lnr}\frac{A_{f,x}}{A_{f,air}} + D_{eff}^{H_2O} S_{air}^{H_2O}\left(-A_{f,x}\frac{\left(p_{f,j,k}^{H_2O} - p_{f,j+1,k}^{H_2O}\right)}{\Delta x} - \left(A_{f,r}\right)_{m+\frac{1}{2}}\frac{\left(p_{f,j,k}^{H_2O} - p_{f,j,k+1}^{H_2O}\right)}{\Delta r}\right)\right]$$

E.2.1.1.2 Case 10

$$V_f = \frac{\pi}{2}(k-1)\Delta r^2 \Delta x$$

$$A_{f,x} = 2\pi(k-1)\Delta r^2$$

$$\left(A_{f,r}\right)_{k-\frac{1}{2}} = \frac{\pi}{2}\left(k-\frac{3}{2}\right)\Delta r \Delta x$$

$$\left(A_{f,r}\right)_{k+\frac{1}{2}} = \frac{\pi}{2}\left(k-\frac{1}{2}\right)\Delta r \Delta x$$

$$V_f\left[\varepsilon S_{air}^{H_2O} + (1-\varepsilon)S_f^{H_2O}\right]\frac{dp_{f,j,k}^{H_2O}}{dt} = J_{prf,lnr}^{H_2O} A_{prf,lnr}\frac{A_{f,x}}{A_{f,air}} - D_{eff}^{H_2O} S_{air}^{H_2O} A_{f,x}\frac{\left(p_{f,j,k}^{H_2O} - p_{f,j+1,k}^{H_2O}\right)}{\Delta x} + D_{eff}^{H_2O} S_{air}^{H_2O}\left(A_{f,r}\right)_{k-\frac{1}{2}}\frac{\left(p_{f,j,k-1}^{H_2O} - p_{f,j,k}^{H_2O}\right)}{\Delta r} - D_{eff}^{H_2O} S_{air}^{H_2O}\left(A_{f,r}\right)_{k+\frac{1}{2}}\frac{\left(p_{f,j,k}^{H_2O} - p_{f,j,k+1}^{H_2O}\right)}{\Delta r}$$

$$\frac{dp_{f,j,k}^{H_2O}}{dt} = \frac{1}{V_f\left[\varepsilon S_{air}^{H_2O} + (1-\varepsilon)S_f^{H_2O}\right]}\left[J_{prf,lnr}^{H_2O} A_{prf,lnr}\frac{A_{f,x}}{A_{f,air}} + D_{eff}^{H_2O} S_{air}^{H_2O}\left(-A_{f,x}\frac{\left(p_{f,j,k}^{H_2O} - p_{f,j+1,k}^{H_2O}\right)}{\Delta x} + \left(A_{f,r}\right)_{k-\frac{1}{2}}\frac{\left(p_{f,j,k-1}^{H_2O} - p_{f,j,k}^{H_2O}\right)}{\Delta r} - \left(A_{f,r}\right)_{k+\frac{1}{2}}\frac{\left(p_{f,j,k}^{H_2O} - p_{f,j,k+1}^{H_2O}\right)}{\Delta r}\right)\right]$$

E.2.1.1.3 Case 11

$$V_f = \frac{\pi}{2}(k-1)\Delta r^2 \Delta x$$

$$A_{f,x} = 2\pi(k-1)\Delta r^2$$

$$\left(A_{f,x}\right)_{k=1:K_{air}} = \pi\left(\left(k-\frac{3}{2}\right)\Delta r\right)^2$$

$$\left(A_{f,r}\right)_{k-\frac{1}{2}} = \frac{\pi}{2}\left(k-\frac{3}{2}\right)\Delta r \Delta x$$

$$\left(A_{f,r}\right)_{k+\frac{1}{2}} = \frac{\pi}{2}\left(k-\frac{1}{2}\right)\Delta r \Delta x$$

$$V_f\left[\varepsilon S_{air}^{H_2O} + (1-\varepsilon)S_f^{H_2O}\right]\frac{dp_{f,j,k}^{H_2O}}{dt}$$

$$= J_{prf,lnr}^{H_2O} A_{prf,lnr}\frac{A_{air} - \left(A_{f,x}\right)_{k=1:K_{air}}}{A_{air}} - D_{eff}^{H_2O} S_{air}^{H_2O} A_{f,x}\frac{\left(p_{f,j,k}^{H_2O} - p_{f,j+1,k}^{H_2O}\right)}{\Delta x}$$

$$+ D_{eff}^{H_2O} S_{air}^{H_2O}\left(A_{f,r}\right)_{k-\frac{1}{2}}\frac{\left(p_{f,j,k-1}^{H_2O} - p_{f,j,k}^{H_2O}\right)}{\Delta r}$$

$$- D_{eff}^{H_2O} S_{air}^{H_2O}\left(A_{f,r}\right)_{k+\frac{1}{2}}\frac{\left(p_{f,j,k}^{H_2O} - p_{f,j,k+1}^{H_2O}\right)}{\Delta r}$$

$$\frac{dp_{f,j,k}^{H_2O}}{dt} = \frac{1}{V_f\left[\varepsilon S_{air}^{H_2O} + (1-\varepsilon)S_f^{H_2O}\right]}\left[J_{prf,lnr}^{H_2O} A_{prf,lnr}\frac{A_{air} - \left(A_{f,x}\right)_{k=1:K_{air}}}{A_{air}}\right.$$

$$+ D_{eff}^{H_2O} S_{air}^{H_2O}\left(-A_{f,x}\frac{\left(p_{f,j,k}^{H_2O} - p_{f,j+1,k}^{H_2O}\right)}{\Delta x} + \left(A_{f,r}\right)_{k-\frac{1}{2}}\frac{\left(p_{f,j,k-1}^{H_2O} - p_{f,j,k}^{H_2O}\right)}{\Delta r}\right.$$

$$\left.\left. - \left(A_{f,r}\right)_{k+\frac{1}{2}}\frac{\left(p_{f,j,k}^{H_2O} - p_{f,j,k+1}^{H_2O}\right)}{\Delta r}\right)\right]$$

E.2.1.2 Matlab Solution

Refer to Appendix B for a digital copy of this numerical solution.

E.2.1.2.1 Script File (Perforation.m)

```
%Script File

clear all

global J K dxf drf Kair;
global MrH2O R;
global rhos E isotherm Aair;
global XTlnr Aprflnr dprflnr;
global kGAB CGAB M0GAB CBET M1BET blin clin;


%System Inputs
%General SIs
MrH2O=0.01802;                          %Molecular mass of water (kg/mol)
R=8.314;                                %Ideal gas constant (m^3.Pa/K/mol)

%Food Powder SIs
Aair=pi*0.2^2;                          %Area of air pocket around perforation (m^2)
rhob=850;                               %Bulk density
rhop=1493;                              %Particle density
rhos=rhop/(1+0.03);                     %Density of solids in the food product (kg/m^3)
E=1-rhob/rhop;                          %Porosity of food product (-)
Xf=0.4;                                 %Distance of water vapour diffusion into food
product in x-direction (m)
Rf=0.5;                                 %Distance of water vapour diffusion into food
product in r-direction (m)

isotherm='gab';                         %Type of moisture (GAB, BET, or lin)

%Isotherm SIs
if lower(isotherm)=='gab'           %GAB Isotherm
    kGAB=1.08;                          %GAB isotherm constant (correcting factor)
    CGAB=12.11;                         %GAB isotherm constant (Guggenheim constant)
    M0GAB=0.051;                        %GAB isotherm constant (monolayer) (kg water/kg
solids)
elseif lower(isotherm)=='bet'       %BET isotherm
    CBET=0;                             %BET isotherm constant
    M1BET=0;                            %BET isotherm constant (monolayer) (kg water/kg
solids)
elseif lower(isotherm)=='lin'       %Linear isotherm
    blin=0;                             %Linear isotherm slope
    clin=0;                             %Linear isotherm intercept
end

%Packaging SIs
XTlnr=82e-6;                            %Total thickness of polymer liner (m)
Aprflnr=pi*(2e-3/2)^2;                  %Surface area of perforation in polymer liner
(m^2)
dprflnr=1e-4;                           %Diameter of perforation in polymer liner (m)

%Model Node SIs
J=10;                                   %Number of nodes in x-direction (-)
dxf=Xf/J;                               %Node width of food product in x-direction (m)

K=10;                                   %Number of nodes in r-direction (-)
drf=Rf/J;                               %Node width of food product in r-direction (m)

Kair=ceil(sqrt(Aair/pi)/drf+1);


%Initial Conditions
Mi=0.03;                                %Initial moisture content of food product (kg
water/kg solids)
Ti=273.15+20;                           %Initial ambient tempearture (*C)

p0i=exp(23.4795-3990.56/(Ti-273.15+233.833));

if lower(isotherm)=='gab'
    pfi=zeros(1,(J+1)*(K+1))+p0i*(-(kGAB*(CGAB-CGAB*M0GAB/Mi-2))-sqrt((kGAB*(CGAB-
CGAB*M0GAB/Mi-2))^2-4*kGAB^2*(1-CGAB)))/(2*kGAB^2*(1-CGAB));
elseif lower(isotherm)=='bet'
```

```
    pfi=zeros(1,(J+1)*(K+1))+p0i*(-(CBET-CBET*M1BET/Mi-2)-sqrt((CBET-CBET*M1BET/Mi-2)^2-4*(1-
CBET)))/(2*(1-CBET));
elseif lower(isotherm)=='lin'
    pfi=zeros(1,(J+1)*(K+1))+p0i*(Mi-clin)/blin;
end

ICs=pfi;

stime=365;                                  %Simulation time (days)


%Solver
options=odeset('RelTol', 1e-0);
[t,D]=ode23s('PerforationFun',[0:24*60^2:stime*24*60^2],ICs,options);


%Plots
%Plot of water vapour pressure in food powder
figure
pfend=D(end,1:(J+1)*(K+1));
pfend=reshape(pfend,J+1,K+1);
contourf(pfend(1:J+1,1:K+1));
axis ij
colorbar;
title(['Water Vapour Pressure in Food Powder after ',num2str(stime),' Days']);
xlabel('k');
ylabel('j');

%Plot of average water vapour pressure in food powder vs time
VfT=pi*Rf^2*Xf;
for i=1:size(D,1)
    pf=reshape(D(i,:),J+1,K+1);
    for j=[1,J+1]
        k=1;
        Vf=pi/8*drf^2*dxf;
        pfVf(j,k)=pf(j,k)*Vf;
        for k=2:K
            Vf=pi*(k-1)*drf^2*dxf;
            pfVf(j,k)=pf(j,k)*Vf;
        end
        k=K+1;
        Vf=pi/2*(k-5/4)*drf^2*dxf;
        pfVf(j,k)=pf(j,k)*Vf;
    end
    for j=2:J
        k=1;
        Vf=pi/4*drf^2*dxf;
        pfVf(j,k)=pf(j,k)*Vf;
        for k=2:K
            Vf=2*pi*(k-1)*drf^2*dxf;
            pfVf(j,k)=pf(j,k)*Vf;
        end
        k=K+1;
        Vf=pi*(k-5/4)*drf^2*dxf;
        pfVf(j,k)=pf(j,k)*Vf;
    end
    pfave(i,1)=sum(sum(pfVf))/VfT;
end
figure
plot(t/(24*60^2),pfave,'b-');
title('Average Water Vapour Pressure in the Food Powder');
xlabel('t (days)');
ylabel('pfave(Pa)');


%Output data to Excel spreadsheet
outputtitle={'t(s)','pfave (Pa)'};
outputdata=[t pfave];
xlswrite('PerforationOutput',outputtitle,'pfave');
xlswrite('PerforationOutput',outputdata,'pfave','A2');
```

E.2.1.2.2 Model Function File (PerforationFun.m)

```
%Model Function File

function dD=PerforationFun(t,D)

global J K dxf drf Kair;
global MrH2O R;
global rhos E isotherm Afair;
global XTlnr Aprflnr dprflnr;
global kGAB CGAB M0GAB CBET M1BET blin clin;


D=reshape(D,J+1,K+1);
pf=D;

dD=zeros(J+1,K+1);


%General CVs
T=273.15+20;                                        %Ambient temperature (K)
RHa=75;                                             %Relative humidity of ambient air (%RH)
p0=exp(23.4795-3990.56/(T-273.15+233.833));         %Saturated vapour pressure of pure water
at T (Pa)
pa=RHa*p0/100;                                      %Partial pressure of water vapour in
ambient air (Pa)
Dair=1.7255e-7*T-2.552e-5;                          %Diffusivity of water vapour in air
(m^2/s)
Sair=1/R/T;                                         %Solubility of water vapour in air
(mol/m^3/Pa)
Deff=0.7*E*Dair;                                    %Effective diffusivity of water vapour in
vapour phase of food product (m^2/s)


%Average Water Vapour Pressure in Air Pocket
j=1;
k=1;
Afx=pi/4*drf^2;
pfAfx(k)=pf(j,k)*Afx;
j=1;
for k=2:Kair-1
    Afx=2*pi*(k-1)*drf^2;
    pfAfx(k)=pf(j,k)*Afx;
end
j=1;
k=Kair;
Afx=Afair-pi*((k-3/2)*drf)^2;
pfAfx(k)=pf(j,k)*Afx;
pap=sum(pfAfx)/Afair;


%Perforation Equations
%Perforation(s) in polymer liner
j=1;
k=1;
if dprflnr<(1e-7)
    Jprflnr=48.5*dprflnr/R/T/XTlnr*(T/1000/MrH2O)^0.5*(pa-pap);
elseif dprflnr>=(1e-7) && dprflnr<(1e-5)
    Jprflnr=Dair*Sair*(pa-pap)/(XTlnr+dprflnr/2);   %Only valid if distance between
perforations >> pore radius
elseif dprflnr>=(1e-5)
    Jprflnr=Dair*Sair*(pa-pap)/XTlnr;               %Only valid if no total pressure
difference across packaging
end


%Finite Difference Approximations for Food Product
%Case 1
for j=2:J
    for k=2:K
        Vf=2*pi*(k-1)*drf^2*dxf;
        Afx=2*pi*(k-1)*drf^2;
        Afr(1)=2*pi*(k-3/2)*drf*dxf;
        Afr(2)=2*pi*(k-1/2)*drf*dxf;
```

```
        Sf=IsothermFun(j,k,pf,p0);
        dpf(j,k)=Deff*Sair/Vf/(E*Sair+(1-E)*Sf)*(Afx*(pf(j-1,k)-pf(j,k))/dxf-Afx*(pf(j,k)-
pf(j+1,k))/dxf+Afr(1)*(pf(j,k-1)-pf(j,k))/drf-Afr(2)*(pf(j,k)-pf(j,k+1))/drf);
    end
end

%Case 2
for j=2:J
    k=1;
    Vf=pi/4*drf^2*dxf;
    Afx=pi/4*drf^2;
    Afr(2)=pi*drf*dxf;
    Sf=IsothermFun(j,k,pf,p0);
    dpf(j,k)=Deff*Sair/Vf/(E*Sair+(1-E)*Sf)*(Afx*(pf(j-1,k)-pf(j,k))/dxf-Afx*(pf(j,k)-
pf(j+1,k))/dxf-Afr(2)*(pf(j,k)-pf(j,k+1))/drf);
end

%Case 3
j=1;
for k=Kair+1:K
    Vf=pi*(k-1)*drf^2*dxf;
    Afx=2*pi*(k-1)*drf^2;
    Afr(1)=pi*(k-3/2)*drf*dxf;
    Afr(2)=pi*(k-1/2)*drf*dxf;
    Sf=IsothermFun(j,k,pf,p0);
    dpf(j,k)=Deff*Sair/Vf/(E*Sair+(1-E)*Sf)*(-Afx*(pf(j,k)-pf(j+1,k))/dxf+Afr(1)*(pf(j,k-1)-
pf(j,k))/drf-Afr(2)*(pf(j,k)-pf(j,k+1))/drf);
end

%Case 4
for j=2:J
    k=K+1;
    Vf=pi*(k-5/4)*drf^2*dxf;
    Afx=pi*(k-5/4)*drf^2;
    Afr(1)=2*pi*(k-3/2)*drf*dxf;
    Sf=IsothermFun(j,k,pf,p0);
    dpf(j,k)=Deff*Sair/Vf/(E*Sair+(1-E)*Sf)*(Afx*(pf(j-1,k)-pf(j,k))/dxf-Afx*(pf(j,k)-
pf(j+1,k))/dxf+Afr(1)*(pf(j,k-1)-pf(j,k))/drf);
end

%Case 5
j=J+1;
for k=2:K
    Vf=pi*(k-1)*drf^2*dxf;
    Afx=2*pi*(k-1)*drf^2;
    Afr(1)=pi*(k-3/2)*drf*dxf;
    Afr(2)=pi*(k-1/2)*drf*dxf;
    Sf=IsothermFun(j,k,pf,p0);
    dpf(j,k)=Deff*Sair/Vf/(E*Sair+(1-E)*Sf)*(Afx*(pf(j-1,k)-pf(j,k))/dxf+Afr(1)*(pf(j,k-1)-
pf(j,k))/drf-Afr(2)*(pf(j,k)-pf(j,k+1))/drf);
end

%Case 6
j=1;
k=1;
Vf=pi/8*drf^2*dxf;
Afx=pi/4*drf^2;
Afr(2)=pi/2*drf*dxf;
Sf=IsothermFun(j,k,pf,p0);
dpf(j,k)=1/Vf/(E*Sair+(1-E)*Sf)*(Jprflnr*Aprflnr*Afx/Afair+Deff*Sair*(-Afx*(pf(j,k)-
pf(j+1,k))/dxf-Afr(2)*(pf(j,k)-pf(j,k+1))/drf));

%Case 7
j=1;
k=K+1;
Vf=pi/2*(k-5/4)*drf^2*dxf;
Afx=pi*(k-5/4)*drf^2;
Afr(1)=pi*(k-3/2)*drf*dxf;
Sf=IsothermFun(j,k,pf,p0);
dpf(j,k)=Deff*Sair/Vf/(E*Sair+(1-E)*Sf)*(-Afx*(pf(j,k)-pf(j+1,k))/dxf+Afr(1)*(pf(j,k-1)-
pf(j,k))/drf);

%Case 8
j=J+1;
k=K+1;
Vf=pi/2*(k-5/4)*drf^2*dxf;
Afx=pi*(k-5/4)*drf^2;
```

```
Afr(1)=pi*(k-3/2)*drf*dxf;
Sf=IsothermFun(j,k,pf,p0);
dpf(j,k)=Deff*Sair/Vf/(E*Sair+(1-E)*Sf)*(Afx*(pf(j-1,k)-pf(j,k))/dxf+Afr(1)*(pf(j,k-1)-
pf(j,k))/drf);

%Case 9
j=J+1;
k=1;
Vf=pi/8*drf^2*dxf;
Afx=pi/4*drf^2;
Afr(2)=pi/2*drf*dxf;
Sf=IsothermFun(j,k,pf,p0);
dpf(j,k)=Deff*Sair/Vf/(E*Sair+(1-E)*Sf)*(Afx*(pf(j-1,k)-pf(j,k))/dxf-Afr(2)*(pf(j,k)-
pf(j,k+1))/drf);

%Case 10
j=1;
for k=2:Kair-1
    Vf=pi*(k-1)*drf^2*dxf;
    Afx=2*pi*(k-1)*drf^2;
    Afr(1)=pi*(k-3/2)*drf*dxf;
    Afr(2)=pi*(k-1/2)*drf*dxf;
    Sf=IsothermFun(j,k,pf,p0);
    dpf(j,k)=1/Vf/(E*Sair+(1-E)*Sf)*(Jprflnr*Aprflnr*Afx/Afair+Deff*Sair*(-Afx*(pf(j,k)-
pf(j+1,k))/dxf+Afr(1)*(pf(j,k-1)-pf(j,k))/drf-Afr(2)*(pf(j,k)-pf(j,k+1))/drf));
end

%Case 11
j=1;
k=Kair;
Vf=pi*(k-1)*drf^2*dxf;
Afx=2*pi*(k-1)*drf^2;
Afxair=Afair-pi*((k-3/2)*drf)^2;
Afr(1)=pi*(k-3/2)*drf*dxf;
Afr(2)=pi*(k-1/2)*drf*dxf;
Sf=IsothermFun(j,k,pf,p0);
dpf(j,k)=1/Vf/(E*Sair+(1-E)*Sf)*(Jprflnr*Aprflnr*Afxair/Afair+Deff*Sair*(-Afx*(pf(j,k)-
pf(j+1,k))/dxf+Afr(1)*(pf(j,k-1)-pf(j,k))/drf-Afr(2)*(pf(j,k)-pf(j,k+1))/drf));


dD=reshape(dpf,(J+1)*(K+1),1);
```

E.2.1.2.3 Solubility of Water Vapour in Food Powder Function File (IsothermFun.m)

```
%Food Product Isotherm Function File

function Sf=IsothermFun(j,k,pf,p0)

global J K dxf drf Kair;
global MrH2O R;
global rhos E isotherm Afair;
global XTlnr Aprflnr dprflnr;
global kGAB CGAB M0GAB CBET M1BET blin clin;


if lower(isotherm)=='gab'           %GAB isotherm
    Sf=rhos/MrH2O*(M0GAB*kGAB^2*CGAB*pf(j,k)/p0^2/(1-kGAB*pf(j,k)/p0)^2/(1-
kGAB*pf(j,k)/p0+kGAB*CGAB*pf(j,k)/p0)+M0GAB*kGAB*CGAB/p0/(1-kGAB*pf(j,k)/p0)/(1-
kGAB*pf(j,k)/p0+kGAB*CGAB*pf(j,k)/p0)-M0GAB*kGAB^2*CGAB*(CGAB-1)*pf(j,k)/p0^2/(1-
kGAB*pf(j,k)/p0)/(1-kGAB*pf(j,k)/p0+kGAB*CGAB*pf(j,k)/p0)^2);
elseif lower(isotherm)=='bet'       %BET isotherm
    Sf=rhos/MrH2O*(M1BET*CBET/p0/(1-pf(j,k)/p0)/(1-pf(j,k)/p0+CBET*pf(j,k)/p0)-
M1BET*CBET*(CBET-1)*pf(j,k)/p0^2/(1-pf(j,k)/p0)/(1-pf(j,k)/p0+CBET*pf(j,k)/p0)^2-
M1BET*CBET*pf(j,k)/p0^2/(1-pf(j,k)/p0)^2/(1-pf(j,k)/p0+CBET*pf(j,k)/p0));
elseif lower(isotherm)=='lin'       %Linear isotherm
    Sf=rhos/MrH2O*blin/p0;
end
```

E.2.2 Error checks

E.2.2.1 Numerical Error Checks

E.2.2.1.1 Time Step

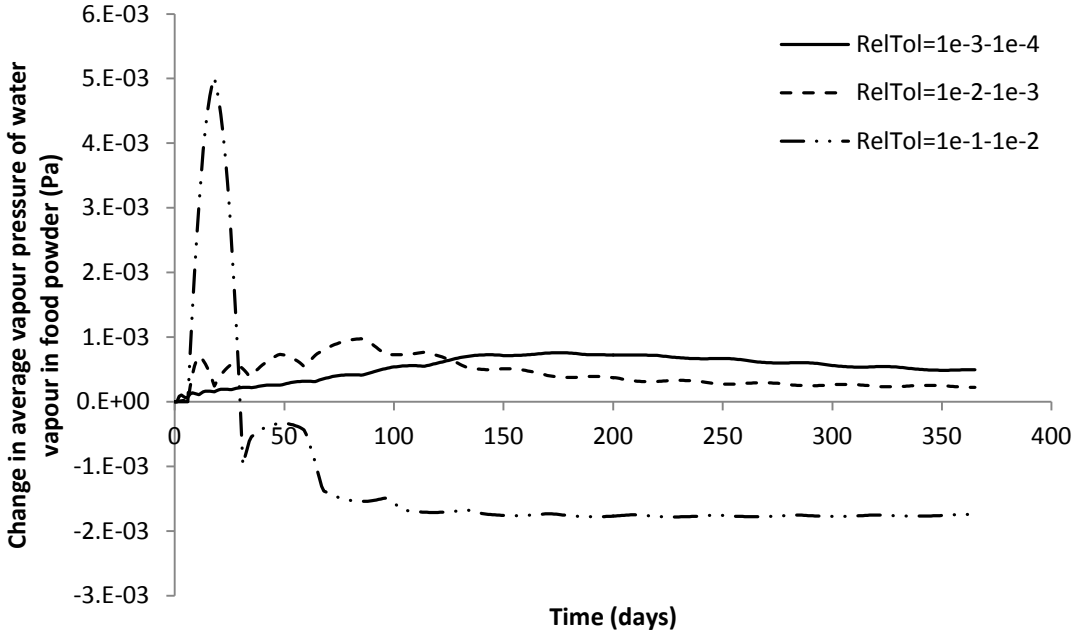

Figure E-3: Plot of change in predicted values of average water vapour pressure in food powder (Pa), with changes to relative error tolerance of MATLAB® solver (RelTol).

As shown in Figure E-3, all changes to relative error tolerance of the MATLAB® solver (RelTol) had relatively insignificant effects on predicted values of average water vapour pressure in the food powder, with no differences greater than 5.1×10^{-3} Pa over the period $0 \leq t \leq 365$ days. Therefore the default RelTol value of 1×10^{-3} should be suitable for use in the model.

E.2.2.1.2 Space Step

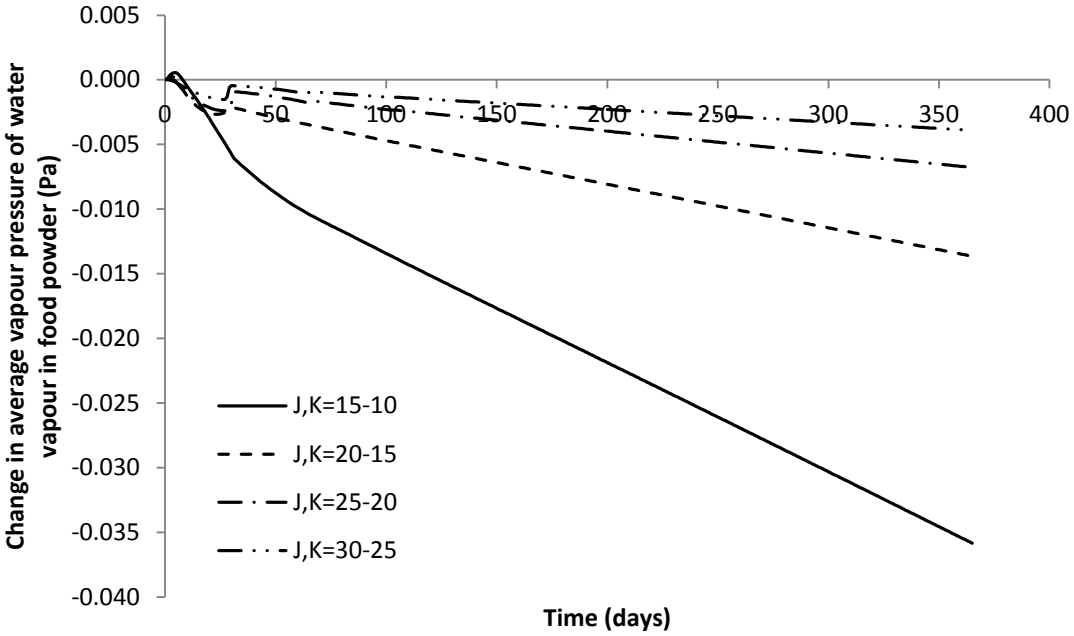

Figure E-4: Plot of change in predicted values of average water vapour pressure in food powder (Pa) with changes to number of nodes in axial (J) and radial (K) directions.

As shown in Figure E-4, changes to the number of nodes in axial and radial directions had relatively insignificant effects on predictions of average water vapour pressure in the food powder, with no differences greater than 0.036×10^{-3} Pa over the period $0 \leq t \leq 365$ days. This is in contrast to the model with no isolated air pocket around the perforation (Section E.1.3.1.2), which is due to the larger area of water vapour entering the system and thus a moisture profile covering of a larger number of nodes. However it should be noted that a similar effect will likely occur if the air pocket is sufficiently small relative to the radial thickness of the food powder being considered. Again, since other approximations are expected to be more significant, a standard 10 nodes in both axial and radial directions were used to allow a reasonable solving time.

E.2.2.2 Mathematical Error Checks

To allow an analytical solution for the water vapour pressure in the food powder, the following changes were made:

- The porosity of the food powder was set to 1 to disable water sorption in the solid phase.
- Only the water vapour pressure profile after 1 minute was considered.
- The number of nodes in the radial direction was increased significantly and the area of the air pocket adjusted to cover all nodes except for the node furthest from the axis of symmetry. This essentially reduced the system to one-dimension. It should be noted that the number of nodes was practically limited by solving time, therefore it was not possible to eliminate the effect of the outer node. However to further reduce this effect, only the water vapour profile along the axis of symmetry was considered.
- The area of perforations in the polymer liner was set to a very high value to ensure the water vapour pressure at the surface of the food powder bordering the air pocket remained equal to the water vapour pressure in the ambient air.

Formulated problem:

$$\left(\varepsilon S_{air}^{H_2O} + (1-\varepsilon) S_f^{H_2O}\left(p_f^{H_2O}\right)\right)\frac{\partial p_f^{H_2O}}{\partial t} = D_{eff}^{H_2O} S_{air}^{H_2O}\frac{\partial^2 p_f^{H_2O}}{\partial x^2}$$

for $t \geq 0,\ 0 < x < X_f$

$$p_f^{H_2O} = p_a^{H_2O}$$

for $t \geq 0,$ *at* $x = 0$

$$\frac{dp_f^{H_2O}}{dx} = 0$$

for $t \geq 0,$ *at* $x = X_f$

$$p_f^{H_2O} = p_{f,i}^{H_2O}$$

for $t = 0,\ 0 < x < X_f$

Analytical solution:

$$Fo = \frac{D_{eff}^{H_2O} t}{{X_f}^2} = \frac{1.754 \times 10^{-5} \times 60}{0.1^2} = 0.1053$$

$$Y = \frac{4}{\pi}\sum_{m=0}^{\infty}\frac{(-1)^m}{2m+1}cos\left[(2m+1)\frac{\pi}{2}\frac{x}{X_f}\right]exp\left[-(2m+1)^2\frac{\pi^2}{4}Fo\right]$$

m	$\frac{(-1)^m}{2m+1}cos\left[(2m+1)\frac{\pi}{2}\frac{x}{X_f}\right]exp\left[-(2m+1)^2\frac{\pi^2}{4}Fo\right]$
0	0.7713
1	-0.03219
2	3.027×10^{-4}
Total	0.7394

$$Y = \frac{4}{\pi}0.7394 = 0.9414$$

$$p_{lnr}^{H_2O} = Y\left(p_{lnr,i}^{H_2O} - p_a^{H_2O}\right) + p_a^{H_2O} = 0.9414(585.2 - 1755.7) + 1755.7 = 653.8 \text{ Pa}$$

This procedure was repeated to calculate the water vapour pressure after 60 seconds for various positions within the food powder.

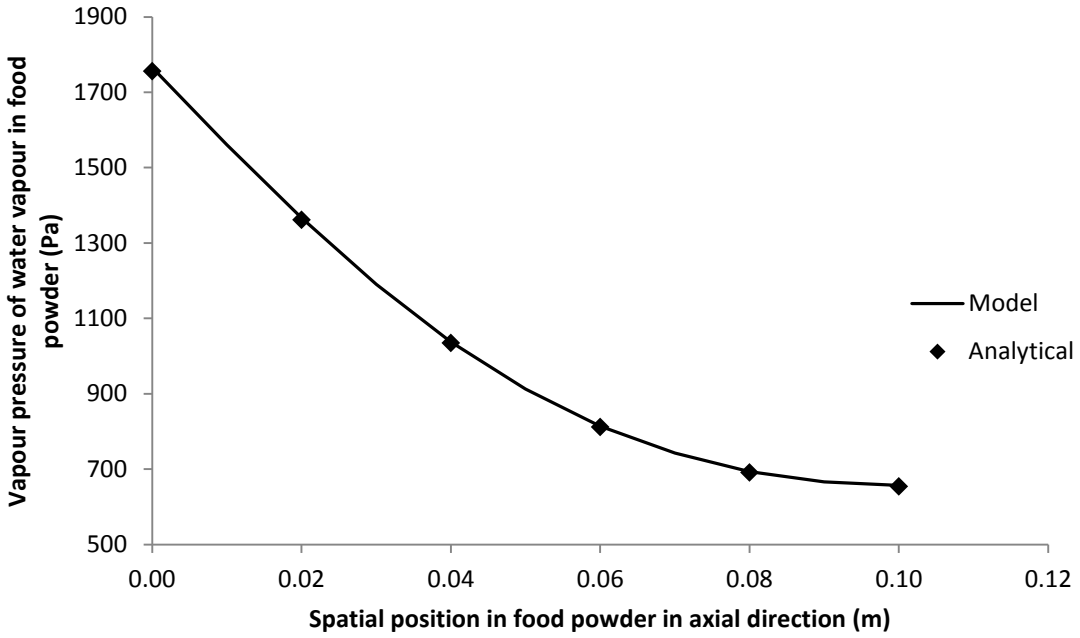

Figure E-5: Comparison of water vapour pressure profile in food powder after 60 seconds as predicted analytically and by the model.

As shown in Figure E-5, the values predicted by the model agree closely with those calculated analytically, suggesting the model is correctly calculating the water vapour pressure in the food powder. A similar solution was not possible for the case of no air pocket, however since the models were essentially identical except for the boundary conditions, similar agreement was expected. Analytical solutions were also not possible for water sorption in the solids phase or moisture transfer radially, although it is believed model validation would provide further verification.

Appendix F

FOOD PACKAGE CONSOLIDATION MODEL

F.1 MATHEMATICAL MODEL FORMULATION

F.1.1 Word Balances and Equations

F.1.1.1 ODE for Volume of Air in Package Headspace

$$p_1 + \frac{1}{2}\rho {v_1}^2 + \rho g h_1 = p_2 + \frac{1}{2}\rho {v_2}^2 + \rho g h_2$$

$$v_1 = 0, h_1 = 0, h_2 = 0$$

$$\therefore p_1 = p_2 + \frac{1}{2}\rho {v_2}^2$$

$$v_2 = \sqrt{\frac{2}{\rho}(p_1 - p_2)}$$

$$p_1 = p_{ph}^{air}$$

$$p_2 = p_{atm}$$

$$\therefore \frac{dV_{air}}{dt} = -A_{prf} v_2 = -A_{prf}\sqrt{\frac{2}{\rho}\left(p_{ph}^{air} - p_{atm}\right)}$$

$$\left[\frac{m^3}{s}\right] = [m^2]\left[\frac{m}{s}\right]$$

F.2 SOLUTION

F.2.1 Analytical Solution

$$\frac{dV_{air}}{dt} = -A_{prf}\sqrt{\frac{2}{\rho}\left(p_{ph}^{air} - p_{atm}\right)}$$

$$\int_{V_{air,i}}^{V_{air}} dV_{air} = \int_{0}^{t} -A_{prf}\sqrt{\frac{2}{\rho}\left(p_{ph}^{air} - p_{atm}\right)}\,dt$$

$$V_{air} - V_{air,i} = -A_{prf}\sqrt{\frac{2}{\rho}\left(p_{ph}^{air} - p_{atm}\right)}t$$

$$V_{air} = V_{air,i} - A_{prf}t\sqrt{\frac{2}{\rho}\left(p_{ph}^{air} - p_{atm}\right)}$$

F.2.2 MATLAB® Solution

Refer to Appendix B for a digital copy of this numerical solution.

F.2.2.1 Script File (Consolidation.m)

```
%Script File

clear all

%System Inputs
Aprf=5.2e-9;                %Total surface area of perforation(s) in packaging (m^2)
mstk=25;                    %Mass pushing down on food package(kg)
g=9.81;                     %Acceleration due to gravity (m/s^2)
Astk=0.09;                  %Surface area of mass in contact with food package(m^2)
patm=101300;                %Atmospheric pressure (Pa)
Mrair=0.02897;              %Molecular mass of dry air (kg/mol)
R=8.314;                    %Ideal gas constant (m^3.Pa/mol/K)
T=273.15+18;                %Absolute temperature (K)

stime=24*60*60;             %Simulation time (seconds)


%CVs
ppkg=mstk*g/Astk;
rhoair=(patm+ppkg)*Mrair/R/T;


%Initial Conditions
```

```
Vairi=0.027;


%Solution
t=(0:stime/100:stime)';
for i=1:size(t)
    Vair(i,1)=Vairi-Aprf*sqrt(2/rhoair*(ppkg))*t(i);
    if Vair(i)<0
        Vair(i)=0;
    end
end


%Plot
figure
plot(t/60^2,Vair,'b-');
title('Volume of Air in Food Package');
xlabel('t (hours)');
ylabel('Vair (m^3)');


%Output data to Excel spreadsheet
outputtitle={'t (s)','V (m^3)'};
outputdata=[t,Vair];
xlswrite('ConsolidationOutput',outputtitle,'sheet1');
xlswrite('ConsolidationOutput',outputdata,'sheet1','A2');
```